

November 2014

PHYSIOLOGICAL MODELS OF GEOBACTER SULFURREDUCTENS AND DESULFOBACTER POSTGATEI TO UNDERSTAND URANIUM REMEDICATION IN SUBSURFACE SYSTEMS

Roberto Orellana
umass

Follow this and additional works at: https://scholarworks.umass.edu/dissertations_2



Part of the [Environmental Microbiology and Microbial Ecology Commons](#), and the [Microbial Physiology Commons](#)

Recommended Citation

Orellana, Roberto, "PHYSIOLOGICAL MODELS OF GEOBACTER SULFURREDUCTENS AND DESULFOBACTER POSTGATEI TO UNDERSTAND URANIUM REMEDIATION IN SUBSURFACE SYSTEMS" (2014). *Doctoral Dissertations*. 278.
https://scholarworks.umass.edu/dissertations_2/278

This Open Access Dissertation is brought to you for free and open access by the Dissertations and Theses at ScholarWorks@UMass Amherst. It has been accepted for inclusion in Doctoral Dissertations by an authorized administrator of ScholarWorks@UMass Amherst. For more information, please contact scholarworks@library.umass.edu.

PHYSIOLOGICAL MODELS OF *GEOBACTER SULFURREDUCTENS* AND
DESULFOBACTER POSTGATEI TO UNDERSTAND URANIUM REMEDIATION IN
SUBSURFACE SYSTEMS

A Dissertation Presented

by

ROBERTO ORELLANA ROMAN

Submitted to the Graduate School of the
University of Massachusetts Amherst in partial fulfillment
of the requirements for the degree of

DOCTOR OF PHILOSOPHY

September 2014

Microbiology Department

© Copyright by Roberto Orellana Roman 2014
All Rights Reserved

PHYSIOLOGICAL MODELS OF *GEOBACTER SULFURREDUCENS* AND
DESULFOBACTER POSTGATEI TO UNDERSTAND URANIUM REMEDIATION IN
SUBSURFACE SYSTEMS

A Dissertation Presented

by

ROBERTO ORELLANA ROMAN

Approved as to style and content by:

Derek R. Lovley, Chair

Kristen M. De Angelis, Member

James F. Holden, Member

Jason M. Tor, Member

John Lopes, Department Head
Microbiology

DEDICATION

Para Loreto, Leonor e Ignacio.

Essentially, all models are wrong, but some are useful.

George E. P. Box

ACKNOWLEDGMENTS

I would like to thank Derek Lovley for being a constant source of guidance, critical thinking and support. I arrived to his lab not having idea of anaerobic bacteria and I have learned a lot throughout these years. I would also like to give thanks to my other committee members; Kristen DeAngelis, Jim Holden, and Jason Tor. They have spent many hours discussing the results and have very valuable insights.

Also I thank to several mentors in the lab Carla Risso, Marzia Miletto, and Melissa Barlett that give me support, advice, and motivation. I thank current and past lab members: Arianna Gray, Sean Murphy, Pier Luc Tremblay, Shabir Dar, Dawn Holmes, Ching Leang, Pravin Shrestha, Toshiyuki Ueki, Jo Philips, Nikhil Malvankar, Tunde Mester, Joy Ward, Manju Sharma and Areen Banerjee for valuable help at all stages of this dissertation. Also, I want to thanks to the researchers from other universities that collaborate along this research. Thanks speacially to Luis Comolli (LBNL), Janet Leavitt (UNM), Kim Hixson, and Mary Lipton (PNNL).

I am highly indebted to my friends Burcu Unal, Jennifer Lin and Jesus Alvelo for help in many things and endless support especially when things got tough. I also have special thanks to the administrative people in the department: Maryanne Wells, Sue Laford, Ruthie Allies and Lorell Perreault for the countless times they save me from administrative issues during grad school. Also, I want to thanks to the department head John Lopes for his interesting conversations about science and soccer. I am grateful for all other students in the department that made my time here easier and enjoyable, especially George Hamaoui, Jennifer Hayashi, Joanne Lau, and Sarah Hensley.

Above all, I owe gratitude especially to my wife, my parents and sister. Without their encouragement, patience and love I would not have been capable of finishing this story with a happy end.

ABSTRACT
PHYSIOLOGICAL MODELS OF *GEOBACTER SULFURREDUCENS* AND
DESULFOBACTER POSTGATEI TO UNDERSTAND URANIUM REMEDIATION IN
SUBSURFACE SYSTEMS

SEPTEMBER 2014

ROBERTO ANDRES ORELLANA ROMAN
B.A., UNIVERSITY OF CHILE

Ph.D., UNIVERSITY OF MASSACHUSETTS AMHERST

Directed by: Professor Derek R. Lovley

Geobacter species are often the predominant Fe(III)-reducing microorganisms in many sedimentary environments due to their capacity for extracellular electron transfer. This exceptional physiological capability allows them to couple acetate oxidation to uranium (U(VI)) reduction, that is one of the most significant interactions between radionuclides and microorganisms that naturally takes place in uranium-contaminated environments. Although this process has been proposed as a promising strategy for the *in situ* bioremediation of uranium-contaminated groundwater, little is known about the molecular mechanisms involved in U(VI) reduction and the interaction between *Geobacter* and other microbial species.

In the first two research chapters, this dissertation aim to study the interaction between *Geobacter sulfurreducens*, a primary model organism to elucidate the physiological capabilities of *Geobacter* species, and U(VI). Our findings presented here suggest that *G. sulfurreducens* requires outer-surface *c*-type cytochromes, but not pili, for

the reduction of uranium, and U(IV), the product of U(VI) reduction was precipitated at the outer cell surface. Our results also suggest that there is not one specific U(VI)-detoxification specific mechanism for uranium detoxification in *G. sulfurreducens*. Rather, resistance to U(VI) appears to be accomplished with multiple stress response systems, that includes detoxification and oxidative stress response, and regulatory networks that facilitate fast adaptation to rapidly changing conditions.

The third research chapter of this dissertation examines the physiology of *Desulfobacter postgatei*, a competitor for acetate during *in situ* bioremediation of subsurface systems at a uranium-contaminated site in Rifle, CO. Our findings suggest that novel enzymatic complexes, such as the energy-converting hydrogenase related complex, Ehr, the proton-translocating ferredoxin:NADP⁺ oxidoreductase, Rnf, and also the NADH-dependent reduced ferredoxin:NADP⁺ oxidoreductase, Nfn, are involved in energy conservation, making *D. postgatei* a major competitor for acetate in several environments.

TABLE OF CONTENTS

	Page
ACKNOWLEDGMENTS	vi
ABSTRACT	vii
LIST OF TABLES	xiii
LIST OF FIGURES	xiv
CHAPTER	
1. INTRODUCTION	1
1.1 Central objective and goals	1
1.2 Bioremediation of uranium contamination	2
1.3 <i>In situ</i> bioremediation of uranium by microbial reduction	3
1.4 <i>Geobacter</i> species	4
1.5 Insights of Uranium reduction by <i>Geobacter sulfurreducens</i>	5
1.6 Physiological response of <i>G. sulfurreducens</i> to environmental relevant levels of Uranium	7
1.7 <i>In situ</i> stimulation of <i>Geobacter</i> towards uranium reduction	7
1.8 Subsurface microbial ecology during <i>in situ</i> bioremediation of uranium-contaminated groundwater	8
2. U(VI) REDUCTION BY A DIVERSITY OF OUTER SURFACE C-TYPE CYTOCHROMES OF <i>GEOBACTER SULFURREDUCTENS</i>	12
2.1 Introduction	12
2.2 Material and methods	14
2.2.1 Bacterial strains, culture conditions, cell suspension	14
2.2.2 Transmission electron microscopy	15
2.2.3 X-Ray Energy Dispersive Spectroscopy	16
2.2.4 Software	16
2.2.5 X-Ray Absorption Near Edge Structure (XANES)	17
2.2.6 qRT-PCR	17
2.3 Results and discussion	18
2.3.1 U(VI) Reduction with Genetically Modified Strains	18
2.3.2 Speciation and Localization of Uranium	19
2.4 Implications	19

3. PROTEOME OF GEOBACTER SULFURREDUCENS IN THE PRESENCE OF U(VI).....	26
3.1 Introduction.....	27
3.2 Material and methods.....	28
3.2.1 Strains and culturing	28
3.2.2 Protein Digestion and Desalting	28
3.2.3 Tandem MS, MS and putative peptide identification	29
3.2.4 Determination of Accurate Mass and Time (AMT) Tags.....	30
3.2.5 Impact of mutations on growth in the presence of U(VI).....	31
3.3 Results.....	31
3.3.1 Proteins involved in growth.....	32
3.3.2 Protein and DNA damage	33
3.3.3 Detoxification and Membrane damage.....	33
3.3.4 Proteins involved in oxidative stress.....	35
3.3.5 Extracellular matrix proteins.....	36
3.3.6 c-type cytochromes	36
3.4 Implications.....	37
4. NOVEL MEMBRANE-BOUND COMPLEXES INVOLVED IN ENERGY CONSERVATION BY THE ACETATE OXIDIZING SULFATE-REDUCING BACTERIUM DESULFOBACTER POSTGATEI.....	48
4.1 Introduction.....	49
4.2 Material and methods.....	50
4.2.1 Organism.....	50
4.2.2 Media and cultivation	51
4.2.3 Chemostat experiments	51
4.2.4 Analytical methods	51
4.2.5 DNA extraction and genome sequencing	52
4.2.6 Genome annotation	52
4.2.7 Metabolic Network Reconstruction	53
4.2.8 Total mRNA extraction.....	54
4.2.9 Illumina sequencing and assembly of Illumina reads	55
4.2.10 Mapping mRNA reads	55
4.3 Results and discussion	56
4.3.1 Energy metabolism	56
4.3.2 Novel membrane-bound complexes found in the genome of <i>D. postgatei</i>	57
4.3.2.1 Qrc (Quinone-reductase) complex.....	57
4.3.2.2 Ehr (Ech-hydrogenase-related) complex	58
4.3.2.3 H ⁺ -translocating ferredoxin:NADP ⁺ oxidoreductase (Rnf complex)	60
4.3.3 <i>In silico</i> metabolic model of <i>D. postgatei</i>	60
4.3.4 Growth kinetics and stoichiometry under electron donor and electron acceptor limitation.....	61
4.3.5 Kinetic of acetate oxidation and sulfate reduction.....	63

4.3.6 Validation of the metabolic model with experimental data	63
4.3.7 <i>In silico</i> characterization of <i>D. postgatei</i> metabolism	65
4.3.8 Monte Carlo sampling of <i>D.postgatei</i> model.....	67
4.3.9 Genome-wide transcriptional response of <i>D.postgatei</i> to different growth rates.....	67
4.3.10 Implications	69
5. CONCLUSION.....	81
APPENDICES	
A. SUPPLEMENTARY INFORMATION U(VI) REDUCTION BY A DIVERSITY OF OUTER SURFACE C-TYPE CYTOCHROMES OF GEOBACTER SULFURREDUCTENS	85
B. SUPPLEMENTARY INFORMATION PROTEOME OF GEOBACTER SULFURREDUCTENS IN THE PRESENCE OF U(VI)	89
C. SUPPLEMENTARY INFORMATION NOVEL MEMBRANE-BOUND COMPLEXES INVOLVED IN ENERGY CONSERVATION BY THE ACETATE OXIDIZING SULFATE-REDUCING BACTERIUM DESULFOBACTER POSTGATEI.....	207
BIBLIOGRAPHY.....	371

LIST OF TABLES

Table	Page
1. Selected proteins with lower relative abundance during exposure to U(VI) compared to the control cells.	43
2. Selected proteins with higher relative abundance during exposure to U(VI) compared to the control cells	45
3. Genes that were differentially expressed at least two fold in <i>D. postgatei</i> growing at 0.032 h ⁻¹ compared to those growing at 0.014 h ⁻¹	77

LIST OF FIGURES

Figure	Page
1.	U(VI)-reducing activity of wild type (wt) and mutant strains of <i>G. sulfurreducens</i> 20
2.	Uranium LIII-edge XANES spectra of uranium associated with 3 strains of <i>G. sulfurreducens</i> and their corresponding fits..... 21
3.	Proportion of Uranium at the different oxidations states after 4 hours cell suspensions 22
4.	TEM pictures showing level of filament production in wild type, Δ BESTZ and Δ pilA..... 23
5.	CryoTEM images of wild-type reducing fumarate, and wild-type, Δ pilA, Δ BESTZ reducing U(VI)..... 24
6.	XEDS of wild-type, Δ pilA, and Δ BESTZ respiring U(VI) 25
7.	Changes in the protein profile as a result of U(VI) exposure 38
8.	Effect of U(VI) on the growth of wild-type..... 39
9.	Effect of U(VI) on the growth of Δ sodA 40
10.	Effect of U(VI) on the growth of Δ GSU2212..... 41
11.	Effect of U(VI) on the growth of Δ GSU2213..... 42
12.	Comparison of the <i>D. postgatei</i> qrc operon to the one in <i>D. vulgaris</i> , <i>D. autotrophicum</i> , and <i>Desulfosarcina</i> sp. BuS5 71
13.	Representation of quinone reduction by Qrc in H ₂ -utilizing SRB and the proposed cytochrome reduction by Qrc in Acetate-utilizing SRB..... 72

14.	Hydrogen cycle in <i>D. vulgaris</i> proposed by Odom and Peck.....	73
15.	Predicted mechanism of Ehr complex and Qrc complex in <i>D. postgatei</i>	74
16.	Schematic metabolic reconstruction of the energy metabolism of <i>D. postgatei</i> .	75
17.	Phenotype Phase Planes analysis (PhPP) of <i>D. postgatei</i> metabolic model	76

CHAPTER 1

INTRODUCTION

1.1 Central objective and goals

Uranium mining, milling, nuclear fuel and weapons manufacturing-related activities have concentrated large quantities of U(VI) in specific areas, resulting in vast zones of contaminated soils and groundwater. Currently, one of the most feasible tools to prevent U(VI) mobility in the environment is *in situ* bioremediation of uranium-contaminated groundwater. This seeks the reduction, by means of microbial respiration, of hexavalent uranium U(VI) to tetravalent uranium U(IV) which is orders of magnitude less soluble. Several sediment-based and *in situ* studies at a uranium-contaminated site in Rifle, CO, have shown that U(VI) reduction can be stimulated with the addition of organic electron donors, such as acetate (1, 2). However a highly efficient and sustainable long-term uranium bioremediation strategy requires a deeper understanding of the *in situ* physiological status of the subsurface community during uranium bioremediation and an identification of the factors potentially limiting U(VI) reduction activity.

The main goal of this dissertation is to address these knowledge gaps by studying the interaction between *Geobacter sulfurreducens* and U(VI) and by studying the physiology of *Desulfobacter postgatei*, its competitor for acetate during *in situ* bioremediation of subsurface systems at a uranium-contaminated site in Rifle, CO.

This project is expected to answer the following research questions:

- i- What are the uranium reductases in *G. sulfurreducens*? Where does U(VI) reduction take place in the cell?
- ii- What is the physiological response of *G. sulfurreducens* in the presence of environmentally relevant concentrations of U(VI)?
- iii- What are the kinetic and stoichiometric parameters that characterize the growth of *Desulfobacter postgatei* under environmental relevant conditions? What are key physiological characteristics that are unknown in the metabolism of *D. postgatei*?

This dissertation is divided into three independent research chapters; each one will correspond to an independent scientific publication. Chapter 1 presents the justification and the background of the study. Chapter 2, 3, and 4, are the main research chapters describing the results and findings from each project. Chapter 2 includes the results about electron transfer mechanism of *Geobacter sulfurreducens* to reduce U(VI), which was recently published (3). Chapter 3 includes the physiological response of *G. sulfurreducens* to environmentally relevant levels of U(VI), which is currently in review by Microbiology Journal. Chapter 4 is devoted to the sulfate-reducing bacteria, *Desulfobacter postgatei* and includes the description of the stoichiometry and kinetics of growth and explores previously unknown metabolic capabilities to conserve energy. Chapter 6 summarizes the findings for the entire study and suggests possible directions for future work.

1.2 Bioremediation of uranium contamination

The use of uranium for nuclear research, fuel production, and weapons manufacturing has resulted in widespread dispersal of an environmental contaminant with a great ecological risk (4). Uranium contamination of sediments and ground/surface water is a serious concern, especially at many former uranium mining and processing facilities (5). At these sites, residual radionuclides have leached into the subsurface threatening the natural environment and human health, both locally and through off-site transport of soluble U(VI) (6). Additional contamination has resulted uranium being released from the combustion of coal as well as from the manufacture and application of phosphate fertilizers (4, 7).

The U.S. Department of Energy's (DOE) Subsurface Science, through the NABIR (Natural and Accelerated Bioremediation Research), EMSP (Environmental Management Science Program), ERSP (Environmental Remediation Sciences Program) and SBR (Subsurface Biogeochemical Research Program) programs, has invested a vast amount of effort to gain a comprehensive and mechanistic understanding of the microbial factors and associated geochemistry controlling uranium mobility in the environment. In several previous studies supported by DOE, a systematic multi-tiered and predictive approach

has been proposed to design strategies for the *in situ* bioremediation of groundwater contaminated with uranium and other toxic metals.

Bioremediation is the application of living or dead organisms to degrade or transform hazardous inorganic and organic contaminants present in the environment (8). It often works by either transforming or degrading contaminants into nonhazardous or less hazardous chemicals. Since, unlike organic compounds, metals and radionuclides cannot be degraded, uranium bioremediation seeks the reduction of U(VI) to U(IV), which is orders of magnitude less soluble than most other U species (9).

There are a number of *ex situ* and *in situ* bioremediation methods currently available. In the *ex situ* approach, also known as “pump and treat methods”, the polluted groundwater is pumped to the surface where it can be treated more easily (10). However, its application in uranium remediation is generally restricted by poor extraction efficiency, the generation of large volumes of toxic uranium waste, and the increased public health and safety risks of bringing uranium contaminants up to the surface (11). On the other hand, the *in situ* approach has been suggested as an attractive alternative strategy for remediation of uranium contaminated subsurface environments due to the fact that is a relatively simple, low cost, effective, and environmentally safe remediation method (7, 11-13). However, this approach still has several challenges. For instance, the addition of extrinsic microbes to the contaminated groundwater may not be a viable option, since foreign microbes may not survive or may not remediate contaminants any better than indigenous microbes (10). Therefore, a significant effort has been made in order to develop and improve the strategies capable to stimulate the indigenous bacteria to reduce mobile U(VI) to the insoluble U(IV). These usually seek to identify the microbes responsible for uranium reduction, expand our understanding about their *in situ* physiological status, enhance the natural microbial environment by adding amendments that make native microbial communities work more effectively towards U(VI) reduction, and integrate the interplay of biology, hydrology, and geochemistry to predictively model the coupled processes in subsurface environments (2, 10, 14).

1.3 *In situ* bioremediation of uranium by microbial reduction

Microbial activity affects the chemical nature of U by altering its solubility, speciation, and sorption properties and thus its bioavailability (15). Some microbes can interact with radionuclides via several mechanisms, some of which may be used as the basis of potential bioremediation strategies. These mechanisms include biosorption, bioaccumulation, biomineralization, microbially enhanced chemisorption and direct enzymatic reduction (16). Among these, the reduction of U(VI) to U(IV) plays a pivotal role in controlling the solubility and mobility of uranium since uraninite, UO_2 , is orders of magnitude less soluble than most other U species (4, 17). Due to its natural occurrence in the environment, applicability, and also due to the greater stability of the reduced form, microbial uranium reduction has become a fundamental baseline behind bioremediation of uranium-contaminated groundwater (16, 18).

The list of bacteria known to reduce U(VI) includes more than 40 species and still is growing (4). Many microorganisms that are able to couple the oxidation of organic compounds to the reduction of Fe(III) are also able to reduce uranium enzymatically (19). Among these, particular attention has been drawn to *Geobacter metallireducens* and *Shewanella putrefaciens* (20) which were the first organisms found to be capable of uranium reduction. Together with *Desulfotomaculum reducens* (21), *Anaeromyxobacter dehalogenans* (22), and *Thermoterrabacterium ferrireducens* (23), they are the only species that can yield enough energy to support growth by uranium reduction. In addition, the sulfate-reducing bacteria *Desulfovibrio desulfuricans*, *D. sulfodismutans*, *D. alaskensis*, *D. vulgaris* and *Desulfomicrobium norvegicum*, and other anaerobes such as *Clostridium* sp. and *Pseudomonas putida* are able to reduce U(VI) enzymatically without conserving energy from these processes (4, 24-28). Nevertheless, other *Geobacter* species, such as *G. lovleyi* and *G. sulfurreducens*, were surprisingly capable to gain enough energy for growth from this process (22).

1.4 *Geobacter* species

Geobacter species are anaerobic iron-reducing bacteria that have received special attention because of their novel electron transfer capabilities. *Geobacter* species have the ability to conserve energy for growth by oxidizing organic compounds coupled to the

reduction of a high variety of electron acceptors (1). This along with its remarkable respiratory versatility (29) allows *Geobacter* to be significant in environments in which Fe(III) reduction is the primary electron-accepting process (30), and more important in many uranium contaminated subsurface environments (7).

Geobacter sulfurreducens, a member of the deltaproteobacteria and of the family *Geobacteraceae*, commonly serves as the model organism for the *Geobacteraceae* in subsurface environments. Since it is closely related to *Geobacter* species that are predominant in subsurface environments (31), it has become one of the most intensively studied metal reducing bacteria (1). This was the first *Geobacter* species whose genome was sequenced (31) and for which a genome-based metabolic model was designed and a genetic system was developed (32). Indeed a substantial number of genome-scale gene expression and proteomic studies have been conducted with *G. sulfurreducens* (33-51).

1.5 Insights of Uranium reduction by *Geobacter sulfurreducens*

Despite the fact that little is known about the nature of this process, *c*-type cytochromes are expected to play a key role in this process (4, 52). Although the first evidence that *c*-type cytochromes were involved in this process was proposed by Lovley et al (1993) (26, 53), the mechanism(s) by which U(VI) is reduced by *Geobacter* species remains still unknown. In this study, the *c*-type cytochromes were oxidized when U(VI) was added to whole cell suspensions of *Geobacter metallireducens*. Afterwards Lloyd and coauthors (2003)(54) showed that deletion of the gene encoding the periplasmic *c*7 cytochrome, PpcA, negatively impacted acetate-dependent U(VI) reduction in *G. sulfurreducens*. Although this evidence suggested that PpcA may play a role in U(VI) reduction, it did not reveal its specific function. Indeed, more recent studies have shown other *c*-type cytochromes play a key role in microbial U(VI) reduction in *G. sulfurreducens* (55). Shelobolina *et al* found that the elimination of two confirmed outer membrane cytochromes and two putative outer membrane cytochromes significantly decreased the ability of *G. sulfurreducens* to reduce U(VI) by 50–60% (52).

There is an increasing body of evidence that suggest that *c*-type cytochromes are essential molecules for U(VI) reduction in other dissimilatory metal reducing bacteria,

such as *Shewanella* and *Desulfovibrio* species (55, 56). For instance, two studies showed that the periplasmic tetraheme *c3* cytochrome was required for U(VI) reduction by species of the sulfate reducing bacteria, *Desulfovibrio vulgaris* (26) and *Desulfovibrio desulfuricans* (28). It was also reported that the iron reducing bacteria, *Shewanella oneidensis* MR-1 mutant lacking the cytochrome *c552* was deficient in its ability to reduce U(VI) (57). Furthermore, it was shown that the failure to complete *c*-type cytochromes maturation impaired U(VI) reduction. Indeed, the deletion of *mtrC* and *omcA*, both outer membrane bound decaheme *c*-type cytochrome, affected significantly U(VI) reduction (55). More interestingly, the same research shows both cytochromes forming a close association with extracellular uranium nanoparticles within EPS.

Despite the different lines of evidence that support an important role of *c*-type cytochromes in U(VI) reduction, it has recently been suggested by others that electrons are directly transferred from the conductive pili of *G. sulfurreducens* (58, 59) to U(VI) (60, 61). Although this evidence contrasts with the finding that pili are not required for the reduction of other soluble extracellular electron acceptors such as Fe(III) citrate or the humic substances analog anthraquinone-2,6-disulfonate (AQDS) (58, 62), further experiments are necessary to resolve this controversy.

Not only are the mechanisms of *G. sulfurreducens* to reduce U(VI) still unclear, but also the site where this reaction occurs remains unknown. Since extracellular electron transfer to minerals, such as Fe(III) and Mn(IV) oxides (20, 29, 63), electrodes (64), and soluble metal species, such as Fe(III) chelated with citrate (65) have been described as one of *Geobacter*'s specialties, it has been assumed that U(VI) reduction mainly takes place at the outer membrane (52). However, contradictory results have hampered our understanding about the location of U(VI) reduction.

Initially, chymotrypsin-treated cells performed uranium reduction at similar rates as untreated cells, while the rate of reduction of insoluble Fe(III) oxides was reduced by 90% (16). Assuming that the chymotrypsin treatment was able to efficiently digest all outer membrane proteins, these results suggested that surface proteins are required for electron transfer to Fe(III) oxides, but not U(VI). In spite of this, more recent studies also suggested a role for periplasmic cytochromes as putative electron shuttles, from central metabolism to the outer membrane, and outer membrane cytochromes as the uranyl

reductases (52). A more compelling argument was revealed in the same study, showing that accumulation of uranium in the periplasm of U(VI) reduction-impaired mutants and wild type. This implies that periplasmic uranium accumulation observed before is unrelated to the capacity for uranium reduction and may instead reflect the ability of uranium to penetrate the outer membrane and react with substances in the periplasm that promote formation of precipitates. Although *Geobacter* species has been identified as an effective means for immobilizing U(VI) in several bioremediation engineered systems, the biomolecular mechanisms of U(VI) reductions by *Geobacter* species are still not well understood.

1.6 Physiological response of *G. sulfurreducens* to environmental relevant levels of U(VI)

U(VI) is both biochemically and radiologically toxic even for microorganisms that use it as a source of energy (4, 66). Despite of its importance as a model to expand the understanding of *in situ* bioremediation of U(VI) contaminated groundwater, the knowledge about the interaction between *Geobacter sulfurreducens* and U(VI) is still highly limited.

There are few studies addressing the effects of U(VI) exposure to anaerobic pure bacterial cultures, and none of them includes *Geobacter* species (67, 68). These studies reported that, in contrast to essential metals that can be imported or extruded depending on current requirements of the cell (69), U(VI) presents a particular challenge to *Geobacter* species. Since there is no evidence for U(VI)-specific transport or protective mechanism, there are many other unspecific physiological traits that may deal with U(VI). Also, the capacity of U(VI) to denature proteins, inactivate functional groups of enzymes, disrupt the cell envelope, and damage DNA remains unknown (70-72).

1.7 *In situ* stimulation of *Geobacter* towards uranium reduction

Initially supported by the The Natural and Accelerated Bioremediation Research (NABIR) program, several efforts have been made to study the potential for stimulating

indigenous U(VI)-reducing microbial communities in subsurface sediments. Early studies evaluated which electron donors might best promote the activity of dissimilatory metal-reducing microorganisms that would reduce the available uranium in subsurface sediments, and which species were the predominant members of the microbial community (12, 31). In these studies, subsurface sediments from a variety of uranium-contaminated sites were incubated under anaerobic conditions with various electron donors added while monitoring metal reduction and microbial community composition over time. In nearly all cases, species belonging to the *Geobacteraceae* became the predominant metal-reducing microorganisms (73, 74). Afterwards, several studies have shown the same predominance of *Geobacter* in the field (7, 30, 75, 76) demonstrating that laboratory incubations of uranium-contaminated sediments yielded useful insights into the microbial processes likely to take place *in situ*.

Another important outcome of the laboratory sediment incubations was that acetate was shown to be the best promoter for microbial metal reduction without stimulating the unwanted growth of fermentative organisms that were not involved in the uranium reduction process and may cause aquifer clogging. These results served as the basis for the design of field experiments at the uranium-contaminated Uranium Mill Tailings Remedial Action (UMTRA) Project site in Rifle, Colorado. These field scale studies have demonstrated the stimulation of uranium bioremediation with added acetate was a repeatable phenomenon and that U(VI) reduction was clearly linked to the presence and activity of microorganisms of the family *Geobacteraceae* (7, 74). The field scale studies indicate an increase in *Geobacter* species by several orders of magnitude in groundwater accompanied by enhanced uranium and Fe (III) reduction for up to 40 days. Furthermore, it was reported that vanadium was also removed from the groundwater via the reduction of V(V) to V(IV), which is consistent with our other work supported by NABIR that *Geobacter* species are also capable of V(V) reduction (77).

1.8 Subsurface microbial ecology during *in situ* bioremediation of uranium-contaminated groundwater

The success of the *in situ* stimulation approach depends on ensuring iron reduction as the predominant terminal electron-accepting process (TEAP) and uranium-reducing bacteria, such as *Geobacter*, as the dominant species in the subsurface for the longest possible time. Although, the first *in situ* experiment reported that *Geobacter* was successfully stimulated for 30-40 days (7), continuing acetate injections at the Rifle field site from year to year have shown that the initial *Geobacter* bloom only lasted for 20 days in subsequent experiments in the same plot and was followed by a more rapid decline of the *Geobacter* and increase of sulfate-reducing bacteria (SRB) (75). Once the sulfate reduction phase had begun, uranium removal was less effective suggesting that the acetate-consuming sulfate-reducing bacteria, such as members of *Desulfobacteraceae* and some Firmicutes present at Rifle site, may not be able to reduce uranium (78). Geochemical monitoring and molecular analysis in sediments and groundwater have shown that due to the high concentrations of sulfate (~8-10 mM), complete oxidizing sulfate-reducing bacteria were able to consume the acetate, thereby limiting the activity of the *Geobacter* and decreasing the overall effectiveness of uranium removal (7). It raises the point that during acetate-amended bioremediation, *Geobacter* must compete for acetate with SRB.

Since Fe(III) reduction is energetically more favorable than SO_4^{2-} reduction, iron-reducing bacteria were expected to outcompete SRB for common electron donors (79). Therefore, it was hypothesized that Fe(III) depletion was the main factor driving the shift from dissimilatory iron reduction to sulfate reduction as the dominant TEAP. To test this hypothesis, microcosm and column studies were conducted using Rifle sediments. These results suggested that both TEAP processes can take place concurrently, even after long periods of acetate amendment, and the lack of Fe(III) availability may not be the primary reason for the *Geobacteraceae* decline (80). Therefore, the mechanism of interaction between the *Geobacter* and SRB is still unknown, and thus supporting the hypothesis that this might be more complex than a competitive thermodynamic interaction.

Due to the advantages of acetate-amended based bioremediation, our current interest in uranium remediation is primarily focused on the interactions of these two specific microbial groups and the significance of their interaction to remediation

strategies. During 2008 and 2009 *in situ* field studies, the diversity, abundance, and metabolic state of the sulfate-reducing community was investigated to better understand the microbial community dynamics involved in the transition from iron to sulfate reduction. Clone libraries based on the *dsrAB* gene, which encode α and β subunits of the dissimilatory (bi)sulfite reductase, indicated that there were three major phylogenetic clusters of SRB at the site: *Desulfobacteraceae*, *Desulfobulbaceae*, and the *Syntrophaceae*-related sulfate reducers. The *Desulfobacteraceae* cluster displays 97% sequence similarity with *Desulfobacter postgatei* (78). The recovered *dsrAB* sequences were used to design primers to assess the abundance and metabolic state of the sulfate-reducing community from estimates of *dsrAB* operon and transcript abundance, respectively. During the sulfate reduction phase the *Desulfobacteraceae*-related SRB were found at an order of magnitude greater abundance than the *Desulfobulbaceae*- and *Syntrophaceae*-related SRB (78). Similarly, the *Desulfobacteraceae* cluster was found to be the most active, as the number of *dsrAB* transcripts was 2 orders of magnitude higher than that of *Desulfobulbaceae* and *Syntrophaceae* clusters (78). More recent studies agreed with these results suggesting that the diversion of acetate flux from *Geobacter* species to *Desulfobacter postgatei* is a likely explanation for the poor performance of the uranium bioremediation strategy under sulfate-reducing conditions (81, 82).

Desulfobacteraceae are the most important players during the sulfate reduction phase. Therefore, the next step to improving remediation strategies is to determine the mechanisms of interaction between these and the *Geobacter* species and ascertain possible changes to the current strategy to improve long-term uranium reduction. However, since no field isolates of acetate-using SRB from the *Desulfobacteraceae* have been cultured, the *Desulfobacter postgatei* strain 2ac9 was used as model organism to get a better understanding of its metabolic potential that drives microbial interactions between *Geobacter* and SRB communities during uranium bioremediation. The availability of *D.postgatei* genome sequence will help to design genome-wide studies to elucidate and compare its global physiological status *in situ* and laboratory incubations. Moreover, together with the availability of genome sequences of relevant *Geobacteraceae* species in Rifle (83), information on the *D. postgatei* genome was

utilized to design a computational metabolic model that can predict the physiological responses under environmental relevant conditions.

CHAPTER 2

U(VI) REDUCTION BY A DIVERSITY OF OUTER SURFACE C-TYPE CYTOCHROMES OF *GEOBACTER SULFURREDUCTENS*

2 Abstract

Early studies with *Geobacter sulfurreducens* suggested that outer-surface *c*-type cytochromes might play a role in U(VI) reduction, but it has recently been suggested that there is substantial U(VI) reduction at the surface of the electrically conductive pili known as microbial nanowires. This phenomenon was further investigated. A strain of *G. sulfurreducens*, known as Aro-5, which produces pili with substantially reduced conductivity, reduced U(VI) nearly as well as wild-type as did a strain in which the gene for PilA, the structural pilin protein, was deleted. In order to reduce rates of U(VI) reduction to levels less than 20% of wild-type it was necessary to delete the genes for the five most abundant outer surface *c*-type cytochromes of *G. sulfurreducens*. X-ray absorption near-edge structure spectroscopy demonstrated that whereas $83 \pm 10\%$ of the uranium associated with wild-type cells correspond to U(IV) after four hours of incubation, with the quintuple mutant $89 \pm 10\%$ of uranium was U(VI). Transmission electron microscopy and X-ray Energy Dispersion Spectroscopy revealed that wild-type cells did not precipitate uranium along pili as previously reported, but U(IV) was precipitated at the outer cell surface. These findings are consistent with previous studies which have suggested that *G. sulfurreducens* requires outer-surface *c*-type cytochromes, but not pili, for the reduction of soluble extracellular electron acceptors.

2.1 Introduction

The mechanisms for U(VI) reduction in *Geobacter* species are of interest because the precipitation of U(VI) to U(IV) is a promising strategy for the *in situ* bioremediation of uranium-contaminated groundwater and *Geobacter* species often predominate in subsurface environments in which U(VI) reduction is stimulated with the addition of organic electron donors (2, 37). The suggestion that electrons are directly transferred from the conductive pili of *Geobacter sulfurreducens* to U(VI) (60, 61) contrasts with the

finding that pili are not required for the reduction of other soluble extracellular electron acceptors such as Fe(III) citrate or the humic substances analog anthraquinone-2,6-disulfonate (AQDS) (58, 62).

Pili are required for long-range electron transport to insoluble electron acceptors in the *Geobacter* species that have been examined to date. This includes reduction of insoluble Fe(III) oxides (58, 84) and electron exchange between syntrophic partners (35, 85) as well as electron conduction through current-producing biofilms (59, 86, 87). This has been attributed to the metallic-like conductivity of the pili (59, 88). For example, a strain of *G. sulfurreducens*, designated Aro-5, which was genetically modified to produce pili with diminished conductivity lacked the capacity for effective Fe(III) oxide reduction and current production (88). In addition to pili, *G. sulfurreducens* requires the multi-heme *c*-type cytochrome, OmcS, for Fe(III) oxide reduction (89). OmcS is specifically localized on the pili (90). Thus, the simplest model for the last steps in Fe(III) oxide reduction is electron transport to OmcS via the pili, with OmcS facilitating electron transfer from the pili to Fe(III) oxide (91, 92). In a similar manner, networks of pili facilitate long-range electron transport through conductive biofilms of *G. sulfurreducens*, but one or more multi-heme cytochromes are required to promote electron transfer from the biofilm to electrodes (87, 93, 94).

Gene deletion studies demonstrated that, in contrast to the requirement of OmcS for Fe(III) oxide reduction, OmcS was not essential for the reduction of Fe(III) citrate or AQDS (62, 89), consistent with the ability of the pili-deficient strain to reduce these electron acceptors (58, 62). In order to significantly reduce the capacity for AQDS reduction it was necessary to delete the genes for five outer-surface *c*-type cytochromes in one strain (58, 62). These included OmcS and the OmcS homolog OmcT, as well as OmcE, OmcZ, and OmcB. Immunolabelling studies have demonstrated that OmcB is embedded in the outer membrane of *G. sulfurreducens* with a portion of the molecule exposed to the extracellular environment (95), whereas as OmcZ (94) and OmcE (89) are localized in the extracellular matrix. The necessity to remove all of these cytochromes suggested that AQDS reduction is rather non-specific. Although deleting just OmcB significantly eliminated the capacity for Fe(III) citrate reduction (96) the OmcB-deficient

mutant adapted over time to reduce Fe(III) citrate in the absence of OmcB with increased expression of other outer-surface cytochromes (97).

A diversity of *c*-type cytochromes can reduce U(VI) *in vitro* (55, 93, 98, 99). Furthermore, *c*-type cytochromes are essential for U(VI) reduction in *Shewanella oneidensis*, which accumulates uranium nanoparticles in association with the outer membrane cytochromes (55). Previous studies also suggested that *c*-type cytochromes exposed on the outer surface of *G. sulfurreducens* were involved in U(VI) reduction (52). An important line of evidence for a potentially important role of pili in U(VI) reduction was the finding that a pilA-deficient mutant reduced U(VI) at a rate ca. one-third the rate that wild-type reduced U(VI) (60). However, the pilA-deficient mutant was also defective in the production of outer-surface *c*-type cytochromes (60), confounding interpretation of the results. These considerations, and the recent availability of the Aro-5 strain, led us to further investigate the hypothesis that pili are a major conduit for electron transfer to U(VI) by *G. sulfurreducens*.

2.2 Material and methods

2.2.1 Bacterial strains, culture conditions, cell suspensions

All strains (Table A1) were obtained from our laboratory collection and were routinely cultured anaerobically in medium with 10 mM acetate as electron donor and 20 mM fumarate as electron acceptor, as previously described (52).

Resting cell suspensions were prepared as previously described (52). Briefly, cells were harvested in late exponential phase with an optical density of 0.25-0.28, washed with buffer and resuspended in buffer containing NaHCO₃ (2.5 g L⁻¹), NH₄Cl (0.25 g L⁻¹), NaH₂PO₄·H₂O (0.006 g L⁻¹), and KCl (0.1 g L⁻¹) at an OD₆₀₀ of 0.075-0.08. Acetate (5mM) and uranyl acetate (1mM) were added as electron donor and acceptor, respectively. Heat-killed controls were prepared by autoclaving the cell suspension for 30 min before the addition of U(VI). Cell suspensions were incubated at 30 °C.

The ability of cells to reduce U(VI) was monitored as the loss of U(VI) over time as previously described (52). Briefly, samples from cell suspensions (100 ul) were taken at

one-hour intervals and diluted in 14.9 ml of anoxic 100 mM bicarbonate and 14.9 ml of anoxic URAPLEX working solution. U(VI) concentrations were quantified with Kinetic Phosphorescence Analyzer (KPA) (Chemcheck Corp., Richland, WA), and the rate of enzymatic U(VI) reduction over 4 h was calculated as described previously (52).

2.2.2 Transmission electron microscopy

For a control survey of cell appendages, cells were harvested by centrifugation at mid-log phase and prepared as previously described (52). Samples were placed on 400-mesh carbon-coated copper grids, incubated for 5 minutes, and then stained with 2 % uranyl acetate. Cell appendages were observed with a JEOL 100 transmission electron microscope at an accelerating voltage of 80 kV. Images were taken digitally using the MaxIm-DL software and analyzed using Image J (<http://rsbweb.nih.gov/ij/index.html>).

For cryo-TEM, 5 μ L aliquots of culture were placed onto lacey carbon grids (Ted Pella 01881, Ted Pella Inc., Redding, CA) that were pre-treated by glow-discharge. The Formvar support was not removed from the lacey carbon. The grids were manually blotted with filter paper and flash frozen with a portable cryo-plunger (100), and stored in liquid nitrogen.

For air-dried samples aliquots of 5 μ L were placed onto continuous carbon-coated Formvar TEM grids (Ted Pella 01753, Ted Pella Inc., Redding, CA) pre-treated grids by glow-discharge. They were blotted after equilibration for 2 min. Cryo-grids were freeze-dried after cryo-TEM imaging. Both air-dried and freeze dried cryo-TEM specimens were used for XEDS analysis as described below.

Cryo-TEM images were acquired on a JEOL-3100-FFC electron microscope equipped with a FEG electron source operating at 300 kV, an Omega energy filter, cryo-transfer stage, and a Gatan 795 4Kx4K CCD camera mounted at the exit of an Electron Decelerator held at a constant voltage of 200 kV (101). The stage was cooled with liquid nitrogen to 80 K during acquisition of all data sets. In order to have a statistically relevant survey, over 100 images were recorded using magnifications of 112Kx, 70Kx, and 42Kx at the CCD giving a pixel size of 0.14 nm, 0.21 nm or 0.375 nm at the specimen, respectively. Underfocus values ranged between 2 μ m \pm 0.5 μ m to 12 μ m \pm 0.5 μ m, and

energy filter widths were typically around $28 \text{ eV} \pm 2 \text{ eV}$. The survey of the grids and the selection of suitable targets for tilt series acquisition were done in low dose diffraction mode through the acquisition of dozens of images.

Two tomographic data sets of Δ pilA were acquired. Tomographic tilt series were acquired under low dose conditions, over an angular range between $+62^\circ$ and -62° , $\pm 2^\circ$ with increments of 2° . Sixty (60) and sixty three (63) images were recorded for these tilt series, acquired semi-automatically with the program Serial-EM (<http://bio3d.colorado.edu/>) adapted to JEOL microscopes. For these tilt series data sets, images were recorded using nominal magnification of 15 kx resulting in 42 kx at the CCD and a pixel size of 0.375 nm at the specimen. The under focus value was set to $12 \mu\text{m} \pm 0.5 \mu\text{m}$, and energy filter widths to 28 eV. The maximum dose used per complete tilt series was approximately $140 \text{ e}^-/\text{\AA}^2$.

2.2.3 X-Ray Energy Dispersive Spectroscopy

High spatial resolution chemical analyses of cell membranes of air-dried samples on continuous carbon-coated Formvar TEM grids and freeze-dried cryo-TEM samples were carried out in the JEOL 2100-F 200 kV Field-Emission Analytical Transmission Electron Microscope (TEM) equipped with Oxford INCA Energy Dispersive Spectroscopy (EDS) X-ray detection system at the Molecular Foundry at Lawrence Berkeley National Laboratory. High angle annular dark field (HAADF) scanning transmission electron microscopy (STEM) images and X-ray elemental line scans were acquired with a 1 nm probe at 120 or 200 kV. The specimens were tilted 10 degrees toward the X-ray detector to optimize the X-ray detection geometry. Collection times were 300 live seconds for each line scan. The EDS line scans on the high contrast regions of the outer membrane clearly demonstrate the localized uranium in this membrane responsible for the increased contrast in the STEM HAADF images.

2.2.4 Software

All tomographic reconstructions were obtained with the program Imod (<http://bio3d.colorado.edu/>) (102). The program ImageJ (NIH, <http://rsb.info.nih.gov/ij/>)

was used for analysis of the 2D image projections. Volume rendering and image analysis of tomographic reconstructions was performed using the open source program ParaView (<http://www.paraview.org/>) and movies were created with the open source package ffmpeg (<http://www.ffmpeg.org/>). The inner membranes of 2 cells of each species were segmented by hand using the program Imod.

2.2.5 X-Ray Absorption Near Edge Structure (XANES) Analyses

The oxidation state of uranium in cell suspensions samples was determined with the X-ray Absorption Near Edge Structure (XANES) spectroscopic method. Cell pellets from the cell suspensions were flash frozen in liquid nitrogen, and shipped on ice. Samples were loaded in Aluminum sample holder with Kapton windows in an anaerobic chamber (2-5% hydrogen, balance nitrogen) at the Stanford Synchrotron Radiation Lightsource (SSRL, SLAC National Accelerator Laboratory, Menlo Park, CA). Immediately prior to analysis, the sample assembly was mounted in a liquid nitrogen cryostat, placed under vacuum, and frozen. U L_{III}-edge transmission spectra were collected at SSRL beamline 4-1, using a Si (220) double-crystal monochromator detuned to reject higher harmonic intensity. Vertical slits in the experimental hutch were set to 0.5 mm during the measurement to insure that the spectrometer resolution was lower than that of the intrinsic core-hole lifetime limitation. Energy calibration was monitored continuously and no drift was detected. XANES spectra were background subtracted and analyzed using ATHENA software (103).

2.2.6 qRT-PCR

Total RNA was extracted with RNeasy Mini kit (Qiagen) from mid-log acetate-fumarate cultures. cDNA was generated with the Enhanced Avian First Strand Synthesis Kit (Sigma-Aldrich, St-Louis, MO, USA) using random primers according to manufacturer's recommendations. The SYBR Green PCR Master Mix (Applied Biosystems, Foster City, CA) and the ABI 7500 Real-Time PCR System were used to amplify and to quantify PCR products from *pilA* with RT_ORF02545_F and

RT_ORF02545_R pair of primers (87). Expression of this gene was normalized with proC expression, a constitutively expressed gene in *G. sulfurreducens* using proC2F and proC77R pair of primers. Relative levels of expression of the studied genes were calculated by the $2^{-\Delta\Delta CT}$ method (76).

2.3 Results and Discussion

2.3.1 U(VI) Reduction with Genetically Modified Strains

Strain Aro-5, which produces pili with diminished conductivity, but still properly localizes outer surface *c*-type cytochromes (88), reduced U(VI) at rates that were only slightly lower and not significantly different than the wild-type rate of 0.23 μM of U(VI) $\text{mg}^{-1} \text{min}^{-1}$ (Figure 1). This result suggested that electron conduction along pili was not an important requirement for U(VI) reduction.

With further investigation, we could not replicate the previously reported findings (60) that the *pilA*-deficient mutant had substantially lower rates of U(VI) reduction than wild-type or that pre-growing cells at 25 °C, a temperature suggested to increase pili production (60) significantly enhanced U(VI) reduction (Figure 1).

Previous studies on the mechanisms for the reduction of anthraquinone-2,6-disulfonate (AQDS), another soluble extracellular electron acceptor, demonstrated that deletion of the genes for multiple outer-surface *c*-type cytochromes was necessary in order to substantially diminish rates of AQDS reduction (62). In a similar manner, deletion of genes of the outer-surface *c*-type cytochromes, OmcB or OmcE, only partially reduced rates of U(VI) reduction (52). A quadruple mutant deficient not only in OmcB and OmcE, but also the outer-surface cytochromes OmcS, and OmcT, still reduced U(VI) at rates (40%) of wild-type (Fig. 1). A quintuple mutant in which *omcZ* was deleted along with *omcB*, *omcE*, *omS*, and *omcT* (ΔBESTZ) only reduced U(VI) at a rate 19% that of wild-type (Fig. 1). This could not be attributed solely to the loss of OmcZ, because a strain in which only *omcZ* was deleted reduced U(VI) at a rate ca. 50% of wild-type (Fig. 1).

Lower rates of U(VI) reduction in the quintuple mutant could not be attributed to an impact on pili production. Transcript abundance of *pilA* relative to the housekeeping gene *proC* was 3.5 (± 0.76) fold higher in the quintuple mutant than wild-type cells and transmission electron microscopy revealed the expression of pili in the quintuple mutant and wild-type, but not in the *pilA*-deficient mutant (Figures 4 and A1).

2.3.2 Speciation and Localization of Uranium

Analysis of cell pellets from the cell-suspension incubations with X-ray absorption near-edge structure spectroscopy (XANES) demonstrated that after 4 hours, $83 \pm 10\%$ of the uranium associated with wild-type cells was U(IV) with the remainder in the U(VI) oxidation state (Figure 2). The percentage of U(IV) was slightly lower in the *pilA* mutant ($63 \pm 10\%$), but the difference was not significantly different. In contrast, $89 \pm 10\%$ of uranium was present as U(VI) in the quintuple mutant (Figure 3).

In contrast to previous reports (60), no U(IV) precipitates associated with the pili of wild-type cells were observed (Figure 5). There was an electron-dense accumulation at the outer membrane of both wild-type and *pilA* mutant, which X-ray Energy Dispersion Spectroscopy (XEDS) confirmed was uranium (Figure 6 and Fig. A2). These precipitates were not detected in cell suspensions provided fumarate rather than U(VI) as an electron acceptor (Fig. 5). There was very little accumulation of uranium on the outer-surface of the quintuple mutant, consistent with the low levels of U(VI) reduction.

2.4 Implications

The results suggest that *G. sulfurreducens* reduces U(VI) much like it reduces AQDS, another soluble, extracellular electron acceptor. A number of outer-surface *c*-type cytochromes appear to contribute to U(VI) reduction. This is analogous to results in *Shewanella oneidensis* (55). Previous results have demonstrated that *G. sulfurreducens* *c*-type cytochromes reduce U(VI) *in vitro*, including OmcS and OmcZ (93, 98). Long-range electron conduction through pili is not necessary for the reduction of other soluble

electron acceptors by *G. sulfurreducens* (58) and is also not expected to be necessary for the reduction of U(VI).

Figures:

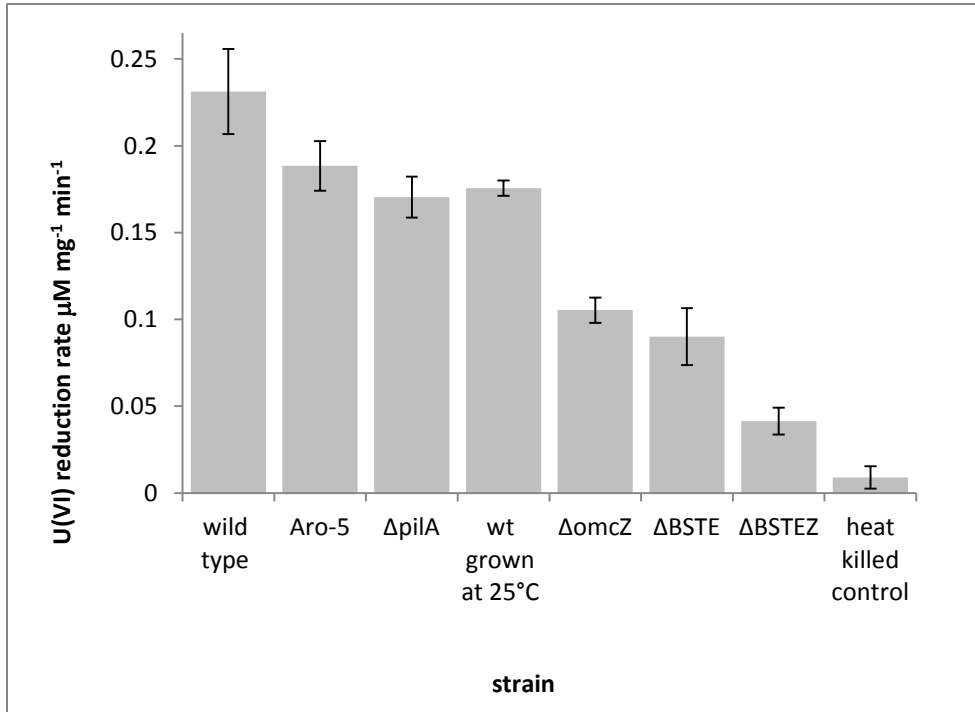


Figure 1: U(VI)-reducing activity of wild type (wt) and mutant strains of *G. sulfurreducens*. Data are means \pm standard deviations (SD) of triplicates.

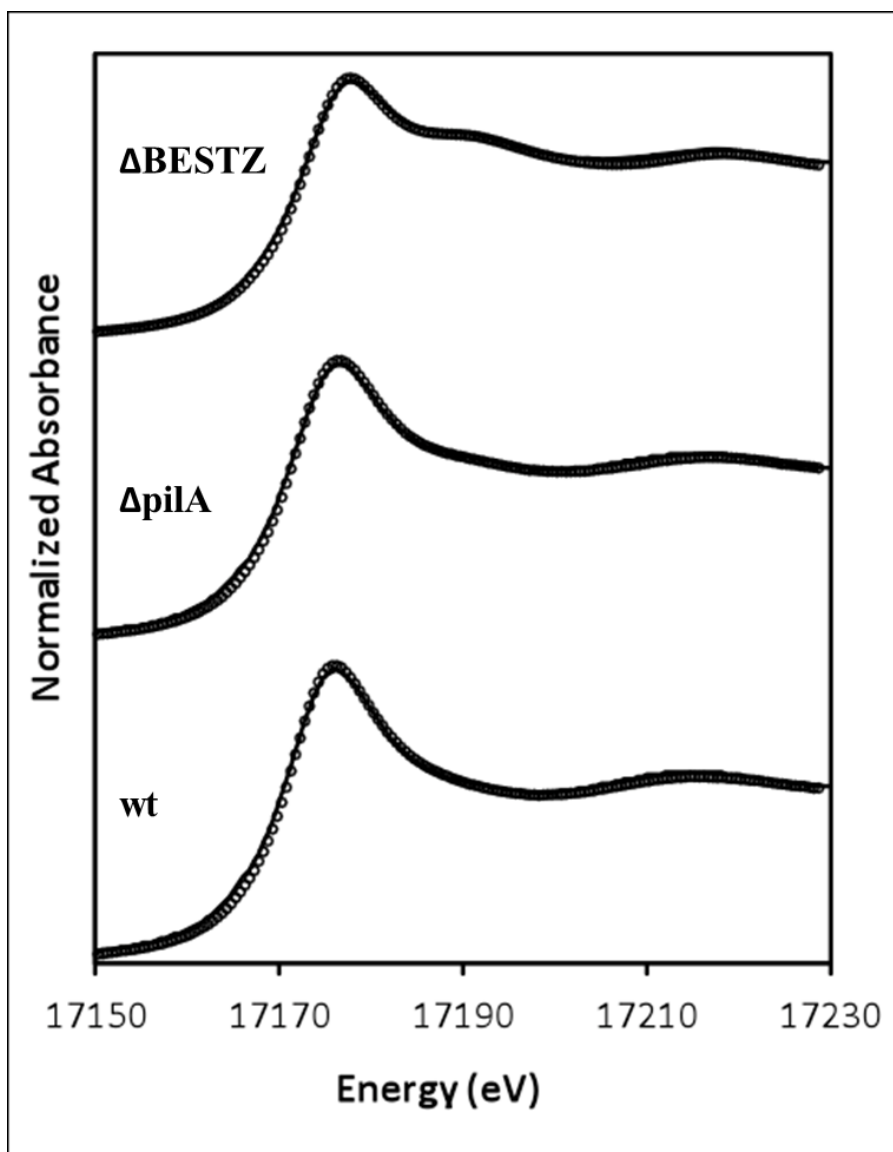


Figure 2: Uranium LIII-edge XANES spectra of uranium associated with 3 strains of *G. sulfurreducens* (circles) and their corresponding fits (lines).

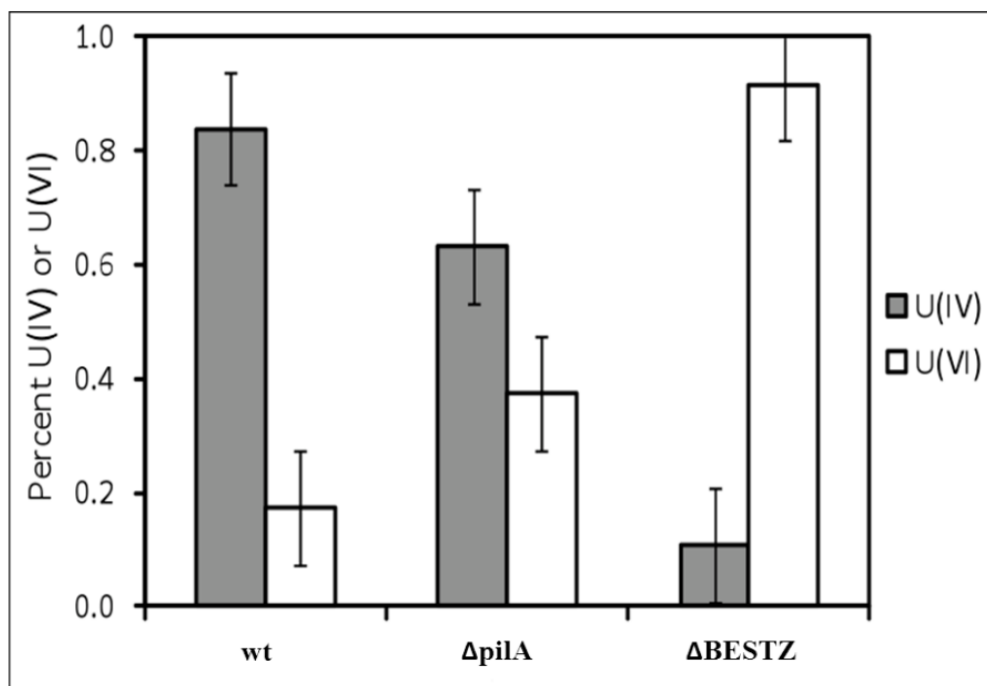


Figure 3: Proportion of Uranium at the different oxidations states: U(IV), gray bars, and U(VI), white bars, after 4 hours cell suspensions.

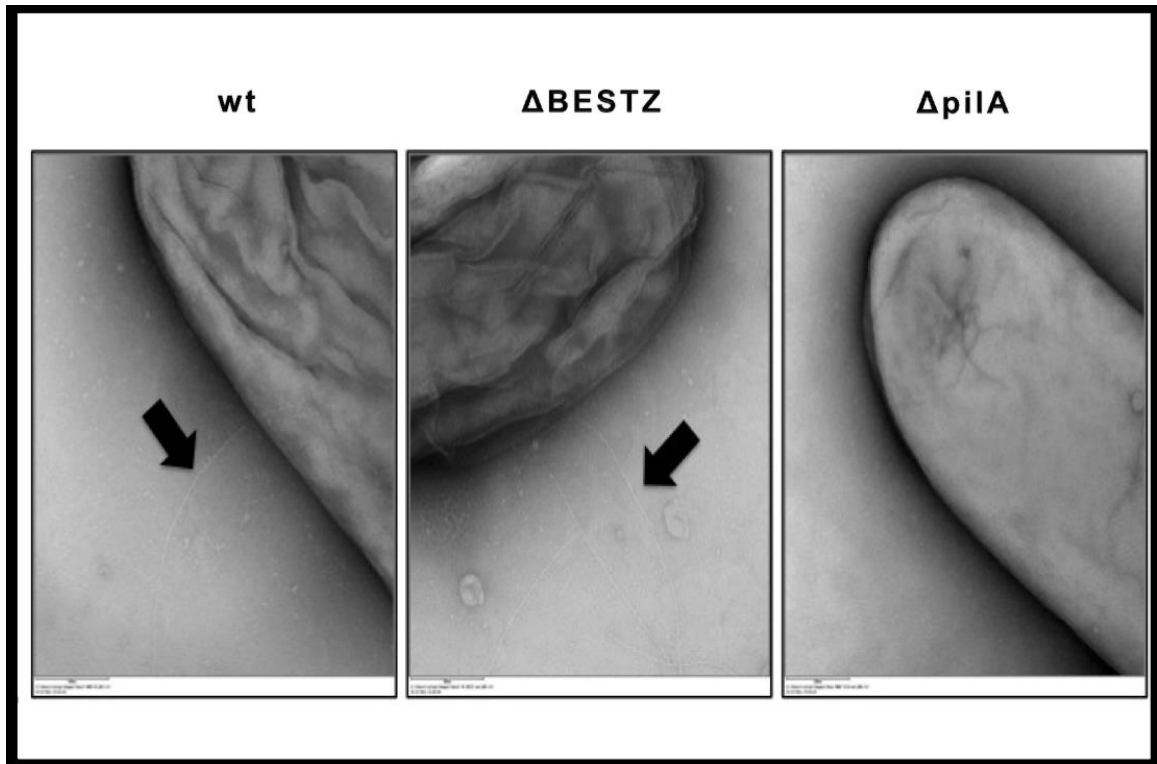


Figure 4: TEM pictures showing level of filament production in wild type(left), Δ BESTZ(middle) and Δ pilA(right).

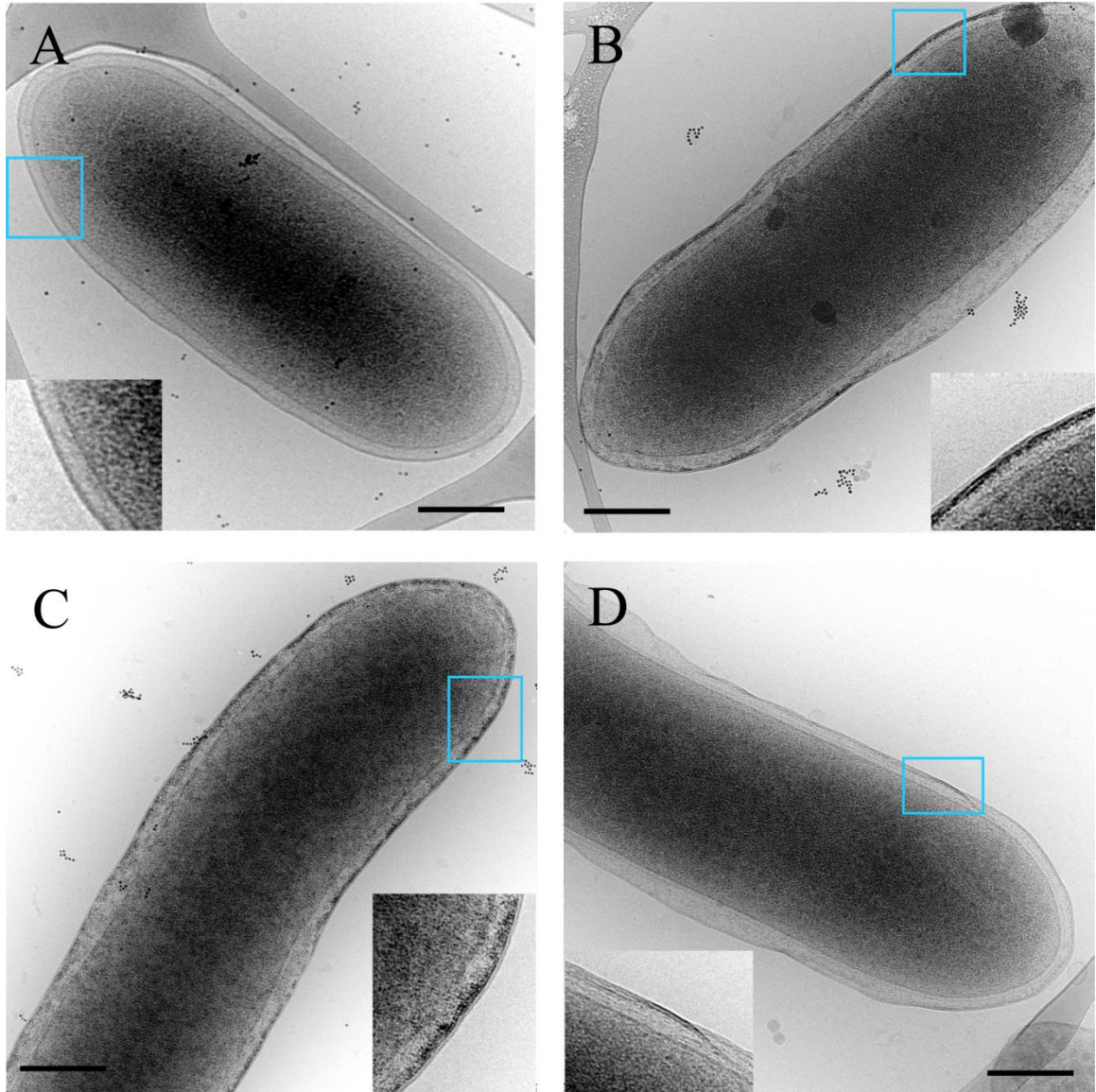


Figure 5: (A) CryoTEM images of wild-type reducing fumarate, and (B) wild-type, (C) $\Delta pilA$, (D) $\Delta BESTZ$ reducing U(VI). (A) The cell wall of *Geobacter* respiring in fumarate is typical of gram-negative bacteria with clear inner and outer membrane and a transparent periplasmic space. (B) and (C): The cell walls of wild-type and $\Delta pilA$ are spanned by irregular patches of high contrast (electron dense) material, mainly at the outer membrane. (D) The cell wall of $\Delta BESTZ$ respiring U(VI) appears to contain significantly less high contrast aggregated material and is closer to wild-type respiring fumarate. On occasion there are irregular patches of aggregates as seen in the inset. Scale bar: 250 nm.

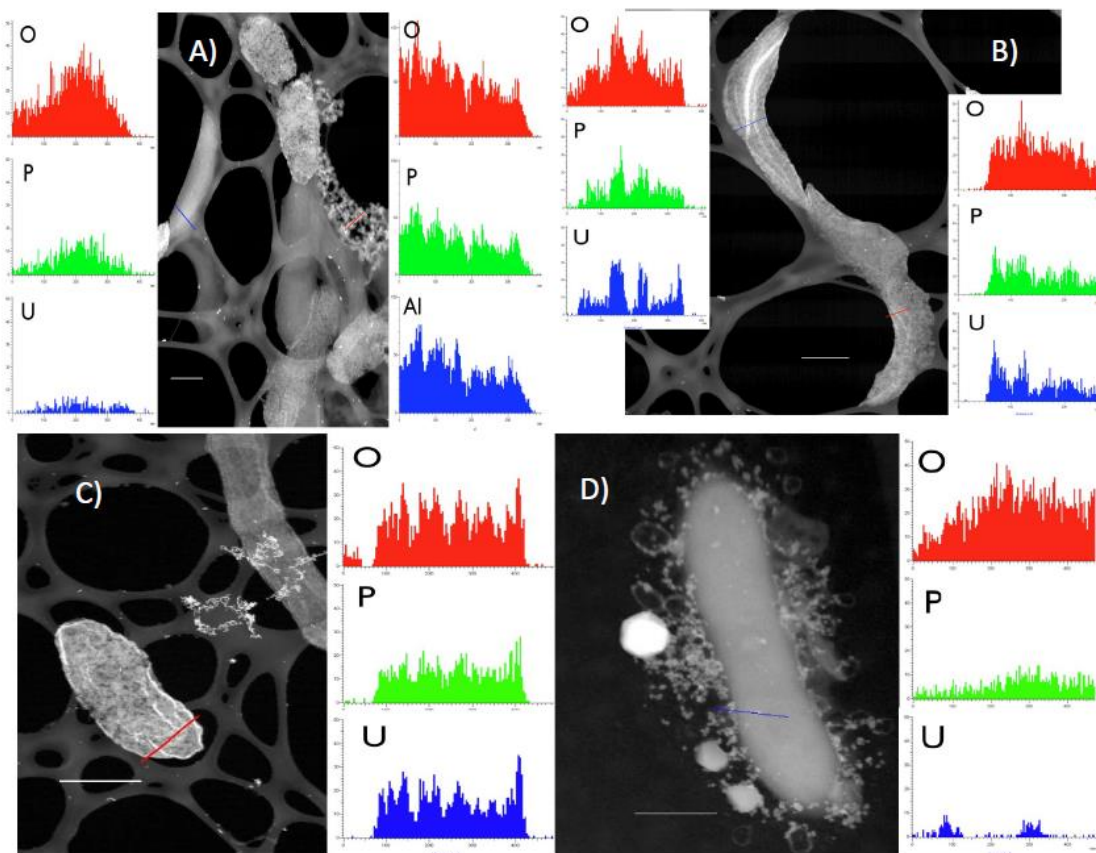


Figure 6: XEDS of (A and B) wild-type, (B) $\Delta pilA$, and (C) $\Delta BESTZ$ respiring U(VI). High angle annular of dark field STEM images of areas of freeze-dried cryo-TEM grids. The “spider web-like” pattern supporting the cells is the lacey carbon support. The scattering from metal aggregates and gold beads appears intensely bright. The red and blue lines indicate the line scanned by the probe. Scale bar: 500 nm. Side panels show x-ray counts of the main elements along the scanned line. The units in the line scans are nm on the x-axis and x-ray counts on the y-axis. For O (oxygen), P (phosphorus) and Al (aluminum) it is the number of x-ray counts in their K alpha peaks, and for U it is the number of counts in the L alpha peak. Uranium counts are significantly above background.

CHAPTER 3

PROTEOME OF GEOBACTER SULFURREDUCTENS IN THE PRESENCE OF U(VI)

3 Abstract *Geobacter* species often play an important role in the *in situ* bioremediation of uranium-contaminated groundwater, but little is known about how these microbes avoid uranium toxicity. To evaluate this further, the proteome of *G. sulfurreducens* exposed to 100 μ M U(VI) acetate was compared with control cells not exposed to U(VI). Of the 1363 proteins detected from these cultures, 203 proteins had higher abundance during exposure to U(VI) compared to the control cells and 148 proteins had lower abundance. U(VI)-exposed cultures expressed lower levels of proteins involved in growth, protein and amino acid biosynthesis, as well as key central metabolism enzymes as a result of the deleterious effect of U(VI) in the growth of *G. sulfurreducens*. In contrast, proteins involved in detoxification, such as several efflux pumps belonging to the RND family, and protection of membrane and proteins, such as chaperons and proteins involved in secretion systems, were in higher abundance in cells exposed to U(VI). Exposing *G. sulfurreducens* to U(VI) resulted in higher abundance of many proteins associated with the oxidative stress response, such as superoxide dismutase and superoxide reductase. A strain in which the gene for superoxide dismutase was deleted grew slower than the wild-type strain in the presence U(VI), but not in its absence. The results suggest that there is not one specific mechanism for uranium detoxification. Rather, multiple general stress responses are induced, which presumably enable *Geobacter* species to tolerate high uranium concentrations.

3.1 Introduction

Uranium contamination of sediments and ground/surface water has become a serious environmental concern, especially at many former uranium mining and processing facilities (4, 5, 66). One strategy for preventing the spread of uranium in the subsurface is to take advantage of the ability of some microorganisms to reduce soluble U(VI) to poorly soluble U(IV) (7, 12, 20, 30, 73, 75, 104). This approach has been investigated in a diversity of subsurface sites (2, 4, 105, 106). In many instances, stimulation of dissimilatory metal reduction with organic electron donors specifically enriches *Geobacter* species which are highly effective in U(VI) reduction (1, 2).

Geobacter sulfurreducens has served as the primary model organism to elucidate the physiological capabilities of *Geobacter* species (1, 107). Gene deletion and uraninite localization studies have suggested that *G. sulfurreducens* reduces U(VI) at the outer cell surface with a diversity of *c*-type cytochromes (3, 52). However, some uranium may enter the cell, and little is known about the physiological response to this uranium. Unlike essential metals that can be imported or extruded depending on requirements of the cell (108), uranium is not expected to be a required nutrient and is likely to be toxic because U(VI) can denature proteins, inactivate functional groups of enzymes, disrupt the cell envelope, and damage DNA (70, 72). There is not yet evidence for U(VI)-specific transport or a protective mechanism in any bacteria, suggesting that physiological systems designed for handling other toxic materials may also deal with U(VI) toxicity.

In this study we employed a genome-scale proteomic analysis and targeted gene deletions to gain insights into the impact of uranium exposure on the physiology of *G. sulfurreducens*. The results suggest that rather than a U(VI)-specific detoxification system, *G. sulfurreducens* utilizes a combination of mechanisms to cope with stress produced by U(VI).

3.2 Materials and Methods

3.2.1 Strains and culturing

Geobacter sulfurreducens strain DL-1(32) as well as Δ sodA (37), Δ GSU2212 (109), Δ GSU2213 (109), Δ BESTZ (62) were obtained from our laboratory culture collection. Cells were routinely grown in anaerobic medium with acetate as the electron donor and fumarate as the electron acceptor (110).

For proteomic analysis of the impact of U(VI) exposure, 100 μ M U(VI)-acetate was added to mid-log phase cultures. Cells were collected by centrifugation at 9,000*g for 15 min at 4°C, washed with 50mM Tris-HCl containing 10 mM MgCl₂ and protease inhibitors and stored at -20 °C until use. Controls received no U(VI) additions.

3.2.2 Protein Digestion and Desalting

For the global trypsin digestion the cells were re-suspended in 4 cell volumes of a denaturation solution of 7 M urea, 2 M thiourea and 5 mM DTT in 50 mM ammonium bicarbonate, pH 7.8. Cells were lysed by bead beating. The cells were mixed with 0.1 mm zirconia/silica beads in a mini-bead beater (Biospec, Bartlesville OK) for 90 s at 4500 rpm. Isolated proteins were diluted with a 10-fold volume of 50 mM ammonium bicarbonate, pH 7.8, CaCl₂ was added to a concentration of 2 mM, and trypsin was added in a w/w ratio of 1:50, trypsin:total protein. The proteins were digested with trypsin for 8 hours at 37 °C. The resulting peptides were desalted with a Supelclean C-18 column (Supelco, St. Louis MO) using a 5% acetonitrile in water wash buffer and an 80% acetonitrile in water elution buffer. The peptides were concentrated to dryness with a SpeedVac (ThermoSavant, Milford MA) and were reconstituted in ~100 μ L of nanopure water. Total peptide concentration was determined with the BCA assay (Pierce, Rockford IL). The peptides were quick frozen in liquid nitrogen and stored at -80°C until further analysis.

3.2.3 Tandem MS, MS and putative peptide identification

The capillary LC system consisted of a pair of syringe pumps (100-ml ISCO model 100DM) and controller (series D ISCO) and an in-house manufactured mixer, capillary column selector, and sample loop for manual injections. Separations were achieved with a 5,000 psi reversed-phase in-house packed capillary (150 μm i.d. \times 360 μm o.d.; Polymicro Technologies, Phoenix) by using two mobile-phase solvents consisting of 0.2% acetic acid and 0.05% trifluoroacetic acid (TFA) in water (A) and 0.1% TFA in 90% acetonitrile/10% water (B). The mobile-phase selection valve was switched from position A to B 10 min after injection, creating an exponential gradient as mobile phase B displaced A in the mixer. Flow through the capillary HPLC column was \sim 1.8 $\mu\text{l}/\text{min}$ when equilibrated to 100% mobile-phase A.

Sample eluate from the HPLC was infused into a conventional ion trap MS (LCQ, ThermoFinnigan, San Jose, CA) operating in a data-dependent MS/MS mode over a 400 to 2000 m/z range. For each cycle, the three most abundant ions from MS analysis were selected for MS/MS analysis by using a collision energy setting of 30%. Dynamic exclusion was used to discriminate against previously analyzed ions. The collision induced dissociation spectra from the conventional ion trap mass spectrometer were analyzed using SEQUEST (111) and the genome sequence of *Geobacter sulfurreducens* (112). Initial peptide identifications (i.e. putative mass and time tags: PMT tags) were based on a minimum cross correlation (Xcorr) score of 1.5 for all peptides identified at least twice in all MS/MS experiments. For peptides only identified once, Xcorr values had to be a minimum of 1.9, 2.2, and 3.5 for charge states of 1+, 2+ and 3+, respectively. All peptides conformed to a tryptic cleavage state on at least one of their termini.

Using the same LC conditions, each sample was further analyzed in triplicate by FTICR-MS. The FTICR mass spectrometers developed at our laboratory use ESI interfaced with an electrodynamic ion funnel assembly coupled to a radio frequency quadrupole for collisional ion focusing and highly efficient ion accumulation and transport to a cylindrical FTICR cell for analysis (113).

3.2.4 Determination of Accurate Mass and Time (AMT) Tags

The peptide library (containing peptide sequence information, elution time information and the theoretical mass) were then compared with the high resolution high accuracy peptide mass and elution time obtained from the FTICR MS runs. These peptides that were matched and verified in this manner were then deemed accurate mass and time (AMT) tags. More details as to AMT tag validation has been previously described (114). Briefly, the resultant FTICR data was processed using the PRISM Data Analysis system, a series of software tools developed in-house. The first step involved de-isotoping the MS data, giving the monoisotopic mass, charge, and intensity of the major peaks in each mass spectrum. Following this, the data was examined in a two-dimensional fashion to find the groups of mass spectral peaks that were observed in sequential spectra. Each group, known as a unique mass class (UMC), has a median mass, central normalized elution time (NET), and abundance estimate, computed by summing the intensities of the MS peaks that comprise the UMC.

The identity of the UMC's was determined by comparing the mass and NET of each UMC with the mass and NET's of all identified peptides ascertained from all prior MS/MS analyses performed on *G.sulfurreducens*. Search tolerances were ± 6 ppm for the mass and $\pm 5\%$ of the total run time for the elution time. Relative abundance values for each peptide were determined from the summed ion current value of all MS scans that detected the peptide eluting. Protein values were represented by the most abundant peptide values observed for each protein.

The abundance values for each protein in each analysis were transformed into a z-score value (also known as the standard row function) to determine those showing significant changes from their average values. The z-score is obtained by using the mean value of each protein across all compared growth conditions, subtracted from each individual protein abundance value and divided by the standard deviation of the values. Generally, z-score values between samples were considered significantly different if the difference was at least 1.5 or greater.

3.2.5 Impact of mutations on growth in the presence of U(VI)

We monitored the growth of the aforementioned strains under the two following conditions “environmental relevant stress” (in the presence of 100 μ M of U(VI) in the form of uranyl acetate) and “severe U(VI) stress” (in the presence of 1 mM of U(VI) in the form of uranyl acetate). Cells were grown in acetate-fumarate medium in anaerobic pressure tubes (32). Each culture was inoculated with 5% mid-log-phase cells. Uranium was added to a final concentration of 100 μ M and 1 mM from a concentrated stock of uranyl acetate (20 mM) dissolved in bicarbonate buffer. An equivalent volume of bicarbonate buffer (41 mM) was added to uranium-free control cultures. During incubation, culture tubes were shaken horizontally to minimize the attachment of cells on the glass. Cell numbers were determined with epifluorescence microscopy utilizing cells stained with acridine orange (0.01%) as previously described (115). In order to have a statistically relevant description of growth, over 8 fields were recorded for each time point in three independent replicate cultures. Images were taken digitally with the SimplePCI software, version 5.3 (C-Imaging Systems, Compix Inc., Mars, PA) and cells were quantified using ImageJ software (NIH, <http://rsb.info.nih.gov/ij/>).

3.3 Results

In order to evaluate how bacterial cells respond to the presence of U(VI), *G. sulfurreducens* three biological replicates were grown anaerobically to mid-log phase, exposed to 100 μ M uranyl acetate for four hours, and then harvested for proteomic analysis. A total of 1363 proteins were detected in cells from these cultures. This represented about 40% of the 3469 predicted protein-encoding open reading frames in the genome of *G. sulfurreducens* (83). There were 203 proteins detected with higher abundance during exposure to U(VI) compared to the control cells not exposed to U(VI) and 148 proteins with lower abundance (Tables B1 and B2). This accounted for 26% of the total proteins detected indicating that protein expression was significantly affected by the presence of U(VI).

Proteins with differential expression in the presence of U(VI) were classified under 17 categories according to their annotation function in the genome (Figure 7, Tables B3-

B19). Proteins associated with energy conservation (26) had the highest number of proteins with greater abundance following uranium exposure, other than proteins with unknown function and hypothetical proteins (58). The majority of proteins that were in lower abundance in the uranium-exposed cells were also annotated as hypothetical proteins (29), proteins of unknown function (24) and proteins involved in energy metabolism (20) (Figure 7; Tables B1 and B2).

3.3.1 Proteins involved in growth

Exposure to U(VI) slightly reduced the growth rate of *G. sulfurreducens* (Figure 8) and many proteins associated with the central metabolism were in lower abundance in cells exposed to U(VI). For example, the expression of citrate synthase (GltA, GSU1106), which is directly correlated with metabolic rates of *G. sulfurreducens* (76, 116, 117), was lower in the presence of U(VI) compared to the untreated control (Table 1), suggesting that metabolism was slower in the presence of U(VI). Phosphoenolpyruvate synthase (PpsA, GSU0803), another enzyme involved in the central metabolism (118), and two subunits of ATP synthase (GSU0108 and GSU0111) were also less abundant when U(VI) was present (Table 1).

It also appeared that protein biosynthesis was less important in the presence of U(VI), which was reflected in the lower abundance of proteins involved in translation, such as GSU1920 (elongation factor Ts), GSU0102 (selenocysteine-specific translation elongation factor), and GSU1516 (translation initiation factor IF-3); as well as several ribosomal proteins, such as RpsG, RplR, RpsT, YfiA, RplX, RpsS, RpsA, RplF, RpsK, and RpsP; and proteins involved in ribosome biogenesis, ObgE and EngB (Table 1). Proteins involved in amino acid biosynthesis, such as GSU1061 (aspartate aminotransferase), GSU3099 (histidinol-phosphate aminotransferase), GSU3095 (imidazole glycerol phosphate synthase subunit HisF), and GSU1828 (chorismate mutase) were also less abundant (Table 1).

3.3.2 Protein and DNA damage

Uranium has high affinity for organic molecules and can form strong bonds with functional groups in proteins (119). The uranium binding can produce conformational changes in proteins (120-122). Uranium ions can generate ligands with functional groups of thiolates as well as carboxylate from acidic amino acids, such as aspartate or glutamate (71, 122, 123). Enzymes in *G. sulfurreducens* that assist in protein folding may help to avoid these potential deleterious effects. For example, exposure to U(VI) resulted in higher expression of the chaperonin GroES (GSU3339), the DnaJ-related molecular chaperone (GSU0014) and the DnaJ adenine nucleotide exchange factor (GrpE, GSU0032) that is involved in the protection and renaturation of heat-labile proteins (Table 2).

The expression of several proteins related to peptide secretion and trafficking were also more abundant in the presence of U(VI). For example, the SecE and SecF (GSU2869 and GSU2616), which belong to the general Sec system, and PulQ (GSU1778) and GspK (GSU0322), which are part of the type II secretion system, were in higher abundance in the presence of U(VI) (Table 2). Previous studies have suggested that the type II secretion system has an essential role in localizing several metal-containing proteins on the outer surface of the cell (1, 112).

Uranium has a high affinity for DNA, which can result in DNA strand breakage and inhibits DNA-protein interactions (121, 123-125). Thus, the exposure to U(VI) could be expected to result in DNA damage. However, only three proteins involved in DNA metabolism, DnaA (GSU3470), TopA (GSU2549), and Ssb-2 (GSU3117), were more abundant following U(VI) exposure (Table 2), and surprisingly RecA (GSU0145), an essential protein for the repair and maintenance of DNA was in lower abundance in the presence of U(VI) (Table 1). This suggests that although some uranium was able to enter the cytoplasm, uranium scavenging enzymes were highly efficient, preventing the subsequent DNA damage.

3.3.3 Detoxification and Membrane damage

Although there are no known uranium-specific detoxification systems in microorganisms, metal efflux pumps for other toxic metals exist (108) and could

conceivably play a role in preventing uranium toxicity. Several efflux pumps in the RND family, which confer metal tolerance by extruding a wide spectrum of metals, were more abundant in cells exposed to U(VI) (Table 2). For example, RND family proteins associated with the CzcABC complex, were triggered by the presence of U(VI). GSU2695 (RND-type efflux pump) and GSU1482 (CzcC, RND-type efflux pump), which correspond to outer membrane proteins able to transport heavy metals across the outer membrane, were more abundant in cells exposed to U(VI). The three membrane fusion proteins, GSU2136 (RND-type efflux pump), GSU2781 (RND-type efflux pump) and GSU0496 (RND-type efflux pump), which span the periplasmic space and funnel cations across it (126), were also in higher abundance in the presence of U(VI) (Table 2). Many other proteins related to binding and transport metals were also significantly more abundant in the presence of U(VI), such as the putative periplasmic tungstate ABC transporter (TupA, GSU2700) which is part of the tungstate transport complex and MgtA (GSU1678) commonly involved in Mg^{2+} transport (Table 2).

Another strategy for heavy metals detoxification is precipitation (4, 127, 128). Several microorganisms are known to use phosphate derived from polyphosphate to precipitate uranium (129). The polyphosphate kinase (Ppk-2, GSU0728), which catalyzes the transfer of phosphate from ATP to form a long-chain polyphosphate, and the exopolyphosphatase (GSU2559), which irreversibly hydrolyzes polyP to form phosphates, were both more abundant in cells exposed to uranium, suggesting a potential role in uranium detoxification (Table 2).

The lipid bilayer of the outer membrane is the most external barrier before the peptidoglycan in *G. sulfurreducens*. This layer is rich in phosphate and carboxylate groups, which may strongly bind U(VI) (129). Many lipoproteins such as GSU1817 (outer membrane lipoprotein, Slp family), GSU0457 (outer membrane lipoprotein LolB) and GSU0157 (lipoprotein) were more abundant in the presence of U(VI). A similar response was observed with proteins involved in peptidoglycan and cell wall biosynthesis, such as Ddl (GSU3066) and MurI (GSU2923), respectively (Table 2).

3.3.4 Proteins involved in oxidative stress

G. sulfurreducens is an aerotolerant anaerobe, with effective mechanisms for dealing with oxidative stress (71, 130). Many proteins that are involved in the typical oxidative stress response in bacteria are also induced in response to other environmental stimuli, such as heat (131, 132), high salt concentrations (133) and heavy metals stress (131, 133-135). A number of proteins associated with the oxidative stress response were more abundant in cells exposed to uranium (Table 2). A possible explanation for this is that glutathione can reduce U(VI) that enters the cells, producing oxidized bisglutathione and hydrogen peroxide (67, 136, 137). This reduction could potentially be catalyzed by two proteins encoding typical 2-Cys subfamily of peroxiredoxins, GSU0352 and GSU3246, and glutaredoxin (GSU1155), which were more highly expressed in cells grown in the presence of U(VI) (Table 2). Homologs of rhodanese-like proteins (GSU0505 and GSU2516) that are involved in the oxidative stress response of *E. coli* (138), were also expressed in higher abundance when U(VI) was present (Table 2). Exposing *G. sulfurreducens* to U(VI) resulted in higher abundance of both superoxide dismutase (SodA, GSU1158) and superoxide reductase (GSU0720) (Table 2). A former transcriptional study of the *Geobacter* species that predominated during *in situ* uranium bioremediation at a field study site in Rifle, CO, reported that the gene encoding the superoxide dismutase (SodA) was highly expressed despite the presence of a highly reduced environment (139). Another study that evaluated the transcriptional expression of the *G. uraniireducens*, an isolate from the site (140), also found that the *sodA* gene was upregulated when the isolate was grown in the contaminated subsurface sediments (104). Both results suggested that the expression of SodA could not only be triggered as a result of oxygen stress, but also other factors in the sediments. Furthermore, the gene encoding the superoxide dismutase was upregulated when cells of the highly uranium tolerant oligotroph, *Caulobacter crescentus*, were exposed to uranium, cadmium, chromate, and dichromate (131), suggesting that this enzyme is involved in the response to a wide range of heavy metals.

In order to evaluate the role of superoxide dismutase in response to U(VI) stress, the growth of a SodA-deficient strain in the presence U(VI) was evaluated (Figure 9). In the absence of U(VI) the growth of the SodA-deficient strain was comparable to that of wild-type (Figure 8). However, in the presence of 100 μ M U(VI) the SodA-deficient

strain grew slower than wild-type (Figure 8). The impact of the loss of SodA was even more apparent in the presence of 1 mM U(VI) (Figure 9).

3.3.5 Extracellular matrix proteins

Two regulatory proteins (GSU2212 and GSU2213) related to the *che5* gene cluster, which has been shown to participate in the synthesis of extracellular matrix and biofilm formation (109), were more abundant in cells exposed to uranium (Table 2). In order to evaluate the potential role of these proteins in response to uranium toxicity cultures in which one of the genes for these proteins was deleted were grown in the presence of uranium (Figure 10 and 11). However, deletion of these genes did not significantly inhibit growth in the presence of uranium, suggesting that these regulatory proteins were not essential for the response to uranium toxicity.

3.3.6 *c*-type cytochromes

Three *c*-type cytochromes (GSU0357, GSU1648, and GSU2801) were expressed with higher abundance when cells were exposed to U(VI) (Table 2). GSU0357 is predicted to be a nitrite reductase. The function of GSU2801 is unknown. GSU2801 is not essential for Fe(III) oxide reduction in *G.sulfurreducens* (84), but, its homolog in *G. metallireducens* had higher transcript abundance in cells grown on Fe(III) oxide than in Fe(III) citrate-grown cells (84). GSU 1648 (*macC*) is predicted to be periplasmic. The gene encoding a *macC* homolog was more highly expressed in *G. uranireducens* grown in a U(VI)-contaminated subsurface than in culture medium (104).

A number of *G. sulfurreducens* outer-surface cytochromes appear to contribute to U(VI) reduction (3, 52). The reduction of U(VI) at the outer surface might be expected to be one mechanism for reducing uranium toxicity because poorly soluble U(IV) is unlikely to enter the cell. To test this concept, studies were conducted with the previously described quintuple mutant (62) in which the genes for the outer-surface *c*-type cytochromes OmcB, OmcE, OmcS, OmcT, and OmcZ were deleted. Although cell suspensions of this quintuple mutant reduced U(VI) at a rate only 18 % that of wild-type

cells (Orellana *et al.*, 2013), this strain grew as well as the wild-type strain in the presence of U(VI) (Figure 1).

3.4 Implications

The ability of *G. sulfurreducens* (this study) and other *Geobacter* species (20) to grow in the presence of mM quantities of uranium is remarkable because it is unlikely that there has ever been any major evolutionary pressure on these organisms to deal with such high concentrations of uranium in natural environments. The differential expression of proteins in the presence of U(VI) did not reveal a specific U(VI)-detoxification system. Rather, resistance to U(VI) appears to be accomplished with multiple stress response systems and regulatory networks that facilitate fast adaptation to rapidly changing conditions. The ability of *Geobacter* species to cope with potential U(VI) toxicity in this manner may be one of the reasons that *Geobacter* species are often one of the most abundant genera of microorganisms during *in situ* uranium bioremediation.

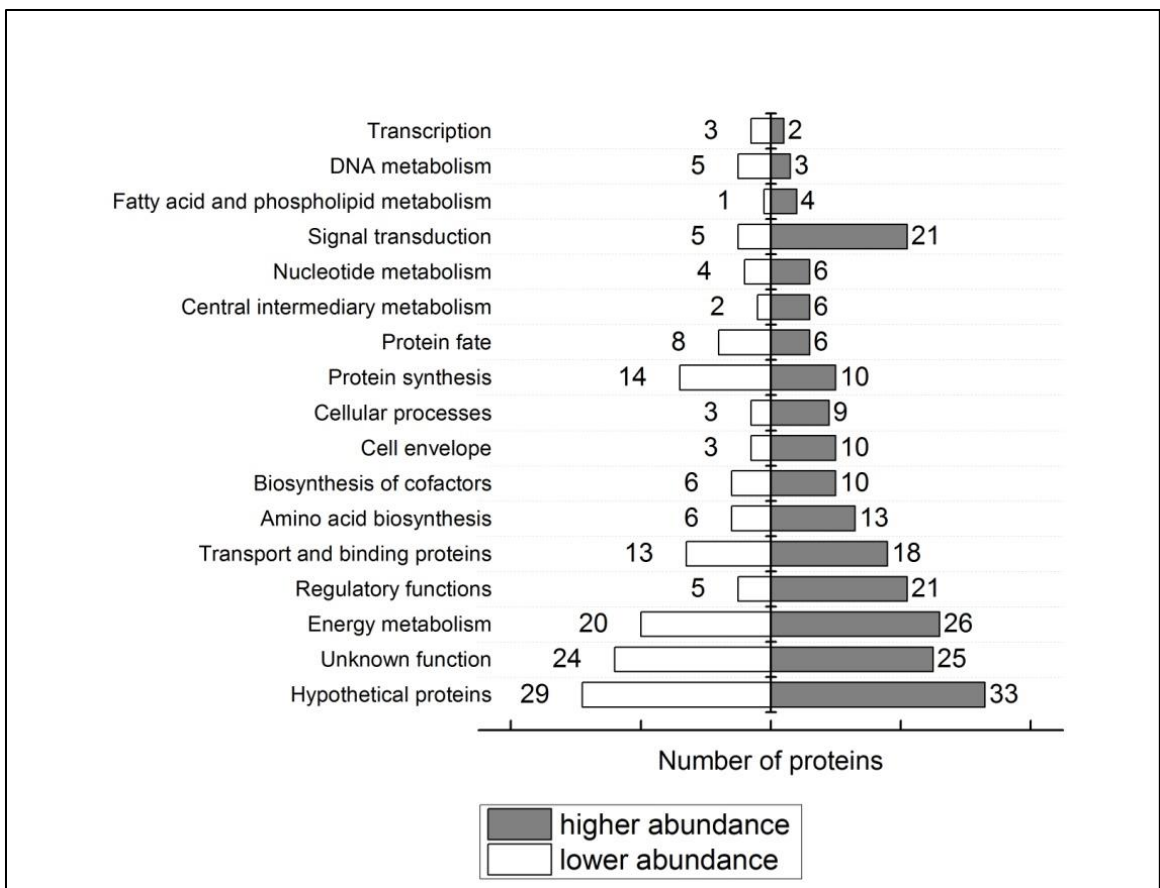


Figure 7: Changes in the protein profile as a result of U(VI) exposure. In the right side, number of proteins with increased relative abundance. In the left side, number of proteins with lower relative abundance. The proteins are grouped according to functional class as defined by the TIGR annotation.

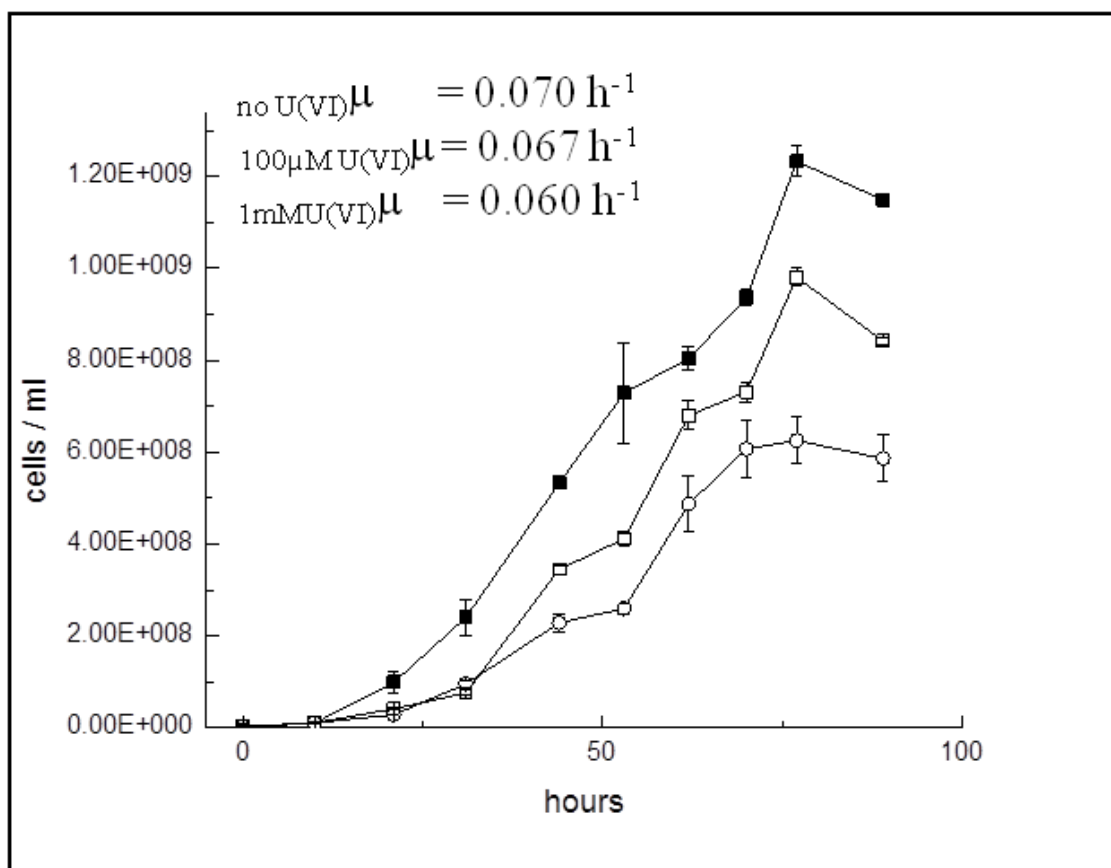


Figure 8: Effect of U(VI) on the growth of wild-type. Solid boxes indicate cultures grown in absence of U(VI). Empty boxes indicate cultures grown in the presence of 100 μM of U(VI). Each point in the curve is the mean from three independent replicate cultures. Bars designate one standard deviation of the mean.

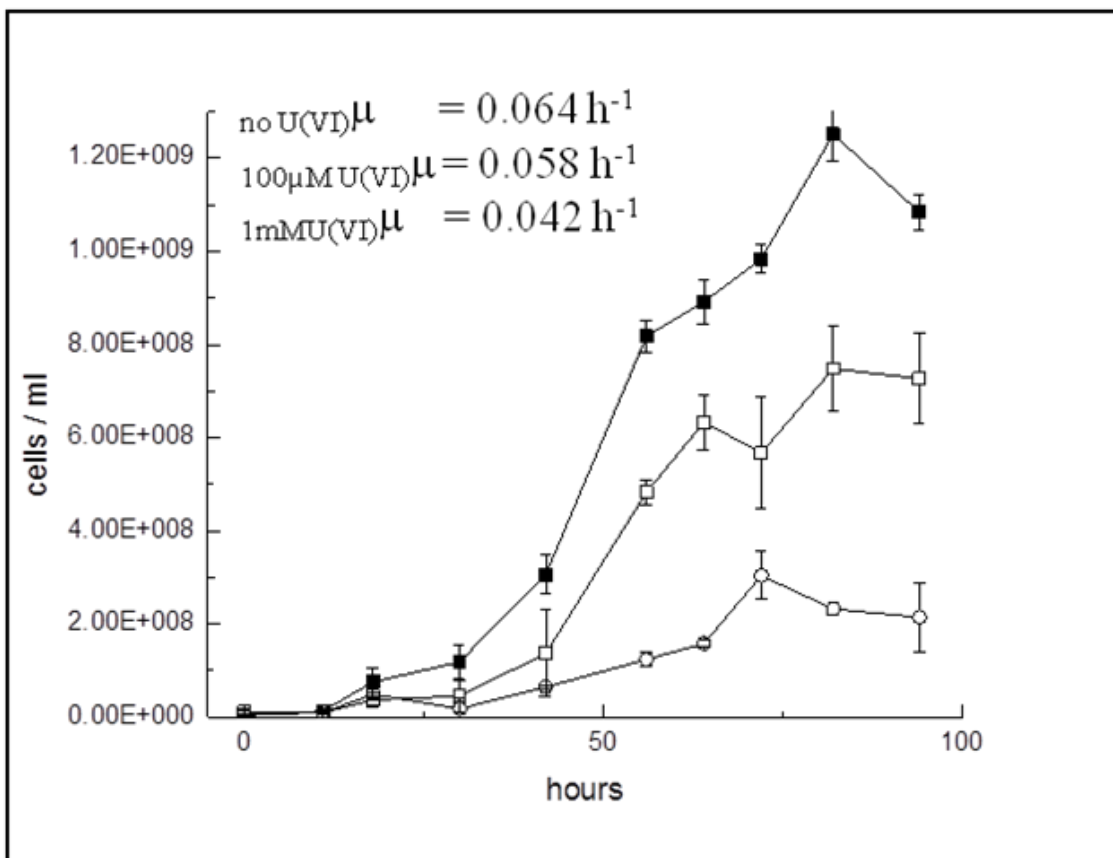


Figure 9: Effect of U(VI) on the growth of ΔsodA . Solid boxes indicate cultures grown in absence of U(VI). Empty boxes indicate cultures grown in the presence of 100 μM of U(VI). Each point in the curve is the mean from three independent replicate cultures. Bars designate one standard deviation of the mean.

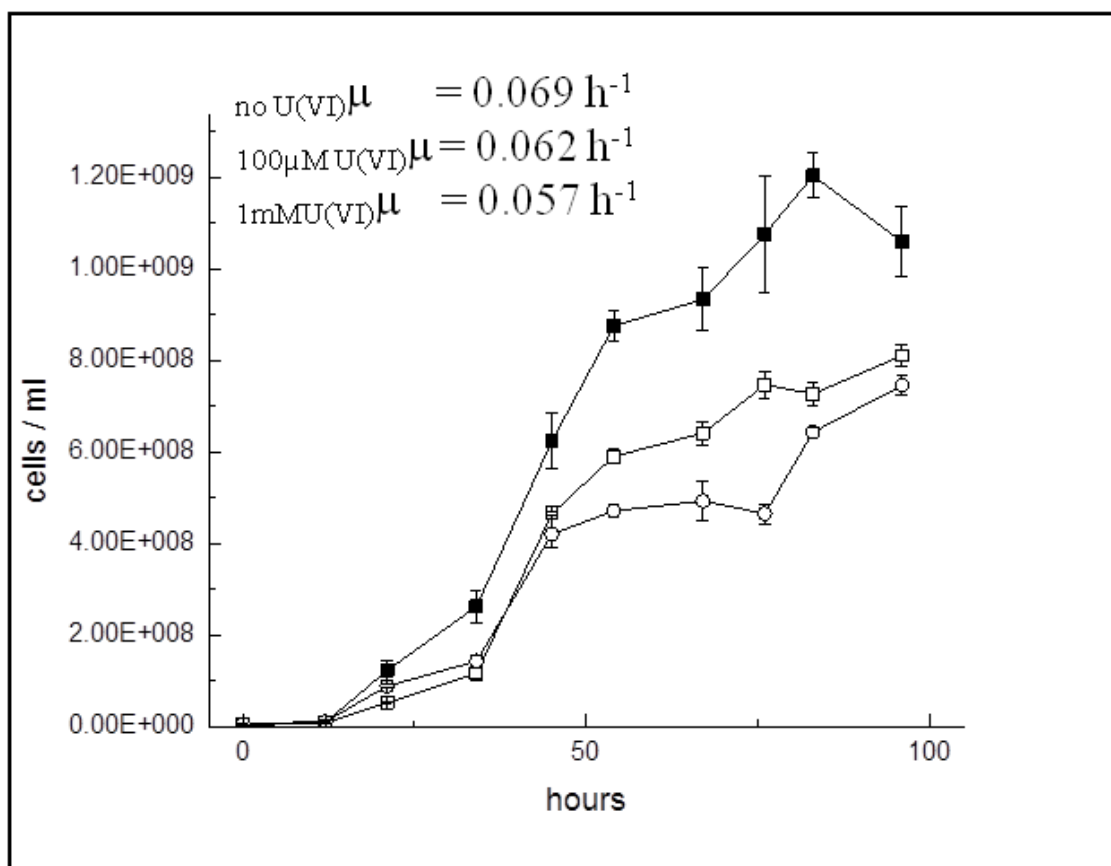


Figure 10: Effect of U(VI) on the growth of Δ GSU2212. Solid boxes indicate cultures grown in absence of U(VI). Empty boxes indicate cultures grown in the presence of 100 μ M of U(VI). Each point in the curve is the mean from three independent replicate cultures. Bars designate one standard deviation of the mean.

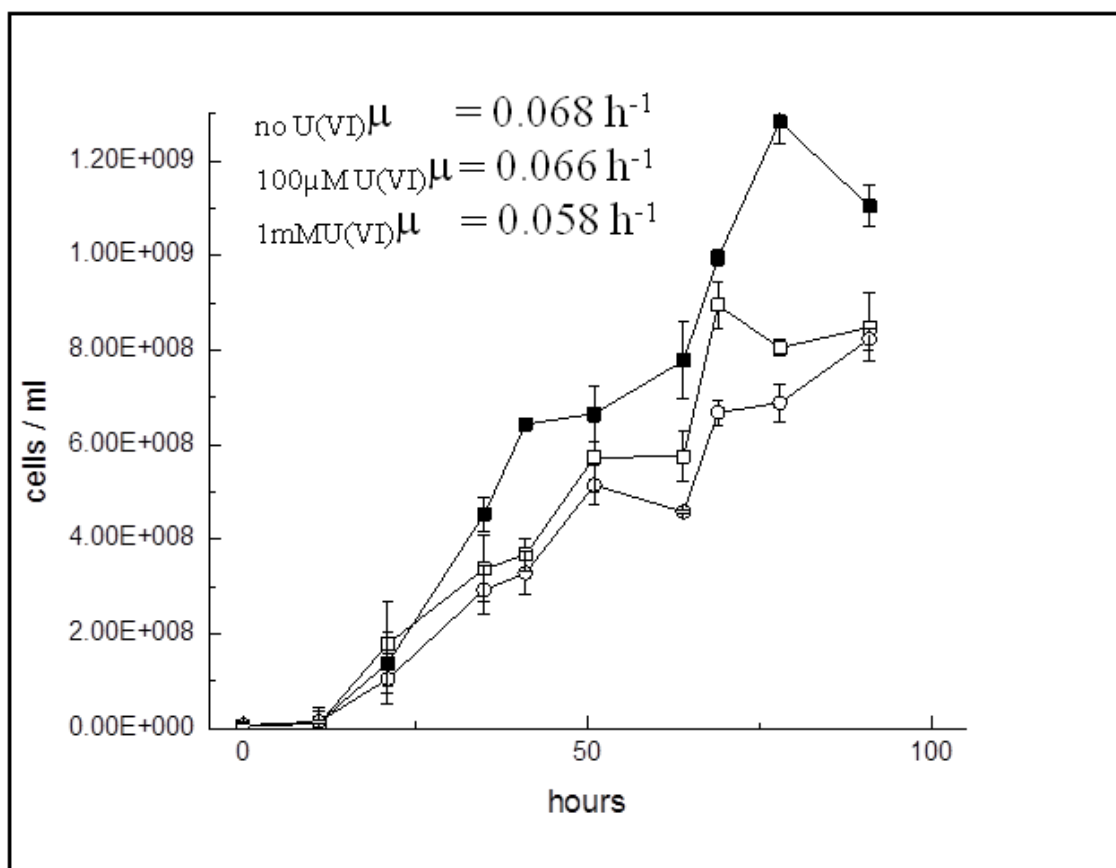


Figure 11: Effect of U(VI) on the growth of Δ GSU2213. Solid boxes indicate cultures grown in absence of U(VI). Empty boxes indicate cultures grown in the presence of 100 μM of U(VI). Each point in the curve is the mean from three independent replicate cultures. Bars designate one standard deviation of the mean.

Table 1: Selected proteins with lower relative abundance during exposure to U(VI) compared to the control cells. The right column indicates the z-score (also called the Standard Row Function). z-score were obtained by using the mean value of each protein across both conditions, subtracted from each individual protein abundance value and divided by the standard deviation of the values. z-score values between samples were considered significantly different if the difference was at least 1.5 or greater.

Locus ID	Gene Annotation	Gene name	z- score difference ($Z_{U(VI)} - Z_{control}$)
Proteins involved in growth			
<i>Central metabolism and energy conservation</i>			
GSU1106	citrate synthase	gltA	-1.65
GSU0803	phosphoenolpyruvate synthase	ppsA	-1.62
GSU0108	ATP synthase F0, B subunit, putative		-1.59
GSU0111	ATP synthase F1, alpha subunit	atpA	-1.74
<i>Translation and protein synthesis</i>			
GSU1920	translation elongation factor Ts	tsf	-1.65
GSU0102	selenocysteine-specific translation elongation factor	selB	-1.70
GSU1516	translation initiation factor IF-3	infC	-1.51
GSU2861	ribosomal protein S7	rpsG	-1.51
GSU2841	ribosomal protein L18	rplR	-1.53
GSU2206	ribosomal protein S20	rpsT	-1.54
GSU1886	ribosomal subunit interface-associated sigma-54	yfiA	-1.55

	modulation protein		
GSU2846	ribosomal protein L24	rplX	-1.57
GSU2853	ribosomal protein S19	rpsS	-1.57
GSU2603	ribosomal protein S1	rpsA	-1.67
GSU2842	ribosomal protein L6	rplF	-1.69
GSU2833	ribosomal protein S11	rpsK	-1.72
GSU0643	ribosomal protein S16	rpsP	-1.73
<i>Ribosome biogenesis</i>			
GSU3213	ribosome biogenesis GTPase ObgE	obgE	-1.74
GSU3013	GTPase EngB	engB	-1.79
<i>Amino acid biosynthesis</i>			
GSU1061	aspartate aminotransferase		-1.53
GSU3099	histidinol-phosphate aminotransferase	hisC	-1.63
GSU3095	Imidazole glycerol phosphate synthase, cyclase subunit	hisF	-1.64
GSU1828	chorismate mutase		-1.66
DNA repair			
GSU0145	recA protein	recA	-1.60

Table 2: Selected proteins with higher relative abundance during exposure to U(VI) compared to the control cells. The right column indicates the z-score (also called the Standard Row Function). z-score were obtained by using the mean value of each protein across both conditions, subtracted from each individual protein abundance value and divided by the standard deviation of the values. z-score values between samples were considered significantly different if the difference was at least 1.5 or greater.

Locus ID	Gene Annotation	Gene name	z- score difference ($z_{U(VI)} - z_{control}$)
Protein and DNA damage			
<i>Protein folding</i>			
GSU3339	chaperonin GroES	groES	1.54
GSU0014	DnaJ-related molecular chaperone		1.82
GSU0032	DnaJ adenine nucleotide exchange factor GrpE	grpE	1.63
<i>Peptide secretion and trafficking</i>			
GSU2869	preprotein translocase, SecE subunit	secE	1.73
GSU2616	protein-export membrane protein SecF	secF	1.50
GSU1778	type II secretion system secretin lipoprotein PulQ	pulQ	1.65
GSU0322	type II secretion system protein GspK	gspK	1.54
<i>DNA protection</i>			
GSU3470	chromosomal replication initiator protein DnaA	dnaA	1.78
GSU2549	DNA topoisomerase I	topA	1.68
GSU3117	single-strand binding protein	ssb-2	1.67

Detoxification and membrane damage			
<i>Detoxification</i>			
GSU2695	efflux pump, RND family, outer membrane protein		1.77
GSU1482	efflux pump, RND family, outer membrane protein		1.81
GSU2136	efflux pump, RND family, membrane fusion protein		1.71
GSU2781	efflux transporter, RND family, MFP subunit		1.64
GSU0496	efflux transporter, RND family, MFP subunit		1.56
GSU2700	tungstate ABC transporter, periplasmic tungstate-binding protein, putative	tupA	1.77
GSU1678	cation-transport ATPase, E1-E2 family	mgtA	1.54
<i>Polyphosphate metabolism</i>			
GSU0728	polyphosphate kinase	ppk-2	1.55
GSU2559	Exopolyphosphatase		1.64
<i>Lipoproteins</i>			
GSU1817	outer membrane lipoprotein, Slp family		1.79
GSU0457	outer membrane lipoprotein LolB, putative		1.76
GSU0157	lipoprotein, putative		1.65
<i>Peptidoglycan and cell wall biosynthesis</i>			
GSU3066	D-alanine--D-alanine ligase	ddl	1.74

GSU2923	glutamate racemase	murI	1.66
Oxidative stress response			
<i>Peroxiredoxins and glutaredoxins</i>			
GSU0352	peroxiredoxin, atypical 2-Cys subfamily	prx-3	1.66
GSU3246	peroxiredoxin, typical 2-Cys subfamily	prx-2	1.80
GSU1155	glutaredoxin family protein		1.77
<i>Rhodanase like proteins</i>			
GSU0505	rhodanese homology domain superfamily protein		1.66
GSU2516	rhodanese homology domain pair protein		1.77
<i>Reduction/oxidation of superoxide</i>			
GSU0720	superoxide reductase		1.78
GSU1158	superoxide dismutase	sodA	1.72
Extracellular matrix proteins			
<i>Chemotaxis</i>			
GSU2212	chemotaxis protein CheY	cheY-5	1.71
GSU2213	GAF domain protein		1.82
c-type cytochromes			
<i>Periplasmic cytochromes</i>			
GSU0357	cytochrome c family protein		1.74
GSU2801	cytochrome c, 5 heme-binding sites		1.72
GSU1648	cytochrome c, 5 heme-binding sites	macC	1.73

CHAPTER 4

NOVEL MEMBRANE-BOUND COMPLEXES INVOLVED IN ENERGY CONSERVATION BY THE ACETATE OXIDIZING SULFATE-REDUCING BACTERIUM *DESULFOBACTER POSTGATEI*

4 Abstract

Desulfobacter postgatei is a pure culture model for the *Desulfobacter* species that plays an important role in sulfate reduction in marine sediments and that have a negative impact on *in situ* uranium bioremediation by outcompeting U(VI)-reducing species for acetate. In order to learn more about the mechanisms by which *D. postgatei* conserves energy from acetate oxidation couple to sulfate reduction, the genome of *D. postgatei* was sequenced and a genome-scale metabolic model was constructed. The model was improved and validated through several iterations of hypothesis generation. The integration of these predictions with bibliographic and experimental data based on continuous-culture system, allowed us to describe novel elements for energy conservation in *D. postgatei*. These included the energy-converting hydrogenase related complex, Ehr, the quinone-reductase complex, Qrc, the proton-translocating ferredoxin:NADP⁺ oxidoreductase, Rnf, and also the NADH-dependent ferredoxin:NADP⁺ oxidoreductase, Nfn. The current version of the model predicts that these complexes actively regulate the transition of the cells into different physiological states, providing also a link between the ferredoxin and NAD(H)/NADP(H) pools. RNA-seq analysis of transcript abundance in cells grown in an acetate-limited chemostat at different growth rates (0.014–0.032 h⁻¹) revealed that many of the genes encoding proteins involved in these complexes were expressed in higher abundance as respiration rates increased. This new understanding of *D. postgatei* energy conservation will substantially improve the modeling of the growth of this organism in marine sediments and subsurface environments and also highlight how genome-scale metabolic modeling, coupled with enhanced genome annotation and experimental studies, can accelerate the study of the physiology of environmentally relevant, but understudied microorganisms.

4.1 Introduction

Sulfate-reducing bacteria (SRB) are a phylogenetically and physiologically diverse group of microorganisms that have in common the use of sulfate as an electron acceptor, which results in the production of sulfide as the end-product (141). SRB are anaerobic microorganisms that are ubiquitous in many anoxic environments where sulfate is available and they represent one of the more ancient metabolic processes (142). These organisms can use several fermentation products as electron donors, including hydrogen and organic compounds such as acetate, ethanol, formate, lactate, pyruvate, malate and succinate (143, 144).

SRB can be divided in two major physiological groups, the ones that incompletely degrade organic compounds to acetate and the ones that completely degrade organic compounds to CO₂ (143). Complete acetate oxidation is an ecophysiological relevant metabolic trait due to the fact that acetate is the most important intermediate in anoxic sediments in which sulfate reduction is the predominant terminal electron-accepting process, such as many marine environments and fresh water sediments with high concentration of sulfate (145-149). The high mineralization observed in those environments, especially in marine sediments with high input of organic matter, is linked to the activity of acetate-oxidizing SRB (150). Indeed, previous evidence has shown that more than 50% of the mineralization of organic carbon is metabolized by sulfate-reducing organisms suggesting that the activity of acetate-oxidizing SRB is central to today's biogeochemical cycling of carbon and sulfur (142, 145).

There are few SRB isolates that are capable of acetate oxidation. Among them, *Desulfobacter postgatei* is the only with a genome sequence available one that uses a modified citric acid cycle. *D. postgatei* strain 2ac9 is a Gram-negative, acetate-oxidizing SRB that was isolated from a brackish water ditch near Jadebusen (North Sea) (151). Acetate is used as both electron-donor and carbon source (152, 153). It can use other electron acceptors other than sulfate for growth including sulfite, thiosulfate and chelated Fe(III) (26). Described as a specialist due to its narrow capabilities to use substrates, *D. postgatei* has been shown to be a good scavenger of acetate. Therefore, it is expected that

this bacterium is widespread in environments limited by carbon availability (154).

Despite the importance of acetate-oxidizing SRB in sulfur and carbon cycles, investigations of their metabolism are scarce. A large part of the present knowledge of sulfate reduction metabolism has been derived from experiments with species belonging to the *Desulfovibrio* genus because a genetic system is available (155-158). In these studies, novel soluble and membrane-bound complexes involved in energy conservation have been recently discovered (155, 159-166), emphasizing our current lack of understanding about the metabolism of SRB. Furthermore, this is augmented by the fact that some of these enzymes might vary in function or directionality under different conditions (156).

Constraint-based modeling is an approach for quantitative prediction of the behavior of complex biological systems and their responses to the environment. To date, this method has been successfully applied to provide physiological and ecological insights on the metabolism of many environmental relevant anaerobic bacteria (118, 167-169) and has been used to optimize its applications in energy production and bioremediation (44, 170). In this work, we applied a systems biology approach to study energy conservation mechanisms of *D. postgatei*. Initially the genome was sequenced and manually annotated, and a genome-scale metabolic model was developed. Then, through validation using chemostat-based experiments and genome-wide transcription analysis, we analyzed the metabolism of *D. postgatei*. Both metabolic predictions and RNA-seq analysis of transcript abundance revealed that novel elements described are involved in energy conservation. These included the energy-converting hydrogenase related complex, Ehr, the proton-translocating ferredoxin:NADP⁺ oxidoreductase, Rnf, the quinone-reductase complex, Qrc, and also the NADH-dependent reduced ferredoxin:NADP⁺ oxidoreductase, Nfn. This new understanding of *D. postgatei* energy conservation will substantially improve the modeling of the growth of this organism in marine sediments and subsurface environments.

4.2 Materials and methods

4.2.1 Organism

Desulfobacter postgatei strain Dangast 2ac9 (DSMZ 2034) was obtained from the German Collection of Microorganisms and Cell Cultures (Deutsche Sammlung von Mikroorganismen und Zellkulturen, DSMZ), Braunschweig, Germany.

4.2.2 Media and cultivation

D. postgatei was grown anaerobically under N₂/CO₂ gas phase as originally described by Widdel and Pfenning (1981) (151) in mineral media supplemented with trace element solution SL10 (171) and vitamin solution (172). Mineral media was reduced with sulfide and bicarbonate was used as buffer. Cultivation was carried out at 30°C. Cultures were grown with 21 mM sodium acetate as the sole source of organic carbon and energy and sodium sulfate (20 mM) as the electron acceptor.

4.2.3 Chemostat experiments

D. postgatei was grown at 30°C in duplicated chemostats in 1-L glass vessels with a 900 ml working volume, within a water bath for temperature control. The culture vessel and all associated tubing were sterilized by autoclaving. The connections between tubes were made with stainless steel Luer fittings (Cole Palmer) and the culture was sampled through a steel canula connected to a stainless steel port. The medium was introduced into the culture vessel at a steady rate with a variable-speed dispensing pump (ISMATEC) and calibrated tubing (PharMed; 1.30 mm internal diameter). The culture media were constantly gassed (50 ml min⁻¹) with a certified mixture of N₂-CO₂ (80:20) passed through heated copper filings to remove any traces of oxygen. The culture exited vertically through a stainless steel canula, pushed by the gas overpressure in the headspace and is collected in the effluent reservoir. The culture was stirred at a constant speed of 600 r.p.m. with a magnetic bar. Steady-state cell growth was obtained after 3

volume refills and was confirmed by a constant cell density and concentrations of acetate and sulfate.

4.2.4 Analytical methods

Protein concentrations were determined as previously described (173). Sulfate concentrations were determined by ion chromatography (174) and fatty acid concentrations by high-pressure liquid chromatography (175). Sulfite concentrations were determined by colorimetry (176). Acetate consumption for cell mass synthesis was calculated according to the equation described before (177). K_s (half saturation constant) was calculated with the Lineweaver-Burk linearization method based on nutrient-limited chemostats (178, 179).

4.2.5 DNA extraction and genome sequencing

DNA for sequencing was extracted using the DNA Isolation Bacterial Protocol available through the JGI (<http://www.jgi.doe.gov>). The quality of DNA extracted was assessed by gel electrophoresis and NanoDrop (ThermoScientific, Wilmington, DE) according to the JGI recommendations, and the quantity was measured using the Quant-iT™ Picogreen assay kit (Invitrogen, Carlsbad, CA) as directed.

The draft genome of *D. postgatei* was generated at the Joint Genome Institute (JGI) using a combination of Sanger and 454 sequencing platforms. All general aspects of library construction and sequencing can be found at <http://www.jgi.doe.gov/>. 454 Pyrosequencing reads were assembled using the Newbler assembler version 1.1.02.15 (Roche). Large Newbler contigs were broken into 2,525 overlapping fragments of 1,000 bp and entered into assembly as pseudo-reads. The sequences were assigned quality scores based on Newbler consensus q -scores with modifications to account for overlap redundancy and to adjust inflated q -scores. A hybrid 454/Sanger assembly was made using the phrap assembler. Possible mis-assemblies were corrected with Dupfinisher or transposon bombing of bridging clones (180). Gaps between contigs were closed by

editing in Consed, custom primer walk or PCR amplification. The error rate of the completed genome sequence is less than 1 in 100,000.

4.2.6 Genome annotation

Genes were identified using a combination of Critica (181) and Glimmer (182) as part of the genome annotation pipeline at Oak Ridge National Laboratory (ORNL), Oak Ridge, Tennessee, USA, followed by a round of manual curation. The predicted CDSs were translated and used to search the National Center for Biotechnology Information (NCBI) nonredundant database (<http://www.ncbi.nlm.nih.gov/genome/3293>), UniProt, TIGRFam, Pfam, PRIAM, KEGG, COG, and InterPro databases. The tRNAScanSE tool (183) was used to find tRNA genes, whereas ribosomal RNAs were found by using BLASTn against the ribosomal RNA databases. The RNA components of the protein secretion complex and the RNaseP were identified by searching the genome for the corresponding Rfam profiles using INFERNAL (139). Additional gene prediction analysis and manual functional annotation was performed within the Integrated Microbial Genomes (IMG) platform (<http://img.jgi.doe.gov/>) developed by the Joint Genome Institute, Walnut Creek, California, USA (184).

4.2.7 Metabolic Network Reconstruction

The initial *D. postgatei* metabolic network was done by the combination of the rapid annotation using subsystem technology (RAST) server [33] and Model SEED pipeline [34]. Refinement of the draft metabolic network was completed with the help of several public databases, including KEGG [35], MetaCyc [36], UniProt [37], BRENDA [38], and TCDB [39]. New assigned open reading frames (ORFs) obtained from RAST annotation in the reconstruction were identified by known physiological features of *D. postgatei* or a local sequence similarity search (BLASTp) [37]. The reactions and genes in the draft model were manually reviewed using the gene annotations and the available biochemical and physiological information. The main features of the metabolism of *D. postgatei* are explained in Appendix C (Table C1).

The resulting network was then subjected to the gap filling process to allow biomass formation under physiological growth conditions. For gap filling, simulations were performed to determine if the networks could synthesize every biomass component and the missing reactions in the pathways were identified as previously described (185). These reactions were reviewed for gene association, or added as non-gene associated reactions to enable the formation of biomass by the reconstructed network.

Biomass compositions in the published *Geobacter sulfurreducens* (118) and *Rhodospirillum rubrum* (169) model were used as a model to create the biomass demand reactions in the initial *D. postgatei* metabolic network. Experiments were carried out to determine the biomass composition (dry basis) of 1 gram of *D. postgatei* cells (Tables C3 to C14). Cultures were grown to a final optical density at 600 nm (OD₆₀₀) of 0.2 to measure DNA, RNA, protein, lipid, and carbohydrate content and dry cell weight. For the dry cell weight, five independent cell pellets from a 500-ml culture samples were resuspended in water and carefully transferred into pre-weighed Eppendorf microcentrifuge tubes, and then dried at 85°C until at least 3 days. The dry weight was measured on a balance with 0.1-mg accuracy (Mettler Toledo; PL303) (Table C3). For the macromolecular composition analysis, the amounts of protein, lipids and carbohydrates were determined by the bicinchoninic acid method (173), the sulfo-phospho-vanillin method (186) and colorimetric analysis (187), respectively (Table C4). DNA content was calculated following methodology explained before (188). RNA content was assumed to be an average between reported values for *G.sulfurreducens* (118) and *E.coli* iAF260(189). The content of LPS (Lipopolysaccharides), inorganic ions, peptidoglycan (murein), and cofactors, prosthetic groups and others were assumed to be similar to the ones reported in *E.coli* iAF260 (189) . The following external metabolites were allowed to freely enter and leave the network for simulations of anaerobic growth on DSMZ 193 media: PO₄³⁻, CO₂, Mn²⁺, Zn²⁺, Cu²⁺, Ca²⁺, Cl⁻, Co²⁺, K⁺, Fe²⁺, Fe³⁺, riboflavin, Mg, cytidine triphosphate, biotin, spermidine, thiamin, folate, vitamin B-12, pantothenate, pyridoxal phosphate, cobinamide, nicotinamide, and lipoate. Also acetate and sulfate were added as electron donor and acceptor, respectively.

4.2.8 Total mRNA extraction

Cells were harvested from the two sets of duplicate 900 mL chemostat run in parallel in two conditions as previously described (190). Briefly, cultures were centrifuged at 4°C for 15 min and pellets were flash frozen and stored at –80°C. The biomass thus obtained were mixed with *RNAlater* (Ambion) as previously described (191) and RNA was extracted with TRIzol (Sigma) as previously described (36).

Total RNA was purified with the MinElute PCR purification kit (Qiagen) prior to rDNase I (Ambion) digestion following the manufacturers' protocol, followed by an additional treatment with the MinElute PCR purification kit. The absence of genomic DNA contamination was verified by 16S rRNA gene analysis as described previously (191). Then the mRNA was isolated with the *MICROBExpress* kit (Ambion), following the manufacturer's protocol. Aliquots of the triplicate mRNA extracts were analyzed with Experion RNA HiSens kit (Bio Rad) for the efficiency of rRNA removal.

4.2.9 Illumina sequencing and assembly of Illumina reads

The mRNA extracts were used to prepare directional multiplex libraries using ScriptSeq™ v2 RNA-Seq library preparation kit (Epicentre) following the manufacturer's protocol and single end sequencing was done using Hi-Seq 2000. All the raw data generated by Illumina sequencing was quality checked by visualization of base quality scores and nucleotide distributions. Then the sequences were sorted out by trimming of reads and read filtering based on base quality score and sequence properties such as primer contaminations, N content and GC bias using PRINSEQ (192).

4.2.10 Mapping mRNA reads

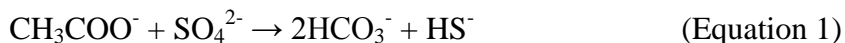
The mRNA sequence reads were first filtered for rRNA sequences and the purified mRNA reads were mapped against already published genome of *Desulfobacter postgatei* (DSM 2034) as described previously (35). For the final expression analysis, the mapped reads were normalized with the RPKM (reads assigned per kilobase of target per million mapped reads) method (193, 194) using ARRAY STAR. Reads from biological

replicates were first compared with each other graphically after mapping onto the template genomes. Biological replicates were highly reproducible (Figures C42a and C42b). Therefore, reads from biological replicates were merged and averaged for all further analysis. Expression levels were considered significant only when the \log_2 RPKM value was \geq median RPKM value (Figure C42c; Table C18). In the co-culture fold changes were computed only for those genes that had \geq median RPKM in one of the samples.

4.3 Results and discussion

4.3.1 Energy metabolism

Biochemical analyses have shown *D. postgatei* couples the oxidation of acetate to the reduction of sulfate through a citric acid cycle, running in reverse (141) (see Appendix C, Figure C1). The stoichiometry of this reaction has a free energy change of -63 kJ per mol of acetate (Equation 1) (141). Since ADP phosphorylation in living cells costs around 70 kJ per mol of substrate (195, 196), previous calculations based on information available before the genome of *D. postgatei* was sequenced predicted that the metabolism should yield a net production of 0.9 mol of ATP per mol of acetate oxidized (197, 198). However, it was difficult to envisage such net production of ATP due to the fact that only 1 ATP per mol of acetate is produced via substrate phosphorylation (153) and there is a requirement of 2 ATP in the activation of sulfate to APS (199).



The question arises of how the electron flow is coupled to the generation of ATP in the metabolism of *D. postgatei*. In order to explain this, Rabus and colleagues (2006) suggested that proton translocation might take place during the reduction of NADP by ferredoxin and the following reduction of quinones by NADPH, allowing an extra production of ATP via chemiosmosis (Figure C7). This hypothesis was based on previous

biochemical experiments that suggested that *D. postgatei* has both succinate dehydrogenase, an enzyme that oxidizes succinate to fumarate, and a membrane-bound NADPH:menaquinone oxidoreductase, an enzyme that reoxidize the NADPH⁺ generated during isocitrate oxidation (152, 198) (Figure C7). Although a ferredoxin:NADP oxidoreductase activity was mainly recovered in the membrane associated fraction, this enzyme was shown not to be involved in proton translocation (198).

Surprisingly, we could not find any homolog for genes encoding NADPH:menaquinone oxidoreductase and ferredoxin:NADP oxidoreductase in the genome sequence of *D. postgatei*. Instead, we found homologs encoding the complete set of subunits of three novel complexes that are related to energy conservation in other species and were not previously described in SRB. The novel complexes are the following: Quinone reductase (Qrc complex), Ech-hydrogenase-related complex (Ehr complex), and H⁺-translocating ferredoxin:NAD⁺ oxidoreductase (Rnf complex). We also found 2 additional complexes that have been previously described in SRB, the Quinone-interacting oxidoreductase (Qmo complex), and the Ferredoxin:NADP oxidoreductase (Nfn complex). All of these complexes have subunits that are predicted to be membrane-bound by TMHMM Server v. 2.0 (<http://www.cbs.dtu.dk/services/TMHMM-2.0/>), with the exception of Nfn complex.

4.3.2 Novel membrane-bound complexes found in the genome of *D. postgatei*

4.3.2.1 Qrc (Quinone-reductase) complex

The membrane-associated Quinone Reductase Complex (Qrc) is composed of four subunits, three periplasmic (QrcABC) and one integral membrane subunit (QrcD). QrcA and QrcB are both membrane-anchored proteins (166). QrcA contains five or six heme binding motifs that interact with *c*-type cytochromes (166). QrcB belongs to the molybdopterin oxidoreductase family, and QrcC contains sixteen conserved Cys residues that binds four Fe-S clusters (161). These clusters are essential for electron transfer between the quinone pool and the catalytic center of the protein. QrcD is an integral membrane protein that belongs to the NrfD/PsrC family (166).

Qrc complex is widely found in other sulfate-reducing *Deltaproteobacteria*, such as *Desulfovibrio vulgaris* and *Desulfobacterium autotrophicum*, however its characterization has been limited to *D. vulgaris* (161). In *D. vulgaris*, periplasmic hydrogenases oxidize hydrogen and donate electrons to periplasmic c_3 cytochromes. Then, *D. vulgaris* Qrc complex transfers electrons from the reduced pool of c_3 cytochromes into the quinone pool (161).

The four subunits of the Qrc were found in the genome of *D. postgatei*. As in *D. vulgaris*, the genes encoding the four sub-units of this complex, *qrcA*, *qrcB*, *qrcC* and *qrcD* are located contiguously on the *D. postgatei* chromosome (Figure 12). Also, the membrane anchored QrcB belongs to the MopB superfamily of proteins, and QrcC has four Fe-S binding motifs. Moreover, the transmembrane-spanning QrcD corresponds to a polysulphide reductase that is predicted to be directly involved in the electrogenic interaction with the quinone pool (161). QrcA corresponds to a cytochrome that in *D. postgatei* and other SRBs contain five heme binding sites, and *D. vulgaris* has six. Surprisingly, the main difference between these complexes is that while the catalytic center (hemes) of the QrcA of *D. vulgaris* is located in the periplasm, in *D. postgatei* is predicted to be located in the cytoplasm (Figure 12). This particular localization of the hemes led us to envisage that the function of the Qrc complex in *D. postgatei* is to oxidize quinones and to reduce the cytoplasmic thiol/disulfide containing protein, DsrC, which is known to interact closely with the cytosolic enzyme dissimilatory sulfite reductase, DsrAB (157). This resembles the function of the Alternative complex (ACIII) described for *Rhodothermus marinus* (200) and *Chloroflexus aurantiacus* (201), a six to eight subunits membrane-bound complex, with the exception that in the Qrc complex the heme-binding sites are located in the cytoplasm. The difference in the localization of QrcA remains similar when comparing the sequences of other H_2 -oxidizing and acetate-oxidizing SRBs suggesting that this modification may be widespread in other δ -Proteobacteria (Figure 12). Therefore, we hypothesize that *D. postgatei* Qrc complex reduces the soluble DsrC with electrons coming from the quinone pool, coupling the opposite reaction than the one characterized in *D. vulgaris* (Figure 13).

4.3.2.2 Ehr (Ech-hydrogenase-related) complex

The ability to oxidize hydrogen is a common feature in the metabolism of several SRBs (143, 202). For instance, H₂-oxidizing SRB, such as *D. vulgaris* and *D. desulfuricans* possess both periplasmic and cytoplasmic hydrogenases (202). Besides its utilization as electron donor, hydrogen has been hypothesized to be involved in a mechanism called “chemiosmotic H₂ cycling” proposed by Odom and Peck (203). During this process, the reducing power resulting from the oxidation of organic acids is transferred to a membrane-bound hydrogenase (Ech) to generate H₂. This gas diffuses to the periplasm and its re-oxidation produces electrons that are shuttled back to the cytoplasm by the Qrc complex. The main goal of this process is to contribute to energy conservation via H⁺ translocation (203, 204) (Figure 14).

Ech hydrogenases belong to the subgroup of multisubunit membrane-bound energy-conserving [NiFe] hydrogenases and has been found in many SRB, such as *D. vulgaris* (205), *D. gigas* (204), and *Desulfotomaculum ruminis* (206) and also methanogens, such as *Methanosarcina barkeri* (207). Surprisingly, we did not detect Ech hydrogenases in the genome of *D. postgatei*. Instead, an Ech-hydrogenase-related (*ehr*) cluster (DespoDRAFT_01512 - DespoDRAFT_01517), previously described in *G. sulfurreducens* (208), was identified. Although sharing similar subunits with high homology, Ech-hydrogenase-related complex is not a [NiFe] hydrogenase because they lack the CxxC motifs containing the cysteine residues key for H₂ oxidation at the N and C terminus of EhrL, the large subunit of the complex (Figures C3 and C4) (208, 209). Although the subunit *D. postgatei* EhrS subunit is 52% similar to the one in *G. sulfurreducens*, its physiological function remains to be revealed. The N-terminal of these subunits seems to be related to Fe-S clusters suggesting that ferredoxins generated during acetate oxidation can be reoxidized with transfer of electrons into the quinone pool in the membrane. Since this is a membrane-bound complex and interacts with Qrc complex, this reaction is a likely to contribute to energy conservation (Figure 15).

To test whether H₂ cycling is important for energy conservation in *D. postgatei*, 10 ppm of hydrogen was supplied to the headspace of growing cultures. There was no hydrogen consumption after the culture was in stationary phase (120 hours), ruling out

the ability of periplasmic hydrogenases to oxidize hydrogen (Figure C8). This result agreed with recent evidence that showed that this process is not important for energy conservation in the closely related *Desulfovibrio alaskensis* (210). Although, this supports our hypothesis that “chemiosmotic H₂ cycling” is not important in *D. postgatei*, further experiments are required to establish the role of this enzyme in energy conservation.

4.3.2.3 H⁺-translocating ferredoxin:NADP⁺ oxidoreductase (Rnf complex)

It was suggested previously that SRB may be able to use electron bifurcation and confurcation to equilibrate reducing equivalents derived from the central metabolism (163, 211). In recent years, the Rnf complex (for *Rhodobacter* nitrogen fixation) has been identified in several microorganisms, including many SRB, suggesting it might be involved in energy conservation. The function of this complex is to provide a link between ferredoxin and NAD(H)/NADP(H) pools (161, 163, 212-217).

Genes encoding the six subunits of the proton-translocating ferredoxin:NADP⁺ oxidoreductase (rnfABCDE) were found in one operon in the genome of *D. postgatei* (Figure C5). As reported for the methanogen *Methanosarcina acetivorans*, a multiheme cytochrome *c* encoding gene with 4–10 hemes was found next to the *rnf* genes (207). Also this *c*-type cytochrome is 71% identical of HRM2_32060 and 28% identical to Dole_2831, a *c*-type cytochrome found after one of the two copies of the *rnf* genes found in the close relatives *Desulfobacterium autotrophicum* and *Desulfococcus oleovorans* Hxd3, respectively (163). In agreement with previous research that showed that *D. postgatei* has a membrane-bound ferredoxin:NADP oxidoreductase, we predict that the Rnf complex of *D. postgatei* is involved in the reoxidation of ferredoxin, generated during 2-oxoglutarate oxidation, to the reduction of NAD⁺ (198). Although previous studies suggested this enzyme was electrically independent, we hypothesized that *D. postgatei* Rnf is involved in proton-motive force generation by the translocation of either protons or sodium ions (Figure 16) (161).

A detailed description of other aspects of the metabolism of *D. postgatei* is provided in Supplementary data (Appendix C).

4.3.3 In silico metabolic model of *D. postgatei*

The manually curated genome was utilized to prepare a genome scale network of the metabolism of *D. postgatei*. The main reconstruction procedure was made following the published protocol [32]. The initial automatic reconstruction made by the rapid annotation using subsystem technology (RAST) server [33] and Model SEED pipeline [34] was further refined by using published biochemical and physiological information. After the model was improved through several iterations of hypothesis generation, the current version contains a matrix with 1084 reactions and 1025 metabolites, including 630 gene-protein-reaction associations.

The metabolic capabilities of the *D. postgatei* network were calculated using flux balance analysis and linear optimization. Energy conservation was calculated as shown in Table C2 (Appendix C). Biomass synthesis was selected as the objective function to be maximized in growth simulations. The biomass function describes the rate at which all of the biomass precursors are made in the correct proportions and also includes growth-associated energy demand (218). This reaction was constructed based on measurements of *D. postgatei* biomass composition (Appendix C, tables C3 to C14) and takes into account the amounts of 79 metabolites, cofactors, precursors, and ions required to synthesize each gram (dry weight) (gdw) of biomass, the proton consumed for reductive reactions, the ATP required for the polymerization (peptide biosynthesis, DNA replication, and RNA polymerization) and biosynthesis of precursors and metabolites. Energy parameters of the metabolic model including GAM (Growth-Associated Maintenance energy) (Tables C13 and C14), and NGAM (Non-Growth Associated Maintenance energy) were also determined (219). The GAM requirement for the *D. postgatei* model was calculated using empirical and physiological information and was equal to 59.72 mmol ATP/gdw h. The NGAM requirement (0.38 mmol ATP/gdw h) was estimated by fitting Y_{ATP} to the hypothetical zero growth condition as described by Pirt (1965) and others (219-221) (Figure C21).

The electron donors (acetate) or acceptors (sulfate) tested were allowed a maximum uptake rate into the network of ~5 mmol/gdw h or as specified in the results. All the simulations resulted in flux values in units of mmol/gdw h.

4.3.4 Growth kinetics and stoichiometry under electron donor and electron acceptor limitation

In order to better understand the dynamic of growth of *D. postgatei*, chemostats were run under nutrient limiting conditions and dilution rates between 0.014 and 0.032 h⁻¹. Under electron donor limitation, basal medium was supplemented with 21.1 mM of sulfate as electron acceptor and 8.5 mM of acetate as electron donor.

The steady state concentrations of acetate were below detection limit at the lower dilution rates indicating that growth was limited by acetate. Up to 7.9 mM of sulfide was produced as a result of sulfate reduction; however this concentration did not seem to affect growth. An average of 13.7 mM of sulfate remained in the medium, indicating the 1:1 stoichiometry of acetate oxidation and sulfate reduction (Equation 1) (Figure C10). Consistent with Monod-type growth, the total biomass remained constant in the range of 44 to 50 mg dw/l and the biomass productivity was linear ($r^2=0.96$) (Figure C9). Growth yield was equal to 5.7 g dw per mmol of acetate consumed (Table C15), slightly higher than 4.3-4.8 g dw per mmol of acetate previously reported on batch cultures (152, 154, 197). Both the specific respiration rate (q_{electron}) and specific acetate consumption rates (q_{acetate}) increased linearly with growth rate in both conditions tested (Figure C11). The efficiency of both acetate and sulfate metabolisms were higher when cultures were limited by acetate, suggesting that electron donor limitation may be more likely to occur in many sedimentary environments where *D. postgatei* is found (154).

Under limitation of sulfate, basal medium was supplemented with 8.5 mM of sulfate as electron acceptor and 21.1 mM of acetate as electron donor. Up to 9.5 mM of sulfide was accumulated in the medium, and an average of 13.7 mM of acetate remained (Figure C10). Sulfate concentration remained at steady state levels only under the lower dilution rates and the total biomass remained constant ~20% lower than acetate-limiting

growth suggesting a more substantial impact on the metabolism of *D. postgatei*, (Figure C12). Biomass productivity remained linear in all dilution rates ($r^2=0.95$).

To the best of our knowledge, *D. postgatei* is not able to assimilate carbon through CO₂ fixation as can its close relative, *Desulfobacter hydrogenophilus* (222). Overall there was ca. 11% assimilation of acetate, which is consistent with other SRB. Under electron donor-limited growth, the majority of acetate (7.4 mM) was funneled into dissimilatory pathways, whereas under electron acceptor-limited growth an smaller fraction (6.3 mM) was used for dissimilation (Tables C15 and C16). This suggests that electron acceptor limitation affected growth more negatively than electron donor limitation.

Growth yield (Y_{ATP}) is a parameter that illustrates how energy can be diverted in several cellular functions other than cell growth. These functions include metabolic pathways shifting, energy spilling, cell motility, osmoregulation, and turnover of macromolecular compounds, among others (221, 223, 224). The Y_{ATP} (mmol ATP/g dw h) increased linearly with the growth rate in both electron donor and electron acceptor limited cultures (Figure C21). The Y_{ATP} values were slightly higher for electron acceptor limited cultures, suggesting that limitation of sulfate required an additional energy input.

Microscopic examination (TEM) revealed that dividing cells were more abundant in the samples collected from *D. postgatei* growing at 0.032 h⁻¹ (Figures C17 and C19). Also, we observed smaller-diameter flagellated cells at dilution rates of 0.014 h⁻¹ as it was observed in similar studies (Figures C18 and C20) (225).

4.3.5 Kinetic of acetate oxidation and sulfate reduction

The half saturation constant (K_s) obtained by Lineweaver-Burk linearization for acetate was 42 μM (Figure C14). This is in agreement with values previously reported (154, 226) and confirms that *D. postgatei* is able to deplete acetate to concentrations that are lower than those produced by most acetoclastic methanogens where sulfate is depleted (143, 226-228). The *D. postgatei* genome contains a gene encoding an acetate permease (DespoDRAFT_03458; AcpA) that transports acetate from the environment to the cytoplasm together with protons (229). The half saturation constant of sulfate (81

μM) (Figure C16) suggests that in marine environments, where *D. postgatei* was originally isolated, the supply of acetate is more limited than sulfate (154).

4.3.6 Validation of the metabolic model with experimental data

Simulations with the *D. postgatei* metabolic model were utilized to make predictions of *D. postgatei* metabolism. An initial *in silico* characterization of a batch-type growth indicates that the model utilizes acetate as the electron donor and sulfate as the electron acceptor, producing hydrogen sulfide as the end product. Other compounds in the culture medium, such as ammonia, were minimally used (Figure C22). This confirms that the metabolic model is able to resemble energy conservation through coupling acetate oxidation to sulfate reduction.

The *D. postgatei* metabolic model was validated by comparing experimental results obtained with chemostats with predicted results from *in silico* simulations. Under electron donor limitation, the predicted values matched well with the experimental data (Figure C23). The average of both experimental and predicted growth yields ($n=6$) for *D. postgatei* growing under acetate limitation was 0.173 mg dw per mM of acetate. However, during sulfate-limiting conditions the predicted growth yield is 0.2 mg dw per mM of sulfate, while the experimental growth yield is 0.32 mg dw per mM of sulfate (Figure C24). This suggests that the metabolism of *D. postgatei* contains other pathways capable of improving the growth yield under electron acceptor limitation that our simulations in the metabolic model do not represent.

The properties of the *D. postgatei* model were further analyzed by Phenotype Phase Planes analysis (PhPP). This analysis aims to study the genotype-phenotype relation, describing the effect of the availability of two key substrates, acetate and sulfate, on the specific growth rate (230, 231). Growth rates of all predicted phenotypes under electron donor limitation were higher than the ones under electron acceptor limitation (Figure 17). Acetate-limited and sulfate-limited growth predictions resulted in five and four different phases, respectively (Figure 17). Each of these phases corresponds to a distinct region that is representative to a metabolic state of the metabolic model. The bottom phases (number 1 in both charts) correspond to unfeasible phenotypes with

specific growth rates close to zero due to the fact that either acetate- and sulfate- specific respiration rates are not enough to meet both biosynthesis of metabolites and ATP maintenance requirement. Regions 2 and 3 correspond to phenotypes to regions limited by the excess of acetate and sulfate, respectively. Region 4 is the area where acetate and sulfate are perfectly balanced and specific growth rate is close to highest. The plateau observed in the acetate-limited simulations suggested that under high access to acetate and sulfate, the set of reactions included in the model can act as ATP-consuming futile cycles (i.e. anapleurotic reactions) (Figure C1). Thus, the *D. postgatei* metabolic model has been validated with physiological data and can be applied in future modeling studies.

4.3.7 *In silico* characterization of *D. postgatei* metabolism

Examination of the metabolic model revealed that the citric acid cycle was the main source of electrons and reducing equivalents that are directed toward sulfate reduction. Considered a “specialist” acetate-oxidizing bacteria, *D. postgatei* has a cascade of reactions involved in acetate activation capable of acting as anapleurotic pathway to ensure the feeding of central metabolism, and also serving as an alternative futile cycle.

In order to gain a better understanding of the metabolic role of these anapleurotic reactions, the flux distribution of reactions in acetate and sulfate-limited chemostats at different growth rates (0.014–0.032 h⁻¹) were examined in detail (Figure C25). In all cases, acetate was predicted to almost exclusively be utilized by succinyl:acetate CoA transferase (~95%) that funnels acetate into citric acid cycle, and small flux was routed to anapleurotic reactions. Indeed, both acetate-CoA ligases (AMP- and ADP-forming) were predicted to be active only under the highest growth rates. Synthesis of pyruvate through acetate kinase, phosphotransacetylase, and pyruvate ferredoxin oxidoreductase were linearly correlated with growth rates in order to meet the increasing requirements of gluconeogenic demand. The flux of these reactions was higher under sulfate-limited conditions, suggesting that these could be utilized as a potential futile cycle and there was more acetate available to fuel biosynthesis pathways. The highest portion of this flux is funneled into oxaloacetate by pyruvate carboxylase towards the biosynthesis of aspartate, asparagine, methionine, threonine, isoleucine, and lysine (Figure C25).

The correlation between the flux of both the citric acid cycle and the sulfate reduction pathway with growth rates in both acetate and sulfate limited simulations (Figures C26 to C37, Number 1 and 2) indicates that both pathways are the source of electrons and reducing equivalents towards energy conservation. However during sulfate limitation the flux of both pathways for each growth rate tested was higher, suggesting that there was an increased energy requirement. This result is consistent with the chemostats studies that showed a lower biomass under electron acceptor limitation (Table C16).

D. postgatei can conserve energy through chemiosmosis and substrate-level phosphorylation by ATP synthase and ATP-citrate lyase, respectively (198). The *D. postgatei* metabolic model predicts that the ATP synthase and ATP-citrate lyase, have the highest flux (7.69 mmol /gdw h and 6.9 mmol /gdw h, respectively) in cells growing at 0.032 h⁻¹ under sulfate limitation (Figures C26 to C37, Number 1 and 4). The flux predicted for acetate-limited growth was 15% lower for ATP synthase and 31% lower for ATP-citrate lyase, confirming the capability of the model to reflect the higher efficiency of *D. postgatei* to incorporate carbon into biomass under electron donor limitation. Furthermore, the flux predicted for both reactions correlated well with the growth rates under both conditions (acetate and sulfate limitation) (Figures C26 to C37, Number 1 and 4).

Interestingly, similar correlation to growth rates were observed for the flux distribution predicted for majority of the novel membrane-bound complexes found in *D. postgatei*. For instance, the Ehr (Ech-hydrogenase-related) complex, the membrane-bound enzyme capable of coupling oxidation of ferredoxins to the reduction of quinones, has a highest predicted flux under sulfate limitation (4.32 mmol /gdw h), while under acetate-limited growth the predicted flux was 34% lower (Figures C26 to C37, Number 6). Both the Qrc (Quinone-reductase) complex and the menaquinol:DsrC oxidoreductase (DrsDSRMKJOP) complex, which their hypothesized function is to oxidize quinones and reduce the cytoplasmic electron carrier, DsrC (Figure 13), have the highest predicted flux of 2.53 mmol /gdw h under sulfate limitation growing at 0.032 h⁻¹. This value is also higher (48%) than the one predicted under acetate-limiting growth (1.7 mmol /gdw h). In agreement with our hypothesis based on the genome analysis, the flux through reactions

that connects the oxidation of ferredoxins (Qrc and Ehr) and quinones (DsrMKJOP) to the reduction of sulfate correlated well with growth rates under both conditions suggesting that these enzymes might also be linked to energy conservation.

The *D.postgatei* model predicted that the flux of the soluble Nfn (NADH-dependent reduced ferredoxin:NADP⁺ oxidoreductase) complex was higher as respiration rates increases, suggesting that this enzyme plays an active role between ferredoxin and NAD(H)/NADP(H) pools (Figures C26 to C37, Number 7). On the other hand, the model predicts there is no flux through H⁺-translocating ferredoxin:NADP⁺ oxidoreductase (Rnf complex) under all conditions utilized to simulate growth. Although this might reflect the incapability of the model to reproduce the intracellular physiological conditions, more experimental evidence is required to evaluate its involvement in energy conservation.

4.3.8 Monte Carlo sampling of *D.postgatei* model

Monte Carlo sampling is an approach to provide insights into the robustness of the genome-scale metabolic network by assessing and quantifying the impact of uncertainty on its predictions. Monte Carlo method (210, 232, 233) was used to examine the ability of the predicted fluxes to maintain specific functions in the face of varying conditions in the *D.postgatei* metabolic model. The flux distributions for a set of reactions were calculated from 2,200 possible solutions and plotted as histograms (Figures C38 to C41). Different trends appear in the distribution analysis of these reactions. For instance, the average flux distribution of the ATP-producing reactions, ATP citrate lyase and ATP synthase, followed a similar trend that the 2-oxoglutarate ferredoxin oxidoreductase, a key enzyme in the citric acid cycle (Figures C38 to C41, Numbers 1, 2 and 3). Also, the flux distribution of the Qrc (Quinone-reductase) complex and the Ehr (Ech-hydrogenase-related) complex followed a similar trend to the one for dissimilatory sulfite reductase (DsrAB) that catalyze the six-electron reduction of sulfite to sulfide (Figures C38 to C41, Numbers 4, 5 and 6). These results supported our previous hypothesis that the flux among all these reactions is likely to be linearly related, representing a high-flux-backbone involved in energy metabolism pathway of *D.postgatei*.

4.3.9 Genome-wide transcriptional response of *D.postgatei* to different growth rates

In order to gain further insight into the physiological status of cells growing under electron donor limitation and to validate the computational predictions of *D. postgatei* metabolic model, the gene transcript abundance of *D. postgatei* growing in continuous culture at dilution rates of 0.032 h⁻¹ and 0.014 h⁻¹ was compared.

In general, transcript levels for genes encoding proteins involved in the central metabolism, sulfate respiration, amino-acid and protein biosynthesis were significantly higher as respiration rates increased. For instance, the gene encoding aconitase A (DespoDRAFT_00181), the enzyme that catalyses the isomeration of citrate to isocitrate, was up-regulated as growth rates increased (Table 3). Also the genes encoding the alpha (DespoDRAFT_00205), beta (DespoDRAFT_00204), gamma (DespoDRAFT_00203), and delta (DespoDRAFT_00106) subunits of the 2-oxoglutarate:ferredoxin oxidoreductase (*kgor*) were also up-regulated (Table 3). This enzyme is often utilized in other anaerobes for the carboxylation of succinyl-CoA to 2-oxoglutarate (234). However in *D. postgatei* this enzyme couples the reverse reaction to the reduction of ferredoxins that are further utilized as reducing equivalents by the membrane-bound complexes Rnf and DsrMKJOP. Therefore, a ferredoxin encoded by DespoDRAFT_00206 within the same operon is also up-regulated at the higher growth rate (Table 3). More interestingly, the gene encoding a succinyl-CoA:acetate CoA transferase, the enzyme that funnels the larger portion of acetate into the citrate acid cycle was also expressed in higher abundance at higher respiration rates (Table 3). The higher expression level of genes involved in the citric acid cycle under higher rate of metabolism agreed with the prediction made by the metabolic model.

Many genes encoding proteins associated with the sulfate reduction pathway were in higher abundance in cells growing at higher growth rates. For instance, the level of *dsrA* (dissimilatory sulfite reductase subunit α) transcripts, which has been proposed as proxy for the metabolic state of SRB (229, 235), was higher at the higher dilution rate (Table 3). The genes encoding four of the five subunits of the transmembrane DsrMKJOP complex (*dsrP*, *dsrO*, *dsrJ*, and *dsrK*) were also up-regulated (Table 3). This novel

complex is conserved in other SRB and has been predicted to link the quinone pool to the soluble DsrC cytochrome (See Appendix C), a key step in the reduction of sulfite. In contrast, lower transcript abundance for genes involved in the uptake of sulfate, such as sulfate permease-like transporter (DespoDRAFT_02318), was found at the highest dilution rate, as compared with the lower dilution rate where ATP hydrolysis coupled to active transport is likely to be minimized (Table 3).

Since cultures at higher dilution rates have increased growth-associated energy consumption, higher levels of transcripts of genes involved in energy conservation were expected. Indeed, genes encoding five subunits of the ATP synthase (DespoDRAFT_01538-01541 and DespoDRAFT_01543) and three subunits of the proton-translocating ferredoxin:NADP⁺ oxidoreductase (Rnf complex) were up-regulated at higher dilution rates (Table 3). This is in agreement with a proteogenomic study of sediments during *in situ* uranium bioremediation at a field study site in Rifle, CO, that found that proteins belonging to the *D. postgatei* Rnf complex were abundantly expressed in sediments after acetate stimulation (81). This supports our hypothesis that Rnf complex might be involved in coupling the reduction of ferredoxins to the translocation of protons. Furthermore, genes encoding four subunits of the quinone-reductase complex (Qrc) and the small subunit of the energy-converting hydrogenase related complex (*ehrS*) were also up-regulated supporting the model prediction that higher metabolic rates demand a higher flux through these reactions (Table 3).

It also appeared that protein biosynthesis was more important at higher growth rates, which was reflected in the higher abundance of transcripts encoding 50S (L2, L10, L14, L18, L20 and L35), 30S (S1, S6, S8, S11, S13, S16 and S21) ribosomal proteins, proteins involved in the aminoacylation of transfer RNAs (*aspS*, *leuS*, *gatA*), and proteins involved in amino acid biosynthesis (DespoDRAFT_00630, DespoDRAFT_00112, DespoDRAFT_00823, DespoDRAFT_01427, DespoDRAFT_01742, DespoDRAFT_01743, DespoDRAFT_02637 and DespoDRAFT_03545) (Table 3).

4.4 Implications

Despite the central role that SRB plays in sulfur and carbon cycles and the number of sequenced genomes of SRB has increased significantly in the recent years, a deeper understanding of the energy metabolism and the electron transfer pathways of sulfate-reducing metabolism remained elusive. Recent studies have shown a range of novel components of the electron transfer pathways underlying the metabolism of SRB that include both novel membrane-bound and cytoplasmic enzymes (156, 157, 163, 165, 236, 237). However, all the experimental evidence has been limited to incomplete-oxidizing *Desulfovibrio* strains for which genetic tools are available.

This study presents three independent lines of evidence (genomic context, genome-scale metabolic network model and global transcriptional analysis) that identify novel enzymes involved in energy conservation. These included the energy-converting hydrogenase related complex, Ehr, the proton-translocating ferredoxin:NADP⁺ oxidoreductase, Rnf, and also the NADH-dependent reduced ferredoxin:NADP⁺ oxidoreductase, Nfn, that were not identified by previous biochemical studies (198). This new understanding of *D. postgatei* energy conservation will substantially improve the modeling of the growth of this organism in marine sediments and subsurface environments, and also shed light on the adaptation strategies that enable specialist microbes, such as *D. postgatei*, to succeed in such competitive niches (238).

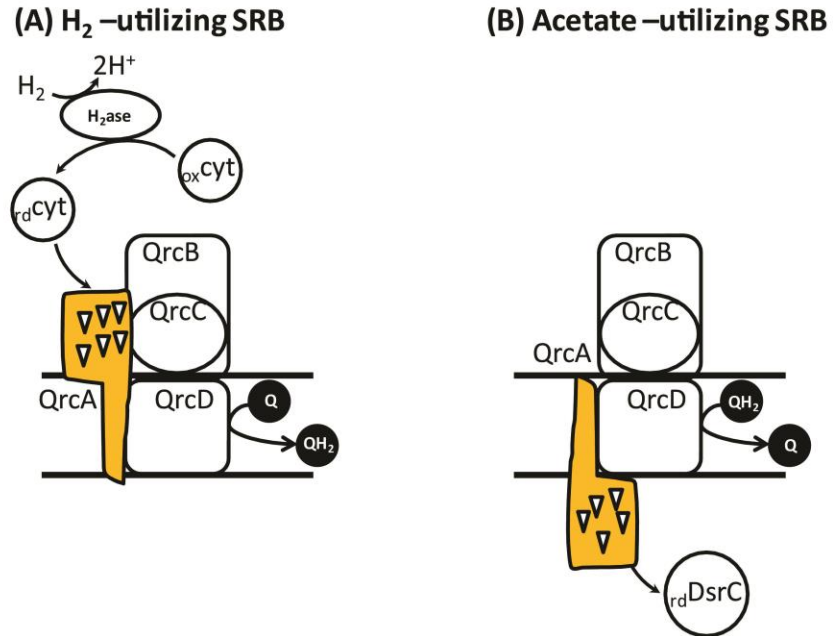


Figure 13: Representation of quinone reduction by Qrc in (A) H₂-utilizing SRB (as *D. vulgaris*, see text) and the proposed cytochrome reduction by Qrc in (B) Acetate utilizing SRB. QH₂, reduced quinone; Q, oxidized quinone; H₂ase, periplasmic hydrogenase. Triangles indicate heme groups of the QrcA subunit.

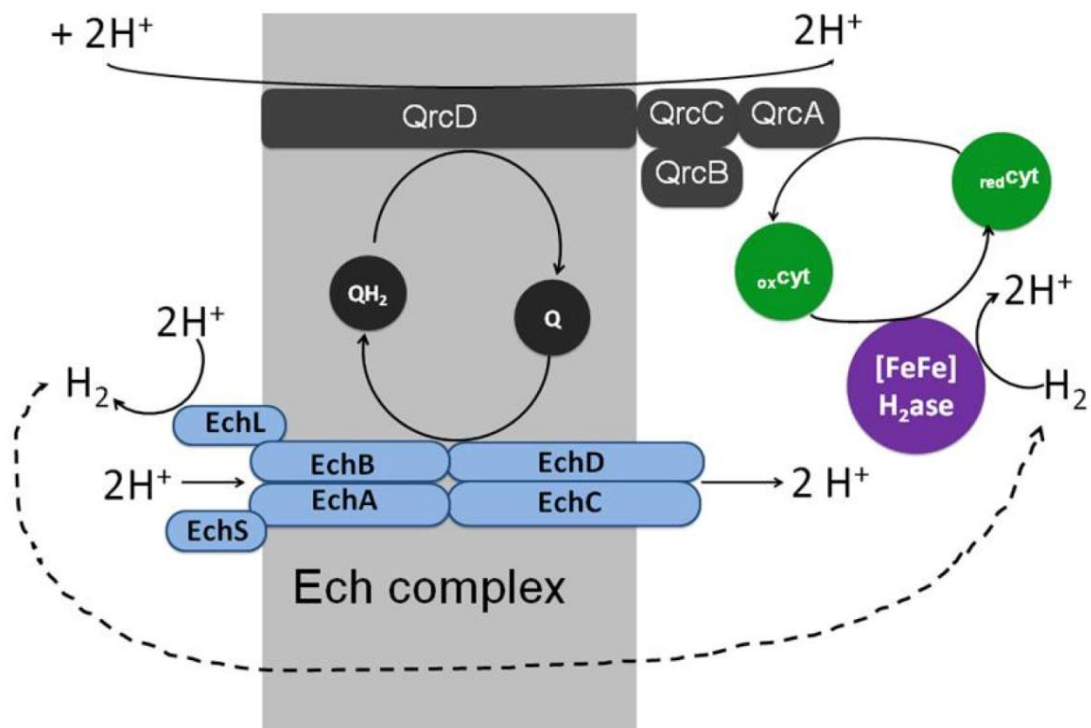


Figure 14: Hydrogen cycle in *D. vulgaris* proposed by Odom and Peck (203). Ech complex in blue and Qrc complex in gray. QH_2 , reduced quinone; Q , oxidized quinone; $red\text{cyt}$, reduced cytochrome, $ox\text{cyt}$, oxidized cytochrome; [FeFe] H_2ase , periplasmic hydrogenase.

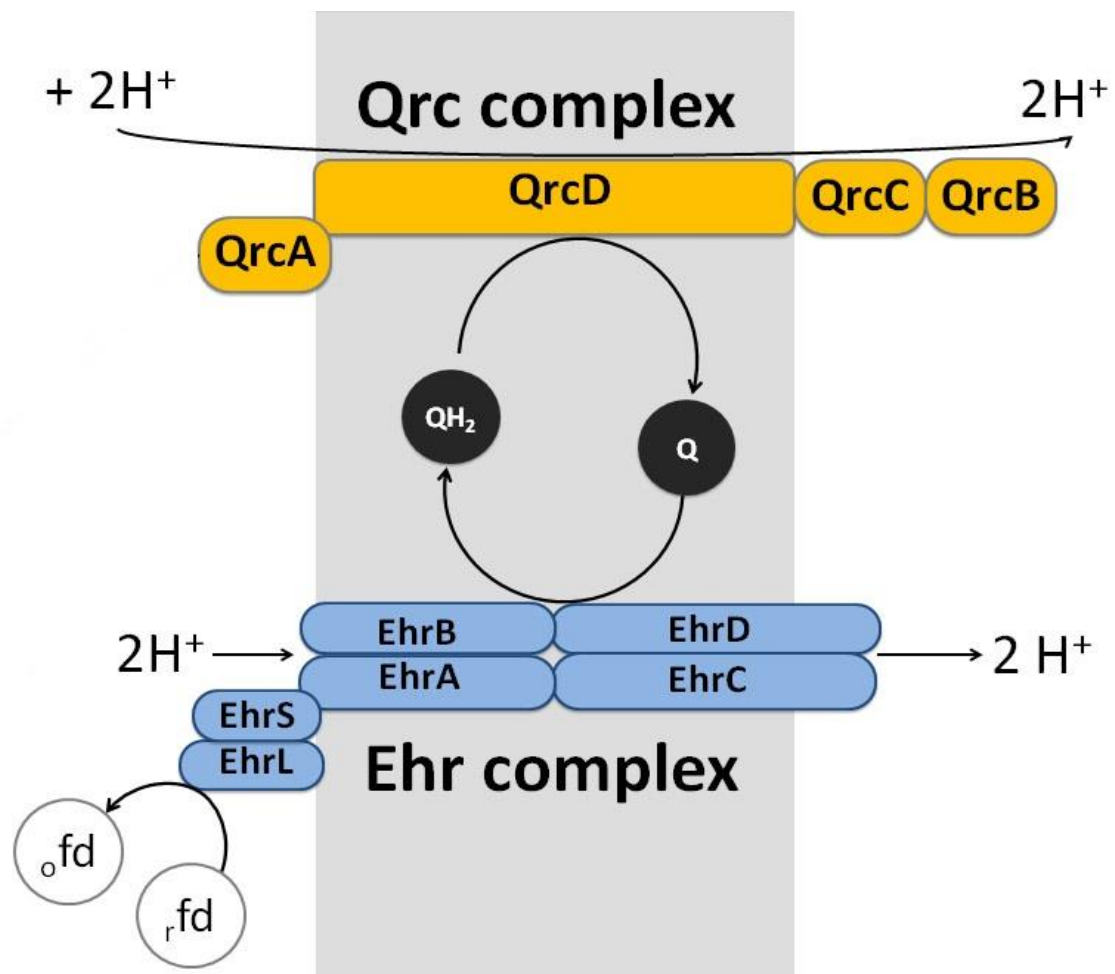


Figure 15: Predicted mechanism of Ehr complex and Qrc complex in *D. postgatei*. Ehr complex in blue and Qrc complex in gray. QH₂, reduced quinone; Q, oxidized quinone;

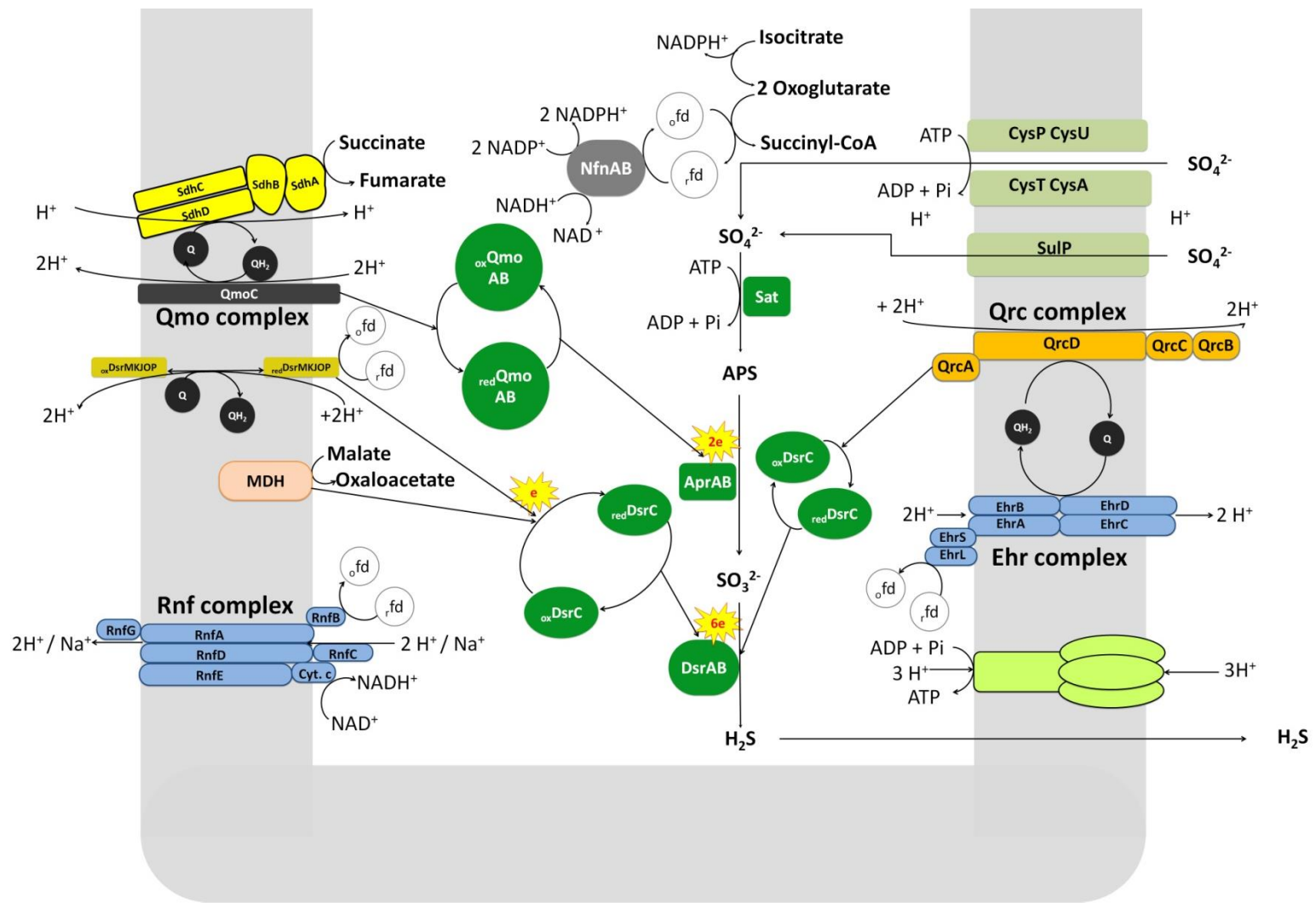


Figure 16: Schematic metabolic reconstruction of the energy metabolism of *D. postgatei*.

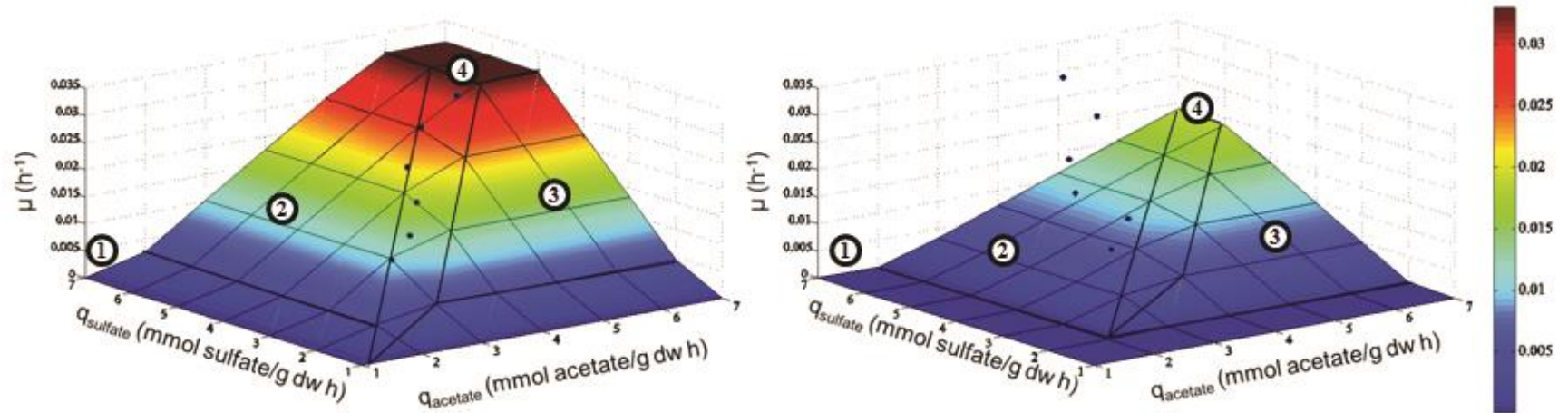


Figure 17: Phenotype Phase Planes analysis (PhPP) of *D. postgatei* metabolic model. The left graph corresponds to simulations made in acetate –limited growth and the right graph corresponds to simulations made in sulfate-limited growth. x-axis corresponds to sulfate specific respiration rate (q_{sulfate}), y-axis corresponds to acetate specific respiration rate (q_{acetate}), and z-axis corresponds to growth rate. Numbers indicate the different phases during growth

Table 3: Selected genes that were differentially expressed at least two fold in *D. postgatei* growing at 0.032 h⁻¹ compared to those growing at 0.014 h⁻¹ (P-value cutoff less than or equal to 0.05). Positive and negative numbers indicate up- and down-regulated genes at 0.032 h⁻¹.

Locus ID	Gene Annotation	Expression level (log2RPKM values)	P-value
<i>Central metabolism</i>			
DespoDRAFT_00181	aconitase A	2.55	0.0261
DespoDRAFT_00205	2-oxoglutarate:ferredoxin oxidoreductase, α subunit (kgorA)	3.648	0.0274
DespoDRAFT_00204	2-oxoglutarate:ferredoxin oxidoreductase, β subunit (kgorB)	3.356	0.0463
DespoDRAFT_00203	2-oxoglutarate:ferredoxin oxidoreductase, γ subunit (kgorC)	3.301	0.0149
DespoDRAFT_00106	2-oxoglutarate:ferredoxin oxidoreductase, delta subunit (kgorD)	2.619	0.0138
DespoDRAFT_00206	ferredoxin	3.876	0.0458
DespoDRAFT_02073	succinyl-CoA:acetate CoA transferase	2.926	0.0241
<i>Sulfate reduction and energy conservation</i>			
DespoDRAFT_01364	sulfite reductase, dissimilatory-type alpha subunit (dsrA)	2.575	0.0326
DespoDRAFT_03015	polysulfide reductase (dsrP)	5.123	0.0175
DespoDRAFT_03016	Fe-S-cluster-containing hydrogenase	4.233	0.0455

	subunit (dsrO)		
DespoDRAFT_03017	cytochrome c (dsrJ)	4.625	0.0447
DespoDRAFT_03018	Fe-S oxidoreductase (dsrK)	3.847	0.0218
DespoDRAFT_02318	Sulfate permease-like transporter (sulP3), high affinity sulfate transporter.	- 2.94	0.0209
DespoDRAFT_01538	ATP synthase F0 subunit b	2.432	0.00692
DespoDRAFT_01539	ATP synthase F1 delta subunit	2.823	0.0274
DespoDRAFT_01540	proton translocating ATP synthase F1 alpha subunit	2.376	0.0449
DespoDRAFT_01541	ATP synthase F1 gamma subunit	2.627	0.0255
DespoDRAFT_01543	ATP synthase F1 epsilon subunit	2.708	0.0464
DespoDRAFT_01996	NADH:ubiquinone oxidoreductase δ subunit (rnfD)	2.603	0.0247
DespoDRAFT_01995	electron transport complex RnfABCDGE type η subunit (rnfG)	2.587	0.0014
DespoDRAFT_01997	NADH:ubiquinone oxidoreductase γ subunit (rnfC)	3.011	0.0361
DespoDRAFT_02815	class III cytochrome C family protein (qrcA)	2.754	0.0413
DespoDRAFT_02816	Anaerobic dehydrogenase typically selenocysteine-containing (qrcB)	2.341	0.0354
DespoDRAFT_02817	Fe-S-cluster-containing hydrogenase subunit (qrcC)	3.301	0.0408
DespoDRAFT_02818	polysulfide reductase (qrcD)	3.166	0.0268

DespoDRAFT_01512	Ech-hydrogenase-related complex (ehrS)	3.696	0.0355
<i>Protein synthesis</i>			
DespoDRAFT_00756	ribosomal protein L35	3.304	0.0161
DespoDRAFT_00757	ribosomal protein L20	2.163	0.0241
DespoDRAFT_01792	ribosomal protein S6	4.357	0.0338
DespoDRAFT_02454	ribosomal protein L10	2.625	0.0337
DespoDRAFT_02465	ribosomal protein L2 bacterial/organelar	2.002	0.0196
DespoDRAFT_02472	ribosomal protein L14 bacterial/organelle	2.351	0.0072
DespoDRAFT_02476	ribosomal protein S8	2.599	0.0431
DespoDRAFT_02478	ribosomal protein L18 bacterial type	2.121	0.0498
DespoDRAFT_02485	30S ribosomal protein S13	2.231	0.0422
DespoDRAFT_02486	30S ribosomal protein S11	2.125	0.0466
DespoDRAFT_02896	ribosomal protein S16	2.795	0.0336
DespoDRAFT_03026	ribosomal protein S21	2.924	0.0355
DespoDRAFT_03476	ribosomal protein S1	2.468	0.0423
DespoDRAFT_00157	aspartyl-tRNA synthetase (aspS)	2.694	0.0365
DespoDRAFT_01802	leucyl-tRNA synthetase (leuS)	2.518	0.0315
DespoDRAFT_02794	glutamyl-tRNA(Gln) amidotransferase C subunit (gatA)	2.308	0.0418
DespoDRAFT_02870	glutamyl-tRNA synthetase	5.392	0.0487
<i>Amino acid biosynthesis</i>			

DespoDRAFT_00630	3-isopropylmalate dehydrogenase	5.944	0.00598
DespoDRAFT_00112	branched-chain amino acid aminotransferase, group II hisC	5.158	0.0325
DespoDRAFT_00823	3-isopropylmalate dehydratase, small subunit	5.844	0.0439
DespoDRAFT_01427	aspartate/tyrosine/aromatic aminotransferase	2.03	0.0248
DespoDRAFT_01742	phosphoserine aminotransferase	6.266	0.0313
DespoDRAFT_01743	D-3-phosphoglycerate dehydrogenase	4.408	0.0317
DespoDRAFT_02637	argininosuccinate synthase	2.676	0.0225
DespoDRAFT_03545	glutamate 5-kinase	2.354	0.0241

CHAPTER 5

CONCLUSION

This dissertation has presented three research projects with the goal of (1) investigating the electron transfer mechanism of *Geobacter sulfurreducens* to reduce U(VI), (2) evaluating the physiological response of *G. sulfurreducens* in the presence of environmental relevant concentrations of U(VI), and (3) understanding the physiology of energy conservation in the sulfate-reducing bacteria *Desulfobacter postgatei*. The integration of these goals seeks to improve our understanding about the interaction between *Geobacter* species, U(VI) and its competitor for acetate, *D. postgatei*, during *in situ* bioremediation of subsurface systems at a uranium-contaminated site in Rifle, CO.

The first research project described the nature of the molecular mechanism by which *G. sulfurreducens* reduces U(VI) through an integrative approach. Although, early studies with *G. sulfurreducens* suggested that outer-surface *c*-type cytochromes might play a role in U(VI) reduction (52), more recent evidence suggested that there is substantial U(VI) reduction at the surface of the electrically conductive pili known as microbial nanowires (60). We found that in order to reduce rates of U(VI) reduction to levels less than 20% of wild-type it was necessary to delete the genes for the five most abundant outer surface *c*-type cytochromes of *G. sulfurreducens*. Furthermore, an strain of *G. sulfurreducens*, known as Aro-5, which produces pili with substantially reduced conductivity, reduced U(VI) nearly as well as wild-type as did a strain in which the gene for PilA, the structural pilin protein, was deleted. We also observed through Transmission electron microscopy and X-ray Energy Dispersion Spectroscopy that wild-type cells did not precipitate uranium along pili as previously reported, but U(IV) was precipitated at the outer cell surface. Our findings are consistent with previous studies which have suggested that *G. sulfurreducens* requires outer-surface *c*-type cytochromes, but not pili, for the reduction of soluble extracellular electron acceptors.

The second research project described the physiological response of a mid-exponential phase culture of *G. sulfurreducens* exposed for four hours to 100 μ M of U(VI) by a global proteomic approach. This results were complemented with the

monitoring of several strains of *G.sulfurreducens* growing under the three following conditions: absence of U(VI), “slight U(VI) stress” (in the presence of 100 μ M of U(VI) in the form of uranyl acetate) and “severe U(VI) stress” (in the presence of 1mM of U(VI) in the form of uranyl acetate). We found that U(VI)-exposed cultures expressed lower levels of proteins involved in growth, protein and amino acid biosynthesis, as a result of the deleterious effect of U(VI). In contrast, proteins involved in detoxification, such as several efflux pumps belonging to the RND family, and protection of membrane and proteins, such as chaperons and proteins involved in secretion systems, were in higher abundance in cells exposed to U(VI). Exposing *G. sulfurreducens* to U(VI) resulted in higher abundance of many proteins associated with the oxidative stress response, such as superoxide dismutase and superoxide reductase. A strain in which the gene for superoxide dismutase was deleted grew slower than the wild-type strain in the presence U(VI), but not in its absence. The results suggest that there is not one specific U(VI)-detoxification system specific mechanism for uranium detoxification. Rather, resistance to U(VI) appears to be accomplished with multiple stress response systems and regulatory networks that facilitate fast adaptation to rapidly changing conditions. The ability of *Geobacter* species to cope with potential U(VI) toxicity in this manner may be one of the reasons that *Geobacter* species are often one of the most abundant genera of microorganisms during *in situ* uranium bioremediation.

The third research project described the physiology of the energy conservation in the sulfate-reducing bacteria *D. postgatei*, a pure culture model for the *Desulfobacter* species that play an important role in sulfate reduction in marine sediments and that have a negative impact on *in situ* uranium bioremediation by outcompeting U(VI)-reducing species for acetate. During this project the genome of *D. postgatei* was sequenced and a genome-scale metabolic model constructed. The annotated genome obtained from the Joint Genome Institute was manually curated, identifying 3773 genes predicted, 3678 of which were predicted to encode proteins. Growing *D. postgatei* in a continuous-culture system under electron donor (acetate) and electron acceptor (sulfate)-limiting conditions provided important physiological data and growth parameters that were incorporated into a genome-scale metabolic model designed to quantitatively explore energy conservation from acetate oxidation coupled to sulfate reduction. The model was improved through

several iterations of hypothesis generation, and integration of experimental and bibliographic data. Through this process, novel elements for energy conservation were discovered. These included the energy-converting hydrogenase related complex, Ehr, the proton-translocating ferredoxin:NADP⁺ oxidoreductase, Rnf, and also the NADH-dependent reduced ferredoxin:NADP⁺ oxidoreductase, Nfn. The current version of the model predicts that these complexes actively regulate the transition of the cells into different physiological states, providing also a link between the ferredoxin and NAD(H)/NADP(H) pools. RNA-seq analysis of transcript abundance in cells grown in an acetate-limited chemostat at different growth rates (0.014–0.032 h⁻¹) revealed that many of the genes encoding proteins involved in these complexes were expressed in higher abundance as respiration rates increased. The future enzymatic characterization of these complexes as well as their interactions with recently characterized enzymes involved in energy conservation (156, 159, 163-165, 236, 237, 240), will increase our understanding of the energy metabolism and the electron transfer pathways of sulfate-reducing bacteria.

The many physiological aspects revealed in this dissertation expanded the physiological framework of *Geobacter* species, increasing the knowledge about microbe–radionuclide interactions and its potential as a powerful tool for *in situ* bioremediation. This dissertation increase the knowledge of the physiology of *D.postgatei* that can serve as a platform to improve our understanding of microbial interactions and their environments, allowing us to predict physiological status and behavior of these two species and tune the electron donor inputs along bioremediation of uranium-contaminated groundwater.

APPENDICES

APPENDIX A

**SUPPLEMENTARY INFORMATION U(VI) REDUCTION BY A DIVERSITY OF
OUTER SURFACE C-TYPE CYTOCHROME OF GEOBACTER
SULFURREDUCTENS**

Table A1: Strains used in this study.

Strain name	Deleted or modified gene(s)	Genbank accession number of deleted or modified gene(s)	Localization	Reference
Δ omcST	omcS; omcT is also not expressed	GI-39997599	OM	(89)
Δ omcZ	omcZ	GI-39997174	OM	(87)
Δ pilA	pilA	GI-39996596	OM	(58)
Δ pilA::cm	-	-	-	(58)
Δ BSTE	omcB, omcS, omcT, omcE	GI-39997831, GI-39997599, GI-39997598, GI-39995725	OM	(62)
Δ BSTEZ	omcB, omcS, omcT, omcE, omcZ	GI-39997831, GI-39997599, GI-39997598, GI-39995725, GI-39997174	OM	(62)
Δ aro-5	Alanine was substituted for each of the five aromatic amino acids in the carboxyl terminus of pilA gene	GI-39996596	C	(88)

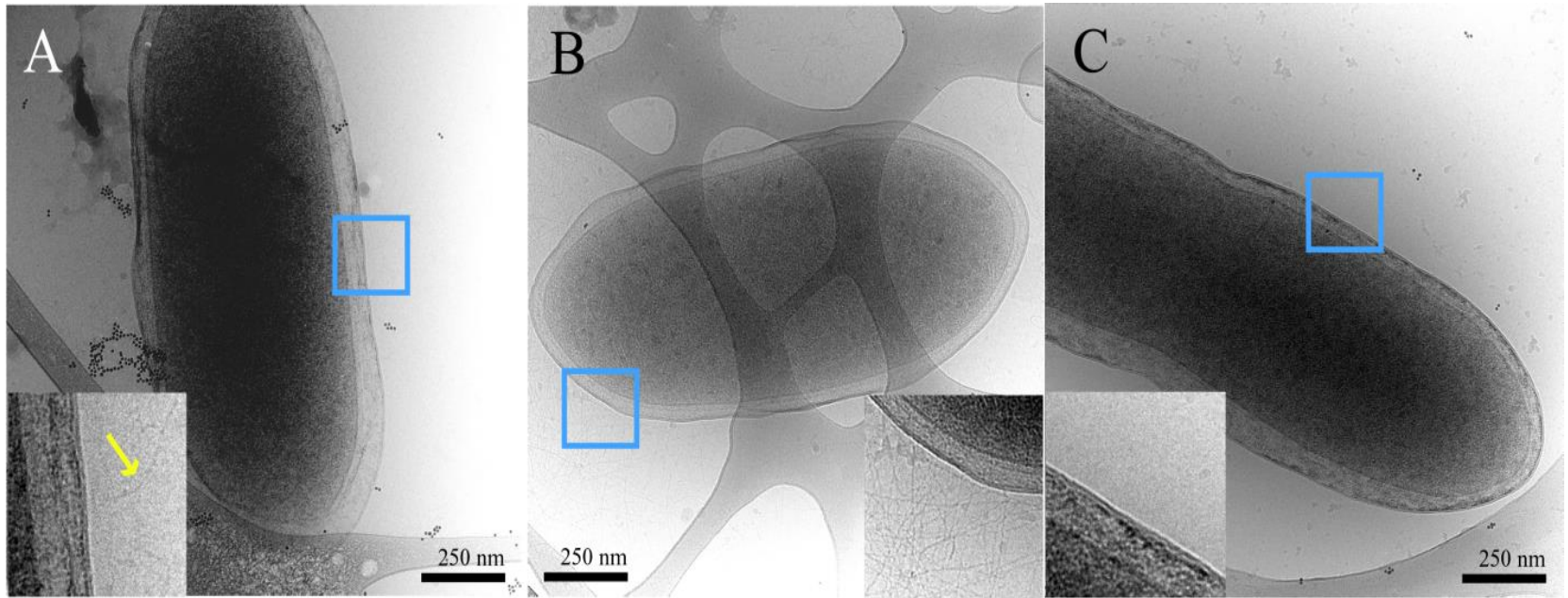


Figure A1: CryoTEM images of (A) wild-type, (B) Δ BESTZ, and (C) Δ pilA cells respiring U(VI). The cell walls and high contrast aggregates were discussed in the context of Fig. 6. We clearly see normal pili distribution in wild type, high abundance of pili in cells of Δ BESTZ, and no pili in Δ pilA. Insets show magnified views of small regions within blue boxes for enhanced view.

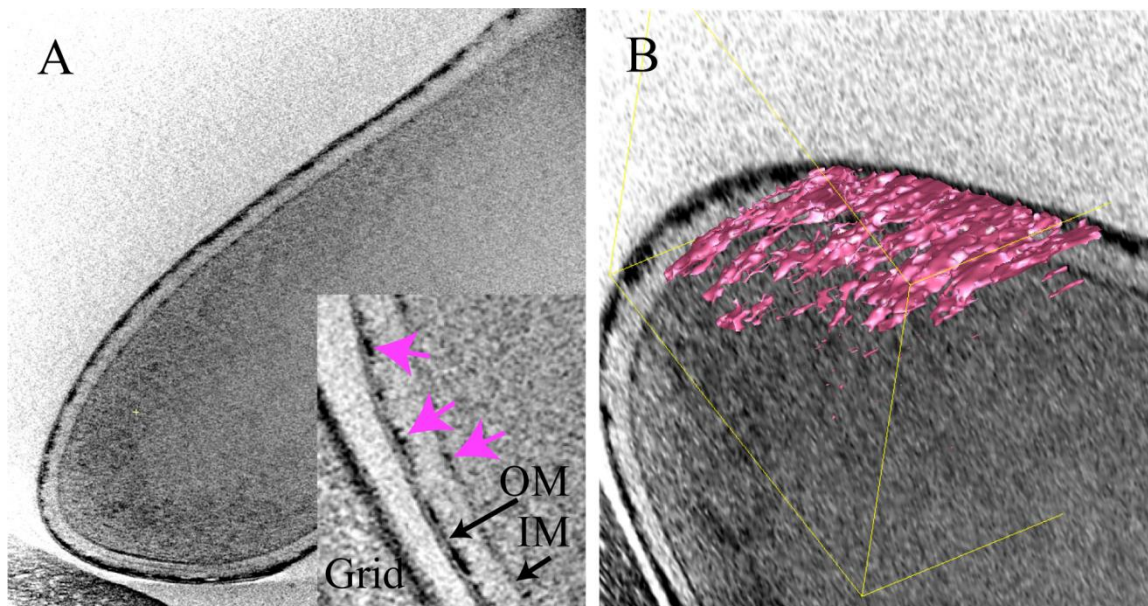


Figure A2: Cryo-ET of $\Delta pilA$ cells respiring U(VI). **A)** Slice through a 3D cryo-ET reconstruction of an intact cell in vitreous ice. The high contrast encasing/spanning the OM is consistent with U deposition, the only high atomic number element (very “electron dense”) added to the cultures. IM: inner membrane; OM: outer membrane; Grid: carbon coated Formvar support. Pink arrows: aggregates at OM and IM. **B)** Slice through a 3D cryo-ET of another cell with. The isosurface rendering in 3D of a region of the high contrast aggregates is shown in dark pink, superimposed on a slice of the same cryo-ET reconstruction in grey-scale. The yellow box outlines the 3D isosurface sub-volume. See XEDS line scans across the cell surface and cell wall in **Figure 6B** unequivocally identifying the aggregates as U. Scale: the width of the periplasmic space is approximately 30 nm.

APPENDIX B

SUPPLEMENTARY INFORMATION PROTEOME OF GEOBACTER SULFURREducENS IN THE PRESENCE

Table B1: Proteins with increased abundance under U(VI) exposure. Δz -score was calculated as follows: (z-score in U treatment - z-score in control).

Locus ID	Symbol	Name	Δz
GSU2213		GAF domain protein	1.82
GSU2429		peptidylprolyl cis-trans isomerase, PpiC-type	1.82
GSU0014		DnaJ-related molecular chaperone	1.82
GSU1737	paaK-2	phenylacetate-CoA ligase	1.81
GSU1482		efflux pump, RND family, outer membrane protein	1.81
GSU1458		TPR domain protein	1.80
GSU3318		conserved hypothetical protein	1.80
GSU3246	prx-2	peroxiredoxin, typical 2-Cys subfamily	1.80
GSU1183		O-acetyl-L-homoserine sulfhydrylase	1.80
GSU1493	pilC	type IV pilus biogenesis protein PilC	1.79
GSU1919	pyrH	uridylate kinase	1.79
GSU3292		transcriptional regulator, Fur family	1.79
GSU0987		conserved hypothetical protein	1.79
GSU1817		outer membrane lipoprotein, Slp family	1.79
GSU0106		chromosome partitioning ATPase Soj	1.79
GSU3077	mraW	SAM-dependent membrane protein methyltransferase MraW	1.78
GSU3470	dnaA	chromosomal replication initiator protein DnaA	1.78
GSU3424		dihydrolipoamide dehydrogenase-related protein	1.78
GSU2980	nikR	nickel-binding domain transcriptional regulator	1.78
GSU0720		superoxide reductase	1.78

GSU0983		phage-related baseplate assembly protein, putative	1.78
GSU2038	pilY1-2	type IV pilus tip-associated adhesin	1.78
GSU1530	hisG-1	ATP phosphoribosyltransferase	1.77
GSU2700	tupA	tungstate ABC transporter, periplasmic tungstate-binding protein, putative	1.77
GSU2666		transcriptional regulator, TetR family	1.77
GSU2695		efflux pump, RND family, outer membrane protein	1.77
GSU0990		hypothetical protein	1.77
GSU1155		glutaredoxin family protein	1.77
GSU0672		conserved hypothetical protein	1.77
GSU0160	dapB	dihydrodipicolinate reductase	1.77
GSU2516		rhodanese homology domain pair protein	1.77
GSU1328		protein of unknown function DUF1255	1.76
GSU0197		oxidoreductase, short chain dehydrogenase/reductase family	1.76
GSU1090		signal transduction protein-related protein, response receiver	1.76
GSU2441		conserved hypothetical protein	1.76
GSU0457		outer membrane lipoprotein LolB, putative	1.76
GSU2821	nifH	nitrogenase iron protein	1.75
GSU0689	hpnN	efflux pump, RND superfamily, putative	1.75
GSU0357		cytochrome c family protein	1.74
GSU2425		O-acetyl-L-homoserine sulfhydrylase	1.74
GSU3066	ddl	D-alanine--D-alanine ligase	1.74
GSU3296	glcD-1	D-lactate/glycolate dehydrogenase, FAD-binding protein, putative	1.74
GSU0483	queC	7-cyano-7-deazaguanine synthase	1.73
GSU3373	rsmB	16S rRNA (5-methyl-C967)-methyltransferase	1.73
GSU2869	secE	preprotein translocase, SecE subunit	1.73
GSU1648	macC	cytochrome c, 5 heme-binding sites	1.73
GSU2062		response receiver-modulated nucleotide cyclase	1.72
GSU1230		ABC transporter, periplasmic substrate-binding protein	1.72

GSU2801		cytochrome c, 5 heme-binding sites	1.72
GSU1089		iron-sulfur cluster-binding protein	1.72
GSU1158	sodA	superoxide dismutase, iron/manganese-containing	1.72
GSU1117		response regulator	1.71
GSU0800		amino acid ABC transporter, periplasmic amino acid-binding protein	1.71
GSU2136		efflux pump, RND family, membrane fusion protein	1.71
GSU1459	ispG	4-hydroxy-3-methylbut-2-en-1-yl diphosphate synthase	1.71
GSU0242	acpP-1	acyl carrier protein	1.71
GSU1827	nadB	L-aspartate oxidase	1.71
GSU0008		response receiver sensor histidine kinase, PAS domain-containing	1.71
GSU3464	gidA	tRNA (5-carboxymethylaminomethyl-2-thio-U34)-formylglycyltransferase	1.71
GSU2212	cheY-5	chemotaxis protein CheY	1.71
GSU0783		nickel-dependent hydrogenase, iron-sulfur cluster-binding protein	1.71
GSU2538	nspC	carboxynorspermidine decarboxylase	1.71
GSU1729		phenylacetate-CoA ligase	1.70
GSU3072	murF	UDP-N-acetylmuramoylalanyl-D-glutamyl-2,6-diaminopimelate-D-alanyl-D-alanyl ligase	1.70
GSU1900		transporter, putative	1.70
GSU2265	fabZ	(3R)-hydroxymyristoyl-(acyl-carrier-protein) dehydratase	1.70
GSU0582		methyl-accepting chemotaxis protein	1.70
GSU1999	hfq	hfq protein	1.70
GSU0869		LysM domain/NLP/P60 family protein	1.69
GSU1845		conserved hypothetical protein	1.69
GSU2437		conserved hypothetical protein	1.69
GSU2814		rubrerythrin	1.69
GSU2938		conserved hypothetical protein	1.69

GSU2477		radical SAM domain-containing iron-sulfur cluster-binding oxidoreductase	1.69
GSU1606	rpiB	ribose-5-phosphate isomerase B, putative	1.68
GSU3423	tkt	transketolase	1.68
GSU3209		protein of unknown function DUF143	1.68
GSU2549	topA	DNA topoisomerase I	1.68
GSU3117	ssb-2	single-strand binding protein	1.67
GSU3134		conserved hypothetical protein	1.67
GSU1942	capL	UDP-N-acetyl-D-galactosamine 6-dehydrogenase, putative	1.67
GSU0601		glycoside hydrolase, putative	1.67
GSU1667		conserved hypothetical protein	1.67
GSU2569	mnmA	tRNA (5-carboxymethylaminomethyl-2-thio-U34)-thioltransferase	1.66
GSU0865		cell division protein DivIVA, putative	1.66
GSU0505		rhodanese homology domain superfamily protein	1.66
GSU1103		AMP-forming acyl-CoA synthetase	1.66
GSU0352	prx-3	peroxiredoxin, atypical 2-Cys subfamily	1.66
GSU2923	murI	glutamate racemase	1.66
GSU3278		conserved hypothetical protein	1.66
GSU1909	ilvC	ketol-acid reductoisomerase	1.66
GSU1706	panC	pantoate--beta-alanine ligase	1.66
GSU1548		hypothetical protein	1.66
GSU0290	fabH-1	3-oxoacyl-(acyl-carrier-protein) synthase III	1.65
GSU1283		conserved hypothetical protein	1.65
GSU0867	ubiE	ubiquinone/menaquinone biosynthesis methyltransferase UbiE, putative	1.65
GSU0157		lipoprotein, putative	1.65
GSU1778	pulQ	type II secretion system secretin lipoprotein PulQ	1.65
GSU1875	ahcY	S-adenosyl-L-homocysteine hydrolase	1.65
GSU0478		ferritin-like domain protein	1.65

GSU3454		radical SAM domain iron-sulfur cluster-binding oxidoreductase	1.64
GSU1584	bioB	biotin synthetase	1.64
GSU0164		conserved hypothetical protein, truncation	1.64
GSU1679		hypothetical protein	1.64
GSU2781		efflux transporter, RND family, MFP subunit	1.64
GSU3410		conserved hypothetical protein	1.64
GSU2559		exopolyphosphatase	1.64
GSU1589	rbfA	ribosome-binding factor A	1.63
GSU1836	glnB	nitrogen regulatory protein P-II	1.63
GSU0585	ycgM	fumarylacetoacetate hydrolase family protein ycgM	1.63
GSU3094	hisE	phosphoribosyl-ATP pyrophosphohydrolase	1.63
GSU2101		glycerol dehydratase, putative	1.63
GSU0032	grpE	DnaJ adenine nucleotide exchange factor GrpE	1.63
GSU2493		NHL repeat domain protein	1.63
GSU1270	pyrR	pyrimidine operon regulatory protein PyrR; uracil phosphoribosyltransferase	1.63
GSU0648	rplS	ribosomal protein L19	1.62
GSU0345	nuoH-1	NADH dehydrogenase I, H subunit	1.62
GSU2906		conserved hypothetical protein	1.62
GSU1614		CoA-binding protein	1.62
GSU2850	rplP	ribosomal protein L16	1.62
GSU3010	cobU	adenosylcobinamide kinase and adenosylcobinamide phosphate guanylyltransferase	1.62
GSU1066	pilY1-1	type IV pilus tip-associated adhesin	1.61
GSU2008		branched-chain amino acid ABC transporter, ATP-binding protein	1.61
GSU2998		conserved hypothetical protein	1.61
GSU0604	thiC-1	4-amino-5-hydroxymethyl-2-methylpyrimidine synthetase	1.61
GSU0152	argF	ornithine carbamoyltransferase	1.61
GSU2761		FAD-dependent glycerol-3-phosphate dehydrogenase subunit	1.61

GSU1415		response regulator	1.61
GSU0189	dbpA	ATP-dependent RNA helicase DbpA	1.61
GSU2286	eno	enolase	1.60
GSU2572	cysE	serine acetyltransferase	1.60
GSU2718	hoxL	bidirectional NAD-reducing hydrogenase, large subunit	1.60
GSU1708		metal-dependent hydrolase, subgroup D	1.60
GSU1855		polysaccharide chain length determinant domain protein	1.60
GSU2051	paaK-3	phenylacetate-coenzyme A ligase	1.60
GSU0933	upp	uracil phosphoribosyltransferase	1.60
GSU0156	argH	argininosuccinate lyase	1.60
GSU3109		transcriptional regulator, IclR family	1.60
GSU1978	epsI	EpsI family protein	1.59
GSU3457		amino acid-binding ACT domain regulatory protein	1.59
GSU2013		phosphoglucomutase/phosphomannomutase family protein	1.59
GSU0599		sensor histidine kinase	1.59
GSU2383	trpE	anthranilate synthase component I	1.59
GSU2106		conserved hypothetical protein	1.59
GSU2012	nifU	nitrogen fixation iron-sulfur cluster assembly protein NifU	1.59
GSU0361		peptidylprolyl cis-trans isomerase, PpiC-type	1.59
GSU1463	aspS	aspartyl-tRNA synthetase	1.58
GSU2789		sensor histidine kinase, PAS, PAS and PAS domain-containing	1.58
GSU0384		ferritin-like domain protein	1.58
GSU1905		cold shock domain family protein	1.58
GSU1642		ferritin-like domain protein	1.58
GSU3395	putA	proline dehydrogenase/delta-1-pyrroline-5-carboxylate dehydrogenase	1.58
GSU3370		transcriptional regulator, GntR family	1.57
GSU2431	nfeD	NfeD-like membrane-bound serine protease	1.57
GSU1632	purB	adenylosuccinate lyase	1.57
GSU1626		transcriptional regulator, GntR family	1.57

GSU3265		sulfite reductase, assimilatory-type	1.56
GSU1427		anti-anti-sigma factor	1.56
GSU0496		efflux transporter, RND family, MFP subunit	1.56
GSU0283		sensor histidine kinase	1.56
GSU0150	argB	acetylglutamate kinase	1.56
GSU2045	valS	valyl-tRNA synthetase	1.56
GSU2742		conserved hypothetical protein	1.55
GSU1467	korD	2-oxoglutarate:ferredoxin oxidoreductase, ferredoxin subunit	1.55
GSU0153	argG	argininosuccinate synthase	1.55
GSU0099	mglA	cell polarity determinant GTPase MglA	1.55
GSU1432		TPR domain protein	1.55
GSU2029	pilP	type IV pilus assembly lipoprotein PilP, putative	1.55
GSU2625		transcriptional regulator, ArsR family	1.55
GSU1108		aldehyde dehydrogenase family protein	1.55
GSU0312		PilZ domain protein	1.55
GSU0728	ppk-2	polyphosphate kinase	1.55
GSU1222		histone deacetylase family protein	1.54
GSU0322	gspK	type II secretion system protein GspK	1.54
GSU1039		sigma-54 dependent DNA-binding response regulator	1.54
GSU1678	mgtA	cation-transport ATPase, E1-E2 family	1.54
GSU1376		conserved hypothetical protein	1.54
GSU3339	groES	chaperonin GroES	1.54
GSU1637	pyrE	orotate phosphoribosyltransferase	1.53
GSU2255		glycosyl transferase, putative	1.53
GSU3199	cheA-3	chemotaxis sensor histidine kinase CheA	1.53
GSU1769		divergent polysaccharide deacetylase domain protein	1.53
GSU2838	rplO	ribosomal protein L15	1.52
GSU1242	aatA	aspartate aminotransferase	1.52
GSU2426		mcbC-like oxidoreductase for polypeptide thioester cyclization	1.52
GSU2583	ycaC	isochorismatase family protein YcaC	1.52

GSU3306		conserved hypothetical protein	1.52
GSU2698		transcriptional regulator, TetR family	1.51
GSU3367	ispF	2C-methyl-D-erythritol 2,4-cyclodiphosphate synthase	1.51
GSU0617		NHL repeat domain lipoprotein	1.51
GSU0644		RNA-binding KH domain protein, putative	1.51
GSU1810	tilS	tRNA(Ile)-lysidine synthetase	1.51
GSU0212		ABC transporter, ATP-binding protein	1.50
GSU2796	etfA	electron transfer flavoprotein, alpha subunit	1.50
GSU0610	purD	phosphoribosylamine--glycine ligase	1.50
GSU0815		ABC transporter, periplasmic substrate-binding protein, MCE family	1.50
GSU1731	livG	branched-chain amino acid ABC transporter, ATP-binding protein	1.50
GSU2377		conserved hypothetical protein	1.50
GSU2616	secF	protein-export membrane protein SecF	1.50
GSU2028	pilQ	type IV pilus biogenesis protein PilQ	1.50
GSU1860	vorB	2-oxoacid:ferredoxin oxidoreductase, thiamin diphosphate-binding subunit	1.50
GSU2089	mreB	rod shape-determining protein MreB	1.50
GSU2875	rpsI	ribosomal protein S9	1.50

Table B2: Proteins with lower abundance under U(VI) exposure. Δz -score was calculated as follows: (z-score in U treatment - z-score in control).

Locus ID	Symbol	Name	Δz
GSU3206		zinc finger transcriptional regulator, TraR/DksA family	-1.50
GSU3314		lipoprotein, putative	-1.50
GSU3207	gpmI	phosphoglycerate mutase, 2,3-bisphosphoglycerate-independent	-1.50
GSU0810		OmpA domain protein	-1.50
GSU2359		glycoside hydrolase, family 57, DUF3536 domain-containing	-1.50
GSU3062		radical SAM domain iron-sulfur cluster-binding oxidoreductase	-1.50

GSU2861	rpsG	ribosomal protein S7	-1.51
GSU1725	sbcC-2	DNA repair exonuclease SbcCD, C subunit, putative	-1.51
GSU1701		diadenosine polyphosphate hydrolase, FHIT domain-containing	-1.51
GSU1516	infC	translation initiation factor IF-3	-1.51
GSU2362		transcriptional regulator, MarR family	-1.52
GSU0547	mutS-2	DNA mismatch repair ATPase MutS-2	-1.52
GSU2697	acrA	efflux pump, RND family, membrane fusion lipoprotein	-1.52
GSU2424		conserved hypothetical protein	-1.52
GSU1061		aspartate aminotransferase	-1.53
GSU2090		conserved hypothetical protein	-1.53
GSU1521	ihfA-1	integration host factor, alpha subunit	-1.53
GSU2372	mcp028	methyl-accepting chemotaxis sensory transducer, putative	-1.53
GSU2841	rplR	ribosomal protein L18	-1.53
GSU1941		sensor histidine kinase, GAF domain-containing	-1.54
GSU0782	hybS	periplasmically oriented, membrane-bound [NiFe]-hydrogenase small subunit	-1.54
GSU2238	gmk	guanylate kinase	-1.54
GSU2206	rpsT	ribosomal protein S20	-1.54
GSU0233		protein of unknown function DUF480	-1.55
GSU1636	purF	glutamine--phosphoribosylpyrophosphate amidotransferase	-1.55
GSU1886	yfiA	ribosomal subunit interface-associated sigma-54 modulation protein	-1.55
GSU2461		conserved hypothetical protein	-1.55
GSU1110	ndk	nucleoside diphosphate kinase	-1.56
GSU0452		sensor histidine kinase	-1.56
GSU3319	ppiA	cytosolic peptidylprolyl cis-trans isomerase, cyclophilin A-like	-1.56
GSU0913	uup	DNA-binding ATPase Uup	-1.57
GSU3059		radical SAM domain iron-sulfur cluster-binding oxidoreductase	-1.57
GSU0921		ribonuclease, Rne/Rng family protein	-1.57
GSU2665		efflux pump, RND family, membrane fusion lipoprotein	-1.57

GSU2004	ubiD-2	UbiD family decarboxylase	-1.57
GSU2846	rplX	ribosomal protein L24	-1.57
GSU1839		phosphatase/phosphohexomutase-related hydrolase	-1.57
GSU2853	rpsS	ribosomal protein S19	-1.57
GSU0023		TPR domain protein	-1.58
GSU1932		SPOR domain protein	-1.58
GSU1337		lipoprotein, putative	-1.58
GSU1743		lipoprotein, putative	-1.58
GSU0169		ABC transporter, ATP-binding protein	-1.58
GSU1345		transcriptional regulator, Rrf2 family	-1.58
GSU1496	pilA	geopilin	-1.58
GSU0108		ATP synthase F0, B subunit, putative	-1.59
GSU2207	holA	DNA polymerase III, delta subunit	-1.59
GSU0894		peptidyl-prolyl cis-trans isomerase, cyclophilin-type	-1.59
GSU0310		phospholipase, patatin family, putative	-1.59
GSU1469	korB	2-oxoglutarate:ferredoxin oxidoreductase, thiamin diphosphate-binding subunit	-1.59
GSU1861	vorA	2-oxoacid:ferredoxin oxidoreductase, alpha subunit	-1.59
GSU1873	pepF	oligoendopeptidase F	-1.59
GSU1479		conserved hypothetical protein	-1.60
GSU2413		ABC transporter, ATP-binding protein	-1.60
GSU2921	metH	5-methyltetrahydrofolate--homocysteine methyltransferase	-1.60
GSU2602	ihfB-2	DNA-binding protein HU	-1.60
GSU0027		ExbD/TolR-related biopolymer transport membrane protein	-1.60
GSU0145	recA	recA protein	-1.60
GSU0442	mqnC-1	dehypoxanthinylfuralosine cyclase, putative	-1.60
GSU1594		zinc-dependent peptidase, PqqL family	-1.61
GSU0771		zinc-dependent oxidoreductase	-1.61
GSU2788		OsmC family protein	-1.62

GSU3092	yqeY	uncharacterized protein YqeY	-1.62
GSU1000		conserved hypothetical protein	-1.62
GSU1868		cysteine desulfurase family protein	-1.62
GSU1790	loN-2	ATP-dependent protease La	-1.62
GSU0803	ppsA	phosphoenolpyruvate synthase	-1.62
GSU2087	gmhA	D-sedoheptulose-7-phosphate isomerase	-1.63
GSU1319		sensor histidine kinase	-1.63
GSU3099	hisC	histidinol-phosphate aminotransferase	-1.63
GSU2973		lipoprotein, putative	-1.63
GSU1278		protein of unknown function DUF1858	-1.63
GSU3405		amino acid ABC transporter, permease protein	-1.63
GSU2248		conserved hypothetical protein	-1.63
GSU2195	guaB	inosine-5-monophosphate dehydrogenase	-1.64
GSU2521	yedF	selenium metabolism protein YedF, putative	-1.64
GSU3111		conserved hypothetical protein	-1.64
GSU0388		conserved hypothetical protein	-1.64
GSU3132	hup	histone-like protein	-1.64
GSU0824		conserved hypothetical protein	-1.64
GSU3095	hisF	imidazoleglycerol phosphate synthase, cyclase subunit	-1.64
GSU1519	pheS	phenylalanyl-tRNA synthetase, alpha subunit	-1.64
GSU1866		PhoH-related ATPase	-1.65
GSU2183		Fic family protein	-1.65
GSU2074		peptidylprolyl cis-trans isomerase, PpiC-type	-1.65
GSU2957	trx-2	thioredoxin family protein	-1.65
GSU1920	tsf	translation elongation factor Ts	-1.65
GSU2191		aldehyde ferredoxin oxidoreductase, tungsten-containing	-1.65
GSU2353		conserved hypothetical protein	-1.66
GSU1106	gltA	citrate synthase	-1.66
GSU2743		cytochrome c, 1 heme-binding site	-1.66
GSU1828		chorismate mutase	-1.66

GSU1002		YcaC-related hydrolase, putative	-1.66
GSU0654	thiF-1	thiamin biosynthesis thiocarboxylate synthase	-1.66
GSU0443		ribonuclease D, putative	-1.66
GSU2603	rpsA	ribosomal protein S1	-1.67
GSU0570		SAM-dependent methyltransferase, type 11	-1.67
GSU1782	pulM	type II secretion system ATPase PulM, putative	-1.67
GSU1311	pgi	glucose-6-phosphate isomerase	-1.67
GSU1468	korA	2-oxoglutarate:ferredoxin oxidoreductase, alpha subunit	-1.68
GSU2842	rplF	ribosomal protein L6	-1.69
GSU2737	OmcB	polyheme membrane-associated cytochrome c	-1.69
GSU1901		conserved hypothetical protein	-1.69
GSU1975		NAD-dependent epimerase/dehydratase family protein	-1.69
GSU2285		membrane-associated metal-dependent phosphohydrolase, HDc domain-containing	-1.70
GSU0102	selB	selenocysteine-specific translation elongation factor	-1.70
GSU1911	ilvB	acetolactate synthase, large subunit, biosynthetic type	-1.71
GSU0915		conserved hypothetical protein	-1.71
GSU1254		hypothetical protein	-1.71
GSU2270	lolE	lipoprotein release ABC transporter, membrane protein	-1.71
GSU2833	rpsK	ribosomal protein S11	-1.72
GSU0949		efflux transporter, RND family, MFP subunit	-1.72
GSU0542		diguanylate cyclase	-1.73
GSU0643	rpsP	ribosomal protein S16	-1.73
GSU1199		nuclease, putative	-1.74
GSU3213	obgE	ribosome biogenesis GTPase ObgE	-1.74
GSU2939		porin, putative	-1.74
GSU0111	atpA	ATP synthase F1, alpha subunit	-1.74
GSU2435	aceF	pyruvate dehydrogenase complex, E2 protein, dihydrolipoamide acetyltransferase	-1.74
GSU1754	kamA	L-lysine 2,3-aminomutase	-1.74

GSU1772	ctpA-2	periplasmic carboxy-terminal processing protease lipoprotein	-1.75
GSU2813	ccpA	cytochrome c peroxidase, 2 heme-binding sites	-1.75
GSU0859	galU	UTP-glucose-1-phosphate uridylyltransferase	-1.75
GSU3190		twin-arginine translocation protein, TatA/E family	-1.75
GSU1304	mcp025	methyl-accepting chemotaxis sensory transducer	-1.75
GSU2360		maltooligosyltrehalose synthase, putative	-1.76
GSU1609		efflux pump, RND family, outer membrane protein	-1.76
GSU2273		conserved hypothetical protein	-1.76
GSU0115	pdxA	4-hydroxythreonine-4-phosphate dehydrogenase	-1.76
GSU3139		protein of unknown function DUF399	-1.76
GSU0816		organic solvent tolerance ABC transporter, ATP-binding protein	-1.76
GSU0355		conserved hypothetical protein	-1.76
GSU1321	trx-1	TlpA family-related protein disulfide reductase lipoprotein	-1.76
GSU3376		response receiver-modulated diguanylate cyclase	-1.77
GSU0488	trxB	thioredoxin reductase	-1.78
GSU0376	gcvH-1	glycine cleavage system H protein	-1.78
GSU1802	yjeF	YjeF-related putative carbohydrate kinase	-1.78
GSU3194	thiL	thiamine monophosphate kinase	-1.79
GSU3013	engB	GTPase EngB	-1.79
GSU1060		conserved hypothetical protein	-1.79
GSU1844		IPT/TIG domain protein, putative	-1.79
GSU2184	ccaC	cytidine-specific tRNA nucleotidyltransferase	-1.79
GSU2019	accC	acetyl-CoA carboxylase, biotin carboxylase	-1.80
GSU1981		conserved hypothetical protein	-1.80
GSU2502		spermine/spermidine synthase family protein	-1.80
GSU2335	usp-4	universal stress protein Usp	-1.81
GSU2835	map	methionine aminopeptidase, type I	-1.81
GSU2187		ABC transporter, permease protein	-1.81

Table B3: Δz -score of proteins involved in protein fate. Δz -score was calculated as follows: (z-score in U treatment - z-score in control).

Locus ID	Symbol	Name	Category	Δz
GSU2869	secE	preprotein translocase, SecE subunit	Protein fate, Protein and peptide secretion and trafficking	1.73
GSU1778	pulQ	type II secretion system secretin lipoprotein PulQ	Protein fate, Protein and peptide secretion and trafficking	1.65
GSU0032	grpE	DnaJ adenine nucleotide exchange factor GrpE	Protein fate, Protein folding and stabilization	1.63
GSU0322	gspK	type II secretion system protein GspK	Protein fate, Protein and peptide secretion and trafficking	1.54
GSU3339	groES	chaperonin GroES	Protein fate, Protein folding and stabilization	1.54
GSU2616	secF	protein-export membrane protein SecF	Protein fate, Protein and peptide secretion and trafficking	1.50
GSU2433		ATP-dependent protease, putative	Protein fate, Degradation of proteins, peptides, and glycopeptides	1.48
GSU2410		heat shock protein, Hsp20 family	Protein fate, Protein folding and stabilization	1.43
GSU2075		subtilisin	Protein fate, Degradation of proteins, peptides, and glycopeptides	1.42
GSU1865		metalloendopeptidase, putative, glycoprotease family	Protein fate, Degradation of proteins, peptides, and	1.29

			glycopeptides	
GSU1791	clpX	ATP-dependent Clp protease, ATP-binding subunit ClpX	Protein fate, Degradation of proteins, peptides, and glycopeptides	1.26
GSU1627	secG	preprotein translocase, SecG subunit	Protein fate, Protein and peptide secretion and trafficking	1.22
GSU2617	secD	protein-export membrane protein SecD	Protein fate, Protein and peptide secretion and trafficking	1.12
GSU1437		peptidase, M48 family	Protein fate, Degradation of proteins, peptides, and glycopeptides	1.12
GSU2021	pepQ-2	xaa-pro dipeptidase	Protein fate, Degradation of proteins, peptides, and glycopeptides	1.12
GSU1792	clpP	ATP-dependent Clp protease, proteolytic subunit ClpP	Protein fate, Degradation of proteins, peptides, and glycopeptides	1.10
GSU0969	ctpA-1	carboxy-terminal processing protease	Protein fate, Degradation of proteins, peptides, and glycopeptides	1.05
GSU0823	ppiC	peptidyl-prolyl cis-trans isomerase C	Protein fate, Protein folding and stabilization	1.04
GSU3348		chaperonin, 33 kDa family	Protein fate, Protein folding and stabilization	0.95
GSU2060		pmbA protein, putative	Protein fate, Protein modification and repair	0.91
GSU2390	htpG	heat shock protein HtpG	Protein fate, Protein folding and stabilization	0.90

GSU0928		peptidase, M16 family	Protein fate, Degradation of proteins, peptides, and glycopeptides	0.90
GSU0332	pepA	aminopeptidase A/I	Protein fate, Degradation of proteins, peptides, and glycopeptides	0.75
GSU0321		general secretion pathway protein L, putative	Protein fate, Protein and peptide secretion and trafficking	0.68
GSU0328	gspE	general secretion pathway protein E	Protein fate, Protein and peptide secretion and trafficking	0.68
GSU0080	degQ	protease degQ	Protein fate, Degradation of proteins, peptides, and glycopeptides	0.57
GSU1132	ftsY	signal recognition particle-docking protein FtsY	Protein fate, Protein and peptide secretion and trafficking	0.56
GSU0330		general secretion pathway protein C, putative	Protein fate, Protein and peptide secretion and trafficking	0.52
GSU0228		peptidyl-prolyl cis-trans isomerase, FKBP-type, putative	Protein fate, Protein folding and stabilization	0.40
GSU0129	def-1	polypeptide deformylase	Protein fate, Protein modification and repair	0.28
GSU3135	lspA	signal peptidase II	Protein fate, Protein and peptide secretion and trafficking	0.26
GSU0306	hypF	hydrogenase maturation protein HypF	Protein fate, Protein modification and repair	0.25
GSU2618		preprotein translocase, YajC	Protein fate, Protein and	0.21

		subunit	peptide secretion and trafficking	
GSU3193	loN-3	ATP-dependent protease La	Protein fate, Degradation of proteins, peptides, and glycopeptides	0.12
GSU1914		membrane-associated zinc metalloprotease, putative	Protein fate, Degradation of proteins, peptides, and glycopeptides	0.09
GSU2837	secY	preprotein translocase, SecY subunit	Protein fate, Protein and peptide secretion and trafficking	0.05
GSU0383		peptidyl-prolyl cis-trans isomerase, FKBP-type	Protein fate, Protein folding and stabilization	0.01
GSU0923	loN-1	ATP-dependent protease La	Protein fate, Degradation of proteins, peptides, and glycopeptides	-0.11
GSU0305	hypB	hydrogenase accessory protein HypB	Protein fate, Protein folding and stabilization	-0.14
GSU2050	secA	preprotein translocase, SecA subunit	Protein fate, Protein and peptide secretion and trafficking	-0.40
GSU2823		HlyD family secretion protein	Protein fate, Protein and peptide secretion and trafficking	-0.51
GSU1267	lepB	signal peptidase I	Protein fate, Protein and peptide secretion and trafficking	-0.52
GSU1524	pcM	protein-L-isoaspartate O-methyltransferase	Protein fate, Protein modification and repair	-0.61
GSU0304	pepN	aminopeptidase N	Protein fate, Degradation of proteins, peptides, and	-0.64

			glycopeptides	
GSU0034	dnaJ	chaperone protein dnaJ	Protein fate, Protein folding and stabilization	-1.07
GSU1610		efflux transporter, RND family, MFP subunit	Protein fate, Protein and peptide secretion and trafficking	-1.08
GSU0927		peptidase, M16 family	Protein fate, Degradation of proteins, peptides, and glycopeptides	-1.08
GSU0658	clpB	ClpB protein	Protein fate, Degradation of proteins, peptides, and glycopeptides	-1.14
GSU0856		peptidase, M48 family	Protein fate, Degradation of proteins, peptides, and glycopeptides	-1.16
GSU0308	hypD	hydrogenase expression/formation protein HypD	Protein fate, Protein folding and stabilization	-1.21
GSU0538		heat shock protein, Hsp20 family	Protein fate, Protein folding and stabilization	-1.22
GSU0642	ffH	signal recognition particle protein	Protein fate, Protein and peptide secretion and trafficking	-1.23
GSU3203		outer membrane lipoprotein carrier protein LolA, putative	Protein fate, Protein and peptide secretion and trafficking	-1.24
GSU3456	def-2	polypeptide deformylase	Protein fate, Protein modification and repair	-1.24
GSU1793	tig	trigger factor	Protein fate, Protein and peptide secretion and trafficking	-1.30

GSU0786		hydrogenase maturation protease	Protein fate, Protein modification and repair	-1.34
GSU3340	groEL	60 kDa chaperonin	Protein fate, Protein folding and stabilization	-1.35
GSU3347		peptidase, U32 family	Protein fate, Degradation of proteins, peptides, and glycopeptides	-1.38
GSU1105	pepQ-1	xaa-pro dipeptidase	Protein fate, Degradation of proteins, peptides, and glycopeptides	-1.44
GSU0033	dnaK	chaperone protein dnaK	Protein fate, Protein folding and stabilization	-1.45
GSU0329		general secretion pathway protein D, putative	Protein fate, Protein and peptide secretion and trafficking	-1.48
GSU3319	ppiA	cytosolic peptidylprolyl cis-trans isomerase, cyclophilin A-like	Protein fate, Protein folding and stabilization	-1.56
GSU0894		peptidyl-prolyl cis-trans isomerase, cyclophilin-type	Protein fate, Protein folding and stabilization	-1.59
GSU1873	pepF	oligoendopeptidase F	Protein fate, Degradation of proteins, peptides, and glycopeptides	-1.59
GSU1594		zinc-dependent peptidase, PqqL family	Protein fate, Degradation of proteins, peptides, and glycopeptides	-1.61
GSU1790	loN-2	ATP-dependent protease La	Protein fate, Degradation of proteins, peptides, and glycopeptides	-1.62
GSU1772	ctpA-2	periplasmic carboxy-terminal processing protease lipoprotein	Protein fate, Degradation of proteins, peptides, and glycopeptides	-1.75

GSU3190		twin-arginine translocation protein, TatA/E family	Protein fate, Protein and peptide secretion and trafficking	-1.75
GSU2835	map	methionine aminopeptidase, type I	Protein fate, Protein modification and repair	-1.81

Table B4: Δz -score of proteins involved in nucleotide and nucleoside metabolism. Δz -score was calculated as follows: (z-score in U treatment - z-score in control)

Locus ID	Symbol	Name	Category	Δz
GSU1919	pyrH	uridylate kinase	Purines, pyrimidines, nucleosides, and nucleotides, Nucleotide and nucleoside interconversions	1.79
GSU0483	queC	7-cyano-7-deazaguanine synthase	Purines, pyrimidines, nucleosides, and nucleotides	1.73
GSU0933	upp	uracil phosphoribosyltransferase	Purines, pyrimidines, nucleosides, and nucleotides, Salvage of nucleosides and nucleotides	1.60
GSU1632	purB	adenylosuccinate lyase	Purines, pyrimidines, nucleosides, and nucleotides, Purine ribonucleotide biosynthesis	1.57
GSU1637	pyrE	orotate phosphoribosyltransferase	Purines, pyrimidines, nucleosides, and nucleotides, Pyrimidine ribonucleotide biosynthesis	1.53

GSU0610	purD	phosphoribosylamine--glycine ligase	Purines, pyrimidines, nucleosides, and nucleotides, Purine ribonucleotide biosynthesis	1.50
GSU3308	purA	adenylosuccinate synthetase	Purines, pyrimidines, nucleosides, and nucleotides, Purine ribonucleotide biosynthesis	1.41
GSU2091	purC	phosphoribosylaminoimidazole-succinocarboxamide synthase	Purines, pyrimidines, nucleosides, and nucleotides, Purine ribonucleotide biosynthesis	1.40
GSU1272	pyrC	dihydroorotase, multifunctional complex type	Purines, pyrimidines, nucleosides, and nucleotides, Pyrimidine ribonucleotide biosynthesis	1.32
GSU2605	cmk	cytidylate kinase	Purines, pyrimidines, nucleosides, and nucleotides, Nucleotide and nucleoside interconversions	1.26
GSU3058		dihydroorotate dehydrogenase, electron transfer subunit, putative	Purines, pyrimidines, nucleosides, and nucleotides, Pyrimidine ribonucleotide biosynthesis	1.18
GSU1756		dihydroorotate dehydrogenase, electron transfer subunit, putative	Purines, pyrimidines, nucleosides, and nucleotides, Pyrimidine ribonucleotide biosynthesis	1.16
GSU1526	apt	adenine phosphoribosyltransferase	Purines, pyrimidines, nucleosides, and	1.11

			nucleotides, Salvage of nucleosides and nucleotides	
GSU3106	thyX	thymidylate synthase, flavin-dependent	Purines, pyrimidines, nucleosides, and nucleotides, 2'-Deoxyribonucleotide metabolism	0.88
GSU1271	pyrB	aspartate carbamoyltransferase	Purines, pyrimidines, nucleosides, and nucleotides, Pyrimidine ribonucleotide biosynthesis	0.83
GSU1755	pyrD	dihydroorotate dehydrogenase	Purines, pyrimidines, nucleosides, and nucleotides, Pyrimidine ribonucleotide biosynthesis	0.41
GSU0611	purE-1	phosphoribosylaminoimidazole carboxylase, catalytic subunit	Purines, pyrimidines, nucleosides, and nucleotides, Purine ribonucleotide biosynthesis	0.26
GSU2194	guaA	GMP synthase	Purines, pyrimidines, nucleosides, and nucleotides, Purine ribonucleotide biosynthesis	0.18
GSU0609	purH	phosphoribosylaminoimidazolecarboxamide formyltransferase/IMP cyclohydrolase	Purines, pyrimidines, nucleosides, and nucleotides, Purine ribonucleotide biosynthesis	0.18
GSU1634		phosphoribosylformylglycinamide synthase II, putative	Purines, pyrimidines, nucleosides, and nucleotides, Purine	0.06

			ribonucleotide biosynthesis	
GSU1112	mtaP	methylthioadenosine phosphorylase	Purines, pyrimidines, nucleosides, and nucleotides, Salvage of nucleosides and nucleotides	0.05
GSU1017		hypoxanthine phosphoribosyltransferase, putative	Purines, pyrimidines, nucleosides, and nucleotides, Salvage of nucleosides and nucleotides	0.04
GSU1895	pyrG	CTP synthase	Purines, pyrimidines, nucleosides, and nucleotides, Pyrimidine ribonucleotide biosynthesis	-0.16
GSU1273	carA	carbamoyl-phosphate synthase, small subunit	Purines, pyrimidines, nucleosides, and nucleotides, Pyrimidine ribonucleotide biosynthesis	-0.31
GSU1276	carB	carbamoyl-phosphate synthase, large subunit	Purines, pyrimidines, nucleosides, and nucleotides, Pyrimidine ribonucleotide biosynthesis	-0.45
GSU1461	pyrF	orotidine 5'-phosphate decarboxylase	Purines, pyrimidines, nucleosides, and nucleotides, Pyrimidine ribonucleotide biosynthesis	-0.47
GSU1759	purN	phosphoribosylglycinamide formyltransferase	Purines, pyrimidines, nucleosides, and nucleotides, Purine ribonucleotide biosynthesis	-0.48

GSU1758	purM	phosphoribosylformylglycinamide cyclo-ligase	Purines, pyrimidines, nucleosides, and nucleotides, Purine ribonucleotide biosynthesis	-0.93
GSU1871		ribonucleoside-diphosphate reductase, putative	Purines, pyrimidines, nucleosides, and nucleotides, 2'-Deoxyribonucleotide metabolism	-1.08
GSU2306	purE-2	phosphoribosylaminoimidazole carboxylase, catalytic subunit	Purines, pyrimidines, nucleosides, and nucleotides, Purine ribonucleotide biosynthesis	-1.27
GSU1635		phosphoribosylformylglycinamide synthase I, putative	Purines, pyrimidines, nucleosides, and nucleotides, Purine ribonucleotide biosynthesis	-1.32
GSU2836	adk	adenylate kinase	Purines, pyrimidines, nucleosides, and nucleotides, Nucleotide and nucleoside interconversions	-1.40
GSU0661	prsA	ribose-phosphate pyrophosphokinase	Purines, pyrimidines, nucleosides, and nucleotides, Purine ribonucleotide biosynthesis	-1.49
GSU2238	gmk	guanylate kinase	Purines, pyrimidines, nucleosides, and nucleotides, Nucleotide and nucleoside interconversions	-1.54

GSU1636	purF	glutamine-- phosphoribosylpyrophosphate amidotransferase	Purines, pyrimidines, nucleosides, and nucleotides, Purine ribonucleotide biosynthesis	-1.55
GSU1110	ndk	nucleoside diphosphate kinase	Purines, pyrimidines, nucleosides, and nucleotides, Nucleotide and nucleoside interconversions	-1.56
GSU2195	guaB	inosine-5-monophosphate dehydrogenase	Purines, pyrimidines, nucleosides, and nucleotides, Purine ribonucleotide biosynthesis	-1.64

Table B5: Δz -score of proteins involved in biosynthesis of cofactors. Δz -score was calculated as follows: (z-score in U treatment - z-score in control)

Locus ID	Symbol	Name	Category	Dz
GSU1459	ispG	4-hydroxy-3-methylbut-2-en-1-yl diphosphate synthase	Biosynthesis of cofactors, prosthetic groups, and carriers, Other	1.71
GSU1827	nadB	L-aspartate oxidase	Biosynthesis of cofactors, prosthetic groups, and carriers, Pyridine nucleotides	1.71
GSU1942	capL	UDP-N-acetyl-D-galactosamine 6- dehydrogenase, putative	Biosynthesis and degradation of surface polysaccharides and lipopolysaccharides	1.67
GSU1706	panC	pantoate--beta-alanine ligase	Biosynthesis of cofactors, prosthetic groups, and carriers, Pantothenate and	1.66

			coenzyme A	
GSU0867	ubiE	ubiquinone/menaquinone biosynthesis methyltransferase UbiE, putative	Biosynthesis of cofactors, prosthetic groups, and carriers, Menaquinone and ubiquinone	1.65
GSU1584	bioB	biotin synthetase	Biosynthesis of cofactors, prosthetic groups, and carriers, Biotin	1.64
GSU3010	cobU	adenosylcobinamide kinase and adenosylcobinamide phosphate guanylyltransferase	Biosynthesis of cofactors, prosthetic groups, and carriers, Heme, porphyrin, and cobalamin	1.62
GSU0604	thiC-1	4-amino-5-hydroxymethyl-2-methylpyrimidine synthetase	Biosynthesis of cofactors, prosthetic groups, and carriers, Thiamine	1.61
GSU2051	paaK-3	phenylacetate-coenzyme A ligase	Biosynthesis of cofactors, prosthetic groups, and carriers, Menaquinone and ubiquinone	1.60
GSU3367	ispF	2C-methyl-D-erythritol 2,4-cyclodiphosphate synthase	Biosynthesis of cofactors, prosthetic groups, and carriers, Other	1.51
GSU1577	cobO	cob(I)alamin adenosyltransferase	Biosynthesis of cofactors, prosthetic groups, and carriers, Heme, porphyrin, and cobalamin	1.49
GSU0588	thiG	thiamine biosynthesis protein ThiG	Biosynthesis of cofactors, prosthetic groups, and carriers, Thiamine	1.43
GSU1691	ribE	6,7-dimethyl-8-ribityllumazine synthase	Biosynthesis of cofactors, prosthetic groups, and	1.41

			carriers, Riboflavin, FMN, and FAD	
GSU2264	lpxA	acyl-(acyl-carrier-protein)--UDP-N-acetylglucosamine O-acyltransferase	Biosynthesis and degradation of surface polysaccharides and lipopolysaccharides	1.40
GSU2289		nicotinate phosphoribosyltransferase, putative	Biosynthesis of cofactors, prosthetic groups, and carriers, Pyridine nucleotides	1.31
GSU2995	cobI	precorrin-2 C20-methyltransferase	Biosynthesis of cofactors, prosthetic groups, and carriers, Heme, porphyrin, and cobalamin	1.31
GSU2241		capsular polysaccharide biosynthesis protein I	Biosynthesis and degradation of surface polysaccharides and lipopolysaccharides	1.25
GSU2011		cysteine desulfurase	Biosynthesis of cofactors, prosthetic groups, and carriers, Other	1.18
GSU1815		NAD-dependent epimerase/dehydratase family protein	Biosynthesis and degradation of surface polysaccharides and lipopolysaccharides	1.17
GSU2256		ADP-heptose--LPS heptosyltransferase II, putative	Biosynthesis and degradation of surface polysaccharides and lipopolysaccharides	1.13
GSU0021	nadA	quinolinate synthetase complex, subunit A	Biosynthesis of cofactors, prosthetic groups, and	1.06

			carriers, Pyridine nucleotides	
GSU2261	lpxB	lipid A disaccharide synthase (lpxB)	Biosynthesis and degradation of surface polysaccharides and lipopolysaccharides	1.01
GSU2996	cobL	precorrin-6y c5,15-methyltransferase	Biosynthesis of cofactors, prosthetic groups, and carriers, Heme, porphyrin, and cobalamin	0.98
GSU0135	hemB	delta-aminolevulinic acid dehydratase	Biosynthesis of cofactors, prosthetic groups, and carriers, Heme, porphyrin, and cobalamin	0.97
GSU0660	ispE	4-diphosphocytidyl-2C-methyl-D-erythritol kinase	Biosynthesis of cofactors, prosthetic groups, and carriers, Other	0.95
GSU1243	coaD	pantetheine-phosphate adenylyltransferase	Biosynthesis of cofactors, prosthetic groups, and carriers, Pantothenate and coenzyme A	0.95
GSU1764	dxs-2	deoxyxylulose-5-phosphate synthase	Biosynthesis of cofactors, prosthetic groups, and carriers, Other	0.93
GSU1720		6-pyruvoyl tetrahydrobiopterin synthase family protein	Biosynthesis of cofactors, prosthetic groups, and carriers, Other	0.91
GSU0337	hemL	glutamate-1-semialdehyde-2,1-aminomutase	Biosynthesis of cofactors, prosthetic groups, and carriers, Heme, porphyrin, and cobalamin	0.88

GSU1896	kdsB	3-deoxy-D-manno-octulosonate cytidyltransferase	Biosynthesis and degradation of surface polysaccharides and lipopolysaccharides	0.84
GSU3460		glycosyl transferase, group 2 family protein	Biosynthesis and degradation of surface polysaccharides and lipopolysaccharides	0.79
GSU0012	hemG	protoporphyrinogen oxidase	Biosynthesis of cofactors, prosthetic groups, and carriers, Heme, porphyrin, and cobalamin	0.79
GSU1804	pdxJ	pyridoxal phosphate biosynthetic protein PdxJ	Biosynthesis of cofactors, prosthetic groups, and carriers, Pyridoxine	0.75
GSU1202		mannose-1-phosphate guanylyltransferase/mannose-6- phosphate isomerase, truncation	Biosynthesis and degradation of surface polysaccharides and lipopolysaccharides	0.73
GSU1915	dxr	1-deoxy-D-xylulose 5-phosphate reductoisomerase	Biosynthesis of cofactors, prosthetic groups, and carriers, Other	0.66
GSU0862	fold-2	fold bifunctional protein	Biosynthesis of cofactors, prosthetic groups, and carriers, Folic acid	0.66
GSU2705	moaB	molybdenum cofactor biosynthesis protein B	Biosynthesis of cofactors, prosthetic groups, and carriers, Molybdopterin	0.65
GSU1317	ispB	octaprenyl-diphosphate synthase	Biosynthesis of cofactors, prosthetic groups, and carriers, Menaquinone and	0.60

			ubiquinone	
GSU0440		3-octaprenyl-4-hydroxybenzoate carboxy-lyase, putative	Biosynthesis of cofactors, prosthetic groups, and carriers, Menaquinone and ubiquinone	0.57
GSU2254		glycosyl transferase, group 2 family protein	Biosynthesis and degradation of surface polysaccharides and lipopolysaccharides	0.46
GSU0626	gmd	GDP-mannose 4,6-dehydratase	Biosynthesis and degradation of surface polysaccharides and lipopolysaccharides	0.46
GSU3286		uroporphyrinogen III synthase/methyltransferase	Biosynthesis of cofactors, prosthetic groups, and carriers, Heme, porphyrin, and cobalamin	0.43
GSU3285	hemC	porphobilinogen deaminase	Biosynthesis of cofactors, prosthetic groups, and carriers, Heme, porphyrin, and cobalamin	0.20
GSU3453	hemE	uroporphyrinogen decarboxylase	Biosynthesis of cofactors, prosthetic groups, and carriers, Heme, porphyrin, and cobalamin	0.20
GSU1894	kdsA	2-dehydro-3- deoxyphosphooctonate aldolase	Biosynthesis and degradation of surface polysaccharides and lipopolysaccharides	0.06
GSU1681		cobyrinic acid a,c-diamide synthase family protein	Biosynthesis of cofactors, prosthetic groups, and	0.05

			carriers, Heme, porphyrin, and cobalamin	
GSU1124	coaBC	phosphopantothenoylcysteine decarboxylase/phosphopantothenate--cysteine ligase	Biosynthesis of cofactors, prosthetic groups, and carriers, Pantothenate and coenzyme A	-0.02
GSU1977		glycosyl transferase, group 2 family protein	Biosynthesis and degradation of surface polysaccharides and lipopolysaccharides	-0.05
GSU1970		polysaccharide biosynthesis protein, putative	Biosynthesis and degradation of surface polysaccharides and lipopolysaccharides	-0.05
GSU3368	ispD	4-diphosphocytidyl-2C-methyl-D-erythritol synthase	Biosynthesis of cofactors, prosthetic groups, and carriers, Other	-0.10
GSU0885		cobyrinic acid a,c-diamide synthase family protein	Biosynthesis of cofactors, prosthetic groups, and carriers, Heme, porphyrin, and cobalamin	-0.10
GSU3284	hemA	glutamyl-tRNA reductase	Biosynthesis of cofactors, prosthetic groups, and carriers, Heme, porphyrin, and cobalamin	-0.11
GSU2992	cobJQ	precorrin-3B C17-methyltransferase/cobyrinic acid synthase	Biosynthesis of cofactors, prosthetic groups, and carriers, Heme, porphyrin, and cobalamin	-0.17
GSU0999		acyl-(acyl-carrier-protein)--UDP-N-acetylglucosamine O-	Biosynthesis and degradation of surface	-0.26

		acyltransferase, putative	polysaccharides and lipopolysaccharides	
GSU3009	cobT	nicotinate-nucleotide--dimethylbenzimidazole phosphoribosyltransferase	Biosynthesis of cofactors, prosthetic groups, and carriers, Heme, porphyrin, and cobalamin	-0.35
GSU3312	hemH	ferrochelatase	Biosynthesis of cofactors, prosthetic groups, and carriers, Heme, porphyrin, and cobalamin	-0.36
GSU2259		3-deoxy-D-manno-octulosonic-acid transferase, putative	Biosynthesis and degradation of surface polysaccharides and lipopolysaccharides	-0.42
GSU2083	rfaA	glucose-1-phosphate thymidyltransferase	Biosynthesis and degradation of surface polysaccharides and lipopolysaccharides	-0.49
GSU3006	cobB	cobyrinic acid a,c-diamide synthase	Biosynthesis of cofactors, prosthetic groups, and carriers, Heme, porphyrin, and cobalamin	-0.49
GSU0686	dxs-1	deoxyxylulose-5-phosphate synthase	Biosynthesis of cofactors, prosthetic groups, and carriers, Other	-0.49
GSU2704	moaC	molybdenum cofactor biosynthesis protein MoaC	Biosynthesis of cofactors, prosthetic groups, and carriers, Molybdopterin	-0.68
GSU3005	thiC-2	thiamine biosynthesis protein ThiC	Biosynthesis of cofactors, prosthetic groups, and carriers, Thiamine	-0.70

GSU1985		outer membrane protein, putative	Biosynthesis and degradation of surface polysaccharides and lipopolysaccharides	-0.70
GSU1816	ugd	UDP-glucose 6-dehydrogenase	Biosynthesis and degradation of surface polysaccharides and lipopolysaccharides	-0.70
GSU1854		UDP-glucose/GDP-mannose dehydrogenase family protein	Biosynthesis and degradation of surface polysaccharides and lipopolysaccharides	-0.78
GSU2337		glycosyl transferase, group 20 family protein	Biosynthesis and degradation of surface polysaccharides and lipopolysaccharides	-0.81
GSU1690	ribA	3,4-dihydroxy-2-butanone 4-phosphate synthase/GTP cyclohydrolase II	Biosynthesis of cofactors, prosthetic groups, and carriers, Riboflavin, FMN, and FAD	-0.82
GSU2243		UDP-N-acetylglucosamine 2-epimerase	Biosynthesis and degradation of surface polysaccharides and lipopolysaccharides	-0.83
GSU2570		cysteine desulfurase	Biosynthesis of cofactors, prosthetic groups, and carriers, Other	-0.83
GSU2085		ADP-heptose synthase	Biosynthesis and degradation of surface polysaccharides and lipopolysaccharides	-0.89

GSU1484		soluble lytic murein transglycosylase, putative	Biosynthesis and degradation of surface polysaccharides and lipopolysaccharides	-0.96
GSU0605		thiamine-phosphate pyrophosphorylase/phosphomethyl pyrimidine kinase	Biosynthesis of cofactors, prosthetic groups, and carriers, Thiamine	-0.98
GSU0074	elbB	enhancing lycopene biosynthesis protein 2	Biosynthesis of cofactors, prosthetic groups, and carriers, Other	-1.02
GSU0652	nadE	NAD ⁺ synthetase	Biosynthesis of cofactors, prosthetic groups, and carriers, Pyridine nucleotides	-1.06
GSU1983		polysaccharide biosynthesis protein, putative	Biosynthesis and degradation of surface polysaccharides and lipopolysaccharides	-1.07
GSU1088		ubiquinone biosynthesis protein AarF, putative	Biosynthesis of cofactors, prosthetic groups, and carriers, Menaquinone and ubiquinone	-1.09
GSU2999	cobH	precorrin-8X methylmutase	Biosynthesis of cofactors, prosthetic groups, and carriers, Heme, porphyrin, and cobalamin	-1.10
GSU3023		glycosyl transferase, group 1/2 family protein	Biosynthesis and degradation of surface polysaccharides and lipopolysaccharides	-1.16
GSU3004		cobalamin biosynthesis protein	Biosynthesis of cofactors,	-1.21

		CbiM	prosthetic groups, and carriers, Heme, porphyrin, and cobalamin	
GSU1936	nadC	nicotinate-nucleotide pyrophosphorylase	Biosynthesis of cofactors, prosthetic groups, and carriers, Pyridine nucleotides	-1.21
GSU2366	rfbB	dTDP-glucose 4,6-dehydratase	Biosynthesis and degradation of surface polysaccharides and lipopolysaccharides	-1.41
GSU2266	lpxD	UDP-3-O-3-hydroxymyristoyl glucosamine N-acyltransferase	Biosynthesis and degradation of surface polysaccharides and lipopolysaccharides	-1.42
GSU1765		geranyltranstransferase	Biosynthesis of cofactors, prosthetic groups, and carriers, Menaquinone and ubiquinone	-1.47
GSU2004	ubiD-2	UbiD family decarboxylase	Biosynthesis of cofactors, prosthetic groups, and carriers, Menaquinone and ubiquinone	-1.57
GSU2087	gmhA	D-sedoheptulose-7-phosphate isomerase	Biosynthesis and degradation of surface polysaccharides and lipopolysaccharides	-1.63
GSU0859	galU	UTP-glucose-1-phosphate uridylyltransferase	Biosynthesis and degradation of surface polysaccharides and lipopolysaccharides	-1.75

GSU2360		maltooligosyltrehalose synthase, putative	Biosynthesis and degradation of surface polysaccharides and lipopolysaccharides	-1.76
GSU0115	pdxA	4-hydroxythreonine-4-phosphate dehydrogenase	Biosynthesis of cofactors, prosthetic groups, and carriers, Pyridoxine	-1.76
GSU3194	thiL	thiamine monophosphate kinase	Biosynthesis of cofactors, prosthetic groups, and carriers, Thiamine	-1.79

Table B6: Δz -score of proteins involved in regulatory functions. Δz -score was calculated as follows: (z-score in U treatment - z-score in control)

Locus ID	Symbol	Name	Category	Dz
GSU3292		transcriptional regulator, Fur family	Regulatory functions, DNA interactions	1.79
GSU0106		chromosome partitioning ATPase Soj	Regulatory functions, Other	1.79
GSU2980	nikR	nickel-binding domain transcriptional regulator	Regulatory functions, DNA interactions	1.78
GSU2666		transcriptional regulator, TetR family	Regulatory functions, DNA interactions	1.77
GSU1117		response regulator	Regulatory functions, Protein interactions	1.71
GSU0008		response receiver sensor histidine kinase, PAS domain-containing	Signal transduction, Two-component systems	1.71
GSU1999	hfq	hfq protein	Regulatory functions, Other	1.70
GSU1836	glnB	nitrogen regulatory protein P-II	Regulatory functions,	1.63

			Protein interactions	
GSU1270	pyrR	pyrimidine operon regulatory protein PyrR; uracil phosphoribosyltransferase	Regulatory functions, Other	1.63
GSU1415		response regulator	Signal transduction, Two-component systems	1.61
GSU3109		transcriptional regulator, IclR family	Regulatory functions, DNA interactions	1.60
GSU3457		amino acid-binding ACT domain regulatory protein	Regulatory functions, Other	1.59
GSU0599		sensor histidine kinase	Regulatory functions, Protein interactions	1.59
GSU2789		sensor histidine kinase, PAS, PAS and PAS domain-containing	Signal transduction, Two-component systems	1.58
GSU3370		transcriptional regulator, GntR family	Regulatory functions, DNA interactions	1.57
GSU1626		transcriptional regulator, GntR family	Regulatory functions, DNA interactions	1.57
GSU1427		anti-anti-sigma factor	Regulatory functions, Protein interactions	1.56
GSU0283		sensor histidine kinase, GAF and GAF domain-containing, nonconserved putative heme-binding site	Signal transduction, Two-component systems	1.56
GSU2625		transcriptional regulator, ArsR family	Regulatory functions, DNA interactions	1.55
GSU1039		sigma-54 dependent DNA-binding response regulator	Signal transduction, Two-component systems	1.54
GSU2698		transcriptional regulator, TetR family	Regulatory functions, DNA interactions	1.51

GSU2815		sensory box histidine kinase	Signal transduction, Two-component systems	1.48
GSU0939		nitrogen regulatory protein P-II, putative	Regulatory functions, Protein interactions	1.44
GSU1414		sensory box histidine kinase/response regulator	Signal transduction, Two-component systems	1.43
GSU1379	fur	ferric uptake regulation protein Fur	Regulatory functions, DNA interactions	1.42
GSU3253		response regulator	Signal transduction, Two-component systems	1.37
GSU1891		response regulator	Signal transduction, Two-component systems	1.18
GSU2816		sensory box histidine kinase/response regulator	Signal transduction, Two-component systems	1.16
GSU0514		transcriptional regulator, IclR family	Regulatory functions, DNA interactions	1.16
GSU2475		sigma-54 dependent transcriptional regulator	Regulatory functions, Protein interactions	1.13
GSU1940		sigma-54 dependent DNA-binding response regulator	Signal transduction, Two-component systems	1.08
GSU0366		transcriptional regulator, putative	Regulatory functions, Other	1.08
GSU3261		response regulator	Signal transduction, Two-component systems	0.82
GSU0682		DNA-binding response regulator, LuxR family	Regulatory functions, DNA interactions	0.79
GSU3363		sigma-54 dependent transcriptional regulator, Fis family	Regulatory functions, Protein interactions	0.79
GSU2483	kdpD	sensor histidine kinase KdpD	Signal transduction, Two-component systems	0.78

GSU3437		sensory box histidine kinase	Signal transduction, Two-component systems	0.67
GSU0735		PTS system IIA component, fructose subfamily	Signal transduction, PTS	0.60
GSU1220		response regulator	Regulatory functions, Protein interactions	0.58
GSU2354		transcriptional regulator, IclR family	Regulatory functions, DNA interactions	0.50
GSU2915		sigma-54 dependent DNA-binding response regulator	Regulatory functions, Protein interactions	0.45
GSU2225		GTP-binding protein Era, putative	Regulatory functions, RNA interactions	0.42
GSU1927		sensory box/response regulator	Signal transduction, Two-component systems	0.41
GSU2287		response regulator	Regulatory functions, Protein interactions	0.40
GSU0881		sensor histidine kinase	Regulatory functions, Protein interactions	0.34
GSU3421		transcriptional regulator, Crp/Fnr family	Regulatory functions, DNA interactions	0.33
GSU1116		GAF domain protein, putative	Regulatory functions, Other	0.32
GSU0732		nucleoside diphosphate kinase regulator protein, putative	Regulatory functions, Other	0.15
GSU2226	era	GTP-binding protein Era	Regulatory functions, RNA interactions	0.12
GSU1658		response regulator/GGDEF domain protein	Signal transduction, Two-component systems	0.10
GSU0149		sensor histidine kinase/response regulator	Signal transduction, Two-component systems	0.10

GSU1129		sigma-54 dependent DNA-binding response regulator	Signal transduction, Two-component systems	0.10
GSU0811	ntrX	nitrogen regulation protein NtrX	Regulatory functions, Other	0.08
GSU0842		sensory box histidine kinase/response regulator	Signal transduction, Two-component systems	0.07
GSU0009		sensory box histidine kinase	Regulatory functions, Small molecule interactions	-0.01
GSU0841		sigma-54 dependent DNA-binding response regulator	Signal transduction, Two-component systems	-0.02
GSU3127		transcriptional regulator, AraC family	Regulatory functions, DNA interactions	-0.05
GSU2219		response regulator	Signal transduction, Two-component systems	-0.18
GSU1320		sigma-54 dependent DNA-binding response regulator	Signal transduction, Two-component systems	-0.21
GSU2991		sensor histidine kinase	Regulatory functions, Protein interactions	-0.22
GSU1655		sensory box histidine kinase/response regulator	Regulatory functions, Small molecule interactions	-0.25
GSU1003	ntrC	nitrogen regulation protein NR(I)	Regulatory functions, DNA interactions	-0.31
GSU0896	tldD	tldD protein	Regulatory functions, Other	-0.33
GSU0303		sensory box protein	Regulatory functions, Small molecule interactions	-0.35
GSU1928		sensor histidine kinase/response	Signal transduction, Two-	-0.57

		regulator	component systems	
GSU0963		sigma-54 dependent DNA-binding response regulator	Signal transduction, Two-component systems	-0.61
GSU1863		transcriptional regulator, Ros/MucR family	Regulatory functions, DNA interactions	-0.64
GSU2262	degT	pleiotropic regulatory protein	Regulatory functions, Other	-0.66
GSU2523		transcriptional regulator, LysR family	Regulatory functions, DNA interactions	-0.67
GSU1119		sensor histidine kinase/response regulator	Signal transduction, Two-component systems	-0.69
GSU1495		sigma-54 dependent DNA-binding response regulator	Signal transduction, Two-component systems	-0.75
GSU1934		transcriptional activator, putative, Baf family	Regulatory functions, DNA interactions	-0.76
GSU0776		sigma-54 dependent DNA-binding response regulator	Signal transduction, Two-component systems	-0.78
GSU3138		sensor histidine kinase/response regulator	Signal transduction, Two-component systems	-0.79
GSU1654		response regulator, putative	Signal transduction, Two-component systems	-0.93
GSU0284	dksA	dnaK suppressor protein	Regulatory functions, DNA interactions	-0.93
GSU0598		sigma-54 dependent DNA-binding response regulator	Regulatory functions, DNA interactions	-0.95
GSU1579		LAO/AO transport system ATPase	Regulatory functions, Protein interactions	-0.95
GSU2947		sensor histidine kinase	Signal transduction, Two-component systems	-0.97
GSU1250		sigma-54 dependent DNA-binding	Signal transduction, Two-	-0.98

		response regulator	component systems	
GSU3087		transcriptional regulator, Sir2 family	Regulatory functions, DNA interactions	-1.05
GSU2046		response regulator	Regulatory functions, Protein interactions	-1.26
GSU2016		sensory box/GGDEF family protein	Regulatory functions, Small molecule interactions	-1.29
GSU1316		response regulator	Signal transduction, Two-component systems	-1.32
GSU1004		sensory box histidine kinase	Regulatory functions, Small molecule interactions	-1.35
GSU1120		response regulator	Regulatory functions, Protein interactions	-1.37
GSU0451		DNA-binding response regulator	Signal transduction, Two-component systems	-1.46
GSU3206		zinc finger transcriptional regulator, TraR/DksA family	Regulatory functions, DNA interactions	-1.50
GSU2362		transcriptional regulator, MarR family	Regulatory functions, DNA interactions	-1.52
GSU1941		sensor histidine kinase, GAF domain-containing	Signal transduction, Two-component systems	-1.54
GSU0452		sensor histidine kinase	Signal transduction, Two-component systems	-1.56
GSU1319		sensor histidine kinase	Regulatory functions, Protein interactions	-1.63

Table B7: Δz -score of hypothetical proteins. Δz -score was calculated as follows: (z-score in U treatment - z-score in control)

Locus ID	Name	Category	Δz
GSU3318		conserved hypothetical protein	1.80
GSU0987		conserved hypothetical protein	1.79
GSU0983		phage-related baseplate assembly protein, putative	1.78
GSU2038	pilY1-2	type IV pilus tip-associated adhesin	1.78
GSU0990		hypothetical protein	1.77
GSU0672		conserved hypothetical protein	1.77
GSU1328		protein of unknown function DUF1255	1.76
GSU2441		conserved hypothetical protein	1.76
GSU1845		conserved hypothetical protein	1.69
GSU2437		conserved hypothetical protein	1.69
GSU2938		conserved hypothetical protein	1.69
GSU3134		conserved hypothetical protein	1.67
GSU1667		conserved hypothetical protein	1.67
GSU3278		conserved hypothetical protein	1.66
GSU1548		hypothetical protein	1.66
GSU1283		conserved hypothetical protein	1.65
GSU0478		ferritin-like domain protein	1.65
GSU0164		conserved hypothetical protein, truncation	1.64
GSU1679		hypothetical protein	1.64
GSU3410		conserved hypothetical protein	1.64
GSU2906		conserved hypothetical protein	1.62
GSU1066	pilY1-1	type IV pilus tip-associated adhesin	1.61
GSU2106		conserved hypothetical protein	1.59
GSU0384		ferritin-like domain protein	1.58
GSU1642		ferritin-like domain protein	1.58
GSU2742		conserved hypothetical protein	1.55
GSU0312		PilZ domain protein	1.55

GSU1376		conserved hypothetical protein	1.54
GSU2255		glycosyl transferase, putative	1.53
GSU1769		divergent polysaccharide deacetylase domain protein	1.53
GSU2426		mcbC-like oxidoreductase for polypeptide thioester cyclization	1.52
GSU3306		conserved hypothetical protein	1.52
GSU2377		conserved hypothetical protein	1.50
GSU0905.1		cold shock DNA/RNA-binding protein	1.49
GSU0141		conserved hypothetical protein	1.47
GSU2647		nucleoside diphosphate sugar epimerase	1.47
GSU2332		conserved hypothetical protein	1.47
GSU3289		ferritin-like domain protein	1.45
GSU0061		conserved hypothetical protein	1.44
GSU0973		conserved hypothetical protein	1.44
GSU1565		conserved hypothetical protein	1.40
GSU0195		protein of unknown function DUF1458	1.39
GSU0302		conserved hypothetical protein	1.38
GSU0086.1		hypothetical	1.37
GSU2713		conserved hypothetical protein	1.37
GSU0511		leucyl aminopeptidase-related protein	1.31
GSU1771		putative DNA/RNA-binding protein	1.30
GSU2564		conserved hypothetical protein	1.25
GSU1971		hypothetical protein	1.25
GSU2639		conserved hypothetical protein	1.24
GSU2710		conserved hypothetical protein	1.22
GSU2298		conserved hypothetical protein	1.21
GSU1872		conserved hypothetical protein	1.19
GSU2970		conserved hypothetical protein	1.15
GSU1969		hypothetical protein	1.12

GSU3403	OmpJ-related porin	1.10
GSU2733	conserved hypothetical protein	1.09
GSU2793	conserved hypothetical protein	1.04
GSU0716	conserved hypothetical protein	1.02
GSU1087	conserved hypothetical protein	1.00
GSU3293	ferritin-like domain protein	0.92
GSU0320	conserved hypothetical protein	0.91
GSU2107	hypothetical protein	0.89
GSU1947	hypothetical protein	0.89
GSU2251	hypothetical protein	0.87
GSU2750	conserved domain protein	0.82
GSU3309	conserved hypothetical protein	0.79
GSU0715	conserved hypothetical protein	0.79
GSU0868	DUF147 domain protein	0.79
GSU0790	conserved hypothetical protein	0.75
GSU2528	conserved hypothetical protein	0.68
GSU1252	multicopper oxidase with phosphopantotheine attachment site	0.63
GSU0874	conserved hypothetical protein	0.61
GSU0005	conserved hypothetical protein	0.60
GSU3185	hypothetical protein	0.59
GSU2276	protein of unknown function DUF1015	0.58
GSU3086	N6-adenine-specific DNA methylase, N12 class	0.56
GSU0540	conserved hypothetical protein	0.54
GSU2002	conserved hypothetical protein	0.50
GSU3085	conserved hypothetical protein	0.47
GSU2035	conserved hypothetical protein	0.42
GSU2500	YVTN family beta-propeller domain protein	0.40
GSU0481	conserved hypothetical protein	0.35
GSU2440	conserved hypothetical protein	0.30
GSU2048	conserved hypothetical protein	0.30

GSU1385		conserved hypothetical protein	0.21
GSU2108		conserved hypothetical protein	0.19
GSU1585		protein of unknown function DUF150	0.16
GSU2644		conserved hypothetical protein	0.16
GSU2747		conserved hypothetical protein	0.14
GSU3351		conserved hypothetical protein	0.13
GSU1263		conserved hypothetical protein	0.11
GSU1876		conserved hypothetical protein	0.07
GSU3105		conserved hypothetical protein	0.06
GSU0165		conserved hypothetical protein, truncation	0.04
GSU3003		conserved hypothetical protein	0.03
GSU2427		conserved hypothetical protein	0.03
GSU1938		conserved hypothetical protein	-0.01
GSU3344		conserved hypothetical protein	-0.02
GSU0476		protein of unknown function DUF185	-0.05
GSU2239		YicC family stress-induced protein TIGR00255	-0.10
GSU2922		conserved hypothetical protein	-0.10
GSU2886.			
1		cytochrome c, 7 heme-binding sites	-0.20
GSU0083		protein of unknown function YfiH (DUF152)	-0.21
GSU3362		conserved hypothetical protein	-0.26
GSU1247		conserved hypothetical protein	-0.27
GSU3358		conserved hypothetical protein	-0.29
GSU0450		protein of unknown function DUF299	-0.34
GSU1333		conserved hypothetical protein	-0.38
GSU1046		conserved hypothetical protein	-0.39
GSU1472		PATAN domain protein	-0.40
GSU2017		periplasmic solute-binding protein	-0.40
GSU2105		predicted ATP-dependent Lon-type protease COG4930	-0.42
GSU2682		conserved hypothetical protein	-0.47

GSU2200		conserved hypothetical protein	-0.49
GSU2347		conserved hypothetical protein	-0.49
GSU2082		putative epimerase	-0.50
GSU1181		conserved hypothetical protein	-0.50
GSU0319		conserved hypothetical protein	-0.51
GSU3243		conserved hypothetical protein	-0.52
GSU2780		conserved hypothetical protein	-0.54
GSU2086		conserved hypothetical protein	-0.57
GSU0934		conserved hypothetical protein	-0.65
GSU1497		conserved hypothetical protein	-0.68
GSU2469		hypothetical protein	-0.70
GSU0849		conserved hypothetical protein	-0.70
GSU3204		protein of unknown function DUF520	-0.71
GSU3301	tmk-2	thymidylate kinase, putative	-0.75
GSU0536		ATP alpha-hydrolase TIGR00268	-0.78
GSU0564		conserved hypothetical protein	-0.79
GSU1850		hypothetical protein	-0.83
GSU0714		hypothetical protein	-0.83
GSU2047		beta-lactamase family protein	-0.84
GSU3275		conserved hypothetical protein	-0.85
GSU1079		hypothetical protein	-0.92
GSU1151		YdjC-like protein	-0.98
GSU1884		P-loop-containing kinase	-1.02
GSU1212		conserved hypothetical protein	-1.04
GSU2496		conserved hypothetical protein	-1.06
GSU1829		conserved hypothetical protein	-1.07
GSU0382		conserved hypothetical protein	-1.08
GSU2405		hypothetical protein	-1.10
GSU3244		conserved hypothetical protein	-1.13
GSU1167		conserved hypothetical protein	-1.14

GSU0882		periplasmic/secreted protein DUF534	-1.14
GSU1073		conserved hypothetical protein	-1.15
GSU3144		conserved hypothetical protein	-1.16
GSU3341	prkA	putative serine protein kinase	-1.19
GSU0737		conserved hypothetical protein	-1.19
GSU3305		conserved hypothetical protein	-1.20
GSU0317		conserved hypothetical protein	-1.22
GSU0081		conserved hypothetical protein	-1.23
GSU1357		conserved hypothetical protein	-1.23
GSU3337		conserved hypothetical protein	-1.24
GSU1360		Sir2 superfamily protein	-1.24
GSU2146		conserved hypothetical protein	-1.25
GSU1282		putative porin	-1.25
GSU0133		conserved hypothetical protein	-1.26
GSU2726		conserved hypothetical protein	-1.28
GSU2193		ferritin-like domain protein	-1.28
GSU0680		DUF748 repeat protein	-1.30
GSU1889	yhbN	conserved hypothetical protein	-1.30
GSU3402		conserved hypothetical protein	-1.31
GSU2675		C1 peptidase family protein	-1.32
GSU0850		protein disulfide bond isomerase, DsbC/DsbG-like	-1.35
GSU0095		conserved hypothetical protein	-1.37
GSU0977		conserved hypothetical protein	-1.43
GSU2518		conserved hypothetical protein	-1.44
GSU1436		conserved hypothetical protein	-1.45
GSU2359		glycoside hydrolase, family 57, DUF3536 domain-containing	-1.50
GSU2424		conserved hypothetical protein	-1.52
GSU2090		conserved hypothetical protein	-1.53
GSU0233		protein of unknown function DUF480	-1.55
GSU2461		conserved hypothetical protein	-1.55

GSU1932		SPOR domain protein	-1.58
GSU1337		lipoprotein, putative	-1.58
GSU0310		phospholipase, patatin family, putative	-1.59
GSU1479		conserved hypothetical protein	-1.60
GSU2788		OsmC family protein	-1.62
GSU1000		conserved hypothetical protein	-1.62
GSU1278		protein of unknown function DUF1858	-1.63
GSU2248		conserved hypothetical protein	-1.63
GSU2521	yedF	selenium metabolism protein YedF, putative	-1.64
GSU3111		conserved hypothetical protein	-1.64
GSU0388		conserved hypothetical protein	-1.64
GSU0824		conserved hypothetical protein	-1.64
GSU2353		conserved hypothetical protein	-1.66
GSU0570		SAM-dependent methyltransferase, type 11	-1.67
GSU1782	pulM	type II secretion system ATPase PulM, putative	-1.67
GSU1901		conserved hypothetical protein	-1.69
GSU0915		conserved hypothetical protein	-1.71
GSU1254		hypothetical protein	-1.71
GSU2273		conserved hypothetical protein	-1.76
GSU3139		protein of unknown function DUF399	-1.76
GSU0355		conserved hypothetical protein	-1.76
GSU1060		conserved hypothetical protein	-1.79
GSU1981		conserved hypothetical protein	-1.80
GSU2998		conserved hypothetical protein	1.61

Table B8: Δz -score of proteins involved in transport. Δz -score was calculated as follows:

(z-score in U treatment - z-score in control)

Locus ID	Symbol	Name	Category	Δz
GSU1482		efflux pump, RND family,	Transport and binding	1.81

		outer membrane protein	proteins, Unknown substrate	
GSU0720		superoxide reductase	Transport and binding proteins, Cations and iron carrying compounds	1.78
GSU2700	tupA	tungstate ABC transporter, periplasmic tungstate-binding protein, putative	Transport and binding proteins, Anions	1.77
GSU2695		efflux pump, RND family, outer membrane protein	Transport and binding proteins, Unknown substrate	1.77
GSU0689	hpnN	efflux pump, RND superfamily, putative	Transport and binding proteins, Cations and iron carrying compounds	1.75
GSU1230		ABC transporter, periplasmic substrate-binding protein	Transport and binding proteins, Unknown substrate	1.72
GSU0800		amino acid ABC transporter, periplasmic amino acid-binding protein	Transport and binding proteins, Amino acids, peptides and amines	1.71
GSU2136		efflux pump, RND family, membrane fusion protein	Transport and binding proteins, Cations and iron carrying compounds	1.71
GSU1900		transporter, putative	Transport and binding proteins, Unknown substrate	1.70
GSU2781		efflux transporter, RND family, MFP subunit	Transport and binding proteins, Unknown substrate	1.64
GSU2008		branched-chain amino acid ABC transporter, ATP-binding protein	Transport and binding proteins, Amino acids, peptides and amines	1.61
GSU1855		polysaccharide chain length determinant domain protein	Transport and binding proteins, Other	1.60
GSU1978	epsI	EpsI family protein	Transport and binding	1.59

			proteins, Unknown substrate	
GSU0496		efflux transporter, RND family, MFP subunit	Transport and binding proteins, Unknown substrate	1.56
GSU1678	mgtA	cation-transport ATPase, E1-E2 family	Transport and binding proteins, Cations and iron carrying compounds	1.54
GSU0212		ABC transporter, ATP-binding protein	Transport and binding proteins, Unknown substrate	1.50
GSU0815		ABC transporter, periplasmic substrate-binding protein, MCE family	Transport and binding proteins, Unknown substrate	1.50
GSU1731	livG	branched-chain amino acid ABC transporter, ATP-binding protein	Transport and binding proteins, Amino acids, peptides and amines	1.50
GSU1332		heavy metal efflux pump, CzcA family	Transport and binding proteins, Cations and iron carrying compounds	1.49
GSU1557		mechanosensitive ion channel family protein	Transport and binding proteins, Unknown substrate	1.45
GSU2260		ABC transporter, ATP-binding protein, MsbA family	Transport and binding proteins, Other	1.43
GSU2351		cation-transport ATPase, E1-E2 family	Transport and binding proteins, Cations and iron carrying compounds	1.42
GSU2452		copper-translocating P-type ATPase	Transport and binding proteins, Cations and iron carrying compounds	1.38
GSU3322	corA-2	magnesium and cobalt transport protein CorA	Transport and binding proteins, Cations and iron carrying compounds	1.35

GSU1775	ftsE	cell division ATP-binding protein FtsE	Transport and binding proteins, Unknown substrate	1.33
GSU1307	ftn	ferritin	Transport and binding proteins, Cations and iron carrying compounds	1.29
GSU1481		multidrug resistance protein, putative	Transport and binding proteins, Other	1.29
GSU1331		efflux transporter, RND family, MFP subunit	Transport and binding proteins, Unknown substrate	1.27
GSU3401		branched-chain amino acid ABC transporter, periplasmic amino acid-binding protein, putative	Transport and binding proteins, Amino acids, peptides and amines	1.26
GSU1165	ptsP	phosphoenolpyruvate-protein phosphotransferase PtsP	Transport and binding proteins, Carbohydrates, organic alcohols, and acids	1.25
GSU1330		metal ion efflux outer membrane protein family protein, putative	Transport and binding proteins, Cations and iron carrying compounds	1.03
GSU3392		branched-chain amino acid ABC transporter, ATP-binding protein	Transport and binding proteins, Amino acids, peptides and amines	0.71
GSU3291		V-type H(+)-translocating pyrophosphatase	Transport and binding proteins, Cations and iron carrying compounds	0.68
GSU1883		PTS system, IIA component, putative	Transport and binding proteins, Carbohydrates, organic alcohols, and acids	0.61
GSU2055		extracellular solute-binding protein, family 7	Transport and binding proteins, Unknown substrate	0.60
GSU0814		outer membrane efflux protein,	Transport and binding	0.55

		putative	proteins, Unknown substrate	
GSU2982		TonB dependent receptor, putative	Transport and binding proteins, Unknown substrate	0.42
GSU1644		ABC transporter, ATP-binding protein	Transport and binding proteins, Unknown substrate	0.42
GSU1501		ABC transporter, ATP-binding protein	Transport and binding proteins, Unknown substrate	0.34
GSU1888		ABC transporter, ATP-binding protein	Transport and binding proteins, Unknown substrate	0.31
GSU0025		tolB protein	Transport and binding proteins, Other	0.26
GSU2352		sodium/solute symporter family protein	Transport and binding proteins, Unknown substrate	0.12
GSU2951		ABC transporter, ATP-binding protein	Transport and binding proteins, Unknown substrate	-0.02
GSU0940		ammonium transporter	Transport and binding proteins, Cations and iron carrying compounds	-0.03
GSU0391		Outer membrane efflux family protein	Transport and binding proteins, Unknown substrate	-0.04
GSU2649		amino acid ABC transporter, amino acid-binding protein	Transport and binding proteins, Amino acids, peptides and amines	-0.04
GSU2985		ABC transporter, ATP-binding protein	Transport and binding proteins, Unknown substrate	-0.16
GSU3406		amino acid ABC transporter, periplasmic amino acid- binding protein	Transport and binding proteins, Amino acids, peptides and amines	-0.19
GSU1730	livF	branched-chain amino acid ABC transporter, ATP-binding	Transport and binding proteins, Amino acids,	-0.21

		protein	peptides and amines	
GSU1341		ABC transporter, ATP-binding protein	Transport and binding proteins, Unknown substrate	-0.21
GSU1162		ABC transporter, ATP-binding protein	Transport and binding proteins, Unknown substrate	-0.21
GSU3391		branched-chain amino acid ABC transporter, ATP-binding protein	Transport and binding proteins, Amino acids, peptides and amines	-0.22
GSU1346	cysP	sulfate ABC transporter, periplasmic sulfate-binding protein	Transport and binding proteins, Anions	-0.23
GSU0210		ABC transporter, permease protein, putative	Transport and binding proteins, Unknown substrate	-0.30
GSU1068		sodium/solute symporter family protein	Transport and binding proteins, Unknown substrate	-0.36
GSU2696		AcrB/AcrD/AcrF family protein	Transport and binding proteins, Other	-0.38
GSU1261		ABC transporter, ATP-binding protein	Transport and binding proteins, Unknown substrate	-0.42
GSU1016		potassium uptake protein, Trk family	Transport and binding proteins, Cations and iron carrying compounds	-0.45
GSU1349	cysA	sulfate ABC transporter, ATP-binding protein	Transport and binding proteins, Anions	-0.57
GSU1445		TonB-dependent receptor, putative	Transport and binding proteins, Cations and iron carrying compounds	-0.60
GSU2751	dcuB	C4-dicarboxylate transporter, anaerobic	Transport and binding proteins, Carbohydrates, organic alcohols, and acids	-0.76

GSU3304		LamB porin family protein, putative	Transport and binding proteins, Porins	-0.81
GSU0028	tolQ	tolQ protein	Transport and binding proteins, Other	-0.88
GSU2782		AcrB/AcrD/AcrF family protein	Transport and binding proteins, Other	-0.91
GSU1735		branched-chain amino acid ABC transporter, periplasmic amino acid-binding protein, putative	Transport and binding proteins, Amino acids, peptides and amines	-0.98
GSU3404		amino acid ABC transporter, ATP-binding protein	Transport and binding proteins, Amino acids, peptides and amines	-1.01
GSU2651		amino acid ABC transporter, ATP-binding protein	Transport and binding proteins, Amino acids, peptides and amines	-1.02
GSU1885	hprK	HPr(Ser) kinase/phosphatase	Transport and binding proteins, Carbohydrates, organic alcohols, and acids	-1.12
GSU1734		branched-chain amino acid ABC transporter, periplasmic amino acid-binding protein, putative	Transport and binding proteins, Amino acids, peptides and amines	-1.13
GSU0392		efflux transporter, RND family, MFP subunit	Transport and binding proteins, Unknown substrate	-1.14
GSU0883		ferric enterobactin receptor, putative	Transport and binding proteins, Cations and iron carrying compounds	-1.16
GSU2005		branched-chain amino acid ABC transporter, periplasmic amino acid-binding protein,	Transport and binding proteins, Amino acids, peptides and amines	-1.16

		putative		
GSU1161		efflux transporter, RND family, MFP subunit	Transport and binding proteins, Unknown substrate	-1.20
GSU0922		ABC transporter, ATP-binding protein	Transport and binding proteins, Unknown substrate	-1.24
GSU1340		ABC transporter, permease protein	Transport and binding proteins, Unknown substrate	-1.28
GSU1070		sodium/solute symporter family protein	Transport and binding proteins, Unknown substrate	-1.32
GSU1578		B12-binding protein	Transport and binding proteins, Other	-1.45
GSU0813		organic solvent tolerance ABC transporter periplasmic protein	Transport and binding proteins, Unknown substrate	-1.49
GSU2697	acrA	efflux pump, RND family, membrane fusion lipoprotein	Transport and binding proteins, Other	-1.52
GSU0913	uup	DNA-binding ATPase Uup	Transport and binding proteins, Unknown substrate	-1.57
GSU2665		efflux pump, RND family, membrane fusion lipoprotein	Transport and binding proteins, Unknown substrate	-1.57
GSU0169		ABC transporter, ATP-binding protein	Transport and binding proteins, Unknown substrate	-1.58
GSU2413		ABC transporter, ATP-binding protein	Transport and binding proteins, Unknown substrate	-1.60
GSU0027		ExbD/TolR-related biopolymer transport membrane protein	Transport and binding proteins, Cations and iron carrying compounds	-1.60
GSU3405		amino acid ABC transporter, permease protein	Transport and binding proteins, Amino acids, peptides and amines	-1.63
GSU2270	lolE	lipoprotein release ABC	Transport and binding	-1.71

		transporter, membrane protein	proteins, Unknown substrate	
GSU0949		efflux transporter, RND family, MFP subunit	Transport and binding proteins, Unknown substrate	-1.72
GSU2939		porin, putative	Transport and binding proteins, Porins	-1.74
GSU1609		efflux pump, RND family, outer membrane protein	Transport and binding proteins, Unknown substrate	-1.76
GSU0816		organic solvent tolerance ABC transporter, ATP-binding protein	Transport and binding proteins, Unknown substrate	-1.76
GSU2187		ABC transporter, permease protein	Transport and binding proteins, Unknown substrate	-1.81

Table B9: Δz -score of proteins involved in energy metabolism. Δz -score was calculated as follows: (z-score in U treatment - z-score in control)

Locus ID	Symbol	Name	Category	Δz
GSU1737	paaK-2	phenylacetate-CoA ligase	Energy metabolism, Other	1.81
GSU3246	prx-2	peroxiredoxin, typical 2-Cys subfamily	Energy metabolism, Electron transport	1.80
GSU1155		glutaredoxin family protein	Energy metabolism, Electron transport	1.77
GSU0357		cytochrome c family protein	Energy metabolism, Electron transport	1.74
GSU3296	glcD-1	D-lactate/glycolate dehydrogenase, FAD-binding protein, putative	Energy metabolism, Other	1.74
GSU1648	macC	cytochrome c, 5 heme-binding sites	Energy metabolism, Electron transport	1.73
GSU2801		cytochrome c, 5 heme-binding	Energy metabolism, Electron	1.72

		sites	transport	
GSU1089		iron-sulfur cluster-binding protein	Energy metabolism, Electron transport	1.72
GSU0783		nickel-dependent hydrogenase, iron-sulfur cluster-binding protein	Energy metabolism, Electron transport	1.71
GSU1729		phenylacetate-CoA ligase	Energy metabolism, Other	1.70
GSU2814		rubrerythrin	Energy metabolism, Electron transport	1.69
GSU1606	rpiB	ribose-5-phosphate isomerase B, putative	Energy metabolism, Pentose phosphate pathway	1.68
GSU3423	tkt	transketolase	Energy metabolism, Pentose phosphate pathway	1.68
GSU0601		glycoside hydrolase, putative	Energy metabolism, Biosynthesis and degradation of polysaccharides	1.67
GSU2101		glycerol dehydratase, putative	Energy metabolism, Fermentation	1.63
GSU0345	nuoH-1	NADH dehydrogenase I, H subunit	Energy metabolism, Electron transport	1.62
GSU2761		FAD-dependent glycerol-3-phosphate dehydrogenase subunit	Energy metabolism, Other	1.61
GSU2286	eno	enolase	Energy metabolism, Glycolysis/gluconeogenesis	1.60
GSU2718	hoxL	bidirectional NAD-reducing hydrogenase, large subunit	Energy metabolism, Electron transport	1.60
GSU2013		phosphoglucomutase/phosphomannomutase family protein	Energy metabolism, Sugars	1.59
GSU3395	putA	proline dehydrogenase/delta-1-	Energy metabolism, Amino	1.58

		pyrroline-5-carboxylate dehydrogenase	acids and amines	
GSU1467	korD	2-oxoglutarate:ferredoxin oxidoreductase, ferredoxin subunit	Energy metabolism, Electron transport	1.55
GSU1108		aldehyde dehydrogenase family protein	Energy metabolism, Fermentation	1.55
GSU0728	ppk-2	polyphosphate kinase	Energy metabolism, Other	1.55
GSU2796	etfA	electron transfer flavoprotein, alpha subunit	Energy metabolism, Electron transport	1.50
GSU1860	vorB	2-oxoacid:ferredoxin oxidoreductase, thiamin diphosphate-binding subunit	Energy metabolism, Fermentation	1.50
GSU0088		heterodisulfide reductase subunit	Energy metabolism, Electron transport	1.48
GSU2192	cbbZ	phosphoglycolate phosphatase	Energy metabolism, Sugars	1.48
GSU2052		indolepyruvate ferredoxin oxidoreductase, beta subunit, putative	Energy metabolism, Fermentation	1.47
GSU2240	galE	UDP-glucose 4-epimerase	Energy metabolism, Sugars	1.47
GSU1707		group II decarboxylase	Energy metabolism, Amino acids and amines	1.44
GSU0804	WrbA	trp repressor binding protein WrbA	Energy metabolism, Electron transport	1.44
GSU3238		Rieske 2Fe-2S family protein	Energy metabolism, Electron transport	1.43
GSU0089		heterodisulfide reductase subunit	Energy metabolism, Electron transport	1.43
GSU2201		cytochrome c family protein	Energy metabolism, Electron transport	1.42

GSU1859		keto/oxoacid ferredoxin oxidoreductase, gamma subunit	Energy metabolism, Fermentation	1.41
GSU2811	hsc	cytochrome c Hsc	Energy metabolism, Electron transport	1.38
GSU2645		cytochrome c family protein	Energy metabolism, Electron transport	1.37
GSU0375	gcvT	glycine cleavage system T protein	Energy metabolism, Amino acids and amines	1.34
GSU3294		rubredoxin-oxygen oxidoreductase, putative	Energy metabolism, Electron transport	1.30
GSU3302		methylmalonyl-CoA mutase, putative	Energy metabolism, Fermentation	1.30
GSU0385		NADH dehydrogenase subunit, putative	Energy metabolism, Electron transport	1.29
GSU0122		nickel-dependent hydrogenase, large subunit	Energy metabolism, Electron transport	1.27
GSU3374	rpe	ribulose-phosphate 3-epimerase	Energy metabolism, Pentose phosphate pathway	1.25
GSU1334		cytochrome c family protein	Energy metabolism, Electron transport	1.25
GSU1305		Glu/Leu/Phe/Val dehydrogenase family protein	Energy metabolism, Amino acids and amines	1.25
GSU2053		indolepyruvate ferredoxin oxidoreductase, alpha subunit, putative	Energy metabolism, Fermentation	1.24
GSU3321		phosphoglucomutase/phosphomannomutase family protein	Energy metabolism, Sugars	1.24
GSU2732		cytochrome c family protein	Energy metabolism, Electron transport	1.23

GSU2706		phosphate acetyltransferase	Energy metabolism, Electron transport	1.22
GSU1372		3-hydroxyisobutyrate dehydrogenase family protein	Energy metabolism, Amino acids and amines	1.21
GSU1416		iron-sulfur cluster-binding protein	Energy metabolism, Electron transport	1.12
GSU0340	nuoC	NADH dehydrogenase I, C subunit	Energy metabolism, Electron transport	1.02
GSU0843		NADH oxidase, putative	Energy metabolism, Electron transport	1.00
GSU1612	gpm	phosphoglycerate mutase	Energy metabolism, Glycolysis/gluconeogenesis	1.00
GSU1739		indolepyruvate ferredoxin oxidoreductase, alpha subunit	Energy metabolism, Fermentation	0.98
GSU3334		cytochrome c family protein, putative	Energy metabolism, Electron transport	0.98
GSU0339	nuoB	NADH dehydrogenase I, B subunit	Energy metabolism, Electron transport	0.97
GSU3254		phosphoglucomutase/phosphomannomutase family protein	Energy metabolism, Sugars	0.96
GSU1703	pfk	6-phosphofructokinase	Energy metabolism, Glycolysis/gluconeogenesis	0.95
GSU2292	ald	alanine dehydrogenase	Energy metabolism, Amino acids and amines	0.94
GSU0350	nuoM-1	NADH dehydrogenase I, M subunit	Energy metabolism, Electron transport	0.88
GSU3281	trx	thioredoxin	Energy metabolism, Electron transport	0.77
GSU0109	atpF	ATP synthase F0, B subunit	Energy metabolism, ATP-proton motive force	0.74

			interconversion	
GSU2449	sucA	2-oxoglutarate dehydrogenase, E1 component	Energy metabolism, TCA cycle	0.73
GSU2428	pyc	pyruvate carboxylase	Energy metabolism, Glycolysis/gluconeogenesis	0.73
GSU1058	sucC	succinyl-CoA synthase, beta subunit	Energy metabolism, TCA cycle	0.68
GSU1113		carbohydrate kinase, PfkB family	Energy metabolism, Sugars	0.68
GSU2707	ackA-1	acetate kinase	Energy metabolism, Fermentation	0.60
GSU2068		6-phosphofructokinase	Energy metabolism, Glycolysis/gluconeogenesis	0.48
GSU2724		cytochrome c family protein	Energy metabolism, Electron transport	0.46
GSU1628		phosphoglycerate kinase/triosephosphate isomerase	Energy metabolism, Glycolysis/gluconeogenesis	0.44
GSU1996		cytochrome c family protein	Energy metabolism, Electron transport	0.42
GSU2098	cooS	carbon monoxide dehydrogenase subunit	Energy metabolism, Other	0.39
GSU1284		cytochrome c, putative	Energy metabolism, Electron transport	0.35
GSU0090		heterodisulfide reductase subunit	Energy metabolism, Electron transport	0.32
GSU2636		alpha-amylase family protein	Energy metabolism, Biosynthesis and degradation of polysaccharides	0.30
GSU0371		carbohydrate phosphorylase	Energy metabolism,	0.29

		family protein	Biosynthesis and degradation of polysaccharides	
GSU0580	ppdK	pyruvate phosphate dikinase	Energy metabolism, Other	0.23
GSU3385	pckA	phosphoenolpyruvate carboxykinase	Energy metabolism, Glycolysis/gluconeogenesis	0.23
GSU1564		Glu/Leu/Phe/Val dehydrogenase family protein	Energy metabolism, Amino acids and amines	0.18
GSU3303		methylmalonyl-CoA epimerase	Energy metabolism, Fermentation	0.17
GSU0594		cytochrome c family protein	Energy metabolism, Electron transport	0.14
GSU2588	lpdA-2	alpha keto acid dehydrogenase complex, E3 component, lipoamide dehydrogenase	Energy metabolism, Amino acids and amines	0.13
GSU2308	scfA	malate oxidoreductase	Energy metabolism, Other	0.13
GSU1660	acnB	aconitate hydratase 2	Energy metabolism, TCA cycle	0.11
GSU3408		L-threonine aldolase, low-specificity	Energy metabolism, Amino acids and amines	0.09
GSU2445		aconitate hydratase, putative	Energy metabolism, TCA cycle	0.09
GSU0466	macA	cytochrome c551 peroxidase	Energy metabolism, Electron transport	0.08
GSU1059	sucD	succinyl-CoA synthase, alpha subunit	Energy metabolism, TCA cycle	0.07
GSU0344		NADH dehydrogenase I, G subunit, putative	Energy metabolism, Electron transport	0.06
GSU0378		glycine cleavage system P protein, subunit 2	Energy metabolism, Amino acids and amines	0.06
GSU0343	nouF	NADH dehydrogenase I, F	Energy metabolism, Electron	0.05

		subunit	transport	
GSU0785		nickel-dependent hydrogenase, large subunit	Energy metabolism, Electron transport	0.02
GSU2918		transketolase, C-terminal subunit	Energy metabolism, Pentose phosphate pathway	0.01
GSU0893		thioredoxin peroxidase	Energy metabolism, Electron transport	0.00
GSU0097		pyruvate ferredoxin/ferredoxin oxidoreductase	Energy metabolism, Fermentation	0.00
GSU2937		cytochrome c family protein	Energy metabolism, Electron transport	-0.06
GSU2872		electron transfer flavoprotein, Etf beta-subunit/FixA family	Energy metabolism, Electron transport	-0.06
GSU0201	iorB	isoquinoline 1-oxidoreductase, beta subunit	Energy metabolism, Fermentation	-0.08
GSU0777	fdnG	formate dehydrogenase, major subunit, selenocysteine- containing	Energy metabolism, Anaerobic	-0.08
GSU1893		carbohydrate isomerase, KpsF/GutQ family	Energy metabolism, Sugars	-0.10
GSU0742		NAD-dependent dehydrogenase subunit	Energy metabolism, Electron transport	-0.17
GSU0346	nuoI-1	NADH dehydrogenase I, I subunit	Energy metabolism, Electron transport	-0.20
GSU0364	cyd-1	cytochrome c3	Energy metabolism, Electron transport	-0.22
GSU2898		high-molecular-weight cytochrome c	Energy metabolism, Electron transport	-0.34
GSU1761		cytochrome c family protein	Energy metabolism, Electron transport	-0.35

GSU3259		cytochrome c family protein	Energy metabolism, Electron transport	-0.36
GSU0349	nuoL-1	NADH dehydrogenase I, L subunit	Energy metabolism, Electron transport	-0.37
GSU2504	OmcS	cytochrome c family protein	Energy metabolism, Electron transport	-0.39
GSU0818		aldehyde dehydrogenase family protein	Energy metabolism, Fermentation	-0.41
GSU0347	nouJ	NADH dehydrogenase I, J subunit	Energy metabolism, Electron transport	-0.43
GSU1176		fumarate reductase, cytochrome b subunit, putative	Energy metabolism, Anaerobic	-0.45
GSU0091		heterodisulfide reductase subunit	Energy metabolism, Electron transport	-0.46
GSU0743		NAD-dependent dehydrogenase subunit	Energy metabolism, Electron transport	-0.48
GSU0592		cytochrome c family protein	Energy metabolism, Electron transport	-0.50
GSU1465	icd	isocitrate dehydrogenase, NADP-dependent	Energy metabolism, TCA cycle	-0.50
GSU0846	acnA	aconitate hydratase 1	Energy metabolism, TCA cycle	-0.54
GSU3444	nuoBC D	NADH dehydrogenase I, B/C/D subunits	Energy metabolism, Electron transport	-0.56
GSU2887		cytochrome c family protein	Energy metabolism, Electron transport	-0.57
GSU0112	atpG	ATP synthase F1, gamma subunit	Energy metabolism, ATP-proton motive force interconversion	-0.58
GSU1451		3-hydroxyisobutyrate	Energy metabolism, Amino	-0.60

		dehydrogenase family protein	acids and amines	
GSU3125		alcohol dehydrogenase, zinc-containing	Energy metabolism, Fermentation	-0.61
GSU1023	glgA-1	glycogen synthase	Energy metabolism, Biosynthesis and degradation of polysaccharides	-0.62
GSU2762	glpK	glycerol kinase	Energy metabolism, Other	-0.71
GSU2448	sucB	2-oxoglutarate dehydrogenase, E2 component, dihydrolipoamide succinyltransferase	Energy metabolism, TCA cycle	-0.72
GSU2076		cytochrome c family protein	Energy metabolism, Electron transport	-0.73
GSU2944		(R)-2-hydroxyglutaryl-CoA dehydratase alpha-subunit, putative	Energy metabolism, Amino acids and amines	-0.74
GSU0333	atpE	ATP synthase F0, C subunit	Energy metabolism, ATP-proton motive force interconversion	-0.75
GSU0674	hcP-1	prismane protein	Energy metabolism, Electron transport	-0.75
GSU2797	etfB	electron transfer flavoprotein, beta subunit	Energy metabolism, Electron transport	-0.77
GSU0509	sfrA	Fe(III) reductase, alpha subunit	Energy metabolism, Anaerobic	-0.81
GSU2731	OmcC	polyheme membrane-associated cytochrome c	Energy metabolism, Anaerobic	-0.84
GSU0110	atpH	ATP synthase F1, delta subunit	Energy metabolism, ATP-proton motive force interconversion	-0.88
GSU3137		cytochrome c family protein	Energy metabolism, Electron	-0.90

			transport	
GSU3256	galT	galactose-1-phosphate uridylyltransferase	Energy metabolism, Sugars	-0.94
GSU2612		rubrerythrin/rubredoxin protein, putative	Energy metabolism, Electron transport	-0.94
GSU1470		keto/oxoacid ferredoxin oxidoreductase, gamma subunit	Energy metabolism, Fermentation	-0.95
GSU2725		cytochrome c family protein	Energy metabolism, Electron transport	-1.01
GSU2446	lpdA-1	2-oxoglutarate dehydrogenase complex, E3 component, lipoamide dehydrogenase	Energy metabolism, TCA cycle	-1.01
GSU2919		transketolase, N-terminal subunit	Energy metabolism, Pentose phosphate pathway	-1.02
GSU3331	pyk	pyruvate kinase	Energy metabolism, Glycolysis/gluconeogenesis	-1.03
GSU1738		indolepyruvate ferredoxin oxidoreductase, beta subunit	Energy metabolism, Fermentation	-1.04
GSU1245		fructose-bisphosphate aldolase, class-II, putative	Energy metabolism, Glycolysis/gluconeogenesis	-1.05
GSU2495		cytochrome c family protein	Energy metabolism, Electron transport	-1.05
GSU2503	OmcT	cytochrome c family protein	Energy metabolism, Electron transport	-1.05
GSU0114	atpC	ATP synthase F1, epsilon subunit	Energy metabolism, ATP- proton motive force interconversion	-1.06
GSU2361		alpha amylase family protein	Energy metabolism, Biosynthesis and degradation	-1.06

			of polysaccharides	
GSU0341	nouD	NADH dehydrogenase I, D subunit	Energy metabolism, Electron transport	-1.06
GSU2066	glgP	glycogen phosphorylase	Energy metabolism, Biosynthesis and degradation of polysaccharides	-1.07
GSU0274		cytochrome c family protein	Energy metabolism, Electron transport	-1.09
GSU0612	ppcA	cytochrome c3	Energy metabolism, Electron transport	-1.16
GSU0342	nuoE-1	NADH dehydrogenase I, E subunit	Energy metabolism, Electron transport	-1.17
GSU1700	maeB	NADP-dependent malic enzyme	Energy metabolism, TCA cycle	-1.18
GSU0510	sfrB	Fe(III) reductase, beta subunit	Energy metabolism, Anaerobic	-1.19
GSU1377		3-hydroxybutyryl-CoA dehydratase	Energy metabolism, Fermentation	-1.20
GSU0087		heterodisulfide reductase, iron-sulfur binding subunit, putative	Energy metabolism, Electron transport	-1.21
GSU0994	fumB	fumarate hydratase, class I	Energy metabolism, TCA cycle	-1.21
GSU0479	aspA	aspartate ammonia-lyase	Energy metabolism, Amino acids and amines	-1.21
GSU0006	gpsA	glycerol-3-phosphate dehydrogenase (NAD(P)+)	Energy metabolism, Other	-1.26
GSU0591		cytochrome c family protein	Energy metabolism, Electron transport	-1.28
GSU1466	mdh	malate dehydrogenase	Energy metabolism, TCA cycle	-1.28
GSU1178	frdB	fumarate reductase, iron-sulfur	Energy metabolism, Anaerobic	-1.30

		protein		
GSU0092		heterodisulfide reductase subunit	Energy metabolism, Electron transport	-1.31
GSU2513		cytochrome c family protein	Energy metabolism, Electron transport	-1.33
GSU0377		glycine cleavage system P protein, subunit 1	Energy metabolism, Amino acids and amines	-1.35
GSU0778	fdnH	formate dehydrogenase, iron-sulfur subunit	Energy metabolism, Anaerobic	-1.37
GSU1397		cytochrome c family protein, putative	Energy metabolism, Electron transport	-1.38
GSU1024	cyd-4	cytochrome c3	Energy metabolism, Electron transport	-1.38
GSU1629	gap	glyceraldehyde 3-phosphate dehydrogenase 1	Energy metabolism, Glycolysis/gluconeogenesis	-1.39
GSU2795		iron-sulfur cluster-binding protein	Energy metabolism, Electron transport	-1.40
GSU1182	malQ	4-alpha-glucanotransferase	Energy metabolism, Biosynthesis and degradation of polysaccharides	-1.41
GSU1177	frdA	fumarate reductase, flavoprotein subunit	Energy metabolism, TCA cycle	-1.42
GSU2637		alcohol dehydrogenase, zinc-containing	Energy metabolism, Fermentation	-1.43
GSU1651	fbP-1	fructose-1,6-bisphosphatase	Energy metabolism, Glycolysis/gluconeogenesis	-1.44
GSU0113	atpD	ATP synthase F1, beta subunit	Energy metabolism, ATP-proton motive force interconversion	-1.49
GSU3207	gpmI	phosphoglycerate mutase, 2,3-	Energy metabolism,	-1.50

		bisphosphoglycerate-independent	Glycolysis/gluconeogenesis	
GSU0782	hybS	periplasmically oriented, membrane-bound [NiFe]-hydrogenase small subunit	Energy metabolism, Electron transport	-1.54
GSU0108		ATP synthase F0, B subunit	Energy metabolism, ATP-proton motive force interconversion	-1.59
GSU1469	korB	2-oxoglutarate:ferredoxin oxidoreductase, thiamin diphosphate-binding subunit	Energy metabolism, Fermentation	-1.59
GSU1861	vorA	2-oxoacid:ferredoxin oxidoreductase, alpha subunit	Energy metabolism, Fermentation	-1.59
GSU0771		zinc-dependent oxidoreductase	Energy metabolism, Fermentation	-1.61
GSU0803	ppsA	phosphoenolpyruvate synthase	Energy metabolism, Glycolysis/gluconeogenesis	-1.62
GSU2957	trx-2	thioredoxin family protein	Energy metabolism, Electron transport	-1.65
GSU1106	gltA	citrate synthase	Energy metabolism, TCA cycle	-1.66
GSU2743		cytochrome c, 1 heme-binding site	Energy metabolism, Electron transport	-1.66
GSU1311	pgi	glucose-6-phosphate isomerase	Energy metabolism, Glycolysis/gluconeogenesis	-1.67
GSU1468	korA	2-oxoglutarate:ferredoxin oxidoreductase, alpha subunit	Energy metabolism, Fermentation	-1.68
GSU2737	OmcB	polyheme membrane-associated cytochrome c	Energy metabolism, Anaerobic	-1.69
GSU1975		NAD-dependent	Energy metabolism, Sugars	-1.69

		epimerase/dehydratase family protein		
GSU0111	atpA	ATP synthase F1, alpha subunit	Energy metabolism, ATP-proton motive force interconversion	-1.74
GSU1754	kamA	L-lysine 2,3-aminomutase	Energy metabolism, Amino acids and amines	-1.74
GSU2813	ccpA	cytochrome c peroxidase, 2 heme-binding sites	Energy metabolism, Electron transport	-1.75
GSU1321	trx-1	TlpA family-related protein disulfide reductase lipoprotein	Energy metabolism, Electron transport	-1.76
GSU0488	trxB	thioredoxin reductase	Energy metabolism, Electron transport	-1.78
GSU0376	gcvH-1	glycine cleavage system H protein	Energy metabolism, Amino acids and amines	-1.78

Table B10: Δz -score of proteins involved in cellular processes. Δz -score was calculated as follows: (z-score in U treatment - z-score in control)

Locus ID	Symbol	Name	Category	Δz
GSU3424		dihydrolipoamide dehydrogenase-related protein	Cellular processes, Detoxification	1.78
GSU1158	sodA	superoxide dismutase, iron/manganese-containing	Cellular processes, Detoxification	1.72
GSU2212	cheY-5	chemotaxis protein CheY	Cellular processes, Chemotaxis and motility	1.71
GSU0582		methyl-accepting chemotaxis protein	Cellular processes, Chemotaxis and motility	1.70
GSU0865		cell division protein DivIVA, putative	Cellular processes, Cell division	1.66

GSU0352	prx-3	peroxiredoxin, atypical 2-Cys subfamily	Cellular processes, Detoxification	1.66
GSU1905		cold shock domain family protein	Cellular processes, Adaptations to atypical conditions	1.58
GSU0099	mgIA	cell polarity determinant GTPase MglA	Cellular processes, Chemotaxis and motility	1.55
GSU3199	cheA-3	chemotaxis sensor histidine kinase CheA	Cellular processes, Chemotaxis and motility	1.53
GSU0581		cold-shock domain family protein	Cellular processes, Adaptations to atypical conditions	1.38
GSU1180	ftsH-1	cell division protein FtsH	Cellular processes, Cell division	1.35
GSU2220	cheW-7	chemotaxis protein CheW	Cellular processes, Chemotaxis and motility	1.26
GSU2100	katG	catalase/oxidase	Cellular processes, Detoxification	1.23
GSU1141		methyl-accepting chemotaxis protein	Cellular processes, Chemotaxis and motility	1.23
GSU0394		AcrB/AcrD/AcrF family protein	Cellular processes, Toxin production and resistance	1.19
GSU3198	cheY-7	chemotaxis protein CheY	Cellular processes, Chemotaxis and motility	1.14
GSU3064	ftsA	cell division protein FtsA	Cellular processes, Cell division	1.12
GSU2367		organic solvent tolerance protein, putative	Cellular processes, Detoxification	1.06
GSU1832	scpA	segregation and condensation protein A	Cellular processes, Cell division	0.78

GSU1492	pilT-4	twitching motility protein PilT	Cellular processes, Chemotaxis and motility	0.58
GSU2657		spore coat protein A	Cellular processes, Sporulation and germination	0.51
GSU1118		universal stress protein family	Cellular processes, Adaptations to atypical conditions	-0.26
GSU0191		cold-shock domain family protein	Cellular processes, Adaptations to atypical conditions	-0.41
GSU1013		chemotaxis MotB protein, putative	Cellular processes, Chemotaxis and motility	-0.41
GSU3196		methyl-accepting chemotaxis protein	Cellular processes, Chemotaxis and motility	-0.50
GSU1899		virulence factor Mce family protein	Cellular processes, Pathogenesis	-0.55
GSU1704		methyl-accepting chemotaxis protein, putative	Cellular processes, Chemotaxis and motility	-0.64
GSU0400		methyl-accepting chemotaxis protein	Cellular processes, Chemotaxis and motility	-0.66
GSU0401		methyl-accepting chemotaxis protein, putative	Cellular processes, Chemotaxis and motility	-0.66
GSU0756		methyl-accepting chemotaxis protein	Cellular processes, Chemotaxis and motility	-0.66
GSU0916		methyl-accepting chemotaxis protein	Cellular processes, Chemotaxis and motility	-0.66
GSU0935		methyl-accepting chemotaxis protein, putative	Cellular processes, Chemotaxis and motility	-0.66
GSU1029		methyl-accepting chemotaxis protein	Cellular processes, Chemotaxis and motility	-0.66

GSU1032		methyl-accepting chemotaxis protein	Cellular processes, Chemotaxis and motility	-0.66
GSU1035		methyl-accepting chemotaxis protein	Cellular processes, Chemotaxis and motility	-0.66
GSU1041		methyl-accepting chemotaxis protein	Cellular processes, Chemotaxis and motility	-0.66
GSU1374	hylB	methyl-accepting chemotaxis protein	Cellular processes, Chemotaxis and motility	-0.66
GSU2579		methyl-accepting chemotaxis protein	Cellular processes, Chemotaxis and motility	-0.66
GSU2652		methyl-accepting chemotaxis protein	Cellular processes, Chemotaxis and motility	-0.66
GSU2942		methyl-accepting chemotaxis protein	Cellular processes, Chemotaxis and motility	-0.66
GSU3156		methyl-accepting chemotaxis protein, putative	Cellular processes, Chemotaxis and motility	-0.66
GSU3200		chemotaxis protein, CheC family	Cellular processes, Chemotaxis and motility	-0.70
GSU0750		methyl-accepting chemotaxis protein, putative	Cellular processes, Chemotaxis and motility	-0.70
GSU0583		methyl-accepting chemotaxis protein	Cellular processes, Chemotaxis and motility	-0.73
GSU1768		ParA family protein	Cellular processes, Cell division	-0.77
GSU1809	ftsH-2	cell division protein FtsH	Cellular processes, Cell division	-0.85
GSU0207		cold-shock domain family protein	Cellular processes, Adaptations to atypical conditions	-0.87
GSU1030		methyl-accepting chemotaxis	Cellular processes, Chemotaxis	-0.91

		protein	and motility	
GSU0766		methyl-accepting chemotaxis protein, putative	Cellular processes, Chemotaxis and motility	-0.97
GSU0098		MglB protein	Cellular processes, Chemotaxis and motility	-1.05
GSU1408		ParA family protein	Cellular processes, Cell division	-1.06
GSU0515		universal stress protein family	Cellular processes, Adaptations to atypical conditions	-1.09
GSU1214		tetracenomycin polyketide synthesis 8-o-methyltransferase, putative	Cellular processes, Toxin production and resistance	-1.10
GSU1033		methyl-accepting chemotaxis protein	Cellular processes, Chemotaxis and motility	-1.14
GSU2550	drpA	DNA processing protein DprA	Cellular processes, DNA transformation	-1.15
GSU2236	relA	GTP pyrophosphokinase	Cellular processes, Adaptations to atypical conditions	-1.25
GSU1130		chromosome segregation SMC protein, putative	Cellular processes, Cell division	-1.28
GSU3112		cell division protein FtsK, putative	Cellular processes, Cell division	-1.31
GSU3063	ftsZ	cell division protein FtsZ	Cellular processes, Cell division	-1.40
GSU2302		trehalose-phosphatase, putative	Cellular processes, Adaptations to atypical conditions	-1.43
GSU2794	mscL	large conductance	Cellular processes,	-1.44

		mechanosensitive channel protein	Adaptations to atypical conditions	
GSU2222	cheA-2	chemotaxis protein CheA	Cellular processes, Chemotaxis and motility	-1.45
GSU0326	gspG	general secretion pathway protein G	Cellular processes, Pathogenesis	-1.48
GSU2372	mcp028	methyl-accepting chemotaxis sensory transducer, putative	Cellular processes, Chemotaxis and motility	-1.53
GSU1304	mcp025	methyl-accepting chemotaxis sensory transducer	Cellular processes, Chemotaxis and motility	-1.75
GSU2335	usp-4	universal stress protein Usp	Cellular processes, Adaptations to atypical conditions	-1.81

Table B11: Δz -score of proteins involved in amino acid biosynthesis. Δz -score was calculated as follows: (z-score in U treatment - z-score in control)

Locus ID	Symbol	Name	Category	Δz
GSU1183		O-acetyl-L-homoserine sulfhydrylase	Amino acid biosynthesis, Aspartate family	1.80
GSU1530	hisG-1	ATP phosphoribosyltransferase	Amino acid biosynthesis, Histidine family	1.77
GSU0160	dapB	dihydrodipicolinate reductase	Amino acid biosynthesis, Aspartate family	1.77
GSU2425		O-acetyl-L-homoserine sulfhydrylase	Amino acid biosynthesis, Aspartate family	1.74
GSU1909	ilvC	ketol-acid reductoisomerase	Amino acid biosynthesis, Pyruvate family	1.66
GSU3094	hisE	phosphoribosyl-ATP pyrophosphohydrolase	Amino acid biosynthesis, Histidine family	1.63
GSU0152	argF	ornithine carbamoyltransferase	Amino acid biosynthesis, Glutamate family	1.61

GSU2572	cysE	serine acetyltransferase	Amino acid biosynthesis, Serine family	1.60
GSU0156	argH	argininosuccinate lyase	Amino acid biosynthesis, Glutamate family	1.60
GSU2383	trpE	anthranilate synthase component I	Amino acid biosynthesis, Aromatic amino acid family	1.59
GSU0150	argB	acetylglutamate kinase	Amino acid biosynthesis, Glutamate family	1.56
GSU0153	argG	argininosuccinate synthase	Amino acid biosynthesis, Glutamate family	1.55
GSU1242	aatA	aspartate aminotransferase	Amino acid biosynthesis, Aspartate family	1.52
GSU0656	ilvE	branched-chain amino acid aminotransferase	Amino acid biosynthesis, Pyruvate family	1.41
GSU3101	hisG-2	ATP phosphoribosyltransferase	Amino acid biosynthesis, Histidine family	1.36
GSU3057	gltA	glutamate synthase (NADPH), homotetrameric	Amino acid biosynthesis, Glutamate family	1.31
GSU0535	cysK	cysteine synthase A	Amino acid biosynthesis, Serine family	1.17
GSU0945	metC-2	cystathionine beta-lyase	Amino acid biosynthesis, Aspartate family	1.16
GSU1906	leuA	2-isopropylmalate synthase	Amino acid biosynthesis, Pyruvate family	1.11
GSU3097	hisH	imidazole glycerol phosphate synthase, glutamine amidotransferase subunit	Amino acid biosynthesis, Histidine family	1.09
GSU1799		aspartate kinase, monofunctional class	Amino acid biosynthesis, Aspartate family	1.06
GSU3158	cysM	cysteine synthase B	Amino acid biosynthesis,	0.91

			Serine family	
GSU3098	hisB	imidazoleglycerol-phosphate dehydratase	Amino acid biosynthesis, Histidine family	0.90
GSU1695	thrC	threonine synthase	Amino acid biosynthesis, Aspartate family	0.88
GSU1820		protein-P-II uridylyltransferase, putative	Amino acid biosynthesis, Glutamate family	0.81
GSU0151	argD	acetylornithine aminotransferase	Amino acid biosynthesis, Glutamate family	0.81
GSU1953	asnB	asparagine synthase, glutamine-hydrolyzing	Amino acid biosynthesis, Aspartate family	0.78
GSU0159	dapA	dihydrodipicolinate synthase	Amino acid biosynthesis, Aspartate family	0.73
GSU2606	aroA	3-phosphoshikimate 1-carboxyvinyltransferase	Amino acid biosynthesis, Aromatic amino acid family	0.66
GSU2049	argJ	glutamate N-acetyltransferase/amino-acid acetyltransferase	Amino acid biosynthesis, Glutamate family	0.55
GSU2025	aroB	3-dehydroquinate synthase	Amino acid biosynthesis, Aromatic amino acid family	0.47
GSU1902		3-isopropylmalate dehydratase, small subunit, putative	Amino acid biosynthesis, Pyruvate family	0.47
GSU2541	proC	pyrroline-5-carboxylate reductase	Amino acid biosynthesis, Glutamate family	0.27
GSU1198	serA	D-3-phosphoglycerate dehydrogenase	Amino acid biosynthesis, Serine family	0.26
GSU0531	dapF	diaminopimelate epimerase	Amino acid biosynthesis, Aspartate family	0.06
GSU2371	trpA	tryptophan synthase, alpha subunit	Amino acid biosynthesis, Aromatic amino acid family	-0.17

GSU3142		phospho-2-dehydro-3-deoxyheptonate aldolase	Amino acid biosynthesis, Aromatic amino acid family	-0.20
GSU2291		phospho-2-dehydro-3-deoxyheptonate aldolase	Amino acid biosynthesis, Aromatic amino acid family	-0.22
GSU0158	lysA	diaminopimelate decarboxylase	Amino acid biosynthesis, Aspartate family	-0.23
GSU1903		3-isopropylmalate dehydratase, large subunit, putative	Amino acid biosynthesis, Pyruvate family	-0.35
GSU1607	glyA	serine hydroxymethyltransferase	Amino acid biosynthesis, Serine family	-0.44
GSU2879	leuB	3-isopropylmalate dehydrogenase	Amino acid biosynthesis, Pyruvate family	-0.59
GSU3333		phospho-2-dehydro-3-deoxyheptonate aldolase	Amino acid biosynthesis, Aromatic amino acid family	-0.63
GSU3096	hisA	phosphoribosylformimino-5-aminoimidazole carboxamide ribotide isomerase	Amino acid biosynthesis, Histidine family	-0.64
GSU2874	argC	N-acetyl-gamma-glutamyl-phosphate reductase	Amino acid biosynthesis, Glutamate family	-0.64
GSU3260		phosphoserine aminotransferase, putative	Amino acid biosynthesis, Serine family	-0.74
GSU3211	proA	gamma-glutamyl phosphate reductase	Amino acid biosynthesis, Glutamate family	-0.87
GSU0215	fold-1	fold bifunctional protein	Amino acid biosynthesis, Aspartate family	-0.96
GSU2379		pyridoxal-phosphate dependent enzyme	Amino acid biosynthesis, Aromatic amino acid family	-1.00
GSU3100	hisD	histidinol dehydrogenase	Amino acid biosynthesis, Histidine family	-1.02
GSU0484	tdcB	threonine and serine	Amino acid biosynthesis,	-1.07

		dehydratase and deaminase, catabolic	Pyruvate family	
GSU2539	LYS1	saccharopine dehydrogenase	Amino acid biosynthesis, Aspartate family	-1.14
GSU1693	hom	homoserine dehydrogenase	Amino acid biosynthesis, Aspartate family	-1.14
GSU1912	ilvD	dihydroxy-acid dehydratase	Amino acid biosynthesis, Pyruvate family	-1.26
GSU2608	pheA	chorismate mutase/prephenate dehydratase	Amino acid biosynthesis, Aromatic amino acid family	-1.31
GSU1910	ilvN	acetolactate synthase, small subunit	Amino acid biosynthesis, Pyruvate family	-1.34
GSU0944	metC-1	cystathionine beta-lyase	Amino acid biosynthesis, Aspartate family	-1.36
GSU1835	glnA	glutamine synthetase, type I	Amino acid biosynthesis, Glutamate family	-1.37
GSU2878		aspartate-semialdehyde dehydrogenase, putative	Amino acid biosynthesis, Aspartate family	-1.45
GSU1531	hisI	phosphoribosyl-AMP cyclohydrolase	Amino acid biosynthesis, Histidine family	-1.46
GSU0486	ilvA	threonine dehydratase	Amino acid biosynthesis, Pyruvate family	-1.49
GSU1061		aspartate aminotransferase	Amino acid biosynthesis, Aspartate family	-1.53
GSU2921	metH	5-methyltetrahydrofolate-- homocysteine methyltransferase	Amino acid biosynthesis, Aspartate family	-1.60
GSU3099	hisC	histidinol-phosphate aminotransferase	Amino acid biosynthesis, Histidine family	-1.63
GSU3095	hisF	imidazoleglycerol phosphate	Amino acid biosynthesis,	-1.64

		synthase, cyclase subunit	Histidine family	
GSU1828		chorismate mutase	Amino acid biosynthesis, Aromatic amino acid family	-1.66
GSU1911	ilvB	acetolactate synthase, large subunit, biosynthetic type	Amino acid biosynthesis, Pyruvate family	-1.71

Table B12: Δz -score of proteins involved in cell envelope metabolism. Δz -score was calculated as follows: (z-score in U treatment - z-score in control)

Locus ID	Symbol	Name	Category	Δz
GSU1493	pilC	type IV pilus biogenesis protein PilC	Cell envelope, Surface structures	1.79
GSU1817		outer membrane lipoprotein, Slp family	Cell envelope, Other	1.79
GSU0457		outer membrane lipoprotein LolB, putative	Cell envelope, Other	1.76
GSU3066	ddl	D-alanine--D-alanine ligase	Cell envelope, Biosynthesis and degradation of murein sacculus and peptidoglycan	1.74
GSU3072	murF	UDP-N- acetylmuramoylalanyl-D- glutamyl-2,6-diaminopimelate- D-alanyl-D-alanyl ligase, frameshifted	Cell envelope, Other	1.70
GSU2923	murI	glutamate racemase	Cell envelope, Biosynthesis and degradation of murein sacculus and peptidoglycan	1.66
GSU2431	nfeD	NfeD-like membrane-bound serine protease	Cell envelope, Other	1.57
GSU2029	pilP	type IV pilus assembly	Cell envelope, Other	1.55

		lipoprotein PilP, putative		
GSU2028	pilQ	type IV pilus biogenesis protein PilQ	Cell envelope, Surface structures	1.50
GSU2089	mreB	rod shape-determining protein MreB	Cell envelope, Biosynthesis and degradation of murein sacculus and peptidoglycan	1.50
GSU0427		lipoprotein, putative	Cell envelope, Other	1.49
GSU3133		penicillin-binding protein, 1A family	Cell envelope, Biosynthesis and degradation of murein sacculus and peptidoglycan	1.48
GSU0543		outer membrane lipoprotein, Slp family, putative	Cell envelope, Other	1.47
GSU2081	mreC	rod shape-determining protein MreC	Cell envelope, Biosynthesis and degradation of murein sacculus and peptidoglycan	1.39
GSU2458		penicillin-binding protein, putative	Cell envelope, Biosynthesis and degradation of murein sacculus and peptidoglycan	1.35
GSU3466		membrane protein, putative	Cell envelope, Other	1.33
GSU2498		lipoprotein, putative	Cell envelope, Other	1.26
GSU0872		lipoprotein, putative	Cell envelope, Other	1.03
GSU0636		membrane protein, putative	Cell envelope, Other	0.89
GSU3068	murC	UDP-N-acetylmuramate--alanine ligase	Cell envelope, Biosynthesis and degradation of murein sacculus and peptidoglycan	0.87
GSU2030		type IV pilus biogenesis protein PilO	Cell envelope, Surface structures	0.87
GSU2305		peptidoglycan-associated lipoprotein	Cell envelope, Other	0.85
GSU1489		membrane protein, putative	Cell envelope, Other	0.58

GSU2208		lipoprotein, putative	Cell envelope, Other	0.56
GSU2268		outer membrane protein, putative	Cell envelope, Other	0.48
GSU1805	glmM	phosphoglucosamine mutase	Cell envelope, Biosynthesis and degradation of murein sacculus and peptidoglycan	0.35
GSU1091		lipoprotein, putative	Cell envelope, Other	0.30
GSU2333		membrane protein, putative	Cell envelope, Other	0.26
GSU3074	murE	UDP-N-acetylmuramoylalanyl-D-glutamyl-2,6-diaminopimelate ligase	Cell envelope, Biosynthesis and degradation of murein sacculus and peptidoglycan	0.13
GSU0456		membrane protein, putative	Cell envelope, Other	0.11
GSU0501		lipoprotein, putative	Cell envelope, Other	-0.06
GSU1783		type IV pilus biogenesis protein PilB, putative	Cell envelope, Surface structures	-0.15
GSU2277		lipoprotein, NLP/P60 family, putative	Cell envelope, Other	-0.16
GSU2552		lipoprotein, putative	Cell envelope, Other	-0.18
GSU0622		membrane protein, putative	Cell envelope, Other	-0.18
GSU2272		lipoprotein, putative	Cell envelope, Other	-0.21
GSU2267		outer membrane protein, putative	Cell envelope, Other	-0.22
GSU1491		type IV pilus biogenesis protein PilB	Cell envelope, Surface structures	-0.35
GSU2031		type IV pilus biogenesis protein PilN	Cell envelope, Surface structures	-0.37
GSU1922		membrane protein, putative	Cell envelope, Other	-0.44
GSU0182		lipoprotein, putative	Cell envelope, Other	-0.48
GSU3462		lipoprotein, putative	Cell envelope, Other	-0.66

GSU0271	glmU	UDP-N-acetylglucosamine pyrophosphorylase	Cell envelope, Biosynthesis and degradation of murein sacculus and peptidoglycan	-0.70
GSU1869		lipoprotein, putative	Cell envelope, Other	-0.73
GSU3102	murA	UDP-N-acetylglucosamine 1-carboxyvinyltransferase	Cell envelope, Biosynthesis and degradation of murein sacculus and peptidoglycan	-0.84
GSU3130		lipoprotein, putative	Cell envelope, Other	-0.85
GSU3069	murG	UDP-N-acetylglucosamine--N-acetylmuramyl-(pentapeptide) pyrophosphoryl-undecaprenol N-acetylglucosamine transferase	Cell envelope, Biosynthesis and degradation of murein sacculus and peptidoglycan	-0.92
GSU0381		lipoprotein, putative	Cell envelope, Other	-0.94
GSU1984		polysaccharide chain length determinant protein, putative	Cell envelope, Other	-1.02
GSU2104		lipoprotein, putative	Cell envelope, Other	-1.06
GSU2032		type IV pilus biogenesis protein PilM	Cell envelope, Surface structures	-1.07
GSU2940		lipoprotein, putative	Cell envelope, Other	-1.12
GSU1229		lipoprotein, putative	Cell envelope, Other	-1.22
GSU3071	murD	UDP-N-acetylmuramoylalanine--D-glutamate ligase	Cell envelope, Biosynthesis and degradation of murein sacculus and peptidoglycan	-1.29
GSU2633		lipoprotein, putative	Cell envelope, Other	-1.30
GSU1153		outer membrane protein, OMP85 family	Cell envelope, Other	-1.38
GSU0733		cell shape-determining protein MreB/Mrl family	Cell envelope, Biosynthesis and degradation of murein sacculus and peptidoglycan	-1.41

GSU0183		lipoprotein, putative	Cell envelope, Other	-1.43
GSU3314		lipoprotein, putative	Cell envelope, Other	-1.50
GSU1743		lipoprotein, putative	Cell envelope, Other	-1.58
GSU2973		lipoprotein, putative	Cell envelope, Other	-1.63

Table B13: Δz -score of proteins involved in central intermediary metabolism. Δz -score was calculated as follows: (z-score in U treatment - z-score in control)

Locus ID	Symbol	Name	Category	Δz
GSU2821	nifH	nitrogenase iron protein	Central intermediary metabolism, Nitrogen fixation	1.75
GSU2538	nspC	carboxynorspermidine decarboxylase	Central intermediary metabolism, Polyamine biosynthesis	1.71
GSU1875	ahcY	S-adenosyl-L-homocysteine hydrolase	Central intermediary metabolism, One-carbon metabolism	1.65
GSU2559		exopolyphosphatase	Central intermediary metabolism, Phosphorus compounds	1.64
GSU2012	nifU	nitrogen fixation iron-sulfur cluster assembly protein NifU	Central intermediary metabolism, Nitrogen fixation	1.59
GSU3265		sulfite reductase, assimilatory-type	Central intermediary metabolism, Sulfur metabolism	1.56
GSU1028		peptidylarginine deiminase-related protein	Central intermediary metabolism, Amino sugars	1.47
GSU0910		aldehyde:ferredoxin oxidoreductase, tungsten-containing	Central intermediary metabolism, Other	1.42
GSU2307		carbonic anhydrase	Central intermediary metabolism, Other	1.18

GSU1716		phosphoadenosine phosphosulfate reductase, putative	Central intermediary metabolism, Sulfur metabolism	1.17
GSU0809		carbonic anhydrase, putative	Central intermediary metabolism, Other	1.16
GSU2819	nifK	nitrogenase molybdenum-iron protein, beta subunit	Central intermediary metabolism, Nitrogen fixation	0.89
GSU2820	nifD	nitrogenase molybdenum-iron protein, alpha chain	Central intermediary metabolism, Nitrogen fixation	0.86
GSU1880	metK	S-adenosylmethionine synthetase	Central intermediary metabolism, Other	0.68
GSU2806	nifEN	nitrogenase molybdenum-iron cofactor biosynthesis protein NifEN	Central intermediary metabolism, Nitrogen fixation	0.66
GSU2803		dinitrogenase iron- molybdenum cofactor family protein	Central intermediary metabolism, Nitrogen fixation	0.64
GSU1672	hprA	glycerate dehydrogenase	Central intermediary metabolism, Other	0.29
GSU1027		glycosyl hydrolase, family 10	Central intermediary metabolism, Nitrogen metabolism	0.19
GSU2975		inorganic pyrophosphatase, manganese-dependent, putative	Central intermediary metabolism, Phosphorus compounds	-0.48
GSU0270	glmS	glucosamine--fructose-6- phosphate aminotransferase (isomerizing)	Central intermediary metabolism, Amino sugars	-0.82
GSU2537	speA	biosynthetic arginine decarboxylase	Central intermediary metabolism, Polyamine biosynthesis	-1.02

GSU0453	pfs	MTA/SAH nucleosidase	Central intermediary metabolism, Other	-1.10
GSU3323	ppk	polyphosphate kinase	Central intermediary metabolism, Phosphorus compounds	-1.19
GSU1717	cysD	sulfate adenylyltransferase, subunit 2	Central intermediary metabolism, Sulfur metabolism	-1.48
GSU2191		aldehyde ferredoxin oxidoreductase, tungsten-containing	Central intermediary metabolism, Other	-1.65
GSU2502		spermine/spermidine synthase family protein	Central intermediary metabolism, Polyamine biosynthesis	-1.80

Table B14: Δz -score of proteins with unknown function. Δz -score was calculated as follows: (z-score in U treatment - z-score in control)

Locus ID	Symbol	Name	Category	Δz
GSU2213		GAF domain protein	Unknown function, General	1.82
GSU2429		peptidylprolyl cis-trans isomerase, PpiC-type	Unknown function, General	1.82
GSU0014		DnaJ-related molecular chaperone	Unknown function, General	1.82
GSU1458		TPR domain protein	Unknown function, General	1.80
GSU3077	mraW	SAM-dependent membrane protein methyltransferase MraW	Unknown function, Enzymes of unknown specificity	1.78
GSU2516		rhodanese homology domain pair	Unknown function,	1.77

		protein	General	
GSU0197		oxidoreductase, short chain dehydrogenase/reductase family	Unknown function, Enzymes of unknown specificity	1.76
GSU1090		signal transduction protein-related protein, response receiver	Unknown function, General	1.76
GSU2062		response receiver-modulated nucleotide cyclase, GGDEF-related domain-containing	Unknown function, General	1.72
GSU0869		LysM domain/NLP/P60 family protein	Unknown function, General	1.69
GSU2477		cobalamin-binding radical SAM domain iron-sulfur cluster-binding oxidoreductase with TPR domain	Unknown function, General	1.69
GSU3209		protein of unknown function DUF143	Unknown function, General	1.68
GSU0505		rhodanese homology domain superfamily protein	Unknown function, General	1.66
GSU0157		lipoprotein, putative	Unknown function, General	1.65
GSU3454		radical SAM domain iron-sulfur cluster-binding oxidoreductase	Unknown function, Enzymes of unknown specificity	1.64
GSU0585	ycgM	fumarylacetoacetate hydrolase family protein ycgM	Unknown function, Enzymes of unknown specificity	1.63
GSU2493		NHL repeat domain protein	Unknown function, General	1.63
GSU1614		CoA-binding protein	Unknown function, General	1.62

GSU1708		metal-dependent hydrolase, subgroup D	Unknown function, Enzymes of unknown specificity	1.60
GSU0361		peptidylprolyl cis-trans isomerase, PpiC-type	Unknown function, General	1.59
GSU1432		TPR domain protein	Unknown function, General	1.55
GSU1222		histone deacetylase family protein	Unknown function, General	1.54
GSU2583	ycaC	isochorismatase family protein YcaC	Unknown function, Enzymes of unknown specificity	1.52
GSU0617		NHL repeat domain lipoprotein	Unknown function, General	1.51
GSU0644		RNA-binding KH domain protein, putative	Unknown function, General	1.51
GSU2610		LysM domain protein	Unknown function, General	1.49
GSU3145		MOSC domain protein	Unknown function, General	1.49
GSU1877		oxidoreductase, 2-nitropropane dioxygenase family	Unknown function, Enzymes of unknown specificity	1.49
GSU1327		homocysteine S-methyltransferase domain protein	Unknown function, General	1.48
GSU0434		ThiI family protein	Unknown function, General	1.47
GSU2476		TPR domain protein	Unknown function, General	1.47
GSU2888		B12-binding domain	Unknown function,	1.46

		protein/radical SAM domain protein	General	
GSU1306		PHP domain protein	Unknown function, General	1.45
GSU0016		PPIC-type PPIASE domain protein	Unknown function, General	1.44
GSU1818		phosphoglycerate mutase family protein	Unknown function, Enzymes of unknown specificity	1.43
GSU0876		diacylglycerol kinase catalytic domain protein	Unknown function, General	1.40
GSU1149		EAL domain protein	Unknown function, General	1.39
GSU2555		dolichyl-phosphate-mannose-protein mannosyltransferase family protein	Unknown function, General	1.38
GSU1997		PDZ domain protein	Unknown function, General	1.37
GSU1801		CBS domain protein	Unknown function, General	1.36
GSU1371		oxidoreductase, FAD/FMN-binding	Unknown function, Enzymes of unknown specificity	1.36
GSU1123		metallo-beta-lactamase family protein	Unknown function, Enzymes of unknown specificity	1.36
GSU3277		lysM domain protein	Unknown function, General	1.35
GSU3240		radical SAM domain protein	Unknown function, Enzymes of unknown	1.35

			specificity	
GSU0235		S1 RNA binding domain protein	Unknown function, General	1.33
GSU3330		NADH-dependent flavin oxidoreductase, Oye family	Unknown function, Enzymes of unknown specificity	1.29
GSU1237		pyridine nucleotide-disulphide oxidoreductase family protein	Unknown function, Enzymes of unknown specificity	1.28
GSU1274		radical SAM domain protein	Unknown function, Enzymes of unknown specificity	1.26
GSU1398		SCO1/SenC family protein	Unknown function, General	1.26
GSU3343		SpoVR-like family protein	Unknown function, General	1.25
GSU1698		TPR domain protein	Unknown function, General	1.25
GSU0162		aromatic aminotransferase, putative	Unknown function, Enzymes of unknown specificity	1.18
GSU2430		SPFH/Band 7 domain protein	Unknown function, General	1.16
GSU0527		trkA domain protein	Unknown function, General	1.12
GSU3157		hydrolase, alpha/beta fold family	Unknown function, Enzymes of unknown specificity	1.08
GSU0217		nitroreductase family protein	Unknown function, Enzymes of unknown	1.05

			specificity	
GSU1925		transport-associated domain protein	Unknown function, General	1.01
GSU1361		Piwi domain protein	Unknown function, General	1.00
GSU2551		LysM domain protein	Unknown function, General	0.99
GSU2536		dienelactone hydrolase family protein	Unknown function, Enzymes of unknown specificity	0.96
GSU2615		TPR domain protein	Unknown function, General	0.96
GSU3461		thioesterase family protein	Unknown function, General	0.90
GSU0015		PPIC-type PPIASE domain protein	Unknown function, General	0.88
GSU1974		DegT/DnrJ/EryC1/StrS family protein	Unknown function, General	0.88
GSU1736		ACT domain protein	Unknown function, General	0.87
GSU1987		TPR domain protein	Unknown function, General	0.86
GSU0029		hydrolase, carbon-nitrogen family	Unknown function, Enzymes of unknown specificity	0.85
GSU0664	ychF	GTP binding protein YchF	Unknown function, General	0.79
GSU2216		PBS lyase HEAT-like repeat protein	Unknown function, General	0.76
GSU0817		transporter membrane protein of	Unknown function,	0.75

		unknown function DUF140	General	
GSU1137		KH domain/HD domain protein	Unknown function, General	0.74
GSU3078		mraZ protein, putative	Unknown function, General	0.74
GSU0331		trypsin domain/PDZ domain protein	Unknown function, General	0.74
GSU0534		Rrf2 family protein	Unknown function, General	0.70
GSU3299		carboxyl transferase domain protein	Unknown function, General	0.70
GSU0273		radical SAM domain protein	Unknown function, Enzymes of unknown specificity	0.70
GSU3450		glutamate synthase-related protein	Unknown function, General	0.64
GSU1195		HD domain protein	Unknown function, General	0.63
GSU3300		biotin-requiring enzyme subunit	Unknown function, Enzymes of unknown specificity	0.60
GSU1590		DHH family/DHHA1 domain protein	Unknown function, General	0.55
GSU0314		general secretion protein E N-terminal domain protein	Unknown function, General	0.50
GSU1968		nucleotidyltransferase family protein	Unknown function, Enzymes of unknown specificity	0.49
GSU3447		AhpC/TSA family protein	Unknown function, General	0.46

GSU3113		metallo-beta-lactamase family protein	Unknown function, Enzymes of unknown specificity	0.46
GSU2745		ATPase, AAA family	Unknown function, General	0.42
GSU3126		oxidoreductase, aldo/keto reductase family	Unknown function, Enzymes of unknown specificity	0.40
GSU1677		AMP-binding enzyme/acyltransferase	Unknown function, Enzymes of unknown specificity	0.36
GSU1138		Ser/Thr protein phosphatase family protein	Unknown function, Enzymes of unknown specificity	0.35
GSU2974		methylenetetrahydrofolate reductase family protein	Unknown function, Enzymes of unknown specificity	0.31
GSU0490		acetyl-CoA hydrolase/transferase family protein	Unknown function, Enzymes of unknown specificity	0.26
GSU0613		ResB-like family protein	Unknown function, General	0.24
GSU1224		TPR domain protein	Unknown function, General	0.23
GSU1937		GGDEF domain/HAMP domain protein	Unknown function, General	0.19
GSU3276		LysM domain protein	Unknown function, General	0.16
GSU1122		HD domain protein	Unknown function, General	0.16

GSU1446		radical SAM domain protein	Unknown function, Enzymes of unknown specificity	0.15
GSU0926		mce-related protein	Unknown function, General	0.15
GSU2010		CBS domain protein	Unknown function, General	0.14
GSU0179		NADPH-dependent FMN reductase domain protein	Unknown function, General	0.03
GSU2282		CBS domain protein	Unknown function, General	-0.06
GSU0174		acetyl-CoA hydrolase/transferase family protein	Unknown function, Enzymes of unknown specificity	-0.08
GSU1721		radical SAM domain protein	Unknown function, Enzymes of unknown specificity	-0.13
GSU2196		hydrolase, putative	Unknown function, Enzymes of unknown specificity	-0.14
GSU1939		GAF domain/His Kinase A domain/HD domain protein	Unknown function, General	-0.15
GSU2527		nitrite/sulfite reductase domain protein	Unknown function, General	-0.17
GSU1982		general secretion pathway protein- related protein	Unknown function, General	-0.23
GSU1842		polysaccharide biosynthesis/export domain protein	Unknown function, General	-0.26
GSU2073		EF hand domain/PKD domain protein	Unknown function, General	-0.29

GSU2547	gid	gid protein	Unknown function, General	-0.31
GSU3191		TPR domain protein	Unknown function, General	-0.31
GSU1114		TPR domain protein	Unknown function, General	-0.34
GSU1150		oxidative cyclase-related protein	Unknown function, General	-0.35
GSU1193		ketose-bisphosphate aldolase family protein	Unknown function, Enzymes of unknown specificity	-0.42
GSU1892		phosphatase, YrbI family	Unknown function, Enzymes of unknown specificity	-0.46
GSU1718		elongation factor Tu GTP binding domain protein	Unknown function, General	-0.50
GSU0480		NifU-like domain protein	Unknown function, General	-0.53
GSU1207		HesB/YadR/YfhF family protein, selenocysteine-containing	Unknown function, General	-0.53
GSU0651		hydrolase, carbon-nitrogen family	Unknown function, Enzymes of unknown specificity	-0.56
GSU2715		fibronectin type III domain protein	Unknown function, General	-0.57
GSU1537		general secretion pathway protein- related protein	Unknown function, General	-0.57
GSU3435		ankyrin repeat protein	Unknown function, General	-0.58
GSU0441		radical SAM domain protein	Unknown function,	-0.59

			Enzymes of unknown specificity	
GSU1587		ribosomal protein L7Ae family protein	Unknown function, General	-0.61
GSU3000		cbiX protein	Unknown function, General	-0.62
GSU1014		smr domain protein	Unknown function, General	-0.63
GSU3007		phosphoglycerate mutase family, putative	Unknown function, Enzymes of unknown specificity	-0.66
GSU0024		OmpA domain protein	Unknown function, General	-0.66
GSU0500	typA	GTP-binding protein TypA	Unknown function, General	-0.67
GSU3378		glutamate-ammonia ligase adenylyltransferase domain protein	Unknown function, General	-0.73
GSU2885		NHL repeat domain protein	Unknown function, General	-0.77
GSU1394		laccase family protein	Unknown function, General	-0.86
GSU1048		SEC-C motif domain protein	Unknown function, General	-0.87
GSU1741		phosphatase, Ppx/GppA family	Unknown function, Enzymes of unknown specificity	-0.89
GSU2571		Rrf2 family protein	Unknown function, General	-0.92
GSU1596		Sua5/YciO/YrdC/YwlC family protein	Unknown function, General	-0.98

GSU1798		2-isopropylmalate synthase/homocitrate synthase family protein	Unknown function, General	-1.02
GSU3280		thioredoxin-related protein	Unknown function, General	-1.06
GSU1338		heavy-metal-associated domain protein	Unknown function, General	-1.08
GSU1210		metallo-beta-lactamase family protein	Unknown function, Enzymes of unknown specificity	-1.10
GSU0825		pirin family protein	Unknown function, General	-1.13
GSU1251		BNR repeat domain protein	Unknown function, General	-1.14
GSU1477		LemA family protein	Unknown function, General	-1.16
GSU1350		thiF family protein	Unknown function, General	-1.16
GSU1904		decarboxylase family protein	Unknown function, Enzymes of unknown specificity	-1.17
GSU0119		glyoxalase family protein	Unknown function, Enzymes of unknown specificity	-1.17
GSU0237		MaoC-like domain protein	Unknown function, General	-1.19
GSU2436		dehydrogenase complex, E1 component, beta subunit	Unknown function, Enzymes of unknown specificity	-1.24
GSU0117		aminotransferase, classes I and II	Unknown function,	-1.24

			Enzymes of unknown specificity	
GSU1166		TPR domain protein	Unknown function, General	-1.26
GSU1945		fibronectin type III domain protein	Unknown function, General	-1.26
GSU2296		HD domain protein	Unknown function, General	-1.27
GSU0448		hydrolase, putative	Unknown function, Enzymes of unknown specificity	-1.28
GSU2063		HD domain protein	Unknown function, General	-1.30
GSU0360		OmpA domain protein	Unknown function, General	-1.35
GSU2977		transaldolase, putative	Unknown function, Enzymes of unknown specificity	-1.39
GSU1266	lepA	GTP-binding protein LepA	Unknown function, General	-1.41
GSU0853		CBS domain protein	Unknown function, General	-1.41
GSU0685		radical SAM domain protein	Unknown function, Enzymes of unknown specificity	-1.42
GSU2442		RelA/SpoT domain protein	Unknown function, General	-1.44
GSU1442		carbonic anhydrase family protein	Unknown function, Enzymes of unknown specificity	-1.44

GSU2263		oxidoreductase, Gfo/Idh/MocA family	Unknown function, Enzymes of unknown specificity	-1.47
GSU0810		OmpA domain protein	Unknown function, General	-1.50
GSU3062		radical SAM domain iron-sulfur cluster-binding oxidoreductase	Unknown function, Enzymes of unknown specificity	-1.50
GSU1701		diadenosine polyphosphate hydrolase, FHIT domain-containing	Unknown function, General	-1.51
GSU3059		radical SAM domain iron-sulfur cluster-binding oxidoreductase	Unknown function, Enzymes of unknown specificity	-1.57
GSU1839		phosphatase/phosphohexomutase-related hydrolase	Unknown function, Enzymes of unknown specificity	-1.57
GSU0023		TPR domain protein	Unknown function, General	-1.58
GSU1345		transcriptional regulator, Rrf2 family	Unknown function, General	-1.58
GSU1496	pilA	geopilin	Unknown function, General	-1.58
GSU0442	mqnC-1	dehypoxanthinylfualosine cyclase, putative	Unknown function, Enzymes of unknown specificity	-1.60
GSU3092	yqeY	uncharacterized protein YqeY	Unknown function, General	-1.62
GSU1868		cysteine desulfurase family protein	Unknown function, Enzymes of unknown specificity	-1.62

GSU1866		PhoH-related ATPase	Unknown function, General	-1.65
GSU2183		Fic family protein	Unknown function, General	-1.65
GSU2074		peptidylprolyl cis-trans isomerase, PpiC-type	Unknown function, General	-1.65
GSU1002		YcaC-related hydrolase, putative	Unknown function, Enzymes of unknown specificity	-1.66
GSU0654	thiF-1	thiamin biosynthesis thiocarboxylate synthase	Unknown function, General	-1.66
GSU2285		membrane-associated metal- dependent phosphohydrolase, HDc domain-containing	Unknown function, General	-1.70
GSU0542		diguanylate cyclase	Unknown function, General	-1.73
GSU3213	obgE	ribosome biogenesis GTPase ObgE	Unknown function, General	-1.74
GSU2435	aceF	pyruvate dehydrogenase complex, E2 protein, dihydrolipoamide acetyltransferase	Unknown function, Enzymes of unknown specificity	-1.74
GSU3376		response receiver-modulated diguanylate cyclase	Unknown function, General	-1.77
GSU1802	yjeF	YjeF-related putative carbohydrate kinase	Unknown function, General	-1.78
GSU3013	engB	GTPase EngB	Unknown function, General	-1.79
GSU1844		IPT/TIG domain protein, putative	Unknown function, General	-1.79

Table B15: Δz -score of proteins involved in protein biosynthesis. Δz -score was calculated as follows: (z-score in U treatment - z-score in control)

Locus ID	Symbol	Name	Category	Δz
GSU3373	rsmB	16S rRNA (5-methyl-C967)-methyltransferase	Protein synthesis, tRNA and rRNA base modification	1.73
GSU3464	gidA	tRNA (5-carboxymethylaminomethyl-2-thio-U34)-formylglycine transferase/reductase	Protein synthesis, tRNA and rRNA base modification	1.71
GSU2569	mnmA	tRNA (5-carboxymethylaminomethyl-2-thio-U34)-thioltransferase	Protein synthesis, tRNA and rRNA base modification	1.66
GSU0648	rplS	ribosomal protein L19	Protein synthesis, Ribosomal proteins: synthesis and modification	1.62
GSU2850	rplP	ribosomal protein L16	Protein synthesis, Ribosomal proteins: synthesis and modification	1.62
GSU1463	aspS	aspartyl-tRNA synthetase	Protein synthesis, tRNA aminoacylation	1.58
GSU2045	valS	valyl-tRNA synthetase	Protein synthesis, tRNA aminoacylation	1.56
GSU2838	rplO	ribosomal protein L15	Protein synthesis, Ribosomal proteins: synthesis and modification	1.52
GSU1810	tilS	tRNA(Ile)-lysine synthetase	Protein synthesis, tRNA and rRNA base modification	1.51

GSU2875	rpsI	ribosomal protein S9	Protein synthesis, Ribosomal proteins: synthesis and modification	1.50
GSU2232	metG	methionyl-tRNA synthetase	Protein synthesis, tRNA aminoacylation	1.46
GSU3366	glnS	glutaminyl-tRNA synthetase	Protein synthesis, tRNA aminoacylation	1.45
GSU3467	rpmH	ribosomal protein L34	Protein synthesis, Ribosomal proteins: synthesis and modification	1.42
GSU3104	prfA	peptide chain release factor 1	Protein synthesis, Translation factors	1.40
GSU1139	tyrS	tyrosyl-tRNA synthetase	Protein synthesis, tRNA aminoacylation	1.39
GSU2844	rpsN	ribosomal protein S14	Protein synthesis, Ribosomal proteins: synthesis and modification	1.38
GSU1918	frr	ribosome recycling factor	Protein synthesis, Translation factors	1.37
GSU2848	rpsQ	ribosomal protein S17	Protein synthesis, Ribosomal proteins: synthesis and modification	1.36
GSU2856	rplD	ribosomal protein L4	Protein synthesis, Ribosomal proteins: synthesis and modification	1.35
GSU2860	fusA-3	translation elongation factor G	Protein synthesis, Translation factors	1.31
GSU3380	gatB	glutamyl-tRNA(Gln) amidotransferase, B subunit	Protein synthesis, tRNA aminoacylation	1.25
GSU1750	infA	translation initiation factor IF-1	Protein synthesis,	1.22

			Translation factors	
GSU3136	ileS	isoleucyl-tRNA synthetase	Protein synthesis, tRNA aminoacylation	1.11
GSU1659	hisS	histidyl-tRNA synthetase	Protein synthesis, tRNA aminoacylation	1.11
GSU2209	leuS	leucyl-tRNA synthetase	Protein synthesis, tRNA aminoacylation	1.11
GSU3379		translation initiation factor, putative, aIF-2BI family	Protein synthesis, Translation factors	0.94
GSU2859	tuf-1	translation elongation factor Tu	Protein synthesis, Translation factors	0.84
GSU3381	gatA	glutamyl-tRNA(Gln) amidotransferase, A subunit	Protein synthesis, tRNA aminoacylation	0.83
GSU1452		RNA methyltransferase, TrmA family	Protein synthesis, tRNA and rRNA base modification	0.60
GSU2839	rpmD	ribosomal protein L30	Protein synthesis, Ribosomal proteins: synthesis and modification	0.54
GSU1709	smpB	SsrA-binding protein	Protein synthesis, Other	0.47
GSU2840	rpsE	ribosomal protein S5	Protein synthesis, Ribosomal proteins: synthesis and modification	0.38
GSU2852	rplV	ribosomal protein L22	Protein synthesis, Ribosomal proteins: synthesis and modification	0.32
GSU1219	gltX	glutamyl-tRNA synthetase	Protein synthesis, tRNA aminoacylation	0.32
GSU3465	trmE	tRNA modification GTPase TrmE	Protein synthesis, tRNA and rRNA base	0.26

			modification	
GSU3205		MiaB-like tRNA modifying enzyme YliG	Protein synthesis, tRNA and rRNA base modification	0.23
GSU1592	rpsO	ribosomal protein S15	Protein synthesis, Ribosomal proteins: synthesis and modification	0.21
GSU1515	thrS	threonyl-tRNA synthetase	Protein synthesis, tRNA aminoacylation	0.12
GSU0662	rplY	ribosoma protein L25	Protein synthesis, Ribosomal proteins: synthesis and modification	0.05
GSU0666	rpsR	ribosomal protein S18	Protein synthesis, Ribosomal proteins: synthesis and modification	0.03
GSU0130	fmt	methionyl-tRNA formyltransferase	Protein synthesis, tRNA aminoacylation	0.01
GSU3307		histidyl-tRNA synthetase, putative	Protein synthesis, tRNA aminoacylation	0.00
GSU2271	lysS	lysyl-tRNA synthetase	Protein synthesis, tRNA aminoacylation	-0.02
GSU1518	rplT	ribosomal protein L20	Protein synthesis, Ribosomal proteins: synthesis and modification	-0.07
GSU0138	prfC	peptide chain release factor 3	Protein synthesis, Translation factors	-0.09
GSU2847	rplN	ribosomal protein L14	Protein synthesis, Ribosomal proteins: synthesis and modification	-0.16
GSU1460	proS	prolyl-tRNA synthetase	Protein synthesis, tRNA	-0.26

			aminoacylation	
GSU2845	rplE	ribosomal protein L5	Protein synthesis, Ribosomal proteins: synthesis and modification	-0.28
GSU2876	rplM	ribosomal protein L13	Protein synthesis, Ribosomal proteins: synthesis and modification	-0.39
GSU1588	infB	translation initiation factor IF-2	Protein synthesis, Translation factors	-0.41
GSU2851	rpsC	ribosomal protein S3	Protein synthesis, Ribosomal proteins: synthesis and modification	-0.48
GSU2234	rpmB	ribosomal protein L28	Protein synthesis, Ribosomal proteins: synthesis and modification	-0.49
GSU0578	glyQ	glycyl-tRNA synthetase, alpha subunit	Protein synthesis, tRNA aminoacylation	-0.54
GSU0668	rplI	ribosomal protein L9	Protein synthesis, Ribosomal proteins: synthesis and modification	-0.64
GSU1517	rpmI	ribosomal protein L35	Protein synthesis, Ribosomal proteins: synthesis and modification	-0.65
GSU1200		ribosomal protein S1	Protein synthesis, Ribosomal proteins: synthesis and modification	-0.67
GSU2834	rpsM	ribosomal protein S13	Protein synthesis, Ribosomal proteins: synthesis and modification	-0.70
GSU2830	rplQ	ribosomal protein L17	Protein synthesis, Ribosomal proteins:	-0.82

			synthesis and modification	
GSU2843	rpsH	ribosomal protein S8	Protein synthesis, Ribosomal proteins: synthesis and modification	-0.83
GSU2865	rplJ	ribosomal protein L10	Protein synthesis, Ribosomal proteins: synthesis and modification	-0.84
GSU2866	rplA	ribosomal protein L1	Protein synthesis, Ribosomal proteins: synthesis and modification	-0.89
GSU3093	rpsU-2	ribosomal protein S21	Protein synthesis, Ribosomal proteins: synthesis and modification	-0.89
GSU1520	pheT	phenylalanyl-tRNA synthetase, beta subunit	Protein synthesis, tRNA aminoacylation	-0.90
GSU1752	efp-2	translation elongation factor P	Protein synthesis, Translation factors	-0.90
GSU2855	rplW	ribosomal protein L23	Protein synthesis, Ribosomal proteins: synthesis and modification	-0.92
GSU2871	tuf-2	translation elongation factor Tu	Protein synthesis, Translation factors	-0.96
GSU0465	efp-1	translation elongation factor P	Protein synthesis, Translation factors	-0.99
GSU1933	fusA-1	translation elongation factor G	Protein synthesis, Translation factors	-1.00
GSU2858	rpsJ	ribosomal protein S10	Protein synthesis, Ribosomal proteins: synthesis and modification	-1.02
GSU0148	alaS	alanyl-tRNA synthetase	Protein synthesis, tRNA	-1.03

			aminoacylation	
GSU2854	rplB	ribosomal protein L2	Protein synthesis, Ribosomal proteins: synthesis and modification	-1.03
GSU1812	argS	arginyl-tRNA synthetase	Protein synthesis, tRNA aminoacylation	-1.09
GSU1833	trpS	tryptophanyl-tRNA synthetase	Protein synthesis, tRNA aminoacylation	-1.11
GSU0579	glyS	glycyl-tRNA synthetase, beta subunit	Protein synthesis, tRNA aminoacylation	-1.12
GSU3235	rpmA	ribosomal protein L27	Protein synthesis, Ribosomal proteins: synthesis and modification	-1.18
GSU3107	rpmE	ribosomal protein L31	Protein synthesis, Ribosomal proteins: synthesis and modification	-1.20
GSU3365	cysS	cysteinyl-tRNA synthetase	Protein synthesis, tRNA aminoacylation	-1.21
GSU1599	rpmF	ribosomal protein L32	Protein synthesis, Ribosomal proteins: synthesis and modification	-1.24
GSU2864	rplL	ribosomal protein L7/L12	Protein synthesis, Ribosomal proteins: synthesis and modification	-1.27
GSU2832	rpsD	ribosomal protein S4	Protein synthesis, Ribosomal proteins: synthesis and modification	-1.33
GSU0037	serS	seryl-tRNA synthetase	Protein synthesis, tRNA aminoacylation	-1.35
GSU2849	rpmC	ribosomal protein L29	Protein synthesis,	-1.37

			Ribosomal proteins: synthesis and modification	
GSU3236	rplU	ribosomal protein L21	Protein synthesis, Ribosomal proteins: synthesis and modification	-1.39
GSU2867	rplK	ribosomal protein L11	Protein synthesis, Ribosomal proteins: synthesis and modification	-1.40
GSU2529	fusA-2	translation elongation factor G	Protein synthesis, Translation factors	-1.41
GSU1921	rpsB	ribosomal protein S2	Protein synthesis, Ribosomal proteins: synthesis and modification	-1.43
GSU0665	rpsF	ribosomal protein S6	Protein synthesis, Ribosomal proteins: synthesis and modification	-1.44
GSU3383	gatC	glutamyl-tRNA(Gln) amidotransferase, C subunit	Protein synthesis, tRNA aminoacylation	-1.45
GSU2857	rplC	ribosomal protein L3	Protein synthesis, Ribosomal proteins: synthesis and modification	-1.47
GSU2861	rpsG	ribosomal protein S7	Protein synthesis, Ribosomal proteins: synthesis and modification	-1.51
GSU1516	infC	translation initiation factor IF-3	Protein synthesis, Translation factors	-1.51
GSU2841	rplR	ribosomal protein L18	Protein synthesis, Ribosomal proteins: synthesis and modification	-1.53
GSU2206	rpsT	ribosomal protein S20	Protein synthesis, Ribosomal proteins:	-1.54

			synthesis and modification	
GSU1886	yfiA	ribosomal subunit associated sigma-54 modulation protein	Protein synthesis, Translation factors	-1.55
GSU2846	rplX	ribosomal protein L24	Protein synthesis, Ribosomal proteins: synthesis and modification	-1.57
GSU2853	rpsS	ribosomal protein S19	Protein synthesis, Ribosomal proteins: synthesis and modification	-1.57
GSU1519	pheS	phenylalanyl-tRNA synthetase, alpha subunit	Protein synthesis, tRNA aminoacylation	-1.64
GSU1920	tsf	translation elongation factor Ts	Protein synthesis, Translation factors	-1.65
GSU2603	rpsA	ribosomal protein S1	Protein synthesis, Ribosomal proteins: synthesis and modification	-1.67
GSU2842	rplF	ribosomal protein L6	Protein synthesis, Ribosomal proteins: synthesis and modification	-1.69
GSU0102	selB	selenocysteine-specific translation elongation factor	Protein synthesis, Translation factors	-1.70
GSU2833	rpsK	ribosomal protein S11	Protein synthesis, Ribosomal proteins: synthesis and modification	-1.72
GSU0643	rpsP	ribosomal protein S16	Protein synthesis, Ribosomal proteins: synthesis and modification	-1.73

Table B16: Δz -score of proteins with extrachromosomal element functions. Δz -score was calculated as follows: (z-score in U treatment - z-score in control)

Locus ID	Symbol	Name	Category	Dz
GSU0053		CRISPR-associated protein, GSU0053 family	Mobile and extrachromosomal element functions, Other	1.17
GSU2280		ISGsu7, transposase OrfA	Mobile and extrachromosomal element functions, Transposon functions	0.60
GSU1387		CRISPR-associated protein, CT1975 family	Mobile and extrachromosomal element functions, Other	0.50
GSU0975		phage tail sheath protein, putative	Mobile and extrachromosomal element functions, Prophage functions	-0.77

Table B17: Δz -score of proteins involved in transcription. Δz -score was calculated as follows: (z-score in U treatment - z-score in control)

Locus ID	Symbol	Name	Category	Δz
GSU1589	rbfA	ribosome-binding factor A	Transcription, RNA processing	1.63
GSU0189	dbpA	ATP-dependent RNA helicase DbpA	Transcription, Other	1.61
GSU1485		ribonuclease R, putative	Transcription, Degradation of RNA	1.22
GSU3239	cafA	ribonuclease G	Transcription, RNA processing	1.07
GSU2237	rpoZ	DNA-directed RNA polymerase,	Transcription, DNA-	0.99

		omega subunit	dependent RNA polymerase	
GSU1887	rpoN	RNA polymerase sigma-54 factor	Transcription, Transcription factors	0.97
GSU1586	nusA	N utilization substance protein A	Transcription, Transcription factors	0.76
GSU3108	rho	transcription termination factor Rho	Transcription, Transcription factors	0.64
GSU1795	rph	ribonuclease PH	Transcription, RNA processing	0.60
GSU3089	rpoD	RNA polymerase sigma factor RpoD	Transcription, Transcription factors	0.58
GSU2868	nusG	transcription antitermination protein NusG	Transcription, Transcription factors	0.52
GSU2831	rpoA	DNA-directed RNA polymerase, alpha subunit	Transcription, DNA-dependent RNA polymerase	0.51
GSU1581		polyA polymerase family protein	Transcription, RNA processing	0.09
GSU2235		endoribonuclease L-PSP, putative	Transcription, Degradation of RNA	-0.19
GSU1277	greA	transcription elongation factor GreA	Transcription, Transcription factors	-0.43
GSU1525		RNA polymerase sigma-70 factor family	Transcription, Transcription factors	-0.55
GSU0522	rhlB	ATP-dependent RNA helicase RhlB	Transcription, Degradation of RNA	-0.60
GSU0914	rhlE-2	ATP-dependent RNA helicase RhlE	Transcription, Other	-0.66
GSU1593	pnp	polyribonucleotide	Transcription, Degradation	-0.91

		nucleotidyltransferase	of RNA	
GSU1692	nusB	N utilization substance protein B	Transcription, Transcription factors	-1.34
GSU2863	rpoB	DNA-directed RNA polymerase, beta subunit	Transcription, DNA- dependent RNA polymerase	-1.44
GSU0921		ribonuclease, Rne/Rng family protein	Transcription, RNA processing	-1.57
GSU0443		ribonuclease D, putative	Transcription, RNA processing	-1.66
GSU2184	ccaC	cytidine-specific tRNA nucleotidyltransferase	Transcription, RNA processing	-1.79

Table B18: Δz -score of proteins involved in fatty acid and phospholipid metabolism. Δz -score was calculated as follows: (z-score in U treatment - z-score in control)

Locus ID	Symbol	Name	Category	Δz
GSU0242	acpP-1	acyl carrier protein	Fatty acid and phospholipid metabolism, Biosynthesis	1.71
GSU2265	fabZ	(3R)-hydroxymyristoyl-(acyl- carrier-protein) dehydratase	Fatty acid and phospholipid metabolism, Biosynthesis	1.70
GSU1103		AMP-forming acyl-CoA synthetase	Fatty acid and phospholipid metabolism, Degradation	1.66
GSU0290	fabH-1	3-oxoacyl-(acyl-carrier-protein) synthase III	Fatty acid and phospholipid metabolism, Biosynthesis	1.65

GSU1402	accA	acetyl-CoA carboxylase, carboxyl transferase, alpha subunit	Fatty acid and phospholipid metabolism, Biosynthesis	1.47
GSU0688	shc-1	squalene-hopene cyclase	Fatty acid and phospholipid metabolism, Other	1.42
GSU1600	plsX	fatty acid/phospholipid synthesis protein PlsX	Fatty acid and phospholipid metabolism, Biosynthesis	1.21
GSU1008	fabI	enoyl-(acyl-carrier-protein) reductase	Fatty acid and phospholipid metabolism, Biosynthesis	0.93
GSU1907	pssA	CDP-diacylglycerol--serine O-phosphatidyltransferase	Fatty acid and phospholipid metabolism, Biosynthesis	0.35
GSU1603	fabG-2	3-oxoacyl-(acyl-carrier-protein) reductase	Fatty acid and phospholipid metabolism, Biosynthesis	0.33
GSU1605	fabF-2	3-oxoacyl-(acyl-carrier-protein) synthase II	Fatty acid and phospholipid metabolism, Biosynthesis	-0.18
GSU2020	accB	acetyl-CoA carboxylase, biotin carboxyl carrier protein	Fatty acid and phospholipid metabolism, Biosynthesis	-0.37
GSU0229	alkK	medium-chain-fatty-acid--CoA ligase	Fatty acid and phospholipid metabolism, Degradation	-0.72
GSU1601	fabH-2	3-oxoacyl-(acyl-carrier-protein) synthase III	Fatty acid and phospholipid metabolism, Biosynthesis	-0.73
GSU3116		1-acyl-sn-glycerol-3-phosphate	Fatty acid and	-0.76

		acyltransferase, putative	phospholipid metabolism, Biosynthesis	
GSU2370	accD	acetyl-CoA carboxylase, carboxyl transferase, beta subunit	Fatty acid and phospholipid metabolism, Biosynthesis	-0.91
GSU0482		cardiolipin synthetase, putative	Fatty acid and phospholipid metabolism, Biosynthesis	-1.16
GSU1604	acpP-2	acyl carrier protein	Fatty acid and phospholipid metabolism, Biosynthesis	-1.38
GSU3313		thiolase, putative	Fatty acid and phospholipid metabolism, Other	-1.45
GSU1602	fabD	malonyl CoA-acyl carrier protein transacylase	Fatty acid and phospholipid metabolism, Biosynthesis	-1.48
GSU2019	accC	acetyl-CoA carboxylase, biotin carboxylase	Fatty acid and phospholipid metabolism, Biosynthesis	-1.80

Table B19: Δz -score of proteins involved in DNA metabolism. Δz -score was calculated as follows: (z-score in U treatment - z-score in control)

Locus ID	Symbol	Name	Category	Δz
GSU3470	dnaA	chromosomal replication initiator protein DnaA	DNA metabolism, DNA replication, recombination, and repair	1.78
GSU2549	topA	DNA topoisomerase I	DNA metabolism, DNA replication, recombination,	1.68

			and repair	
GSU3117	ssb-2	single-strand binding protein	DNA metabolism, DNA replication, recombination, and repair	1.67
GSU1746	ihfB	integration host factor, beta subunit	DNA metabolism, DNA replication, recombination, and repair	1.47
GSU1539	xth	exodeoxyribonuclease III	DNA metabolism, DNA replication, recombination, and repair	1.45
GSU0890	ligA	DNA ligase, NAD-dependent	DNA metabolism, DNA replication, recombination, and repair	1.45
GSU0541	polA	DNA polymerase I	DNA metabolism, DNA replication, recombination, and repair	1.29
GSU3090	dnaG	DNA primase	DNA metabolism, DNA replication, recombination, and repair	1.17
GSU2829		deoxyribodipyrimidine photolyase, putative	DNA metabolism, DNA replication, recombination, and repair	1.07
GSU3371		AP endonuclease, family 2	DNA metabolism, DNA replication, recombination, and repair	0.77
GSU0094	dnaX	DNA polymerase III, gamma and tau subunits	DNA metabolism, DNA replication, recombination, and repair	0.73
GSU2001	mutL	DNA mismatch repair protein MutL	DNA metabolism, DNA replication, recombination, and repair	0.39

GSU0004	gyrA	DNA gyrase, A subunit	DNA metabolism, DNA replication, recombination, and repair	0.20
GSU3266		DNA helicase II, putative	DNA metabolism, DNA replication, recombination, and repair	0.05
GSU0017	mfd	transcription-repair coupling factor	DNA metabolism, DNA replication, recombination, and repair	-0.14
GSU1822		DNA mismatch repair protein MutS	DNA metabolism, DNA replication, recombination, and repair	-0.26
GSU1766	xseB	exodeoxyribonuclease VII, small subunit	DNA metabolism, Degradation of DNA	-0.43
GSU0001	dnaN	DNA polymerase III, beta subunit	DNA metabolism, DNA replication, recombination, and repair	-0.43
GSU2230	holB	DNA polymerase III, delta prime subunit	DNA metabolism, DNA replication, recombination, and repair	-0.58
GSU1401	dnaE	DNA polymerase III, alpha subunit	DNA metabolism, DNA replication, recombination, and repair	-0.87
GSU1326	recG	ATP-dependent DNA helicase RecG	DNA metabolism, DNA replication, recombination, and repair	-1.01
GSU0003	gyrB	DNA gyrase, B subunit	DNA metabolism, DNA replication, recombination	-1.05
GSU2064	recN	DNA repair protein RecN	DNA metabolism, DNA replication, recombination	-1.06
GSU0143		competence/damage-inducible	DNA metabolism, DNA	-1.09

		protein CinA	replication, recombination, and repair	
GSU1044		mutT/nudix family protein	DNA metabolism, DNA replication, recombination, and repair	-1.38
GSU1076	ruvA	Holliday junction DNA helicase RuvA	DNA metabolism, DNA replication, recombination, and repair	-1.41
GSU1725	sbcC-2	DNA repair exonuclease SbcCD, C subunit, putative	DNA metabolism, DNA replication, recombination, and repair	-1.51
GSU0547	mutS-2	DNA mismatch repair ATPase MutS-2	DNA metabolism, Other	-1.52
GSU1521	ihfA-1	integration host factor, alpha subunit	DNA metabolism, DNA replication, recombination, and repair	-1.53
GSU2207	hola	DNA polymerase III, delta subunit	DNA metabolism, DNA replication, recombination, and repair	-1.59
GSU2602	ihfB-2	DNA-binding protein HU	DNA metabolism, Chromosome-associated proteins	-1.60
GSU0145	recA	recA protein	DNA metabolism, DNA replication, recombination, and repair	-1.60
GSU3132	hup	histone-like protein	DNA metabolism, Chromosome-associated proteins	-1.64
GSU1199		nuclease, putative	DNA metabolism, Degradation of DNA	-1.74

APPENDIX C

SUPPLEMENTARY INFORMATION NOVEL MEMBRANE-BOUND COMPLEXES INVOLVED IN ENERGY CONSERVATION BY THE ACETATE OXIDIZING SULFATE-REDUCING BACTERIUM *DESULFOBACTER* *POSTGATEI*

Genome sequence the sulfate reducing bacteria *Desulfobacter postgatei*

General Features of the *D. postgatei* Genome

Together with *Desulfobacter curvatus* (<http://www.ncbi.nlm.nih.gov/bioproject/?term=169816>), the one of *D. postgatei* is the second acetate-oxidizing, sulfate-reducing bacteria whose genome sequence has been completely sequenced. The genome of *D. postgatei* 2ac9 consist of a single, circular chromosome of 3,974,658 base pairs (bp) (Accession NZ_CM001488 NZ_AGJR02000000). The automated annotation process identified 3,773 genes predicted, 3,678 were proteins coding genes, 95 RNAs, and 238 were predicted as pseudogenes (Table C1). The majority of the intact protein-coding genes (2,742) were assigned with a putative function while the remaining ones (936) were annotated as hypothetical proteins.

Table C1: Genome statistics of *Desulfobacter postgatei*

Attribute	Value	% of total
Genome size (bp)	3,974,658	100.00%
DNA coding number of bases (bp)	3,419,080	86.02%
DNA G+C number of bases	1,874,851	47.17%
Extrachromosomal elements	0	
Genes total number	3,773	100.00%
Protein coding genes	3,678	97.48%
RNA genes	95	2.52%
Pseudo genes	238	6.31%

Protein coding genes with function prediction	2,742	72.67%
Protein coding genes without function prediction	936	24.81%

Energy metabolism

D. postgatei grows heterotrophically using acetate as electron donor for sulfate reduction as sole energy source (241). Therefore, they thrive in habitats where acetate and sulfate are permanently available (242). Although many components of its central metabolism were already described by biochemical experiments, the genome sequence and subsequent results obtained by this study revealed novel features that are relevant for energy metabolism, including the H⁺-translocating ferredoxin:NAD⁺ oxidoreductase (Rnf complex), Quinone-interacting oxidoreductase (Qmo complex), NADH-dependent reduced ferredoxin:NADP⁺ oxidoreductase (Nfn complex), Ech-hydrogenase-related complex (Ehr complex), and Quinone reductase (Qrc complex). Relevant features of the carbon and energy metabolism of *D.postgatei* are explained in the following sections.

Acetate uptake

Mainly, acetate enters the cell by active transportation across the cell membrane using the proton or sodium gradient (243). In environments where acetate concentration is low, acetate uptake likely proceeds via active transport. In contrast, in environments in which acetate is available in high concentration, this likely enters to the cell through passive form, associates with a proton in the periplasm and diffuses through the membrane as acetic acid (243).

Sulfate uptake

Since sulfate reduction takes place in the cytoplasm and the membrane of *D. postgatei* is not permeable to sulfate ions, sulfate has to be transported into the cell by an active specific transporter (242). The genome annotation suggested there are different types of uptake system for sulfate in *D. postgatei* depending upon the environmental conditions. For instance, in environments where sulfate concentrations are low, such as freshwater, sulfate uptake might be performed via the high-affinity proton-driven

symporters, SulP (DespoDRAFT_02318), and the ABC-type transport system, cysATP (DespoDRAFT_01411). In environments where sulfate concentrations are often high, such as brackish and marine mud, uptake of sulfate is likely to be driven by an energy-independent sodium translocation (244).

Citric Acid Cycle

Initial characterization of the central metabolism of *D.postgatei* has revealed that all enzymes for a citric acid cycle were found (245). However, further experiments have shown an unusual utilization of a reductive citric acid cycle in reverse, similar to those observed in green sulfur bacteria (245-247) that allow the net production of 1 ATP via substrate phosphorylation (248). Briefly, the citric acid cycle in *D.postgatei* can be explained in the following steps.

Initially, acetate is activated via succinyl-CoA:acetate CoA transferase (DespoDRAFT_02073) to acetyl-CoA and succinate. The acetyl-CoA is taken by the reversible ATP citrate lyase generating citrate and one additional mol of ATP by substrate level phosphorylation (153). The DespoDRAFT_02935 and DespoDRAFT_02936 are contiguous genes encoding the alpha and beta subunits of ATP citrate lyase, respectively. This step is a peculiarity of *D.postgatei* metabolism because the formation of citrate is catalyzed rather by citrate synthase in many other acetate-oxidizing bacteria and ATP citrate lyase was hypothesized to be restricted to only autotrophic bacteria (246, 249).

Genes for aconitate hydratase (DespoDRAFT_00706), a NADP-dependent isocitrate dehydrogenase (DespoDRAFT_00291) and the four subunits of 2-oxoglutarate ferredoxin oxidoreductase (DespoDRAFT_00203 - DespoDRAFT_00206) were also found in the genome as they were previously described *D.postgatei* (246). The 2-oxoglutarate ferredoxin oxidoreductase catalyzes the reversible decarboxylation of 2-oxoglutarate to form succinyl-CoA. As another peculiarity of the *D.postgatei* metabolism, this step is mediated by ferredoxin, instead of NAD, as many other anaerobes (250). Genes for the three subunits of the membrane bound succinate dehydrogenase (DespoDRAFT_02909 - DespoDRAFT_02911) were found located contiguously in the genome. Because succinate oxidation is coupled to the reduction of

quinones in an endergonic reaction, succinate dehydrogenase contains a *b*-type cytochrome subunit traversing the membrane capable of reversibly transferring electrons to quinone and use the proton gradient as a source of energy (229). The reversible hydration of fumarate is carried out by a cytoplasmic fumarate hydratase (DespoDRAFT_00633) and the oxidation of malate is catalyzed by a membrane-bound malate dehydrogenase (DespoDRAFT_00212). Previous biochemical studies suggested that malate oxidation could not be coupled to the reduction of NAD or NADP and due to the limited redox potential, this reaction could not also be coupled to proton translocation (246). Therefore, we hypothesized that DsrC, a cytoplasmic disulfide enzyme that interacts directly with the dissimilatory sulfite reductase, couples the direct oxidation of malate to the reduction of sulfite (163). In synthesis, the citric acid cycle in *D. postgatei* yields one reduced NADPH, one reduced ferredoxin, one reduced quinone, and one electron utilized in the reduction of DsrC in addition to the 1 mol of ATP produced by the ATP citrate lyase (Figure C1).

Anapleurotic reactions

Anapleurotic pathway is a set of important reactions that connect, bypass and replenish citric acid cycle intermediates that have been utilized as building blocks for anabolic purposes (251). Labeling and physiological studies have previously shown that *D. postgatei* contains the same anapleurotic sequence for the citric acid cycle found in *Desulfuromonas acetoxidans*. This pathway goes from acetate to phosphoenolpyruvate (acetate → acetyl-P → acetyl-CoA → pyruvate → phosphoenolpyruvate) (Figure C1)(248).

Genes encoding the key enzymes for this set of reactions were found in the genome of *D. postgatei* (Figure C1). The phosphorylation of acetate is catalyzed by acetate kinase, *ackr*, and the conversion of acetyl-P to acetyl-CoA by phosphate transacetylase, *pta*. Two further pathways for the activation of acetate, the ADP-forming acetate-CoA ligase, *acs1*, and the AMP-forming acetate-CoA ligase, *acs2*, were identified. The conversion of acetyl-CoA into pyruvate is catalyzed by pyruvate ferredoxin oxidoreductase, *por*. The phosphorylation of pyruvate to phosphoenolpyruvate can be carried out by three different enzymes. Genes encoding for the enzymes pyruvate

kinase, pyruvate phosphate dikinase, and phosphoenolpyruvate synthase were also identified. Pyruvate carboxylase and phosphoenolpyruvate carboxylase appear to be the main connection between this set of reactions and the citric acid cycle (Figure C1).

As in the Fe(III)-reducing bacteria, *Geobacter sulfurreducens*, anapleurotic reactions have two distinguishable features. They can alternate pathways and provide metabolic redundancy that enables *D.postgatei* to resist potential events of genetic perturbation which is essential to maintain the robustness of its specialist metabolism (252-254). We hypothesized that the anapleurotic reactions can also be utilized as futile cycles to counteract the overproduction of ATP under certain conditions, allowing bacteria to regulate catabolic and anabolic functions.

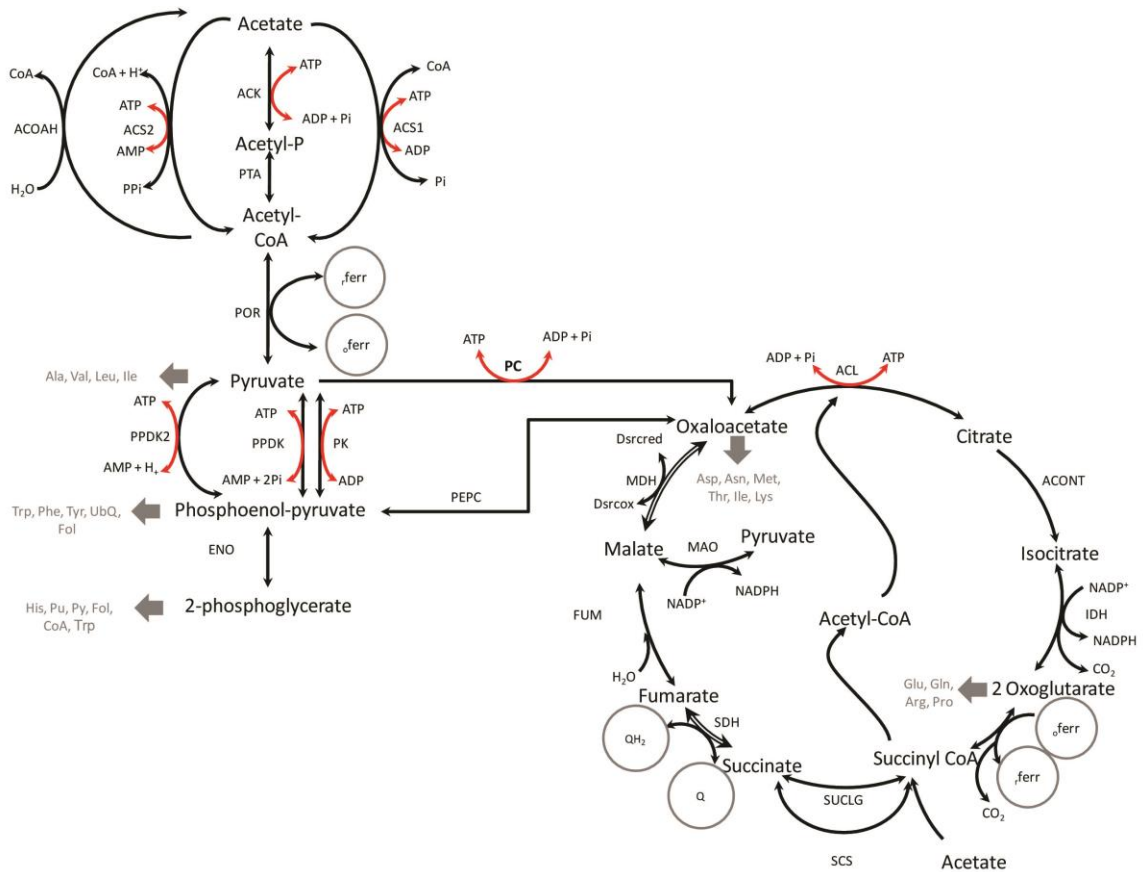


Figure C1: Anapleurotic reactions and the citric acid cycle of *D.postgatei*. Arrows directions indicate the reversibility of the reactions. Striped arrows indicate that the

reaction is predicted to be catalyzed by a membrane-bound enzyme. Red arrows indicate reactions that produce or consume ATP. In circles are the reducing equivalents, QH₂: reduced quinone, Q: oxidized quinone, _rferr: reduced ferredoxin, and _oferr: oxidized ferredoxin. The abbreviations indicate the name of each reaction. Abbreviations and the locus name of the genes encoding these enzymes are the following: ACK, Acetate kinase (DespoDRAFT_00806); PTA, Phosphotransacetylase (DespoDRAFT_00751); ACS1, Acetate-CoA ligase (ADP-forming) (DespoDRAFT_00221); ACS2, Acetate-CoA ligase (AMP-forming) (DespoDRAFT_00810); ACOAH, Acetyl-CoA hydrolase (DespoDRAFT_00482); POR, Pyruvate ferredoxin oxidoreductase (DespoDRAFT_02687, DespoDRAFT_02688, and DespoDRAFT_00515); PK, Pyruvate kinase (DespoDRAFT_02186); PPK, Pyruvate phosphate dikinase (DespoDRAFT_02139); PPK2, Phosphoenolpyruvate synthase (DespoDRAFT_00514); PC, Pyruvate carboxylase (DespoDRAFT_00286 and DespoDRAFT_01944); PEPC, Phosphoenolpyruvate carboxylase (DespoDRAFT_00104); ENO, Enolase (DespoDRAFT_03029); SUCLG, Succinyl:acetate CoA transferase (DespoDRAFT_02073); SCS, Succinyl-CoA synthetase (DespoDRAFT_02935 and DespoDRAFT_02936); ACL, ATP-dependent citrate lyase (DespoDRAFT_00153 and DespoDRAFT_00154); ACONT, Aconitase (DespoDRAFT_00181 and DespoDRAFT_00706); IDH, Isocitrate dehydrogenase (DespoDRAFT_00291); KGOR, 2-oxoglutarate ferredoxin oxidoreductase (DespoDRAFT_00203, DespoDRAFT_00204, DespoDRAFT_00205, and DespoDRAFT_00206); SDH, Succinate dehydrogenase (DespoDRAFT_02909, DespoDRAFT_02910, and DespoDRAFT_02911); FUM, Fumarate hydratase (DespoDRAFT_00633); MDH, Malate dehydrogenase (DespoDRAFT_00292) and MAO, Malate oxidoreductase (DespoDRAFT_02908). Biomass building blocks are indicated in gray. The abbreviations are the following: Trp, Tryptophan; Phe, Phenylalanine; Tyr, Tyrosine; UbQ, Ubiquinone; Fol, Folate; Pu, Purines; Py, Pyrimidines; CoA, Coenzyme A; Asp, Aspartate; Asn, Asparagine; Met, Methionine; Thr, Threonine; Ile, Isoleucine; Lys, Lysine; Glu, Glutamate; Gln, Glutamine; Arg, Arginine; Pro, Proline; Ala, Alanine; Val, Valine and Leu, Leucine.

Sulfate reduction

D. postgatei can utilize sulfate, sulfite, and thiosulfate as electron acceptors to produce hydrogen sulfide (242). The pathway of sulfate reduction involves the same set of reactions than other SBR previously characterized (250). Briefly, once sulfate enters the cell, it is activated via sulfate adenylyltransferase, *sat*, to form adenosine 5'-phosphosulfate (APS). In the following step, APS is reduced to sulfite by adenosine 5-phosphosulfate reductase, *aprA* and *aprB*. The final step of sulfate reduction, sulfite reduction, is carried out by dissimilatory sulfite reductase, *dsrA* and *dsrB*. Since one of the remaining question in the metabolism of *D.postgatei* correspond to the nature of electron donors utilized by these enzymes, we focused our analysis on the complexes that have been recently described in other SBR and have been found for the first time in *D. postgatei*.

QmoABC complex

From a thermodynamic point of view, sulfate reduction is not an easy task. The redox potential of the sulfate/sulfite couple is extremely low (-516 mV) making sulfate very unwilling to accept electrons (255). Therefore, *D.postgatei* has to spend 2 moles of ATP to produce adenosine phosphosulfate (APS) from sulfate to allow its reduction by intracellular electron mediators, such as ferredoxin or NADH (-398 mV and -314 mV, respectively) (199). As mentioned before, the activation of sulfate is catalyzed by a sulfate adenylyltransferase, encoded by DespoDRAFT_02886 (*sat*). In the following step, APS is reduced to sulfite by adenosine 5-phosphosulfate reductase, encoded by DespoDRAFT_00746 (*aprA*) and DespoDRAFT_00747 (*aprB*)(163).

Previous studies in the sulfate-reducing bacteria *Desulfovibrio desulfuricans* have shown that electrons utilized by APS reductase derive from QmoABC, a recently described complex that is essential for sulfate reduction (256, 257). This complex mediates the electron transfer from the reduced quinone pools to the reduction of APS (Figure 4)(256, 258).

Genes encoding the three subunits of this complex were found in the genome of *D.postgatei* contiguously to adenosine phosphosulfate reductase, *aprA*, as in other SRBs

(163). Further experiments in *D.desulfuricans* showed that QmoABC (for Quinone-interacting membrane-bound oxidoreductase) complex and the APS reductase interacts directly, however they failed to detect electron transfer between only the two enzymes, suggesting that bifurcation or confurcation mechanism could be involved (256). This has been supported by the fact that membrane potential cannot drive electron transfer from the periplasm-facing transmembrane, QmoC, to the cytoplasmic AprAB, and a more energetically favorable reaction, such as ferredoxin oxidation, must be utilized (256). The transmembrane member of the QmoABC complex, the cytochrome *b* containing QmoC, is the hypothesized responsible to couple this reaction to chemiosmotic energy conservation (161). The role of QmoABC in energy conservation and sulfate reduction and its interactions with other enzymes deserves further consideration.

DsrMKJOP complex

A second membrane-bound complex, DsrMKJOP, transfers the electrons derived from oxidation of electron donor to sulfite, the product resulting from APS reduction. Likewise QmoABC, the DsrMKJOP complex is also involved in generation of proton motive force (259). This transmembrane complex is composed by five subunit DsrP, DsrO, DsrJ, DsrK, and DsrM and its function is to couple the oxidation of quinones to the reduction of the cytoplasmic electron carrier, DsrC, that further delivers two electrons to the dissimilatory sulfite reductase enzyme, DsrAB (155, 157) (Figure 4).

Genes encoding the two subunits of the dissimilatory sulfite reductase A and B, DespoDRAFT_01364, and DespoDRAFT_01365, were found to be located contiguously as in other sulfate SRB (Figure C2) (211, 260-263). With few exceptions, both DsrMKJOP and QmoABC complexes are conserved in the genomes of sulfate-reducing bacteria described so far. In those microorganisms that lack these complexes, a simpler version of them is present (261).

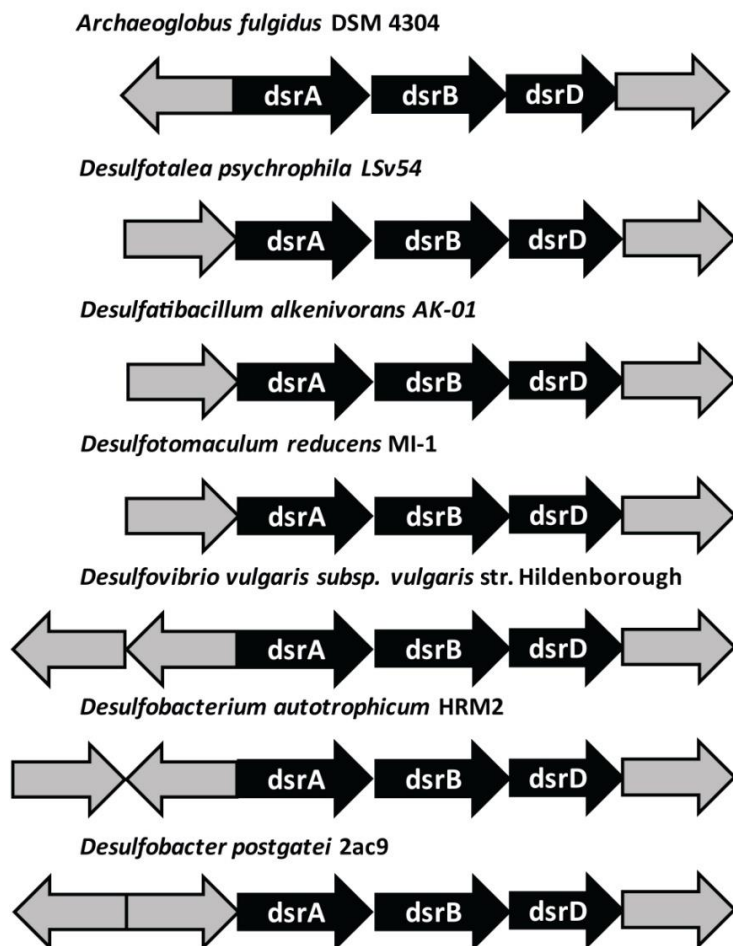


Figure C2: Genomic context of the *dsr* genes of *D.postgatei* and comparison with other SRB.

Nfn (NADH-dependent reduced ferredoxin:NADP⁺ oxidoreductase) complex

Reverse electron bifurcation, also known as electron confurcation, has been proposed as a mechanism that allows that the endergonic reduction of APS by reduced quinone is coupled to its exergonic reduction by a low-potential soluble electron donor, such as ferredoxin (255). This mechanism aims to increase the yield of reduced ferredoxin, which can be further used by Rnf complex to pump additional ions into the periplasm towards to energy conservation (240, 264).

Electron confurcation by Nfn complex was formerly described in *Clostridium kluuyveri* (264), and homologs for the two subunits have been found in the genomes of *D. vulgaris* Hildenborough and *D. alaskensis* G20 (240). Genes encoding the two subunits

of the soluble NADH-dependent reduced ferredoxin:NADP⁺ oxidoreductase A (DespoDRAFT_02087) and B (DespoDRAFT_02088) were found to be located contiguously in the genome of *D. postgatei*. Since *D.postgatei* central metabolism contains a NADPH⁺-dependent isocitrate dehydrogenase (DespoDRAFT_00291, Figure C1), we predict Nfn complex provides a link between two moles of NADPH⁺ toward to the reduction of one ferredoxin and one NAD.

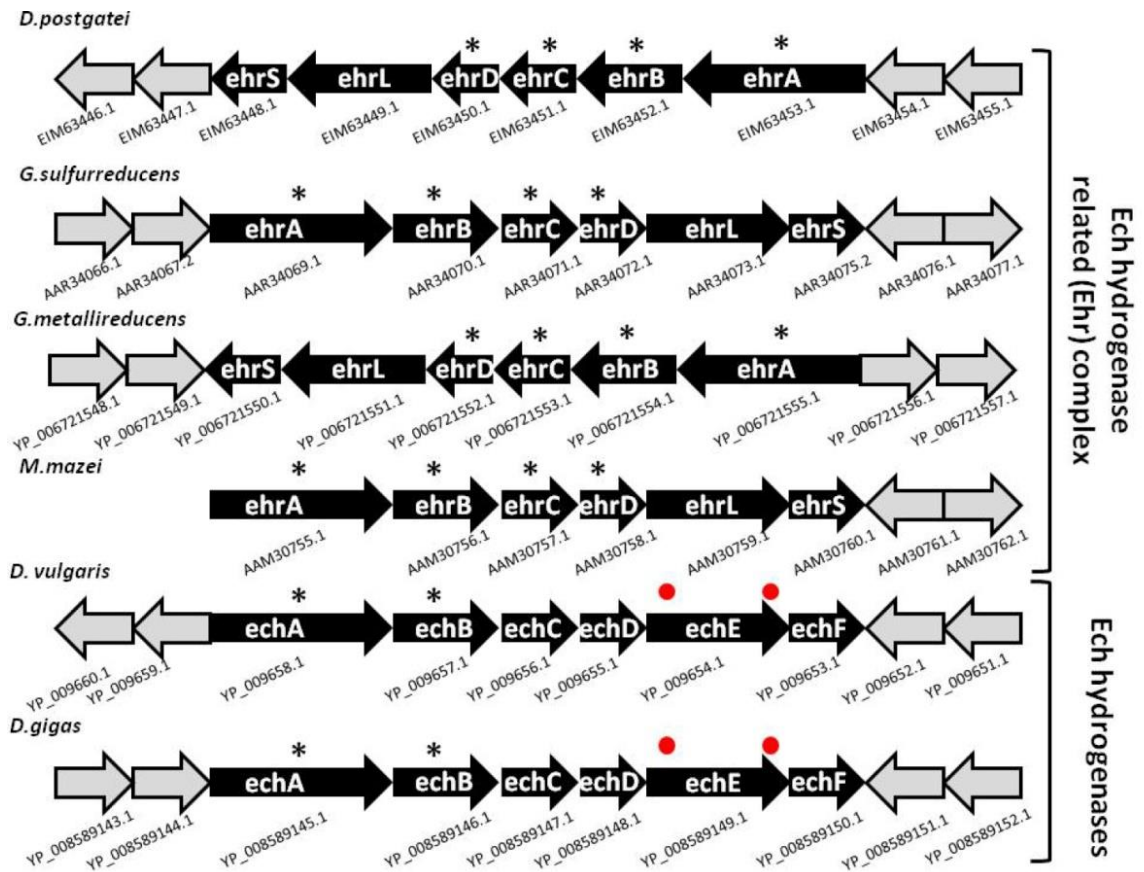


Figure C3: Comparison of the Ech hydrogenases in *D.vulgaris* and *D.gigas* with the Ech-hydrogenase-related (Ehr) complex present in *D.postgatei*, *G.sulfurreducens*, *G.metallireducens*, and *M.mazei*. The subunits encoding Ech hydrogenases and Ech-hydrogenase-related are in black. Asterisk marks indicate the trans-membrane helix(ces) predicted by TMHMM Server v. 2.0 (239). Red circles indicate CxxC motifs containing the cysteine residues in the N- and C-termini.

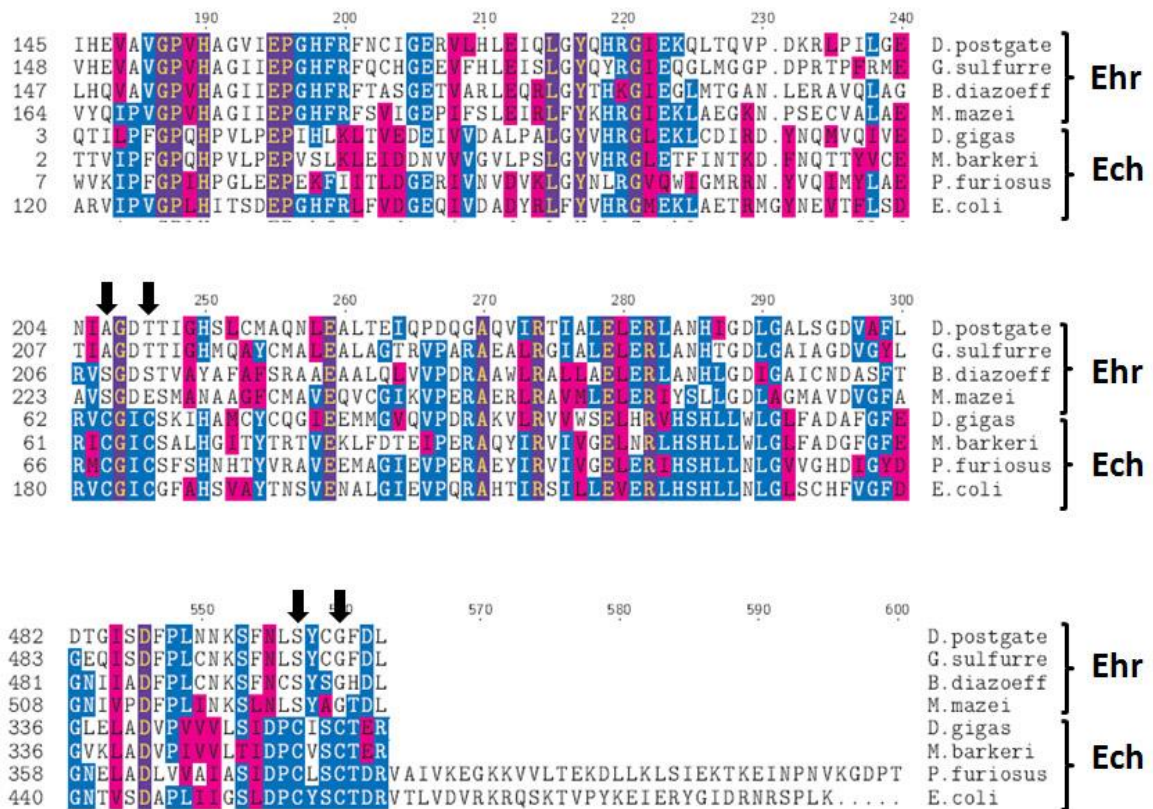


Figure C4: Alignment of the N- and C-termini of representative Ech (EchL) and Ehr (EhrL) large subunits. Identical residues are indicated in purple and similar residues are indicated in blue and pink. The arrows indicate the critical NiFe centre-binding residues of Ech hydrogenases in the N- and C-termini. References or accession numbers for the various ech and ehr clusters are as follows: *E. coli* hyf (265), *Methanosarcina barkeri* ech (266), *Pyrococcus furiosus* mbh (267), *Desulfovibrio gigas* (204), *G. sulfurreducens* ehr (208), *Methanosarcina mazei* ehr (AAM30759) and *Bradyrhizobium diazoefficiens* ehr (BAC51608).

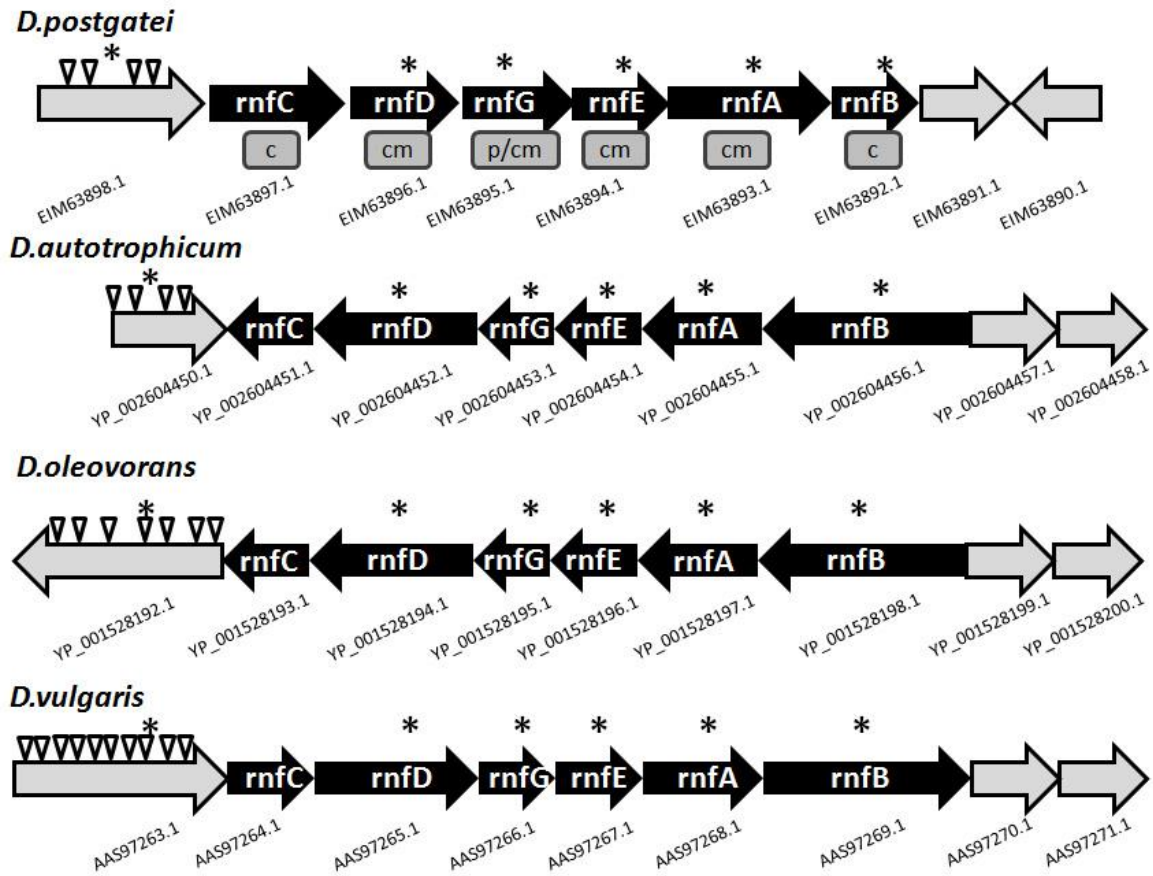


Figure C5: Comparison of the *D. postgatei* *rnf* cluster (DespoDRAFT_01992 - DespoDRAFT_01997) to those of *D. autotrophicum* (211), *D. oleovorans* (163), and *D. vulgaris* (268). The subunits encoding for the H⁺-translocating ferredoxin:NAD⁺ oxidoreductase (Rnf complex) are in black. Gray boxes below *D. postgatei* *rnf* cluster show the localization of each subunit predicted by PSORTB (269); c stands for Cytoplasmic, cm stands for Cytoplasmic Membrane, and p for Periplasmic. Asterisk marks indicate the trans-membrane helix(es) predicted by TMHMM Server v. 2.0 (239). Triangles indicate the CXXCH motif for the *c*-type cytochrome found besides the *rnf* cluster.

Response to environmental challenges

The genome of *D. postgatei* revealed its potential to respond to a variety of environmental stimuli. We found 40 putative genes coding for sensor histidine kinase, and 22 chemotaxis related genes. *In contrast* with previous observations, *D. postgatei*

seems to be motile by flagella under conditions where nutrients were nearly depleted (Figure C18 and Figure C20) (242). The genes for flagella biosynthesis are mainly arranged in the two clusters, DespoDRAFT_00538-DespoDRAFT_00610 and DespoDRAFT_02845-DespoDRAFT_02854, and chemotaxis genes are located adjacent to the first one (Figure C6).

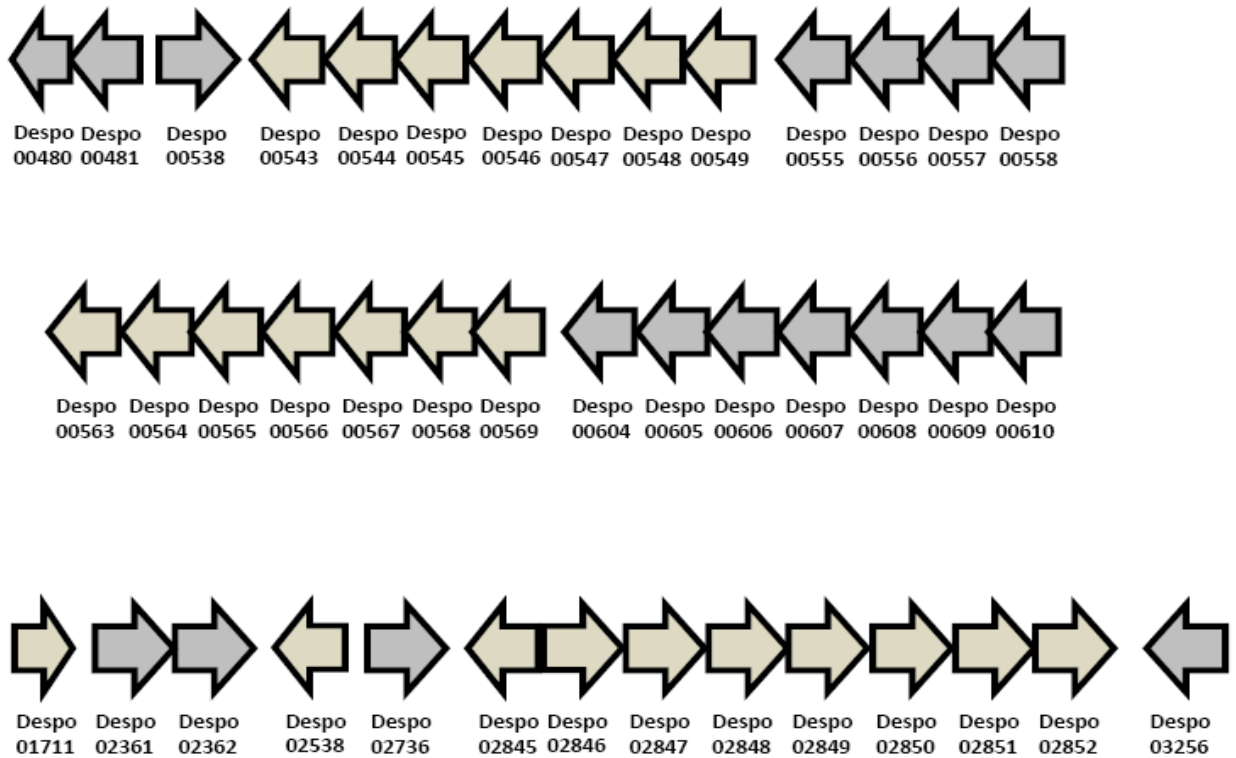


Figure C6: Two gene encoding flagella in the genome of *D. postgatei*. Cluster #1: DespoDRAFT_00480, flagellar motor protein; DespoDRAFT_00481, flagellar motor component; DespoDRAFT_00538, flagellar protein FlaG; DespoDRAFT_00543, flagellar basal-body P-ring protein; DespoDRAFT_00544, flagellar basal body L-ring protein; DespoDRAFT_00545, flagella basal body P-ring formation protein FlgA; DespoDRAFT_00546, flagellar basal-body rod protein FlgG; DespoDRAFT_00547, flagellar hook-basal body protein; DespoDRAFT_00548, uncharacterized protein, cytoplasmic domain of flagellar protein FhlB like protein; DespoDRAFT_00549, Flagellar hook-length control protein FliK; DespoDRAFT_00555, flagellar GTP-binding protein; DespoDRAFT_00556, flagellar biosynthesis protein FlhA; DespoDRAFT_00557, flagellar biosynthetic protein FlhB; DespoDRAFT_00558,

flagellar biosynthetic protein FliR; DespoDRAFT_00563, flagellar biosynthetic protein FliQ; DespoDRAFT_00564, flagellar biosynthetic protein FliP; DespoDRAFT_00565, flagellar biosynthetic protein FliO; DespoDRAFT_00566, flagellar motor switch protein FliN; DespoDRAFT_00567, flagellar motor switch protein FliM; DespoDRAFT_00568, flagellar basal body-associated protein; DespoDRAFT_00569, flagellar hook-length control protein; DespoDRAFT_00604, flagellar biosynthesis/type III secretory pathway protein; DespoDRAFT_00605, flagellar motor switch protein FliG; DespoDRAFT_00606, flagellar basal-body M-ring protein/flagellar hook-basal body protein FliF; DespoDRAFT_00607, flagellar hook-basal body complex protein FliE; DespoDRAFT_00608, flagellar basal-body rod protein FlgC; DespoDRAFT_00609, flagellar basal-body rod protein FlgB; DespoDRAFT_00610, response regulator with CheY-like receiver. Cluster #2: DespoDRAFT_01711, Flagellar basal body-associated protein FliL; DespoDRAFT_02361, flagellar motor component; DespoDRAFT_02362, flagellar motor protein; DespoDRAFT_02538, flagellar biosynthesis anti-sigma factor FlgM; DespoDRAFT_02736, flagellar motor protein; DespoDRAFT_02845, flagellin/flagellar hook associated protein; DespoDRAFT_02846, flagellar capping protein; DespoDRAFT_02847, flagellar biosynthetic protein FliS; DespoDRAFT_02848, hypothetical protein; DespoDRAFT_02849, flagellar protein FlaG; DespoDRAFT_02850, hypothetical protein; DespoDRAFT_02851, flagellar hook capping protein; DespoDRAFT_02852, flagellar hook-basal body protein; DespoDRAFT_03256, flagellar basal body rod protein

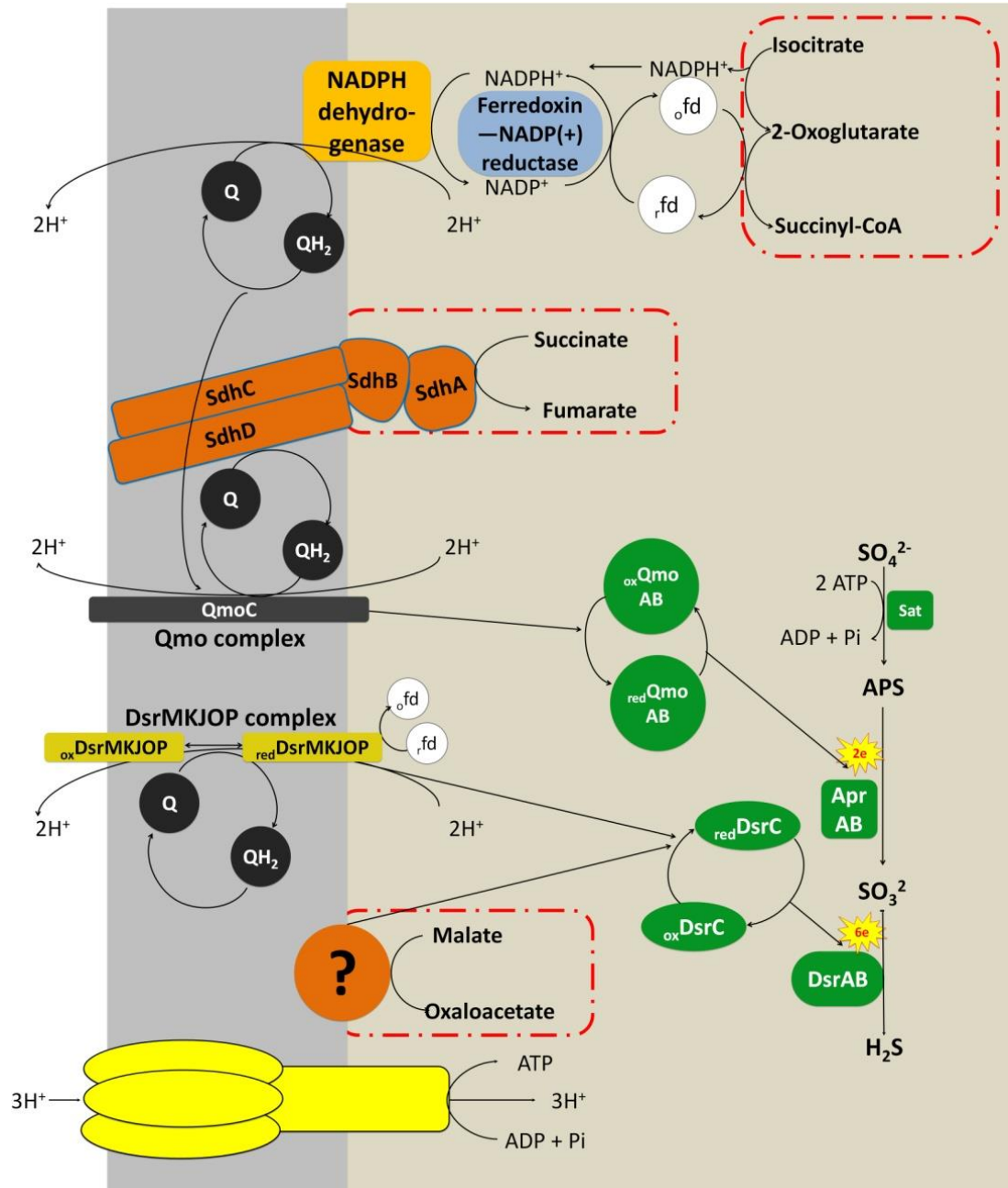


Figure C7: Schematic metabolic reconstruction of energy metabolism of *D. postgatei* based on biochemical experiments proposed by Rabus and colleagues (2006) (250). Red boxes indicate reactions that belong to the citric acid cycle. QH₂: reduced quinone, Q: oxidized quinone, _rferr: reduced ferredoxin, and _oferr: oxidized ferredoxin.

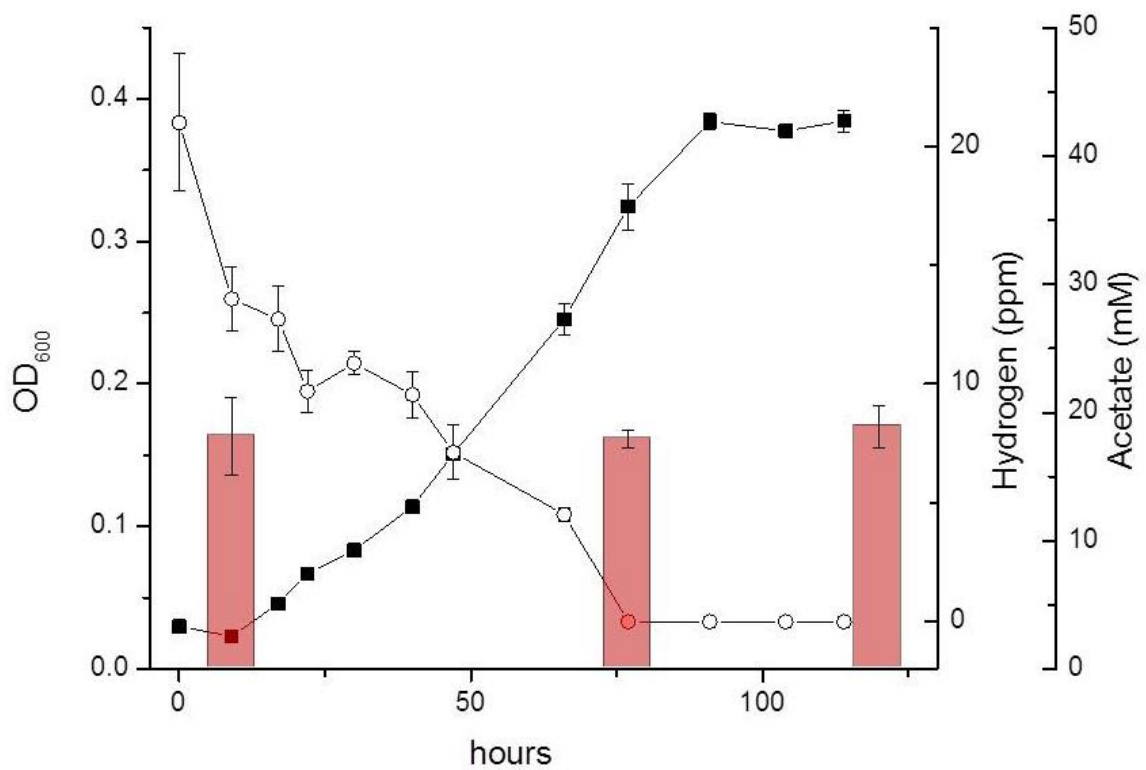


Figure C8: Acetate and hydrogen consumption by *D.postgatei*. Batch culture of *D.postgatei* using acetate (21 mM) and sulfate (20 mM) as electron donor and acceptor, respectively.

Table C2: Proton translocation and ATP production of sulfate reduction coupled to acetate oxidation in *D. postgatei*.

Proton translocation	Per mol of acetate or sulfate	Comments
Sulfate transport	0 H ⁺	SRB membrane is not freely permeable to sulfate ions, sulfate is transported together with 2 Na ⁺ ions (244).
	-2 H ⁺	Under sulfate limitation, sulfate is transported together with 2 H ⁺ (241, 270).
Acetate transport	0 H ⁺	Acetate freely diffuses across the membrane when acetate is abundant (243).
	-1 H ⁺	Under acetate limitation, acetate transport consumes 1 H ⁺ or Na ⁺ per acetate (229).
Sulfate activation	-2 ATP	2 moles of ATP are required for the activation of sulfate to APS (153, 271).
APS reduction	+2 H ⁺	1 H ⁺ per electron is translocated along APS reduction (2 electrons). Proton translocation across the membrane is driven by the membrane bound QmoC complex (229).
Sulfite reduction	+6 H ⁺	DsrMKJOP complex links reoxidation of membrane-bound quinones to proton translocation in ratio of 1H ⁺ per electron (272).
Succinate oxidation	-2 H ⁺	Succinate oxidation to fumarate (E' = +0.033V) with menaquinone (E'=-0.074V) is endergonic. Therefore H ⁺ translocation from the periplasm served as a source of energy to carry out this reaction (250).
Ferredoxin oxidation – NADP ⁺ reduction	+2 H ⁺	RNF complex is predicted to translocate 2H ⁺ per ferredoxin reoxidized (229).
NADH oxidation	+1 to +2 H ⁺	Ehr complex is predicted to translocate 1-2 H ⁺ per ferredoxin reoxidized.

N# protons translocated	+7 H ⁺	
N# ATP produced	2.33	We assumed that H ⁺ /ATP ratio of the <i>D.postgatei</i> ATP synthase is 3.
N# ATP consumed	-2	
Net ATP production by electron transport chain	0.33	
Electron donor oxidation	+1	ATP-citrate lyase produces 1 ATP via substrate level phosphorylation (153)
ATP yield	1.33	

Calculations of *D.postgatei* Cell Composition

The shape of *D. postgatei* cell is reported to be rod shape to ellipsoidal cells with an average size of 1-1.5 by 1.7-2.5 μm with rounded ends (242). Therefore, assuming a radio of the volume of one cell is 0.75μm and 0.5μm, the volume of a single cell is 0.78 μm³.

$$Volumen = \frac{4}{3} \pi * a^2 * b ;$$

where *a* correspond to the radio of the minor axis, and *b* correspond to the radio of the major axis;

$$Volumen = \frac{4}{3} \pi * (0.5\mu m)^2 * 0.75\mu m$$

$$Volumen = 0.785 \mu m^3$$

Assuming that cell density of a cells is equal to the density of water = 1 g/ml, the mass of one cell of *D. postgatei* is

$$Mass = 1 \frac{g}{cm^3} * 0.785\mu m^3 * \left(\frac{1cm}{10mm}\right)^3 * \left(\frac{1mm}{1000\mu m}\right)^3$$

$$Mass = 7.85 * 10^{-13} \text{ g}$$

Since usually a bacterial cell has 70% of water (273), the dry weight of a single cell is $2.35 * 10^{-13} \text{ g}$.

The length of *D. postgatei* genome is 3,974,658 base pairs, and assuming that 1 base pair has a molecular weight of 666 g/mol, the molar mass of the genome is 2,647,122,228 g/mol. Since, 1 mole of nucleotides is equal to $6.023 * 10^{23}$ molecules of nucleotides, the mass of the complete genome of *D.postgatei* is equal to $4.39 * 10^{-15} \text{ g}$. Therefore, the percentage of DNA in 1 gram of dry cell mass is

$$= \left(\frac{4.39 * 10^{-15} \text{ g}}{2.35 * 10^{-13} \text{ g}} * 100 \right) = 1.9\%$$

Table C3: Dry weighth of *D. postgatei* Culture

Biomass (OD ₆₀₀)	mgdw ml ⁻¹ biomass
0.2	0.037
0.2	0.050
0.2	0.034
0.2	0.030
0.2	0.027
Average	0.036

Table C4: Overall Macromolecular Composition of a *D. postgatei* Cell

Biomass component	Percent (%)
Proteins	53.1
Lipids	5.5
DNA	1.9
RNA	15.3
Carbohydrates (includes Glycogen)	14.1
LPS	3.4
Peptidoglycan (murein)	2.5
Cofactors, prosthetic groups and Others	2.9
Inorganic Ions	1.4

Table C5: Protein Composition of 1 Gram of *D. postgatei* Cell

Aminoacids		count in genome	prevalence (P%)	MW (g/mol)	P * MW	% (by weight)	Content (mmol/gDW)
Alanine	Ala	93,198	8.0%	89.05	7.126	5.5%	0.358425385
Arginine	Arg	59,189	5.1%	175.11	8.899	6.9%	0.227631925
Asparagine	Asn	47,353	4.1%	132.05	5.369	4.1%	0.182112462
Aspartic Acid	Asp	67,251	5.8%	132.04	7.624	5.9%	0.258637155
Cysteine	Cys	15,364	1.3%	121.02	1.596	1.2%	0.059087616
Glutamic Acid	Glu	71,752	6.2%	146.05	8.998	6.9%	0.275947319
Glutamine	Gln	42,456	3.6%	146.07	5.325	4.1%	0.163279342
Glycine	Gly	82,274	7.1%	75.03	5.300	4.1%	0.316413337
Histidine	His	24,486	2.1%	155.07	3.260	2.5%	0.094169446
Isoleucine	Ile	84,989	7.3%	131.07	9.564	7.4%	0.326854815
Leucine	Leu	112,435	9.7%	131.09	12.655	9.8%	0.432407972
Lysine	lys	75,414	6.5%	147.11	9.525	7.4%	0.290030816
Methionine	Met	31,933	2.7%	149.05	4.087	3.2%	0.122809479
Phenylalanine	Phe	53,245	4.6%	165.08	7.547	5.8%	0.204772202
proline	Pro	50,044	4.3%	115.06	4.944	3.8%	0.192461641
Serine	Ser	69,185	5.9%	105.40	6.261	4.8%	0.266075026
Threonine	Thr	62,587	5.4%	119.06	6.398	4.9%	0.240700118
Tryptophan	Trp	12,000	1.0%	204.09	2.103	1.6%	0.046150182
Tyrosine	Tyr	34,499	3.0%	181.07	5.363	4.1%	0.132677926

Valine	Val	75,037	6.4%	117.08	7.543	5.8%	0.288580931
Sum		1,164,691.0	100.0%	2,736.7	129.5	100.0%	4.479225094

Table C6: Lipid composition of 1 gram of *D. postgatei* Cell.

Name	Formula	Charge	Content (g/gDW)	MW (g/mol)	Content (mmol/gDW)
Fatty acid (Iso-C14:0)	C14H27O2	-1	0.0046	227.3	0.001035476
Iso-C14:0 CoA Isotetradecanoyl-CoA	C35H59N7O17P3 S	-3	0.0046	241.3	0.001099253
Fatty acid (Iso-C15:0)	C15H29O2	-1	0.0046	241.39	0.001099663
Iso-C15:0 CoA Isopentadecanoyl-CoA	C36H61N7O17P3 S	-3	0.0046	988.8	0.004504524
Fatty acid (Anteiso-C15:0)	C15H29O2	-1	0.0046	241.39	0.001099663
Anteiso-C15:0 CoA Anteisopentadecanoyl-CoA	C36H61N7O17P3 S	-3	0.0046	988.8	0.004504524
Fatty acid (iso-C16:0)	C16H31O2	-1	0.0046	255.4	0.001163486
Iso-C16:0 CoA Isohexadecanoyl-CoA	C37H63N7O17P3 S	-3	0.0046	1005.9	0.004582424
Fatty acid (Iso-C17:0)	C17H33O2	-1	0.0046	269.44	0.001227446
Iso-C17:0 CoA Isoheptadecanoyl-CoA	C38H65N7O17P3 S	-3	0.0046	1016.946	0.004632744
Fatty acid (Anteiso-C17:0)	C17H33O2	-1	0.0046	269.44	0.001227446
Anteiso-C17:0 CoA Anteisoheptadecanoyl-CoA	C38H65N7O17P3 S	-3	0.0046	1016.946	0.004632744

Table C7: DNA composition of 1 gram of *D. postgatei* Cell.

Component	Units in the genome	prevalence (P%)	MW (g/mol)	P * MW	% (by weight)	Content (mmol/gDW)
dATP	954,547	27.10	487.00	13195.39	27.3	0.010466
dCTP	820,821	23.30	462.99	10787.39	22.3	0.008999
dGTP	877,597	24.91	503.00	12530.24	25.9	0.009622
dTTP	869,964	24.69	477.99	11803.65	24.4	0.009538
Total	3,522,929	100		48316.66	100.0	0.0386

Table C8: RNA composition of 1 gram of *D. postgatei* Cell.

Component	Units in the genome	prevalence (P%)	MW (g/mol)	P * MW	% (by weight)	Content (mmol/gDW)
ATP	869,964	24.69	503.00	12421.25	25.1	0.076155
CTP	877,597	24.91	478.98	11931.87	24.1	0.076823
GTP	820,821	23.30	518.99	12092.15	24.5	0.071853
UTP	954,547	27.10	479.97	13004.92	26.3	0.083559
Total	3,522,929	100		49450.19	100.0	0.3084

Table C9: Carbohydrate composition of 1 gram of *D. postgatei* Cell.

Carbohydrate	Content (g/gDW)	MW (g/mol)	Content (mmol/gDW)
Ribose	0.013143	150.13	0.001973
Heptose	0.013143	210.18	0.002762
Glucose	0.013143	180.16	0.002368
Galactose	0.013143	180.16	0.002368
Rhamnose	0.013143	164.16	0.002158
Glucosamine	0.013143	179.17	0.002355
Glycogen	0.013143	666.5	0.00876
Total			0.02274

Table C10: Cofactor composition of 1 gram of *D. postgatei* Cell.

Component	Content (mmol/gDW)	Comments
Putrescine	0.0262	Assumed to be the same quantities than <i>Dehalococcoides</i> model (188)
Homospermidine	0.0047	
Acetyl-CoA	0.0001	
CoA	0.000006	
NAD	3.547	
NADH	3.547	
NADP	0.000335	
NADPH	0.000112	
Succinyl-CoA	0.000003	Assumed to be the same quantities than <i>Dehalococcoides</i> model (188)
AMP	0.001	
ADP	0.002	
ATP	0.004	
5,6,7,8-tetrahydrofolate	0.0001	
Adenosylcobalamin	0.0047	

Table C11: Murein composition of 1 gram of *D. postgatei* Cell.

Compound ID	Amount building block required (μmol)	Content (g/gDW)	MW (g/mol)	Content (mmol/gDW)
Building Blocks				
UDP-NAG	27.6	0.004166667	607	0.002529167
UDP-NAM	27.6	0.004166667	607	0.002529167
L-Alanine	27.6	0.004166667	89.05	0.000371042
D-Alanine	27.6	0.004166667	89.05	0.000371042
m-Diaminopimelic acid	27.6	0.004166667	190.2	0.0007925
D-Glutamic acid	27.6	0.004166667	146.05	0.000608542

Table C12: LPS composition of 1 gram of *D. postgatei* Cell.

Components	Amount building block required (μmol)	Content (g/gDW)	MW (g/mol)	Content (mmol/gDW)
Lipid A building blocks				
TDP-glucosamine	15.7	0.003584956	179	0.000641707
Fatty Acid -ACP (b-OH-myristic, etc)	47	0.010732035	228.37	0.002450875
CDP-ethanolamine	7.8	0.001781061	446.24	0.000794781
Core building blocks				
CMP-KDO	23.5	0.005366017	238.19	0.001278132
ADP-heptose	23.5	0.005366017	210.18	0.00112783
UDP-glucose	15.7	0.003584956	180.16	0.000645866
CDP-ethanolamine	15.7	0.003584956	61.08	0.000218969

Table C13: Energy Cost for processing and Polymerization of Macromolecules of bacterial cells

Process	mmol / gDW	mmol ATP / mmol ^a	mmol ATP / g DW
Protein			
Energy for activation and incorporation	4.479	4.000	17.917
Energy for mRNA synthesis		0.200	0.895
Energy for proofreading		0.100	0.447
Energy for assembly and modification		0.024	0.108
Lipids			
Energy for synthesis of phosphatidylethanolamine	0.031	1.000	0.031
DNA			
Energy for unwinding the helix	0.039	1.000	0.039
Energy for Proofreading		0.350	0.014
Energy for discontinuous synthesis		0.006	0.000
Energy for negative supercoiling		0.005	0.000
Energy for methylation		0.001	0.000
RNA			
Energy for discarding segments	0.308	0.380	0.117
Energy for modifications		0.022	0.007
Carbohydrates (includes Glycogen)			
Energy for Synthesis of carbohydrates	0.023	8.000	0.182
LPS			
Energy for LPS assembly	0.007	1.000	0.007
Peptidoglycan (Murein)			
Energy for forming the pentapeptide	0.007	0.833	0.006
Total Cost			19.7698

Table C14: Biosynthetic Cost of making 1 mmol of each of these building blocks (mmol/mmol)

Building block	quantity in 1 g dried cells (mmol/gDW)	Cost of making 1 mmol of each of these building blocks (mmol/mmol)					
		ATP/ mmol	ATP	NADPH/ mmol	NADPH	NADH /mmol	NADH
Alanine	0.358425385	0	0	1	0.35842538	0	0
Arginine	0.227631925	7	1.593423474	4	0.91052769	-1	-1.593423474
Asparagine	0.182112462	3	0.546337387	1	0.18211246	0	0
Aspartic Acid	0.258637155	0	0	1	0.25863715	0	0
Cysteine	0.059087616	4	0.236350463	5	0.29543807	-1	-0.236350463
Glutamic Acid	0.275947319	0	0	1	0.27594731	0	0
Glutamine	0.163279342	1	0.163279342	1	0.16327934	0	0
Glycine	0.316413337	0	0	1	0.31641333	-1	0
Histidine	0.094169446	6	0.565016673	1	0.09416944	-3	-1.695050019
Isoleucine	0.326854815	2	0.65370963	5	1.63427407	0	0
Leucine	0.432407972	0	0	2	0.86481594	-1	0
Lysine	0.290030816	2	0.580061632	4	1.16012326	0	0
Methionine	0.122809479	7	0.859666353	8	0.98247583	0	0
Phenylalanine	0.204772202	1	0.204772202	2	0.40954440	0	0
proline	0.192461641	1	0.192461641	3	0.57738492	0	0
Serine	0.266075026	0	0	1	0.26607502	-1	0
Threonine	0.240700118	2	0.481400236	3	0.72210035	0	0

Tryptophan	0.046150182	5	0.230750908	3	0.13845054	-2	-0.461501816
Tyrosine	0.132677926	1	0.132677926	2	0.26535585	-1	-0.132677926
Valine	0.288580931	0	0	2	0.57716186	0	0
SubTotal			6.439907867		10.4527123		-4.119003698
RNA nucleotides							
ATP	0.076155147	11	0.837706619	1	0.07615514	-3	-0.228465441
CTP	0.076823327	13	0.998703248	0	0	-3	-0.23046998
GTP	0.071853254	9	0.646679284	1	0.07185325	0	0
UTP	0.083559397	7	0.584915779	1	0.08355939	0	0
SubTotal			3.068004929		0.23156779		-0.458935422
DNA nucleotides							
dATP	0.010465663	11	0.115122288	2	0.02093132	-3	-0.031396988
dCTP	0.008999489	13	0.116993362	1	0.00899948	-3	-0.026998468
dGTP	0.009621982	9	0.086597838	2	0.01924396	0	0
dTTP	0.009538294	10.5	0.100152084	3	0.02861488	0	0
SubTotal			0.418865571		0.07778965		-0.058395456
Lipid components							
total fatty acids	0.030809395	7.2	0.221827645	14	0.43133153	0	0
			0.221827645		0.43133153		0
LPS components							
TDP-glucosamine	0.000641707	2	0.001283414	0	0	0	0
Fatty Acid -ACP (b-	0.002450875	6	0.014705249	11	0.02695962	0	0

OH-myristic, etc)							
CDP-ethanolamine	0.000794781	3	0.002384342	1	0.00079478	-1	-0.000794781
CMP-KDO	0.001278132	2	0.002556263	0	0	0	0
ADP-heptose	0.00112783	1	0.00112783	-4	-0.0045113	0	0
UDP-glucose	0.000645866	1	0.000645866	0	0	0	0
CDP-ethanolamine	0.000218969	3	0.000656907	-1	-0.0002189	1	0.000218969
SubTotal			0.023359871		0.02302411		-0.000575812
Murein components							
UDP-NAG	0.002529167	3	0.0075875	0	0	0	0
UDP-NAM	0.002529167	4	0.010116667	1	0.00252916	0	0
L-Alanine	0.000371042	0	0	0	0	1	0.000371042
D-Alanine	0.000371042	0	0	0	0	1	0.000371042
m-Diaminopimelic acid	0.0007925	2	0.001585	3	0.0023775	0	0
D-Glutamic acid	0.000608542	0	0	0	0	1	0.000608542
			0.019289167		0.00490666		0.001350625
Carbohydrates							
Ribose	0.001973137	1	0.001973137	0	0	0	0
Heptose	0.002762366	1	0.002762366	0	0	0	0
Glucose	0.002367817	1	0.002367817	0	0	0	0
Galactose	0.002367817	1	0.002367817	0	0	0	0
Rhamnose	0.002157531	1	0.002157531	0	0	0	0
Glucosamine	0.002354806	1	0.002354806	0	0	0	0

Glycogen	0.008759714	1	0.008759714	0	0	0	0
SubTotal			0.022743189		0		0
			ATP		NADPH		NADH
Total			10.21399824		11.2213320		-4.635559762

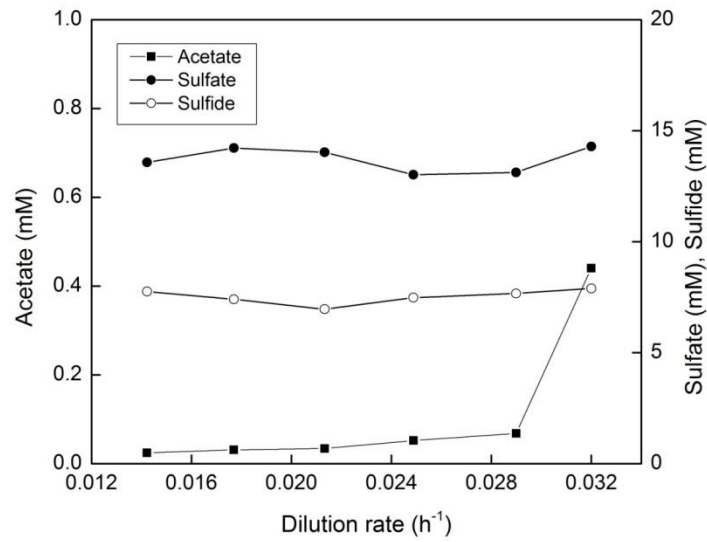


Figure C9: Influence of the growth rate on steady state values of acetate concentration (close squares), sulfate concentration (closed circles), and sulfide concentration (open circles) in acetate-limiting chemostats under sulfate reduction.

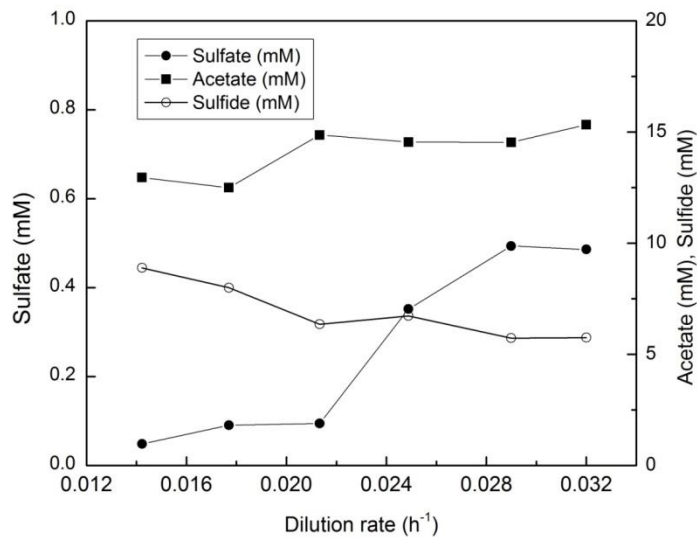


Figure C10: Influence of the growth rate on steady state values of acetate concentration (close squares), sulfate concentration (closed circles), and sulfide concentration (open circles) in sulfate-limiting chemostats under sulfate reduction.

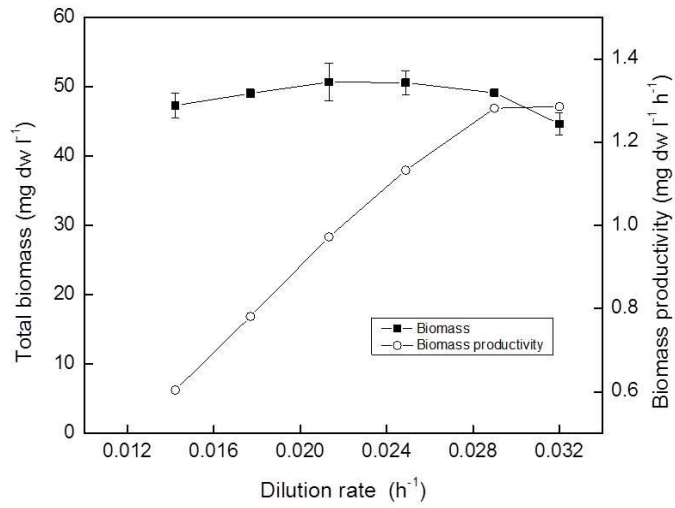


Figure C11: Influence of the growth rate on steady state values of biomass (close squares) and biomass productivity (open circles) in acetate-limiting chemostats under sulfate reduction.

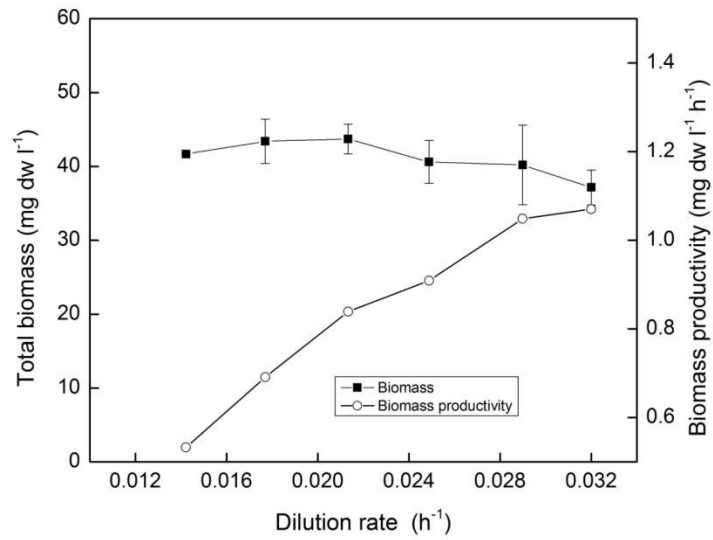


Figure C12: Influence of the growth rate on steady state values of biomass (close squares) and biomass productivity (open circles) in sulfate-limiting chemostats under sulfate reduction.

Table C15: Total biomass, biomass productivity, specific respiration rates and Yield in acetate-limited chemostats.

D (hr ⁻¹)	Total biomass (mg dw/l)	Biomass productivity (mg dw/l h)	Acetate assimilated (%)	Acetate dissimilated (%)	q _{acetate} (mmol acetate/g dw h)	q _{sulfate} (mmol SO ₄ /g dw h)	Y _{acetate} (mg dw/mM consumed)	Y _{sulfate} (mg dw/mM consumed)
0.032	44.646	1.286	11.32%	88.68%	5.1988	4.4040	5.54	6.54
0.029	49.125	1.282	11.91%	88.09%	4.4776	4.2449	5.83	6.15
0.025	50.576	1.132	12.24%	87.76%	3.7401	3.5885	5.99	6.24
0.021	50.671	0.973	12.23%	87.77%	3.2067	2.6842	5.99	7.15
0.018	49.044	0.781	11.84%	88.16%	2.7508	2.2414	5.79	7.11
0.014	47.286	0.604	11.40%	88.60%	2.2906	2.0394	5.58	6.27

Table C16: Total biomass, biomass productivity, specific respiration rates and Yield in sulfate-limited chemostats.

D (hr ⁻¹)	Total biomass (mg dw/l)	Biomass productivity (mg dw/l h)	Acetate assimilated (%)	Acetate dissimilated (%)	q _{acetate} (mmol acetate/g dw h)	q _{sulfate} (mmol SO ₄ /g dw h)	Y _{acetate} (mg dw/mM consumed)	Y _{sulfate} (mg dw/mM consumed)
0.032	37.158	1.070	13.11%	86.89%	4.4886	6.2114	6.42	4.64
0.029	40.199	1.049	12.49%	87.51%	4.2692	5.1958	6.11	5.02
0.025	40.604	0.909	12.64%	87.36%	3.6214	4.4934	6.18	4.98
0.021	43.724	0.839	14.30%	85.70%	2.7432	3.6897	7.00	5.20
0.018	43.397	0.691	10.29%	89.71%	3.1642	3.0867	5.03	5.16
0.014	41.679	0.533	10.43%	89.57%	2.5045	2.5915	5.10	4.93

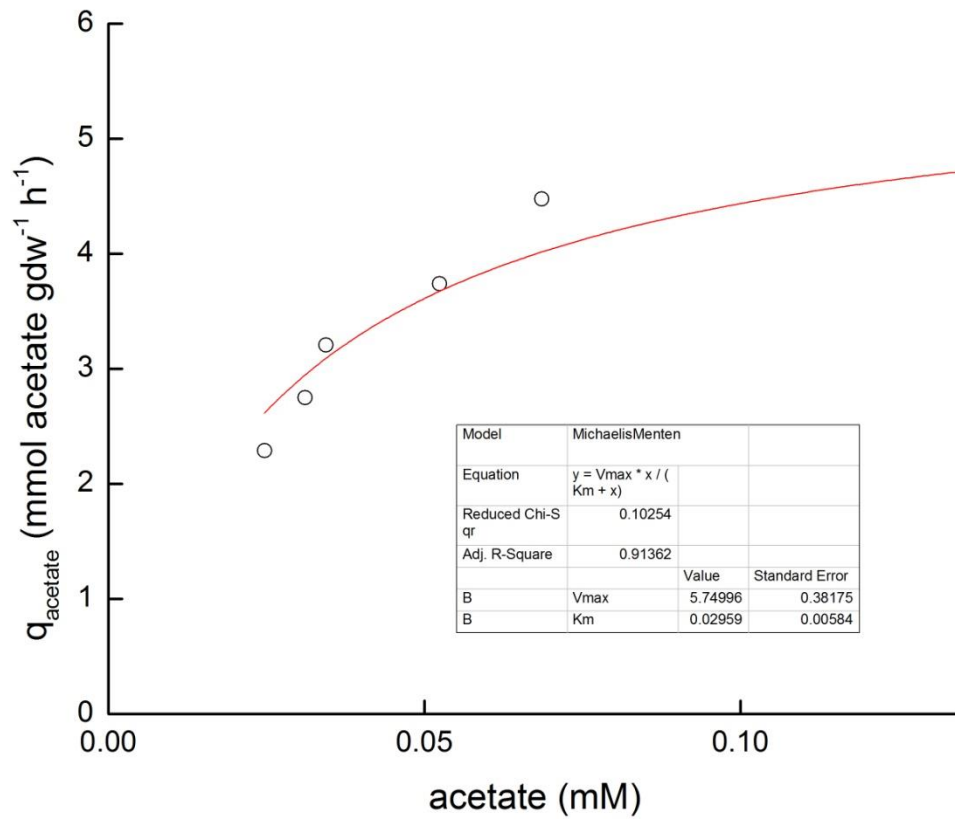


Figure C13: Michaelis-Menten type relationship that represents the effect of acetate concentrations and specific acetate consumption rates under acetate-limited conditions. Each point represents the average of triplicate measurements

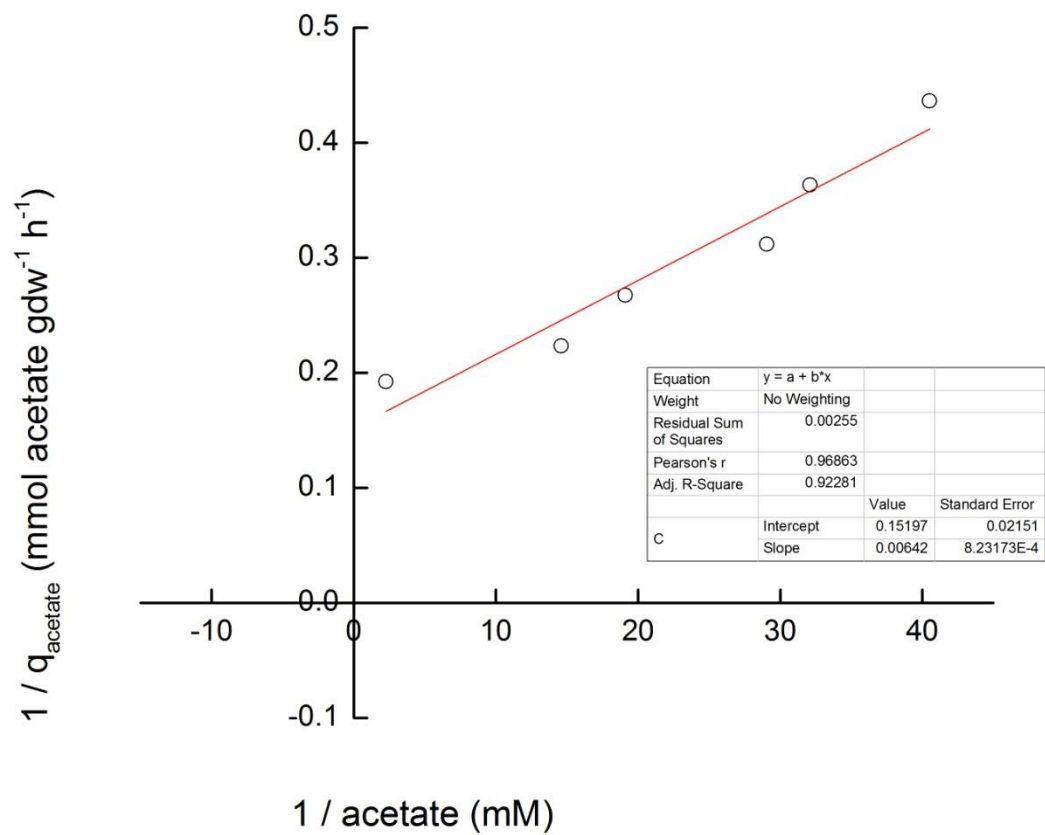


Figure C14: Lineweaver-Burk Linearization plot of the same data as Figure C13.

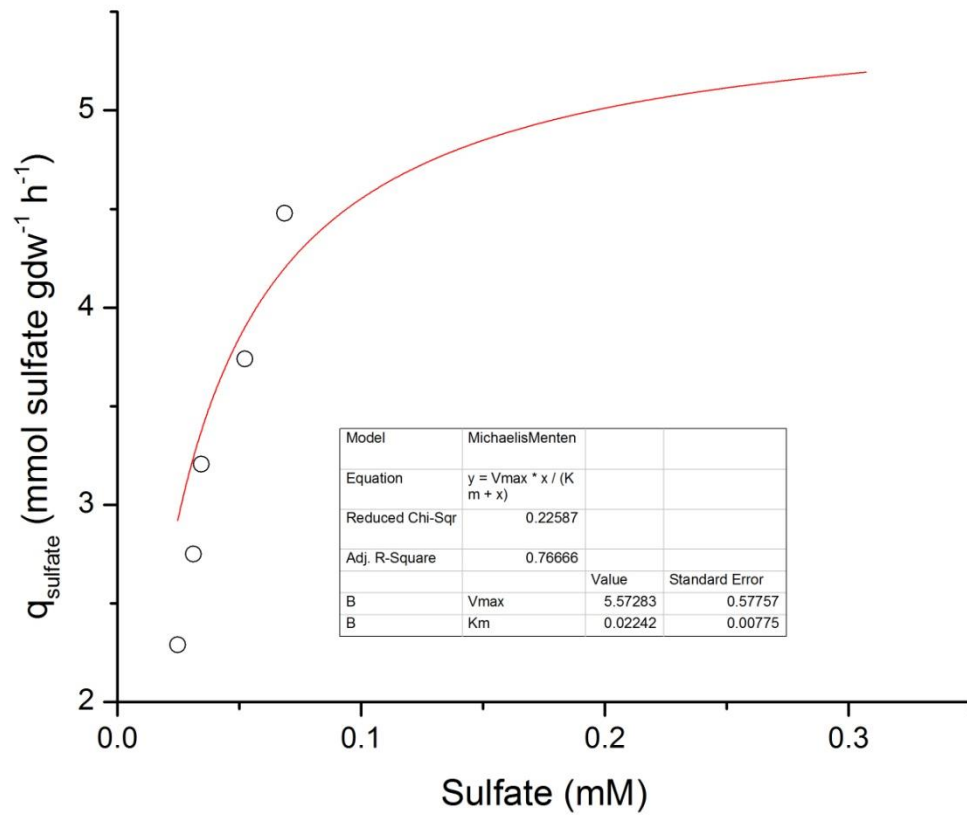


Figure C15: Michaelis-Menten type relationship that represents the effect of sulfate concentrations and specific sulfate consumption rates under sulfate-limited conditions. Each point represents the average of triplicate measurements.

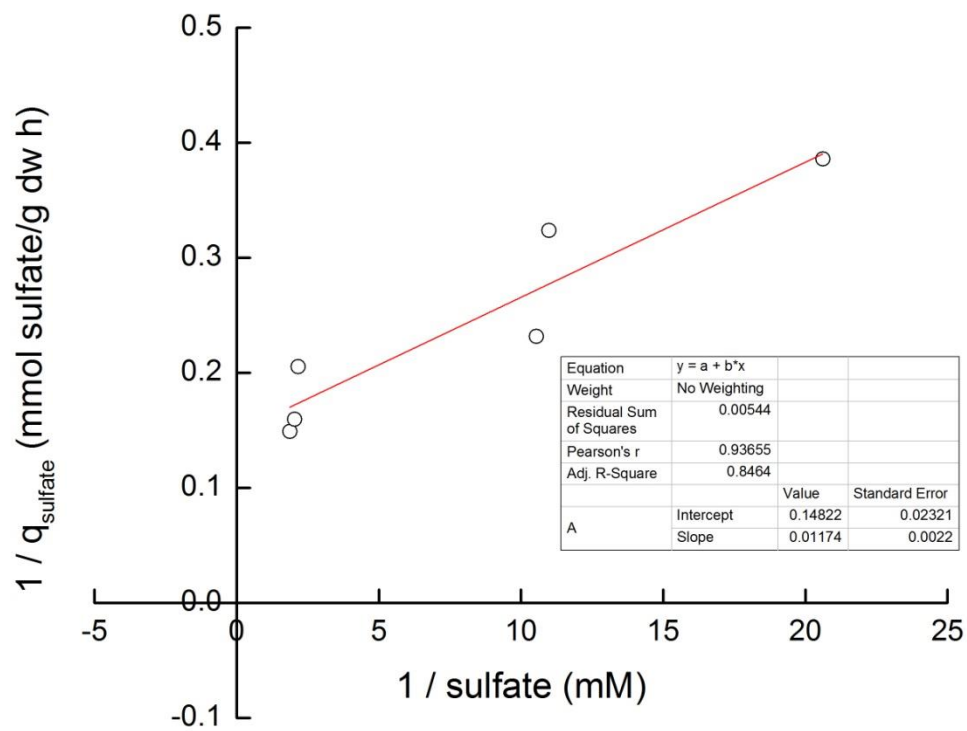


Figure C16: Lineweaver-Burk Linearization plot of the same data as Figure C15.

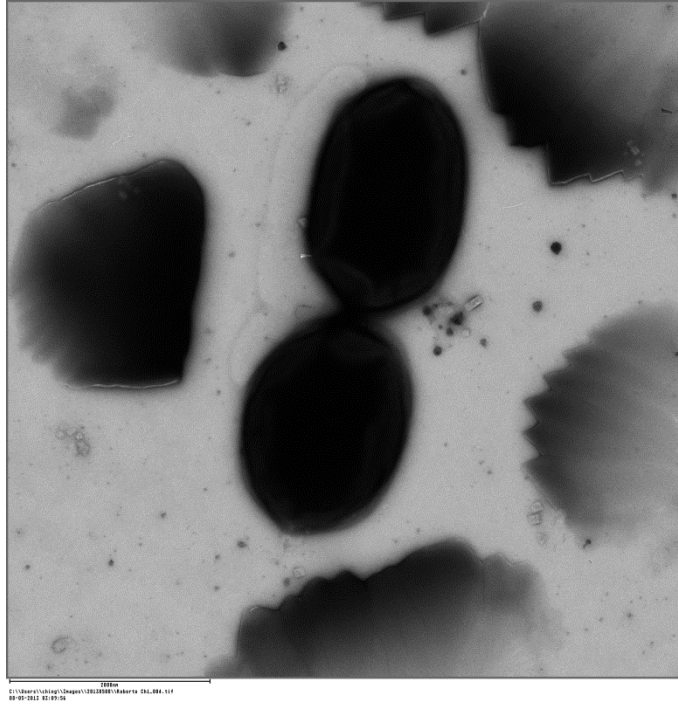


Figure C17: Transmission Electron Microscopy image of *D.postgatei* during growth in acetate-limiting chemostats at $D= 0.032 \text{ h}^{-1}$

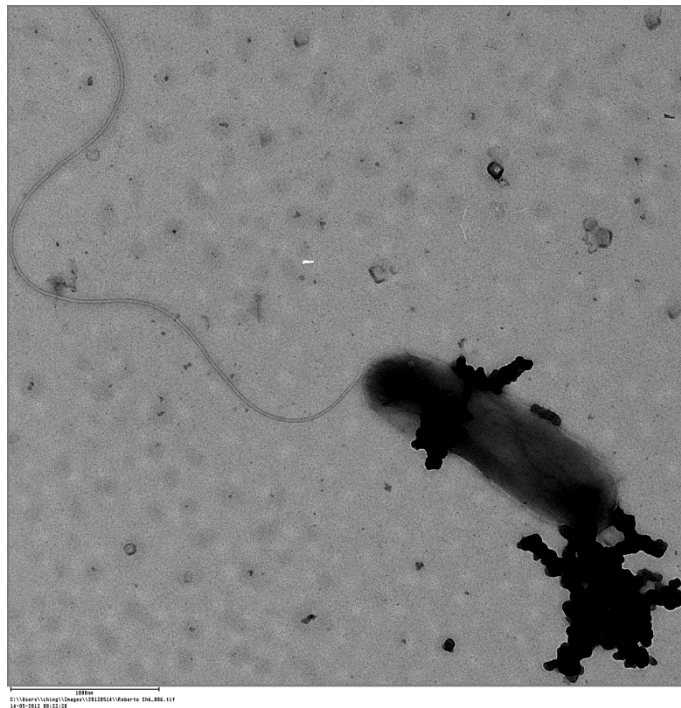


Figure C18: Transmission Electron Microscopy image of *D.postgatei* during growth in acetate-limiting chemostats at $D= 0.014 \text{ h}^{-1}$

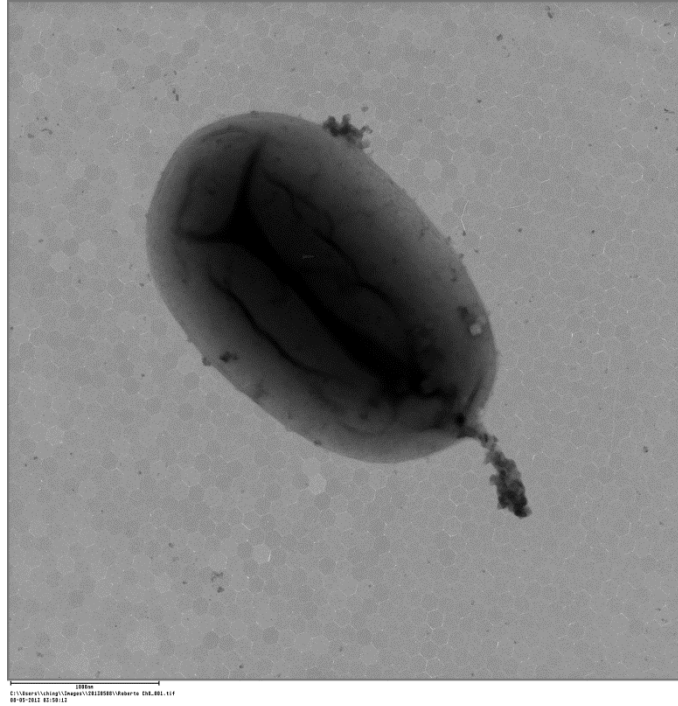


Figure C19: Transmission Electron Microscopy image of *D. postgatei* during growth in sulfate-limiting chemostats at $D= 0.032 \text{ h}^{-1}$

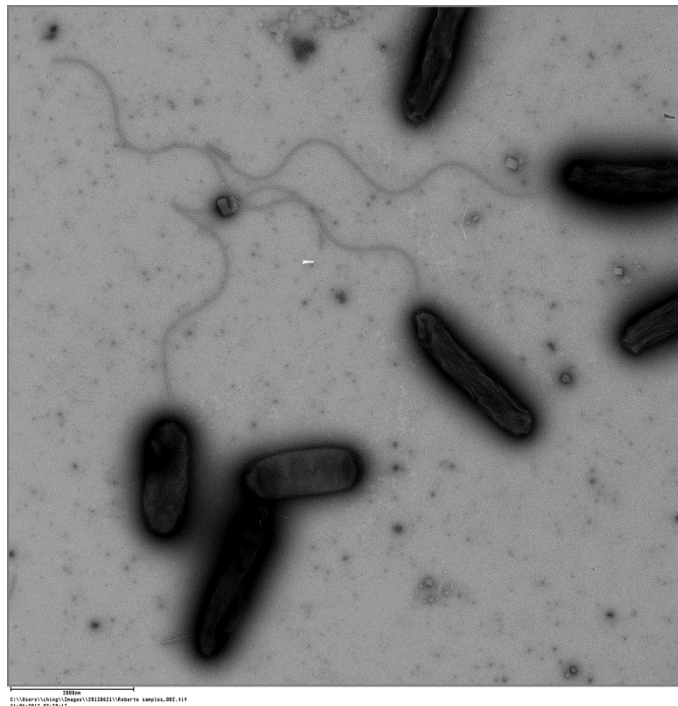


Figure C20: Transmission Electron Microscopy image of *D. postgatei* during growth in sulfate-limiting chemostats at $D= 0.014 \text{ h}^{-1}$

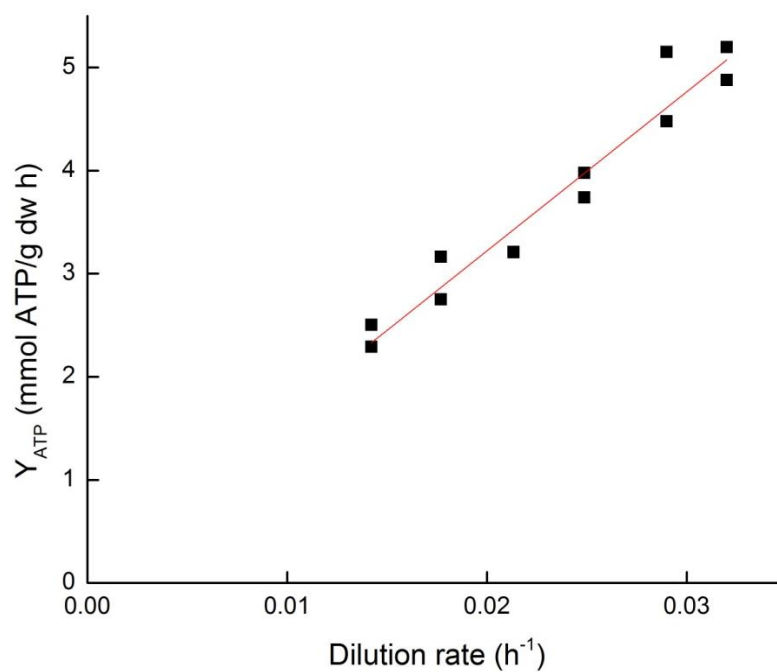


Figure C21: Y_{ATP} values of continuous cultures of *D.postgatei* during growth in both acetate and sulfate-limiting conditions. A projection drawn from the correlation to the Y-axis indicates the quantity of energy that is devoted to NGAM (Non-Growth Associated Maintenance energy).

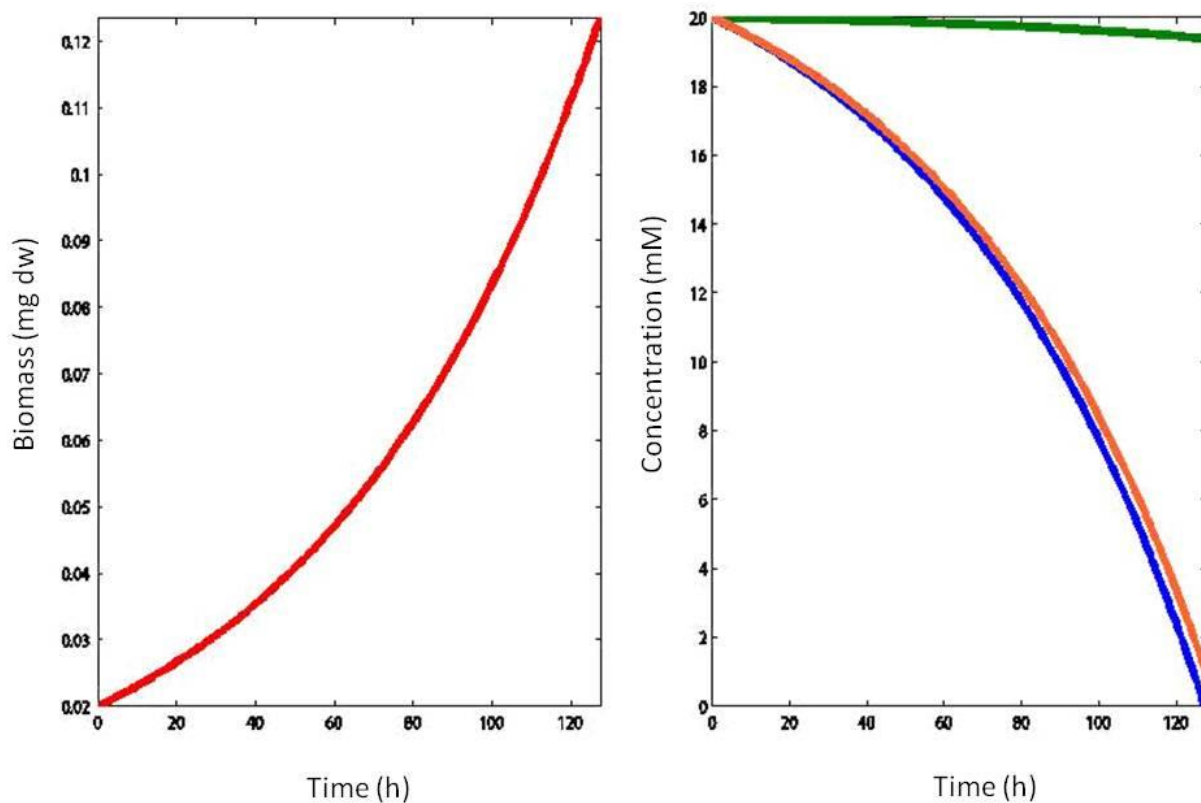


Figure C22: Dynamic flux balance analysis of *D.postgatei* model. The left graph indicates the biomass generation (red) and the right the acetate (blue), sulfate (orange), and ammonia (green) concentrations as a function of time.

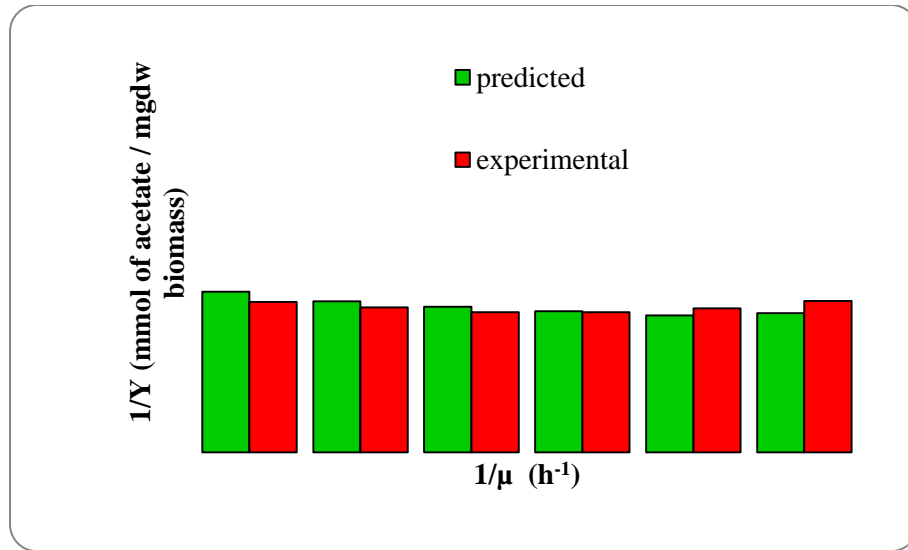


Figure C23: Validation of the *D.postgatei* metabolic model with experimental data. Reciprocal plot of predicted and experimental growth yields ($1/Y$) versus growth rates ($1/\mu$) in acetate limited chemostats.

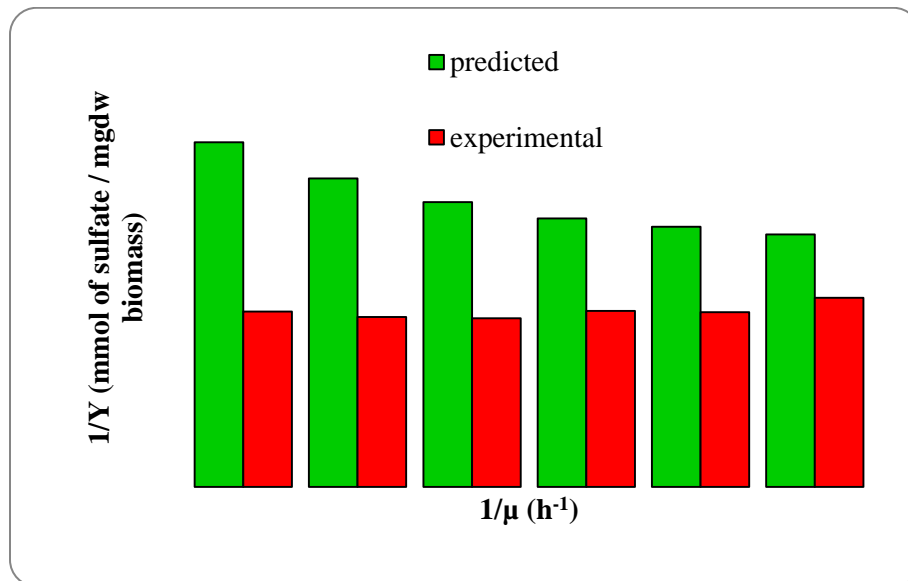


Figure C24: Validation of the *D.postgatei* metabolic model with experimental data. Reciprocal plot of predicted and experimental growth yields ($1/Y$) versus growth rates ($1/\mu$) in sulfate limited chemostats.

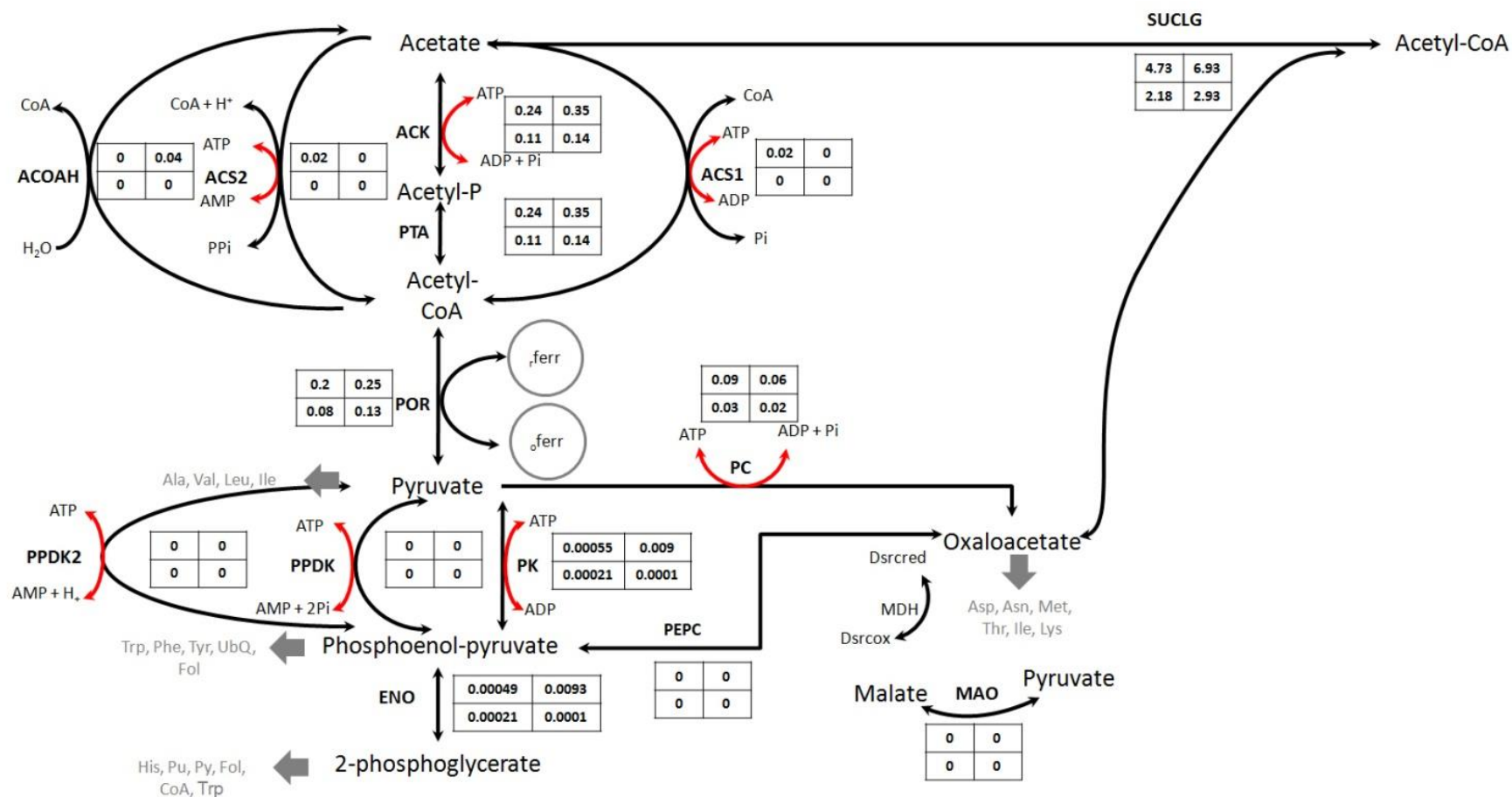


Figure C25: *In silico* flux estimation of a set of reactions responsible for acetate oxidation. The boxes besides the reactions correspond to the flux predicted per each reaction (mmol/gdw h) for *D.postgatei* cultures growing in chemostats. The numbers on the left column of the boxes correspond to acetate limited cultures growing at $D= 0.032 \text{ h}^{-1}$ (up) and $D= 0.014 \text{ h}^{-1}$ (down). The numbers on the right column correspond to sulfate limited cultures growing at $D= 0.032 \text{ h}^{-1}$ (up) and $D= 0.014 \text{ h}^{-1}$ (down). Abbreviations are the following: ACK, Acetate kinase; ACS1, Acetate-CoA ligase (ADP-forming); ACS2, Acetate-CoA ligase

(AMP-forming); POR, Pyruvate ferredoxin oxidoreductase; PK, Pyruvate kinase; PPDK, Pyruvate phosphate dikinase; PPDK2, Phosphoenolpyruvate synthase; PEPC, Phosphoenolpyruvate carboxylase; ENO, Enolase; MDH, Malate dehydrogenase ; MAO, Malate oxidoreductase, and SUCLG, Succinyl:acetate CoA transferase.

Note: for Figures C26 to C37, the numbers inside each metabolic representation indicate (1) citric acid cycle, (2) sulfate reduction pathway, (3) anapleurotic reactions, (4) ATP synthase, (5) Qrc (Quinone-reductase) complex, (6) Ehr (Ech-hydrogenase-related) complex, (7) Rnf (H⁺-translocating ferredoxin:NADP⁺ oxidoreductase) and Nfn (Ferredoxin:NADP oxidoreductase) complex. Abbreviations are the following: atp, ATP; 3pg, 3-Phospho-D-glycerate; 13dpg, 3-Phospho-D-glyceroyl phosphate; adp, ADP; ru5p-D, D-Ribulose 5-phosphate; n2, nitrogen; pan, Pantothenate; 2pg, D-Glycerate 2-phosphate; ac, Acetate; accoa, Acetyl-CoA; acon-C, cis-Aconitate; actp, Acetyl phosphate; adp, ADP; akg, 2-Oxoglutarate; amp, Adenosine Monophosphate; aps, Adenosine 5'-phosphosulfate; cit, Citrate; co2, carbon dioxide; coa, Coenzyme A; dhap, Dihydroxyacetone phosphate; DsrCred, DsrC cytochrome - reduced; DsrCrox, DsrC cytochrome - oxidized; e4p, D-Erythrose 4-phosphate; f6p, D-Fructose 6-phosphate; Fdox, Oxidized ferredoxin; fdp, D-Fructose 1,6-bisphosphate; Fdred, Reduced ferredoxin; fol, folate; for, Formate; fum, Fumarate; g3p, Glyceraldehyde 3-phosphate; glu-L, L-Glutamate; h, H⁺; h2o, H₂O; h2s, H₂S; icit, Isocitrate; mal-L, L-Malate; mk, Quinone; mkh2, Quinol, nad, Nicotinamide adenine dinucleotide; nadh, Nicotinamide adenine dinucleotide - reduced; nadp, Nicotinamide adenine dinucleotide phosphate; nadph, Nicotinamide adenine dinucleotide phosphate - reduced; nh4, Ammonium; oaa, Oxaloacetate; pep, Phosphoenolpyruvate; pi, Phosphate; pyr, Pyruvate; r5p, alpha-D-Ribose 5-phosphate; s7p, Sedoheptulose 7-phosphate; so3, SO₃; so4, SO₄; succ, Succinate; succoa, Succinyl-CoA; xu5p-D, D-Xylulose 5-phosphate.

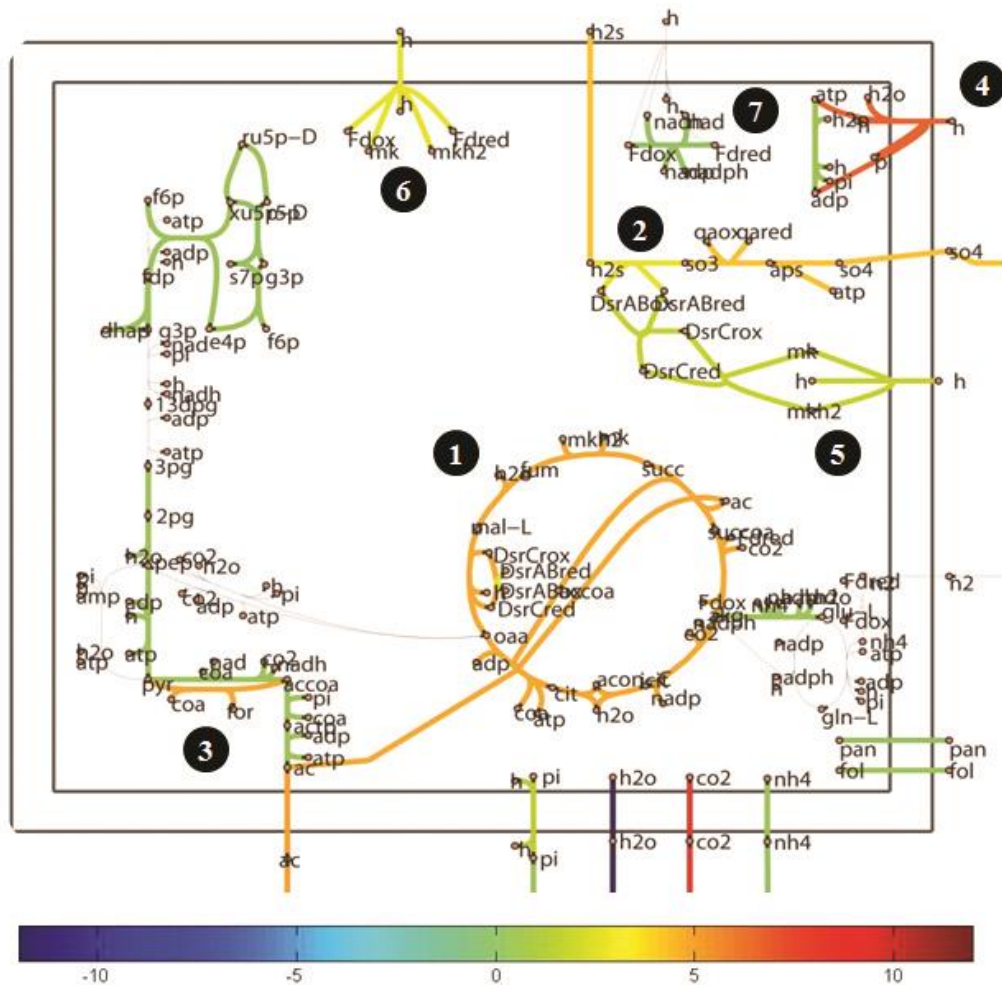


Figure C26: Representative portion of the metabolism of *D. postgatei* growing under electron donor limitation at 0.032 h^{-1} . The color of the line between metabolites indicates the flux rate for each reaction in mmol/gdw h (see numbers in color bar).

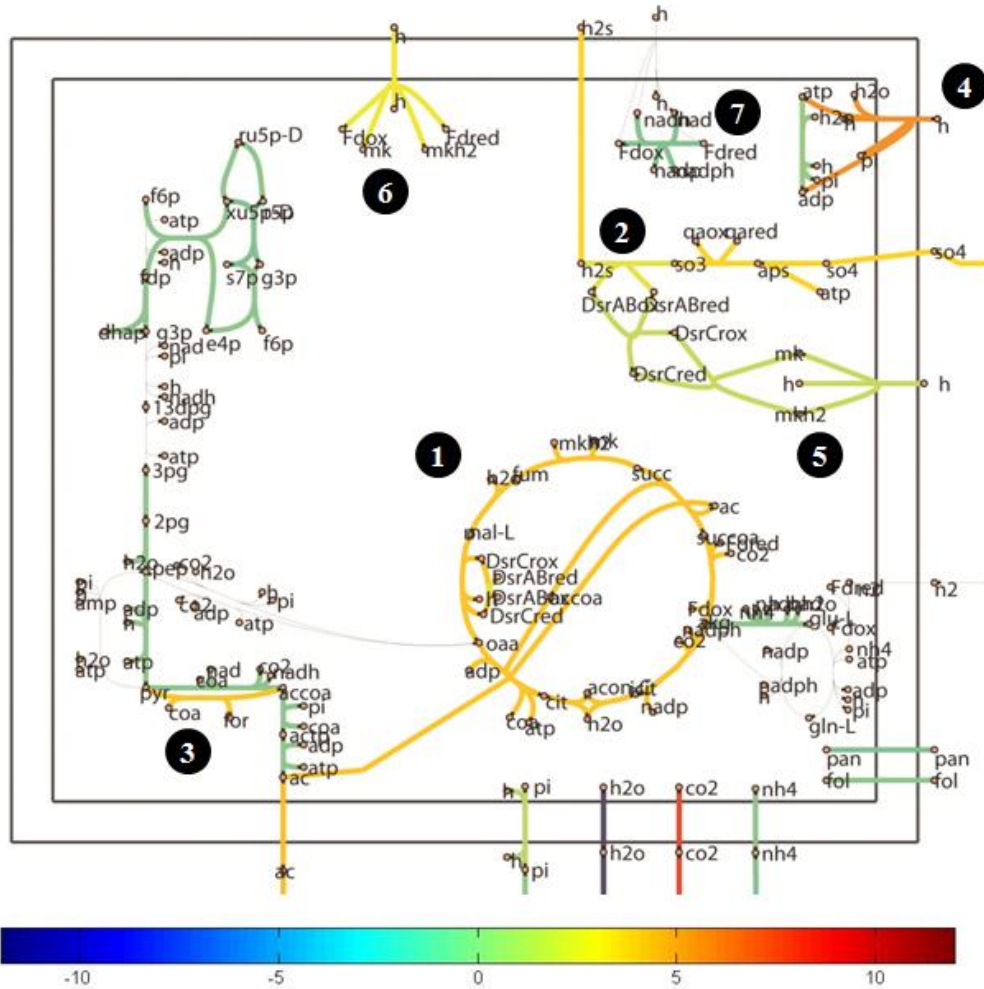


Figure C27: Representative portion of the metabolism of *D. postgatei* growing under electron donor limitation at 0.028 h^{-1} . The color of the line between metabolites indicates the flux rate for each reaction in mmol/gdw h (see numbers in color bar).

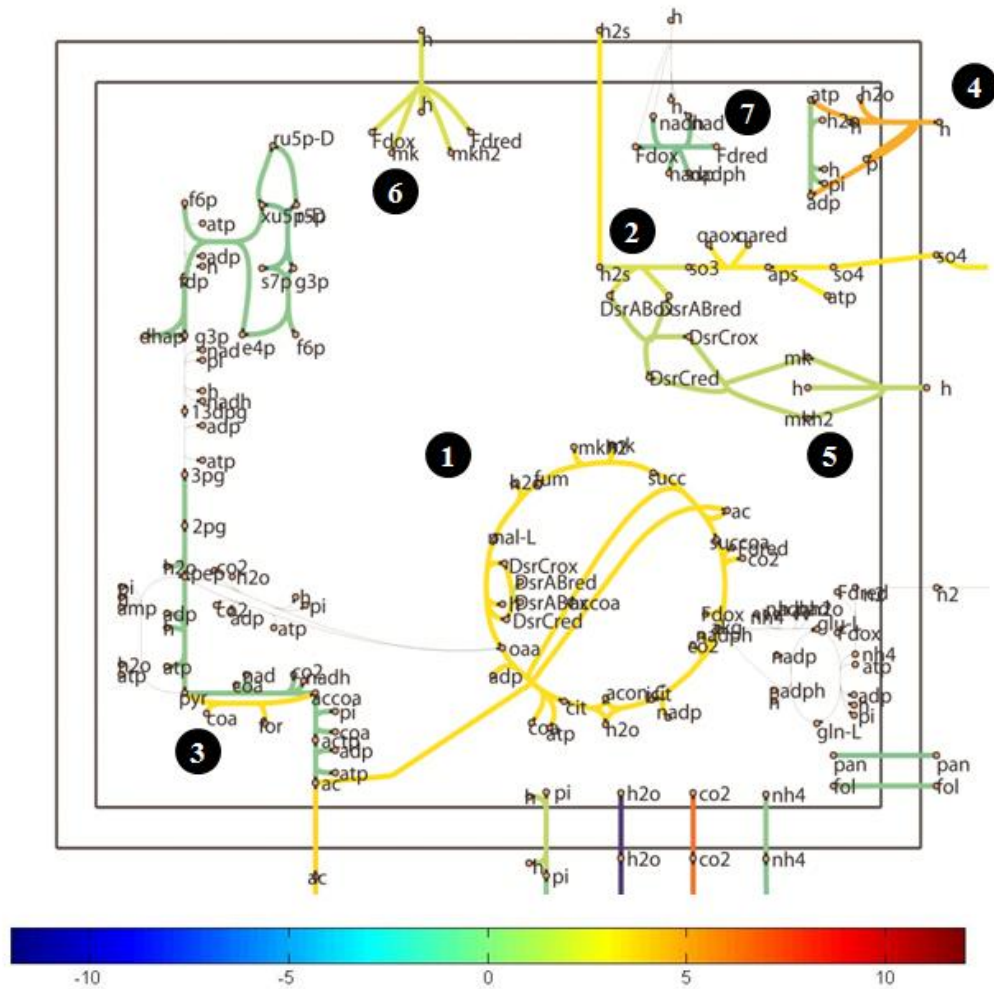


Figure C28: Representative portion of the metabolism of *D. postgatei* growing under electron donor limitation at 0.024 h^{-1} . The color of the line between metabolites indicates the flux rate for each reaction in mmol/gdw h (see numbers in color bar).

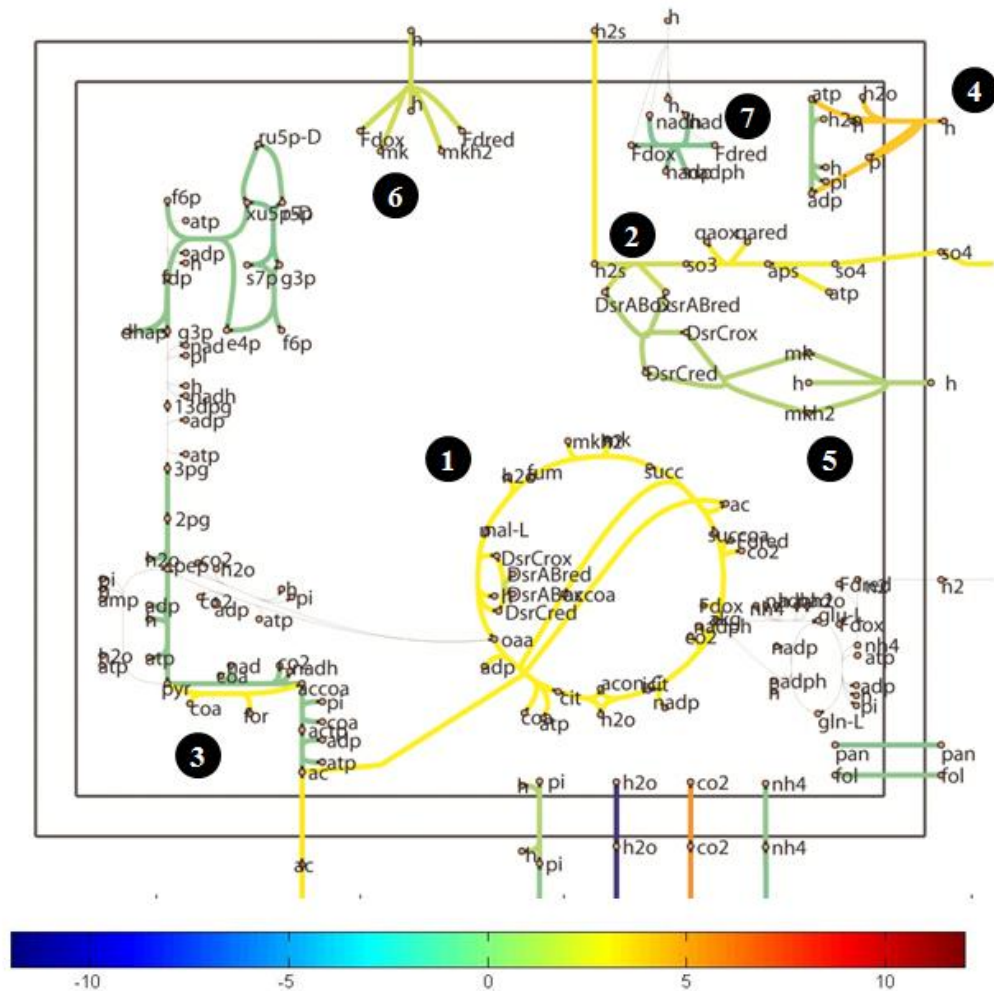


Figure C29: Representative portion of the metabolism of *D. postgatei* growing under electron donor limitation at 0.021 h^{-1} . The color of the line between metabolites indicates the flux rate for each reaction in mmol/gdw h (see numbers in color bar).

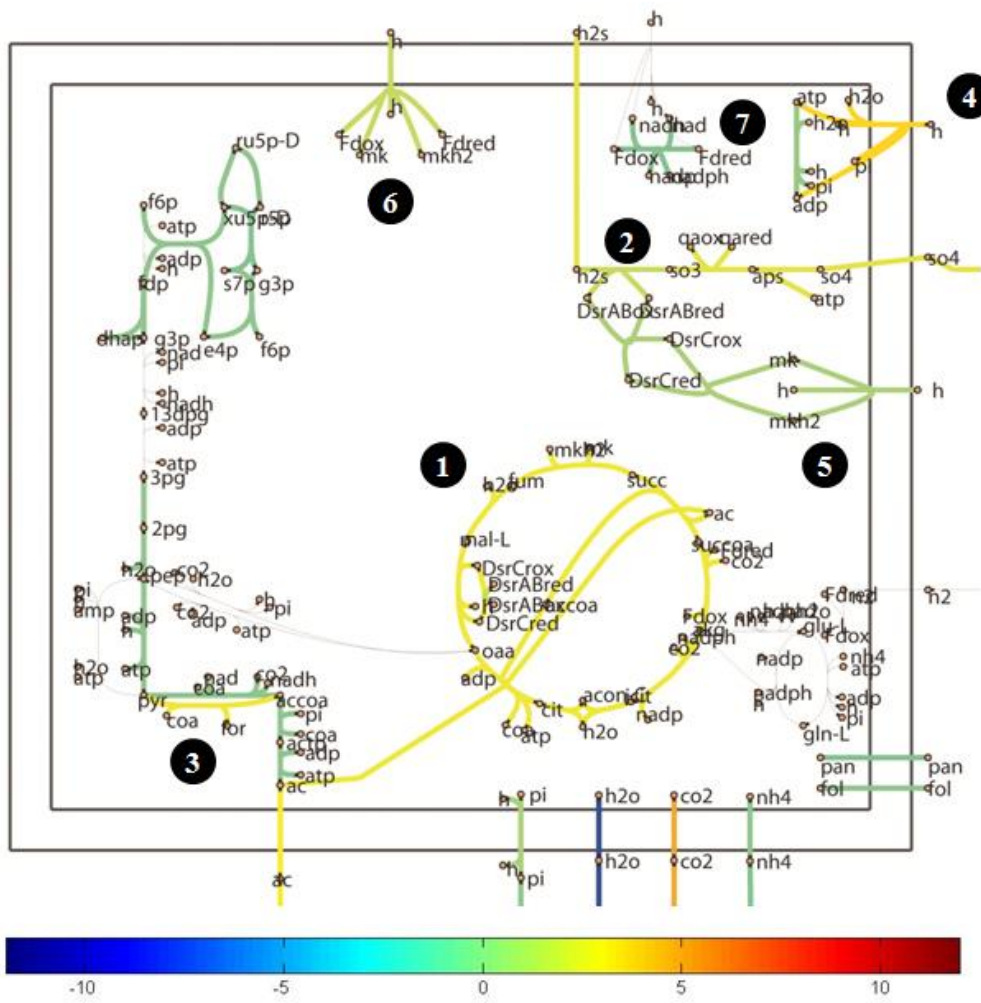


Figure C30: Representative portion of the metabolism of *D.postgatei* growing under electron donor limitation at 0.017 h^{-1} . The color of the line between metabolites indicates the flux rate for each reaction in mmol/gdw h (see numbers in color bar).

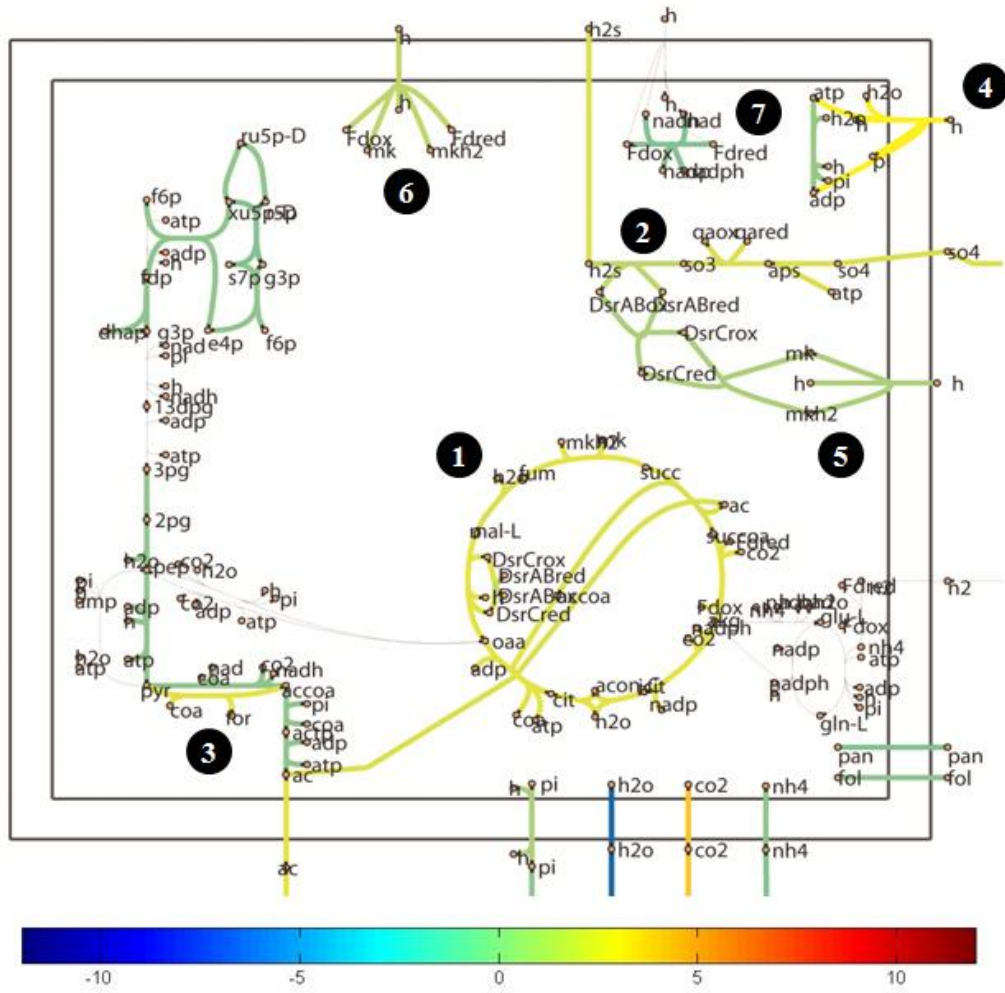


Figure C31: Representative portion of the metabolism of *D. postgatei* growing under electron donor limitation at 0.014 h^{-1} . The color of the line between metabolites indicates the flux rate for each reaction in mmol/gdw h (see numbers in color bar).

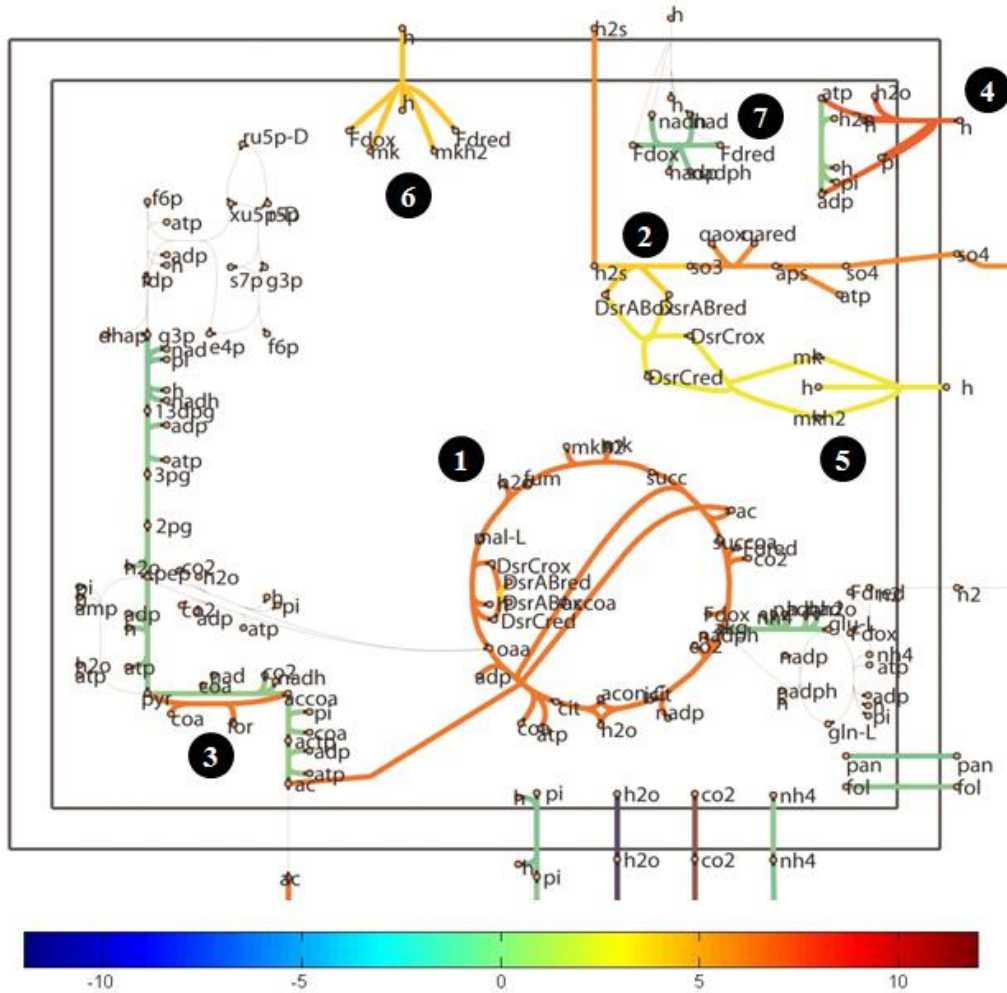


Figure C32: Representative portion of the metabolism of *D. postgatei* growing under electron acceptor limitation at 0.032 h^{-1} . The color of the line between metabolites indicates the flux rate for each reaction in mmol/gdw h (see numbers in color bar).

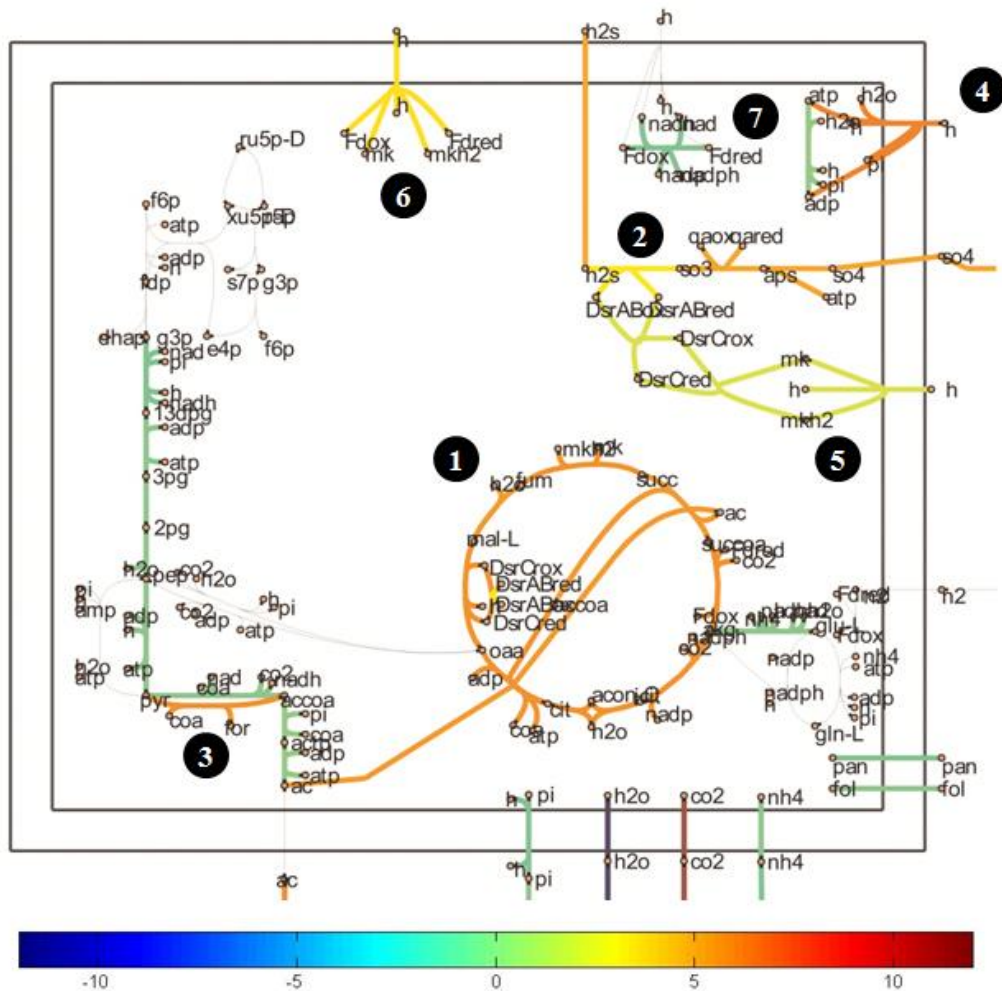


Figure C33: Representative portion of the metabolism of *D. postgatei* growing under electron acceptor limitation at 0.028 h^{-1} . The color of the line between metabolites indicates the flux rate for each reaction in mmol/gdw h (see numbers in color bar).

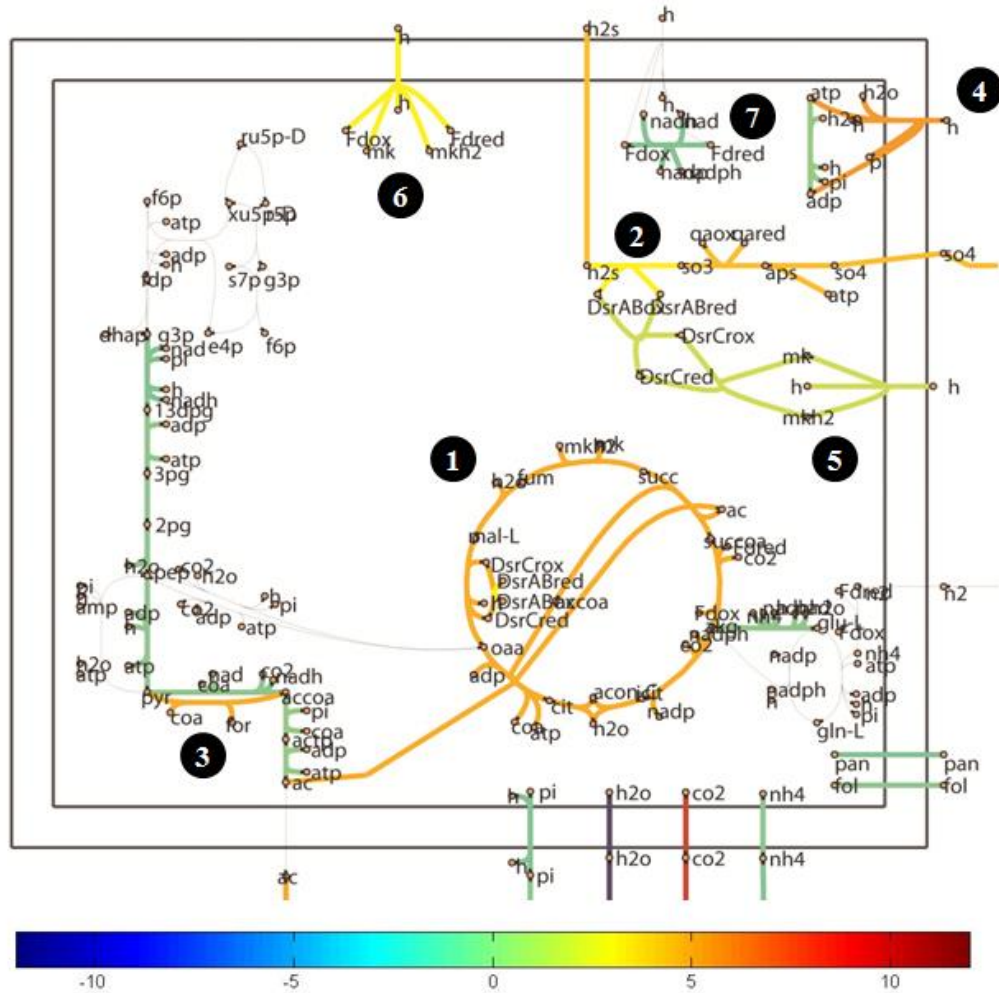


Figure C34: Representative portion of the metabolism of *D. postgatei* growing under electron acceptor limitation at 0.024 h⁻¹. The color of the line between metabolites indicates the flux rate for each reaction in mmol/gdw h (see numbers in color bar).

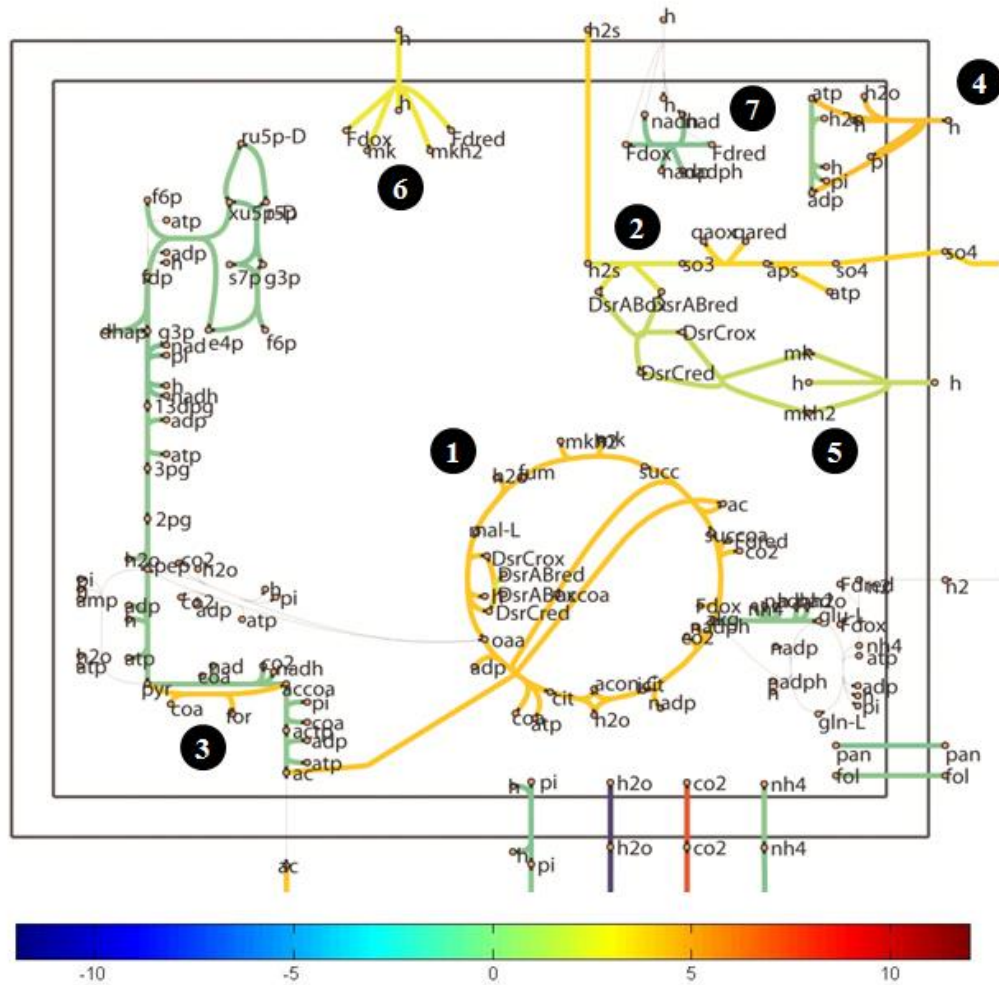


Figure C35: Representative portion of the metabolism of *D. postgatei* growing under electron acceptor limitation at 0.021 h^{-1} . The color of the line between metabolites indicates the flux rate for each reaction in mmol/gdw h (see numbers in color bar).

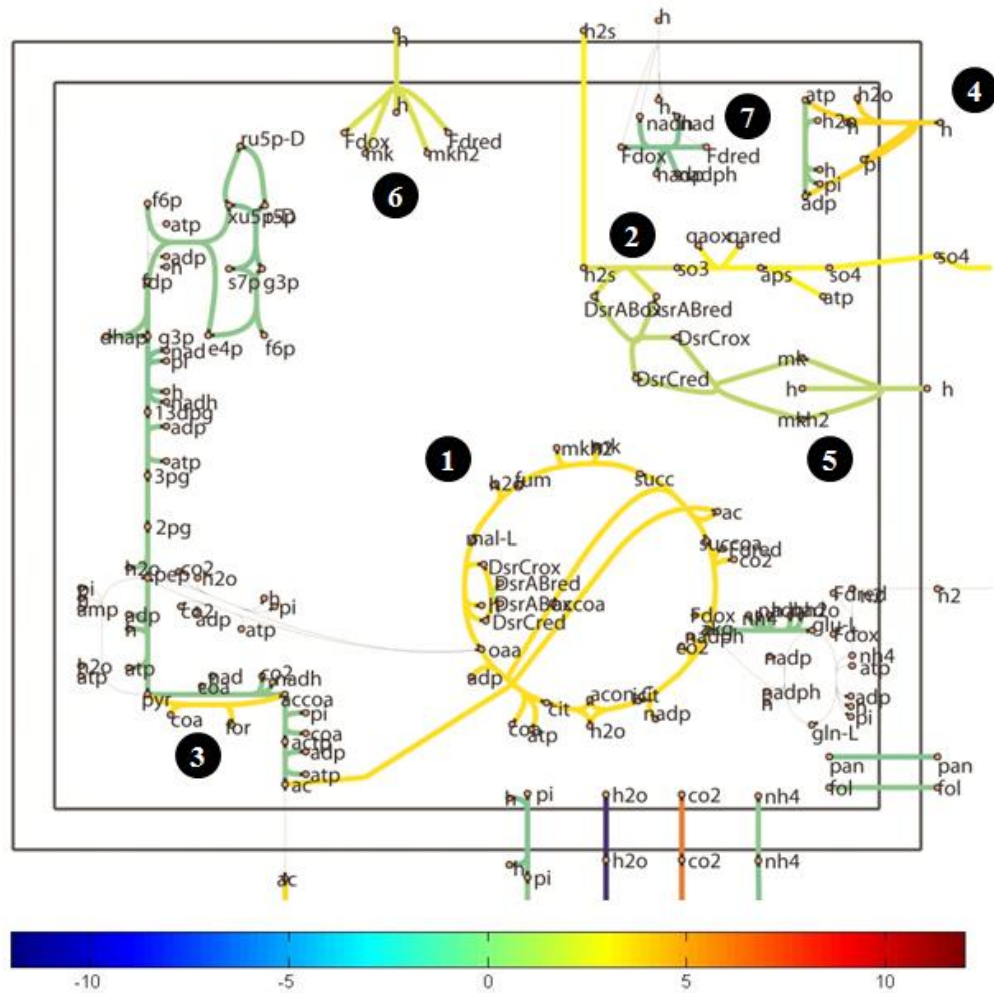


Figure C36: Representative portion of the metabolism of *D. postgatei* growing under electron acceptor limitation at 0.017 h^{-1} . The color of the line between metabolites indicates the flux rate for each reaction in mmol/gdw h (see numbers in color bar).

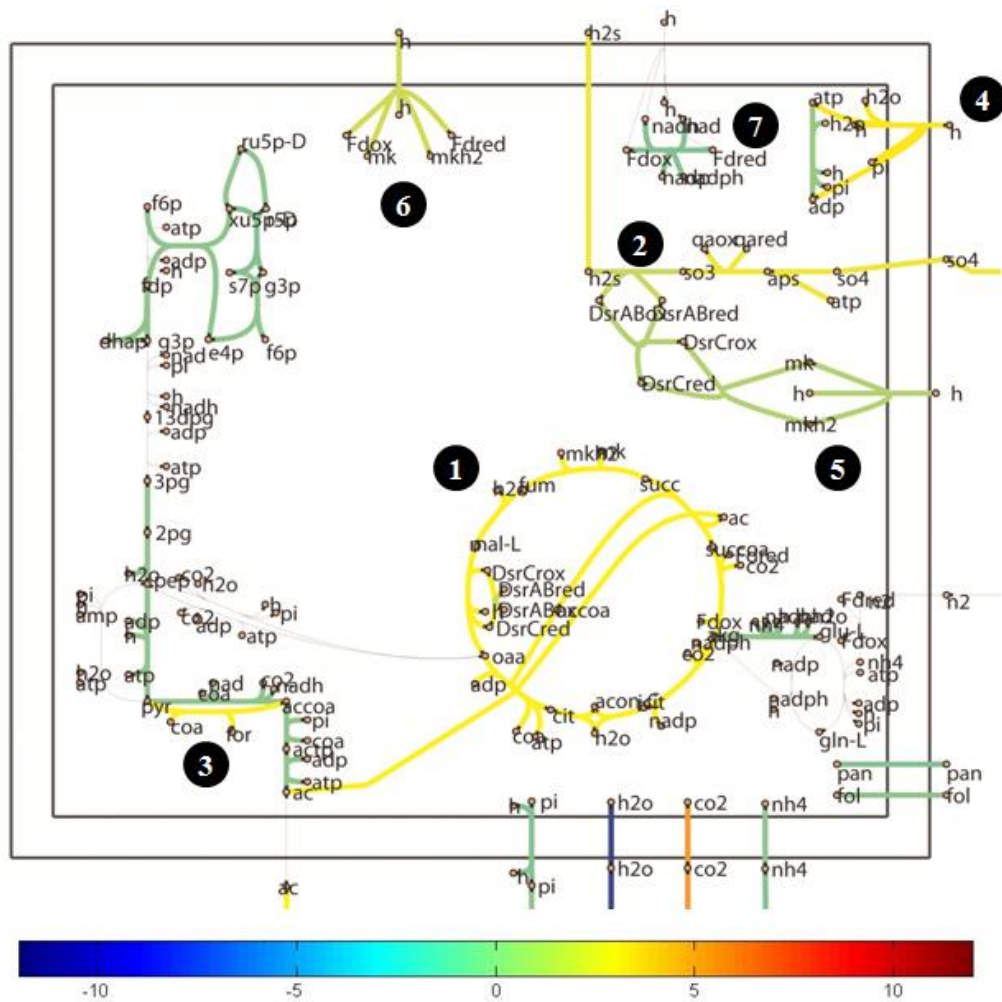


Figure C37: Representative portion of the metabolism of *D. postgatei* growing under electron acceptor limitation at 0.014 h^{-1} . The color of the line between metabolites indicates the flux rate for each reaction in mmol/gdw h (see numbers in color bar).

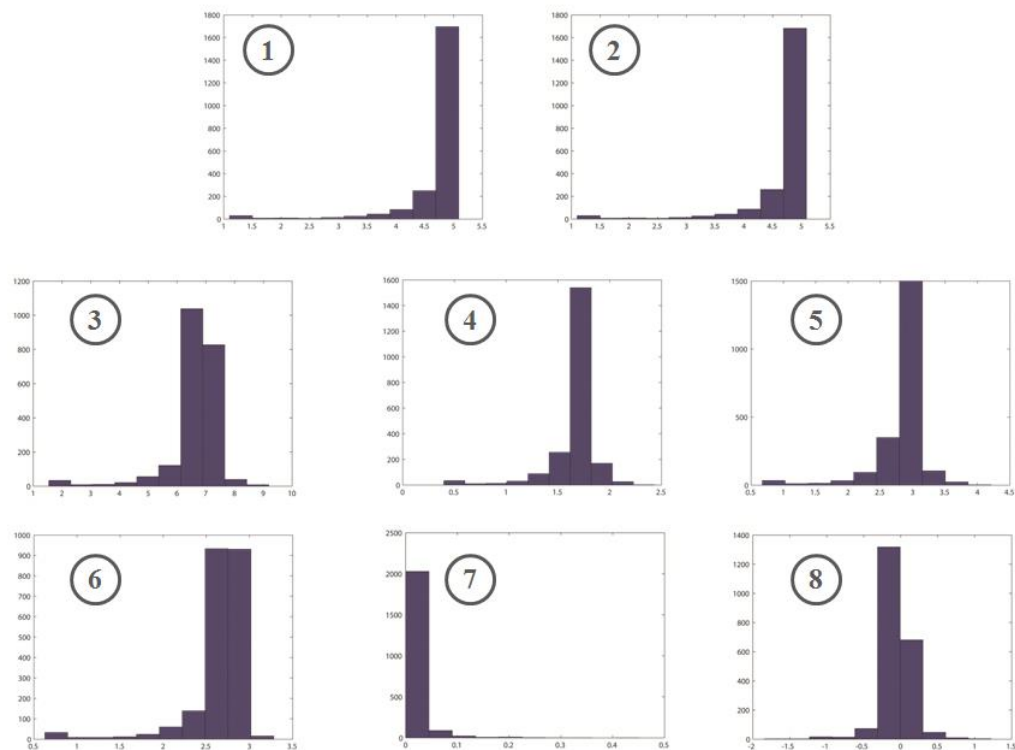


Figure C38: Probability flux distributions of *D.postgatei* growing under electron donor limitation at 0.032 h^{-1} . The *D.postgatei* metabolic model with imposed maximum and minimum constraints on each flux was sampled using the *in silico* Monte Carlo procedure. The histograms of each reaction represent the distribution of solutions (y-axis) with respect to each reaction flux (x-axis, in mmol/gdw h). Reactions correspond as following: (1) ATP citrate lyase, (2) 2-oxoglutarate ferredoxin oxidoreductase, (3) ATP synthase, (4) Qrc complex, (5) Ferredoxin:menaquinone oxidoreductase, (6) Dissimilatory sulfite reductase, (7) H^+ -translocating ferredoxin: NAD^+ oxidoreductase (Rnf), (8) NADH-dependent ferredoxin:NADP oxidoreductase (Nfn).

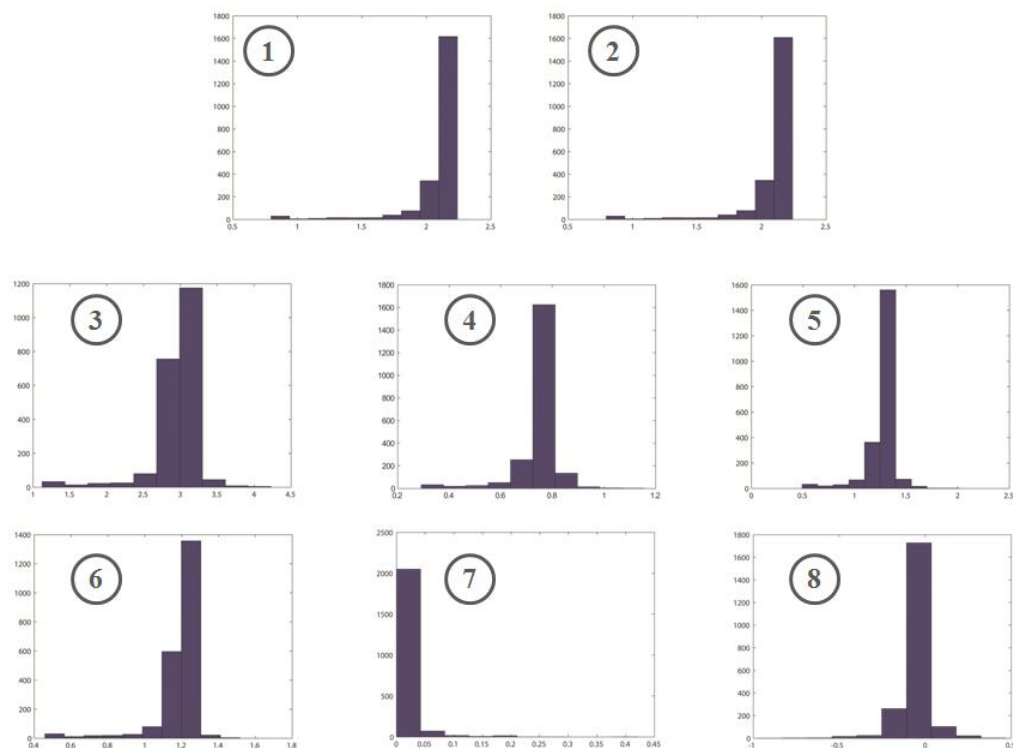


Figure C39: Probability flux distributions of *D.postgatei* growing under electron donor limitation at 0.014 h^{-1} . The *D.postgatei* metabolic model with imposed maximum and minimum constraints on each flux was sampled using the *in silico* Monte Carlo procedure. The histograms of each reaction represent the distribution of solutions (y-axis) with respect to each reaction flux (x-axis, in mmol/gdw h). Reactions correspond as following: (1) ATP citrate lyase, (2) 2-oxoglutarate ferredoxin oxidoreductase, (3) ATP synthase, (4) Qrc complex, (5) Ferredoxin:menaquinone oxidoreductase, (6) Dissimilatory sulfite reductase, (7) H⁺-translocating ferredoxin:NAD⁺ oxidoreductase (Rnf), (8) NADH-dependent ferredoxin:NADP oxidoreductase (Nfn).

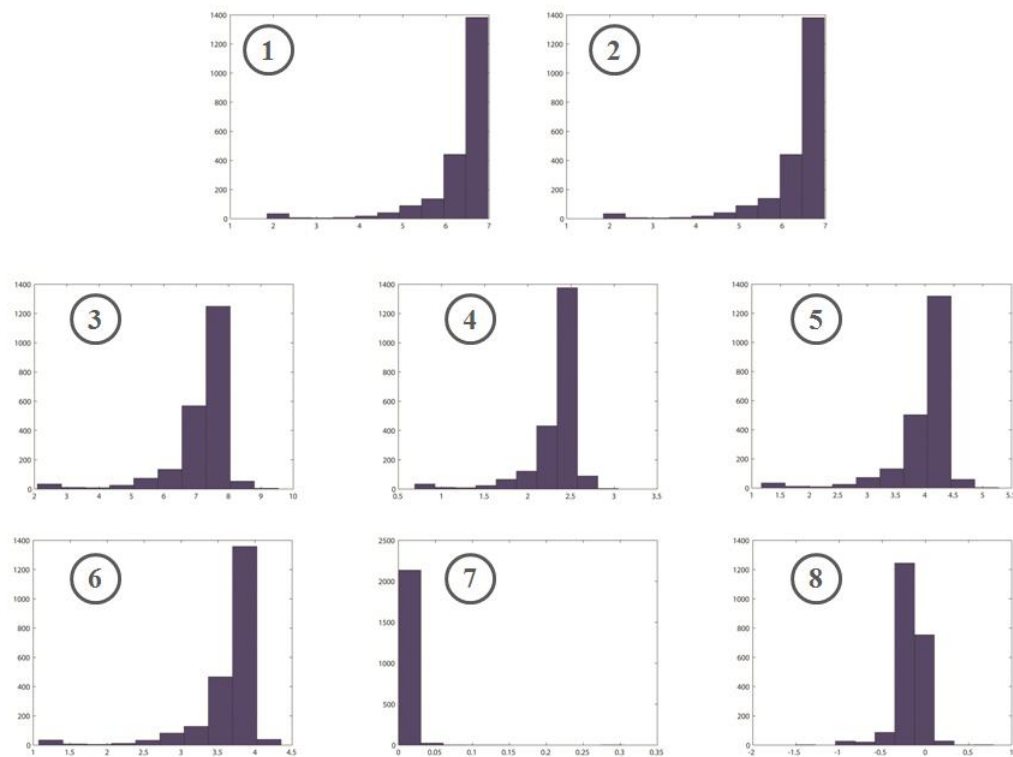


Figure C40: Probability flux distributions of *D.postgatei* growing under electron acceptor limitation at 0.032 h^{-1} . The *D.postgatei* metabolic model with imposed maximum and minimum constraints on each flux was sampled using the *in silico* Monte Carlo procedure. The histograms of each reaction represent the distribution of solutions (y-axis) with respect to each reaction flux (x-axis, in mmol/gdw h). Reactions correspond as following: (1) ATP citrate lyase, (2) 2-oxoglutarate ferredoxin oxidoreductase, (3) ATP synthase, (4) Qrc complex, (5) Ferredoxin:menaquinone oxidoreductase, (6) Dissimilatory sulfite reductase, (7) H⁺-translocating ferredoxin:NAD⁺ oxidoreductase (Rnf), (8) NADH-dependent ferredoxin:NADP oxidoreductase (Nfn).

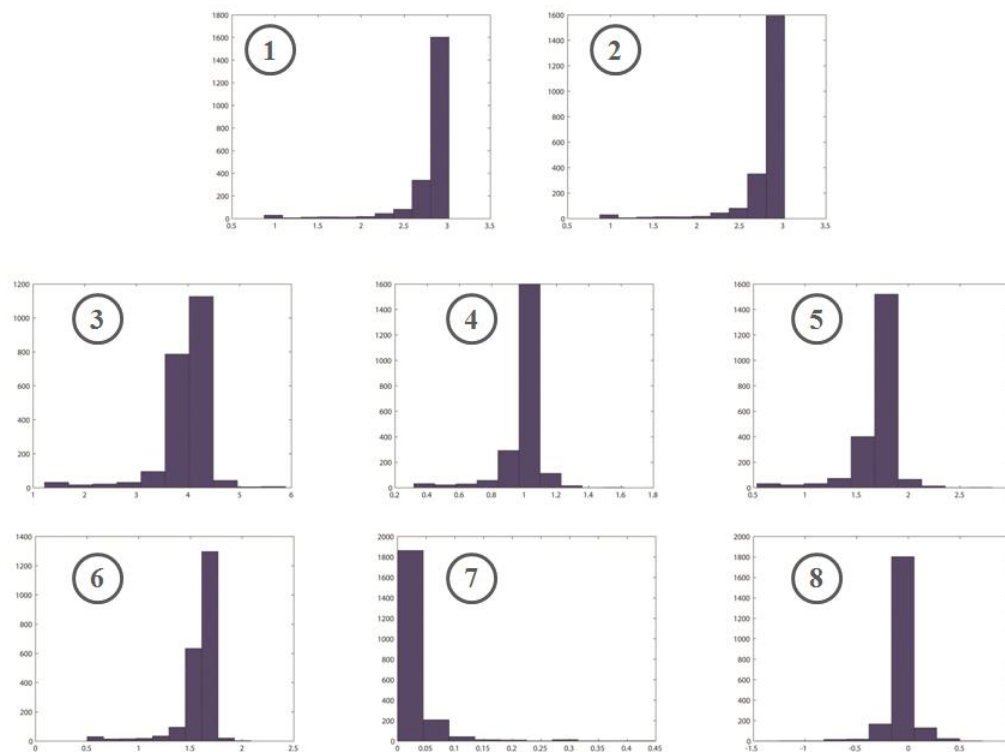


Figure C41: Probability flux distributions of *D.postgatei* growing under electron acceptor limitation at 0.014 h^{-1} . The *D.postgatei* metabolic model with imposed maximum and minimum constraints on each flux was sampled using the *in silico* Monte Carlo procedure. The histograms of each reaction represent the distribution of solutions (y-axis) with respect to each reaction flux (x-axis, in mmol/gdw h). Reactions correspond as following: (1) ATP citrate lyase, (2) 2-oxoglutarate ferredoxin oxidoreductase, (3) ATP synthase, (4) Qrc complex, (5) Ferredoxin:menaquinone oxidoreductase, (6) Dissimilatory sulfite reductase, (7) H⁺-translocating ferredoxin:NAD⁺ oxidoreductase (Rnf), (8) NADH-dependent ferredoxin:NADP oxidoreductase (Nfn).

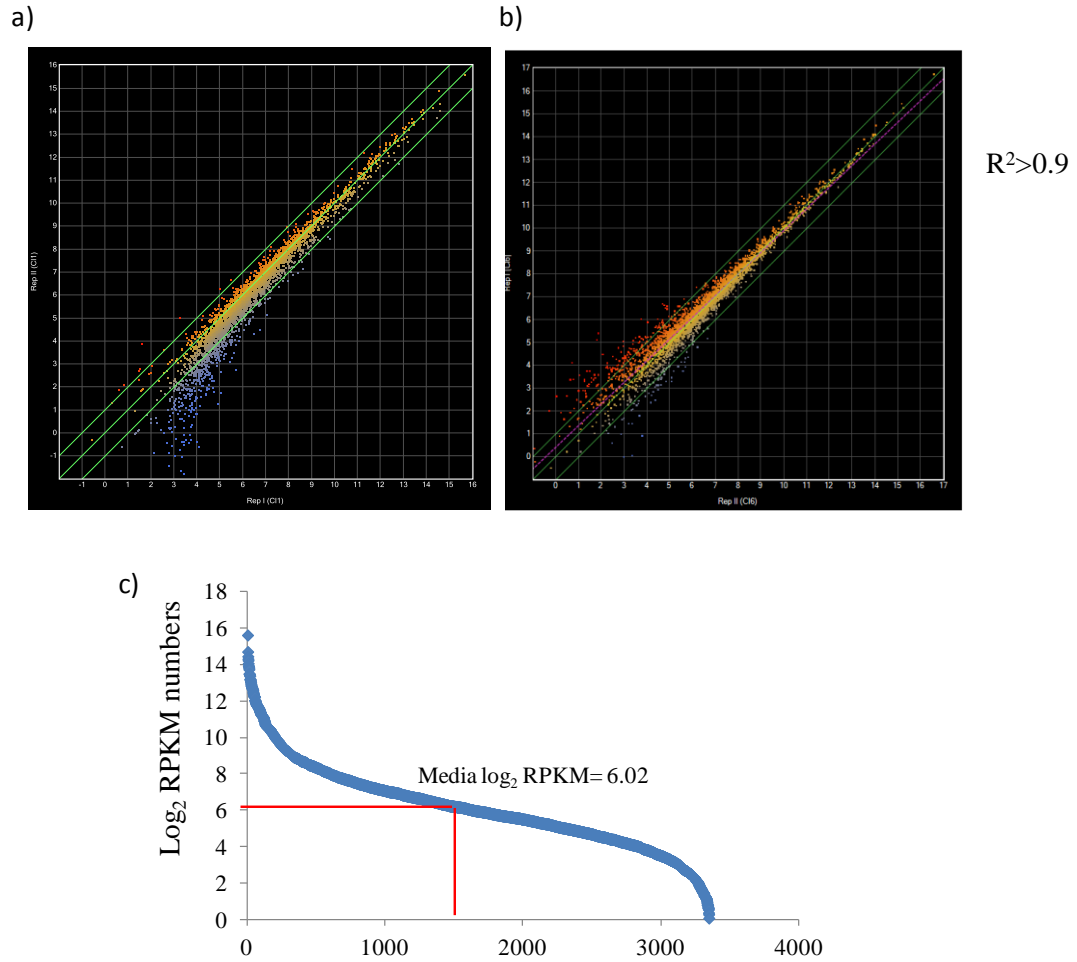


Figure C42 (a) Scatter plot showing comparison of gene expression levels in replicate culture of *D. postgatei* growing under electron donor (acetate) limitation at (a)0.032 h⁻¹ and (b)0.014 h⁻¹. Each data point on the scatter plot represents an individual gene and is plotted based on its expression level in both of the selected experiments. Median log₂ RPKM value calculation. Only the gene expression levels above the median log₂ RPKM values were treated as the significant expression.

Table C18: Genes that were differentially expressed at least two fold in *D. postgatei* growing at 0.032 h⁻¹ compared to those growing at 0.014 h⁻¹ (P-value cutoff less than or equal to 0.05). Positive and negative numbers indicate up- and down-regulated genes at 0.032 h⁻¹.

Locus tag	Function	Fold change	P value
DespoDRAFT_00001	hypothetical protein	-1.457	0.431
DespoDRAFT_00002	hypothetical protein	-1.505	0.608
DespoDRAFT_00003	hypothetical protein	-1.51	0.586
DespoDRAFT_00009	transcriptional regulator	1.145	0.103
DespoDRAFT_00011	hypothetical protein	-6.588	0.24
DespoDRAFT_00014	hypothetical protein	1.708	0.36
DespoDRAFT_00020	hypothetical protein	-1.488	0.28
DespoDRAFT_00023	putative addiction module killer protein	-1.349	0.502
DespoDRAFT_00024	putative addiction module antidote protein	-1.914	0.0557
DespoDRAFT_00028	transcriptional regulator containing GAF, AAA-type ATPase, and DNA binding domains	1.197	0.336
DespoDRAFT_00031	hypothetical protein	-1.522	0.472
DespoDRAFT_00032	HD superfamily phosphohydrolase	1.485	0.498
DespoDRAFT_00033	hypothetical protein	-3.654	0.383
DespoDRAFT_00034	glyceraldehyde-3-phosphate dehydrogenase/erythrose-4-phosphate dehydrogenase	-1.483	0.119
DespoDRAFT_00035	Pyruvate kinase	-1.411	0.112
DespoDRAFT_00036	hypothetical protein	-1.243	0.16
DespoDRAFT_00037	Pyruvate kinase	-1.195	0.783
DespoDRAFT_00038	hypothetical protein	1.199	0.766
DespoDRAFT_00039	putative permease	1.059	0.95
DespoDRAFT_00040	response regulator with CheY-like receiver, AAA-type ATPase, and DNA-binding domains	-3.349	0.0957
DespoDRAFT_00041	vitamin B12 dependent methionine synthase	-1.065	0.611
DespoDRAFT_00042	Homocysteine S-methyltransferase	1.207	0.16
DespoDRAFT_00043	hypothetical protein	-1.386	0.679
DespoDRAFT_00044	signal transduction histidine kinase	-2.14	0.187
DespoDRAFT_00045	diguanylate cyclase (GGDEF) domain-containing protein	-1.922	0.095
DespoDRAFT_00048	hypothetical protein	-1.416	NaN
DespoDRAFT_00049	glycogen synthase	-1.402	0.27
DespoDRAFT_00050	ADP-ribose pyrophosphatase	-1.496	0.0743
DespoDRAFT_00054	cobalamin biosynthesis protein CbiK, Co ²⁺ chelatase	-1.002	0.994

DespoDRAFT_00055	putative metal-binding protein	1.153	0.616
DespoDRAFT_00056	putative phosphohydrolase	-1.312	0.287
DespoDRAFT_00057	P-type ATPase, translocating	1.087	0.688
DespoDRAFT_00058	hypothetical protein	1.978	0.344
DespoDRAFT_00059	putative domain HDIG-containing protein	-1.149	0.565
DespoDRAFT_00060	peptide chain release factor 2	-1.142	0.359
DespoDRAFT_00061	apolipoprotein N-acyltransferase	1.361	0.557
DespoDRAFT_00062	Response regulator receiver domain protein, histidine kinase	-2.166	0.317
DespoDRAFT_00063	molecular chaperone (small heat shock protein)	-1.226	0.861
DespoDRAFT_00064	ATP-dependent protease La	-1.52	0.294
DespoDRAFT_00065	rare lipoprotein A	-1.164	0.721
DespoDRAFT_00066	histidinol-phosphate phosphatase family protein	1.063	0.875
DespoDRAFT_00067	helicase, putative, RecD/TraA family	1.186	0.759
DespoDRAFT_00068	hypothetical protein	1.344	0.334
DespoDRAFT_00069	hypothetical protein	#VALUE!	NaN
DespoDRAFT_00070	transcription termination factor	1.752	0.126
DespoDRAFT_00071	ATP-dependent protease La	1.292	0.09
DespoDRAFT_00072	endopeptidase Clp ATP-binding regulatory subunit ClpX	-1.071	0.553
DespoDRAFT_00073	ATP-dependent Clp protease, proteolytic subunit ClpP	-1.354	0.0359
DespoDRAFT_00074	trigger factor	2.275	0.00431
DespoDRAFT_00076	site-specific recombinase XerD	1.101	0.949
DespoDRAFT_00077	TraX protein	-2.368	0.574
DespoDRAFT_00078	hypothetical protein	-1.275	NaN
DespoDRAFT_00079	hypothetical protein	1.038	0.985
DespoDRAFT_00080	hypothetical protein	#VALUE!	NaN
DespoDRAFT_00081	hypothetical protein	-1.499	0.456
DespoDRAFT_00082	hypothetical protein	-2.889	0.0827
DespoDRAFT_00085	hypothetical protein	-1.249	0.616
DespoDRAFT_00086	zonula occludens toxin	1.544	NaN
DespoDRAFT_00087	Protein of unknown function (DUF2523)	#VALUE!	NaN
DespoDRAFT_00088	hypothetical protein	-5.315	0.48
DespoDRAFT_00089	hypothetical protein	-3.603	0.336
DespoDRAFT_00090	hypothetical protein	-1.92	0.664
DespoDRAFT_00091	hypothetical protein	#VALUE!	NaN
DespoDRAFT_00092	hypothetical protein	-1.743	NaN
DespoDRAFT_00093	Helix-turn-helix protein	1.198	0.751
DespoDRAFT_00094	hypothetical protein	1.516	0.701
DespoDRAFT_00095	hypothetical protein	-1.451	0.494
DespoDRAFT_00096	hypothetical protein	-1.849	0.127
DespoDRAFT_00097	hypothetical protein	-1.871	0.123

DespoDRAFT_00098	hypothetical protein	-1.09	0.942
DespoDRAFT_00099	hypothetical protein	-2.627	0.156
DespoDRAFT_00100	phosphate ABC transporter, phosphate-binding protein	6.279	0.0556
DespoDRAFT_00101	phosphate ABC transporter, permease protein PstC	-1.11	0.691
DespoDRAFT_00102	phosphate ABC transporter, permease protein PstA	-1.183	0.834
DespoDRAFT_00103	phosphate ABC transporter, ATP-binding protein	-1.204	0.384
DespoDRAFT_00104	Phosphoenolpyruvate carboxylase	1.167	0.785
DespoDRAFT_00105	hypothetical protein	1.556	0.177
DespoDRAFT_00106	2-oxoacid:acceptor oxidoreductase, delta subunit	2.619	0.0138
DespoDRAFT_00107	2-Oxoglutarate:ferredoxin oxidoreductase a subunit	2.721	0.053
DespoDRAFT_00108	2-Oxoglutarate:ferredoxin oxidoreductase b subunit	2.829	0.0723
DespoDRAFT_00109	2-oxoacid:acceptor oxidoreductase, gamma subunit; pyruvate/2-ketoisovalerate family	2.156	0.0523
DespoDRAFT_00110	acyl-CoA dehydrogenase	3.476	0.0347
DespoDRAFT_00111	putative transcriptional regulator with cupin domain	4.09	0.06
DespoDRAFT_00112	branched-chain amino acid aminotransferase, group II	5.158	0.0325
DespoDRAFT_00113	radical SAM domain iron- sulfur cluster-binding oxidoreductase	1.961	0.177
DespoDRAFT_00114	metal-dependent hydrolase	-1.558	0.267
DespoDRAFT_00115	response regulator containing a CheY-like receiver domain and an HTH DNA-binding domain	-1.416	0.0587
DespoDRAFT_00116	hypothetical protein	-1.453	0.21
DespoDRAFT_00117	hypothetical protein	-1.594	0.0676
DespoDRAFT_00118	membrane-bound serine protease (ClpP class)	-5.071	0.254
DespoDRAFT_00119	membrane-bound serine protease (ClpP class)	-1.838	0.116
DespoDRAFT_00120	Mn-dependent transcriptional regulator	-3.113	0.0344
DespoDRAFT_00121	putative DNA-binding protein	-2.943	0.0586
DespoDRAFT_00122	histidinol dehydrogenase	1.321	0.276
DespoDRAFT_00124	hypothetical protein	1.017	0.987
DespoDRAFT_00126	ATP synthase, F1 beta subunit	-3.213	0.103
DespoDRAFT_00127	alternate F1F0 ATPase, F1 subunit epsilon	-2.338	0.0229
DespoDRAFT_00128	ATP synthase, F0F1 subunit	-3.234	0.0509
DespoDRAFT_00129	F1/F0 ATPase,subunit 2	-3.062	0.433

DespoDRAFT_00130	ATP synthase, F0 Alpha subunit	-1.608	0.387
DespoDRAFT_00131	ATP synthase, F0 subunit c	-4.885	0.227
DespoDRAFT_00132	FOF1-type ATP synthase, beta subunit	-2.798	0.0951
DespoDRAFT_00133	ATP synthase, F1 beta subunit	-2.51	0.0925
DespoDRAFT_00134	ATP synthase, F1 beta subunit	-3.488	0.181
DespoDRAFT_00135	hypothetical protein	-1.069	0.936
DespoDRAFT_00136	apurinic endonuclease APN1	3.373	0.21
DespoDRAFT_00137	putative efflux protein, MATE family	2.231	0.664
DespoDRAFT_00138	nicotinate-nucleotide-- dimethylbenzimidazole phosphoribosyltransferase	4.643	0.225
DespoDRAFT_00139	DNA/RNA helicase, superfamily II	-1.064	0.663
DespoDRAFT_00140	hydrogenase assembly chaperone HypC/HupF	-1.422	0.442
DespoDRAFT_00141	(NiFe) hydrogenase maturation protein HypF	-1.261	0.766
DespoDRAFT_00142	hydrogenase expression/formation protein HypD	#VALUE!	1
DespoDRAFT_00143	hydrogenase expression/formation protein HypE	1.198	0.221
DespoDRAFT_00144	RNA polymerase-binding protein DksA	-1.872	0.106
DespoDRAFT_00145	ribonuclease III	-1.154	0.103
DespoDRAFT_00146	histone acetyltransferase	1.796	0.148
DespoDRAFT_00147	2' 5' RNA ligase family protein	-1.8	0.501
DespoDRAFT_00148	putative polymerase with PALM domain, HD hydrolase domain and Zn ribbon	-1.303	0.498
DespoDRAFT_00151	hypothetical protein	1.664	0.108
DespoDRAFT_00152	ATP:corrinoid adenosyltransferase	1.723	0.103
DespoDRAFT_00153	ATP citrate lyase alpha subunit (AclA)	1.191	0.262
DespoDRAFT_00154	ATP citrate lyase beta subunit (AclB)	1.098	0.426
DespoDRAFT_00155	hypothetical protein	-1.3	0.458
DespoDRAFT_00156	histidyl-tRNA synthetase	2.936	0.0592
DespoDRAFT_00157	aspartyl-tRNA synthetase	2.694	0.0365
DespoDRAFT_00158	cell division topological specificity factor MinE	-1.162	0.282
DespoDRAFT_00159	septum site-determining protein MinD	1.086	0.331
DespoDRAFT_00160	septum formation inhibitor	-1.233	0.0497
DespoDRAFT_00161	histidine kinase, Response regulator receiver domain protein, histidine kinase	-2.029	0.0676
DespoDRAFT_00162	response regulator containing a CheY-like receiver domain and an HTH DNA-binding domain	-1.776	0.176
DespoDRAFT_00163	3-dehydroquinate synthase	1.079	0.585
DespoDRAFT_00164	rubrerythrin	-1.219	0.507
DespoDRAFT_00165	thioredoxin	1.059	0.733

DespoDRAFT_00166	thioredoxin-disulfide reductase	-1.107	0.143
DespoDRAFT_00167	outer membrane assembly lipoprotein YfiO	1.009	0.952
DespoDRAFT_00168	ribosomal protein L28	1.375	0.458
DespoDRAFT_00169	PhoH family protein	1.248	0.778
DespoDRAFT_00170	(p)ppGpp synthetase, RelA/SpoT family	1.101	0.755
DespoDRAFT_00171	prolyl-tRNA synthetase, family I	-1.179	0.0185
DespoDRAFT_00172	1-hydroxy-2-methyl-2-(E)-butenyl 4-diphosphate synthase	-1.117	0.0635
DespoDRAFT_00173	type I restriction-modification system methyltransferase subunit	-1.018	0.959
DespoDRAFT_00174	hypothetical protein	1.309	0.774
DespoDRAFT_00175	restriction endonuclease S subunit	-1.74	0.763
DespoDRAFT_00177	DnaJ-class molecular chaperone with C-terminal Zn finger domain	-2.325	0.146
DespoDRAFT_00178	hypothetical protein	-1.656	NaN
DespoDRAFT_00179	molecular chaperone (small heat shock protein)	-4.425	0.383
DespoDRAFT_00181	aconitase A	2.552	0.0261
DespoDRAFT_00182	putative permease	2.219	0.583
DespoDRAFT_00183	saccharopine dehydrogenase-like oxidoreductase	-1.393	0.482
DespoDRAFT_00184	glucokinase	1.137	0.935
DespoDRAFT_00185	methylase involved in ubiquinone/menaquinone biosynthesis	-1.035	0.965
DespoDRAFT_00186	D-alanine aminotransferase	1.286	0.315
DespoDRAFT_00187	alanine racemase	1.31	0.386
DespoDRAFT_00189	hypothetical protein	1.043	0.972
DespoDRAFT_00192	hypothetical protein	-1.437	0.128
DespoDRAFT_00193	acetyl-CoA hydrolase	-1.2	0.557
DespoDRAFT_00194	hypothetical protein	-1.261	0.203
DespoDRAFT_00195	Protein of unknown function (DUF2914)	-1.225	0.862
DespoDRAFT_00196	hypothetical protein	1.044	0.986
DespoDRAFT_00197	putative Acetyl-CoA synthetase	-1.53	0.221
DespoDRAFT_00198	hypothetical protein	-1.295	0.345
DespoDRAFT_00199	membrane-associated lipoprotein involved in thiamine biosynthesis	1.067	0.782
DespoDRAFT_00200	Pyridoxamine 5"-phosphate oxidase	-1.291	0.21
DespoDRAFT_00201	PAS domain S-box	1.138	0.897
DespoDRAFT_00202	response regulator with CheY-like receiver domain and winged-helix DNA-binding domain	-1.419	0.381
DespoDRAFT_00203	2-oxoacid:ferredoxin oxidoreductase, gamma subunit	3.301	0.0149
DespoDRAFT_00204	2-Oxoglutarate:ferredoxin oxidoreductase beta subunit	3.356	0.0463

DespoDRAFT_00205	2-oxoglutarate ferredoxin oxidoreductase subunit alpha	3.648	0.0274
DespoDRAFT_00206	ferredoxin	3.876	0.0458
DespoDRAFT_00207	glycosyl transferase	-1.056	0.748
DespoDRAFT_00208	beta-lactamase domain protein	-1.102	0.651
DespoDRAFT_00210	glycyl-tRNA synthetase, dimeric type	-1.516	0.218
DespoDRAFT_00211	isoleucine patch superfamily enzyme, carbonic anhydrase/acetyltransferase	1.981	0.108
DespoDRAFT_00212	heterodisulfide reductase, subunit B	2.164	0.137
DespoDRAFT_00213	hypothetical protein	1.956	0.0254
DespoDRAFT_00214	citrate lyase beta subunit	-1.635	0.128
DespoDRAFT_00215	dihydrolipoamide dehydrogenase	-2.195	0.101
DespoDRAFT_00216	lipoate-protein ligase A	-1.767	0.181
DespoDRAFT_00217	phosphopantetheine-containing protein	-2.802	0.108
DespoDRAFT_00218	pyruvate/2-oxoglutarate dehydrogenase complex, dihydrolipoamide acyltransferase component	-2.637	0.173
DespoDRAFT_00219	pyruvate/2-oxoglutarate dehydrogenase complex, dehydrogenase component beta subunit	-3.73	0.105
DespoDRAFT_00220	pyruvate dehydrogenase E1 component, alpha subunit	-3.077	0.029
DespoDRAFT_00221	acetyl-CoA synthetase	-2.402	0.237
DespoDRAFT_00222	hypothetical protein	1.25	0.794
DespoDRAFT_00224	P-type ATPase, translocating	-1.056	0.661
DespoDRAFT_00227	hypothetical protein	#VALUE!	NaN
DespoDRAFT_00228	diguanylate cyclase (GGDEF) domain-containing protein	-3.113	0.122
DespoDRAFT_00229	micrococcal nuclease-like nuclease	-1.987	0.0556
DespoDRAFT_00230	ribosomal protein L11 methylase	1.436	0.478
DespoDRAFT_00231	hypothetical protein	1.966	0.0801
DespoDRAFT_00232	Uncharacterized protein family (UPF0153)	2.174	0.0729
DespoDRAFT_00233	tRNA modification GTPase TrmE	1.568	0.109
DespoDRAFT_00234	putative RNA-binding protein	1.146	0.651
DespoDRAFT_00235	membrane protein insertase, YidC/Oxa1 family, N-terminal domain	1.409	0.0846
DespoDRAFT_00236	hypothetical protein	1.628	0.42
DespoDRAFT_00237	ribonuclease P protein component	1.099	0.42
DespoDRAFT_00238	ribosomal protein L34, bacterial type	1.77	0.166
DespoDRAFT_00239	ribonuclease, Rne/Rng family	-1.204	0.501
DespoDRAFT_00240	radical SAM-linked protein/radical SAM family uncharacterized protein	1.074	0.786
DespoDRAFT_00241	asparaginyl-tRNA synthetase	-1.999	0.0477
DespoDRAFT_00242	ribosome small subunit-dependent GTPase A	-2.198	0.0646

DespoDRAFT_00244	uncharacterized Blt101-like protein	-1.981	0.344
DespoDRAFT_00245	FKBP-type peptidyl-prolyl cis-trans isomerase	2.348	0.0541
DespoDRAFT_00246	response regulator containing a CheY-like receiver domain and an HD-GYP domain	-1.039	0.85
DespoDRAFT_00247	methylase involved in ubiquinone/menaquinone biosynthesis	-1.288	0.444
DespoDRAFT_00248	radical SAM domain iron-sulfur cluster-binding oxidoreductase, putative	1.068	0.827
DespoDRAFT_00249	tRNA nucleotidyltransferase/poly(A) polymerase	1.138	0.521
DespoDRAFT_00250	phosphoserine phosphatase SerB	1.205	0.099
DespoDRAFT_00251	hypothetical protein	-1.642	0.251
DespoDRAFT_00252	cold shock protein	1.693	0.172
DespoDRAFT_00253	queuosine biosynthesis protein QueC	1.603	0.309
DespoDRAFT_00254	organic radical activating enzyme	1.682	0.0536
DespoDRAFT_00255	queuosine biosynthesis protein QueD	1.12	0.818
DespoDRAFT_00256	homocysteine/selenocysteine methylase (S-methylmethionine-dependent)	-1.771	0.197
DespoDRAFT_00258	hypothetical protein	-1.616	0.0652
DespoDRAFT_00259	hypoxanthine phosphoribosyltransferase	-1.831	0.0493
DespoDRAFT_00260	DnaJ-class molecular chaperone with C-terminal Zn finger domain	-1.916	0.00851
DespoDRAFT_00261	glucose-inhibited division protein A	1.368	0.14
DespoDRAFT_00262	flavoprotein	2.148	0.387
DespoDRAFT_00263	ATPase component of ABC transporters with duplicated ATPase domain	3.236	0.235
DespoDRAFT_00267	hypothetical protein	1.848	NaN
DespoDRAFT_00269	diguanylate cyclase (GGDEF) domain-containing protein	-2.511	0.00271
DespoDRAFT_00270	aspartate/tyrosine/aromatic aminotransferase	1.294	0.034
DespoDRAFT_00271	putative Fe-S oxidoreductase	-1.108	0.104
DespoDRAFT_00272	glutamine synthetase adenylyltransferase	-1.814	0.0348
DespoDRAFT_00273	DisA bacterial checkpoint controller nucleotide-binding protein	-1.749	0.219
DespoDRAFT_00274	NAD-dependent aldehyde dehydrogenase	-2.091	0.0459
DespoDRAFT_00275	hypothetical protein	-2.405	0.38
DespoDRAFT_00277	carbamoyl-phosphate synthase, small subunit	1.447	0.356
DespoDRAFT_00278	carbamoyl-phosphate synthase, large subunit	1.108	0.149
DespoDRAFT_00279	amidophosphoribosyltransferase	1.949	0.159
DespoDRAFT_00280	putative Fe-S oxidoreductase	1.787	0.0963
DespoDRAFT_00281	serine protease inhibitor	1.047	0.782

DespoDRAFT_00282	transposase	1.524	0.399
DespoDRAFT_00283	molecular chaperone (small heat shock protein)	-4.155	0.0612
DespoDRAFT_00284	molecular chaperone (small heat shock protein)	-5.676	0.0355
DespoDRAFT_00285	hypothetical protein	#VALUE!	NaN
DespoDRAFT_00286	Pyruvate carboxylase	1.318	0.0605
DespoDRAFT_00287	putative N6-adenine-specific DNA methylase	-1.004	0.981
DespoDRAFT_00289	Rhodopirellula transposase	-2.109	0.261
DespoDRAFT_00290	putative domain HDIG-containing protein	1.593	0.774
DespoDRAFT_00291	Isocitrate dehydrogenase	1.824	0.083
DespoDRAFT_00292	lactate dehydrogenase-like oxidoreductase / Malate dehydrogenase	-1.262	0.164
DespoDRAFT_00294	transcriptional regulator	-3.513	0.2
DespoDRAFT_00295	acyl-CoA synthetase (NDP forming)	-2.668	0.0682
DespoDRAFT_00296	3-methyl-2-oxobutanoate hydroxymethyltransferase	-1.833	0.107
DespoDRAFT_00297	coenzyme F420-dependent NADP oxidoreductase	-2.251	0.018
DespoDRAFT_00298	putative Zn-dependent peptidase, insulinase	-1.686	0.00575
DespoDRAFT_00299	hypothetical protein	-2.079	0.228
DespoDRAFT_00300	dimethyladenosine transferase	-1.751	0.0568
DespoDRAFT_00301	HD-GYP domain-containing protein	-1.393	0.426
DespoDRAFT_00302	nicotinamidase-like amidase	-1.154	0.74
DespoDRAFT_00303	nicotinate phosphoribosyltransferase	-1.396	0.488
DespoDRAFT_00304	radical SAM protein, TIGR01212 family	-1.469	0.375
DespoDRAFT_00305	RRM domain-containing RNA-binding protein	2.997	0.33
DespoDRAFT_00306	putative methyltransferase	3.223	NaN
DespoDRAFT_00307	hypothetical protein	7.816	0.0387
DespoDRAFT_00308	DNA/RNA helicase, superfamily II	2.934	NaN
DespoDRAFT_00309	cold shock protein	5.552	0.0834
DespoDRAFT_00310	Putative exonuclease, RdgC	5.54	0.0909
DespoDRAFT_00311	hypothetical protein	3.21	0.0861
DespoDRAFT_00312	ribose-phosphate pyrophosphokinase	1.789	0.199
DespoDRAFT_00314	peptidyl-prolyl cis-trans isomerase (rotamase) - cyclophilin family	2.173	0.036
DespoDRAFT_00315	hypothetical protein	3.034	0.186
DespoDRAFT_00316	Na ⁺ -transporting NADH:ubiquinone oxidoreductase, subunit NqrA	-2.803	0.0586
DespoDRAFT_00317	NADH:ubiquinone oxidoreductase, Na(+)-translocating, B subunit	-3.02	0.16
DespoDRAFT_00318	Na ⁺ -transporting NADH:ubiquinone oxidoreductase, subunit NqrC	-2.895	0.14

DespoDRAFT_00319	NADH:ubiquinone oxidoreductase, Na(+)-translocating, D subunit	-4.84	0.333
DespoDRAFT_00320	NADH:ubiquinone oxidoreductase, Na(+)-translocating, E subunit	-4.164	0.333
DespoDRAFT_00321	NADH:ubiquinone oxidoreductase, Na(+)-translocating, F subunit	-2.005	0.0905
DespoDRAFT_00322	dihydroorotate dehydrogenase family protein	-1.332	0.192
DespoDRAFT_00323	2-polyprenylphenol hydroxylase-like oxidoreductase	-1.545	0.281
DespoDRAFT_00324	orotate phosphoribosyltransferase	-1.495	0.103
DespoDRAFT_00325	periplasmic component of amino acid ABC-type transporter/signal transduction system	1.127	0.815
DespoDRAFT_00326	pantothenate kinase, type III	1.087	0.616
DespoDRAFT_00327	YbbR-like protein	1.597	0.606
DespoDRAFT_00328	dihydropteroate synthase	1.214	0.13
DespoDRAFT_00329	ATP-dependent metalloprotease FtsH	-1.304	0.298
DespoDRAFT_00330	tRNA(Ile)-lysidine synthetase	1.301	0.33
DespoDRAFT_00331	O-6-methylguanine DNA methyltransferase	#VALUE!	NaN
DespoDRAFT_00332	putative dehydrogenase	3.528	0.125
DespoDRAFT_00333	isopropylmalate/homocitrate/citramalate synthase	3.534	0.0616
DespoDRAFT_00334	hypothetical protein	-1.508	0.246
DespoDRAFT_00335	molybdenum-pterin binding domain protein	1.237	0.162
DespoDRAFT_00336	putative permease	-1.749	0.0466
DespoDRAFT_00337	Kef-type K ⁺ transport system, predicted NAD-binding component	-1.917	0.0661
DespoDRAFT_00338	signal transduction histidine kinase	-1.087	0.892
DespoDRAFT_00339	response regulator with CheY-like receiver, AAA-type ATPase, and DNA-binding domains	-1.155	0.661
DespoDRAFT_00340	hypothetical protein	2.801	NaN
DespoDRAFT_00341	potassium uptake protein, TrkH family	-1.345	0.84
DespoDRAFT_00342	K ⁺ transport system, NAD-binding component	-1.04	0.959
DespoDRAFT_00343	ABC-type multidrug transport system, permease component	1.303	0.233
DespoDRAFT_00344	ABC-type multidrug transport system, permease component	1.247	0.513
DespoDRAFT_00345	ABC-type multidrug transport system, ATPase component	1.045	0.633
DespoDRAFT_00346	multidrug resistance efflux pump	1.294	0.182
DespoDRAFT_00348	hypothetical protein	1.493	0.345
DespoDRAFT_00349	hypothetical protein	-1.098	0.629
DespoDRAFT_00350	hypothetical protein	-1.047	0.896

DespoDRAFT_00354	hypothetical protein	-2.552	0.0931
DespoDRAFT_00356	hypothetical protein	-4.061	0.0309
DespoDRAFT_00357	hypothetical protein	-2.268	0.0838
DespoDRAFT_00358	restriction endonuclease S subunit	-2.069	0.149
DespoDRAFT_00359	AAA+ family ATPase	-2.425	0.108
DespoDRAFT_00360	subtilisin-like serine protease	-2.537	0.0759
DespoDRAFT_00361	hypothetical protein	-2.86	0.106
DespoDRAFT_00362	Fic/DOC family protein	-3.404	0.112
DespoDRAFT_00363	type I site-specific deoxyribonuclease, HsdR family	-2.385	0.0353
DespoDRAFT_00364	regulatory P domain of subtilisin-like proprotein convertases	-3.424	0.0568
DespoDRAFT_00365	hypothetical protein	1.033	0.835
DespoDRAFT_00366	putative domain HDIG-containing protein	-1.391	0.331
DespoDRAFT_00367	prepilin-type N-terminal cleavage/methylation domain-containing protein	-1.782	0.185
DespoDRAFT_00368	Fe-S oxidoreductase	-2.677	0.068
DespoDRAFT_00369	leucyl aminopeptidase	-1.667	0.128
DespoDRAFT_00370	A/G-specific adenine glycosylase	-1.296	0.721
DespoDRAFT_00371	putative transcriptional regulator with HTH domain	-1.178	0.665
DespoDRAFT_00374	exonuclease SbcD	-2.551	0.42
DespoDRAFT_00375	ATPase involved in DNA repair	-3.437	0.518
DespoDRAFT_00376	methyl-accepting chemotaxis protein	1.424	0.425
DespoDRAFT_00377	hypothetical protein	1.984	0.507
DespoDRAFT_00378	acetyl-CoA hydrolase	1.342	0.466
DespoDRAFT_00379	hypothetical protein	1.222	NaN
DespoDRAFT_00380	hypothetical protein	5.061	NaN
DespoDRAFT_00381	molybdopterin-guanine dinucleotide biosynthesis protein MobB	1.416	NaN
DespoDRAFT_00382	hypothetical protein	1.491	0.72
DespoDRAFT_00383	pantoate--beta-alanine ligase	1.774	0.155
DespoDRAFT_00385	prevent-host-death family protein	-2.857	0.336
DespoDRAFT_00386	toxin-antitoxin system, toxin component, Txe/YoeB family	-2.426	0.161
DespoDRAFT_00387	Kef-type K ⁺ transport system. predicted NAD-binding component	-1.248	0.745
DespoDRAFT_00388	hypothetical protein	-1.385	0.445
DespoDRAFT_00389	imidazole glycerol phosphate synthase, glutamine amidotransferase subunit	1.234	0.177
DespoDRAFT_00390	putative domain HDIG-containing protein	-1.621	0.095
DespoDRAFT_00391	chemotaxis protein	-1.865	0.177
DespoDRAFT_00392	single stranded DNA-binding protein	-1.178	0.146
DespoDRAFT_00393	DNA gyrase, B subunit	-1.005	0.877

DespoDRAFT_00394	DNA polymerase III, beta subunit	1.199	0.231
DespoDRAFT_00395	hypothetical protein	-1.57	0.0717
DespoDRAFT_00396	anaerobic ribonucleoside-triphosphate reductase activating protein	-1.206	0.42
DespoDRAFT_00397	anaerobic ribonucleoside-triphosphate reductase	1.035	0.559
DespoDRAFT_00398	hypothetical protein	-1.599	0.429
DespoDRAFT_00399	NTP pyrophosphohydrolase	-1.752	0.324
DespoDRAFT_00400	molecular chaperone of HSP90 family	1.905	0.0539
DespoDRAFT_00401	ribosomal protein S12 methylthiotransferase RimO	2.192	0.145
DespoDRAFT_00402	geranylgeranyl pyrophosphate synthase	2.291	0.0725
DespoDRAFT_00403	hypothetical protein	1.918	0.0678
DespoDRAFT_00405	SH3 domain-containing protein	1.124	0.636
DespoDRAFT_00406	diguanylate cyclase (GGDEF) domain-containing protein	-1.334	0.758
DespoDRAFT_00407	hypothetical protein	-1.006	0.997
DespoDRAFT_00408	hypothetical protein	-1.079	0.844
DespoDRAFT_00409	sugar phosphate permease	-1.124	0.877
DespoDRAFT_00410	5"/3"-nucleotidase SurE	-1.056	0.724
DespoDRAFT_00411	transcriptional regulator	-1.808	0.195
DespoDRAFT_00412	Xaa-Pro aminopeptidase	-2.401	0.193
DespoDRAFT_00413	indolepyruvate ferredoxin oxidoreductase, alpha/beta subunit	2.005	0.112
DespoDRAFT_00414	2-oxoacid:ferredoxin oxidoreductase, gamma subunit	3.384	0.0842
DespoDRAFT_00415	coenzyme F390 synthetase	1.128	0.159
DespoDRAFT_00416	TRAP-type C4-dicarboxylate transport system, periplasmic component	4.295	0.0162
DespoDRAFT_00417	TRAP-type C4-dicarboxylate transport system, small permease component	1.937	0.112
DespoDRAFT_00418	TRAP transporter, DctM subunit	2.776	0.0711
DespoDRAFT_00419	hypothetical protein	1.534	0.0859
DespoDRAFT_00420	ornithine/acetylornithine aminotransferase	1.674	0.183
DespoDRAFT_00421	hypothetical protein	-1.537	0.164
DespoDRAFT_00423	integrase family protein	1.497	NaN
DespoDRAFT_00427	polyphosphate:AMP phosphotransferase	-1.825	0.0451
DespoDRAFT_00428	HNH endonuclease	1.147	0.503
DespoDRAFT_00429	hypothetical protein	-1.037	0.963
DespoDRAFT_00430	CheY-like receiver domain-containing protein	-2.475	0.0378
DespoDRAFT_00431	glutamate dehydrogenase/leucine dehydrogenase	1.159	0.351
DespoDRAFT_00432	response regulator containing a CheY-like receiver domain and an HTH DNA-binding	-2.061	0.102

	domain		
DespoDRAFT_00433	NAD-specific glutamate dehydrogenase	1.039	0.91
DespoDRAFT_00434	ABC-type nitrate/sulfonate/bicarbonate transport system, periplasmic component	-3.442	0.12
DespoDRAFT_00435	ABC-type nitrate/sulfonate/bicarbonate transport system, permease component	-1.704	0.627
DespoDRAFT_00436	ABC-type multidrug transport system, ATPase component	-3.054	0.494
DespoDRAFT_00437	putative Fe-S oxidoreductase	1.925	0.345
DespoDRAFT_00438	hypothetical protein	1.571	0.216
DespoDRAFT_00439	C-terminal processing peptidase	1.069	0.0417
DespoDRAFT_00440	membrane-bound metallopeptidase	1.14	0.124
DespoDRAFT_00441	cell division protein	1.659	0.355
DespoDRAFT_00442	putative ATPase involved in cell division	-1.085	0.785
DespoDRAFT_00443	hydrolase, TatD family	2.263	0.257
DespoDRAFT_00444	twin arginine-targeting protein translocase, TatA/E family	1.86	0.173
DespoDRAFT_00445	(protein-PII) uridylyltransferase	1.431	0.246
DespoDRAFT_00446	nitrogen regulatory protein PII	2.126	0.16
DespoDRAFT_00447	glutamine synthetase, type I	-1.149	0.228
DespoDRAFT_00448	membrane-bound lytic murein transglycosylase B	1.438	0.597
DespoDRAFT_00449	hypothetical protein	-1.415	0.812
DespoDRAFT_00451	extracellular solute-binding protein, family 3	-1.477	0.349
DespoDRAFT_00456	integrase family protein	-1.691	0.553
DespoDRAFT_00457	hypothetical protein	#VALUE!	NaN
DespoDRAFT_00459	PAS domain S-box/diguanylate cyclase (GGDEF) domain-containing protein	1.495	0.282
DespoDRAFT_00460	butyrate kinase	-2.259	0.079
DespoDRAFT_00461	acyl-CoA synthetase/AMP-acid ligase	-1.749	0.0465
DespoDRAFT_00462	ABC-type multidrug transport system, ATPase and permease component	-1.493	0.335
DespoDRAFT_00463	ABC-type multidrug transport system, ATPase and permease component	-1.02	0.889
DespoDRAFT_00464	deoxycytidine triphosphate deaminase	-1.208	0.724
DespoDRAFT_00465	hypothetical protein	-1.451	0.695
DespoDRAFT_00466	quinolinate synthetase complex, A subunit	1.213	0.0353
DespoDRAFT_00467	outer membrane lipoprotein-sorting protein	1.493	0.166
DespoDRAFT_00468	acyl-CoA synthetase (AMP-forming)/AMP-acid ligase II	1.446	0.0223
DespoDRAFT_00469	chaperone protein DnaK	1.115	0.497
DespoDRAFT_00470	molecular chaperone GrpE (heat shock protein)	-2.537	0.116

DespoDRAFT_00472	anti-anti-sigma regulatory factor (antagonist of anti-sigma factor)	-1.629	0.324
DespoDRAFT_00473	hypothetical protein	-2.092	0.112
DespoDRAFT_00474	hypothetical protein	-5.042	0.209
DespoDRAFT_00475	NADH:flavin oxidoreductase	-1.146	0.346
DespoDRAFT_00476	cation diffusion facilitator family transporter	-1.295	0.411
DespoDRAFT_00477	phosphatidylserine synthase	-1.189	0.28
DespoDRAFT_00478	putative radical SAM protein YgiQ	-1.027	0.925
DespoDRAFT_00479	arabinose efflux permease family protein	1.481	0.615
DespoDRAFT_00480	flagellar motor protein	-1.66	0.726
DespoDRAFT_00481	flagellar motor component	-2.568	0.302
DespoDRAFT_00482	acetyl-CoA hydrolase	-3.153	0.0349
DespoDRAFT_00483	transcription elongation factor	-1.799	0.134
DespoDRAFT_00484	hypothetical protein	-3.229	0.00283
DespoDRAFT_00485	response regulator with CheY-like receiver, AAA-type ATPase, and DNA-binding domains	-1.079	0.897
DespoDRAFT_00486	signal transduction histidine kinase	-1.676	0.652
DespoDRAFT_00488	ABC-type antimicrobial peptide transport system, ATPase component	-1.772	0.118
DespoDRAFT_00489	ABC-type transport system, involved in lipoprotein release, permease component	-1.591	0.279
DespoDRAFT_00490	hypothetical protein	-1.907	0.164
DespoDRAFT_00491	hypothetical protein	-1.268	0.685
DespoDRAFT_00492	hypothetical protein	-1.174	0.676
DespoDRAFT_00494	TIGR04076 family protein	-1.408	0.532
DespoDRAFT_00495	transcriptional regulator	-1.319	0.616
DespoDRAFT_00496	RND family efflux transporter, MFP subunit	-1.772	0.257
DespoDRAFT_00497	ABC-type transport system, involved in lipoprotein release, permease component	-2.109	0.057
DespoDRAFT_00498	ABC-type antimicrobial peptide transport system, ATPase component	-1.223	0.756
DespoDRAFT_00499	efflux transporter, outer membrane factor lipoprotein, NodT family	-1.606	0.444
DespoDRAFT_00500	CBS-domain-containing membrane protein	3.691	0.294
DespoDRAFT_00501	CBS-domain-containing membrane protein	2.01	0.443
DespoDRAFT_00502	hypothetical protein	-3.393	0.0637
DespoDRAFT_00503	dissimilatory sulfite reductase (desulfovirdin), alpha/beta subunit	-1.732	0.106
DespoDRAFT_00504	hypothetical protein	-1.638	0.0635
DespoDRAFT_00505	nitrate/TMAO reductase, membrane-bound tetraheme cytochrome c subunit	-4.026	0.0609
DespoDRAFT_00506	PAS domain S-box	-3.562	0.0605

DespoDRAFT_00507	hydroxylamine reductase	-3.231	0.0416
DespoDRAFT_00508	beta-lactamase domain protein	-1.799	0.295
DespoDRAFT_00509	iron-sulfur cluster biosynthesis protein, NifU-like protein	1.525	0.424
DespoDRAFT_00510	universal stress protein UspA-like protein	-1.225	0.691
DespoDRAFT_00511	pyruvate/2-oxoglutarate dehydrogenase complex, dehydrogenase component alpha subunit	-1.774	0.231
DespoDRAFT_00512	pyruvate/2-oxoglutarate dehydrogenase complex, dehydrogenase component beta subunit	-1.755	0.0956
DespoDRAFT_00513	CBS-domain-containing membrane protein	-1.17	0.0786
DespoDRAFT_00514	phosphoenolpyruvate synthase	-1.184	0.432
DespoDRAFT_00515	Pyruvate ferredoxin oxidoreductase	-1.277	0.143
DespoDRAFT_00516	hypothetical protein	-1.702	0.0932
DespoDRAFT_00517	putative sugar kinase	1.614	0.0853
DespoDRAFT_00518	phosphoribosylanthranilate isomerase	1.77	0.154
DespoDRAFT_00519	threonine dehydrogenase-like Zn-dependent dehydrogenase	2.303	0.0857
DespoDRAFT_00520	DhnA-type fructose-1, 6-bisphosphate aldolase-like enzyme	2.496	0.0742
DespoDRAFT_00521	uncharacterized protein involved in formation of curli polymers	1.386	0.0465
DespoDRAFT_00522	transcriptional regulator	1.621	0.181
DespoDRAFT_00523	RND family efflux transporter, MFP subunit	1.318	0.431
DespoDRAFT_00524	hydrophobe/amphiphile efflux-1 (HAE1) family transporter	1.456	0.14
DespoDRAFT_00525	efflux transporter, outer membrane factor lipoprotein, NodT family	1.402	0.619
DespoDRAFT_00527	catalase	-2.708	0.045
DespoDRAFT_00528	alpha/beta superfamily hydrolase	-2.872	0.0736
DespoDRAFT_00530	cytosine deaminase-like metal-dependent hydrolase	-2.94	0.038
DespoDRAFT_00531	xanthine dehydrogenase, iron-sulfur cluster and FAD-binding subunit A	-2.85	0.108
DespoDRAFT_00532	xanthine dehydrogenase, molybdopterin-binding subunit B	-3.868	0.0464
DespoDRAFT_00533	glutamate dehydrogenase/leucine dehydrogenase	-2.687	0.286
DespoDRAFT_00534	radical SAM domain iron-sulfur cluster-binding oxidoreductase	1.521	0.0951
DespoDRAFT_00535	glutamate dehydrogenase/leucine dehydrogenase	-1.536	0.134
DespoDRAFT_00536	ORF6N domain-containing protein	-2.415	0.127

DespoDRAFT_00537	SagB-type dehydrogenase domain protein	-3.072	0.182
DespoDRAFT_00538	flagellar protein FlaG	-2.584	0.151
DespoDRAFT_00539	hypothetical protein	-1.26	0.221
DespoDRAFT_00540	carbon storage regulator CsrA	-1.384	0.602
DespoDRAFT_00541	FlgN protein	-1.413	0.505
DespoDRAFT_00542	Rod binding protein	1.342	0.685
DespoDRAFT_00543	flagellar basal-body P-ring protein	-1.248	0.332
DespoDRAFT_00544	flagellar basal body L-ring protein	-1.261	0.344
DespoDRAFT_00545	flagella basal body P-ring formation protein FlgA	-1.877	0.0162
DespoDRAFT_00546	flagellar basal-body rod protein FlgG	-1.618	0.0966
DespoDRAFT_00547	flagellar hook-basal body protein	-1.596	0.139
DespoDRAFT_00548	uncharacterized protein, cytoplasmic domain of flagellar protein FhlB like protein	-1.101	0.956
DespoDRAFT_00549	Flagellar hook-length control protein FliK	-1.827	0.594
DespoDRAFT_00550	hypothetical protein	-1.797	0.723
DespoDRAFT_00551	hypothetical protein	-4.209	0.0834
DespoDRAFT_00552	hypothetical protein	-2.806	0.0201
DespoDRAFT_00553	RNA polymerase sigma factor, FliA/WhiG family	-1.475	0.339
DespoDRAFT_00554	ATPase involved in chromosome partitioning	-2.531	0.122
DespoDRAFT_00555	flagellar GTP-binding protein	-1.636	0.0576
DespoDRAFT_00556	flagellar biosynthesis protein FlhA	-1.624	0.0662
DespoDRAFT_00557	flagellar biosynthetic protein FlhB	-1.823	0.457
DespoDRAFT_00558	flagellar biosynthetic protein FliR	-1.133	0.894
DespoDRAFT_00559	response regulator containing a CheY-like receiver domain and a GGDEF domain	-1.247	0.547
DespoDRAFT_00560	Response regulator receiver domain protein, histidine kinase	-2.195	0.125
DespoDRAFT_00561	PAS domain S-box	-1.292	0.541
DespoDRAFT_00562	PAS domain S-box	-1.225	0.499
DespoDRAFT_00563	flagellar biosynthetic protein FliQ	-1.086	0.88
DespoDRAFT_00564	flagellar biosynthetic protein FliP	-1.512	0.428
DespoDRAFT_00565	flagellar biosynthetic protein FliO	1.181	0.844
DespoDRAFT_00566	flagellar motor switch protein FliN	1.357	0.741
DespoDRAFT_00567	flagellar motor switch protein FliM	-1.599	0.104
DespoDRAFT_00568	flagellar basal body-associated protein	-1.598	0.083
DespoDRAFT_00569	flagellar hook-length control protein	-2.976	0.0973
DespoDRAFT_00570	pyridoxal-phosphate dependent TrpB-like enzyme	4.516	0.0254
DespoDRAFT_00571	PAS domain S-box	-1.008	0.986
DespoDRAFT_00572	NAD(P)H-nitrite reductase	1.127	0.898
DespoDRAFT_00573	transcriptional regulator	-2.39	0.128
DespoDRAFT_00574	ketol-acid reductoisomerase	2.603	0.127

DespoDRAFT_00575	serine/threonine protein kinase	1.433	0.299
DespoDRAFT_00576	putative phosphoesterase	-1.112	0.923
DespoDRAFT_00577	cytochrome c peroxidase	-35.472	0.00271
DespoDRAFT_00579	hypothetical protein	1.194	0.493
DespoDRAFT_00581	cold shock protein	8.288	0.125
DespoDRAFT_00583	hypothetical protein	1.656	0.396
DespoDRAFT_00584	Phytochelatin synthase	1.128	0.801
DespoDRAFT_00585	hypothetical protein	-1.012	0.963
DespoDRAFT_00586	adenylate cyclase	-1.153	0.836
DespoDRAFT_00587	lipoate synthase	-1.093	0.748
DespoDRAFT_00588	lipoate-protein ligase B	-2.217	0.131
DespoDRAFT_00589	putative permease	-1.103	0.512
DespoDRAFT_00590	hypothetical protein	2.093	0.0873
DespoDRAFT_00591	hydro-lyase, Fe-S type, tartrate/fumarate subfamily, hydro-lyase family enzyme, Fe-S type tartrate/fumarate subfamily	1.601	0.0741
DespoDRAFT_00592	dihydrofolate reductase	1.39	0.126
DespoDRAFT_00593	hypothetical protein	1.337	0.0199
DespoDRAFT_00594	putative membrane protein	1.28	0.486
DespoDRAFT_00595	DNA modification methylase	1.49	0.0904
DespoDRAFT_00596	hypothetical protein	-1.892	0.107
DespoDRAFT_00598	peroxiredoxin	-1.607	0.133
DespoDRAFT_00599	hypothetical protein	-1.471	0.217
DespoDRAFT_00600	putative exonuclease of the beta-lactamase fold involved in RNA processing	-1.508	0.147
DespoDRAFT_00601	hypothetical protein	-2.082	0.14
DespoDRAFT_00603	ATPase FliI/YscN family	-2.055	0.107
DespoDRAFT_00604	flagellar biosynthesis/type III secretory pathway protein	-1.673	0.157
DespoDRAFT_00605	flagellar motor switch protein FliG	-1.759	0.0853
DespoDRAFT_00606	flagellar basal-body M-ring protein/flagellar hook-basal body protein FliF	-2.346	0.0243
DespoDRAFT_00607	flagellar hook-basal body complex protein FliE	-2.762	0.119
DespoDRAFT_00608	flagellar basal-body rod protein FlgC	-2.927	0.034
DespoDRAFT_00609	flagellar basal-body rod protein FlgB	-3.635	0.0536
DespoDRAFT_00610	response regulator with CheY-like receiver, AAA-type ATPase, and DNA-binding domains	-1.738	0.195
DespoDRAFT_00611	hypothetical protein	-2.103	0.0957
DespoDRAFT_00612	response regulator with CheY-like receiver, AAA-type ATPase, and DNA-binding domains	-3.105	0.0291
DespoDRAFT_00613	response regulator with CheY-like receiver, AAA-type ATPase, and DNA-binding domains	-2.852	0.0522

	domains		
DespoDRAFT_00614	putative inhibitor of MCP methylation, CheC	-2.746	0.0334
DespoDRAFT_00615	PilZ domain-containing protein	-4.881	0.086
DespoDRAFT_00616	putative domain HDIG-containing protein	-3.186	0.127
DespoDRAFT_00617	transcriptional regulator	-1.21	0.61
DespoDRAFT_00618	diaminopimelate decarboxylase	1.001	0.987
DespoDRAFT_00619	acetyl-CoA hydrolase	-2.092	0.197
DespoDRAFT_00620	tRNA-dihydrouridine synthase	-1.496	0.686
DespoDRAFT_00622	glycosyl transferase	2.364	0.0412
DespoDRAFT_00623	excinuclease ABC, A subunit	-1.325	0.0464
DespoDRAFT_00624	di-/tricarboxylate transporter	-1.811	0.085
DespoDRAFT_00626	hypothetical protein	-2.456	0.0896
DespoDRAFT_00627	hypothetical protein	-1.638	0.0582
DespoDRAFT_00628	small-conductance mechanosensitive channel	-1.034	0.96
DespoDRAFT_00629	aspartate/tyrosine/aromatic aminotransferase	1.882	0.0995
DespoDRAFT_00630	3-isopropylmalate dehydrogenase	5.944	0.00598
DespoDRAFT_00633	Fumarate hydratase	-1.884	0.2
DespoDRAFT_00634	hypothetical protein	-2.255	0.0493
DespoDRAFT_00635	sugar phosphate isomerase/epimerase	1.118	0.877
DespoDRAFT_00636	cobalamin biosynthesis protein CobD	-1.572	0.825
DespoDRAFT_00637	PLP-dependent enzyme, histidinol-phosphate/aromatic aminotransferase or cobyrinic acid decarboxylase	-1.423	0.622
DespoDRAFT_00638	cobalamin-5-phosphate synthase	-1.207	0.811
DespoDRAFT_00639	adenosyl cobinamide kinase/adenosyl cobinamide phosphate guanylyltransferase	-1.236	0.672
DespoDRAFT_00640	hypothetical protein	1.76	NaN
DespoDRAFT_00641	ParB-like nuclease	5.84	NaN
DespoDRAFT_00642	hypothetical protein	-1.396	0.649
DespoDRAFT_00644	putative transcriptional regulator containing CBS domains	1.17	0.518
DespoDRAFT_00645	sodium ion-translocating decarboxylase, beta subunit	-1.169	0.442
DespoDRAFT_00646	hypothetical protein	-1.455	0.396
DespoDRAFT_00647	acetyl-CoA carboxylase, carboxyltransferase component (subunits alpha and beta)	-1.499	0.0799
DespoDRAFT_00648	acetyl/propionyl-CoA carboxylase, alpha subunit	-1.779	0.301
DespoDRAFT_00649	acyl-CoA dehydrogenase	-1.448	0.143
DespoDRAFT_00650	ABC-type cobalamin/Fe ³⁺ -siderophore	-2.368	0.614

	transport system, ATPase component		
DespoDRAFT_00652	ABC-type Fe ³⁺ -hydroxamate transport system, periplasmic component	-1.044	0.934
DespoDRAFT_00653	cytosine deaminase-like metal-dependent hydrolase	2.685	0.33
DespoDRAFT_00654	hypothetical protein	-1.912	0.201
DespoDRAFT_00655	hypothetical protein	-4.763	0.0463
DespoDRAFT_00656	transcriptional regulator containing GAF, AAA-type ATPase, and DNA binding domains	-1.916	0.0847
DespoDRAFT_00658	arabinose efflux permease family protein	1.054	0.969
DespoDRAFT_00659	DNA repair protein RadA	2.339	0.131
DespoDRAFT_00660	23S rRNA methylase	1.703	0.0644
DespoDRAFT_00661	DNA-binding regulatory protein, YebC/PmpR family	2.773	0.0568
DespoDRAFT_00662	hypothetical protein	-1.558	0.142
DespoDRAFT_00663	hypothetical protein	-2.363	0.0681
DespoDRAFT_00664	hypothetical protein	-1.045	0.982
DespoDRAFT_00665	transposase family protein	-1.821	0.167
DespoDRAFT_00666	hypothetical protein	-1.285	0.0958
DespoDRAFT_00667	NADH:flavin oxidoreductase, flavin dependent.	-1.57	0.125
DespoDRAFT_00668	hypothetical protein	-1.17	0.345
DespoDRAFT_00669	GTP-binding protein TypA/BipA	-1.135	0.177
DespoDRAFT_00670	outer membrane lipoprotein	-1.119	0.484
DespoDRAFT_00671	hypothetical protein	#VALUE!	NaN
DespoDRAFT_00672	Protein of unknown function (DUF2589)	2.017	NaN
DespoDRAFT_00673	hypothetical protein	1.276	0.104
DespoDRAFT_00674	uncharacterized protein involved in tellurite resistance	-1.055	0.533
DespoDRAFT_00675	hypothetical protein	-1.141	0.277
DespoDRAFT_00676	hypothetical protein	-1.33	0.095
DespoDRAFT_00677	putative membrane protein	-1.382	0.263
DespoDRAFT_00678	putative spermidine synthase with an N-terminal membrane domain	-1.203	0.804
DespoDRAFT_00679	primosomal protein N"	1.491	0.411
DespoDRAFT_00680	putative ATPase (AAA+ superfamily)	-1.006	0.997
DespoDRAFT_00683	hypothetical protein	-1.558	0.48
DespoDRAFT_00684	type I restriction enzyme R protein	1.447	0.758
DespoDRAFT_00688	penicillin-binding protein, 1A family	1.751	0.0557
DespoDRAFT_00690	phosphoribosyl-AMP cyclohydrolase	1.692	0.148
DespoDRAFT_00691	ATP phosphoribosyltransferase	1.442	0.193
DespoDRAFT_00692	Aspartate transaminase	1.194	0.224

DespoDRAFT_00693	ribosome biogenesis GTP-binding protein YsxC/EngB	1.072	0.921
DespoDRAFT_00694	GTP-binding protein Era	1.297	0.323
DespoDRAFT_00695	restriction endonuclease	1.477	0.155
DespoDRAFT_00696	hypothetical protein	1.335	0.203
DespoDRAFT_00697	7-cyano-7-deazaguanine reductase	1.395	0.767
DespoDRAFT_00698	putative TIM-barrel protein, nifR3 family	1.635	0.193
DespoDRAFT_00699	DNA repair photolyase	6.477	0.227
DespoDRAFT_00700	hypothetical protein	6.561	0.122
DespoDRAFT_00701	PAS domain S-box	-1.365	0.309
DespoDRAFT_00704	small-conductance mechanosensitive channel	-1.351	0.438
DespoDRAFT_00705	magnesium Mg(2+) and cobalt Co(2+) transport protein CorA	-2.084	0.219
DespoDRAFT_00706	Aconitate dehydrogenase	-2.208	0.0586
DespoDRAFT_00707	K+ transport system, NAD-binding component	-2.197	0.155
DespoDRAFT_00708	nitroreductase	-1.989	0.0231
DespoDRAFT_00709	acyl-CoA hydrolase	-1.717	0.219
DespoDRAFT_00710	PEP-CTERM putative exosortase interaction domain-containing protein	2.1	0.14
DespoDRAFT_00711	hypothetical protein	2.53	NaN
DespoDRAFT_00712	Protein of unknown function (DUF2958)	#VALUE!	NaN
DespoDRAFT_00713	hypothetical protein	3.352	NaN
DespoDRAFT_00714	hypothetical protein	-2.054	NaN
DespoDRAFT_00715	antirestriction protein	-1.415	0.886
DespoDRAFT_00716	hypothetical protein	2.878	NaN
DespoDRAFT_00717	hypothetical protein	1.362	NaN
DespoDRAFT_00718	hypothetical protein	-3.126	NaN
DespoDRAFT_00719	hypothetical protein	#VALUE!	NaN
DespoDRAFT_00720	hypothetical protein	1.247	0.914
DespoDRAFT_00721	hypothetical protein	-1.562	0.586
DespoDRAFT_00722	bacterial nucleoid DNA-binding protein	1.308	0.723
DespoDRAFT_00726	ammonium transporter	-1.59	0.463
DespoDRAFT_00727	hypothetical protein	-1.549	0.357
DespoDRAFT_00728	SOS regulatory protein LexA	-1.825	0.146
DespoDRAFT_00729	hypothetical protein	-2.209	0.0635
DespoDRAFT_00730	class III cytochrome C family protein	-1.556	0.0325
DespoDRAFT_00731	ABC-type molybdenum transport system, ATPase component/photorepair protein PhrA	-1.641	0.126
DespoDRAFT_00732	hypothetical protein	2.177	0.144
DespoDRAFT_00734	hypothetical protein	#VALUE!	NaN
DespoDRAFT_00735	acetyl-CoA acetyltransferase	-2.184	0.0229
DespoDRAFT_00736	3-hydroxyacyl-CoA dehydrogenase	-1.533	0.0476

DespoDRAFT_00737	hypothetical protein	1.569	0.0829
DespoDRAFT_00738	hypothetical protein	1.99	0.175
DespoDRAFT_00739	PAS domain S-box	1.791	0.457
DespoDRAFT_00740	Protein of unknown function (DUF2868)	1.004	0.957
DespoDRAFT_00741	protein of unknown function (DUF3482)	1.103	0.609
DespoDRAFT_00743	QmoC	1.699	0.0468
DespoDRAFT_00744	QmoB / polyferredoxin, heterodixulfide reductase subunit A	1.558	0.0952
DespoDRAFT_00745	QmoA / FAD dependent oxidoreductase	1.408	0.193
DespoDRAFT_00746	AprA: adenylylsulfate reductase, alpha subunit	1.474	0.146
DespoDRAFT_00747	AprB: adenylylsulfate reductase, beta subunit	1.909	0.0447
DespoDRAFT_00748	putative Fe-S oxidoreductase	2.55	0.0743
DespoDRAFT_00749	dehydrogenase of unknown specificity	1.325	0.591
DespoDRAFT_00750	transcriptional regulator	-1.056	0.777
DespoDRAFT_00751	Phosphotransacetylase	1.146	0.459
DespoDRAFT_00752	Uncharacterized protein family (UPF0153)	2.811	0.0634
DespoDRAFT_00753	deoxyguanosinetriphosphate triphosphohydrolase, putative	1.964	0.377
DespoDRAFT_00754	cytosine/adenosine deaminase	1.913	0.149
DespoDRAFT_00755	translation initiation factor IF-3	1.472	0.538
DespoDRAFT_00756	ribosomal protein L35	3.304	0.0161
DespoDRAFT_00757	ribosomal protein L20	2.163	0.0241
DespoDRAFT_00758	phenylalanyl-tRNA synthetase, alpha subunit	1.301	0.046
DespoDRAFT_00759	phenylalanyl-tRNA synthetase, beta subunit	1.774	0.0723
DespoDRAFT_00761	hypothetical protein	1.184	0.271
DespoDRAFT_00762	transcription termination factor NusA	1.171	0.156
DespoDRAFT_00763	translation initiation factor IF-2	1.153	0.327
DespoDRAFT_00764	ribosome-binding factor A	1.042	0.752
DespoDRAFT_00765	tRNA pseudouridine 55 synthase	1.226	0.482
DespoDRAFT_00766	ribosomal protein S15	2.181	0.307
DespoDRAFT_00767	polyribonucleotide nucleotidyltransferase	1.749	0.0681
DespoDRAFT_00768	metal-dependent hydrolase, beta-lactamase superfamily I	1.239	0.568
DespoDRAFT_00769	hypothetical protein	-2.12	0.257
DespoDRAFT_00770	hypothetical protein	-1.679	0.537
DespoDRAFT_00771	sigma-54 interacting regulator	-1.341	0.466
DespoDRAFT_00772	helicase, type I site-specific restriction-modification system restriction subunit	-1.577	0.242
DespoDRAFT_00773	hypothetical protein	-1.476	0.112
DespoDRAFT_00774	type I restriction-modification system methyltransferase subunit	-1.238	0.313
DespoDRAFT_00775	restriction endonuclease S subunit	-1.466	0.352

DespoDRAFT_00776	Protein of unknown function (DUF3696)	-1	0.999
DespoDRAFT_00777	hypothetical protein	1.053	0.896
DespoDRAFT_00779	efflux transporter, outer membrane factor lipoprotein, NodT family	1.06	0.685
DespoDRAFT_00780	RND family efflux transporter, MFP subunit	1.281	0.102
DespoDRAFT_00781	cation/multidrug efflux pump	1.815	0.283
DespoDRAFT_00783	xanthine and CO dehydrogenases maturation factor, XdhC/CoxF family	-1.051	0.494
DespoDRAFT_00784	putative MobA-like protein	1.213	0.16
DespoDRAFT_00785	fructose-2, 6-bisphosphatase	-1.913	0.345
DespoDRAFT_00786	NAD-dependent aldehyde dehydrogenase	-1.65	0.0242
DespoDRAFT_00787	aerobic-type carbon monoxide dehydrogenase, large subunit CoxL/CutL-like protein	1.008	0.964
DespoDRAFT_00789	hypothetical protein	-1.571	NaN
DespoDRAFT_00791	methylase involved in ubiquinone/menaquinone biosynthesis	1.459	0.455
DespoDRAFT_00792	molecular chaperone (small heat shock protein)	1.452	0.516
DespoDRAFT_00793	molecular chaperone (small heat shock protein)	1.193	0.822
DespoDRAFT_00793	formylmethanofuran dehydrogenase subunit E	1.747	0.48
DespoDRAFT_00795	TRAP transporter, DctM subunit	3.327	0.161
DespoDRAFT_00796	TRAP-type C4-dicarboxylate transport system, small permease component	3.377	0.117
DespoDRAFT_00797	TRAP-type C4-dicarboxylate transport system, periplasmic component	1.491	0.0194
DespoDRAFT_00798	diguanylate cyclase (GGDEF) domain/uncharacterized domain HDIG-containing protein	-1.544	0.503
DespoDRAFT_00799	hydrogenase maturation protease	-4.665	0.0881
DespoDRAFT_00800	Ni, Fe-hydrogenase I large subunit	-1.897	0.0791
DespoDRAFT_00801	hydrogenase (NiFe) small subunit HydA	-1.556	0.143
DespoDRAFT_00802	hypothetical protein	-2.497	0.124
DespoDRAFT_00803	acyl-CoA thioester hydrolase, YbgC/YbaW family	1.226	0.721
DespoDRAFT_00804	nitroreductase	1.157	0.697
DespoDRAFT_00805	soluble P-type ATPase	1.422	0.498
DespoDRAFT_00806	Acetate kinase	1.142	0.2
DespoDRAFT_00807	crcB protein ; Cis-regulatory element	-1.506	0.696
DespoDRAFT_00808	hypothetical protein	-1.65	0.411
DespoDRAFT_00809	response regulator with CheY-like receiver, AAA-type ATPase, and DNA-binding	-1.396	0.122

	domains		
DespoDRAFT_00810	acetate--CoA ligase	1.011	0.717
DespoDRAFT_00811	apsK ATP sulphurylase/adenylylsulfate kinase	-1.373	0.17
DespoDRAFT_00812	putative Zn-dependent hydrolase of beta-lactamase fold	1.044	0.832
DespoDRAFT_00813	Fe-S-cluster-containing hydrogenase subunit	2.088	0.0362
DespoDRAFT_00814	hypothetical protein	-1.126	0.194
DespoDRAFT_00815	putative domain HDIG-containing protein	-1.067	0.435
DespoDRAFT_00816	family 3 adenylate cyclase	-1.096	0.818
DespoDRAFT_00817	response regulator receiver domain protein	-1.976	0.344
DespoDRAFT_00818	adenylate cyclase	-2.318	0.392
DespoDRAFT_00819	HDOD domain-containing protein	-1.847	0.181
DespoDRAFT_00820	hypothetical protein	1.235	0.804
DespoDRAFT_00821	putative transcriptional regulator	7.106	0.0789
DespoDRAFT_00822	homoaconitate hydratase family protein/3-isopropylmalate dehydratase, large subunit	4.791	0.037
DespoDRAFT_00823	3-isopropylmalate dehydratase, small subunit	5.844	0.0439
DespoDRAFT_00824	hypothetical protein	1.637	0.419
DespoDRAFT_00825	hypothetical protein	2.22	0.248
DespoDRAFT_00826	putative amidophosphoribosyltransferase	1.331	0.641
DespoDRAFT_00827	hypothetical protein	-1.037	0.93
DespoDRAFT_00828	hypothetical protein	-1.57	0.0947
DespoDRAFT_00830	NAD(+) kinase	#VALUE!	1
DespoDRAFT_00831	DNA polymerase I	1.455	0.338
DespoDRAFT_00832	hypothetical protein	1.982	0.135
DespoDRAFT_00833	phosphoribosylglycinamide formyltransferase, formyltetrahydrofolate-dependent	2.172	0.158
DespoDRAFT_00834	putative signal transduction protein containing EAL and modified HD-GYP domains	1.778	0.282
DespoDRAFT_00835	pheromone shutdown-related protein TraB	1.333	0.241
DespoDRAFT_00836	hypothetical protein	1.06	0.89
DespoDRAFT_00837	hypothetical protein	-1.006	0.979
DespoDRAFT_00838	DNA repair protein RecN	1.041	0.482
DespoDRAFT_00839	putative regulatory protein, FmdB family	-1.031	0.929
DespoDRAFT_00840	glycerophosphoryl diester phosphodiesterase	-1.579	0.209
DespoDRAFT_00844	acyl dehydratase	-1.199	0.537
DespoDRAFT_00845	PAS domain S-box	-2.262	0.0572
DespoDRAFT_00846	acyl-CoA dehydrogenase	2.301	0.101

DespoDRAFT_00847	acetyl-CoA acetyltransferase	2.749	0.0467
DespoDRAFT_00848	3-hydroxyacyl-CoA dehydrogenase	2.339	0.0687
DespoDRAFT_00849	metal-dependent hydrolase, beta-lactamase superfamily II	-1.235	0.846
DespoDRAFT_00850	putative permease	1.298	0.449
DespoDRAFT_00851	enoyl-CoA hydratase/carnithine racemase	-1.516	0.28
DespoDRAFT_00852	arabinose efflux permease family protein	-1.858	0.0912
DespoDRAFT_00853	DNA/RNA helicase, superfamily I	-1.085	0.876
DespoDRAFT_00854	phosphomannomutase	1.033	0.731
DespoDRAFT_00855	putative bacitracin resistance protein	1.87	0.472
DespoDRAFT_00856	outer membrane protein/peptidoglycan-associated (lipo)protein	1.251	0.14
DespoDRAFT_00857	DnaK suppressor protein	1.157	0.661
DespoDRAFT_00858	LL-diaminopimelate aminotransferase	1.029	0.857
DespoDRAFT_00859	hypothetical protein	1.953	0.085
DespoDRAFT_00860	Glutamine amidotransferases class-II	4.667	0.0303
DespoDRAFT_00861	glutamate synthase family protein	2.647	0.0438
DespoDRAFT_00862	NADPH-dependent glutamate synthase beta chain-like oxidoreductase	2.667	0.00525
DespoDRAFT_00863	bacteriocin propeptide, TIGR03798 family	-2.213	0.182
DespoDRAFT_00864	molybdenum ABC transporter, periplasmic molybdate-binding protein	-1.335	0.107
DespoDRAFT_00865	CysU ABC-type sulfate transport system, permease component (molybdate ABC transporter, permease protein)	-1.061	0.884
DespoDRAFT_00866	molybdenum ABC transporter, ATP-binding protein	-1.285	0.42
DespoDRAFT_00867	CoA-substrate-specific enzyme activase, putative	2.254	0.214
DespoDRAFT_00868	hypothetical protein	1.028	0.983
DespoDRAFT_00869	putative RND superfamily exporter	-4.662	0.276
DespoDRAFT_00870	hypothetical protein	-1.795	0.41
DespoDRAFT_00871	putative hydrolase or acyltransferase of alpha/beta superfamily	-1.057	0.612
DespoDRAFT_00872	Zn-dependent protease with chaperone function	-1.583	0.0613
DespoDRAFT_00874	transcriptional regulator	1.28	0.471
DespoDRAFT_00875	1, 4-alpha-glucan branching enzyme	-4.66	0.0572
DespoDRAFT_00876	glycogen/starch/alpha-glucan phosphorylase	-4.513	0.0145
DespoDRAFT_00877	1, 4-alpha-glucan branching enzyme	-2.188	0.0512
DespoDRAFT_00878	glycogen synthase	-3.248	0.112
DespoDRAFT_00879	glycogen debranching enzyme	-4.953	0.0222
DespoDRAFT_00880	aspartate-semialdehyde dehydrogenase, gamma-proteobacterial	2.103	0.0508
DespoDRAFT_00881	collagenase-like protease	-1.136	0.71

DespoDRAFT_00882	phosphomethylpyrimidine kinase	-1.937	0.0645
DespoDRAFT_00885	methyl-accepting chemotaxis protein	-2.842	0.449
DespoDRAFT_00886	putative NAD(P)H quinone oxidoreductase, PIG3 family	-1.235	0.0661
DespoDRAFT_00887	amino acid transporter	-1.03	0.942
DespoDRAFT_00888	RND family efflux transporter, MFP subunit	-1.58	0.338
DespoDRAFT_00889	hydrophobe/amphiphile efflux-1 (HAE1) family transporter/efflux transporter, outer membrane factor (OMF) lipoprotein NodT fam>	-1.289	0.257
DespoDRAFT_00890	methyltransferase family protein	-1.346	0.783
DespoDRAFT_00891	hypothetical protein	1.334	0.303
DespoDRAFT_00892	hypothetical protein	-1.109	0.76
DespoDRAFT_00893	hypothetical protein	-1.253	0.685
DespoDRAFT_00894	dienelactone hydrolase-like enzyme	-1.848	0.0813
DespoDRAFT_00895	cobalamin biosynthesis protein CbiK, Co2+ chelatase	1.353	0.26
DespoDRAFT_00896	ABC-type Fe3+-siderophore transport system, permease component	1.061	0.61
DespoDRAFT_00897	ABC-type cobalamin/Fe3+-siderophore transport system, ATPase component	1.334	0.653
DespoDRAFT_00898	ABC-type Fe3+-hydroxamate transport system, periplasmic component	1.76	0.316
DespoDRAFT_00899	cobyrinic acid a, c-diamide synthase	1.375	0.32
DespoDRAFT_00900	precorrin isomerase	-1.541	0.00435
DespoDRAFT_00901	precorrin-2 C20-methyltransferase	-1.087	0.69
DespoDRAFT_00902	hypothetical protein	1.276	0.845
DespoDRAFT_00903	cobalamin biosynthesis protein CbiD	-1.832	0.394
DespoDRAFT_00904	type I site-specific deoxyribonuclease, HsdR family	-1.042	0.917
DespoDRAFT_00905	restriction endonuclease S subunit	-1.198	0.909
DespoDRAFT_00906	type I restriction system adenine methylase HsdM	1.428	0.583
DespoDRAFT_00907	hypothetical protein	-2.868	NaN
DespoDRAFT_00908	putative periplasmic lipoprotein (DUF2279)	1.209	0.818
DespoDRAFT_00909	precorrin-6y C5, 15-methyltransferase (decarboxylating), CbiE subunit, precorrin-6Y C5, 15-methyltransferase (decarboxylating)	-1.068	0.836
DespoDRAFT_00910	hypothetical protein	-1.218	0.793
DespoDRAFT_00911	growth inhibitor	-1.619	0.105
DespoDRAFT_00912	precorrin-4 C11-methyltransferase	-2.148	0.136
DespoDRAFT_00913	cobalamin biosynthesis protein CbiG	-1.569	0.665
DespoDRAFT_00914	precorrin-3B C17-methyltransferase	-2.001	0.527

DespoDRAFT_00915	cobyric acid synthase CobQ	-1.988	0.24
DespoDRAFT_00916	Helix-turn-helix protein	-2.237	0.622
DespoDRAFT_00917	HipA-like protein	-4.008	0.112
DespoDRAFT_00918	universal stress protein UspA-like protein	-4.033	0.172
DespoDRAFT_00919	hypothetical protein	-2.699	0.194
DespoDRAFT_00920	methyltransferase, cyclopropane fatty acid synthase	-1.955	0.0854
DespoDRAFT_00921	flavin-dependent dehydrogenase	-1.555	0.147
DespoDRAFT_00922	molybdopterin biosynthesis enzyme	-1.344	0.262
DespoDRAFT_00923	response regulator with CheY-like receiver, AAA-type ATPase, and DNA-binding domains	-2.205	0.159
DespoDRAFT_00924	PAS domain S-box	-3.622	0.112
DespoDRAFT_00925	hypothetical protein	-3.619	0.12
DespoDRAFT_00926	hypothetical protein	-2.594	0.108
DespoDRAFT_00927	putative permease	-1.464	0.143
DespoDRAFT_00928	hypothetical protein	-1.508	0.112
DespoDRAFT_00929	NADPH-dependent glutamate synthase beta chain-like oxidoreductase	-3.808	0.03
DespoDRAFT_00930	Fe-S-cluster-containing hydrogenase subunit	-5.659	0.0421
DespoDRAFT_00931	Thiosulfate reductase, putative	-5.702	0.0162
DespoDRAFT_00932	putative membrane-bound metal-dependent hydrolase (DUF457)	-1.608	0.477
DespoDRAFT_00933	alanine dehydrogenase	-1.977	0.135
DespoDRAFT_00934	putative SAM-dependent methyltransferase	1.296	0.449
DespoDRAFT_00935	hypothetical protein	-1.044	0.928
DespoDRAFT_00936	putative N6-adenine-specific DNA methylase	2.748	0.11
DespoDRAFT_00937	putative regulatory protein, FmdB family	3.532	0.127
DespoDRAFT_00938	hypothetical protein	5.855	0.1
DespoDRAFT_00939	dinitrogenase iron-molybdenum cofactor biosynthesis protein	6.845	0.0473
DespoDRAFT_00940	P-loop ATPase, MinD superfamily	4.29	0.02
DespoDRAFT_00941	P-loop ATPase, MinD superfamily	3.522	0.0463
DespoDRAFT_00942	hypothetical protein	1.605	0.175
DespoDRAFT_00943	phospho-2-dehydro-3-deoxyheptonate aldolase	3.068	0.126
DespoDRAFT_00944	protein of unknown function (DUF697)	1.17	0.702
DespoDRAFT_00945	hypothetical protein	-1.403	0.635
DespoDRAFT_00946	hypothetical protein	-1.023	0.973
DespoDRAFT_00947	hypothetical protein	1.459	0.398
DespoDRAFT_00948	hypothetical protein	-1.137	0.825
DespoDRAFT_00949	hypothetical protein	-1.419	0.677
DespoDRAFT_00950	hypothetical protein	-1.765	0.691

DespoDRAFT_00951	putative membrane protein	-3.745	0.181
DespoDRAFT_00952	hypothetical protein	#VALUE!	NaN
DespoDRAFT_00953	putative RNA-binding protein containing KH domain, possibly ribosomal protein	1.314	0.333
DespoDRAFT_00954	Zn-dependent hydrolase, glyoxylase	-1.164	0.347
DespoDRAFT_00955	GTP-binding protein YchF	1.319	0.41
DespoDRAFT_00956	hypothetical protein	-1.12	0.652
DespoDRAFT_00957	molybdenum cofactor synthesis domain protein	1.085	0.722
DespoDRAFT_00958	pyrimidine operon attenuation protein/uracil phosphoribosyltransferase	-1.092	0.594
DespoDRAFT_00959	molybdopterin-guanine dinucleotide biosynthesis protein A	-1.516	0.153
DespoDRAFT_00960	molybdopterin converting factor, large subunit	-1.573	0.138
DespoDRAFT_00961	molybdenum cofactor biosynthesis protein MoaC	-1.622	0.201
DespoDRAFT_00962	hypothetical protein	-1.293	0.166
DespoDRAFT_00963	membrane-bound lytic murein transglycosylase	-1.011	0.931
DespoDRAFT_00964	hypothetical protein	-3.744	0.235
DespoDRAFT_00965	histidine kinase, Response regulator receiver domain protein	-11.152	0.128
DespoDRAFT_00966	hypothetical protein	-17.009	0.107
DespoDRAFT_00967	hypothetical protein	-1.226	NaN
DespoDRAFT_00968	methyl-accepting chemotaxis protein	-2.031	0.0477
DespoDRAFT_00969	Hpt domain-containing protein	-2.121	0.158
DespoDRAFT_00970	response regulator containing a CheY-like receiver domain and an HD-GYP domain	-2.027	0.146
DespoDRAFT_00971	hypothetical protein	-2.74	0.493
DespoDRAFT_00972	phosphate transport system regulatory protein PhoU	2.75	0.0578
DespoDRAFT_00973	response regulator with CheY-like receiver domain and winged-helix DNA-binding domain	-1.212	0.557
DespoDRAFT_00974	PAS domain S-box	1.257	0.442
DespoDRAFT_00976	Plasmid pRiA4b ORF-3-like protein	1.199	0.504
DespoDRAFT_00977	hypothetical protein	-1.733	0.106
DespoDRAFT_00978	ATPase involved in DNA repair	1.476	0.401
DespoDRAFT_00979	TIGR02436 family protein	2.683	0.48
DespoDRAFT_00980	exonuclease SbcD	-1.13	0.508
DespoDRAFT_00981	hypothetical protein	-1.182	0.672
DespoDRAFT_00982	restriction endonuclease	1.46	0.247
DespoDRAFT_00983	hypothetical protein	#VALUE!	NaN
DespoDRAFT_00984	hypothetical protein	1.217	0.47

DespoDRAFT_00985	hypothetical protein	1.301	0.367
DespoDRAFT_00986	adenine specific DNA methylase Mod	1.327	0.388
DespoDRAFT_00987	hypothetical protein	-1.046	0.937
DespoDRAFT_00988	DNA/RNA helicase, superfamily II, SNF2 family	1.137	0.42
DespoDRAFT_00989	DNA-binding protein, excisionase family	1.518	0.35
DespoDRAFT_00990	putative addiction module killer protein	-1.375	0.431
DespoDRAFT_00991	putative addiction module antidote protein	-1.751	0.0496
DespoDRAFT_00992	putative TIM-barrel fold metal-dependent hydrolase	1.128	0.335
DespoDRAFT_00993	siroheme synthase, N-terminal domain	1.219	0.0936
DespoDRAFT_00994	ABC-type transport system involved in cytochrome c biogenesis, permease component	-1.184	0.332
DespoDRAFT_00995	glutamyl-tRNA reductase	1.428	0.108
DespoDRAFT_00996	penicillin-binding protein 1B	1.242	0.423
DespoDRAFT_00997	hypothetical protein	2.602	0.311
DespoDRAFT_00998	hypothetical protein	-1	0.999
DespoDRAFT_01000	ABC-type Fe ³⁺ transport system, permease component	1.257	0.756
DespoDRAFT_01001	hypothetical protein	1.26	0.284
DespoDRAFT_01002	acyl-CoA synthetase (AMP-forming)/AMP-acid ligase II	2.072	0.0644
DespoDRAFT_01003	cupin domain-containing protein	3.164	0.0728
DespoDRAFT_01004	signal transduction histidine kinase	1.26	0.448
DespoDRAFT_01005	HRDC domain-containing protein	1.244	0.732
DespoDRAFT_01006	hypothetical protein	-1.12	0.893
DespoDRAFT_01007	DNA/RNA helicase, superfamily II SNF2 family	1.377	0.262
DespoDRAFT_01008	DNA-methyltransferase Dcm	1.12	0.818
DespoDRAFT_01009	DNA mismatch endonuclease Vsr	-1.085	0.854
DespoDRAFT_01010	hypothetical protein	-1.318	0.623
DespoDRAFT_01011	plasmid maintenance system killer protein	1.224	0.705
DespoDRAFT_01012	addiction module antidote protein, HigA family	1.419	0.668
DespoDRAFT_01014	cold shock protein	-2.354	0.107
DespoDRAFT_01015	DNA/RNA helicase superfamily II	1.956	0.0897
DespoDRAFT_01016	hypothetical protein	6.635	0.249
DespoDRAFT_01017	hypothetical protein	-1.352	NaN
DespoDRAFT_01018	23S RNA-specific pseudouridylate synthase	1.502	0.556
DespoDRAFT_01020	Alkaline phosphatase	1.632	0.394
DespoDRAFT_01021	putative multitransmembrane protein	-1.011	0.987
DespoDRAFT_01022	putative Zn-dependent protease	-1.306	0.0838
DespoDRAFT_01023	general secretion pathway protein F	1.109	0.741
DespoDRAFT_01024	hypothetical protein	1.384	0.147

DespoDRAFT_01025	Sulfate ATPase (ABC-type multidrug transport system ATPase component)	-1.341	0.0625
DespoDRAFT_01026	ABC-type multidrug transport system permease component	-1.655	0.673
DespoDRAFT_01027	phosphoesterase MJ0936 family	-1.793	0.337
DespoDRAFT_01028	Zn-dependent protease with chaperone function	1.196	0.672
DespoDRAFT_01029	bacterial nucleoid DNA-binding protein	3.879	0.0123
DespoDRAFT_01030	adenylosuccinate lyase	1.073	0.361
DespoDRAFT_01031	uncharacterized protein PH0010 family	1.155	0.218
DespoDRAFT_01032	TrpR-related protein YerC/YecD	-1.888	0.0681
DespoDRAFT_01033	putative phosphoesterase (MutT family)	1.003	0.987
DespoDRAFT_01034	hypothetical protein	1.447	0.493
DespoDRAFT_01036	nucleoside-diphosphate-sugar epimerase	-1.735	0.209
DespoDRAFT_01037	putative membrane protein	-1.409	0.53
DespoDRAFT_01038	putative signal transduction protein	-1.242	0.503
DespoDRAFT_01039	protein affecting phage T7 exclusion by the F plasmid	-1.858	0.104
DespoDRAFT_01040	leucyl/phenylalanyl-tRNA--protein transferase	-1.206	0.369
DespoDRAFT_01041	ATP-dependent Clp protease ATP-binding subunit clpA	-1.941	0.0651
DespoDRAFT_01042	hypothetical protein	-1.089	0.776
DespoDRAFT_01043	preprotein translocase SecA subunit	-1.447	0.108
DespoDRAFT_01044	metalloendopeptidase-like membrane protein	-1.289	0.233
DespoDRAFT_01045	N-acetyl-gamma-glutamyl-phosphate reductase common form	1.905	0.023
DespoDRAFT_01046	putative phosphatase C-terminal domain of histone macro H2A1 like protein	-1.86	0.112
DespoDRAFT_01047	TRAP transporter solute receptor TAXI family	1.189	0.086
DespoDRAFT_01048	TRAP transporter 4TM/12TM fusion protein	-1.782	0.127
DespoDRAFT_01049	universal stress protein UspA-like protein	-1.545	0.0657
DespoDRAFT_01051	NTP pyrophosphohydrolase	-1.562	0.172
DespoDRAFT_01052	Zn-dependent protease with chaperone function	-1.213	0.436
DespoDRAFT_01053	hypothetical protein	2.504	0.149
DespoDRAFT_01054	iron-sulfur cluster biosynthesis protein NifU-like protein	2.672	0.0828
DespoDRAFT_01055	putative RNA-binding protein (contains KH domain)	-1.885	0.365
DespoDRAFT_01056	ABC-type uncharacterized transport system periplasmic component	-1.982	0.0852

DespoDRAFT_01057	hypothetical protein	-1.106	0.847
DespoDRAFT_01058	arabinose efflux permease family protein	1.237	0.823
DespoDRAFT_01059	putative amino acid racemase	1.273	0.686
DespoDRAFT_01060	serine phosphatase RsbU regulator of sigma subunit	-1.292	0.61
DespoDRAFT_01061	serine phosphatase RsbU regulator of sigma subunit	-1.115	0.909
DespoDRAFT_01062	Protein of unknown function (DUF3124)	-1.178	0.498
DespoDRAFT_01063	response regulator with CheY-like receiver AAA-type ATPase and DNA-binding domains	-2.381	0.0828
DespoDRAFT_01064	GSPII_E-like protein	-1.847	0.0881
DespoDRAFT_01065	ATPase involved in chromosome partitioning	-2.166	0.106
DespoDRAFT_01066	beta-hydroxyacid dehydrogenase, 3-hydroxyisobutyrate dehydrogenase	-1.36	0.261
DespoDRAFT_01067	pterin-4a-carbinolamine dehydratase	-3.703	0.00938
DespoDRAFT_01068	drug resistance transporter, Bcr/CflA subfamily	-1.984	0.143
DespoDRAFT_01069	putative membrane protein	-2.132	0.0591
DespoDRAFT_01070	nucleotidyltransferase/DNA polymerase involved in DNA repair	-1.961	0.205
DespoDRAFT_01071	ABC-type dipeptide transport system, periplasmic component	2.635	0.0698
DespoDRAFT_01072	oligopeptide/dipeptide ABC transporter, ATP-binding protein	1.922	0.38
DespoDRAFT_01073	cold shock protein	1.2	0.417
DespoDRAFT_01074	oligopeptide/dipeptide ABC transporter, ATP-binding protein	2.655	0.214
DespoDRAFT_01075	hypothetical protein	-2.6	NaN
DespoDRAFT_01076	hypothetical protein	1.082	0.777
DespoDRAFT_01077	parvulin-like peptidyl-prolyl isomerase	1.288	0.0326
DespoDRAFT_01078	Mg ²⁺ transporter MgtE	-1.106	0.713
DespoDRAFT_01079	DNA repair protein RecO	1.924	0.251
DespoDRAFT_01080	putative kinase, galactokinase/mevalonate kinase	1.031	0.918
DespoDRAFT_01081	hypothetical protein	1.284	0.207
DespoDRAFT_01082	uridine phosphorylase	1.129	0.603
DespoDRAFT_01083	DNA ligase, NAD-dependent	-1.027	0.824
DespoDRAFT_01084	signal recognition particle-docking protein FtsY	1.67	0.122
DespoDRAFT_01085	diguanylate cyclase (GGDEF) domain-containing protein	-1.12	0.687
DespoDRAFT_01086	6-phosphofructokinase	-1.211	0.464

DespoDRAFT_01087	putative heme d1 biosynthesis radical SAM protein NirJ2	-1.184	0.141
DespoDRAFT_01088	delta-aminolevulinic acid dehydratase	1.109	0.468
DespoDRAFT_01089	putative heme d1 biosynthesis radical SAM protein NirJ1	1.545	0.0302
DespoDRAFT_01090	ATP-dependent protease Clp, ATPase subunit	-1.773	0.0682
DespoDRAFT_01091	hypothetical protein	3.746	0.291
DespoDRAFT_01093	protein translocase, SecG subunit	1.459	0.0316
DespoDRAFT_01094	triosephosphate isomerase	1.628	0.42
DespoDRAFT_01095	glyceraldehyde-3-phosphate dehydrogenase, type I	1.391	0.188
DespoDRAFT_01096	phosphotransferase system, mannose/fructose-specific component IIA	1.186	0.534
DespoDRAFT_01097	putative P-loop-containing kinase	-1.227	0.134
DespoDRAFT_01098	phosphotransferase system mannitol/fructose-specific IIA component (Ntr-type)	-1.075	0.77
DespoDRAFT_01099	ribosomal subunit interface protein	1.184	0.325
DespoDRAFT_01100	RNA polymerase sigma-54 factor	1.125	0.116
DespoDRAFT_01101	ABC-type (unclassified) transport system, ATPase component	-1.041	0.228
DespoDRAFT_01102	hypothetical protein	1.03	0.851
DespoDRAFT_01103	hypothetical protein	1.79	0.374
DespoDRAFT_01104	3-deoxy-D-manno-octulosonate 8-phosphate phosphatase, YrbI family	2.318	0.0682
DespoDRAFT_01105	3-deoxy-8-phosphooctulonate synthase	2.932	0.0893
DespoDRAFT_01106	metalloendopeptidase-like membrane protein	1.022	0.867
DespoDRAFT_01107	hypothetical protein	-1.025	0.671
DespoDRAFT_01108	signal peptidase I	-1.084	0.851
DespoDRAFT_01109	aspartate carbamoyltransferase	1.268	0.169
DespoDRAFT_01110	dihydroorotase, multifunctional complex type	1.31	0.0424
DespoDRAFT_01111	hypothetical protein	-1.343	0.394
DespoDRAFT_01112	hypothetical protein	-1.137	0.751
DespoDRAFT_01113	response regulator with CheY-like receiver, AAA-type ATPase and DNA-binding domains	-1.123	0.505
DespoDRAFT_01114	prepilin-type N-terminal cleavage/methylation domain-containing protein	-4.713	0.0511
DespoDRAFT_01115	ABC-type multidrug transport system, ATPase component	-2.311	0.0347
DespoDRAFT_01116	hypothetical protein	-2.695	0.0936

DespoDRAFT_01117	hypothetical protein	-1.72	0.329
DespoDRAFT_01118	Protein of unknown function (DUF2893)	-1.418	0.471
DespoDRAFT_01119	protein of unknown function (DUF1814)	-1.634	0.568
DespoDRAFT_01121	prevent-host-death family protein	-1.243	0.852
DespoDRAFT_01123	restriction endonuclease	1.3	0.498
DespoDRAFT_01124	hypothetical protein	1.151	0.783
DespoDRAFT_01125	hypothetical protein	1.778	0.578
DespoDRAFT_01126	hypothetical protein	-1.087	0.832
DespoDRAFT_01127	hypothetical protein	-1.96	0.042
DespoDRAFT_01128	hypothetical protein	-1.143	0.847
DespoDRAFT_01129	hypothetical protein	-1.246	0.513
DespoDRAFT_01130	hypothetical protein	-1.724	0.188
DespoDRAFT_01131	hypothetical protein	-1.843	0.0405
DespoDRAFT_01132	prepilin-type N-terminal cleavage/methylation domain-containing protein	-2.348	0.0824
DespoDRAFT_01133	prepilin-type N-terminal cleavage/methylation domain-containing protein	-3.092	0.168
DespoDRAFT_01134	prepilin-type N-terminal cleavage/methylation domain-containing protein	-3.758	0.128
DespoDRAFT_01135	thiamine biosynthesis protein ThiC	1.23	0.196
DespoDRAFT_01136	hypothetical protein	1.4	0.0644
DespoDRAFT_01137	phosphopantothencysteine decarboxylase/phosphopantothenate--cysteine ligase	1.01	0.778
DespoDRAFT_01138	uracil-DNA glycosylase	1.651	0.0757
DespoDRAFT_01139	site-specific recombinase XerD	-1.046	0.871
DespoDRAFT_01140	ATP-dependent protease HslVU, peptidase subunit	1.282	0.298
DespoDRAFT_01141	ATP-dependent protease HslVU, ATPase subunit	2.049	0.0841
DespoDRAFT_01142	acetylglutamate kinase	1.505	0.0477
DespoDRAFT_01143	acetylornithine/succinylornithine aminotransferase	1.505	0.261
DespoDRAFT_01144	ornithine carbamoyltransferase	1.565	0.17
DespoDRAFT_01145	argininosuccinate lyase	1.48	0.2
DespoDRAFT_01146	hypothetical protein	1.715	0.0462
DespoDRAFT_01147	2-amino-4-hydroxy-6-hydroxymethyldihydropteridine pyrophosphokinase	6.107	0.0248
DespoDRAFT_01148	fructose-6-phosphate aldolase, TalC/MipB family	4.815	0.029
DespoDRAFT_01151	hypothetical protein	-1.827	0.231

DespoDRAFT_01155	putative transcriptional regulator	1.129	NaN
DespoDRAFT_01156	DNA polymerase III epsilon subunit-like 3'-5' exonuclease	-1.146	0.963
DespoDRAFT_01157	hypothetical protein	1.119	NaN
DespoDRAFT_01158	phage regulatory protein, rha family	-1.564	0.856
DespoDRAFT_01159	CO dehydrogenase maturation factor	-1.284	NaN
DespoDRAFT_01161	type IV secretory pathway, VirB2 component (pilin)	-1.646	NaN
DespoDRAFT_01162	type IV secretory pathway, VirB4 component	-1.517	0.809
DespoDRAFT_01163	P-type conjugative transfer protein TrbJ	-3.766	0.216
DespoDRAFT_01164	hypothetical protein	-3.369	0.136
DespoDRAFT_01165	P-type conjugative transfer protein TrbL	1.173	0.944
DespoDRAFT_01166	type IV secretory pathway, TrbF component	-1.401	0.847
DespoDRAFT_01167	P-type conjugative transfer protein TrbG	-1.096	0.972
DespoDRAFT_01168	Conjugal transfer protein TrbH	-2.003	NaN
DespoDRAFT_01169	type IV secretory pathway, VirB10 component	-1.85	0.796
DespoDRAFT_01170	DNA topoisomerase III	-1.19	0.921
DespoDRAFT_01171	hypothetical protein	1.447	0.682
DespoDRAFT_01172	antirestriction protein	-1.129	0.931
DespoDRAFT_01173	type IV secretory pathway, VirD4 component	-1.506	0.805
DespoDRAFT_01174	type IV secretory pathway, protease TraF	1.746	NaN
DespoDRAFT_01175	P-type conjugative transfer ATPase TrbB	-1.401	0.749
DespoDRAFT_01176	Ribbon-helix-helix protein, copG family	#VALUE!	NaN
DespoDRAFT_01177	relaxase/mobilization nuclease	1.056	0.972
DespoDRAFT_01178	hypothetical protein	-1.635	NaN
DespoDRAFT_01179	cytotoxic translational repressor of toxin-antitoxin stability system	-3.567	0.0993
DespoDRAFT_01180	putative transcriptional regulator with C-terminal CBS domains	-3.341	0.0464
DespoDRAFT_01181	hypothetical protein	-2.276	0.148
DespoDRAFT_01182	hypothetical protein	-2.548	0.142
DespoDRAFT_01183	methylase involved in ubiquinone/menaquinone biosynthesis	-2.45	0.134
DespoDRAFT_01184	DnaJ-class molecular chaperone with C-terminal Zn finger domain	-1.743	0.435
DespoDRAFT_01185	hypothetical protein	1.144	0.827
DespoDRAFT_01186	serine/threonine protein kinase	-1.082	0.929
DespoDRAFT_01187	hypothetical protein	1.513	0.631
DespoDRAFT_01188	putative ATPase	1.485	0.359
DespoDRAFT_01189	hypothetical protein	2.151	0.42
DespoDRAFT_01190	hypothetical protein	1.202	0.48

DespoDRAFT_01191	hypothetical protein	-1.107	0.842
DespoDRAFT_01192	hypothetical protein	1.091	0.911
DespoDRAFT_01193	S23 ribosomal protein	-3.178	0.0202
DespoDRAFT_01194	hypothetical protein	-1.802	0.109
DespoDRAFT_01195	putative transcriptional regulator with HTH domain	-1.59	0.0571
DespoDRAFT_01196	hypothetical protein	-1.096	0.685
DespoDRAFT_01197	hypothetical protein	1.103	0.537
DespoDRAFT_01198	restriction endonuclease S subunit	1.009	0.946
DespoDRAFT_01199	type I restriction-modification system methyltransferase subunit	-1.001	0.999
DespoDRAFT_01200	hypothetical protein	-2.087	0.066
DespoDRAFT_01201	hypothetical protein	-1.251	0.315
DespoDRAFT_01202	type I restriction-modification system methyltransferase subunit	1.528	0.171
DespoDRAFT_01203	hypothetical protein	#VALUE!	NaN
DespoDRAFT_01204	hypothetical protein	-5.136	NaN
DespoDRAFT_01206	site-specific recombinase XerD	-2.702	0.135
DespoDRAFT_01207	hypothetical protein	3.24	0.173
DespoDRAFT_01208	DNA polymerase III epsilon subunit-like 3'-5' exonuclease	3.171	0.435
DespoDRAFT_01209	hypothetical protein	-1.425	NaN
DespoDRAFT_01210	phage regulatory protein, rha family	3.686	0.219
DespoDRAFT_01211	CobQ/CobB/MinD/ParA nucleotide binding domain-containing protein	-1.134	0.913
DespoDRAFT_01212	hypothetical protein	-1.054	0.971
DespoDRAFT_01213	type IV secretory pathway, VirB2 component (pilin)	2.495	NaN
DespoDRAFT_01215	Rhodopirellula transposase	-1.452	0.832
DespoDRAFT_01216	P-type conjugative transfer protein TrbJ	-1.349	0.867
DespoDRAFT_01217	hypothetical protein	-5.2	0.234
DespoDRAFT_01218	P-type conjugative transfer protein TrbL	2.139	NaN
DespoDRAFT_01219	type IV secretory pathway, TrbF component	2.336	NaN
DespoDRAFT_01220	P-type conjugative transfer protein TrbG	8.646	NaN
DespoDRAFT_01221	Conjugal transfer protein TrbH	#VALUE!	NaN
DespoDRAFT_01222	type IV secretory pathway, VirB10 component	1.117	0.968
DespoDRAFT_01223	hypothetical protein	-1.912	NaN
DespoDRAFT_01224	DNA topoisomerase III	-1.433	0.751
DespoDRAFT_01225	hypothetical protein	-5.004	0.11
DespoDRAFT_01226	antirestriction protein	-1.424	0.808
DespoDRAFT_01227	type IV secretory pathway, VirD4 component	-1.28	0.818
DespoDRAFT_01228	type IV secretory pathway, protease TraF	-1.193	0.875

DespoDRAFT_01229	P-type conjugative transfer ATPase TrbB	-1.343	0.903
DespoDRAFT_01230	TrbM	-2.5	0.574
DespoDRAFT_01231	Ribbon-helix-helix protein, copG family	3.056	NaN
DespoDRAFT_01232	relaxase/mobilization nuclease	-1.322	0.696
DespoDRAFT_01233	hypothetical protein	1.216	0.718
DespoDRAFT_01234	nuclease-like protein protein kinase family protein	1.012	0.98
DespoDRAFT_01238	hypothetical protein	-1.244	0.707
DespoDRAFT_01239	abortive infection bacteriophage resistance protein	-1.078	0.934
DespoDRAFT_01240	putative metal-dependent hydrolase	1.797	0.177
DespoDRAFT_01241	type I site-specific deoxyribonuclease HsdR family	1.081	0.827
DespoDRAFT_01242	restriction endonuclease S subunit	-1.613	0.485
DespoDRAFT_01243	type I restriction-modification system methyltransferase subunit	2.242	0.14
DespoDRAFT_01244	secondary thiamine-phosphate synthase enzyme	-1.645	0.373
DespoDRAFT_01245	hypothetical protein	-2.104	0.122
DespoDRAFT_01248	hypothetical protein	-1.144	0.828
DespoDRAFT_01250	transposase	#VALUE!	NaN
DespoDRAFT_01252	hypothetical protein	-1.402	0.583
DespoDRAFT_01253	site-specific recombinase XerD	-1.323	0.747
DespoDRAFT_01254	regulator of stationary/sporulation gene expression	-1.58	0.387
DespoDRAFT_01255	putative nucleic-acid-binding protein	-1.739	0.195
DespoDRAFT_01257	hypothetical protein	-1.565	0.248
DespoDRAFT_01260	tyrosyl-tRNA synthetase	1.659	0.432
DespoDRAFT_01261	nicotinamidase-like amidase	-1.436	0.283
DespoDRAFT_01262	putative permease	-1.597	0.486
DespoDRAFT_01263	Protein of unknown function (DUF3124)	-1.349	0.545
DespoDRAFT_01264	hypothetical protein	-1.584	0.421
DespoDRAFT_01265	hypothetical protein	-1.454	0.227
DespoDRAFT_01266	hypothetical protein	-1.901	0.444
DespoDRAFT_01267	Protein of unknown function (DUF3102)	-1.658	0.61
DespoDRAFT_01268	hypothetical protein	-1.57	0.424
DespoDRAFT_01269	putative transcription factor, MBF1 like protein	1.811	NaN
DespoDRAFT_01270	hypothetical protein	-2.496	0.586
DespoDRAFT_01272	hypothetical protein	1.34	0.706
DespoDRAFT_01273	hypothetical protein	-1.092	0.893
DespoDRAFT_01274	hypothetical protein	-1.345	0.758
DespoDRAFT_01275	hypothetical protein	-2.93	0.0594
DespoDRAFT_01276	hypothetical protein	-1.634	0.464
DespoDRAFT_01277	hypothetical protein	1.641	0.334

DespoDRAFT_01278	site-specific recombinase XerD	-1.395	0.746
DespoDRAFT_01279	hypothetical protein	2.091	NaN
DespoDRAFT_01280	hypothetical protein	1.007	NaN
DespoDRAFT_01281	hypothetical protein	-1.535	0.847
DespoDRAFT_01282	hypothetical protein	-1.155	0.952
DespoDRAFT_01283	hypothetical protein	1.508	0.622
DespoDRAFT_01284	site-specific recombinase, DNA invertase Pin	-1.435	0.471
DespoDRAFT_01286	transposase	-1.012	0.963
DespoDRAFT_01287	glycogen synthase	-2.281	0.189
DespoDRAFT_01288	acetyl-CoA hydrolase	-2.386	0.0837
DespoDRAFT_01289	Kef-type K ⁺ transport system, predicted NAD-binding component	-1.865	0.166
DespoDRAFT_01290	cyclic nucleotide-binding protein	-1.95	0.402
DespoDRAFT_01291	transcription elongation factor	-1.778	0.247
DespoDRAFT_01292	Ribosomal protein S27	-1.819	0.133
DespoDRAFT_01293	hypothetical protein	-2.655	0.0608
DespoDRAFT_01294	hypothetical protein	-4.583	0.0637
DespoDRAFT_01295	response regulator with CheY-like receiver, AAA-type ATPase, and DNA-binding domains	1.361	0.771
DespoDRAFT_01297	di-/tricarboxylate transporter	-2.514	0.504
DespoDRAFT_01298	hypothetical protein	-1.98	0.27
DespoDRAFT_01299	glyceraldehyde-3-phosphate dehydrogenase type I	-1.267	0.345
DespoDRAFT_01300	dehydrogenase of unknown specificity	-1.415	0.14
DespoDRAFT_01301	glycogen/starch/alpha-glucan phosphorylase	-1.415	0.489
DespoDRAFT_01302	membrane protein MarC family	-1.049	0.921
DespoDRAFT_01303	hypothetical protein	-1.926	0.701
DespoDRAFT_01306	hypothetical protein	1.706	NaN
DespoDRAFT_01307	response regulator with CheY-like receiver AAA-type ATPase and DNA-binding domains	-1.355	0.728
DespoDRAFT_01309	response regulator with CheY-like receiver AAA-type ATPase and DNA-binding domains	-2.644	0.619
DespoDRAFT_01310	signal transduction histidine kinase	-1.246	0.826
DespoDRAFT_01311	iron-sulfur cluster repair di-iron protein	-2.623	0.0636
DespoDRAFT_01312	hypothetical protein	-4.595	0.129
DespoDRAFT_01313	transcriptional regulator	-2.622	0.0489
DespoDRAFT_01314	RND family efflux transporter MFP subunit	-2.927	0.187
DespoDRAFT_01315	ABC-type transport system involved in lipoprotein release permease component	-2.674	0.0489

DespoDRAFT_01316	ABC-type antimicrobial peptide transport system ATPase component	-2.608	0.111
DespoDRAFT_01317	efflux transporter outer membrane factor lipoprotein NodT family	-2.044	0.316
DespoDRAFT_01318	polyferredoxin	1.573	0.719
DespoDRAFT_01320	hypothetical protein	-3.653	0.0475
DespoDRAFT_01321	hypothetical protein	-1.005	0.997
DespoDRAFT_01322	Retron-type reverse transcriptase	-1.2	0.746
DespoDRAFT_01324	Retron-type reverse transcriptase	-1.919	0.352
DespoDRAFT_01327	Protein of unknown function (DUF1566)	-1.166	0.769
DespoDRAFT_01328	copper/silver-translocating P-type ATPase	-1.466	0.128
DespoDRAFT_01329	hypothetical protein	-3.195	0.0574
DespoDRAFT_01330	hypothetical protein	-6.784	0.0951
DespoDRAFT_01331	putative membrane protein	-9.034	0.212
DespoDRAFT_01332	Positive regulator of sigma E activity	-9.733	0.106
DespoDRAFT_01333	response regulator with CheY-like receiver AAA-type ATPase and DNA-binding domains	-1.206	0.645
DespoDRAFT_01334	histidine kinase	-1.357	0.538
DespoDRAFT_01336	hypothetical protein	-1.132	0.934
DespoDRAFT_01337	hypothetical protein	-5.431	0.0531
DespoDRAFT_01338	nitrate/TMAO reductase membrane-bound tetraheme cytochrome c subunit	-3.72	0.125
DespoDRAFT_01339	PAS domain S-box	-3.166	0.084
DespoDRAFT_01340	hydroxylamine reductase	-2.691	0.126
DespoDRAFT_01341	putative Nitric oxide reductase	-3.154	0.08
DespoDRAFT_01342	hydrid cluster protein-associated redox disulfide domain	-1.365	0.748
DespoDRAFT_01343	cAMP-binding protein	1.103	0.931
DespoDRAFT_01346	hypothetical protein	-2.015	NaN
DespoDRAFT_01347	site-specific recombinase XerD	-3.553	0.199
DespoDRAFT_01349	hypothetical protein	1.045	NaN
DespoDRAFT_01350	hypothetical protein	1.815	0.47
DespoDRAFT_01352	hypothetical protein	-3.126	NaN
DespoDRAFT_01353	hypothetical protein	-1.784	0.284
DespoDRAFT_01354	diaminopimelate epimerase	-2.047	0.256
DespoDRAFT_01355	hypothetical protein	-11.838	0.0298
DespoDRAFT_01356	hypothetical protein	-1.796	0.219
DespoDRAFT_01357	DNA/RNA helicase superfamily I	-1.433	0.237
DespoDRAFT_01358	hypothetical protein	1.103	0.804
DespoDRAFT_01359	soluble lytic murein transglycosylase-like protein	-1.453	0.125
DespoDRAFT_01360	UTP-glucose-1-phosphate uridylyltransferase	-1.794	0.0981
DespoDRAFT_01361	putative Fe-S oxidoreductase	1.357	0.21

DespoDRAFT_01362	dihydrodipicolinate synthase	1.385	0.187
DespoDRAFT_01363	putative selenocysteine protein	1.875	0.108
DespoDRAFT_01364	dsrA: sulfite reductase, dissimilatory-type alpha subunit	2.575	0.0326
DespoDRAFT_01365	dsrB: sulfite reductase, dissimilatory-type beta subunit	2.194	0.0834
DespoDRAFT_01366	dsrD: sulfite reductase, dissimilatory-type delta subunit	1.172	0.212
DespoDRAFT_01367	cobyrinic acid a c-diamide synthase	1.259	0.183
DespoDRAFT_01368	putative xylanase/chitin deacetylase	1.748	0.283
DespoDRAFT_01370	hypothetical protein	-2.37	0.0603
DespoDRAFT_01371	putative membrane protein involved in D-alanine export	1.335	0.62
DespoDRAFT_01372	hypothetical protein	-1.255	0.575
DespoDRAFT_01373	hypothetical protein	-2.596	NaN
DespoDRAFT_01374	radical SAM additional 4Fe4S-binding domain protein	1.812	0.465
DespoDRAFT_01375	MMPL family	1.276	0.605
DespoDRAFT_01376	glycosyltransferase involved in LPS biosynthesis	1.743	0.394
DespoDRAFT_01377	putative membrane protein	1.524	0.623
DespoDRAFT_01378	hypothetical protein	1.355	0.362
DespoDRAFT_01379	hypothetical protein	-1.302	0.431
DespoDRAFT_01380	acyl carrier protein	-1.289	0.503
DespoDRAFT_01381	soluble lytic murein transglycosylase-like protein	-1.861	0.138
DespoDRAFT_01382	hypothetical protein	1.038	0.924
DespoDRAFT_01383	hypothetical protein	-1.169	0.498
DespoDRAFT_01384	3-hydroxymyristoyl/3-hydroxydecanoyl-(acyl carrier protein) dehydratase	-1.085	0.781
DespoDRAFT_01385	acyl carrier protein	1.19	0.714
DespoDRAFT_01386	EDD domain protein DegV family	1.518	0.346
DespoDRAFT_01387	putative thioesterase	1.391	0.658
DespoDRAFT_01388	hypothetical protein	2.826	0.104
DespoDRAFT_01389	3-oxoacyl-(acyl-carrier-protein) synthase	1.282	0.306
DespoDRAFT_01390	Tfp pilus assembly protein PilF	-1.046	0.199
DespoDRAFT_01391	hypothetical protein	-1.901	0.0729
DespoDRAFT_01392	hypothetical protein	-2.685	0.0895
DespoDRAFT_01393	methylase involved in ubiquinone/menaquinone biosynthesis	1.075	0.834
DespoDRAFT_01394	hypothetical protein	2.694	0.0435
DespoDRAFT_01395	acetyl-CoA synthetase (AMP-forming)/AMP-acid ligase II	2.521	0.082
DespoDRAFT_01396	3-oxoacyl-(acyl-carrier-protein) synthase	2.416	0.227
DespoDRAFT_01397	1-acyl-sn-glycerol-3-phosphate	1.414	0.622

	acyltransferase		
DespoDRAFT_01398	3-oxoacyl-(acyl-carrier-protein) synthase	2.401	0.29
DespoDRAFT_01399	3-oxoacyl-(acyl-carrier-protein) synthase	2.383	0.0965
DespoDRAFT_01400	acyl-CoA thioester hydrolase YbgC/YbaW family	2.304	0.424
DespoDRAFT_01401	hypothetical protein	2.595	0.023
DespoDRAFT_01402	glycosyl transferase	2.25	0.122
DespoDRAFT_01403	Lauroyl/myristoyl acyltransferase	-1.123	0.856
DespoDRAFT_01404	UDP-N-acetylmuramyl pentapeptide phosphotransferase/UDP-N-acetylglucosamine-1-phosphate transferase	1.393	0.476
DespoDRAFT_01405	NAD dependent epimerase/dehydratase family protein	1.765	0.471
DespoDRAFT_01406	UDP-N-acetylglucosamine 1-carboxyvinyltransferase	1.401	0.0634
DespoDRAFT_01407	DNA internalization-related competence protein ComEC/Rec2	-1.658	0.449
DespoDRAFT_01408	hypothetical protein	-1.039	0.935
DespoDRAFT_01409	CoA-substrate-specific enzyme activase putative	-1.61	0.0463
DespoDRAFT_01410	putative integral membrane protein	1.248	0.63
DespoDRAFT_01411	CysA: sulfate/thiosulfate import ATP-binding protein CysA	1.418	0.184
DespoDRAFT_01412	ABC-type transport system involved in resistance to organic solvents periplasmic component	1.709	0.241
DespoDRAFT_01413	surface lipoprotein	-1.097	0.685
DespoDRAFT_01415	hypothetical protein	1.78	0.128
DespoDRAFT_01417	putative amidohydrolase	-1.085	0.836
DespoDRAFT_01418	transcriptional regulator	-1.011	0.917
DespoDRAFT_01419	dsrC: sulfite reductase, dissimilatory-type gamma subunit	1.676	0.146
DespoDRAFT_01420	tRNA isopentenyltransferase MiaA	1.434	0.421
DespoDRAFT_01423	ABC-type branched-chain amino acid transport system periplasmic component	1.291	0.625
DespoDRAFT_01424	6-phosphofructokinase	-1.876	0.000688
DespoDRAFT_01425	KpsF/GutQ family protein	-1.281	0.336
DespoDRAFT_01426	hypothetical protein	2.771	0.0852
DespoDRAFT_01427	aspartate/tyrosine/aromatic aminotransferase	2.03	0.0248
DespoDRAFT_01428	pseudouridylate synthase I	-1.04	0.923
DespoDRAFT_01429	putative quinone oxidoreductase YhdH/YhfP family	1.822	0.414
DespoDRAFT_01430	aspA aspartate ammonia-lyase	-2.312	0.0709

DespoDRAFT_01432	response regulator with CheY-like receiver domain and winged-helix DNA-binding domain	-1.108	0.235
DespoDRAFT_01433	signal transduction histidine kinase	-1.313	0.276
DespoDRAFT_01434	periplasmic serine protease Do/DeqQ family	-1.344	0.104
DespoDRAFT_01435	glutaredoxin-like protein	-2.097	0.135
DespoDRAFT_01437	parvulin-like peptidyl-prolyl isomerase	1.609	0.108
DespoDRAFT_01438	PilZ domain-containing protein	-1.958	0.412
DespoDRAFT_01439	hypothetical protein	1.719	0.283
DespoDRAFT_01440	hypothetical protein	-1.027	0.95
DespoDRAFT_01441	C-terminal processing peptidase	-1.397	0.223
DespoDRAFT_01442	ribosome biogenesis GTP-binding protein YlqF	-1.116	0.578
DespoDRAFT_01443	hypothetical protein	-1.626	0.312
DespoDRAFT_01444	inositol monophosphatase/fructose-1 6-bisphosphatase family protein	-1.132	0.71
DespoDRAFT_01445	soluble lytic murein transglycosylase-like protein	-1.039	0.795
DespoDRAFT_01446	hypothetical protein	1.035	0.964
DespoDRAFT_01447	hypothetical protein	1.195	0.347
DespoDRAFT_01448	GMP synthase (glutamine-hydrolyzing)	-1.056	0.61
DespoDRAFT_01449	hypothetical protein	-1.079	0.914
DespoDRAFT_01450	type I secretion system ABC transporter PrtD family	2.528	0.103
DespoDRAFT_01451	type I secretion system ABC transporter PrtD family	3.258	0.0265
DespoDRAFT_01452	ABC-type protease/lipase transport system ATPase and permease component	2.056	0.128
DespoDRAFT_01453	type I secretion membrane fusion protein HlyD family	2.657	0.0417
DespoDRAFT_01454	glycosyltransferase	1.674	0.196
DespoDRAFT_01455	hypothetical protein	-1.426	0.152
DespoDRAFT_01456	hypothetical protein	-6.736	0.0193
DespoDRAFT_01457	methylase involved in ubiquinone/menaquinone biosynthesis	-1.62	0.162
DespoDRAFT_01458	hypothetical protein	1.034	0.856
DespoDRAFT_01459	hypothetical protein	1.029	0.666
DespoDRAFT_01460	hypothetical protein	1.061	0.829
DespoDRAFT_01461	hypothetical protein	#VALUE!	NaN
DespoDRAFT_01464	hypothetical protein	-2.787	0.0806
DespoDRAFT_01465	Protein of unknown function (DUF2442)	-3.051	0.114
DespoDRAFT_01467	hypothetical protein	-3.502	0.0935
DespoDRAFT_01471	Protein of unknown function (DUF2442)	-1.269	0.316
DespoDRAFT_01472	hypothetical protein	-1.827	0.412

DespoDRAFT_01473	hypothetical protein	-2.978	0.104
DespoDRAFT_01474	hypothetical protein	-1.048	0.96
DespoDRAFT_01475	hypothetical protein	-1.29	0.193
DespoDRAFT_01476	group II intron maturase family protein	-1.132	0.31
DespoDRAFT_01477	Rhodopirellula transposase	-11.61	0.332
DespoDRAFT_01478	hypothetical protein	-3.769	0.0564
DespoDRAFT_01479	hypothetical protein	-3.768	0.0436
DespoDRAFT_01481	Peptidase M10 serralyisin	-4.113	0.131
DespoDRAFT_01484	SapC	2.57	0.0573
DespoDRAFT_01485	hypothetical protein	-2.981	0.029
DespoDRAFT_01486	hypothetical protein	-2.556	0.0523
DespoDRAFT_01487	Matrixin	-1.91	0.173
DespoDRAFT_01488	hypothetical protein	-1.609	0.0919
DespoDRAFT_01489	GDP-D-mannose dehydratase	2.666	0.179
DespoDRAFT_01490	GDP-mannose 4 6-dehydratase	3.018	0.0949
DespoDRAFT_01491	ABC-type polysaccharide/polyol phosphate export system permease component	2.23	0.0973
DespoDRAFT_01492	glycosyltransferase	2.255	0.31
DespoDRAFT_01493	ABC-type polysaccharide/polyol phosphate transport system ATPase component	2.452	0.0999
DespoDRAFT_01494	glycosyltransferase	1.327	0.596
DespoDRAFT_01495	methylase involved in ubiquinone/menaquinone biosynthesis	1.153	0.746
DespoDRAFT_01496	glycosyltransferase	2.784	0.104
DespoDRAFT_01499	transposase	3.619	0.434
DespoDRAFT_01500	hypothetical protein	-1.14	NaN
DespoDRAFT_01501	hypothetical protein	-1.719	0.488
DespoDRAFT_01502	hypothetical protein	-1.357	0.576
DespoDRAFT_01503	Arylsulfotransferase (ASST)	1.203	0.298
DespoDRAFT_01504	glycosyl transferase	-1.045	0.922
DespoDRAFT_01505	putative membrane protein	-1.347	0.88
DespoDRAFT_01506	hypothetical protein	-1.156	0.828
DespoDRAFT_01507	putative membrane protein involved in D-alanine export	1.415	0.702
DespoDRAFT_01508	hypothetical protein	1.456	0.186
DespoDRAFT_01509	translation elongation factor P	2.944	0.0537
DespoDRAFT_01510	outer membrane protein	1.637	0.125
DespoDRAFT_01511	hypothetical protein	2.894	0.425
DespoDRAFT_01512	Ech-hydrogenase-related complex EhrS / Ni Fe-hydrogenase III small subunit	3.696	0.0355
DespoDRAFT_01513	Ni Fe-hydrogenase III large subunit	2.69	0.0536
DespoDRAFT_01514	formate hydrogenlyase subunit 3/multisubunit Na ⁺ /H ⁺ antiporter MnhD subunit	2.365	0.0878
DespoDRAFT_01515	hydrogenase 4 membrane component (E)	1.727	0.119

DespoDRAFT_01516	formate hydrogenlyase subunit 4	2.567	0.284
DespoDRAFT_01517	formate hydrogenlyase subunit 3/multisubunit Na ⁺ /H ⁺ antiporter MnhD subunit	2.133	0.0893
DespoDRAFT_01518	isoleucine patch superfamily enzyme carbonic anhydrase/acetyltransferase	-1.549	0.0658
DespoDRAFT_01519	anaerobic dehydrogenase typically selenocysteine-containing	1.036	0.881
DespoDRAFT_01520	potassium uptake protein TrkH family	-1.209	0.331
DespoDRAFT_01521	K ⁺ transport system NAD-binding component	1.125	0.747
DespoDRAFT_01522	di-/tricarboxylate transporter	3.272	0.0538
DespoDRAFT_01523	hypothetical protein	1.77	0.361
DespoDRAFT_01524	hypothetical protein	1.589	0.514
DespoDRAFT_01525	transcriptional regulator containing PAS AAA-type ATPase	1.201	0.525
DespoDRAFT_01526	collagenase-like protease	-1.036	0.867
DespoDRAFT_01527	cupin domain-containing protein	-1.006	0.986
DespoDRAFT_01528	hypothetical protein	1.581	0.256
DespoDRAFT_01529	hypothetical protein	-1.173	0.54
DespoDRAFT_01530	putative MccF-like protein (microcin C7 resistance)	-1.325	0.293
DespoDRAFT_01531	penicillin-binding protein beta-lactamase class C	-1.241	0.29
DespoDRAFT_01532	cell shape determining protein MreB/Mrl family	1.114	0.59
DespoDRAFT_01533	rod shape-determining protein MreC	1.744	0.235
DespoDRAFT_01534	hypothetical protein	-1.049	0.948
DespoDRAFT_01535	penicillin-binding protein 2	2.725	0.136
DespoDRAFT_01536	rod shape-determining protein RodA	2.34	0.26
DespoDRAFT_01537	F0F1-type ATP synthase beta subunit	2.759	0.0578
DespoDRAFT_01538	ATP synthase F0 subunit b	2.432	0.00692
DespoDRAFT_01539	ATP synthase F1 delta subunit	2.823	0.0274
DespoDRAFT_01540	proton translocating ATP synthase F1 alpha subunit	2.376	0.0449
DespoDRAFT_01541	ATP synthase F1 gamma subunit	2.627	0.0255
DespoDRAFT_01542	ATP synthase F1 beta subunit	3.385	0.0607
DespoDRAFT_01543	ATP synthase F1 epsilon subunit	2.708	0.0464
DespoDRAFT_01544	N-acetylglucosamine-1-phosphate uridylyltransferase/acetyltransferase	1.635	0.126
DespoDRAFT_01545	hypothetical protein	-1.29	0.286
DespoDRAFT_01546	Cell division protein ZapA	-1.044	0.959
DespoDRAFT_01547	hypothetical protein	1.633	0.165
DespoDRAFT_01548	tyrosyl-tRNA synthetase	1.69	0.0496
DespoDRAFT_01555	phosphopantetheine-containing protein	1.322	0.568

DespoDRAFT_01556	3-oxoacyl-(acyl-carrier-protein) synthase	1.228	0.54
DespoDRAFT_01557	Fe-S oxidoreductase	-1.046	0.963
DespoDRAFT_01558	hypothetical protein	-1.206	0.861
DespoDRAFT_01559	outer membrane lipoprotein-sorting protein	-1.625	0.307
DespoDRAFT_01560	dehydrogenase of unknown specificity	1.043	0.909
DespoDRAFT_01561	hypothetical protein	-1.388	0.655
DespoDRAFT_01562	hypothetical protein	1.446	0.567
DespoDRAFT_01563	Ni Fe-hydrogenase I large subunit	-1.155	0.732
DespoDRAFT_01564	hydrogenase (NiFe) small subunit HydA	-2.541	0.159
DespoDRAFT_01565	methyl-accepting chemotaxis protein	-1.083	0.926
DespoDRAFT_01566	hypothetical protein	-2.466	0.0545
DespoDRAFT_01567	ABC-type transport system involved in Fe-S cluster assembly permease component	-1.269	0.347
DespoDRAFT_01568	ABC-type transport system involved in Fe-S cluster assembly ATPase component	-1.191	0.23
DespoDRAFT_01569	oligopeptide/dipeptide ABC transporter ATP-binding protein	1.408	0.619
DespoDRAFT_01570	ABC-type dipeptide/oligopeptide/nickel transport system permease component	2.197	NaN
DespoDRAFT_01571	ABC-type dipeptide/oligopeptide/nickel transport system permease component	2.055	0.478
DespoDRAFT_01572	ABC-type dipeptide transport system periplasmic component	18.241	0.0948
DespoDRAFT_01573	methylase involved in ubiquinone/menaquinone biosynthesis	4.843	0.17
DespoDRAFT_01574	outer membrane receptor protein	6.213	0.102
DespoDRAFT_01575	hypothetical protein	1.584	NaN
DespoDRAFT_01576	TonB family protein	1.401	0.791
DespoDRAFT_01577	biopolymer transport protein	-1.414	NaN
DespoDRAFT_01578	biopolymer transport protein	-1.155	0.916
DespoDRAFT_01579	biopolymer transport protein	4.083	0.36
DespoDRAFT_01580	Protein of unknown function (DUF3450)	-1.095	NaN
DespoDRAFT_01581	NhaP-type Na ⁺ (K ⁺)/H ⁺ antiporter	-1.437	0.452
DespoDRAFT_01582	superoxide dismutase	-2.029	0.0407
DespoDRAFT_01583	universal stress protein UspA-like protein	-2.789	0.00982
DespoDRAFT_01584	diaminopimelate decarboxylase	-2.405	0.051
DespoDRAFT_01585	biotin carboxylase	-2.51	0.0831
DespoDRAFT_01586	hypothetical protein	-1.999	0.0499
DespoDRAFT_01587	hypothetical protein	-2.144	0.133
DespoDRAFT_01588	hypothetical protein	-2.063	0.148
DespoDRAFT_01589	response regulator with CheY-like receiver AAA-type ATPase and DNA-binding domains	1.11	0.734
DespoDRAFT_01590	hypothetical protein	-1.196	0.62
DespoDRAFT_01591	DnaK suppressor protein	1.596	0.249

DespoDRAFT_01592	hypothetical protein	1.312	0.17
DespoDRAFT_01593	coenzyme F420-reducing hydrogenase delta subunit	1.448	0.202
DespoDRAFT_01594	FAD/FMN-dependent dehydrogenase	1.204	0.39
DespoDRAFT_01598	hypothetical protein	1.172	0.834
DespoDRAFT_01599	hypothetical protein	-2.568	NaN
DespoDRAFT_01600	hypothetical protein	-1.336	0.135
DespoDRAFT_01601	outer membrane protein assembly complex YaeT protein	-1.014	0.959
DespoDRAFT_01602	universal stress protein UspA-like protein	1.145	0.79
DespoDRAFT_01603	glutamyl- or glutaminyl-tRNA synthetase	1.173	0.354
DespoDRAFT_01604	PilZ domain-containing protein	1.23	0.512
DespoDRAFT_01605	DNA topoisomerase I bacterial	2.417	0.00846
DespoDRAFT_01606	DNA protecting protein DprA	1.903	0.449
DespoDRAFT_01607	tol-pal system protein YbgF	2.134	0.28
DespoDRAFT_01608	preprotein translocase subunit SecF	3.038	0.0465
DespoDRAFT_01609	hypothetical protein	1.777	0.133
DespoDRAFT_01610	diaminopimelate decarboxylase	1.772	0.0925
DespoDRAFT_01611	asparagine synthase (glutamine-hydrolyzing)	1.405	0.128
DespoDRAFT_01612	acyltransferase family protein	1.432	0.206
DespoDRAFT_01613	PEP-CTERM/exosortase 1-associated glycosyltransferase Daro_2409 family	1.092	0.79
DespoDRAFT_01614	transposase family protein	-1.183	0.672
DespoDRAFT_01615	putative methicillin resistance protein	-1.104	0.783
DespoDRAFT_01616	hypothetical protein	-2.141	0.169
DespoDRAFT_01617	hypothetical protein	-1.523	0.236
DespoDRAFT_01618	diaminopimelate decarboxylase	-1.135	0.783
DespoDRAFT_01619	asparagine synthase (glutamine-hydrolyzing)	-1.087	0.61
DespoDRAFT_01621	acyltransferase family protein	-1.001	0.998
DespoDRAFT_01622	PEP-CTERM/exosortase 1-associated glycosyltransferase Daro_2409 family	-3.081	0.13
DespoDRAFT_01623	transposase family protein	-1.5	0.663
DespoDRAFT_01624	putative methicillin resistance protein	1.749	0.48
DespoDRAFT_01625	hypothetical protein	1.186	0.653
DespoDRAFT_01626	hypothetical protein	-1.581	0.348
DespoDRAFT_01629	diaminopimelate decarboxylase	-3.195	0.347
DespoDRAFT_01631	asparagine synthase (glutamine-hydrolyzing)	-1.606	0.0502
DespoDRAFT_01632	acyltransferase family protein	-2.546	0.112
DespoDRAFT_01633	PEP-CTERM/exosortase 1-associated glycosyltransferase Daro_2409 family	-1.726	0.0638
DespoDRAFT_01634	transposase family protein	-2.173	0.25
DespoDRAFT_01635	putative methicillin resistance protein	-1.909	0.0439

DespoDRAFT_01636	hypothetical protein	-2.872	0.139
DespoDRAFT_01637	hypothetical protein	-1.687	0.128
DespoDRAFT_01638	diaminopimelate decarboxylase	-1.638	0.199
DespoDRAFT_01639	asparagine synthase (glutamine-hydrolyzing)	-1.251	0.291
DespoDRAFT_01640	acyltransferase family protein	-1.664	0.125
DespoDRAFT_01641	PEP-CTERM/exosortase 1-associated glycosyltransferase Daro_2409 family	-2.219	0.0657
DespoDRAFT_01642	transposase family protein	-2.193	0.131
DespoDRAFT_01643	putative methicillin resistance protein	-1.42	0.1
DespoDRAFT_01644	hypothetical protein	-1.279	0.0393
DespoDRAFT_01645	aspA asparagine synthase	-1.064	0.669
DespoDRAFT_01646	lipid A core-O-antigen ligase-like enzyme	-1.362	0.206
DespoDRAFT_01647	glycosyltransferase	-1.334	0.412
DespoDRAFT_01648	putative xylanase/chitin deacetylase	-1.372	0.203
DespoDRAFT_01649	hypothetical protein	-1.097	0.522
DespoDRAFT_01650	sulfotransferase family protein	1.275	0.555
DespoDRAFT_01651	glycosyl transferase	-2.802	0.141
DespoDRAFT_01652	exopolysaccharide biosynthesis protein	-1.714	0.219
DespoDRAFT_01653	membrane protein involved in the export of O-antigen and teichoic acid	-1.263	0.61
DespoDRAFT_01654	hypothetical protein	-1.004	0.99
DespoDRAFT_01655	protein involved in cellulose biosynthesis (CelD)	1.127	0.661
DespoDRAFT_01656	hypothetical protein	1.101	0.605
DespoDRAFT_01657	hypothetical protein	-1.057	0.783
DespoDRAFT_01658	diaminopimelate decarboxylase	-1.238	0.182
DespoDRAFT_01659	asparagine synthase (glutamine-hydrolyzing)	-1.241	0.361
DespoDRAFT_01660	acyltransferase family protein	-1.302	0.498
DespoDRAFT_01661	PEP-CTERM/exosortase 1-associated glycosyltransferase Daro_2409 family	-1.477	0.157
DespoDRAFT_01663	putative methicillin resistance protein	-1.17	0.656
DespoDRAFT_01664	hypothetical protein	-1.255	0.236
DespoDRAFT_01669	hypothetical protein	-1.307	0.568
DespoDRAFT_01670	hypothetical protein	-1.399	0.383
DespoDRAFT_01671	hypothetical protein	1.183	0.63
DespoDRAFT_01672	hypothetical protein	-1.457	0.083
DespoDRAFT_01673	hypothetical protein	-1.859	0.128
DespoDRAFT_01674	putative nucleotidyltransferase	-2.302	0.269
DespoDRAFT_01676	putative transcriptional regulator with HTH domain	-1.844	0.0897
DespoDRAFT_01677	nucleotidyltransferase substrate binding protein HI0074 family	1.128	0.855
DespoDRAFT_01678	nucleotidyltransferase family protein	-1.328	0.369

DespoDRAFT_01679	putative transcriptional regulator with HTH domain	-1.159	0.846
DespoDRAFT_01680	hypothetical protein	1.6	0.596
DespoDRAFT_01681	hypothetical protein	1.448	0.468
DespoDRAFT_01682	UDP-N-acetylglucosamine 2-epimerase	-1.075	0.638
DespoDRAFT_01683	nucleotide sugar dehydrogenase	1.345	0.185
DespoDRAFT_01684	polysaccharide deactylase family protein PEP-CTERM locus subfamily	-1.346	0.62
DespoDRAFT_01685	eight transmembrane protein EpsH putative exosortase	-1.454	0.262
DespoDRAFT_01686	EpsI family protein	-1.967	0.0636
DespoDRAFT_01687	hypothetical protein	-1.619	0.156
DespoDRAFT_01688	periplasmic protein involved in polysaccharide export	-1.186	0.325
DespoDRAFT_01689	sugar transferase PEP-CTERM system associated/exopolysaccharide biosynthesis polyprenyl glycosylphosphotransferase	-1.446	0.461
DespoDRAFT_01690	capsular exopolysaccharide biosynthesis protein	1.086	0.922
DespoDRAFT_01691	uncharacterized protein involved in exopolysaccharide biosynthesis	-1.079	0.774
DespoDRAFT_01692	nucleoside-diphosphate-sugar epimerase	-1.051	0.833
DespoDRAFT_01693	CAAX amino terminal protease family	-1.535	0.498
DespoDRAFT_01694	type II secretory pathway component ExeA (predicted ATPase)	-1.293	0.655
DespoDRAFT_01695	hypothetical protein	-1.592	0.314
DespoDRAFT_01696	hypothetical protein	-1.218	0.646
DespoDRAFT_01697	Lhr-like helicase	-1.175	0.514
DespoDRAFT_01698	Protein of unknown function (DUF2791)	1.075	0.545
DespoDRAFT_01699	ATPase	1.228	0.107
DespoDRAFT_01700	hypothetical protein	2.828	0.0658
DespoDRAFT_01701	lysophospholipase L1-like esterase	-1.189	0.534
DespoDRAFT_01702	ABC-type antimicrobial peptide transport system ATPase component	3.266	0.559
DespoDRAFT_01703	putative ABC-type transport system involved in lysophospholipase L1 biosynthesis permease component	1.443	0.499
DespoDRAFT_01704	hypothetical protein	1.019	0.886
DespoDRAFT_01705	uncharacterized protein involved in tolerance to divalent cations	-1.051	0.871
DespoDRAFT_01706	hypothetical protein	-1.697	0.154
DespoDRAFT_01707	UDP-glucose-4-epimerase	1.003	0.987
DespoDRAFT_01708	hypothetical protein	-1.83	0.143
DespoDRAFT_01709	hypothetical protein	-1.853	0.199
DespoDRAFT_01710	transcriptional regulator	-1.614	0.259

DespoDRAFT_01711	Flagellar basal body-associated protein FliL	-1.516	0.129
DespoDRAFT_01712	thiamine pyrophosphokinase	-1.161	0.651
DespoDRAFT_01713	putative permease	2.129	0.0887
DespoDRAFT_01714	putative permease	1.573	0.386
DespoDRAFT_01715	3-deoxy-D-manno-octulosonic-acid transferase	2.574	0.0756
DespoDRAFT_01716	tetraacyldisaccharide 4"-kinase	1.856	0.141
DespoDRAFT_01717	Lauroyl/myristoyl acyltransferase	1.061	0.808
DespoDRAFT_01718	lipopolysaccharide heptosyltransferase II	1.441	0.251
DespoDRAFT_01719	ADP-heptose:LPS heptosyltransferase	1.917	0.198
DespoDRAFT_01720	glycosyl transferase	1.072	0.931
DespoDRAFT_01721	putative glycosyltransferase	-1.587	0.174
DespoDRAFT_01722	hypothetical protein	-1.398	0.467
DespoDRAFT_01723	lipid A core-O-antigen ligase-like enzyme	-1.505	0.425
DespoDRAFT_01724	glycosyltransferase	-1.045	0.949
DespoDRAFT_01725	hypothetical protein	-1.507	0.255
DespoDRAFT_01726	glycosyltransferase	-1.186	0.506
DespoDRAFT_01727	glycosyltransferase	-1.086	0.847
DespoDRAFT_01728	3-deoxy-D-manno-octulosonate cytidyltransferase	-1.091	0.424
DespoDRAFT_01729	alcohol dehydrogenase class IV	-1.149	0.262
DespoDRAFT_01730	putative PLP-dependent enzyme possibly involved in cell wall biogenesis	1.351	0.101
DespoDRAFT_01731	Fe-S oxidoreductase	-1.911	0.0484
DespoDRAFT_01732	putative oxygen-independent coproporphyrinogen III oxidase	1.388	0.485
DespoDRAFT_01733	selenocysteine-specific elongation factor SelB	-1.578	0.148
DespoDRAFT_01734	hypothetical protein	-1.257	0.602
DespoDRAFT_01736	cytidylate kinase	-1.265	0.0672
DespoDRAFT_01738	inorganic pyrophosphatase/exopolyphosphatase	1.913	0.101
DespoDRAFT_01739	acyl-CoA synthetase (AMP-forming)/AMP-acid ligase II	-1.544	0.322
DespoDRAFT_01740	cobalt ABC transporter permease protein CbiQ	-1.291	0.653
DespoDRAFT_01741	ABC-type cobalt transport system ATPase component	1.025	0.985
DespoDRAFT_01742	phosphoserine aminotransferase	6.266	0.0313
DespoDRAFT_01743	D-3-phosphoglycerate dehydrogenase	4.408	0.0317
DespoDRAFT_01744	rare lipoprotein A	2.36	0.0466
DespoDRAFT_01745	Transglycosylase	2.177	0.165
DespoDRAFT_01746	hypothetical protein	1.995	0.372
DespoDRAFT_01747	hypothetical protein	-1.785	0.0145
DespoDRAFT_01748	N-carbamoylputrescine amidase	-1.424	0.106

DespoDRAFT_01749	peptidylarginine deiminase-like enzyme	1.284	0.156
DespoDRAFT_01750	spermidine/putrescine-binding periplasmic protein	3.588	0.0635
DespoDRAFT_01751	ABC-type spermidine/putrescine transport system permease component II	1.196	0.867
DespoDRAFT_01752	ABC-type spermidine/putrescine transport system permease component I	2.356	0.319
DespoDRAFT_01753	CysA: sulfate/thiosulfate import ATP-binding protein CysA	1.96	0.59
DespoDRAFT_01754	transcriptional regulator	2.065	0.619
DespoDRAFT_01755	SH3 domain protein	1.439	0.0862
DespoDRAFT_01756	L-aspartate oxidase	1.187	0.32
DespoDRAFT_01757	Phosphoglucomutase	1.151	0.52
DespoDRAFT_01758	putative periplasmic lipoprotein (DUF2279)	-1.476	0.202
DespoDRAFT_01759	ribonucleoside-diphosphate reductase adenosylcobalamin-dependent	1.021	0.853
DespoDRAFT_01760	carbonic anhydrase	1.234	0.502
DespoDRAFT_01761	hypothetical protein	-1.609	0.515
DespoDRAFT_01762	TIR domain-containing protein	-1.633	0.108
DespoDRAFT_01763	MoxR-like ATPase	1.088	0.591
DespoDRAFT_01764	hypothetical protein	1.248	0.658
DespoDRAFT_01766	Retron-type reverse transcriptase	1.597	0.622
DespoDRAFT_01767	hypothetical protein	-1.203	0.14
DespoDRAFT_01768	hypothetical protein	-1.314	0.0852
DespoDRAFT_01769	cobalamin biosynthesis CbiM protein	-2.131	0.173
DespoDRAFT_01770	ABC-type Co ²⁺ transport system permease component	-3.693	0.151
DespoDRAFT_01771	ABC-type Co ²⁺ transport system periplasmic component	-4.297	0.068
DespoDRAFT_01772	methyltransferase cyclopropane fatty acid synthase	-3.832	0.0637
DespoDRAFT_01773	acyl-CoA synthetase/AMP-acid ligase	2.244	0.0149
DespoDRAFT_01774	1-acyl-sn-glycerol-3-phosphate acyltransferase	1.792	0.449
DespoDRAFT_01775	hypothetical protein	-1.006	0.993
DespoDRAFT_01776	putative GTPase	-1.442	0.0728
DespoDRAFT_01777	hypothetical protein	-1.565	0.183
DespoDRAFT_01778	hypothetical protein	-1.931	0.173
DespoDRAFT_01779	hypothetical protein	-2.259	0.227
DespoDRAFT_01780	hypothetical protein	-1.328	0.428
DespoDRAFT_01781	hypothetical protein	-1.823	0.273
DespoDRAFT_01782	hypothetical protein	-1.587	0.229
DespoDRAFT_01783	excinuclease ABC A subunit	-1.206	0.442
DespoDRAFT_01784	4-hydroxythreonine-4-phosphate dehydrogenase	-1.142	0.463

DespoDRAFT_01785	chromosomal replication initiator protein DnaA	1.762	0.141
DespoDRAFT_01786	hypothetical protein	1.054	0.944
DespoDRAFT_01787	GTP-binding protein HflX	2.157	0.199
DespoDRAFT_01788	replicative DNA helicase	1.797	0.0451
DespoDRAFT_01789	ribosomal protein L9	3.111	0.0659
DespoDRAFT_01790	putative membrane protein	4.514	0.0438
DespoDRAFT_01791	ribosomal protein S18	3.823	0.0582
DespoDRAFT_01792	ribosomal protein S6	4.357	0.0338
DespoDRAFT_01793	TIGR02688 family protein	-1.443	0.774
DespoDRAFT_01796	hypothetical protein	1.404	0.205
DespoDRAFT_01797	putative ATPase	1.286	0.614
DespoDRAFT_01798	Eco57I restriction endonuclease	1.054	0.73
DespoDRAFT_01799	protein of unknown function (DUF1788)	-1.214	0.848
DespoDRAFT_01800	Putative inner membrane protein (DUF1819)	1.045	0.948
DespoDRAFT_01801	hypothetical protein	1.913	0.109
DespoDRAFT_01802	leucyl-tRNA synthetase	2.518	0.0315
DespoDRAFT_01803	hypothetical protein	2.059	0.193
DespoDRAFT_01804	ribosomal protein S20	1.617	0.505
DespoDRAFT_01805	hypothetical protein	-1.013	0.984
DespoDRAFT_01806	septum formation initiator	-1.288	0.191
DespoDRAFT_01807	hypothetical protein	-1.872	0.0466
DespoDRAFT_01808	hypothetical protein	-1.482	0.273
DespoDRAFT_01810	Uncharacterized protein family (UPF0153)	1.096	0.634
DespoDRAFT_01811	hypothetical protein	2.59	0.275
DespoDRAFT_01812	LysM domain-containing protein	2.07	0.159
DespoDRAFT_01813	phosphoribosylanthranilate isomerase	2.174	0.0634
DespoDRAFT_01814	Indole-3-glycerol phosphate synthase	2.283	0.219
DespoDRAFT_01815	anthranilate phosphoribosyltransferase	2.108	0.0338
DespoDRAFT_01816	glutamine amidotransferase of anthranilate synthase or aminodeoxychorismate synthase	3.12	0.0573
DespoDRAFT_01817	anthranilate/para-aminobenzoate synthase component I	2.897	0.0682
DespoDRAFT_01818	hypothetical protein	1.767	0.47
DespoDRAFT_01819	hypothetical protein	#VALUE!	NaN
DespoDRAFT_01820	Fe-S oxidoreductase	1.345	0.57
DespoDRAFT_01821	competence/damage-inducible protein CinA-like protein	-1.112	0.69
DespoDRAFT_01822	outer membrane protein/peptidoglycan-associated (lipo)protein	-1.151	0.343
DespoDRAFT_01823	prolyl oligopeptidase family protein	-1.699	0.272
DespoDRAFT_01824	23S rRNA (uracil-5-)-methyltransferase RumA	3.722	0.225
DespoDRAFT_01825	acetyl-CoA hydrolase	-2.726	0.131

DespoDRAFT_01826	hypothetical protein	-4.427	0.102
DespoDRAFT_01827	3, 4-dihydroxy-2-butanone 4-phosphate synthase	-1.272	0.692
DespoDRAFT_01828	hypothetical protein	1.242	0.819
DespoDRAFT_01829	hypothetical protein	-1.253	0.818
DespoDRAFT_01830	type II secretory pathway, component PulC	-1.491	0.583
DespoDRAFT_01831	hypothetical protein	-2.144	0.18
DespoDRAFT_01832	hypothetical protein	-2.758	0.172
DespoDRAFT_01833	ATPase involved in chromosome partitioning	-2.681	0.116
DespoDRAFT_01834	hypothetical protein	-2.965	0.305
DespoDRAFT_01835	P-type ATPase translocating	-2.347	0.0242
DespoDRAFT_01836	universal stress protein UspA-like protein	-2.353	0.111
DespoDRAFT_01837	molybdopterin biosynthesis enzyme	1.156	0.782
DespoDRAFT_01840	aerobic-type carbon monoxide dehydrogenase large subunit CoxL/CutL-like protein	-1.532	0.00982
DespoDRAFT_01842	tyrosine recombinase XerD	-1.632	0.0725
DespoDRAFT_01843	transcription-repair coupling factor Mfd	2.647	0.128
DespoDRAFT_01845	soluble lytic murein transglycosylase-like protein	-1.198	0.209
DespoDRAFT_01847	hypothetical protein	-1.956	0.234
DespoDRAFT_01848	sugar phosphate permease	-1.474	0.236
DespoDRAFT_01849	putative divalent heavy-metal cations transporter	1.631	0.153
DespoDRAFT_01850	putative dithiol-disulfide isomerase involved in polyketide biosynthesis	-1.44	0.349
DespoDRAFT_01851	cupin domain-containing protein	2.114	0.112
DespoDRAFT_01852	putative membrane protein	1.894	0.381
DespoDRAFT_01853	ubiquinone/menaquinone biosynthesis methyltransferase	2.123	0.0465
DespoDRAFT_01854	chaperone protein DnaJ	1.513	0.0945
DespoDRAFT_01855	queuosine biosynthesis protein QueD	1.088	0.721
DespoDRAFT_01856	FAD-dependent dehydrogenase	-1.016	0.963
DespoDRAFT_01857	hypothetical protein	1.692	0.535
DespoDRAFT_01858	molecular chaperone	1.561	0.0437
DespoDRAFT_01859	hypothetical protein	-1.154	0.317
DespoDRAFT_01860	hypothetical protein	1.488	0.0729
DespoDRAFT_01861	hypothetical protein	1.962	0.264
DespoDRAFT_01862	GrpE protein	2.113	0.148
DespoDRAFT_01863	hypothetical protein	2.248	0.138
DespoDRAFT_01864	membrane protein AbrB duplication	2.478	0.105
DespoDRAFT_01865	ATPase component of ABC transporters with duplicated ATPase domain	1.052	0.785
DespoDRAFT_01866	hypothetical protein	1.222	0.851

DespoDRAFT_01867	chloride channel protein EriC	1.167	0.663
DespoDRAFT_01868	DNA-binding protein excisionase family	-1.218	0.0828
DespoDRAFT_01869	hypothetical protein	-2.201	0.489
DespoDRAFT_01870	growth inhibitor	-1.295	0.0675
DespoDRAFT_01871	hypothetical protein	1.308	0.475
DespoDRAFT_01872	DNA modification methylase	2.152	0.139
DespoDRAFT_01873	Restriction endonuclease XhoI	1.601	0.239
DespoDRAFT_01874	Lhr-like helicase	1.457	0.498
DespoDRAFT_01875	Protein of unknown function (DUF2791)	1.317	0.505
DespoDRAFT_01876	tellurite resistance protein	-1.108	0.816
DespoDRAFT_01877	hypothetical protein	-1.406	0.113
DespoDRAFT_01878	hypothetical protein	-1.488	0.0951
DespoDRAFT_01879	hypothetical protein	-1.5	0.468
DespoDRAFT_01880	putative signal-transduction protein containing cAMP-binding and CBS domains	-2.259	0.102
DespoDRAFT_01881	hypothetical protein	-1.113	0.903
DespoDRAFT_01882	nitroreductase	-1.377	0.633
DespoDRAFT_01883	hypothetical protein	#VALUE!	NaN
DespoDRAFT_01884	hypothetical protein	#VALUE!	NaN
DespoDRAFT_01887	putative addiction module antidote protein	-1.231	0.475
DespoDRAFT_01890	hypothetical protein	-1.636	0.291
DespoDRAFT_01891	hypothetical protein	-1.875	0.151
DespoDRAFT_01892	growth inhibitor	-2.734	0.15
DespoDRAFT_01893	hypothetical protein	-2.869	0.134
DespoDRAFT_01894	putative small protein	-1.591	0.295
DespoDRAFT_01895	phage-related protein	-1.543	0.104
DespoDRAFT_01896	hypothetical protein	-1.553	0.632
DespoDRAFT_01897	PEP-CTERM putative exosortase interaction domain-containing protein	-1.332	0.677
DespoDRAFT_01898	methylase involved in ubiquinone/menaquinone biosynthesis	-1.39	0.489
DespoDRAFT_01899	hypothetical protein	1.19	0.651
DespoDRAFT_01900	glycosyl transferase UDP-glucuronosyltransferase	1.19	0.832
DespoDRAFT_01901	hypothetical protein	-1.221	0.731
DespoDRAFT_01902	hypothetical protein	-1.498	0.53
DespoDRAFT_01903	ABC-type transport system, involved in lipoprotein release permease component	-2.396	0.148
DespoDRAFT_01904	ABC-type antimicrobial peptide transport system, ATPase component	-3.183	0.0381
DespoDRAFT_01905	hypothetical protein	-2.859	0.0964
DespoDRAFT_01906	dinucleotide-utilizing enzyme possibly involved in molybdopterin or thiamin biosynthesis	-2.775	0.0637

DespoDRAFT_01907	putative PEP-CTERM/exosortase system-associated acyltransferase	-2.638	0.0831
DespoDRAFT_01908	Protein of unknown function (DUF1329)	-2.68	0.231
DespoDRAFT_01909	hypothetical protein	-2.362	0.127
DespoDRAFT_01910	hypothetical protein	-1.727	0.148
DespoDRAFT_01911	response regulator with CheY-like receiver AAA-type ATPase and DNA-binding domains	-1.502	0.453
DespoDRAFT_01912	histidine kinase	-1.526	0.471
DespoDRAFT_01913	hypothetical protein	-3.532	0.125
DespoDRAFT_01914	response regulator with CheY-like receiver AAA-type ATPase and DNA-binding domains	-3.323	0.0696
DespoDRAFT_01915	chemotaxis protein	-3.243	0.0339
DespoDRAFT_01916	chemotaxis protein histidine kinase-like protein	-3.236	0.1
DespoDRAFT_01917	3-deoxy-7-phosphoheptulonate synthase class II	-1.136	0.0829
DespoDRAFT_01918	putative amidohydrolase	-1.384	0.128
DespoDRAFT_01919	D-heptose-1-phosphate adenyltransferase	-1.488	0.0659
DespoDRAFT_01920	uncharacterized protein YfiH family	-1.27	0.476
DespoDRAFT_01921	selenium donor protein	-1.407	0.285
DespoDRAFT_01922	Putative F0F1-ATPase subunit	1.41	0.445
DespoDRAFT_01923	ATP synthase I chain	1.845	0.26
DespoDRAFT_01924	F0F1-type ATP synthase alpha subunit	2.137	0.0807
DespoDRAFT_01925	ATP synthase F0 subunit c	1.263	0.435
DespoDRAFT_01926	hypothetical protein	-1.376	0.167
DespoDRAFT_01927	ATPase involved in chromosome partitioning	-1.039	0.944
DespoDRAFT_01928	HAMP domain-containing protein histidine kinase GAF domain-containing protein	-1.493	0.478
DespoDRAFT_01929	di-/tricarboxylate transporter	-1.768	0.324
DespoDRAFT_01930	ACT domain-containing protein	1.546	0.148
DespoDRAFT_01931	coenzyme F390 synthetase	2.352	0.0662
DespoDRAFT_01932	enoyl-CoA hydratase/carnithine racemase	2.766	0.108
DespoDRAFT_01933	N-acetylmuramoyl-L-alanine amidase	1.692	0.17
DespoDRAFT_01934	DNA mismatch repair protein MutS	1.11	0.0162
DespoDRAFT_01935	hypothetical protein	1.265	0.512
DespoDRAFT_01936	putative phosphoesterase ICC	1.532	0.364
DespoDRAFT_01937	imidazolonepropionase	-1.025	0.963
DespoDRAFT_01938	histidine ammonia-lyase	1.036	0.934
DespoDRAFT_01939	formyltetrahydrofolate deformylase	1.959	0.0708
DespoDRAFT_01940	hypothetical protein	1.218	0.926
DespoDRAFT_01941	hypothetical protein	-1.035	0.968

DespoDRAFT_01942	D-isomer specific 2-hydroxyacid dehydrogenase NAD-binding protein	-1.151	0.783
DespoDRAFT_01943	birA biotin-(acetyl-CoA-carboxylase) ligase	1.344	0.356
DespoDRAFT_01944	Pyruvate carboxylase	1.259	0.185
DespoDRAFT_01947	2-oxoacid:ferredoxin oxidoreductase gamma subunit	-2.309	0.0859
DespoDRAFT_01948	Zn-dependent hydrolase glyoxylase	-1.368	0.294
DespoDRAFT_01949	hypothetical protein	-1.584	0.41
DespoDRAFT_01950	hypothetical protein	1.286	0.383
DespoDRAFT_01951	carbonic anhydrase	2.817	0.0466
DespoDRAFT_01952	ATP-dependent exoDNAse (exonuclease V) alpha subunit/helicase superfamily I member	1.365	0.48
DespoDRAFT_01953	bacterial nucleoid DNA-binding protein	2.537	0.199
DespoDRAFT_01954	methyl-accepting chemotaxis protein	-2.417	0.0543
DespoDRAFT_01955	anti-anti-sigma regulatory factor (antagonist of anti-sigma factor)	-3.074	0.156
DespoDRAFT_01956	response regulator with CheY-like receiver domain and winged-helix DNA-binding domain	-2.451	0.238
DespoDRAFT_01957	chemotaxis protein histidine kinase-like protein	-2.007	0.26
DespoDRAFT_01958	chemotaxis signal transduction protein	-2.503	0.157
DespoDRAFT_01959	methylase of chemotaxis methyl-accepting protein	-3.289	0.0895
DespoDRAFT_01960	chemotaxis response regulator containing a CheY-like receiver domain and a methylesterase domain	-2.25	0.0639
DespoDRAFT_01961	chemotaxis protein	-3.102	0.0291
DespoDRAFT_01962	signal transduction histidine kinase	-1.245	0.776
DespoDRAFT_01963	hypothetical protein	-4.257	0.0842
DespoDRAFT_01964	outer membrane receptor for ferrienterochelin and colicins	1.148	0.546
DespoDRAFT_01965	uncharacterized Fe-S center protein	-2.021	0.113
DespoDRAFT_01966	signal transduction histidine kinase	-1.744	0.221
DespoDRAFT_01967	hypothetical protein	1.383	0.185
DespoDRAFT_01968	response regulator with CheY-like receiver AAA-type ATPase and DNA-binding domains	-1.438	0.498
DespoDRAFT_01969	hypothetical protein	-1.325	0.35
DespoDRAFT_01970	hypothetical protein	1.973	0.434
DespoDRAFT_01971	AICAR transformylase/IMP cyclohydrolase PurH	2.437	0.0638
DespoDRAFT_01972	AICAR transformylase/IMP cyclohydrolase PurH	1.619	0.104

DespoDRAFT_01974	putative transcriptional regulator	1.32	0.663
DespoDRAFT_01975	small redox-active disulfide protein 2	1.252	0.452
DespoDRAFT_01976	putative permease	-1.108	0.501
DespoDRAFT_01978	cyclic nucleotide-binding protein	-1.479	0.43
DespoDRAFT_01979	Rhodanese-related sulfurtransferase	1.486	0.118
DespoDRAFT_01980	cation diffusion facilitator family transporter	-1.082	0.761
DespoDRAFT_01981	Rhodanese-related sulfurtransferase	-1.009	0.977
DespoDRAFT_01982	putative permease	-1.086	0.896
DespoDRAFT_01984	hypothetical protein	-1.859	0.0242
DespoDRAFT_01988	PEP-CTERM putative exosortase interaction domain-containing protein	-2.258	0.112
DespoDRAFT_01989	exoribonuclease R	1.216	0.605
DespoDRAFT_01990	hypothetical protein	-2.205	0.155
DespoDRAFT_01991	hypothetical protein	1.004	0.999
DespoDRAFT_01992	electron transporter RnfB	2.788	0.0806
DespoDRAFT_01993	Rnf A subunit	2.923	0.0696
DespoDRAFT_01994	Rnf E subunit	2.122	0.0828
DespoDRAFT_01995	electron transport complex RnfABCDGE type G subunit	2.587	0.0014
DespoDRAFT_01996	NADH:ubiquinone oxidoreductase subunit RnfD	2.603	0.0247
DespoDRAFT_01997	NADH:ubiquinone oxidoreductase subunit RnfC	3.011	0.0361
DespoDRAFT_01998	class III cytochrome C family protein	2.569	0.0592
DespoDRAFT_01999	Positive regulator of sigma E activity	-1.077	0.93
DespoDRAFT_02000	hypothetical protein	-1.99	0.111
DespoDRAFT_02002	hypothetical protein	-8.471	0.0462
DespoDRAFT_02003	histidine kinase	-1.581	0.0951
DespoDRAFT_02004	response regulator with CheY-like receiver domain and winged-helix DNA-binding domain	-1.413	0.0682
DespoDRAFT_02005	hypothetical protein	1.071	0.673
DespoDRAFT_02006	Fe-S oxidoreductase	1.136	0.0731
DespoDRAFT_02007	nitroreductase	-1.007	0.96
DespoDRAFT_02008	non-canonical purine NTP pyrophosphatase rdgB/HAM1 family	-1.168	0.149
DespoDRAFT_02009	RNA methyltransferase TrmH family group 1	4.356	0.187
DespoDRAFT_02010	hypothetical protein	-1.915	0.261
DespoDRAFT_02011	hypothetical protein	-2.002	0.194
DespoDRAFT_02012	putative nucleoside-diphosphate sugar epimerase	-1.655	0.147
DespoDRAFT_02013	flavoprotein (flavodoxin)	1.307	0.319
DespoDRAFT_02014	Rnf C subunit	1.641	0.0808

DespoDRAFT_02015	Rnf D subunit	1.967	0.0992
DespoDRAFT_02016	Rnf G subunit	1.608	0.292
DespoDRAFT_02017	Rnf E subunit	1.148	0.42
DespoDRAFT_02018	Rnf A subunit	4.14	0.201
DespoDRAFT_02019	Rnf B subunit	2.326	0.108
DespoDRAFT_02020	TIGR00730 family protein	1.128	0.631
DespoDRAFT_02021	Flp pilus assembly protein TadD	1.192	0.225
DespoDRAFT_02022	PEP-CTERM putative exosortase interaction domain-containing protein	-2.618	0.0262
DespoDRAFT_02023	Xaa-Pro aminopeptidase	-2.28	0.0338
DespoDRAFT_02024	lactoylglutathione lyase-like lyase	-1.892	0.307
DespoDRAFT_02025	hypothetical protein	-2.936	0.0509
DespoDRAFT_02026	polyferredoxin	-2.348	0.0773
DespoDRAFT_02027	hypothetical protein	-4.157	0.283
DespoDRAFT_02028	histidine kinase Response regulator receiver domain protein histidine kinase	-1.412	0.251
DespoDRAFT_02029	ABC-type uncharacterized transport system periplasmic component	-1.545	0.225
DespoDRAFT_02030	hypothetical protein	-1.057	0.738
DespoDRAFT_02031	uncharacterized protein involved in formate dehydrogenase formation	-1.19	0.282
DespoDRAFT_02032	integral membrane protein MviN	1.305	0.746
DespoDRAFT_02033	hypothetical protein	-1.62	0.521
DespoDRAFT_02034	universal stress protein UspA-like protein	-1.111	0.661
DespoDRAFT_02035	methylase involved in ubiquinone/menaquinone biosynthesis	-1.532	0.156
DespoDRAFT_02036	mannose-1-phosphate guanylyltransferase/mannose-6-phosphate isomerase	-1.179	0.307
DespoDRAFT_02037	putative transcriptional regulator	-1.008	0.931
DespoDRAFT_02038	dynamain family protein	1.449	0.365
DespoDRAFT_02039	hypothetical protein	-1.077	0.873
DespoDRAFT_02040	putative membrane protein	-1.073	0.881
DespoDRAFT_02041	Dicarboxylate transport	-1.577	0.581
DespoDRAFT_02042	hypothetical protein	1.077	0.929
DespoDRAFT_02043	hypothetical protein	-1.014	0.955
DespoDRAFT_02044	hypothetical protein	1.574	0.123
DespoDRAFT_02045	hypothetical protein	-2.076	0.057
DespoDRAFT_02048	negative regulator of beta-lactamase expression	1.351	0.467
DespoDRAFT_02049	DNA segregation ATPase FtsK/SpoIIIE family	-1.293	0.411
DespoDRAFT_02050	Protein of unknown function (DUF3108)	-1.034	0.448
DespoDRAFT_02051	Sua5/YciO/YrdC/YwlC family protein	-2.523	0.412

DespoDRAFT_02052	phosphoribosylamine--glycine ligase/phosphoribosylaminoimidazole carboxylase PurE protein	1.043	0.664
DespoDRAFT_02053	D-alanine--D-alanine ligase	1.082	0.0583
DespoDRAFT_02054	hypothetical protein	1.554	0.176
DespoDRAFT_02055	translation elongation factor EF-G	1.799	0.0674
DespoDRAFT_02056	putative Zn-dependent protease	1.101	0.752
DespoDRAFT_02057	putative inhibitor of MCP methylation CheC	2.115	0.359
DespoDRAFT_02058	putative ABC-type transport system permease component	-1.414	0.613
DespoDRAFT_02060	hypothetical protein	1.25	0.534
DespoDRAFT_02061	ABC-type proline/glycine betaine transport system periplasmic component	-15.818	0.0291
DespoDRAFT_02062	ABC-type proline/glycine betaine transport system permease component	-11.172	0.0829
DespoDRAFT_02063	glycine betaine/L-proline transport ATP binding subunit	-9.18	0.0465
DespoDRAFT_02064	cyclic nucleotide-binding protein	1.207	0.461
DespoDRAFT_02065	hypothetical protein	2.611	0.107
DespoDRAFT_02066	sodium ion-translocating decarboxylase beta subunit	1.217	0.45
DespoDRAFT_02067	selT/selW/selH selenoprotein domain protein	1.306	0.671
DespoDRAFT_02068	signal transduction histidine kinase regulating C4-dicarboxylate transport system	1.569	0.425
DespoDRAFT_02069	Cytochrome c bacterial	-1.647	0.0381
DespoDRAFT_02070	putative thiosulfate reductase	-1.102	0.531
DespoDRAFT_02071	carboxynorspermidine decarboxylase	5.711	0.119
DespoDRAFT_02072	saccharopine dehydrogenase-like oxidoreductase	4.021	0.1
DespoDRAFT_02073	succinyl-CoA:acetate CoA transferase	2.926	0.0241
DespoDRAFT_02075	hypothetical protein	2.527	0.27
DespoDRAFT_02076	NAD(P)H-nitrite reductase	2.358	0.0842
DespoDRAFT_02077	protein of unknown function (DUF309)	-1.529	0.475
DespoDRAFT_02080	hypothetical protein	2.002	NaN
DespoDRAFT_02081	Transposase IS66 family	2.209	0.422
DespoDRAFT_02082	Transposase IS66 family	-1.739	0.29
DespoDRAFT_02083	class III cytochrome C family protein	-2.993	0.146
DespoDRAFT_02084	thymidylate kinase	-1.916	0.0619
DespoDRAFT_02086	putative RNA-binding protein	-2.66	0.125
DespoDRAFT_02087	NfnA, the alpha subunit of NADH-dependent ferredoxin:NADP oxidoreductase	-1.311	0.345
DespoDRAFT_02088	NfnB, the beta subunit of NADH-dependent ferredoxin:NADP oxidoreductase	-1.48	0.0861

DespoDRAFT_02089	Rhodanese-related sulfurtransferase	-1.005	0.993
DespoDRAFT_02090	phosphoenolpyruvate carboxykinase (GTP)	-1.044	0.33
DespoDRAFT_02091	putative metal-dependent phosphoesterase PHP family	-1.013	0.929
DespoDRAFT_02092	hypothetical protein	-3.563	NaN
DespoDRAFT_02093	hypothetical protein	-1.227	0.311
DespoDRAFT_02094	copper/silver-translocating P-type ATPase heavy metal-translocating P-type ATPase Cd/Co/Hg/Pb/Zn-transporting	-2.036	0.0197
DespoDRAFT_02095	copper chaperone	-4.692	0.061
DespoDRAFT_02096	cytochrome c biogenesis protein	1.115	0.747
DespoDRAFT_02097	Dinitrogenase reductase ADP- ribosyltransferase (DRAT)	-2.625	0.0807
DespoDRAFT_02098	ADP-ribosyl-(dinitrogen reductase) hydrolase	-2.446	0.0767
DespoDRAFT_02099	2-keto-4-pentenoate hydratase/2-oxohepta- 3-ene-1,7-dioic acid hydratase	-1.421	0.256
DespoDRAFT_02100	hypothetical protein	-4.187	0.0659
DespoDRAFT_02106	hypothetical protein	-3.034	0.0363
DespoDRAFT_02107	glycosyl transferase	-2.631	0.471
DespoDRAFT_02108	Protein of unknown function (DUF3047)	-1.853	0.498
DespoDRAFT_02109	hypothetical protein	-2.366	0.291
DespoDRAFT_02110	pyruvate/2-oxoglutarate dehydrogenase complex dihydrolipoamide dehydrogenase component	-5.399	0.0647
DespoDRAFT_02111	glycosidase	-3.315	0.0883
DespoDRAFT_02112	hypothetical protein	-2.088	0.151
DespoDRAFT_02113	hypothetical protein	-1.178	0.795
DespoDRAFT_02114	beta-ketoacyl synthase	2.158	0.0355
DespoDRAFT_02115	3-oxoacyl-(acyl-carrier-protein) synthase III	-1.464	0.136
DespoDRAFT_02116	probable alpha/beta hydrolase (EC:3.4.11.5)	2.036	0.423
DespoDRAFT_02117	hypothetical protein	-1.547	0.263
DespoDRAFT_02118	acyl-CoA synthetase (AMP-forming)/AMP- acid ligase II	-1.198	0.624
DespoDRAFT_02119	hypothetical protein	-2.132	0.0974
DespoDRAFT_02120	hypothetical protein	-102.868	0.0476
DespoDRAFT_02121	Fe-S oxidoreductase	2.519	0.57
DespoDRAFT_02122	sugar phosphate permease	2.892	0.177
DespoDRAFT_02123	ribulose-phosphate 3-epimerase	2.237	0.298
DespoDRAFT_02124	ribosomal RNA small subunit methyltransferase RsmB	2.962	0.119
DespoDRAFT_02125	methionyl-tRNA formyltransferase	2.491	0.0705
DespoDRAFT_02126	peptide deformylase	1.593	0.224
DespoDRAFT_02127	riboflavin kinase/FMN adenylyltransferase	2.974	0.00985
DespoDRAFT_02129	MiaB-like tRNA modifying enzyme	-1	0.999

DespoDRAFT_02130	tRNA (5-methylaminomethyl-2-thiouridylate)-methyltransferase	1.286	0.314
DespoDRAFT_02131	putative ferredoxin	1.657	0.0354
DespoDRAFT_02132	PAS domain S-box	-1.209	0.236
DespoDRAFT_02134	hypothetical protein	-1.892	0.133
DespoDRAFT_02135	hypothetical protein	-1.465	0.432
DespoDRAFT_02136	response regulator with CheY-like receiver AAA-type ATPase and DNA-binding domains	-1.267	0.651
DespoDRAFT_02137	hypothetical protein	-1.811	0.17
DespoDRAFT_02139	Pyruvate phosphate dikinase	1.433	0.105
DespoDRAFT_02140	ATPase component of ABC transporters with duplicated ATPase domain	2.007	0.0129
DespoDRAFT_02141	hypothetical protein	-1.249	0.315
DespoDRAFT_02142	type IV-A pilus assembly ATPase PilB	-1.541	0.124
DespoDRAFT_02143	cytochrome c biogenesis factor	-1.002	0.963
DespoDRAFT_02144	diguanylate cyclase (GGDEF) domain/uncharacterized domain HDIG-containing protein	-2.237	0.038
DespoDRAFT_02145	hypothetical protein	-1.669	0.307
DespoDRAFT_02146	nitrogen regulatory protein PII	-2.119	0.103
DespoDRAFT_02147	ammonium transporter	1.127	0.428
DespoDRAFT_02148	hypothetical protein	-1.139	0.918
DespoDRAFT_02149	PAS domain S-box	-1.237	0.35
DespoDRAFT_02151	uncharacterized Fe-S center protein	1.152	0.282
DespoDRAFT_02152	ATP-binding cassette protein ChvD family	-1.014	0.32
DespoDRAFT_02153	superfamily II RNA helicase	1.265	0.261
DespoDRAFT_02154	1, 4-dihydroxy-2-naphthoate octaprenyltransferase	1.216	0.699
DespoDRAFT_02155	adenosine deaminase	-4.672	0.104
DespoDRAFT_02156	response regulator with CheY-like receiver, AAA-type ATPase, and DNA-binding domains	1.029	0.959
DespoDRAFT_02157	hypothetical protein	-1.184	0.732
DespoDRAFT_02158	pyridoxal phosphate enzyme YggS family	1.492	0.216
DespoDRAFT_02159	MAF protein	1.115	0.698
DespoDRAFT_02160	RNA methyltransferase RsmE family	-1.191	0.217
DespoDRAFT_02162	Na ⁺ /H ⁺ antiporter	5.027	0.00851
DespoDRAFT_02163	monovalent cation/proton antiporter MnhG/PhaG subunit	-3.077	0.36
DespoDRAFT_02164	multisubunit Na ⁺ /H ⁺ antiporter MnhF subunit	-1.535	0.696
DespoDRAFT_02165	multisubunit Na ⁺ /H ⁺ antiporter MnhE subunit	-1.469	0.593

DespoDRAFT_02166	formate hydrogenlyase subunit 3/multisubunit Na ⁺ /H ⁺ antiporter MnhD subunit	-1.542	0.476
DespoDRAFT_02167	multisubunit Na ⁺ /H ⁺ antiporter MnhC subunit	-1.151	0.723
DespoDRAFT_02168	multisubunit Na ⁺ /H ⁺ antiporter MnhB subunit	-1.171	NaN
DespoDRAFT_02169	NADH:ubiquinone oxidoreductase subunit 5 (chain L)/multisubunit Na ⁺ /H ⁺ antiporter MnhA subunit	-2.712	0.0407
DespoDRAFT_02170	putative membrane protein	-2.847	0.0572
DespoDRAFT_02171	universal stress protein UspA-like protein	-1.932	0.0365
DespoDRAFT_02172	glycoside/pentoside/hexuronide transporter	-1.904	0.0949
DespoDRAFT_02173	hypothetical protein	-1.304	0.185
DespoDRAFT_02174	hypothetical protein	-2.034	0.0912
DespoDRAFT_02175	Na ⁺ /H ⁺ antiporter NhaD-like permease	-1.644	0.61
DespoDRAFT_02176	diaminopimelate decarboxylase	1.334	0.426
DespoDRAFT_02177	Na ⁺ /phosphate symporter	1.175	0.154
DespoDRAFT_02178	hypothetical protein	-1.101	0.929
DespoDRAFT_02179	hypothetical protein	1.544	0.0213
DespoDRAFT_02180	translation elongation factor EF-G	1.481	0.235
DespoDRAFT_02181	16S rRNA (guanine(527)-N(7))- methyltransferase GidB	2.763	0.367
DespoDRAFT_02182	isoleucyl-tRNA synthetase	2.355	0.0742
DespoDRAFT_02183	lipoprotein signal peptidase	1.092	0.929
DespoDRAFT_02184	prolipoprotein diacylglycerol transferase	2.571	0.294
DespoDRAFT_02185	DNA polymerase III delta subunit	1.62	0.0734
DespoDRAFT_02186	Pyruvate kinase	2.295	0.0705
DespoDRAFT_02187	putative domain HDIG-containing protein	-1.124	0.352
DespoDRAFT_02188	PAS domain S-box/diguanylate cyclase (GGDEF) domain-containing protein	-1.741	0.235
DespoDRAFT_02189	ABC-type phosphate transport system periplasmic component	-1.4	0.162
DespoDRAFT_02190	cyclic nucleotide-binding protein	-1.067	0.79
DespoDRAFT_02191	hypothetical protein	1.675	0.33
DespoDRAFT_02192	RNA methyltransferase RsmE family	1.03	0.941
DespoDRAFT_02193	FAD/FMN-dependent dehydrogenase	-1.317	0.466
DespoDRAFT_02194	peptide chain release factor 3	1.978	0.0805
DespoDRAFT_02197	hypothetical protein	-1.397	0.262
DespoDRAFT_02204	HIT family hydrolase diadenosine tetraphosphate hydrolase	-2.149	0.158
DespoDRAFT_02205	NAD-dependent protein deacetylase SIR2 family	-2.212	0.244
DespoDRAFT_02206	hypothetical protein	-1.813	0.16
DespoDRAFT_02207	putative membrane protein	-1.443	0.179

DespoDRAFT_02208	glycine cleavage system protein P	-1.983	0.134
DespoDRAFT_02209	glycine cleavage system protein P	-1.754	0.0451
DespoDRAFT_02210	glycine cleavage system H protein	-1.861	0.142
DespoDRAFT_02211	glycine cleavage system T protein (aminomethyltransferase)	-2.128	0.0573
DespoDRAFT_02212	transcriptional regulator	-1.857	0.221
DespoDRAFT_02213	response regulator with CheY-like receiver AAA-type ATPase and DNA-binding domains	-4.631	0.0213
DespoDRAFT_02214	response regulator with CheY-like receiver AAA-type ATPase and DNA-binding domains	-8.851	0.0149
DespoDRAFT_02215	3-oxoacyl-(acyl-carrier-protein) synthase III	2.383	0.0805
DespoDRAFT_02216	glucose-6-phosphate isomerase	-1.386	0.536
DespoDRAFT_02217	hypothetical protein	1.092	0.651
DespoDRAFT_02218	phosphoglucosamine mutase	-1.163	0.188
DespoDRAFT_02219	ABC-type uncharacterized transport system permease component	1.021	0.909
DespoDRAFT_02220	FtsH-interacting integral membrane protein	-1.39	0.0601
DespoDRAFT_02221	hypothetical protein	-1.541	0.677
DespoDRAFT_02222	hypothetical protein	1.207	NaN
DespoDRAFT_02223	hypothetical protein	-1.877	NaN
DespoDRAFT_02224	phage regulatory protein rha family	-1.115	0.91
DespoDRAFT_02225	CobQ/CobB/MinD/ParA nucleotide binding domain-containing protein	-1.691	0.24
DespoDRAFT_02227	type IV secretory pathway VirB2 component (pilin)	-2.93	0.486
DespoDRAFT_02228	Type IV secretory pathway VirB3-like protein	#VALUE!	NaN
DespoDRAFT_02231	putative nucleotidyltransferase	-2.584	0.419
DespoDRAFT_02235	nucleotidyltransferase substrate binding protein HI0074 family	1.366	0.69
DespoDRAFT_02236	hypothetical protein	#VALUE!	NaN
DespoDRAFT_02237	hypothetical protein	-1.476	0.131
DespoDRAFT_02238	CBS domain-containing protein	-1.243	0.227
DespoDRAFT_02240	putative hydrolase or acyltransferase of alpha/beta superfamily	-1.22	0.52
DespoDRAFT_02241	ADP-ribose pyrophosphatase	-1.636	0.412
DespoDRAFT_02242	NAD-dependent protein deacetylase SIR2 family	-2.29	0.119
DespoDRAFT_02243	23S rRNA m2A2503 methyltransferase	-2.509	0.21
DespoDRAFT_02244	membrane protein TerC possibly involved in tellurium resistance	2.795	0.128
DespoDRAFT_02245	D-alanyl-D-alanine carboxypeptidase	-1.089	0.847
DespoDRAFT_02246	Fe-S oxidoreductase	1.287	0.321

DespoDRAFT_02247	transketolase	1.493	0.0759
DespoDRAFT_02248	secondary thiamine-phosphate synthase enzyme	1.019	0.964
DespoDRAFT_02249	cytochrome c biogenesis factor	-1.398	0.177
DespoDRAFT_02250	hypothetical protein	1.169	0.557
DespoDRAFT_02251	tetratricopeptide repeat protein	-1.495	0.228
DespoDRAFT_02252	hypothetical protein	-1.14	0.836
DespoDRAFT_02253	hypothetical protein	-1.09	0.835
DespoDRAFT_02254	hypothetical protein	1.539	0.291
DespoDRAFT_02255	ABC-type multidrug transport system ATPase component	3.365	0.0857
DespoDRAFT_02256	ABC transporter	2.092	0.0497
DespoDRAFT_02257	ABC-type uncharacterized transporter	1.431	0.0829
DespoDRAFT_02258	hypothetical protein	1.351	0.0168
DespoDRAFT_02259	1-acyl-sn-glycerol-3-phosphate acyltransferase	1.075	0.725
DespoDRAFT_02260	mraZ protein	-1.122	0.331
DespoDRAFT_02261	S-adenosyl-methyltransferase MraW	-1.64	0.0945
DespoDRAFT_02262	Cell division protein FtsL	-1.451	0.133
DespoDRAFT_02263	cell division protein FtsI/penicillin-binding protein 2	-1.85	0.0409
DespoDRAFT_02264	UDP-N-acetylmuramyl-tripeptide synthetase/UDP-N-acetylmuramoyl-tripeptide--D-alanyl-D-alanine ligase	-1.259	0.451
DespoDRAFT_02265	phospho-N-acetylmuramoyl-pentapeptide-transferase	-1.539	0.224
DespoDRAFT_02266	UDP-N-acetylmuramoylalanine--D-glutamate ligase	-1.094	0.843
DespoDRAFT_02267	cell division protein FtsW	-1.953	0.0709
DespoDRAFT_02268	undecaprenyldiphospho-muramoylpentapeptide beta-N-acetylglucosaminyltransferase	1.026	0.911
DespoDRAFT_02269	UDP-N-acetylmuramate--alanine ligase	1.099	0.732
DespoDRAFT_02270	UDP-N-acetylenolpyruvoylglucosamine reductase	1.115	0.771
DespoDRAFT_02271	cell division septal protein	-1.084	0.772
DespoDRAFT_02272	cell division protein FtsA	1.438	0.0992
DespoDRAFT_02273	cell division protein FtsZ	-1.326	0.377
DespoDRAFT_02274	DNA/RNA helicase superfamily II	4.325	0.0217
DespoDRAFT_02276	hypothetical protein	-1.903	0.217
DespoDRAFT_02277	hypothetical protein	-2.884	0.181
DespoDRAFT_02280	putative nucleoside-diphosphate sugar epimerase	-2.257	0.198
DespoDRAFT_02281	putative flavin-nucleotide-binding protein	1.606	0.829

DespoDRAFT_02282	histidine kinase, Response regulator receiver domain protein, histidine kinase GAF domain-containing protein	1.1	0.894
DespoDRAFT_02283	putative NAD/FAD-binding protein	-2.32	0.16
DespoDRAFT_02284	methyltransferase, cyclopropane fatty acid synthase	-2.624	0.134
DespoDRAFT_02285	dehydrogenase of unknown specificity	-6.502	0.0123
DespoDRAFT_02286	hypothetical protein	-4.719	0.00976
DespoDRAFT_02287	hypothetical protein	-5.26	0.0759
DespoDRAFT_02288	hypothetical protein	-1.188	0.228
DespoDRAFT_02289	MIP family channel protein	-1.058	0.538
DespoDRAFT_02291	hypothetical protein	-1.585	0.156
DespoDRAFT_02292	hypothetical protein	-1.88	0.219
DespoDRAFT_02294	hypothetical protein	1.044	0.944
DespoDRAFT_02298	methylase involved in ubiquinone/menaquinone biosynthesis	1.092	0.835
DespoDRAFT_02299	CBS domain-containing protein	1.212	0.771
DespoDRAFT_02300	lipid-A-disaccharide synthase	3.124	0.172
DespoDRAFT_02301	hypothetical protein	1.781	0.188
DespoDRAFT_02302	acyl-(acyl-carrier-protein)--UDP-N-acetylglucosamine O-acyltransferase	2.198	0.205
DespoDRAFT_02303	UDP-3-O-(3-hydroxymyristoyl) glucosamine N-acyltransferase	1.028	0.914
DespoDRAFT_02304	outer membrane protein	2.049	0.116
DespoDRAFT_02305	outer membrane protein assembly complex YaeT protein	1.545	0.38
DespoDRAFT_02306	ABC-type antimicrobial peptide transport system ATPase component	1.719	0.315
DespoDRAFT_02307	lipoprotein releasing system transmembrane protein LolC/E family	2.194	0.245
DespoDRAFT_02308	lysyl-tRNA synthetase (class II)	2.165	0.059
DespoDRAFT_02309	heterodisulfide reductase subunit B	3.988	0.173
DespoDRAFT_02310	Nitrate reductase gamma subunit	5.035	0.0634
DespoDRAFT_02311	signal transduction histidine kinase nitrogen specific	-1.027	0.96
DespoDRAFT_02312	type II secretory pathway component PulF	-1.665	0.311
DespoDRAFT_02313	tRNA nucleotidyltransferase/poly(A) polymerase	-1.821	0.298
DespoDRAFT_02314	tryptophanyl-tRNA synthetase	2.633	0.0777
DespoDRAFT_02315	pseudouridine synthase family protein	-1.131	0.466
DespoDRAFT_02316	glutamate N-acetyltransferase/amino-acid acetyltransferase	1.166	0.326
DespoDRAFT_02317	transcriptional regulator	-1.738	0.202
DespoDRAFT_02318	Sulfate permease-like transporter MFS superfamily (Sulp3), high affinity sulfate	-2.94	0.0209

	transporter.		
DespoDRAFT_02319	response regulator with CheY-like receiver AAA-type ATPase and DNA-binding domains	-2.154	0.0353
DespoDRAFT_02320	histidine kinase	-2.581	0.0679
DespoDRAFT_02321	response regulator with CheY-like receiver AAA-type ATPase and DNA-binding domains	-1.837	0.236
DespoDRAFT_02322	hypothetical protein	-1.292	0.283
DespoDRAFT_02323	response regulator with CheY-like receiver AAA-type ATPase and DNA-binding domains	-2.472	0.0786
DespoDRAFT_02328	hypothetical protein	1.782	0.387
DespoDRAFT_02329	3-deoxy-D-manno-octulosonic-acid transferase	1.019	0.973
DespoDRAFT_02330	ABC-type multidrug transport system ATPase and permease component	2.221	0.186
DespoDRAFT_02331	hypothetical protein	-1.187	0.514
DespoDRAFT_02332	hypothetical protein	1.761	0.502
DespoDRAFT_02333	TIGR00255 family protein	-1.08	0.743
DespoDRAFT_02334	hypothetical protein	-1.147	0.484
DespoDRAFT_02335	guanylate kinase	-1.014	0.979
DespoDRAFT_02336	rRNA methylase putative group 3	1.442	0.0946
DespoDRAFT_02337	putative amidophosphoribosyltransferase	-1.544	0.676
DespoDRAFT_02338	DNA/RNA helicase superfamily II	1.543	0.261
DespoDRAFT_02339	hypothetical protein	1.34	0.707
DespoDRAFT_02340	abortive infection bacteriophage resistance protein	1.092	0.486
DespoDRAFT_02341	adenine-specific DNA methylase containing a Zn-ribbon	1.633	0.311
DespoDRAFT_02342	putative ATPase (AAA+ superfamily)	1.439	0.255
DespoDRAFT_02343	glucosamine 6-phosphate synthetase	1.844	0.0797
DespoDRAFT_02344	cell division protein FtsI/penicillin-binding protein 2	3.263	0.086
DespoDRAFT_02345	protein containing C-terminal region/beta chain of methionyl-tRNA synthetase	1.373	0.108
DespoDRAFT_02346	putative PSP1-like protein	-1.033	0.864
DespoDRAFT_02347	DNA polymerase III delta" subunit	1.114	0.775
DespoDRAFT_02348	bacterial nucleoid DNA-binding protein	1.583	0.186
DespoDRAFT_02349	transcription antiterminator	1.467	0.734
DespoDRAFT_02350	organic solvent tolerance protein OstA	1.908	0.193
DespoDRAFT_02351	cysteine synthase	1.769	0.0488
DespoDRAFT_02352	hypothetical protein	2.388	0.21
DespoDRAFT_02353	iron sulfur cluster binding protein (4Fe-4S	1.925	0.29

	ferredoxin family protein)		
DespoDRAFT_02354	DMT(drug/metabolite transporter) superfamily permease	2.641	0.0945
DespoDRAFT_02357	DMT(drug/metabolite transporter) superfamily permease	2.182	NaN
DespoDRAFT_02359	hypothetical protein	-1.027	0.965
DespoDRAFT_02360	hypothetical protein	1.127	0.498
DespoDRAFT_02361	flagellar motor component	1.178	0.302
DespoDRAFT_02362	flagellar motor protein	-1.759	0.177
DespoDRAFT_02363	hypothetical protein	-1.631	0.728
DespoDRAFT_02364	PilZ domain-containing protein	-1.463	0.361
DespoDRAFT_02365	hypothetical protein	-1.076	0.929
DespoDRAFT_02368	hypothetical protein	-1.887	0.522
DespoDRAFT_02372	YgiT-type zinc finger domain protein	-1.977	0.224
DespoDRAFT_02373	putative Fe-S oxidoreductase	-1.096	0.497
DespoDRAFT_02374	recombination protein RecR	-1.018	0.959
DespoDRAFT_02375	DNA-binding protein YbaB/EbfC family	1.233	0.414
DespoDRAFT_02376	DNA polymerase III subunit gamma/tau	1.308	0.348
DespoDRAFT_02377	general secretion pathway protein G	1.18	0.33
DespoDRAFT_02378	prepilin-type N-terminal cleavage/methylation domain-containing protein	1.256	0.257
DespoDRAFT_02379	prepilin-type N-terminal cleavage/methylation domain-containing protein	-1	0.998
DespoDRAFT_02380	prepilin-type N-terminal cleavage/methylation domain-containing protein	-1.241	0.494
DespoDRAFT_02381	type II secretory pathway component PulK	-1.403	0.167
DespoDRAFT_02382	General secretion pathway protein L (GspL)	1.068	0.893
DespoDRAFT_02383	General secretion pathway M protein	2.462	0.337
DespoDRAFT_02384	general secretion pathway protein D	1.531	0.0734
DespoDRAFT_02385	general secretory pathway protein E	1.705	0.341
DespoDRAFT_02386	hypothetical protein	1.004	0.98
DespoDRAFT_02387	hydroxylamine reductase	-5.076	0.0727
DespoDRAFT_02390	NAD+ synthetase	1.568	0.176
DespoDRAFT_02391	rRNA methylase	1.819	0.59
DespoDRAFT_02392	hypothetical protein	1.361	0.427
DespoDRAFT_02393	fructose-bisphosphate aldolase class II	-1.511	0.0359
DespoDRAFT_02394	ABC-type dipeptide transport system periplasmic component	-1.904	0.0773
DespoDRAFT_02395	ABC-type dipeptide/oligopeptide/nickel transport system permease component	-2.081	0.19
DespoDRAFT_02396	ABC-type dipeptide/oligopeptide/nickel	1.044	0.943

	transport system permease component		
DespoDRAFT_02397	ABC-type dipeptide/oligopeptide/nickel transport system ATPase component	1.232	0.788
DespoDRAFT_02398	ABC-type dipeptide/oligopeptide/nickel transport system ATPase component	-1.045	0.891
DespoDRAFT_02399	SH3 domain-containing protein	1.133	0.623
DespoDRAFT_02400	purine nucleoside phosphorylase I	-1.23	0.49
DespoDRAFT_02401	hypothetical protein	-1.129	0.287
DespoDRAFT_02402	hypothetical protein	-1.567	0.536
DespoDRAFT_02403	response regulator with CheY-like receiver AAA-type ATPase and DNA-binding domains	-1.452	0.695
DespoDRAFT_02404	anion transporter	1.098	0.927
DespoDRAFT_02405	hypothetical protein	1.088	NaN
DespoDRAFT_02406	outer membrane protein/peptidoglycan-associated (lipo)protein	-1.087	0.638
DespoDRAFT_02407	response regulator with CheY-like receiver AAA-type ATPase and DNA-binding domains	-1.451	0.343
DespoDRAFT_02408	histidine kinase HAMP domain-containing protein histidine kinase	-1.51	0.138
DespoDRAFT_02409	response regulator with CheY-like receiver AAA-type ATPase and DNA-binding domains	1.291	0.375
DespoDRAFT_02410	histidine kinase Response regulator receiver domain protein histidine kinase	1.141	0.738
DespoDRAFT_02411	anion transporter	-1.036	0.922
DespoDRAFT_02412	response regulator with CheY-like receiver AAA-type ATPase and DNA-binding domains	-1.34	0.284
DespoDRAFT_02413	response regulator with CheY-like receiver AAA-type ATPase and DNA-binding domains	-1.054	0.922
DespoDRAFT_02414	histidine kinase	-1.99	0.498
DespoDRAFT_02416	universal stress protein UspA-like protein	-5.806	0.0788
DespoDRAFT_02417	universal stress protein UspA-like protein	-2.528	0.0122
DespoDRAFT_02419	hypothetical protein	-4.09	0.183
DespoDRAFT_02420	methionine-R-sulfoxide reductase/methionine-S-sulfoxide reductase	-3.306	0.102
DespoDRAFT_02422	response regulator with CheY-like receiver AAA-type ATPase and DNA-binding domains	1.227	0.545
DespoDRAFT_02423	protein-tyrosine-phosphatase	-1.119	0.792
DespoDRAFT_02424	polyphosphate kinase 1	-1.871	0.101
DespoDRAFT_02425	ribosome-associated GTPase EngA	-2.082	0.029

DespoDRAFT_02426	AAA ATPase	-1.633	0.327
DespoDRAFT_02427	hypothetical protein	1.251	0.65
DespoDRAFT_02428	putative permease	1.259	0.352
DespoDRAFT_02429	DNA gyrase A subunit	1.049	0.764
DespoDRAFT_02430	DNA repair protein radc	-1.597	0.0691
DespoDRAFT_02431	hypothetical protein	-1.391	0.469
DespoDRAFT_02432	3-phosphoglycerate kinase	-1.167	0.429
DespoDRAFT_02433	hypothetical protein	-1.431	0.145
DespoDRAFT_02434	acetyltransferase N-acetylglutamate synthase	-1.848	0.165
DespoDRAFT_02436	response regulator with CheY-like receiver AAA-type ATPase and DNA-binding domains	-2.106	0.33
DespoDRAFT_02437	methylase of chemotaxis methyl-accepting protein	-1.829	0.364
DespoDRAFT_02438	chemotaxis response regulator containing a CheY-like receiver domain and a methylesterase domain	-2.875	0.177
DespoDRAFT_02439	chemotaxis signal transduction protein	-3.166	0.0438
DespoDRAFT_02440	chemotaxis protein histidine kinase-like protein	-2.902	0.0571
DespoDRAFT_02441	collagenase-like protease	1.046	0.833
DespoDRAFT_02443	soluble lytic murein transglycosylase-like protein	2.323	0.235
DespoDRAFT_02448	ribosomal protein L33	-1.435	0.157
DespoDRAFT_02450	preprotein translocase SecE subunit	-1.03	0.921
DespoDRAFT_02451	transcription termination/antitermination factor NusG	-1.011	0.963
DespoDRAFT_02452	50S ribosomal protein L11	1.493	0.22
DespoDRAFT_02453	ribosomal protein L1	1.345	0.116
DespoDRAFT_02454	ribosomal protein L10	2.625	0.0337
DespoDRAFT_02455	ribosomal protein L7/L12	2.28	0.068
DespoDRAFT_02456	DNA-directed RNA polymerase beta subunit	-1.068	0.345
DespoDRAFT_02457	DNA-directed RNA polymerase beta" subunit predominant form	1.148	0.233
DespoDRAFT_02458	ribosomal protein S12 bacterial/organelle	1.414	0.193
DespoDRAFT_02459	ribosomal protein S7 bacterial/organelle	2.016	0.156
DespoDRAFT_02460	translation elongation factor TU	1.787	0.08
DespoDRAFT_02461	ribosomal protein S10 bacterial/organelle	1.947	0.0475
DespoDRAFT_02462	50S ribosomal protein L3 bacterial	1.546	0.0587
DespoDRAFT_02463	50S ribosomal protein L4 bacterial/organelle	1.771	0.0521
DespoDRAFT_02464	ribosomal protein L23	1.863	0.143
DespoDRAFT_02465	ribosomal protein L2 bacterial/organelle	2.002	0.0196

DespoDRAFT_02466	ribosomal protein S19 bacterial/organelle	2.492	0.0756
DespoDRAFT_02467	ribosomal protein L22 bacterial type	1.866	0.127
DespoDRAFT_02468	ribosomal protein S3 bacterial type	1.832	0.0361
DespoDRAFT_02469	ribosomal protein L16 bacterial/organelle	1.703	0.101
DespoDRAFT_02470	ribosomal protein L29	1.945	0.0724
DespoDRAFT_02471	30S ribosomal protein S17	1.981	0.0472
DespoDRAFT_02472	ribosomal protein L14 bacterial/organelle	2.351	0.0072
DespoDRAFT_02473	ribosomal protein L24 bacterial/organelle	2.478	0.132
DespoDRAFT_02474	ribosomal protein L5	2.145	0.0564
DespoDRAFT_02475	ribosomal protein S14	2.22	0.11
DespoDRAFT_02476	ribosomal protein S8	2.599	0.0431
DespoDRAFT_02477	ribosomal protein L6 bacterial type	2.486	0.0605
DespoDRAFT_02478	ribosomal protein L18 bacterial type	2.121	0.0498
DespoDRAFT_02479	ribosomal protein S5 bacterial/organelle type	2.505	0.0778
DespoDRAFT_02480	ribosomal protein L30 bacterial/organelle	2.45	0.1
DespoDRAFT_02481	ribosomal protein L15 bacterial/organelle	1.646	0.143
DespoDRAFT_02482	preprotein translocase SecY subunit	1.573	0.0724
DespoDRAFT_02483	translation initiation factor IF-1	2.009	0.0887
DespoDRAFT_02484	ribosomal protein L36 bacterial type	1.416	0.298
DespoDRAFT_02485	30S ribosomal protein S13	2.231	0.0422
DespoDRAFT_02486	30S ribosomal protein S11	2.125	0.0466
DespoDRAFT_02487	ribosomal protein S4 bacterial/organelle type	2.566	0.0773
DespoDRAFT_02488	DNA-directed RNA polymerase alpha subunit	1.999	0.0474
DespoDRAFT_02489	ribosomal protein L17	1.439	0.214
DespoDRAFT_02490	hypothetical protein	1.801	0.473
DespoDRAFT_02491	molybdenum cofactor biosynthesis protein A	1.863	0.11
DespoDRAFT_02492	uroporphyrin-III C-methyltransferase	2.161	0.0518
DespoDRAFT_02493	porphobilinogen deaminase	2.571	0.0565
DespoDRAFT_02494	putative regulatory protein FmdB family	3.44	0.0471
DespoDRAFT_02495	amidohydrolase	-1.971	0.0439
DespoDRAFT_02496	hypothetical protein	1.56	0.0989
DespoDRAFT_02497	phosphoheptose isomerase	1.346	0.212
DespoDRAFT_02498	tetratricopeptide repeat protein	-2.453	0.119
DespoDRAFT_02499	seryl-tRNA(Sec) selenium transferase	-1.249	0.402
DespoDRAFT_02500	putative domain HDIG-containing protein	-1.332	0.346
DespoDRAFT_02501	diguanylate cyclase (GGDEF) domain-containing protein	-1.096	0.855
DespoDRAFT_02502	orotidine 5"-phosphate decarboxylase subfamily 1	1.206	0.224
DespoDRAFT_02503	aspartate kinase monofunctional class	4.095	0.0278
DespoDRAFT_02504	ATPase YjeE family	1.187	0.814

DespoDRAFT_02505	yjeF-like protein	-1.024	0.935
DespoDRAFT_02506	3-methyladenine DNA glycosylase	1.138	0.368
DespoDRAFT_02507	ABC-type uncharacterized transport system permease and ATPase component	-1.231	0.235
DespoDRAFT_02508	hypothetical protein	1.862	0.0608
DespoDRAFT_02509	putative metal-binding protein	1.663	0.148
DespoDRAFT_02510	2-C-methyl-D-erythritol 2 4-cyclodiphosphate synthase	1.371	0.134
DespoDRAFT_02511	cysteinyl-tRNA synthetase	1.744	0.0862
DespoDRAFT_02512	glutaminyt-tRNA synthetase	1.337	0.0894
DespoDRAFT_02513	putative CoA-binding protein	1.875	0.382
DespoDRAFT_02514	excinuclease ABC B subunit	-1.335	0.145
DespoDRAFT_02515	hypothetical protein	-1.478	0.285
DespoDRAFT_02516	Protein of unknown function (DUF2442)	-2.461	0.128
DespoDRAFT_02518	PKD domain protein	1.3	0.644
DespoDRAFT_02520	Retron-type reverse transcriptase	3.173	0.0301
DespoDRAFT_02522	cysteine protease	1.856	0.298
DespoDRAFT_02523	PEP-CTERM putative exosortase interaction domain-containing protein	-2.925	0.182
DespoDRAFT_02524	rubredoxin	-1.412	0.537
DespoDRAFT_02525	putative nucleotidyltransferase	1.548	0.506
DespoDRAFT_02526	hypothetical protein	1.069	0.898
DespoDRAFT_02527	excinuclease ABC C subunit	-1.233	0.0833
DespoDRAFT_02528	ribosomal protein S1	2.352	0.0525
DespoDRAFT_02529	putative HAD superfamily hydrolase	1.921	0.188
DespoDRAFT_02530	PAS domain S-box	1.117	0.824
DespoDRAFT_02531	pyridoxine 5"-phosphate synthase	1.064	0.851
DespoDRAFT_02532	metalloprotein YbeY/UPF0054 family	-1.069	0.923
DespoDRAFT_02533	putative domain HDIG-containing protein	1.44	0.409
DespoDRAFT_02534	phosphate starvation-inducible protein PhoH predicted ATPase	1.95	0.219
DespoDRAFT_02535	putative membrane protein required for colicin V production	-1.048	0.86
DespoDRAFT_02536	MazG family protein	-1.138	0.33
DespoDRAFT_02537	hypothetical protein	-4.125	0.0859
DespoDRAFT_02538	flagellar biosynthesis anti-sigma factor FlgM	-1.786	0.174
DespoDRAFT_02539	hypothetical protein	-1.375	0.123
DespoDRAFT_02540	fructose/tagatose bisphosphate aldolase	-1.543	0.157
DespoDRAFT_02541	transcriptional regulator	2.172	0.0352
DespoDRAFT_02542	Fe-S oxidoreductase	5.746	0.0165
DespoDRAFT_02543	Electron transfer flavoprotein beta subunit	3.515	0.0522
DespoDRAFT_02544	electron transfer flavoprotein alpha subunit	3.568	0.0122
DespoDRAFT_02545	thymidylate synthase	-1.15	0.653
DespoDRAFT_02546	putative ATPase (AAA+ superfamily)	1.013	0.829

DespoDRAFT_02547	hypothetical protein	1.504	0.324
DespoDRAFT_02548	Protein of unknown function (DUF3423)	1.097	0.651
DespoDRAFT_02549	CRISPR-associated endonuclease Cas1	-3.398	0.685
DespoDRAFT_02550	hypothetical protein	2.239	NaN
DespoDRAFT_02551	hypothetical protein	-2.762	0.467
DespoDRAFT_02552	hypothetical protein	-1.229	0.782
DespoDRAFT_02553	hypothetical protein	-2.134	0.115
DespoDRAFT_02554	hypothetical protein	-1.791	0.262
DespoDRAFT_02555	hypothetical protein	-1.458	0.155
DespoDRAFT_02556	Protein of unknown function (DUF1703)	-1.006	0.986
DespoDRAFT_02557	CRISPR-associated endoribonuclease Cas2	1.062	0.801
DespoDRAFT_02558	CRISPR type III-A/MTUBE-associated RAMP protein Csm5	1.545	0.401
DespoDRAFT_02559	hypothetical protein	1.413	0.544
DespoDRAFT_02560	CRISPR type III-A/MTUBE-associated RAMP protein Csm3	1.342	0.307
DespoDRAFT_02561	CRISPR type III-A/MTUBE-associated protein Csm2	2.227	0.381
DespoDRAFT_02562	CRISPR-associated protein Cas10/Csm1 subtype III-A/MTUBE	1.142	0.489
DespoDRAFT_02563	CRISPR-associated protein TM1812 family	1.483	0.216
DespoDRAFT_02564	hypothetical protein	2.416	0.227
DespoDRAFT_02565	hypothetical protein	1.727	0.664
DespoDRAFT_02567	putative CRISPR-associated protein APE2256 family	-1.138	0.649
DespoDRAFT_02568	CRISPR-associated protein TM1812 family	-1.342	0.138
DespoDRAFT_02569	CRISPR type III-B/RAMP module RAMP protein Cmr6	-1.178	0.314
DespoDRAFT_02570	CRISPR type III-B/RAMP module-associated protein Cmr5	1.158	0.778
DespoDRAFT_02571	CRISPR type III-B/RAMP module RAMP protein Cmr4	-1.31	0.664
DespoDRAFT_02572	CRISPR-associated protein	-1.344	0.421
DespoDRAFT_02573	CRISPR-associated protein Cas10/Cmr2 subtype III-B	-1.186	0.719
DespoDRAFT_02574	CRISPR type III-B/RAMP module RAMP protein Cmr1	-1.503	0.139
DespoDRAFT_02575	hypothetical protein	-2.012	0.233
DespoDRAFT_02576	hypothetical protein	-1.209	0.755
DespoDRAFT_02577	hypothetical protein	1.228	0.61
DespoDRAFT_02578	methylase involved in ubiquinone/menaquinone biosynthesis	-1.335	0.669
DespoDRAFT_02579	anaerobic dehydrogenase typically selenocysteine-containing	1.283	0.71
DespoDRAFT_02580	class III cytochrome C family protein	1.495	0.162

DespoDRAFT_02581	twin arginine targeting protein translocase subunit TatC	-1.091	0.56
DespoDRAFT_02582	Sec-independent protein secretion pathway component	1.165	0.653
DespoDRAFT_02583	DNA/RNA helicase superfamily II	1.443	0.154
DespoDRAFT_02584	putative integral membrane protein	-1.635	0.142
DespoDRAFT_02585	DivIVA domain protein	-1.366	0.282
DespoDRAFT_02586	pilus retraction protein PilT	-1.116	0.644
DespoDRAFT_02587	pilus retraction protein PilT	-1.561	0.116
DespoDRAFT_02588	hypothetical protein	-1.289	0.313
DespoDRAFT_02589	hypothetical protein	-1.334	0.583
DespoDRAFT_02590	penicillin-binding protein, 1A family	1.232	0.159
DespoDRAFT_02591	sporulation related protein	1.896	0.143
DespoDRAFT_02592	hypothetical protein	-3.688	0.0734
DespoDRAFT_02593	hypothetical protein	-3.102	0.152
DespoDRAFT_02594	hypothetical protein	-1.315	0.124
DespoDRAFT_02595	selenium metabolism protein YedF	-1.155	0.467
DespoDRAFT_02596	putative Fe-S oxidoreductase	-1.953	0.402
DespoDRAFT_02597	tRNA-dihydrouridine synthase	-1.127	0.874
DespoDRAFT_02598	hypothetical protein	-3.031	0.0873
DespoDRAFT_02599	putative virion core protein (lumpy skin disease virus)	-2.026	0.0478
DespoDRAFT_02600	Fe ²⁺ /Zn ²⁺ uptake regulation protein	1.498	0.145
DespoDRAFT_02601	hypothetical protein	1.99	0.18
DespoDRAFT_02603	hypothetical protein	1.773	0.183
DespoDRAFT_02604	response regulator with CheY-like receiver AAA-type ATPase and DNA-binding domains	-1.291	0.024
DespoDRAFT_02605	signal transduction histidine kinase	-1.246	0.0616
DespoDRAFT_02606	type IV pilus assembly protein PilM	-3.974	0.054
DespoDRAFT_02607	Tfp pilus assembly protein PilN	-3.181	0.0861
DespoDRAFT_02608	Tfp pilus assembly protein PilO	-3.35	0.0492
DespoDRAFT_02609	Tfp pilus assembly protein PilP	-4.313	0.0661
DespoDRAFT_02610	type IV pilus secretin PilQ/competence protein	-3.294	0.067
DespoDRAFT_02611	Tfp pilus assembly protein PilF	-2.315	0.431
DespoDRAFT_02612	hypothetical protein	-1.992	0.193
DespoDRAFT_02613	threonine synthase	-1.148	0.292
DespoDRAFT_02614	seryl-tRNA synthetase	-1.011	0.936
DespoDRAFT_02615	5, 10-methenyltetrahydrofolate synthetase	1.33	0.377
DespoDRAFT_02616	K ⁺ transport system NAD-binding component	1.028	0.896
DespoDRAFT_02617	protein-L-isoaspartate and D-aspartate O-methyltransferase	-1.372	0.176
DespoDRAFT_02618	putative membrane protein	1.274	0.791

DespoDRAFT_02619	HD-GYP domain-containing protein	1.8	0.157
DespoDRAFT_02620	disulfide bond chaperone	1.147	0.229
DespoDRAFT_02621	periplasmic component of amino acid ABC-type transporter/signal transduction system	-2.224	0.107
DespoDRAFT_02622	PAS domain S-box	-3.076	0.0832
DespoDRAFT_02623	Flavin reductase	1.124	0.235
DespoDRAFT_02624	Mg chelatase-related protein	-1.311	0.51
DespoDRAFT_02625	UDP-3-O-acyl N-acetylglucosamine deacetylase	1.251	0.317
DespoDRAFT_02626	hypothetical protein	-1.374	0.649
DespoDRAFT_02627	PAS domain S-box	-1.089	0.922
DespoDRAFT_02628	response regulator with CheY-like receiver AAA-type ATPase and DNA-binding domains	1.272	0.418
DespoDRAFT_02629	RNA methyltransferase RsmD family	1.913	0.672
DespoDRAFT_02630	pantetheine-phosphate adenyltransferase	2.746	0.275
DespoDRAFT_02631	transcriptional regulator	1.535	0.128
DespoDRAFT_02632	N-methylhydantoinase A/acetone carboxylase beta subunit	-1.443	0.0946
DespoDRAFT_02633	deacetylase histone deacetylase/acetoin utilization protein	-1.433	0.316
DespoDRAFT_02634	lysyl-tRNA synthetase-like protein GenX	-1.17	0.773
DespoDRAFT_02635	HD-GYP domain-containing protein	1.221	0.54
DespoDRAFT_02636	Fe-S oxidoreductase	1.911	0.125
DespoDRAFT_02637	argininosuccinate synthase	2.676	0.0225
DespoDRAFT_02638	hypothetical protein	-1.163	0.607
DespoDRAFT_02639	hypothetical protein	-3	0.268
DespoDRAFT_02640	putative transcriptional regulator	-2.293	0.079
DespoDRAFT_02641	hypothetical protein	-2.67	0.0588
DespoDRAFT_02642	translation elongation factor P/translation initiation factor 5A	4.23	0.102
DespoDRAFT_02643	inorganic pyrophosphatase/exopolyphosphatase	1.127	0.79
DespoDRAFT_02644	pyruvate/2-oxoglutarate dehydrogenase complex dihydrolipoamide dehydrogenase component	-1.14	0.608
DespoDRAFT_02645	isoleucine patch superfamily enzyme carbonic anhydrase/acetyltransferase	1.275	0.298
DespoDRAFT_02646	hypothetical protein	4.98	0.0339
DespoDRAFT_02647	Na ⁺ /H ⁺ antiporter NhaD-like permease	-1.36	0.47
DespoDRAFT_02648	exonuclease DNA polymerase III epsilon subunit family	-2.198	0.471
DespoDRAFT_02650	Protein of unknown function (DUF3375)	-1.847	0.0852
DespoDRAFT_02651	hypothetical protein	-1.744	0.401
DespoDRAFT_02652	hypothetical protein	-1.875	0.0592

DespoDRAFT_02653	hypothetical protein	-1.585	0.411
DespoDRAFT_02655	hypothetical protein	-1.005	0.964
DespoDRAFT_02656	cupin domain-containing protein	-1.016	0.935
DespoDRAFT_02657	hypothetical protein	1.361	NaN
DespoDRAFT_02658	IS66 Orf2 like protein	-1.712	NaN
DespoDRAFT_02660	transposase family protein	-1.63	0.606
DespoDRAFT_02661	hypothetical protein	-1.55	0.0952
DespoDRAFT_02662	putative periplasmic or secreted lipoprotein	-1.096	0.88
DespoDRAFT_02663	hypothetical protein	1.22	0.791
DespoDRAFT_02664	site-specific recombinase XerD	-2.063	0.345
DespoDRAFT_02666	hypothetical protein	-2.953	0.221
DespoDRAFT_02667	hypothetical protein	-1.73	0.229
DespoDRAFT_02671	Mn-dependent transcriptional regulator	1.795	0.103
DespoDRAFT_02672	ATP-dependent protease La	1.374	0.0586
DespoDRAFT_02673	sugar kinase ribokinase	5.501	0.128
DespoDRAFT_02674	S-adenosylmethionine synthetase	3.861	0.0315
DespoDRAFT_02675	adenosylhomocysteinase	3.689	0.0254
DespoDRAFT_02676	hypothetical protein	-1.798	0.0484
DespoDRAFT_02677	radical SAM superfamily enzyme dinitrogenase iron-molybdenum cofactor biosynthesis protein	-6.03	0.0797
DespoDRAFT_02678	glycosidase	-3.775	0.086
DespoDRAFT_02679	sugar kinase ribokinase	-7.227	0.122
DespoDRAFT_02680	HAD-superfamily hydrolase subfamily IIB	-8.802	0.0226
DespoDRAFT_02681	HAD-superfamily hydrolase subfamily IIB	-6.045	0.058
DespoDRAFT_02682	exopolyphosphatase	1.556	0.23
DespoDRAFT_02683	Ribbon-helix-helix protein copG family	-1.441	0.478
DespoDRAFT_02684	hypothetical protein	-1.281	0.227
DespoDRAFT_02685	ATPase involved in chromosome partitioning	-1.202	0.317
DespoDRAFT_02686	hypothetical protein	-1.199	0.553
DespoDRAFT_02687	Pyruvate ferredoxin oxidoreductase	-1.564	0.155
DespoDRAFT_02688	Pyruvate ferredoxin oxidoreductase	-1.167	0.126
DespoDRAFT_02689	alpha-hydroxyacid dehydrogenase FMN- dependent L-lactate dehydrogenase	1.07	0.488
DespoDRAFT_02691	hypothetical protein	-1.167	0.332
DespoDRAFT_02692	nucleoside-diphosphate-sugar epimerase	1.4	0.307
DespoDRAFT_02693	aminopeptidase N	-1.413	0.134
DespoDRAFT_02694	uncharacterized protein involved in an early stage of isoprenoid biosynthesis	-1.766	0.0997
DespoDRAFT_02695	nucleotide sugar dehydrogenase	-1.976	0.118
DespoDRAFT_02696	hypothetical protein	-4.332	0.0636
DespoDRAFT_02697	KamA family protein	-1.713	0.107
DespoDRAFT_02699	putative O-methyltransferase	1.675	0.193
DespoDRAFT_02700	putative RNA-binding protein containing	-1.11	0.619

	Zn ribbon		
DespoDRAFT_02701	HflK protein	1.764	0.0743
DespoDRAFT_02702	HflC protein	1.425	0.145
DespoDRAFT_02703	protein of unknown function (DUF1713)	-1.312	0.457
DespoDRAFT_02704	hypothetical protein	-1.316	0.672
DespoDRAFT_02705	putative regulatory protein FmdB family	1.068	0.722
DespoDRAFT_02706	Co-chaperonin GroES	2.431	0.0551
DespoDRAFT_02707	chaperonin GroL	1.706	0.0586
DespoDRAFT_02708	TolQ protein	1.54	0.041
DespoDRAFT_02709	TolR protein	1.313	0.18
DespoDRAFT_02710	TolA protein	-1.004	0.982
DespoDRAFT_02711	tol-pal system beta propeller repeat protein TolB	2.375	0.0679
DespoDRAFT_02712	peptidoglycan-associated lipoprotein	1.503	0.148
DespoDRAFT_02713	tol-pal system protein YbgF	1.114	0.412
DespoDRAFT_02714	holliday junction resolvasome, endonuclease subunit	-1.03	0.842
DespoDRAFT_02715	holliday junction resolvasome DNA-binding subunit	-1.092	0.534
DespoDRAFT_02716	Holliday junction DNA helicase RuvB subunit	1.607	0.099
DespoDRAFT_02717	ribosomal protein L13 bacterial type	2.649	0.111
DespoDRAFT_02718	ribosomal protein S9	2.261	0.0841
DespoDRAFT_02719	exonuclease I	1.199	0.18
DespoDRAFT_02720	bacterial nucleoid DNA-binding protein	1.406	0.42
DespoDRAFT_02721	putative inhibitor of MCP methylation CheC	-1.386	0.298
DespoDRAFT_02722	Zn-dependent hydrolase glyoxylase	-1.015	0.873
DespoDRAFT_02723	peroxiredoxin	-2.43	0.0243
DespoDRAFT_02724	putative peroxiredoxin	-2.079	0.0681
DespoDRAFT_02725	prepilin signal peptidase PulO-like peptidase	1.427	0.283
DespoDRAFT_02726	ATP-dependent protease La	1.556	0.0869
DespoDRAFT_02727	universal bacterial protein YeaZ	1.428	0.354
DespoDRAFT_02728	phosphatidylserine decarboxylase precursor-related protein	-1.141	0.438
DespoDRAFT_02729	transcription elongation factor GreA	1.02	0.924
DespoDRAFT_02730	DNA-directed RNA polymerase omega subunit	1.005	0.986
DespoDRAFT_02731	putative ATPase of the PP-loop superfamily implicated in cell cycle control	-1.106	0.819
DespoDRAFT_02732	TIGR00294 family protein	-1.47	0.145
DespoDRAFT_02733	D-alanyl-D-alanine carboxypeptidase (penicillin-binding protein 4)	-1.264	0.721
DespoDRAFT_02734	hypothetical protein	-1.719	0.494

DespoDRAFT_02735	hypothetical protein	-3.402	0.104
DespoDRAFT_02736	flagellar motor protein	-1.964	0.0947
DespoDRAFT_02737	glucose-1-phosphate thymidyltransferase short form	1.155	0.228
DespoDRAFT_02738	dTDP-4-dehydrorhamnose 3 5-epimerase	1.068	0.935
DespoDRAFT_02739	dTDP-4-dehydrorhamnose reductase	1.416	0.364
DespoDRAFT_02740	ABC-type uncharacterized transport system periplasmic component	1.751	0.0709
DespoDRAFT_02741	signal transduction histidine kinase	2.009	0.321
DespoDRAFT_02742	response regulator with CheY-like receiver AAA-type ATPase and DNA-binding domains	-1.194	0.0331
DespoDRAFT_02743	outer membrane cobalamin receptor protein	1.179	0.685
DespoDRAFT_02744	putative nucleoside-diphosphate sugar epimerase	1.478	0.222
DespoDRAFT_02745	General secretion pathway protein K	-4.044	0.172
DespoDRAFT_02758	hypothetical protein	1.498	0.864
DespoDRAFT_02759	hypothetical protein	-1.419	0.385
DespoDRAFT_02761	TIGR00268 family protein	-1.64	0.0752
DespoDRAFT_02762	nucleoside diphosphate kinase	8	0.0904
DespoDRAFT_02763	dephospho-CoA kinase	1.042	0.886
DespoDRAFT_02764	transcription termination factor Rho	-1.069	0.461
DespoDRAFT_02765	ribosomal protein L31	1.71	0.169
DespoDRAFT_02766	peptide chain release factor 1	2.016	0.0631
DespoDRAFT_02767	protein-(glutamine-N5) methyltransferase release factor-specific	1.462	0.152
DespoDRAFT_02768	ribosomal protein S2	1.281	0.104
DespoDRAFT_02769	translation elongation factor Ts	1.193	0.259
DespoDRAFT_02770	uridylate kinase	1.666	0.113
DespoDRAFT_02771	ribosome recycling factor	1.795	0.101
DespoDRAFT_02772	undecaprenyl diphosphate synthase	1.393	0.275
DespoDRAFT_02773	CDP-diglyceride synthetase	1.781	0.0823
DespoDRAFT_02774	1-deoxy-D-xylulose 5-phosphate reductoisomerase	2.016	0.172
DespoDRAFT_02775	putative membrane-associated Zn-dependent protease	1.904	0.112
DespoDRAFT_02776	phosphoribosylformylglycinamide (FGAM) synthase synthetase domain	1.324	0.0604
DespoDRAFT_02777	phosphoribosylformylglycinamide (FGAM) synthase glutamine amidotransferase domain	1.463	0.528
DespoDRAFT_02778	putative endoIII-related endonuclease	1.99	0.0339
DespoDRAFT_02779	proline dehydrogenase	1.319	0.435
DespoDRAFT_02781	hypothetical protein	1.335	0.631

DespoDRAFT_02782	PEP-CTERM putative exosortase interaction domain-containing protein	1.4	0.405
DespoDRAFT_02783	hypothetical protein	-1.378	0.222
DespoDRAFT_02784	hypothetical protein	1.104	0.651
DespoDRAFT_02785	DNA segregation ATPase FtsK/SpoIIIE family	1.36	0.494
DespoDRAFT_02786	putative O-methyltransferase	1.155	0.692
DespoDRAFT_02787	uncharacterized iron-regulated protein	1.194	0.166
DespoDRAFT_02788	hypothetical protein	-1.806	0.0674
DespoDRAFT_02791	hypothetical protein	1.589	0.173
DespoDRAFT_02792	arginyl-tRNA synthetase	1.443	0.217
DespoDRAFT_02793	cell division protein	-1.171	0.35
DespoDRAFT_02794	glutamyl-tRNA(Gln) and/or aspartyl-tRNA(Asn) amidotransferase C subunit	2.308	0.0418
DespoDRAFT_02795	glutamyl-tRNA(Gln) and/or aspartyl-tRNA(Asn) amidotransferase A subunit	1.479	0.286
DespoDRAFT_02796	hypothetical protein	2.547	0.182
DespoDRAFT_02797	hypothetical protein	2.551	0.194
DespoDRAFT_02798	DNA mismatch repair protein MutL	4.668	0.184
DespoDRAFT_02799	uncharacterized protein involved in formation of curli polymers	2.384	0.0231
DespoDRAFT_02800	hypothetical protein	-1.27	0.144
DespoDRAFT_02801	transposase	1.147	0.433
DespoDRAFT_02802	PAS domain S-box	-1.037	0.544
DespoDRAFT_02803	hypothetical protein	-27.97	0.00749
DespoDRAFT_02805	adenylosuccinate synthase	1.042	0.629
DespoDRAFT_02806	cytosine/adenosine deaminase	2.046	0.112
DespoDRAFT_02807	glutamate-1-semialdehyde-2, 1-aminomutase	1.559	0.046
DespoDRAFT_02808	UDP-N-acetylmuramate:L-alanyl-gamma-D-glutamyl-meso-diaminopimelate ligase	1.412	0.128
DespoDRAFT_02809	hypothetical protein	2.075	0.229
DespoDRAFT_02810	hemerythrin-like metal-binding domain-containing protein	1.468	0.0811
DespoDRAFT_02811	hypothetical protein	1.152	0.598
DespoDRAFT_02812	exodeoxyribonuclease V alpha subunit	1.048	0.855
DespoDRAFT_02813	ResB protein required for cytochrome c biosynthesis	1.343	0.0453
DespoDRAFT_02814	cytochrome c-type biogenesis protein CcsB	2.55	0.166
DespoDRAFT_02815	QrcA class III cytochrome C family protein	2.754	0.0413
DespoDRAFT_02816	QrcB anaerobic dehydrogenase typically selenocysteine-containing	2.341	0.0354
DespoDRAFT_02817	QrcC Fe-S-cluster-containing hydrogenase subunit	3.301	0.0408
DespoDRAFT_02818	QrcD protein / polysulfide reductase	3.166	0.0268

DespoDRAFT_02819	hypothetical protein	1.75	0.157
DespoDRAFT_02820	pilus biosynthesis protein HicB	-5.998	0.029
DespoDRAFT_02821	putative nucleic-acid-binding protein	-1.578	0.0863
DespoDRAFT_02822	hypothetical protein	-2.001	0.0708
DespoDRAFT_02823	Protein of unknown function (DUF1703)	-3.261	0.0569
DespoDRAFT_02824	putative transcription regulator containing HTH domain	-3.075	0.0605
DespoDRAFT_02825	hypothetical protein	-2.368	0.103
DespoDRAFT_02826	hypothetical protein	-1.119	0.59
DespoDRAFT_02827	integrase family protein	-1.827	0.486
DespoDRAFT_02828	DNA replication protein	-1.563	NaN
DespoDRAFT_02831	growth inhibitor	-2.293	0.389
DespoDRAFT_02832	hypothetical protein	-4.719	0.2
DespoDRAFT_02833	putative transcription regulator containing HTH domain	-1.422	0.75
DespoDRAFT_02835	Transposase IS66 family	1.418	0.402
DespoDRAFT_02836	hypothetical protein	1.324	0.661
DespoDRAFT_02837	putative PLP-dependent enzyme possibly involved in cell wall biogenesis	1.006	0.985
DespoDRAFT_02839	endonuclease IV	1.237	0.818
DespoDRAFT_02840	acetyltransferase	1.206	0.627
DespoDRAFT_02841	N-acetylneuraminate synthase	-1.186	0.435
DespoDRAFT_02842	CMP-N-acetylneuraminic acid synthetase	-1.139	0.759
DespoDRAFT_02843	methyltransferase family protein	-1.179	0.749
DespoDRAFT_02844	Fe-S oxidoreductase	-1.155	0.91
DespoDRAFT_02845	flagellin/flagellar hook associated protein	-2.089	0.157
DespoDRAFT_02846	flagellar capping protein	-1.237	0.773
DespoDRAFT_02847	flagellar biosynthetic protein FliS	-1.008	0.993
DespoDRAFT_02848	hypothetical protein	-1.967	0.494
DespoDRAFT_02849	flagellar protein FlaG	-1.322	0.171
DespoDRAFT_02850	hypothetical protein	#VALUE!	NaN
DespoDRAFT_02851	flagellar hook capping protein	-7.839	0.0635
DespoDRAFT_02852	flagellar hook-basal body protein	-4.173	0.0131
DespoDRAFT_02853	flagellar hook-associated protein FlgK	-3.761	0.166
DespoDRAFT_02854	flagellar hook-associated protein 3	-3.934	0.108
DespoDRAFT_02855	hypothetical protein	-2.001	0.0381
DespoDRAFT_02856	glutamyl-tRNA(Gln) and/or aspartyl-tRNA(Asn) amidotransferase B subunit	1.472	0.298
DespoDRAFT_02857	hypothetical protein	1.094	0.901
DespoDRAFT_02858	S-adenosylmethionine:tRNA ribosyltransferase-isomerase	1.04	0.841
DespoDRAFT_02859	tRNA-guanine transglycosylase queuosine-34-forming	-1.101	0.701
DespoDRAFT_02860	hydrogenase nickel insertion protein HypA	-1.54	0.107
DespoDRAFT_02861	hydrogenase accessory protein HypB	-1.222	0.337

DespoDRAFT_02862	putative dioxygenase	-1.416	0.54
DespoDRAFT_02863	SprT-like family	1.482	0.201
DespoDRAFT_02864	NAD-dependent protein deacetylase SIR2 family	2.45	0.155
DespoDRAFT_02865	YeeE/YedE family protein (DUF395)	-1.478	0.22
DespoDRAFT_02866	YeeE/YedE family protein (DUF395)	-1.545	0.0537
DespoDRAFT_02867	diacylglycerol kinase	-1.511	0.267
DespoDRAFT_02868	hypothetical protein	1.498	0.294
DespoDRAFT_02869	putative xylanase/chitin deacetylase	1.166	0.353
DespoDRAFT_02870	glutamyl-tRNA synthetase	5.392	0.0487
DespoDRAFT_02871	ribosomal protein L32	5.356	0.0728
DespoDRAFT_02872	acyl carrier protein	4.103	0.0483
DespoDRAFT_02873	ribose 5-phosphate isomerase B	2.78	0.0846
DespoDRAFT_02874	glycine/serine hydroxymethyltransferase	2.192	0.073
DespoDRAFT_02875	deoxycytidylate deaminase	2.489	0.113
DespoDRAFT_02876	transcriptional regulator NrdR	2.382	0.0838
DespoDRAFT_02877	riboflavin biosynthesis protein RibD	1.368	0.155
DespoDRAFT_02878	riboflavin synthase alpha subunit	1.266	0.231
DespoDRAFT_02879	GTP cyclohydrolase II/3 4-dihydroxy-2-butanone 4-phosphate synthase	1.756	0.119
DespoDRAFT_02880	6, 7-dimethyl-8-ribityllumazine synthase	1.339	0.084
DespoDRAFT_02881	transcription antitermination factor NusB	1.701	0.0354
DespoDRAFT_02882	Zn-dependent hydrolase glyoxylase	1.31	0.157
DespoDRAFT_02884	Protein of unknown function (DUF1573)	3.146	0.0823
DespoDRAFT_02885	haloacid dehalogenase superfamily enzyme subfamily IA	2.229	0.114
DespoDRAFT_02886	sat ATP sulphurylase	1.401	0.172
DespoDRAFT_02887	Sulfate (and Phosphate) permease	1.453	0.0982
DespoDRAFT_02888	putative S-adenosylmethionine-dependent methyltransferase YraL family	2.624	0.468
DespoDRAFT_02889	putative endonuclease related to Holliday junction resolvase	7.383	0.0901
DespoDRAFT_02890	ribonuclease HII	3.128	0.108
DespoDRAFT_02891	ribosomal protein L19	3.537	0.053
DespoDRAFT_02892	hypothetical protein	2.748	0.0381
DespoDRAFT_02893	tRNA (guanine-N1)-methyltransferase	2.441	0.0728
DespoDRAFT_02894	16S rRNA processing protein RimM	1.952	0.176
DespoDRAFT_02895	putative RNA-binding protein (contains KH domain)	1.773	0.146
DespoDRAFT_02896	ribosomal protein S16	2.795	0.0336
DespoDRAFT_02897	signal recognition particle protein	2.141	0.0414
DespoDRAFT_02898	23S rRNA m2A2503 methyltransferase	-1.162	0.399
DespoDRAFT_02899	growth inhibitor	-1.788	0.0241
DespoDRAFT_02900	growth regulator	-1.082	0.514

DespoDRAFT_02901	putative tRNA(5-methylaminomethyl-2-thiouridylate) methyltransferase with PP-loop ATPase domain	5.026	0.228
DespoDRAFT_02902	coenzyme F390 synthetase	1.5	0.194
DespoDRAFT_02903	ABC-type branched-chain amino acid transport system ATPase component	1.707	0.0932
DespoDRAFT_02904	ABC-type branched-chain amino acid transport system ATPase component	1.179	0.592
DespoDRAFT_02905	ABC-type branched-chain amino acid transport system permease component	1.387	0.653
DespoDRAFT_02906	branched-chain amino acid ABC-type transport system permease component	1.629	0.108
DespoDRAFT_02907	ABC-type branched-chain amino acid transport system periplasmic component	1.757	0.0998
DespoDRAFT_02908	Malate oxidoreductase	-1.833	0.132
DespoDRAFT_02909	succinate dehydrogenase Gamma subunit	1.695	0.103
DespoDRAFT_02910	succinate dehydrogenase a subunit	1.854	0.083
DespoDRAFT_02911	succinate dehydrogenase Beta subunit	1.542	0.108
DespoDRAFT_02912	hypothetical protein	1.115	0.547
DespoDRAFT_02913	putative signal-transduction protein containing cAMP-binding and CBS domains	-1.058	0.882
DespoDRAFT_02914	Cache domain protein	1.891	0.271
DespoDRAFT_02916	Transposase IS66 family	#VALUE!	NaN
DespoDRAFT_02917	hypothetical protein	-29.501	0.0466
DespoDRAFT_02918	hypothetical protein	-7.582	0.0951
DespoDRAFT_02919	hypothetical protein	-1.722	0.702
DespoDRAFT_02920	hypothetical protein	2.681	0.346
DespoDRAFT_02921	ActP acetate permease / putative symporter	1.789	0.496
DespoDRAFT_02922	hypothetical protein	1.618	0.659
DespoDRAFT_02923	dynamamin family protein	1.525	0.194
DespoDRAFT_02924	formate/nitrite transporter family protein	1.104	0.816
DespoDRAFT_02925	hypothetical protein	1.124	0.596
DespoDRAFT_02926	putative membrane protein	-3.22	0.0802
DespoDRAFT_02927	transposase family protein	-3.859	0.0559
DespoDRAFT_02928	PAS domain S-box	-1.037	0.888
DespoDRAFT_02929	hypothetical protein	1.119	NaN
DespoDRAFT_02932	FAD/FMN-dependent dehydrogenase	1.667	0.106
DespoDRAFT_02933	Fe-S oxidoreductase	-1.114	0.341
DespoDRAFT_02934	putative membrane protein	-3.379	0.112
DespoDRAFT_02935	succinyl-CoA synthetase, alpha subunit	-2.705	0.104
DespoDRAFT_02936	succinyl-CoA synthetase, beta subunit	-1.224	0.186
DespoDRAFT_02937	hypothetical protein	-2.183	0.114
DespoDRAFT_02938	Protein of unknown function (DUF3478)	-1.348	0.454
DespoDRAFT_02939	hypothetical protein	-1.12	0.745
DespoDRAFT_02940	hypothetical protein	1.256	0.619

DespoDRAFT_02941	hypothetical protein	-1.049	0.763
DespoDRAFT_02942	CRISPR-associated protein Cas2	-1.311	0.26
DespoDRAFT_02943	CRISPR-associated endonuclease Cas1	-1.199	0.172
DespoDRAFT_02944	CRISPR-associated protein Cas5	-1.122	0.365
DespoDRAFT_02945	CRISPR-associated protein Cas7/Cse4/CasC	1.022	0.583
DespoDRAFT_02946	CRISPR-associated protein Cas6/Cse3/CasE	-1.101	0.0709
DespoDRAFT_02947	CRISPR type I-E protein CasB	-1.132	0.427
DespoDRAFT_02948	CRISPR type I-E protein CasA	-1.704	0.101
DespoDRAFT_02949	CRISPR-associated helicase Cas3/CRISPR-associated endonuclease Cas3-HD	-1.621	0.136
DespoDRAFT_02950	hypothetical protein	-1.743	0.327
DespoDRAFT_02951	putative Zn peptidase	-1.849	0.113
DespoDRAFT_02952	succinate-semialdehyde dehydrogenase	-1.506	0.0915
DespoDRAFT_02953	TRAP transporter solute receptor TAXI family	-2.279	0.0676
DespoDRAFT_02954	type II secretory pathway component ExeA (predicted ATPase)	-3.669	0.212
DespoDRAFT_02955	glyceraldehyde-3-phosphate dehydrogenase/erythrose-4-phosphate dehydrogenase	1.387	0.647
DespoDRAFT_02956	formyltetrahydrofolate synthetase	1.364	0.227
DespoDRAFT_02957	5, 10-methylene-tetrahydrofolate dehydrogenase/methenyl tetrahydrofolate cyclohydrolase	1.873	0.201
DespoDRAFT_02958	protein of unknown function (DUF1844)	1.197	0.691
DespoDRAFT_02959	4-diphosphocytidyl-2C-methyl-D-erythritol kinase	1.469	0.319
DespoDRAFT_02961	ribose-phosphate pyrophosphokinase	1.506	0.158
DespoDRAFT_02962	ribosomal protein L25 Ctc-form	1.583	0.112
DespoDRAFT_02963	peptidyl-tRNA hydrolase	1.429	0.117
DespoDRAFT_02964	CarD-like transcriptional regulator	1.332	0.346
DespoDRAFT_02965	pseudouridine synthase RluA family	1.248	0.622
DespoDRAFT_02966	RNA methyltransferase TrmH family group 1	2.016	0.525
DespoDRAFT_02967	D-tyrosyl-tRNA(Tyr) deacylase	-1.926	0.701
DespoDRAFT_02968	histidinol phosphate phosphatase HisJ family	2.398	0.455
DespoDRAFT_02969	glycosyltransferase	-1.174	0.893
DespoDRAFT_02970	ATP-dependent chaperone ClpB	-1.6	0.0626
DespoDRAFT_02971	PAS domain S-box	-1.822	0.0952
DespoDRAFT_02972	ferredoxin	-3.432	0.00355
DespoDRAFT_02973	hypothetical protein	-4.767	0.0205
DespoDRAFT_02974	hypothetical protein	-5.456	0.0452

DespoDRAFT_02975	transglutaminase-like enzyme predicted cysteine protease	-1.506	0.651
DespoDRAFT_02976	PAS domain S-box	-1.036	0.844
DespoDRAFT_02977	histidine kinase Response regulator receiver domain protein histidine kinase	-1.833	0.359
DespoDRAFT_02978	phosphoenolpyruvate-protein phosphotransferase	-1.032	0.923
DespoDRAFT_02979	hypothetical protein	-1.524	0.731
DespoDRAFT_02980	PAS domain-containing protein	1.27	NaN
DespoDRAFT_02981	diguanylate cyclase (GGDEF) domain-containing protein	-1.495	0.679
DespoDRAFT_02984	integrase family protein	-1.575	0.733
DespoDRAFT_02985	hypothetical protein	-2.166	0.0794
DespoDRAFT_02986	outer membrane protein/peptidoglycan-associated (lipo)protein	-1.763	0.178
DespoDRAFT_02987	response regulator containing a CheY-like receiver domain and an HD-GYP domain	1.151	0.787
DespoDRAFT_02990	Retron-type reverse transcriptase	1.663	0.0777
DespoDRAFT_02992	nuclease-like protein	-1.808	0.329
DespoDRAFT_02993	ABC-type antimicrobial peptide transport system permease component	-1.599	0.0861
DespoDRAFT_02994	ABC-type antimicrobial peptide transport system ATPase component	-1.149	0.852
DespoDRAFT_02995	RND family efflux transporter	-1.071	0.884
DespoDRAFT_02996	efflux transporter outer membrane factor lipoprotein NodT family	-1.126	0.815
DespoDRAFT_02997	hypothetical protein	-1.634	0.615
DespoDRAFT_02998	hypothetical protein	1.782	0.0215
DespoDRAFT_02999	hypothetical protein	-8.894	0.0474
DespoDRAFT_03000	hypothetical protein	-1.101	0.625
DespoDRAFT_03001	acetyl-CoA carboxylase carboxyltransferase component (subunits alpha and beta)	-1.016	0.751
DespoDRAFT_03002	hypothetical protein	1.437	0.489
DespoDRAFT_03003	pyruvate/oxaloacetate carboxyltransferase	1.276	0.218
DespoDRAFT_03004	hypothetical protein	-1.569	0.0841
DespoDRAFT_03006	hypothetical protein	-1.036	0.777
DespoDRAFT_03007	2, 3-bisphosphoglycerate-independent phosphoglycerate mutase	-1	0.994
DespoDRAFT_03008	iojap-like ribosome-associated protein	-1.337	0.596
DespoDRAFT_03009	nicotinate/nicotinamide nucleotide adenylyltransferase	1.809	0.514
DespoDRAFT_03010	Obg family GTPase CgtA	-2.029	0.122
DespoDRAFT_03011	ribosomal protein L27	1.85	0.0675
DespoDRAFT_03012	ribosomal protein L21	3.154	0.116

DespoDRAFT_03013	alkylphosphonate utilization operon protein PhnA	1.612	0.0704
DespoDRAFT_03014	hypothetical protein	1.154	0.562
DespoDRAFT_03015	dsrP	5.123	0.0175
DespoDRAFT_03016	dsrO, putative	4.233	0.0455
DespoDRAFT_03017	dsrJ; cytochrome c	4.652	0.0447
DespoDRAFT_03018	dsrK; Fe-S oxidoreductase	3.847	0.0218
DespoDRAFT_03019	dsrM	3.297	0.0556
DespoDRAFT_03020	hypothetical protein	3.588	0.0242
DespoDRAFT_03021	Lipid A 3-O-deacylase (PagL)	2.181	0.164
DespoDRAFT_03022	methylase involved in ubiquinone/menaquinone biosynthesis	3.058	0.187
DespoDRAFT_03023	glycosyltransferase	1.884	0.349
DespoDRAFT_03025	folylpolyglutamate synthase/dihydrofolate synthase	3.782	0.00431
DespoDRAFT_03026	ribosomal protein S21	2.924	0.0355
DespoDRAFT_03027	adenylate kinase family protein	1.845	0.0464
DespoDRAFT_03028	DNA/RNA helicase superfamily I	-2.58	0.337
DespoDRAFT_03029	Enolase	1.439	0.0138
DespoDRAFT_03030	CTP synthase	1.422	0.128
DespoDRAFT_03031	transcriptional regulator	1.583	0.44
DespoDRAFT_03032	N-methylhydantoinase B/acetone carboxylase alpha subunit	-1.257	0.431
DespoDRAFT_03033	putative methyltransferase YaeB/AF_0241 family	-1.269	0.307
DespoDRAFT_03034	protein of unknown function (DUF1083)	-1.13	0.529
DespoDRAFT_03035	3-hydroxymyristoyl/3-hydroxydecanoyl-(acyl carrier protein) dehydratase	2.48	0.0801
DespoDRAFT_03036	polyketide synthase family protein	2.903	0.0482
DespoDRAFT_03037	PfaD family protein	1.643	0.193
DespoDRAFT_03038	ABC-type nitrate/sulfonate/bicarbonate/thiamine transport system ATPase component	-1.835	0.132
DespoDRAFT_03039	ABC-type nitrate/sulfonate/bicarbonate transport/thiamine system permease component	-2.542	0.0565
DespoDRAFT_03040	ABC-type nitrate/sulfonate/bicarbonate transport/thiamine system periplasmic component	-1.987	0.125
DespoDRAFT_03041	biotin synthase-like enzyme	-1.482	0.186
DespoDRAFT_03042	rubrerythrin	-1.122	0.43
DespoDRAFT_03043	Retron-type reverse transcriptase	-1.128	0.221
DespoDRAFT_03044	transcription elongation factor	-1.818	0.0812
DespoDRAFT_03045	Ribosomal protein S27	-2.502	0.577
DespoDRAFT_03046	hypothetical protein	-3.959	0.0904

DespoDRAFT_03047	hypothetical protein	-2.451	0.157
DespoDRAFT_03051	hypothetical protein	1.395	0.691
DespoDRAFT_03053	hypothetical protein	-5.774	0.106
DespoDRAFT_03054	putative glycosyltransferase	-14.387	0.42
DespoDRAFT_03055	putative glycosyltransferase	-7.612	0.335
DespoDRAFT_03056	glycosyltransferase	-5.695	0.289
DespoDRAFT_03057	hypothetical protein	-6.455	0.194
DespoDRAFT_03058	hypothetical protein	-6.252	0.341
DespoDRAFT_03059	hypothetical protein	-5.057	0.104
DespoDRAFT_03060	hypothetical protein	-2.417	0.0253
DespoDRAFT_03061	hypothetical protein	-4.194	0.108
DespoDRAFT_03063	hypothetical protein	-5.133	0.101
DespoDRAFT_03064	transposase IS605 OrfB family central region	-2.345	0.147
DespoDRAFT_03065	putative glycosyltransferase	-2.413	0.136
DespoDRAFT_03066	hypothetical protein	-2.897	0.116
DespoDRAFT_03067	glycosyltransferase	-1.562	0.599
DespoDRAFT_03068	citrate synthase	-2.031	0.148
DespoDRAFT_03069	glycosyl transferase	-2.176	0.334
DespoDRAFT_03070	hypothetical protein	-1.825	0.295
DespoDRAFT_03071	hypothetical protein	-1.997	0.337
DespoDRAFT_03073	hypothetical protein	-2.549	0.387
DespoDRAFT_03075	GDP-mannose 4 6-dehydratase	-1.75	0.483
DespoDRAFT_03076	nucleoside-diphosphate-sugar epimerase	-2.058	0.525
DespoDRAFT_03077	mannose-1-phosphate guanylyltransferase/mannose-6-phosphate isomerase	-1.62	0.228
DespoDRAFT_03078	hypothetical protein	-1.752	0.06
DespoDRAFT_03079	hypothetical protein	-1.09	0.407
DespoDRAFT_03085	hypothetical protein	-1.621	0.448
DespoDRAFT_03086	hypothetical protein	-1.574	0.156
DespoDRAFT_03087	hypothetical protein	-1.949	0.332
DespoDRAFT_03088	plasmid stability protein	-1.241	0.538
DespoDRAFT_03089	putative nucleic acid-binding protein	-1.351	0.514
DespoDRAFT_03090	hypothetical protein	1.204	0.0658
DespoDRAFT_03091	hypothetical protein	-1.206	0.689
DespoDRAFT_03092	PemK-like protein	-1.273	0.776
DespoDRAFT_03093	dTDP-D-glucose 4 6-dehydratase	2.176	NaN
DespoDRAFT_03095	putative nucleotidyltransferase	-1.178	0.823
DespoDRAFT_03096	hypothetical protein	-1.201	0.458
DespoDRAFT_03097	dTDP-glucose 4 6-dehydratase	-1.293	0.149
DespoDRAFT_03098	dTDP-4-dehydrorhamnose reductase	-1.476	0.0989
DespoDRAFT_03099	glucose-1-phosphate thymidyltransferase short form	-1.151	0.484
DespoDRAFT_03100	dTDP-4-dehydrorhamnose 3, 5-epimerase	-1.617	0.179

DespoDRAFT_03101	methyltransferase family protein	-1.099	0.714
DespoDRAFT_03103	hypothetical protein	1.526	0.61
DespoDRAFT_03104	hypothetical protein	2.162	NaN
DespoDRAFT_03105	transposase	-1.376	0.505
DespoDRAFT_03106	hypothetical protein	-1.007	NaN
DespoDRAFT_03111	apsK ATP sulphurylase/adenylylsulfate kinase	6.229	NaN
DespoDRAFT_03112	hypothetical protein	-1.509	0.368
DespoDRAFT_03113	hypothetical protein	-2.072	0.187
DespoDRAFT_03114	hypothetical protein	-2.131	0.0981
DespoDRAFT_03116	putative membrane protein	-1.839	0.249
DespoDRAFT_03117	nucleoside-diphosphate-sugar epimerase	-2.488	0.442
DespoDRAFT_03119	putative transcriptional regulator with HTH domain	1.697	0.443
DespoDRAFT_03123	hypothetical protein	1.497	NaN
DespoDRAFT_03124	hypothetical protein	-2.758	0.285
DespoDRAFT_03126	D-heptose-7- phosphate 1-kinase	2.348	0.112
DespoDRAFT_03127	phosphoserine phosphatase/homoserine phosphotransferase	1.995	0.173
DespoDRAFT_03128	homoserine dehydrogenase	1.924	0.0253
DespoDRAFT_03129	phosphoribosylaminoimidazole synthetase	-1.247	0.235
DespoDRAFT_03130	putative glycoprotease GCP	-1.184	0.314
DespoDRAFT_03131	beta-glucosidase-like glycosyl hydrolase	-1.494	0.157
DespoDRAFT_03132	DisA bacterial checkpoint controller nucleotide-binding protein	1.092	0.758
DespoDRAFT_03133	SH3 domain protein	1.258	0.431
DespoDRAFT_03134	outer membrane protein	1.184	0.675
DespoDRAFT_03135	hypothetical protein	1.768	0.0834
DespoDRAFT_03136	uncharacterized protein possibly involved in aromatic compounds catabolism	1.327	0.146
DespoDRAFT_03137	shikimate kinase	#VALUE!	0.993
DespoDRAFT_03138	3-phosphoshikimate 1-carboxyvinyltransferase	-1.083	0.319
DespoDRAFT_03139	shikimate 5-dehydrogenase	1.146	0.194
DespoDRAFT_03140	monofunctional chorismate mutase	1.39	0.119
DespoDRAFT_03141	phosphopantetheinyl transferase	1.316	0.775
DespoDRAFT_03143	putative polymerase with PALM domain HD hydrolase domain and Zn ribbon	1.477	0.125
DespoDRAFT_03144	(E)-4-hydroxy-3-methyl-but-2-enyl pyrophosphate reductase	1.073	0.826
DespoDRAFT_03145	ParB-like partition protein	1.616	0.227
DespoDRAFT_03146	ATPase involved in chromosome partitioning	1.442	0.0364
DespoDRAFT_03147	ATP-dependent helicase HrpA	-1.587	0.0709
DespoDRAFT_03148	YgiT-type zinc finger domain protein	-2.593	0.0779

DespoDRAFT_03149	hypothetical protein	-2.524	0.141
DespoDRAFT_03150	hypothetical protein	-3.706	0.0219
DespoDRAFT_03153	hypothetical protein	-1.156	0.796
DespoDRAFT_03154	protein encoded in hypervariable junctions of pilus gene clusters	-1.438	0.524
DespoDRAFT_03156	PEP-CTERM putative exosortase interaction domain-containing protein	-1.544	0.336
DespoDRAFT_03157	hypothetical protein	-1.397	0.672
DespoDRAFT_03158	peptidase T-like protein	-1.169	0.389
DespoDRAFT_03159	TIGR00299 family protein	1.361	0.106
DespoDRAFT_03160	phosphatidylglycerophosphatase A-like protein	1.341	0.426
DespoDRAFT_03161	protein RecA	2.085	0.0995
DespoDRAFT_03162	alanine--tRNA ligase	1.895	0.14
DespoDRAFT_03163	ABC-type uncharacterized transport system permease component	3.041	0.0541
DespoDRAFT_03164	ABC-type uncharacterized transport system permease component	2.622	0.133
DespoDRAFT_03166	hypothetical protein	1.271	0.579
DespoDRAFT_03167	long-chain fatty acid transport protein	1.545	0.0995
DespoDRAFT_03173	glycosyltransferase	1.774	0.664
DespoDRAFT_03174	hypothetical protein	-2.944	NaN
DespoDRAFT_03175	RecA-superfamily ATPase possibly involved in signal transduction	-1.618	0.073
DespoDRAFT_03176	KaiB domain-containing protein	-1.506	0.57
DespoDRAFT_03177	PAS domain S-box	-2.217	0.0881
DespoDRAFT_03178	histidine kinase Response regulator receiver domain protein histidine kinase GAF domain-containing protein	-1.983	0.0869
DespoDRAFT_03179	arsenite efflux pump ACR3-like permease	-2.33	0.0164
DespoDRAFT_03180	methylase of chemotaxis methyl-accepting protein	1.487	0.432
DespoDRAFT_03181	chemotaxis response regulator containing a CheY-like receiver domain and a methylesterase domain	1.271	0.248
DespoDRAFT_03182	chemotaxis protein histidine kinase-like protein	1.625	0.182
DespoDRAFT_03183	PAS domain S-box	1.488	0.285
DespoDRAFT_03184	methyl-accepting chemotaxis protein	2.224	0.0698
DespoDRAFT_03185	chemotaxis signal transduction protein	2.793	0.116
DespoDRAFT_03186	response regulator with CheY-like receiver AAA-type ATPase and DNA-binding domains	1.036	0.867
DespoDRAFT_03187	response regulator with CheY-like receiver AAA-type ATPase and DNA-binding	-1.32	0.536

	domains		
DespoDRAFT_03188	hypothetical protein	-1.572	0.373
DespoDRAFT_03189	CoA-substrate-specific enzyme activase putative	-1.839	0.182
DespoDRAFT_03190	Benzoyl-CoA reductase/2-hydroxyglutaryl-CoA dehydratase subunit BcrC/BadD/HgdB	-1.473	0.0403
DespoDRAFT_03191	Fe-S oxidoreductase	2.456	0.0595
DespoDRAFT_03192	hypothetical protein	1.085	0.242
DespoDRAFT_03193	hypothetical protein	1.59	0.147
DespoDRAFT_03194	hypothetical protein	-1.413	0.45
DespoDRAFT_03195	DNA/RNA helicase superfamily II SNF2 family	-1.405	0.188
DespoDRAFT_03196	hypothetical protein	-1.31	0.357
DespoDRAFT_03197	PAS domain S-box	1.055	0.935
DespoDRAFT_03198	hypothetical protein	-1.545	0.437
DespoDRAFT_03199	D-alanyl-D-alanine carboxypeptidase	-1.032	0.741
DespoDRAFT_03200	transcriptional accessory protein	1.19	0.477
DespoDRAFT_03201	chaperonin GroL	-1.83	0.083
DespoDRAFT_03202	acetyltransferase	1.895	0.714
DespoDRAFT_03203	ATP-grasp enzyme D-alanine-D-alanine ligase	1.059	0.958
DespoDRAFT_03204	ATP-grasp enzyme D-alanine-D-alanine ligase	1.73	0.421
DespoDRAFT_03205	KamA family protein	1.11	0.917
DespoDRAFT_03206	ATP-dependent protease La	-1.009	0.986
DespoDRAFT_03207	ATPase involved in chromosome partitioning	-11.654	0.00258
DespoDRAFT_03209	molecular chaperone (small heat shock protein)	-5.738	0.0463
DespoDRAFT_03210	1, 4-alpha-glucan branching enzyme	-7.425	0.0342
DespoDRAFT_03211	hypothetical protein	1.045	NaN
DespoDRAFT_03217	hypothetical protein	-1.161	0.915
DespoDRAFT_03218	hypothetical protein	-1.292	0.846
DespoDRAFT_03219	hypothetical protein	-2.487	0.381
DespoDRAFT_03220	hypothetical protein	-1.842	0.309
DespoDRAFT_03221	hypothetical protein	-1.668	0.525
DespoDRAFT_03222	hypothetical protein	-1.827	0.518
DespoDRAFT_03223	hypothetical protein	-1.87	0.592
DespoDRAFT_03224	putative endonuclease containing a URI domain	-1.776	0.347
DespoDRAFT_03225	hypothetical protein	-1.192	0.886
DespoDRAFT_03226	site-specific recombinase DNA invertase Pin	-2.556	0.119
DespoDRAFT_03227	hypothetical protein	-1.762	0.189

DespoDRAFT_03228	hypothetical protein	1.222	NaN
DespoDRAFT_03229	hypothetical protein	-1.635	NaN
DespoDRAFT_03230	hypothetical protein	-3.126	NaN
DespoDRAFT_03231	PAS domain S-box	-2.513	0.148
DespoDRAFT_03232	hypothetical protein	-3.805	0.107
DespoDRAFT_03233	molecular chaperone (small heat shock protein)	-24.987	0.135
DespoDRAFT_03234	PAS domain-containing protein	-8.047	0.0569
DespoDRAFT_03235	hypothetical protein	-2.453	NaN
DespoDRAFT_03236	hypothetical protein	-14.984	0.0674
DespoDRAFT_03238	putative regulatory protein FmdB family	-3.088	0.0413
DespoDRAFT_03239	hypothetical protein	-1.75	0.12
DespoDRAFT_03240	D-alanine aminotransferase	-2.44	0.12
DespoDRAFT_03241	uncharacterized protein involved in cysteine biosynthesis	-1.081	0.842
DespoDRAFT_03242	hypothetical protein	-1.707	0.282
DespoDRAFT_03243	hypothetical protein	1.635	0.349
DespoDRAFT_03244	polyferredoxin heterodixulfide reductase subunit A	1.863	0.0192
DespoDRAFT_03245	coenzyme F420-reducing hydrogenase delta subunit	2.325	0.068
DespoDRAFT_03246	Methylene-tetrahydrofolate reductase	1.803	0.00623
DespoDRAFT_03247	5, 10-methylenetetrahydrofolate reductase	2.077	0.0387
DespoDRAFT_03248	iron-sulfur cluster biosynthesis protein NifU-like protein	1.37	0.577
DespoDRAFT_03249	hypothetical protein	-2.366	0.0477
DespoDRAFT_03250	Zn-dependent hydrolase glyoxylase	-1.598	0.152
DespoDRAFT_03251	S-adenosylmethionine decarboxylase proenzyme	2.212	0.21
DespoDRAFT_03252	spermidine synthase	4.295	0.0805
DespoDRAFT_03253	acetyltransferase	-1.238	0.0992
DespoDRAFT_03254	hypothetical protein	-1.089	0.545
DespoDRAFT_03255	cell wall-associated hydrolase invasion-associated protein	-1.523	0.297
DespoDRAFT_03256	flagellar basal body rod protein	-1.938	0.233
DespoDRAFT_03257	SprA-related family	-1.939	0.109
DespoDRAFT_03258	imidazoleglycerol-phosphate dehydratase	1.046	0.902
DespoDRAFT_03259	DNA primase catalytic core	1.103	0.142
DespoDRAFT_03260	RNA polymerase sigma factor sigma-70 family	1.624	0.0447
DespoDRAFT_03262	dinuclear metal center protein YbgI/SA1388 family	1.747	0.375
DespoDRAFT_03263	Zn-ribbon protein	1.249	0.497
DespoDRAFT_03265	HPr-related phosphotransferase system component	-1.251	0.426

DespoDRAFT_03266	2-C-methyl-D-erythritol 4-phosphate cytidyltransferase	1.136	0.808
DespoDRAFT_03267	ABC-type nitrate/sulfonate/bicarbonate transport system periplasmic component	-3.835	0.0437
DespoDRAFT_03268	hypothetical protein	-1.174	0.663
DespoDRAFT_03269	putative Ser protein kinase	-2.361	0.0523
DespoDRAFT_03270	hypothetical protein	-2.829	0.08
DespoDRAFT_03271	hypothetical protein	-2.31	0.229
DespoDRAFT_03272	putative Ser protein kinase	-2.114	0.0613
DespoDRAFT_03273	response regulator containing a CheY-like receiver domain and an HD-GYP domain	-1.705	0.11
DespoDRAFT_03274	single-stranded-DNA-specific exonuclease RecJ	1.953	0.286
DespoDRAFT_03275	hypothetical protein	-1.709	0.312
DespoDRAFT_03276	tRNA-N(6)-(isopentenyl)adenosine-37 thiotransferase enzyme MiaB	1.236	0.0574
DespoDRAFT_03277	methionine aminopeptidase type I	-1.101	0.771
DespoDRAFT_03278	1-acyl-sn-glycerol-3-phosphate acyltransferase	2.055	0.149
DespoDRAFT_03279	nitrogenase iron protein	-3.079	0.0244
DespoDRAFT_03280	nifD nitrogenase molybdenum-iron protein alpha chain	-1.681	0.262
DespoDRAFT_03281	nifK nitrogenase molybdenum-iron protein beta chain	2.291	0.653
DespoDRAFT_03282	nifE nitrogenase MoFe cofactor biosynthesis protein NifE	-1.039	0.964
DespoDRAFT_03283	nifK2 Nitrogenase molybdenum-iron protein	-1.002	0.998
DespoDRAFT_03284	nifB nitrogenase cofactor biosynthesis protein NifB	-1.56	0.696
DespoDRAFT_03285	ferredoxin	1.096	NaN
DespoDRAFT_03286	isopropylmalate/homocitrate/citramalate synthase	-5.555	0.176
DespoDRAFT_03287	PEP-CTERM putative exosortase interaction domain-containing protein	-2.68	0.105
DespoDRAFT_03288	uncharacterized protein MTH1187 family	1.018	0.628
DespoDRAFT_03289	ATP dependent DNA ligase-like protein	-2.111	0.0636
DespoDRAFT_03290	ribulose-5-phosphate 4-epimerase-like epimerase or aldolase	-2.584	0.0556
DespoDRAFT_03291	response regulator with CheY-like receiver AAA-type ATPase and DNA-binding domains	-5.7	0.225
DespoDRAFT_03292	signal transduction histidine kinase	-3.047	0.0636
DespoDRAFT_03294	ABC-type cobalt transport system permease component CbiQ	1.686	0.79
DespoDRAFT_03295	ABC-type cobalt transport system ATPase	1.127	0.286

	component		
DespoDRAFT_03296	hypothetical protein	-1.122	0.847
DespoDRAFT_03297	birA biotin-(acetyl-CoA-carboxylase) ligase	1.821	0.349
DespoDRAFT_03298	putative Rossmann fold nucleotide-binding protein	-1.072	0.216
DespoDRAFT_03299	hypothetical protein	-1.292	0.205
DespoDRAFT_03300	glycogen/starch/alpha-glucan phosphorylase	-1.423	0.0893
DespoDRAFT_03301	dTDP-glucose 4 6-dehydratase	-2.057	0.066
DespoDRAFT_03302	Protein of unknown function (DUF1703)	-2.582	0.0261
DespoDRAFT_03303	protein of unknown function (DUF1902)	-2.731	0.111
DespoDRAFT_03304	putative exonuclease of the beta-lactamase fold involved in RNA processing	-2.553	0.0675
DespoDRAFT_03305	hypothetical protein	-2.083	0.414
DespoDRAFT_03306	PIN domain-containing protein	-2.089	0.227
DespoDRAFT_03307	putative nucleotidyltransferase	-2.051	0.231
DespoDRAFT_03308	hypothetical protein	-2.43	0.104
DespoDRAFT_03309	YgiT-type zinc finger domain protein	-1.906	0.0606
DespoDRAFT_03310	restriction endonuclease	-1.6	0.0964
DespoDRAFT_03311	addiction module antidote protein HigA family	-1.847	0.259
DespoDRAFT_03312	plasmid maintenance system killer protein	-2.194	0.0362
DespoDRAFT_03314	hypothetical protein	1.34	0.228
DespoDRAFT_03317	Protein of unknown function (DUF2281)	-1.918	0.0522
DespoDRAFT_03318	growth inhibitor	-1.972	0.135
DespoDRAFT_03319	addiction module antidote protein HigA family	-2.03	0.18
DespoDRAFT_03320	putative nucleotidyltransferase	1.028	0.954
DespoDRAFT_03321	hypothetical protein	-1.706	0.0913
DespoDRAFT_03322	hypothetical protein	-2.167	0.143
DespoDRAFT_03324	hypothetical protein	-1.89	0.373
DespoDRAFT_03325	hypothetical protein	-2.34	0.116
DespoDRAFT_03326	hypothetical protein	-2.856	0.182
DespoDRAFT_03327	hypothetical protein	-2.395	0.13
DespoDRAFT_03328	putative kinase galactokinase/mevalonate kinase	-1.815	0.12
DespoDRAFT_03329	glucose-1-phosphate cytidyltransferase	-1.704	0.132
DespoDRAFT_03330	nucleoside-diphosphate-sugar epimerase	-2.193	0.0676
DespoDRAFT_03331	dTDP-4-dehydrorhamnose 3, 5-epimerase	-2.646	0.0704
DespoDRAFT_03332	NAD dependent epimerase/dehydratase family protein	-1.59	0.145
DespoDRAFT_03333	nucleoside-diphosphate-sugar epimerase	-2.004	0.0345
DespoDRAFT_03335	Na+-driven multidrug efflux pump	-4.475	0.0111
DespoDRAFT_03336	hypothetical protein	-1.584	0.432

DespoDRAFT_03337	hypothetical protein	-2.326	0.0604
DespoDRAFT_03339	Na ⁺ -driven multidrug efflux pump	-2.856	0.125
DespoDRAFT_03341	hypothetical protein	#VALUE!	NaN
DespoDRAFT_03342	glycosyltransferase	-2.095	0.177
DespoDRAFT_03343	hypothetical protein	-2.985	0.149
DespoDRAFT_03345	coenzyme F390 synthetase	-1.288	0.249
DespoDRAFT_03346	hypothetical protein	-1.124	0.661
DespoDRAFT_03347	glycosyltransferase	-1.746	0.237
DespoDRAFT_03348	Heparinase II/III-like protein	-1.499	0.281
DespoDRAFT_03349	nucleotide sugar dehydrogenase	-1.681	0.086
DespoDRAFT_03351	glycosyltransferase	-2.866	0.0437
DespoDRAFT_03353	hypothetical protein	-1.415	0.473
DespoDRAFT_03354	putative nucleic acid-binding protein	-1.399	0.103
DespoDRAFT_03355	hypothetical protein	-2.299	0.182
DespoDRAFT_03357	hypothetical protein	-2.418	0.332
DespoDRAFT_03358	transposase	-2.419	0.0805
DespoDRAFT_03359	exopolysaccharide biosynthesis polyprenyl glycosylphosphotransferase	-2.112	0.109
DespoDRAFT_03360	hypothetical protein	-3.475	0.0806
DespoDRAFT_03362	PilZ domain-containing protein	1.565	0.335
DespoDRAFT_03363	hypothetical protein	-2.058	0.0635
DespoDRAFT_03364	hypothetical protein	-1.148	0.436
DespoDRAFT_03365	periplasmic protein involved in polysaccharide export	-1.411	0.112
DespoDRAFT_03366	uncharacterized protein involved in exopolysaccharide biosynthesis	-1.557	0.157
DespoDRAFT_03367	lipid A core-O-antigen ligase-like enzyme	-1.155	0.254
DespoDRAFT_03368	hypothetical protein	-1.116	0.603
DespoDRAFT_03369	hypothetical protein	-1.085	0.711
DespoDRAFT_03370	hypothetical protein	-1.733	0.235
DespoDRAFT_03371	hypothetical protein	-1.019	0.977
DespoDRAFT_03372	FAD-dependent dehydrogenase	-1.097	0.877
DespoDRAFT_03373	putative pyridoxal-dependent aspartate 1-decarboxylase	1.871	0.128
DespoDRAFT_03374	hypothetical protein	-2.584	0.409
DespoDRAFT_03375	ribosomal subunit interface protein	-2.147	0.379
DespoDRAFT_03376	arginine kinase	-1.615	0.386
DespoDRAFT_03377	hypothetical protein	1.45	0.468
DespoDRAFT_03378	MoxR-like ATPase	1.405	0.0248
DespoDRAFT_03379	hypothetical protein	1.225	0.16
DespoDRAFT_03380	hypothetical protein	1.225	0.41
DespoDRAFT_03381	Mg-chelatase subunit ChlD	-1.096	0.772
DespoDRAFT_03382	von Willebrand factor type A-like protein	1.08	0.828
DespoDRAFT_03383	tetratricopeptide repeat protein	-2.188	0.0728
DespoDRAFT_03384	glycerol-3-phosphate dehydrogenase	2.704	0.199

DespoDRAFT_03385	putative signal transduction protein	1.783	0.104
DespoDRAFT_03386	ribonuclease HI	1.218	0.143
DespoDRAFT_03387	hypothetical protein	-2.085	0.086
DespoDRAFT_03388	ABC-type transport system involved in resistance to organic solvents auxiliary component	-2.6	0.0193
DespoDRAFT_03389	phosphate ABC transporter permease protein PstC	-1.212	0.768
DespoDRAFT_03390	phosphate ABC transporter permease protein PstA	1.149	0.779
DespoDRAFT_03391	ABC-type phosphate transport system periplasmic component	-1.291	0.434
DespoDRAFT_03392	phosphate ABC transporter ATP-binding protein	1.036	0.954
DespoDRAFT_03393	hypothetical protein	1.083	0.711
DespoDRAFT_03394	exodeoxyribonuclease III	1.017	0.931
DespoDRAFT_03395	ferredoxin-thioredoxin reductase catalytic subunit	-1.314	0.0952
DespoDRAFT_03396	glutaredoxin-like protein	-1.438	0.166
DespoDRAFT_03397	hypothetical protein	-1.676	0.0728
DespoDRAFT_03398	desulfoferredoxin	-2.048	0.0493
DespoDRAFT_03399	TIGR01777 family protein	-1.737	0.102
DespoDRAFT_03400	hypothetical protein	-1.217	0.59
DespoDRAFT_03401	exopolyphosphatase-like enzyme	-1.552	0.086
DespoDRAFT_03402	rubredoxin	-1.873	0.0706
DespoDRAFT_03403	cytochrome d oxidase cyd subunit II	-1.088	0.733
DespoDRAFT_03404	cytochrome bd-type quinol oxidase subunit 1	-1.651	0.0134
DespoDRAFT_03405	Protein of unknown function DUF255	2.587	0.261
DespoDRAFT_03406	5"-deoxy-5"-methylthioadenosine phosphorylase	1.878	0.108
DespoDRAFT_03407	adenine phosphoribosyltransferase	1.555	0.193
DespoDRAFT_03408	hypothetical protein	1.542	0.324
DespoDRAFT_03409	exodeoxyribonuclease V gamma subunit	1.096	0.597
DespoDRAFT_03410	exodeoxyribonuclease V beta subunit	-1.244	0.133
DespoDRAFT_03411	putative membrane protein	-1.785	0.0709
DespoDRAFT_03412	protein of unknown function (DUF2760)	1.336	0.127
DespoDRAFT_03413	molecular chaperone	1.447	0.0827
DespoDRAFT_03414	molecular chaperone	1.112	0.456
DespoDRAFT_03415	hypothetical protein	-1.221	0.395
DespoDRAFT_03418	hypothetical protein	1.027	0.951
DespoDRAFT_03419	putative membrane protein	1.586	0.596
DespoDRAFT_03420	Rhodanese-related sulfurtransferase	1.037	0.413
DespoDRAFT_03421	hypothetical protein	2.825	0.0335
DespoDRAFT_03422	hypothetical protein	-1.018	0.922

DespoDRAFT_03423	L-threonine 3-dehydrogenase	-2.125	0.0224
DespoDRAFT_03424	7-keto-8-aminopelargonate synthetase-like enzyme	-2.251	0.186
DespoDRAFT_03425	hypothetical protein	-1.852	0.0753
DespoDRAFT_03426	hypothetical protein	2.46	0.111
DespoDRAFT_03427	hypothetical protein	-2.189	0.188
DespoDRAFT_03428	diguanylate cyclase (GGDEF) domain-containing protein	-1.297	0.185
DespoDRAFT_03429	hypothetical protein	-2.215	0.0328
DespoDRAFT_03430	ABC-type nitrate/sulfonate/bicarbonate transport system periplasmic component	-1.882	0.0336
DespoDRAFT_03431	ABC-type nitrate/sulfonate/bicarbonate transport system permease component	-1.669	0.253
DespoDRAFT_03432	ABC-type nitrate/sulfonate/bicarbonate transport system periplasmic component	1.156	0.773
DespoDRAFT_03433	ABC-type nitrate/sulfonate/bicarbonate transport system ATPase component	-2.915	0.29
DespoDRAFT_03434	ABC-type nitrate/sulfonate/bicarbonate transport system periplasmic component	-2.599	0.135
DespoDRAFT_03435	putative unusual protein kinase	-1.812	0.1
DespoDRAFT_03436	hypothetical protein	-1.559	0.103
DespoDRAFT_03437	acyl-CoA dehydrogenase	1.233	0.0826
DespoDRAFT_03438	metal-dependent hydrolase beta-lactamase superfamily I	-1.364	0.443
DespoDRAFT_03439	Major Facilitator Superfamily transporter	-1.381	0.737
DespoDRAFT_03440	hypothetical protein	2.369	0.285
DespoDRAFT_03441	hypothetical protein	-1.838	0.644
DespoDRAFT_03442	putative transcriptional regulator	-1.584	0.397
DespoDRAFT_03443	HipA domain-containing protein	-1.329	0.0952
DespoDRAFT_03444	Rhodopirellula transposase	2.454	0.16
DespoDRAFT_03445	Rhodopirellula transposase	1.007	0.96
DespoDRAFT_03446	hypothetical protein	1.017	0.886
DespoDRAFT_03447	Zn-dependent oxidoreductase NADPH:quinone reductase	-1.408	0.16
DespoDRAFT_03449	ADP-ribosylglycohydrolase	-2.705	0.00432
DespoDRAFT_03450	putative transcriptional regulator	-2.075	0.0409
DespoDRAFT_03451	deoxyribodipyrimidine photolyase	-2.098	0.0935
DespoDRAFT_03452	methylase involved in ubiquinone/menaquinone biosynthesis	-2.278	0.0841
DespoDRAFT_03453	methylase involved in ubiquinone/menaquinone biosynthesis	-1.627	0.0381
DespoDRAFT_03454	putative transcription activator	-3.937	0.0145
DespoDRAFT_03455	hypothetical protein	-1.589	0.503
DespoDRAFT_03456	transposase	-1.021	0.968
DespoDRAFT_03457	hypothetical protein	-1.003	0.998

DespoDRAFT_03458	Acetate permease	-1.004	0.993
DespoDRAFT_03459	hypothetical protein	-1.334	0.783
DespoDRAFT_03462	glycosyltransferase	-1.071	0.488
DespoDRAFT_03463	dTDP-4-dehydrothamnose 3, 5-epimerase-like enzyme	-2.109	0.534
DespoDRAFT_03466	putative glycosyltransferase	-2.551	0.108
DespoDRAFT_03467	hypothetical protein	-1.594	0.138
DespoDRAFT_03468	DnaJ-class molecular chaperone with C-terminal Zn finger domain	-1.206	0.273
DespoDRAFT_03469	dihydrodipicolinate reductase	1.741	0.0949
DespoDRAFT_03470	Nucleoside-diphosphate-sugar pyrophosphorylase family protein	2.053	0.263
DespoDRAFT_03471	glycerol-3-phosphate O-acyltransferase	1.15	0.402
DespoDRAFT_03472	hypothetical protein	1.278	0.611
DespoDRAFT_03473	hypothetical protein	-1.692	0.0734
DespoDRAFT_03474	histidinol-phosphate aminotransferase	3.642	0.159
DespoDRAFT_03475	cytidylate kinase	3.502	0.0282
DespoDRAFT_03476	ribosomal protein S1	2.468	0.0423
DespoDRAFT_03477	signal peptide peptidase SppA, 36K type	1.012	0.847
DespoDRAFT_03478	Sua5/YciO/YrdC/YwIC family protein	1.842	0.0614
DespoDRAFT_03479	6-phosphofructokinase	2.074	0.0557
DespoDRAFT_03480	inosine-5"-monophosphate dehydrogenase	1.465	0.249
DespoDRAFT_03481	DNA-directed DNA polymerase III PolC	1.295	0.0575
DespoDRAFT_03482	putative periplasmic or secreted lipoprotein	1.34	0.309
DespoDRAFT_03483	hypothetical protein	-2.078	0.143
DespoDRAFT_03484	protein with DnaJ-like domain	1.366	0.269
DespoDRAFT_03485	hypothetical protein	-1.078	0.884
DespoDRAFT_03486	valyl-tRNA synthetase	-1.064	0.531
DespoDRAFT_03487	nicotinate-nucleotide pyrophosphorylase	1.006	0.99
DespoDRAFT_03488	hypothetical protein	1.139	0.802
DespoDRAFT_03489	hypothetical protein	-3.126	NaN
DespoDRAFT_03490	hypothetical protein	-1.605	0.273
DespoDRAFT_03492	hypothetical protein	-1.933	0.12
DespoDRAFT_03493	diguanylate cyclase (GGDEF) domain-containing protein	-1.306	0.411
DespoDRAFT_03494	GTP-binding protein LepA	1.013	0.853
DespoDRAFT_03495	2-isopropylmalate synthase/homocitrate synthase family protein	2.786	0.0565
DespoDRAFT_03496	acetolactate synthase small subunit	3.656	0.0162
DespoDRAFT_03497	acetolactate synthase large subunit biosynthetic type	2.923	0.0438
DespoDRAFT_03498	dihydroxy-acid dehydratase	1.329	0.0737
DespoDRAFT_03499	hypothetical protein	-1.827	0.112
DespoDRAFT_03501	hypothetical protein	1.354	0.763
DespoDRAFT_03502	NCAIR mutase-like protein	1.438	0.18

DespoDRAFT_03504	histidine kinase	-1.081	0.898
DespoDRAFT_03505	response regulator containing a CheY-like receiver domain and an HTH DNA-binding domain	1.05	0.937
DespoDRAFT_03506	cytochrome c peroxidase	-2.482	0.698
DespoDRAFT_03507	hypothetical protein	-4.313	0.0311
DespoDRAFT_03508	methyltransferase putative	1.12	0.892
DespoDRAFT_03509	Protein of unknown function (DUF1698)	-1.22	0.753
DespoDRAFT_03510	hypothetical protein	-4.475	0.216
DespoDRAFT_03511	arginase	-1.159	0.812
DespoDRAFT_03512	helicase family protein with metal-binding cysteine cluster	1.022	0.88
DespoDRAFT_03514	exopolyphosphatase-like enzyme	1.096	0.143
DespoDRAFT_03515	hypothetical protein	1.527	0.158
DespoDRAFT_03516	dGTP triphosphohydrolase	1.829	0.166
DespoDRAFT_03517	ATPase involved in chromosome partitioning	1.153	0.284
DespoDRAFT_03518	hypothetical protein	-1.652	0.111
DespoDRAFT_03519	tetratricopeptide repeat protein	1.087	0.816
DespoDRAFT_03520	DNA-directed RNA polymerase sigma subunit (sigma70/sigma32)	1.064	0.616
DespoDRAFT_03521	phosphoribosylaminoimidazole-succinocarboxamide synthase	-1.045	0.835
DespoDRAFT_03522	putative transcriptional regulator	1.165	0.0837
DespoDRAFT_03523	hypothetical protein	1.433	0.35
DespoDRAFT_03524	translation elongation factor-like GTPase	1.851	0.085
DespoDRAFT_03525	hemolysin A	2.81	0.099
DespoDRAFT_03526	1-deoxy-D-xylulose-5-phosphate synthase	1.801	0.0821
DespoDRAFT_03527	geranylgeranyl pyrophosphate synthase	1.328	0.532
DespoDRAFT_03528	exodeoxyribonuclease VII small subunit	1.714	0.24
DespoDRAFT_03529	exodeoxyribonuclease VII large subunit	1.302	0.36
DespoDRAFT_03530	sugar phosphate isomerase/epimerase	-1.029	0.944
DespoDRAFT_03531	Rhodanese-related sulfurtransferase	-1.791	0.191
DespoDRAFT_03532	pyridine nucleotide-disulfide oxidoreductase family protein	-1.892	0.0842
DespoDRAFT_03533	hypothetical protein	-2.336	0.204
DespoDRAFT_03534	methylase involved in ubiquinone/menaquinone biosynthesis	-2.387	0.0983
DespoDRAFT_03535	hypothetical protein	-1.501	0.271
DespoDRAFT_03537	signal transduction histidine kinase	-2.11	0.147
DespoDRAFT_03538	esterase/lipase	-2.277	0.0816
DespoDRAFT_03539	acyl-CoA dehydrogenase	-1.38	0.0937
DespoDRAFT_03540	hypothetical protein	1.46	0.355
DespoDRAFT_03541	FRG domain protein	1.944	0.121
DespoDRAFT_03542	putative methyltransferase YaeB/AF_0241	1.155	0.676

	family		
DespoDRAFT_03543	oligoendopeptidase F	1.048	0.71
DespoDRAFT_03544	gamma-glutamyl phosphate reductase	1.234	0.17
DespoDRAFT_03545	glutamate 5-kinase	2.354	0.0241
DespoDRAFT_03547	hypothetical protein	-1.262	0.631
DespoDRAFT_03548	penicilin amidase	-1.867	0.0414
DespoDRAFT_03549	phage shock protein C	-1.878	0.128
DespoDRAFT_03550	hypothetical protein	-1.778	0.149
DespoDRAFT_03551	phage shock protein A	-2.3	0.0633
DespoDRAFT_03552	psp operon transcriptional activator PspF	-2.225	0.0111
DespoDRAFT_03553	LysM repeat-containing protein	-1.735	0.461
DespoDRAFT_03554	YeeE/YedE family protein (DUF395)	1.327	0.184
DespoDRAFT_03555	putative redox protein regulator of disulfide bond formation	1.183	0.134
DespoDRAFT_03556	Protein of unknown function (DUF3343)	1.011	0.937
DespoDRAFT_03557	putative sugar kinase	1.109	0.501
DespoDRAFT_03558	hypothetical protein	1.223	0.746
DespoDRAFT_03559	L-asparaginase/GlutRNAGln amidotransferase subunit D	1.174	0.646
DespoDRAFT_03560	protein-tyrosine-phosphatase	1.735	0.272
DespoDRAFT_03561	isochorismate synthase	1.526	0.344
DespoDRAFT_03562	ATPase involved in chromosome partitioning	-1.2	0.585
DespoDRAFT_03563	hypothetical protein	1.135	0.894
DespoDRAFT_03564	hypothetical protein	-1.051	0.866
DespoDRAFT_03565	AIPR protein	-1.405	0.277
DespoDRAFT_03566	Transposase IS66 family	-5.497	0.108
DespoDRAFT_03567	Protein of unknown function (DUF3089)	-5.044	0.0487
DespoDRAFT_03568	hypothetical protein	-1.62	0.467
DespoDRAFT_03569	putative peptidoglycan-binding domain-containing protein	-1.716	0.162
DespoDRAFT_03570	hypothetical protein	-1.478	0.276
DespoDRAFT_03571	2-succinyl-5-enolpyruvyl-6-hydroxy-3-cyclohexene-1-carboxylic-acid synthase	-1.834	0.0831
DespoDRAFT_03572	dihydroxynaphthoate synthase	-1.409	0.354
DespoDRAFT_03573	enolase superfamily enzyme related to L-alanine-DL-glutamate epimerase	-1.737	0.116
DespoDRAFT_03574	acyl-CoA synthetase (AMP-forming)/AMP-acid ligase II	-2.081	0.225
DespoDRAFT_03575	hypothetical protein	-1.147	0.345
DespoDRAFT_03576	indolepyruvate ferredoxin oxidoreductase alpha subunit	-1.114	0.534
DespoDRAFT_03577	2-oxoacid:ferredoxin oxidoreductase gamma subunit	-1.017	0.964
DespoDRAFT_03578	3-dehydroquininate dehydratase type II	-1.314	0.227

DespoDRAFT_03579	Mg-dependent DNase	-1.169	0.309
DespoDRAFT_03580	dinucleotide-utilizing enzyme possibly involved in molybdopterin or thiamin biosynthesis	-1.206	0.644
DespoDRAFT_03581	hypothetical protein	2.321	0.331
DespoDRAFT_03586	hypothetical protein	-1.563	NaN
DespoDRAFT_03587	hypothetical protein	1.833	NaN
DespoDRAFT_03589	hypothetical protein	-2.382	0.445
DespoDRAFT_03593	addiction module antidote protein HigA family	-4.674	0.325
DespoDRAFT_03594	hypothetical protein	-2.49	0.131
DespoDRAFT_03595	transcriptional regulator	2.07	0.29
DespoDRAFT_03596	tryptophan synthase beta subunit	3.606	0.0403
DespoDRAFT_03597	tryptophan synthase alpha subunit	2.794	0.137
DespoDRAFT_03598	S-methyl-5-thioribose-1-phosphate isomerase	1.24	0.651
DespoDRAFT_03599	transcriptional regulator	1.563	0.41
DespoDRAFT_03600	Fe-S oxidoreductase	-1.063	0.906
DespoDRAFT_03601	hypothetical protein	-1.198	0.653
DespoDRAFT_03602	ABC-type metal ion transport system periplasmic component/surface adhesin	-1.729	0.23
DespoDRAFT_03603	ATPase component of Mn/Zn ABC-type transporter	-1.137	0.0733
DespoDRAFT_03604	ABC-type Mn ²⁺ /Zn ²⁺ transport system permease component	-1.748	0.0264
DespoDRAFT_03605	urocanate hydratase	-1.897	0.0753
DespoDRAFT_03606	acyl-CoA synthetase (AMP-forming)/AMP-acid ligase II	1.484	0.58
DespoDRAFT_03607	Fe ²⁺ transport system protein A	-1.426	0.161
DespoDRAFT_03608	ferrous iron transporter FeoB	1.884	0.144
DespoDRAFT_03609	hypothetical protein	1.906	0.301
DespoDRAFT_03610	methylase involved in ubiquinone/menaquinone biosynthesis	1.102	0.843
DespoDRAFT_03611	3-hydroxyacyl-CoA dehydrogenase	-1.387	0.0128
DespoDRAFT_03612	acetyl-CoA acetyltransferase	-1.627	0.158
DespoDRAFT_03613	universal stress protein UspA-like protein	-1.685	0.0338
DespoDRAFT_03614	signal transduction histidine kinase	-5.631	0.0708
DespoDRAFT_03615	hypothetical protein	-3.129	0.506
DespoDRAFT_03616	hypothetical protein	-1.085	0.854
DespoDRAFT_03617	hypothetical protein	-1.284	0.253
DespoDRAFT_03623	hypothetical protein	1.436	NaN
DespoDRAFT_03624	hypothetical protein	-1.139	0.846
DespoDRAFT_03625	hydroxyethylthiazole kinase sugar kinase family	-1.467	0.582
DespoDRAFT_03628	Protein of unknown function DUF55	-1.415	0.886

DespoDRAFT_03630	uncharacterized protein MTH1187 family	-1.694	0.158
DespoDRAFT_03631	thiamine monophosphate synthase	-1.746	0.167
DespoDRAFT_03632	protein of unknown function (DUF364)	-1.583	0.254
DespoDRAFT_03633	thioredoxin	-1.606	0.19
DespoDRAFT_03635	signal transduction histidine kinase nitrate/nitrite-specific	-1.625	0.449
DespoDRAFT_03636	uncharacterized protein, possibly involved in aromatic compounds catabolism	2.548	0.276
DespoDRAFT_03637	phosphoribosylformimino-5- aminoimidazole carboxamide ribotide isomerase eukaryotic type	1.133	0.748
DespoDRAFT_03638	ABC-type uncharacterized transport system auxiliary component	3.527	0.419
DespoDRAFT_03639	ABC-type transport system involved in resistance to organic solvents, periplasmic component	1.56	0.0333
DespoDRAFT_03640	ABC-type transport system involved in resistance to organic solvents ATPase component	-1.051	0.756
DespoDRAFT_03641	putative integral membrane protein	1.213	0.448
DespoDRAFT_03642	purine nucleoside phosphorylase	-1.958	0.425
DespoDRAFT_03643	putative membrane protein	-1.634	0.472
DespoDRAFT_03644	ribosomal protein L11 methyltransferase	1.264	0.355
DespoDRAFT_03645	signal transduction histidine kinase	-1.282	0.504
DespoDRAFT_03646	response regulator containing a CheY-like receiver domain and an HTH DNA-binding domain	-1.627	0.0684
DespoDRAFT_03647	acyl-CoA synthetase (AMP-forming)/AMP- acid ligase II	-1.13	0.674
DespoDRAFT_03648	hydroxyethylthiazole kinase sugar kinase family	-1.05	0.847
DespoDRAFT_03649	Mn ²⁺ /Fe ²⁺ transporter NRAMP family	1.26	0.664
DespoDRAFT_03650	protein chain release factor B	-1.102	0.716
DespoDRAFT_03651	hypothetical protein	1.139	0.931
DespoDRAFT_03652	RND family efflux transporter	-1.729	0.0307
DespoDRAFT_03653	ABC-type antimicrobial peptide transport system ATPase component	-2.284	0.203
DespoDRAFT_03654	ABC-type transport system involved in lipoprotein release permease component	-1.995	0.515
DespoDRAFT_03655	ABC-type transport system involved in lipoprotein release permease component	-1.932	0.648
DespoDRAFT_03656	phosphatidylserine decarboxylase	3.025	NaN
DespoDRAFT_03657	Prolipoprotein diacylglyceryl transferase	1.34	0.878
DespoDRAFT_03658	hypothetical protein	#VALUE!	NaN
DespoDRAFT_03659	acyl-CoA thioesterase II	-1.907	0.489

DespoDRAFT_03660	periplasmic component of amino acid ABC-type transporter/signal transduction system	1.125	0.783
DespoDRAFT_03661	small-conductance mechanosensitive channel	1.787	0.0803
DespoDRAFT_03663	dihydroorotate dehydrogenase	-1.595	0.0291
DespoDRAFT_03664	hypothetical protein	1.011	0.924
DespoDRAFT_03665	hypothetical protein	1.087	0.629
DespoDRAFT_03666	hypothetical protein	1.436	0.206
DespoDRAFT_03667	hypothetical protein	-1.388	0.122
DespoDRAFT_03669	TIGR01777 family protein	-1.742	0.0448
DespoDRAFT_03670	hypothetical protein	-1.107	0.176
DespoDRAFT_03671	Zn-dependent hydrolase glyoxylase	-1.41	0.18
DespoDRAFT_03673	cysteine desulfurase NifS	-1.71	0.0858
DespoDRAFT_03674	Fe-S cluster assembly protein NifU	-2.342	0.0467
DespoDRAFT_03675	TIGR02757 family protein	-1.521	0.128
DespoDRAFT_03676	K ⁺ -dependent Na ⁺ exchanger related-protein	-1.008	0.993
DespoDRAFT_03677	hypothetical protein	-1.069	0.936
DespoDRAFT_03678	pyrroline-5-carboxylate reductase (proC)	-1.914	0.0723
DespoDRAFT_03679	hypothetical protein	-3.559	0.0413
DespoDRAFT_03680	rubredoxin	-3.538	0.0509
DespoDRAFT_03681	chorismate synthase	-1.702	0.227
DespoDRAFT_03682	sigma-54 interacting regulator	-1.043	0.956
DespoDRAFT_03683	beta-ketoacyl synthase family protein acyltransferase family protein phosphopantetheine-containing protein	1.824	0.0332
DespoDRAFT_03684	phosphopantetheinyl transferase	1.378	0.0958
DespoDRAFT_03685	response regulator with CheY-like receiver AAA-type ATPase and DNA-binding domains	-16.288	0.0337
DespoDRAFT_03686	tetratricopeptide repeat protein	-18.462	0.0383
DespoDRAFT_03687	hypothetical protein	-43.147	0.104
DespoDRAFT_03688	putative Fe-S oxidoreductase	-49.794	0.0463
DespoDRAFT_03689	hypothetical protein	-84.061	0.0731
DespoDRAFT_03690	hypothetical protein	-53.439	0.0902
DespoDRAFT_03691	Ig-like domain-containing surface protein	-41.827	0.0875
DespoDRAFT_03692	Phage tail protein	-83.573	0.0963
DespoDRAFT_03693	Baseplate J-like protein	-71.037	0.159
DespoDRAFT_03694	Baseplate J-like protein	-71.463	0.0826
DespoDRAFT_03695	phage baseplate assembly protein W	-90.216	0.0733
DespoDRAFT_03696	hypothetical protein	-59.868	0.0467
DespoDRAFT_03698	phage protein D	-43.42	0.0408
DespoDRAFT_03699	hypothetical protein	-79.847	0.119
DespoDRAFT_03700	hypothetical protein	-99.796	0.108
DespoDRAFT_03701	hypothetical protein	-108.093	0.00853
DespoDRAFT_03702	AAA+ family ATPase	-92.893	0.0863

DespoDRAFT_03703	hypothetical protein	-112.027	0.0964
DespoDRAFT_03704	putative phage tail region protein	-157.538	0.0265
DespoDRAFT_03705	phage tail sheath protein FI	-97.677	0.0543
DespoDRAFT_03706	hypothetical protein	-186.056	0.00262
DespoDRAFT_03707	hypothetical protein	-98.865	0.0586
DespoDRAFT_03708	putative phage tail region protein	-92.353	0.00136
DespoDRAFT_03709	phage tail sheath protein FI	-95.675	0.0254
DespoDRAFT_03710	phage tail sheath protein FI	-66.537	0.00802
DespoDRAFT_03711	hypothetical protein	-65.612	0.0561
DespoDRAFT_03712	hypothetical protein	-52.23	0.0433
DespoDRAFT_03713	hypothetical protein	-80.282	0.0397
DespoDRAFT_03714	cAMP-binding protein	-2.089	0.398
DespoDRAFT_03715	hypothetical protein	1.835	0.679
DespoDRAFT_03716	peptidyl-prolyl cis-trans isomerase (rotamase) - cyclophilin family	1.295	0.0851
DespoDRAFT_03717	monofunctional biosynthetic peptidoglycan transglycosylase	-1.315	0.186
DespoDRAFT_03718	hypothetical protein	1.954	0.227
DespoDRAFT_03719	phosphohistidine phosphatase SixA	-1.481	0.327
DespoDRAFT_03720	hypothetical protein	1.955	0.138
DespoDRAFT_03721	peroxiredoxin	-1.317	0.229
DespoDRAFT_03722	universal stress protein UspA-like protein	-1.643	0.186
DespoDRAFT_03723	hypothetical protein	-1.306	0.155
DespoDRAFT_03725	hypothetical protein	-2.217	0.134
DespoDRAFT_03727	transposase	-1.678	0.298
DespoDRAFT_03728	hypothetical protein	-1.145	0.272
DespoDRAFT_03729	hypothetical protein	-1.305	0.225
DespoDRAFT_03730	hypothetical protein	-1.801	0.106
DespoDRAFT_03731	transposase	-2.052	0.0452
DespoDRAFT_03732	transposase	-1.449	0.262
DespoDRAFT_03734	prevent-host-death family protein	1.42	0.268
DespoDRAFT_03736	hypothetical protein	-1.489	0.292
DespoDRAFT_03737	VRR-NUC domain-containing protein	1.758	0.24
DespoDRAFT_03738	hypothetical protein	-1.021	0.971
DespoDRAFT_03739	hypothetical protein	-1.434	0.0952
DespoDRAFT_03740	putative transcriptional regulator	-2.482	0.157
DespoDRAFT_03741	hypothetical protein	2.895	0.5
DespoDRAFT_03743	hypothetical protein	-1.544	0.628
DespoDRAFT_03744	hypothetical protein	-1.396	NaN
DespoDRAFT_03745	hypothetical protein	-1.908	0.662
DespoDRAFT_03746	hypothetical protein	1.582	0.61
DespoDRAFT_03747	hypothetical protein	-1.177	0.273
DespoDRAFT_03748	hypothetical protein	-1.765	0.111
DespoDRAFT_03749	hypothetical protein	-3.931	0.158
DespoDRAFT_03750	site-specific recombinase DNA invertase	-3.003	0.0958

	Pin		
DespoDRAFT_03751	hypothetical protein	-5.274	0.186
DespoDRAFT_03752	hypothetical protein	-2.172	0.258
DespoDRAFT_03753	hypothetical protein	-1.771	0.188
DespoDRAFT_03754	site-specific recombinase DNA invertase Pin	-2.162	0.0965
DespoDRAFT_03755	NAD(P)H-nitrite reductase	1.046	0.103
DespoDRAFT_03756	prephenate dehydrogenase	-1.159	0.445
DespoDRAFT_03757	response regulator with CheY-like receiver AAA-type ATPase and DNA-binding domains	-1.497	0.267
DespoDRAFT_03758	signal transduction histidine kinase	-1.108	0.744
DespoDRAFT_03759	hypothetical protein	-3.866	0.036
DespoDRAFT_03760	2-keto-4-pentenoate hydratase/2-oxohepta- 3-ene-1, 7-dioic acid hydratase	-1.212	0.199
DespoDRAFT_03761	hypothetical protein	-1.065	0.959
DespoDRAFT_03762	trypsin-like serine protease with C-terminal PDZ domain	-1.8	0.443
DespoDRAFT_03763	thiamine biosynthesis protein ThiF family 2	-1.994	0.0681
DespoDRAFT_03764	thiazole biosynthesis protein ThiH	-2.995	0.0888
DespoDRAFT_03765	putative enzyme of thiazole biosynthesis	-2.01	0.0982
DespoDRAFT_03766	thiamine biosynthesis protein ThiS	-2.079	0.0601
DespoDRAFT_03767	diaminopimelate epimerase	1.249	0.691
DespoDRAFT_03768	ribonuclease D	2.151	0.141
DespoDRAFT_03769	threonyl-tRNA synthetase	1.609	0.0835
DespoDRAFT_03770	metal-dependent hydrolase beta-lactamase superfamily II	1.152	0.447
DespoDRAFT_03771	Mg/Co/Ni transporter MgtE with CBS domain	-1.261	0.176
DespoDRAFT_03772	universal stress protein UspA-like protein	-1.204	0.214
DespoDRAFT_03773	hypothetical protein	-1.997	0.253

BIBLIOGRAPHY

1. **Lovley DR, Ueki T, Zhang T, Malvankar NS, Shrestha PM, Flanagan KA, Aklujkar M, Butler JE, Giloteaux L, Rotaru AE, Holmes DE, Franks AE, Orellana R, Risso C, Nevin KP.** 2011. *Geobacter*: the microbe electric's physiology, ecology, and practical applications. *Adv Microb Physiol* **59**:1-100.
2. **Williams KH, Bargar JR, Lloyd JR, Lovley DR.** 2012. Bioremediation of uranium-contaminated groundwater: a systems approach to subsurface biogeochemistry. *Curr Opin Biotech* **24**:1-9.
3. **Orellana R, Leavitt JJ, Comolli LR, Csencsits R, Janot N, Flanagan KA, Gray AS, Leang C, Izallalen M, Mester T, Lovley DR.** 2013. U(VI) Reduction by a Diversity of Outer Surface C-Type Cytochromes of *Geobacter sulfurreducens*. *Appl Environ Microbiol*.
4. **Wall JD, Krumholz LR.** 2006. Uranium reduction. *Annu Rev Microbiol* **60**:149-166.
5. **Bradford GR, Bakhtar D, Westcot D.** 1990. Uranium, Vanadium, and Molybdenum in Saline Waters of California. *J. Environ. Qual.* **19**:105-108.
6. **Shelobolina ES, Sullivan SA, O'Neill KR, Nevin KP, Lovley DR.** 2004. Isolation, Characterization, and U(VI)-Reducing Potential of a Facultatively Anaerobic, Acid-Resistant Bacterium from Low-pH, Nitrate- and U(VI)-Contaminated Subsurface Sediment and Description of *Salmonella subterranea* sp. nov. *Appl Environ Microb* **70**:2959-2965.
7. **Anderson RT, Vrionis HA, Ortiz-Bernad I, Resch CT, Long PE, Dayvault R, Karp K, Marutzky S, Metzler DR, Peacock A, White DC, Lowe M, Lovley DR.** 2003. Stimulating the in situ activity of *Geobacter* species to remove uranium from the groundwater of a uranium-contaminated aquifer. *Appl Environ Microb* **69**:5884-5891.
8. **Konhauser K.** 2007. Introduction to geomicrobiology. Blackwell Pub., Malden, MA.
9. **Lawrence Berkeley National Laboratory USDoEOoB, Environmental Research N, Accelerated Bioremediation Research P.** 1999. Bioremediation of metals and radionuclides : what it is and how ti works. [Lawrence Berkeley National Laboratory], [Berkeley, CA].
10. **Watanabe ME.** 2001. Can bioremediation bounce back? *Nat Biotech* **19**:1111-1115.
11. **Beyenal H, Sani RK, Peyton BM, Dohnalkova AC, Amonette JE, Lewandowski Z.** 2004. Uranium Immobilization by Sulfate-Reducing Biofilms. *Environ Sci Technol* **38**:2067-2074.
12. **Finneran KT, Anderson RT, Nevin KP, Lovley DR.** 2002. Potential for Bioremediation of Uranium-Contaminated Aquifers with Microbial U(VI) Reduction. *Soil and Sediment Contamination: An International Journal* **11**:339-357.
13. **Vishnivetskaya TA, Brandt CC, Madden AS, Drake MM, Kostka JE, Akob DM, Küsel K, Palumbo AV.** 2010. Microbial Community Changes in Response to Ethanol or Methanol Amendments for U(VI) Reduction. *Appl Environ Microb* **76**:5728-5735.

14. **Zhuang K, Ma E, Lovley DR, Mahadevan R.** 2012. The design of long-term effective uranium bioremediation strategy using a community metabolic model. *Biotechnology and Bioengineering* **109**:2475-2483.
15. **Francis A.** 2008. Microbial transformations of uranium in wastes and implication on its mobility, p. 713-722. *In* Merkel B, Hasche-Berger A (ed.), *Uranium, Mining and Hydrogeology*. Springer Berlin Heidelberg.
16. **Keith-Roach MJ, Livens FR.** 2002. Interactions of microorganisms with radionuclides. Elsevier, Amsterdam ; New York.
17. **Bargar JR, Bernier-Latmani R, Giammar DE, Tebo BM.** 2008. Biogenic Uraninite Nanoparticles and Their Importance for Uranium Remediation. *Elements* **4**:407-412.
18. **Lovley DR.** 2003. Cleaning up with genomics: Applying molecular biology to bioremediation. *Nat Rev Microbiol* **1**:35-44.
19. **Wilkins MJ, Livens FR, Vaughan DJ, Lloyd JR.** 2006. The impact of Fe(III)-reducing bacteria on uranium mobility. *Biogeochemistry* **78**:125-150.
20. **Lovley DR, Phillips EJP, Gorby YA, Landa ER.** 1991. Microbial Reduction of Uranium. *Nature* **350**:413-416.
21. **Tebo BM, Obraztsova AY.** 1998. Sulfate-reducing bacterium grows with Cr(VI), U(VI), Mn(IV), and Fe(III) as electron acceptors. *Fems Microbiol Lett* **162**:193-198.
22. **Sanford RA, Wu Q, Sung Y, Thomas SH, Amos BK, Prince EK, Löffler FE.** 2007. Hexavalent uranium supports growth of *Anaeromyxobacter dehalogenans* and *Geobacter* spp. with lower than predicted biomass yields. *Environmental Microbiology* **9**:2885-2893.
23. **Khijniak TV, Slobodkin AI, Coker V, Renshaw JC, Livens FR, Bonch-Osmolovskaya EA, Birkeland NK, Medvedeva-Lyalikova NN, Lloyd JR.** 2005. Reduction of uranium(VI) phosphate during growth of the thermophilic bacterium *Thermoterrabacterium ferrireducens*. *Appl Environ Microb* **71**:6423-6426.
24. **Francis AJ, Dodge CJ, Lu F, Halada GP, Clayton CR.** 1994. XPS and XANES Studies of Uranium Reduction by *Clostridium* sp. *Environ Sci Technol* **28**:636-639.
25. **Lovley DR, Phillips EJP.** 1992. Reduction of Uranium by *Desulfovibrio desulfuricans*. *Appl Environ Microb* **58**:850-856.
26. **Lovley DR, Roden EE, Phillips EJP, Woodward JC.** 1993. Enzymatic Iron and Uranium Reduction by Sulfate-Reducing Bacteria. *Mar Geol* **113**:41-53.
27. **Barton LL, Choudhury K, Thomson BM, Steenhoudt K, Groffman AR.** 1996. Bacterial reduction of soluble uranium: The first step of in situ immobilization of uranium. *Radioact Waste Manag* **20**:141-151.
28. **Payne RB, Gentry DA, Rapp-Giles BJ, Casalot L, Wall JD.** 2002. Uranium reduction by *Desulfovibrio desulfuricans* strain G20 and a cytochrome c3 mutant. *Appl Environ Microb* **68**:3129-3132.
29. **Lovley DR, Holmes DE, Nevin KP.** 2004. Dissimilatory Fe(III) and Mn(IV) reduction. *Adv Microb Physiol* **49**:219-286.
30. **Holmes DE, O'Neil RA, Vrionis HA, N'Guessan LA, Ortiz-Bernad I, Larrahondo MJ, Adams LA, Ward JA, Nicoll JS, Nevin KP, Chavan MA,**

- Johnson JP, Long PE, Lovley DR.** 2007. Subsurface clade of Geobacteraceae that predominates in a diversity of Fe(III)-reducing subsurface environments. *ISME J* **1**:663-677.
31. **Snoeyenbos-West OL, Nevin KP, Anderson RT, Lovley DR.** 2000. Enrichment of Geobacter Species in Response to Stimulation of Fe(III) Reduction in Sandy Aquifer Sediments. *Microb Ecol* **39**:153-167.
32. **Coppi MV, Leang C, Sandler SJ, Lovley DR.** 2001. Development of a genetic system for *Geobacter sulfurreducens*. *Appl Environ Microb* **67**:3180-3187.
33. **Methe BA, Webster J, Nevin K, Butler J, Lovley DR.** 2005. DNA microarray analysis of nitrogen fixation and Fe(III) reduction in *Geobacter sulfurreducens*. *Appl Environ Microb* **71**:2530-2538.
34. **Aklujkar M, Coppi MV, Leang C, Kim B-C, Chavan MA, Perpetua LA, Giloteaux L, Liu A, Holmes D.** 2013. Proteins involved in electron transfer to Fe(III) and Mn(IV) oxides by *Geobacter sulfurreducens* and *Geobacter uraniireducens*. *Microbiology*.
35. **Shrestha PM, Rotaru A-E, Summers ZM, Shrestha M, Liu F, Lovley DR.** 2013. Transcriptomic and genetic analysis of direct interspecies electron transfer. *Appl Environ Microb*.
36. **Rotaru A-E, Shrestha PM, Liu F, Ueki T, Nevin K, Summers ZM, Lovley DR.** 2012. Interspecies electron transfer via H₂ and formate rather than direct electrical connections in co-cultures of *Pelobacter carbinolicus* and *Geobacter sulfurreducens*. *Appl Environ Microb*.
37. **Strycharz SM, Glaven RH, Coppi MV, Gannon SM, Perpetua LA, Liu A, Nevin KP, Lovley DR.** 2011. Gene expression and deletion analysis of mechanisms for electron transfer from electrodes to *Geobacter sulfurreducens*. *Bioelectrochemistry* **80**:142-150.
38. **Qiu Y, Cho BK, Park YS, Lovley D, Palsson BO, Zengler K.** 2010. Structural and operational complexity of the *Geobacter sulfurreducens* genome. *Genome research* **20**:1304-1311.
39. **Krushkal J, Juarez K, Barbe JF, Qu Y, Andrade A, Puljic M, Adkins RM, Lovley DR, Ueki T.** 2010. Genome-wide survey for PilR recognition sites of the metal-reducing prokaryote *Geobacter sulfurreducens*. *Gene* **469**:31-44.
40. **Juárez K, Byoung-Chan K, Nevin K, Olvera L, Reguera G, Lovley DR, Methé BA.** 2009. PilR, a Transcriptional Regulator for Pilin and Other Genes Required for Fe(III) Reduction in *Geobacter sulfurreducens*. *Journal of Molecular Microbiology & Biotechnology* **16**:146-158.
41. **Leang C, Krushkal J, Ueki T, Puljic M, Sun J, Juarez K, Nunez C, Reguera G, DiDonato R, Postier B, Adkins RM, Lovley DR.** 2009. Genome-wide analysis of the RpoN regulon in *Geobacter sulfurreducens*. *Bmc Genomics* **10**.
42. **Ding YHR, Hixson KK, Aklujkar MA, Lipton MS, Smith RD, Lovley DR, Mester T.** 2008. Proteome of *Geobacter sulfurreducens* grown with Fe(III) oxide or Fe(III) citrate as the electron acceptor. *Bba-Proteins Proteom* **1784**:1935-1941.
43. **Mahadevan R, Yan B, Postier B, Nevin KP, Woodard TL, O'Neil R, Coppi MV, Methe BA, Krushkal J.** 2008. Characterizing regulation of metabolism in *Geobacter sulfurreducens* through genome-wide expression data and sequence analysis. *Omics* **12**:33-+.

44. **Izallalen M, Mahadevan R, Burgard A, Postier B, Didonato R, Sun J, Schilling CH, Lovley DR.** 2008. *Geobacter sulfurreducens* strain engineered for increased rates of respiration. *Metab Eng* **10**:267-275.
45. **Kim BC, Postier BL, DiDonato RJ, Chaudhuri SK, Nevin KP, Lovley DR.** 2008. Insights into genes involved in electricity generation in *Geobacter sulfurreducens* via whole genome microarray analysis of the OmcF-deficient mutant. *Bioelectrochemistry* **73**:70-75.
46. **Yan B, Lovley DR, Krushkal J.** 2007. Genome-wide similarity search for transcription factors and their binding sites in a metal-reducing prokaryote *Geobacter sulfurreducens*. *Biosystems* **90**:421-441.
47. **Krushkal J, Yan B, DiDonato L, Puljic M, Nevin K, Woodard T, Adkins R, Methé B, Lovley D.** 2007. Genome-wide expression profiling in *Geobacter sulfurreducens*: identification of Fur and RpoS transcription regulatory sites in a rel Gsu mutant. *Funct Integr Genomics* **7**:229-255.
48. **Holmes DE, Chaudhuri SK, Nevin KP, Mehta T, Methe BA, Liu A, Ward JE, Woodard TL, Webster J, Lovley DR.** 2006. Microarray and genetic analysis of electron transfer to electrodes in *Geobacter sulfurreducens*. *Environmental Microbiology* **8**:1805-1815.
49. **Ding YHR, Hixson KK, Giometti CS, Stanley A, Esteve-Nunez A, Khare T, Tollaksen SL, Zhu WH, Adkins JN, Lipton MS, Smith RD, Mester T, Lovley DR.** 2006. The proteome of dissimilatory metal-reducing microorganism *Geobacter sulfurreducens* under various growth conditions. *Bba-Proteins Proteom* **1764**:1198-1206.
50. **Nunez C, Esteve-Nunez A, Giometti C, Tollaksen S, Khare T, Lin W, Lovley DR, Methe BA.** 2006. DNA microarray and proteomic analyses of the RpoS regulon in *Geobacter sulfurreducens*. *J Bacteriol* **188**:2792-2800.
51. **Krushkal J, Puljic M, Bin Y, Barbe JF, Mahadevan R, Postier B, O'Neil RA, Reguera G, Ching L, DiDonato LN, Nunez C, Methe BA, Adkins RM, Lovley DR.** 2008. Genome Regions Involved in Multiple Regulatory Pathways Identified Using GSEL, A Genome-Wide Database of Regulatory Sequence Elements of *Geobacter sulfurreducens*, p. 424-431.
52. **Shelobolina ES, Coppi MV, Korenevsky AA, DiDonato LN, Sullivan SA, Konishi H, Xu HF, Leang C, Butler JE, Kim BC, Lovley DR.** 2007. Importance of c-type cytochromes for U(VI) reduction by *Geobacter sulfurreducens*. *BMC Microbiology* **7**:7-16.
53. **Lovley DR.** 1993. Dissimilatory metal reduction. *Annu Rev Microbiol* **47**:263-290.
54. **Lloyd JR, Leang C, Hodges Myerson AL, Coppi MV, Cuifo S, Methe B, Sandler SJ, Lovley DR.** 2003. Biochemical and genetic characterization of PpcA, a periplasmic c-type cytochrome in *Geobacter sulfurreducens*. *Biochem J* **369**:153-161.
55. **Marshall MJ, Beliaev AS, Dohnalkova AC, Kennedy DW, Shi L, Wang Z, Boyanov MI, Lai B, Kemner KM, McLean JS, Reed SB, Culley DE, Bailey VL, Simonson CJ, Saffarini DA, Romine MF, Zachara JM, Fredrickson JK.** 2006. c-Type Cytochrome-Dependent Formation of U(IV) Nanoparticles by *Shewanella oneidensis*. *PLoS Biol* **4**:e268.

56. **Payne RB, Casalot L, Rivere T, Terry JH, Larsen L, Giles BJ, Wall JD.** 2004. Interaction between uranium and the cytochrome *c3* of *Desulfovibrio desulfuricans* strain G20. *Arch Microbiol* **181**:398-406.
57. **Wade Jr R, DiChristina TJ.** 2000. Isolation of U(VI) reduction-deficient mutants of *Shewanella putrefaciens*. *Fems Microbiol Lett* **184**:143-148.
58. **Reguera G, McCarthy KD, Mehta T, Nicoll JS, Tuominen MT, Lovley DR.** 2005. Extracellular electron transfer via microbial nanowires. *Nature* **435**:1098-1101.
59. **Malvankar NS, Vargas M, Nevin KP, Franks AE, Leang C, Kim BC, Inoue K, Mester T, Covalla SF, Johnson JP, Rotello VM, Tuominen MT, Lovley DR.** 2011. Tunable metallic-like conductivity in microbial nanowire networks. *Nature Nanotechnology* **6**:573-579.
60. **Cologgi DL, Lampa-Pastirk S, Speers AM, Kelly SD, Reguera G.** 2011. Extracellular reduction of uranium via *Geobacter* conductive pili as a protective cellular mechanism. *Proceedings of the National Academy of Sciences of the United States of America* **108**:15248-15252.
61. **Reguera G.** 2012. Electron transfer at the cell-uranium interface in *Geobacter* spp. *Biochemical Society transactions* **40**:1227-1232.
62. **Voordeckers JW, Kim BC, Izallalen M, Lovley DR.** 2010. Role of *Geobacter sulfurreducens* Outer Surface *c*-Type Cytochromes in Reduction of Soil Humic Acid and Anthraquinone-2,6-Disulfonate. *Appl Environ Microbiol* **76**:2371-2375.
63. **Gralnick JA, Newman DK.** 2007. Extracellular respiration. *Mol Microbiol* **65**:1-11.
64. **Lovley DR.** 2006. Bug juice: harvesting electricity with microorganisms. *Nat Rev Microbiol* **4**:497-508.
65. **Coppi MV, O'Neil RA, Leang C, Kaufmann F, Methe BA, Nevin KP, Woodard TL, Liu A, Lovley DR.** 2007. Involvement of *Geobacter sulfurreducens* SfrAB in acetate metabolism rather than intracellular, respiration-linked Fe(III) citrate reduction. *Microbiol-Sgm* **153**:3572-3585.
66. **Schnug E, Haneklaus S.** 2008. Dispersion of uranium in the environment by fertilization, p. 45-52. *In* Merkel B, Hasche-Berger A (ed.), *Uranium, Mining and Hydrogeology*. Springer Berlin Heidelberg.
67. **Hu P, Brodie EL, Suzuki Y, McAdams HH, Andersen GL.** 2005. Whole-genome transcriptional analysis of heavy metal stresses in *Caulobacter crescentus*. *J Bacteriol* **187**:8437-8449.
68. **Bencheikh-Latmani R, Williams SM, Haucke L, Criddle CS, Wu LY, Zhou JZ, Tebo BM.** 2005. Global transcriptional profiling of *Shewanella oneidensis* MR-1 during Cr(VI) and U(VI) reduction. *Appl Environ Microb* **71**:7453-7460.
69. **Nies DH, Silver S.** 1995. Ion Efflux Systems Involved in Bacterial Metal Resistances. *J Ind Microbiol* **14**:186-199.
70. **Canovas D, Cases I, de Lorenzo V.** 2003. Heavy metal tolerance and metal homeostasis in *Pseudomonas putida* as revealed by complete genome analysis. *Environmental Microbiology* **5**:1242-1256.
71. **Van Horn JD, Huang H.** 2006. Uranium(VI) bio-coordination chemistry from biochemical, solution and protein structural data. *Coordin Chem Rev* **250**:765-775.

72. **Nies DH.** 1999. Microbial heavy-metal resistance. *Appl Microbiol Biot* **51**:730-750.
73. **Snoeyenbos-West O, Van Praagh CG, Lovley DR.** 2001. *Trichlorobacter thiogenes* Should Be Renamed as a *Geobacter* Species. *Appl Environ Microb* **67**:1020-1022.
74. **Holmes DE, Finneran KT, O'Neil RA, Lovley DR.** 2002. Enrichment of Members of the Family *Geobacteraceae* Associated with Stimulation of Dissimilatory Metal Reduction in Uranium-Contaminated Aquifer Sediments. *Appl Environ Microb* **68**:2300-2306.
75. **Vrionis HA, Anderson RT, Ortiz-Bernad I, O'Neill KR, Resch CT, Peacock AD, Dayvault R, White DC, Long PE, Lovley DR.** 2005. Microbiological and Geochemical Heterogeneity in an In Situ Uranium Bioremediation Field Site. *Appl Environ Microb* **71**:6308-6318.
76. **Holmes DE, Nevin KP, O'Neil RA, Ward JE, Adams LA, Woodard TL, Vrionis HA, Lovley DR.** 2005. Potential for Quantifying Expression of the *Geobacteraceae* Citrate Synthase Gene To Assess the Activity of *Geobacteraceae* in the Subsurface and on Current-Harvesting Electrodes. *Appl Environ Microb* **71**:6870-6877.
77. **Ortiz-Bernad I, Anderson RT, Vrionis HA, Lovley DR.** 2004. Resistance of Solid-Phase U(VI) to Microbial Reduction during In Situ Bioremediation of Uranium-Contaminated Groundwater. *Appl Environ Microb* **70**:7558-7560.
78. **Miletto M, Williams KH, N'Guessan AL, Lovley DR.** 2011. Molecular Analysis of the Metabolic Rates of Discrete Subsurface Populations of Sulfate Reducers. *Appl Environ Microb* **77**:6502-6509.
79. **Chapelle FH, Lovley DR.** 1992. Competitive-Exclusion of Sulfate Reduction by Fe(II)-Reducing Bacteria - a Mechanism for Producing Discrete Zones of High-Iron Ground-Water. *Ground Water* **30**:29-36.
80. **Barlett M, Moon HS, Peacock AA, Hedrick DB, Williams KH, Long PE, Lovley D, Jaffe PR.** 2012. Uranium reduction and microbial community development in response to stimulation with different electron donors. *Biodegradation* **23**:535-546.
81. **Handley KM, VerBerkmoes NC, Steefel CI, Williams KH, Sharon I, Miller CS, Frischkorn KR, Chourey K, Thomas BC, Shah MB, Long PE, Hettich RL, Banfield JF.** 2013. Biostimulation induces syntrophic interactions that impact C, S and N cycling in a sediment microbial community. *Isme Journal* **7**:800-816.
82. **Handley KM, Wrighton KC, Piceno YM, Andersen GL, DeSantis TZ, Williams KH, Wilkins MJ, N'Guessan AL, Peacock A, Bargar J, Long PE, Banfield JF.** 2012. High-density PhyloChip profiling of stimulated aquifer microbial communities reveals a complex response to acetate amendment. *Fems Microbiol Ecol* **81**:188-204.
83. **Methé BA, Nelson KE, Eisen JA, Paulsen IT, Nelson W, Heidelberg JF, Wu D, Wu M, Ward N, Beanan MJ, Dodson RJ, Madupu R, Brinkac LM, Daugherty SC, DeBoy RT, Durkin AS, Gwinn M, Kolonay JF, Sullivan SA, Haft DH, Selengut J, Davidsen TM, Zafar N, White O, Tran B, Romero C, Forberger HA, Weidman J, Khouri H, Feldblyum TV, Utterback TR, Van**

- Aken SE, Lovley DR, Fraser CM.** 2003. Genome of *Geobacter sulfurreducens*: Metal Reduction in Subsurface Environments. *Science* **302**:1967-1969.
84. **Smith JA, Lovley DR, Tremblay P-L.** 2013. Outer Cell Surface Components Essential for Fe(III) Oxide Reduction by *Geobacter metallireducens*. *Appl Environ Microbiol* **79**:901-907.
85. **Summers ZM, Fogarty HE, Leang C, Franks AE, Malvankar NS, Lovley DR.** 2010. Direct Exchange of Electrons Within Aggregates of an Evolved Syntrophic Coculture of Anaerobic Bacteria. *Science* **330**:1413-1415.
86. **Reguera G, Nevin KP, Nicoll JS, Covalla SF, Woodard TL, Lovley DR.** 2006. Biofilm and Nanowire Production Leads to Increased Current in *Geobacter sulfurreducens* Fuel Cells. *Appl Environ Microbiol* **72**:7345-7348.
87. **Nevin KP, Kim BC, Glaven RH, Johnson JP, Woodard TL, Methe BA, DiDonato RJ, Covalla SF, Franks AE, Liu A, Lovley DR.** 2009. Anode Biofilm Transcriptomics Reveals Outer Surface Components Essential for High Density Current Production in *Geobacter sulfurreducens* Fuel Cells. *PLoS One* **4**:e5628.
88. **Vargas M, Malvankar NS, Tremblay P-L, Leang C, Smith JA, Patel P, Synoeyenbos-West O, Nevin KP, Lovley DR.** 2013. Aromatic Amino Acids Required for Pili Conductivity and Long-Range Extracellular Electron Transport in *Geobacter sulfurreducens*. *mBio* **4**:e00210-00213.
89. **Mehta T, Coppi MV, Childers SE, Lovley DR.** 2005. Outer membrane *c*-type cytochromes required for Fe(III) and Mn(IV) oxide reduction in *Geobacter sulfurreducens*. *Appl Environ Microbiol* **71**:8634-8641.
90. **Leang C, Qian XL, Mester T, Lovley DR.** 2010. Alignment of the *c*-Type Cytochrome OmcS along Pili of *Geobacter sulfurreducens*. *Appl Environ Microbiol* **76**:4080-4084.
91. **Lovley DR.** 2011. Live wires: direct extracellular electron exchange for bioenergy and the bioremediation of energy-related contamination. *Energ Environ Sci* **4**:4896-4906.
92. **Lovley DR.** 2012. Long-range electron transport to Fe(III) oxide via pili with metallic-like conductivity. *Biochem. Soc. Trans* **40**:1186-1190.
93. **Inoue K, Qian XL, Morgado L, Kim BC, Mester T, Izallalen M, Salgueiro CA, Lovley DR.** 2010. Purification and Characterization of OmcZ, an Outer-Surface, Octaheme *c*-Type Cytochrome Essential for Optimal Current Production by *Geobacter sulfurreducens*. *Appl Environ Microbiol* **76**:3999-4007.
94. **Inoue K, Leang C, Franks AE, Woodard TL, Nevin KP, Lovley DR.** 2011. Specific localization of the *c*-type cytochrome OmcZ at the anode surface in current-producing biofilms of *Geobacter sulfurreducens*. *Environmental Microbiology Reports* **3**:211-217.
95. **Qian XL, Reguera G, Mester T, Lovley DR.** 2007. Evidence that OmcB and OmpB of *Geobacter sulfurreducens* are outer membrane surface proteins. *Fems Microbiol Lett* **277**:21-27.
96. **Leang C, Coppi MV, Lovley DR.** 2003. OmcB, a *c*-type polyheme cytochrome, involved in Fe(III) reduction in *Geobacter sulfurreducens*. *J Bacteriol* **185**:2096-2103.

97. **Leang C, Adams LA, Chin KJ, Nevin KP, Methe BA, Webster J, Sharma ML, Lovley DR.** 2005. Adaptation to disruption of the electron transfer pathway for Fe(III) reduction in *Geobacter sulfurreducens*. *J Bacteriol* **187**:5918-5926.
98. **Qian XL, Mester T, Morgado L, Arakawa T, Sharma ML, Inoue K, Joseph C, Salgueiro CA, Maroney MJ, Lovley DR.** 2011. Biochemical characterization of purified OmcS, a *c*-type cytochrome required for insoluble Fe(III) reduction in *Geobacter sulfurreducens*. *Biochimica Et Biophysica Acta-Bioenergetics* **1807**:404-412.
99. **Lovley DR, Widman PK, Woodward JC, Phillips EJP.** 1993. Reduction of Uranium by Cytochrome *c*3 of *Desulfovibrio vulgaris*. *Appl Environ Microbiol* **59**:3572-3576.
100. **Comolli LR, Duarte R, Baum D, Luef B, Downing KH, Larson DM, Csencsits R, Banfield JF.** 2012. A portable cryo-plunger for on-site intact cryogenic microscopy sample preparation in natural environments. *Microsc Res Tech* **75**:829-836.
101. **Downing KH, Mooney PE.** 2008. A charge coupled device camera with electron decelerator for intermediate voltage electron microscopy. *Rev Sci Instrum* **79**:043702-043710
102. **Kremer JR, Mastronarde DN, McIntosh JR.** 1996. Computer visualization of three-dimensional image data using IMOD. *Journal of Structural Biology* **116**:71-76.
103. **Ravel B, Newville M.** 2005. Athena, Artemis, Hephaestus: Data Analysis for X-Ray Absorption Spectroscopy Using Ifeffit. *Journal of Synchrotron Radiation* **12**:537-541.
104. **Holmes DE, O'Neil RA, Chavan MA, N'Guessan LA, Vrionis HA, Perpetua LA, Larrahondo MJ, DiDonato R, Liu A, Lovley DR.** 2009. Transcriptome of *Geobacter uraniireducens* growing in uranium-contaminated subsurface sediments. *ISME J* **3**:216-230.
105. **Converse BJ, Wu T, Findlay RH, Roden EE.** 2013. U(VI) reduction in sulfate-reducing subsurface sediments amended with ethanol or acetate. *Appl Environ Microbiol* **79**:4173-4177.
106. **Newsome L, Morris K, Lloyd JR.** 2014. The biogeochemistry and bioremediation of uranium and other priority radionuclides. *Chemical Geology* **363**:164-184.
107. **Mahadevan R, Palsson BØ, Lovley DR.** 2011. *In situ* to *in silico* and back: elucidating the physiology and ecology of *Geobacter* spp. using genome-scale modelling. *Nat Rev Micro* **9**:39-50.
108. **Nies DH.** 2013. RND-efflux pumps for metal cations. Norwich: Horizon Scientific Press Ltd.
109. **Tran HT.** 2009. Investigation of chemotaxis genes and their functions in *Geobacter* species, p. xiii, 143 p. University of Massachusetts Amherst, Amherst, Mass.
110. **Caccavo F, Lonergan DJ, Lovley DR, Davis M, Stolz JF, Mcinerney MJ.** 1994. *Geobacter sulfurreducens* sp. nov., a Hydrogen-Oxidizing and Acetate-Oxidizing Dissimilatory Metal-Reducing Microorganism. *Appl Environ Microbiol* **60**:3752-3759.

111. **Eng JK, McCormack AL, Yates JR.** 1994. An Approach to Correlate Tandem Mass-Spectral Data of Peptides with Amino-Acid-Sequences in a Protein Database. *J Am Soc Mass Spectr* **5**:976-989.
112. **Mehta T, Childers SE, Glaven R, Lovley DR, Mester T.** 2006. A putative multicopper protein secreted by an atypical type II secretion system involved in the reduction of insoluble electron acceptors in *Geobacter sulfurreducens*. *Microbiology* **152**:2257-2264.
113. **Harkewicz R, Belov ME, Anderson GA, Pasa-Tolic L, Masselon CD, Prior DC, Udseth HR, Smith RD.** 2002. ESI-FTICR mass spectrometry employing data-dependent external ion selection and accumulation. *J Am Soc Mass Spectr* **13**:144-154.
114. **Lipton MS, Pasa-Tolic L, Anderson GA, Anderson DJ, Auberry DL, Battista KR, Daly MJ, Fredrickson J, Hixson KK, Kostandarithes H, Masselon C, Markillie LM, Moore RJ, Romine MF, Shen YF, Stritmatter E, Tolic N, Udseth HR, Venkateswaran A, Wong LK, Zhao R, Smith RD.** 2002. Global analysis of the *Deinococcus radiodurans* proteome by using accurate mass tags. *Proceedings of the National Academy of Sciences of the United States of America* **99**:11049-11054.
115. **Lovley DR, Phillips EJP.** 1988. Novel mode of microbial energy metabolism: organic carbon oxidation coupled to dissimilatory reduction of iron or manganese. *Appl Environ Microbiol* **54**:1472-1480.
116. **Yun J, Ueki T, Miletto M, Lovley DR.** 2011. Monitoring the Metabolic Status of *Geobacter* Species in Contaminated Groundwater by Quantifying Key Metabolic Proteins with *Geobacter*-Specific Antibodies. *Appl Environ Microbiol* **77**:4597-4602.
117. **Wilkins MJ, Callister SJ, Miletto M, Williams KH, Nicora CD, Lovley DR, Long PE, Lipton MS.** 2011. Development of a biomarker for *Geobacter* activity and strain composition; Proteogenomic analysis of the citrate synthase protein during bioremediation of U(VI). *Microb Biotechnol* **4**:55-63.
118. **Mahadevan R, Bond DR, Butler JE, Esteve-Nuñez A, Coppi MV, Palsson BO, Schilling CH, Lovley DR.** 2006. Characterization of Metabolism in the Fe(III)-Reducing Organism *Geobacter sulfurreducens* by Constraint-Based Modeling. *Appl Environ Microbiol* **72**:1558-1568.
119. **Maezato Y, Blum P.** 2012. Survival of the Fittest: Overcoming Oxidative Stress at the Extremes of Acid, Heat and Metal. *Life* **2**:229-242.
120. **Gray C.** 1994. Electron Microscopy of Protein-Nucleic Acid Complexes, p. 347-356. *In* Geoff Kneale G (ed.), *DNA-Protein Interactions*, vol. 30. Humana Press.
121. **Yazzie M, Gamble SL, Civitello ER, Stearns DM.** 2003. Uranyl acetate causes DNA single strand breaks in vitro in the presence of ascorbate (vitamin C). *Chem Res Toxicol* **16**:524-530.
122. **Mallika G, Barry R.** 2002. *Microbial Resistance Mechanisms for Heavy Metals and Metalloids*, Heavy Metals In The Environment. CRC Press.
123. **Zobel CR, Beer M.** 1961. Electron stains. I. Chemical studies on the interaction of DNA with uranyl salts. *J Biophys Biochem Cytol* **10**:335-346.
124. **Hartsock WJ, Cohen JD, Segal DJ.** 2007. Uranyl acetate as a direct inhibitor of DNA-binding proteins. *Chem Res Toxicol* **20**:784-789.

125. **Matsuda E, Nakajima A.** 2012. Effect of catechins and tannins on depleted uranium-induced DNA strand breaks. *Journal of Radioanalytical and Nuclear Chemistry* **293**:711-714.
126. **Kim EH, Nies DH, McEvoy MM, Rensing C.** 2011. Switch or Funnel: How RND-Type Transport Systems Control Periplasmic Metal Homeostasis. *J Bacteriol* **193**:2381-2387.
127. **Lloyd JR, Lovley DR.** 2001. Microbial detoxification of metals and radionuclides. *Curr Opin Biotech* **12**:248-253.
128. **Gadd GM.** 2010. Metals, minerals and microbes: geomicrobiology and bioremediation. *Microbiology* **156**:609-643.
129. **Merroun ML, Selenska-Pobell S.** 2008. Bacterial interactions with uranium: An environmental perspective. *J Contam Hydrol* **102**:285-295.
130. **Lin WC, Coppi MV, Lovley DR.** 2004. *Geobacter sulfurreducens* Can Grow with Oxygen as a Terminal Electron Acceptor. *Appl Environ Microbiol* **70**:2525-2528.
131. **Geslin C, Llanos J, Prieur D, Jeanthon C.** 2001. The manganese and iron superoxide dismutases protect *Escherichia coli* from heavy metal toxicity. *Res Microbiol* **152**:901-905.
132. **Privalle CT, Fridovich I.** 1987. Induction of Superoxide Dismutase in *Escherichia coli* by Heat Shock. *Proceedings of the National Academy of Sciences of the United States of America* **84**:2723-2726.
133. **Bernhardt J, Volker U, Volker A, Antelmann H, Schmid R, Mach H, Hecker M.** 1997. Specific and general stress proteins in *Bacillus subtilis* - A two-dimensional protein electrophoresis study. *Microbiology* **143**:999-1017.
134. **Chourey K, Thompson MR, Morrell-Falvey J, VerBerkmoes NC, Brown SD, Shah M, Zhou JZ, Doktycz M, Hettich RL, Thompson DK.** 2006. Global molecular and morphological effects of 24-hour chromium(VI) exposure on *Shewanella oneidensis* MR-1. *Appl Environ Microbiol* **72**:6331-6344.
135. **Roux M, Coves J.** 2002. The iron-containing superoxide dismutase of *Ralstonia metallidurans* CH34. *Fems Microbiol Lett* **210**:129-133.
136. **Pourahmad J, Ghashang M, Ettehadi HA, Ghalandari R.** 2006. A search for cellular and molecular mechanisms involved in depleted uranium (DU) toxicity. *Environmental Toxicology* **21**:349-354.
137. **Smirnova GV, Oktyabrsky ON.** 2005. Glutathione in Bacteria. *Biochemistry (Moscow)* **70**:1199-1211.
138. **Farr SB, Kogoma T.** 1991. Oxidative Stress Responses in *Escherichia coli* and *Salmonella typhimurium*. *Microbiol Rev* **55**:561-585.
139. **Mouser PJ, Holmes DE, Perpetua LA, DiDonato R, Postier B, Liu A, Lovley DR.** 2009. Quantifying expression of *Geobacter* spp. oxidative stress genes in pure culture and during *in situ* uranium bioremediation. *ISME J* **3**:454-465.
140. **Shelobolina ES, Vrionis HA, Findlay RH, Lovley DR.** 2008. *Geobacter uraniireducens* sp. nov., isolated from subsurface sediment undergoing uranium bioremediation. *International Journal of Systematic and Evolutionary Microbiology* **58**:1075-1078.
141. **Thauer RK, Mollerzinkhan D, Spormann AM.** 1989. Biochemistry of acetate catabolism in anaerobic chemotrophic bacteria. *Annu Rev Microbiol* **43**:43-67.

142. **Mussmann M, Richter M, Lombardot T, Meyerdierks A, Kuever J, Kube M, Glöckner FO, Amann R.** 2005. Clustered Genes Related to Sulfate Respiration in Uncultured Prokaryotes Support the Theory of Their Concomitant Horizontal Transfer. *J Bacteriol* **187**:7126-7137.
143. **Muyzer G, Stams AJM.** 2008. The *ecology* and biotechnology of sulphate-reducing bacteria. *Nat Rev Micro* **6**:441-454.
144. **Hao OJ, Chen JM, Huang L, Buglass RL.** 1996. Sulfate reducing bacteria. *Critical Reviews in Environmental Science and Technology* **26**:155-187.
145. **Jorgensen BB.** 1982. Mineralization of Organic-Matter in the Sea Bed - the Role of Sulfate Reduction. *Nature* **296**:643-645.
146. **Chapelle FH, McMahan PB.** 1991. Geochemistry of Dissolved Inorganic Carbon in a Coastal-Plain Aquifer .1. Sulfate from Confining Beds as an Oxidant in Microbial Co-2 Production. *J Hydrol* **127**:85-108.
147. **Brown CJ, Coates JD, Schoonen MAA.** 1999. Localized sulfate-reducing zones in a coastal plain aquifer. *Ground Water* **37**:505-516.
148. **Goevert D, Conrad R.** 2010. Stable carbon isotope fractionation by acetotrophic sulfur-reducing bacteria. *Fems Microbiol Ecol* **71**:218-225.
149. **Thauer RK, Postgate JR.** 1982. Dissimilatory Sulfate Reduction with Acetate as Electron-Donor. *Philos T Roy Soc B* **298**:467-&.
150. **Fenchel TM, Jørgensen BB.** 1977. Detritus Food Chains of Aquatic Ecosystems: The Role of Bacteria, p. 1-58. *In* Alexander M (ed.), *Advances in Microbial Ecology*, vol. 1. Springer US.
151. **Widdel F, Pfennig N.** 1981. Studies on dissimilatory sulfate-reducing bacteria that decompose fatty acids. *Arch. Microbiol.* **129**:395-400.
152. **Thauer RK.** 1988. Citric-acid cycle, 50 years on. *European Journal of Biochemistry* **176**:497-508.
153. **Möller D, Schauder R, Fuchs G, Thauer RK.** 1987. Acetate oxidation to CO₂ via a citric acid cycle involving an ATP Citrate lyase - a mechanism for the synthesis of ATP via substrate level phosphorylation in *Desulfobacter postgatei* growing on acetate and sulfate. *Arch. Microbiol.* **148**:202-207.
154. **Ingvorsen K, Zehnder AJ, Jørgensen BB.** 1984. Kinetics of sulfate and acetate uptake by *Desulfobacter postgatei*. *Appl Environ Microbiol* **47**:403-408.
155. **Pires RH, Venceslau SS, Morais F, Teixeira M, Xavier AV, Pereira IAC.** 2006. Characterization of the *Desulfovibrio desulfuricans* ATCC 27774 DsrMKJOP complex - A membrane-bound redox complex involved in the sulfate respiratory pathway. *Biochemistry* **45**:249-262.
156. **Meyer B, Kuehl J, Deutschbauer AM, Price MN, Arkin AP, Stahl DA.** 2013. Variation among *Desulfovibrio* Species in Electron Transfer Systems Used for Syntrophic Growth. *J Bacteriol* **195**:990-1004.
157. **Venceslau SS, Cort JR, Baker ES, Chu RK, Robinson EW, Dahl C, Saraiva LM, Pereira IAC.** 2013. Redox states of *Desulfovibrio vulgaris* DsrC, a key protein in dissimilatory sulfite reduction. *Biochem Bioph Res Co* **441**:732-736.
158. **Keller KL, Bender KS, Wall JD.** 2009. Development of a Markerless Genetic Exchange System for *Desulfovibrio vulgaris* Hildenborough and Its Use in Generating a Strain with Increased Transformation Efficiency. *Appl Environ Microbiol* **75**:7682-7691.

159. **Meyer B, Kuehl JV, Price MN, Ray J, Deutschbauer AM, Arkin AP, Stahl DA.** 2014. The energy-conserving electron transfer system used by *Desulfovibrio alaskensis* strain G20 during pyruvate fermentation involves reduction of endogenously formed fumarate and cytoplasmic and membrane-bound complexes, Hdr-Flox and Rnf. *Environmental Microbiology*:n/a-n/a.
160. **Oliveira TF, Vorrhein C, Matias PM, Venceslau SS, Pereira IAC, Archer M.** 2008. The Crystal Structure of *Desulfovibrio vulgaris* Dissimilatory Sulfite Reductase Bound to DsrC Provides Novel Insights into the Mechanism of Sulfate Respiration. *J. Biol. Chem.* **283**:34141-34149.
161. **Venceslau SS, Lino RR, Pereira IAC.** 2010. The Qrc Membrane Complex, Related to the Alternative Complex III, Is a Menaquinone Reductase Involved in Sulfate Respiration. *J. Biol. Chem.* **285**:22774-22783.
162. **Keller KL, Wall JD.** 2011. Genetics and molecular biology of the electron flow for sulfate respiration in *Desulfovibrio*. *Front Microbiol* **2**.
163. **Pereira IAC, Ramos AR, Grein F, Marques MC, da Silva SM, Venceslau SS.** 2011. A comparative genomic analysis of energy metabolism in sulfate reducing bacteria and archaea. *Front Microbiol* **2**.
164. **Ramos AR, Keller KL, Wall JD, Pereira IAC.** 2012. The membrane QmoABC complex interacts directly with the dissimilatory adenosine 5'-phosphosulfate reductase sulfate reducing bacteria. *Front Microbiol* **3**.
165. **Venceslau SS, Stockdreher Y, Dahl C, Pereira IAC.** 2014. The “bacterial heterodisulfide” DsrC is a key protein in dissimilatory sulfur metabolism. *Biochimica et Biophysica Acta (BBA) - Bioenergetics*.
166. **Grein F, Ramos AR, Venceslau SS, Pereira IAC.** 2013. Unifying concepts in anaerobic respiration: Insights from dissimilatory sulfur metabolism. *Biochimica Et Biophysica Acta-Bioenergetics* **1827**:145-160.
167. **Sun J, Sayyar B, Butler JE, Pharkya P, Fahland TR, Famili I, Schilling CH, Lovley DR, Mahadevan R.** 2009. Genome-scale constraint-based modeling of *Geobacter metallireducens*. *Bmc Syst Biol* **3**.
168. **Sun J, Haveman SA, Bui O, Fahland TR, Lovley DR.** 2010. Constraint-based modeling analysis of the metabolism of two *Pelobacter* species. *Bmc Syst Biol* **4**.
169. **Risso C, Sun J, Zhuang K, Mahadevan R, Deboy R, Ismail W, Shrivastava S, Huot H, Kothari S, Daugherty S, Bui O, Schilling CH, Lovley DR, Methe BA.** 2009. Genome-scale comparison and constraint-based metabolic reconstruction of the facultative anaerobic Fe(III)-reducer *Rhodoferrax ferrireducens*. *Bmc Genomics* **10**.
170. **Zhuang K, Izallalen M, Mouser P, Richter H, Risso C, Mahadevan R, Lovley DR.** 2011. Genome-scale dynamic modeling of the competition between *Rhodoferrax* and *Geobacter* in anoxic subsurface environments. *Isme Journal* **5**:305-316.
171. **Widdel F, Pfennig N.** 1982. Studies on dissimilatory sulfate-reducing bacteria that decompose fatty acids II. Incomplete oxidation of propionate by *Desulfobulbus propionicus* gen. nov., sp. nov. *Arch. Microbiol.* **131**:360-365.
172. **DSMZ** 2014, posting date. List of growth media used at DSMZ. [Online.]

173. **Brown RE, Jarvis KL, Hyland KJ.** 1989. Protein measurement using bicinchoninic acid: elimination of interfering substances. *Analytical Biochemistry* **180**:136-139.
174. **Lovley DR, Phillips EJP.** 1994. Novel Processes for Anaerobic Sulfate Production from Elemental Sulfur by Sulfate-Reducing Bacteria. *Appl Environ Microbiol* **60**:2394-2399.
175. **Esteve-Nunez A, Rothermich M, Sharma M, Lovley D.** 2005. Growth of *Geobacter sulfurreducens* under nutrient-limiting conditions in continuous culture. *Environmental Microbiology* **7**:641-648.
176. **Cordruwisch R.** 1985. A Quick Method for the Determination of Dissolved and Precipitated Sulfides in Cultures of Sulfate-Reducing Bacteria. *J Microbiol Meth* **4**:33-36.
177. **Galushko AS, Schink B.** 2000. Oxidation of acetate through reactions of the citric acid cycle by *Geobacter sulfurreducens* in pure culture and in syntrophic coculture. *Arch. Microbiol.* **174**:314-321.
178. **Tempest DW, Neijssel OM.** 1984. The Status of Y_{atp} and Maintenance Energy as Biologically Interpretable Phenomena. *Annu Rev Microbiol* **38**:459-486.
179. **Hazeu W, Bijleveld W, Grotenhuis JTC, Kakes E, Kuenen JG.** 1986. Kinetics and energetics of reduced sulfur oxidation by chemostat cultures of *Thiobacillus ferrooxidans*. *Antonie van Leeuwenhoek* **52**:507-518.
180. **Han C, Chain P.** 2006. Finishing Repetitive Regions Automatically with Dupfinisher, p. 142-147.
181. **Badger JH, Olsen GJ.** 1999. CRITICA: Coding region identification tool invoking comparative analysis. *Mol Biol Evol* **16**:512-524.
182. **Delcher AL, Harmon D, Kasif S, White O, Salzberg SL.** 1999. Improved microbial gene identification with GLIMMER. *Nucleic Acids Res* **27**:4636-4641.
183. **Lowe TM, Eddy SR.** 1997. tRNAscan-SE: a program for improved detection of transfer RNA genes in genomic sequence. *Nucleic Acids Res* **25**:955-964.
184. **Markowitz VM, Mavromatis K, Ivanova NN, Chen IMA, Chu K, Kyrpides NC.** 2009. IMG ER: a system for microbial genome annotation expert review and curation. *Bioinformatics* **25**:2271-2278.
185. **Kumar VS, Dasika MS, Maranas CD.** 2007. Optimization based automated curation of metabolic reconstructions. *Bmc Bioinformatics* **8**.
186. **Izard J, Limberger RJ.** 2003. Rapid screening method for quantitation of bacterial cell lipids from whole cells. *J Microbiol Meth* **55**:411-418.
187. **Ashwell G.** 1957. Colorimetric Analysis of Sugars. *Method Enzymol* **3**:73-105.
188. **Islam MA, Edwards EA, Mahadevan R.** 2010. Characterizing the Metabolism of *Dehalococcoides* with a Constraint-Based Model. *Plos Comput Biol* **6**.
189. **Feist AM, Henry CS, Reed JL, Krummenacker M, Joyce AR, Karp PD, Broadbelt LJ, Hatzimanikatis V, Palsson BO.** 2007. A genome-scale metabolic reconstruction for *Escherichia coli* K-12 MG1655 that accounts for 1260 ORFs and thermodynamic information. *Mol Syst Biol* **3**.
190. **Méthé BA, Webster J, Nevin K, Butler J, Lovley DR.** 2005. DNA Microarray Analysis of Nitrogen Fixation and Fe(III) Reduction in *Geobacter sulfurreducens*. *Appl Environ Microbiol* **71**:2530-2538.

191. **Shrestha PM, Kube M, Reinhardt R, Liesack W.** 2009. Transcriptional activity of paddy soil bacterial communities. *Environ Microbiol* **11**:960-970.
192. **Schmieder R, Edwards R.** 2011. Quality control and preprocessing of metagenomic datasets. *Bioinformatics* **27**:863-864.
193. **Mortazavi A, Williams BA, Mccue K, Schaeffer L, Wold B.** 2008. Mapping and quantifying mammalian transcriptomes by rna-seq. *Nat Meth.* 8 p. *Nature Methods*:8.
194. **Klevebring D, Bjursell M, Emanuelsson O, Lundeberg J.** 2010. In-depth transcriptome analysis reveals novel TARs and prevalent antisense transcription in human cell lines. *Plos One* **5**:e9762.
195. **Buckel W, Thauer RK.** 2013. Energy conservation via electron bifurcating ferredoxin reduction and proton/Na⁺ translocating ferredoxin oxidation. *Biochimica Et Biophysica Acta-Bioenergetics* **1827**:94-113.
196. **Thauer RK, Jungermann K, Decker K.** 1977. Energy conservation in chemotrophic anaerobic bacteriad. *Bacteriological reviews* **41**:100-180.
197. **Rabus R, Hansen T, Widdel F.** 2006. Dissimilatory Sulfate- and Sulfur-Reducing Prokaryotes, p. 659-768. *In* Dworkin M, Falkow S, Rosenberg E, Schleifer K-H, Stackebrandt E (ed.), *The Prokaryotes*. Springer New York.
198. **Möller-Zinkhan D, Thauer RK.** 1988. Membrane-bound NADPH dehydrogenase and ferredoxin:NADP oxidoreductase activity involved in electron transport during acetate oxidation to CO₂ in *Desulfobacter postgatei*. *Arch. Microbiol.* **150**:145-154.
199. **Postgate J.** 1995. Breathless niches. *Nature* **377**:26-26.
200. **Pereira MM, Refojo PN, Hreggvidsson GO, Hjorleifsdottir S, Teixeira M.** 2007. The alternative complex III from *Rhodothermus marinus* – A prototype of a new family of quinol:electron acceptor oxidoreductases. *FEBS Letters* **581**:4831-4835.
201. **Gao XL, Xin YY, Blankenship RE.** 2009. Enzymatic activity of the alternative complex III as a menaquinol: auracyanin oxidoreductase in the electron transfer chain of *Chloroflexus aurantiacus*. *FEBS Letters* **583**:3275-3279.
202. **Barton L, Hamilton WA.** 2007. Sulphate-reducing bacteria : environmental and engineered systems. Cambridge University Press, Cambridge ; New York.
203. **Odom JM, Peck HD.** 1981. Hydrogen cycling as a general mechanism for energy coupling in the sulfate-reducing bacteria, *Desulfovibrio sp.* *Fems Microbiol Lett* **12**:47-50.
204. **Rodrigues R, Valente FMA, Pereira IAC, Oliveira S, Rodrigues-Pousada C.** 2003. A novel membrane-bound Ech [NiFe] hydrogenase in *Desulfovibrio gigas*. *Biochem Bioph Res Co* **306**:366-375.
205. **Caffrey SA, Park HS, Voordouw JK, He Z, Zhou J, Voordouw G.** 2007. Function of periplasmic hydrogenases in the sulfate-reducing bacterium *Desulfovibrio vulgaris* Hildenborough. *J Bacteriol* **189**:6159-6167.
206. **Spring S, Visser M, Lu M, Copeland A, Lapidus A, Lucas S, Cheng JF, Han C, Tapia R, Goodwin LA, Pitluck S, Ivanova N, Land M, Hauser L, Larimer F, Rohde M, Goker M, Detter JC, Kyrpides NC, Woyke T, Schaap PJ, Plugge CM, Muyzer G, Kuever J, Pereira IAC, Parshina SN, Bernier-Latmani R, Stams AJM, Klenk HP.** 2012. Complete genome sequence of the

- sulfate-reducing firmicute *Desulfotomaculum ruminis* type strain (DLT). *Stand Genomic Sci* **7**:304-319.
207. **Welte C, Kratzer C, Deppenmeier U.** 2010. Involvement of Ech hydrogenase in energy conservation of *Methanosarcina mazei*. *Febs J* **277**:3396-3403.
208. **Coppi MV.** 2005. The hydrogenases of *Geobacter sulfurreducens*: a comparative genomic perspective. *Microbiology* **151**:1239-1254.
209. **Vignais PM, Billoud B.** 2007. Occurrence, classification, and biological function of hydrogenases: An overview. *Chem Rev* **107**:4206-4272.
210. **Price ND, Schellenberger J, Palsson BO.** 2004. Uniform sampling of steady-state flux spaces: Means to design experiments and to interpret enzymopathies. *Biophys J* **87**:2172-2186.
211. **Strittmatter AW, Liesegang H, Rabus R, Decker I, Amann J, Andres S, Henne A, Fricke WF, Martinez-Arias R, Bartels D, Goesmann A, Krause L, Puhler A, Klenk HP, Richter M, Schuler M, Glockner FO, Meyerdierks A, Gottschalk G, Amann R.** 2009. Genome sequence of *Desulfobacterium autotrophicum* HRM2, a marine sulfate reducer oxidizing organic carbon completely to carbon dioxide. *Environmental Microbiology* **11**:1038-1055.
212. **McInerney MJ, Rohlin L, Mouttaki H, Kim U, Krupp RS, Rios-Hernandez L, Sieber J, Struchtemeyer CG, Bhattacharyya A, Campbell JW, Gunsalus RP.** 2007. The genome of *Syntrophus aciditrophicus*: life at the thermodynamic limit of microbial growth. *Proc Natl Acad Sci U S A* **104**:7600-7605.
213. **Muller V, Imkamp F, Biegel E, Schmidt S, Dilling S.** 2008. Discovery of a Ferredoxin : NAD(+)-Oxidoreductase (Rnf) in *Acetobacterium woodii* - A novel potential coupling site in acetogens. *Ann Ny Acad Sci* **1125**:137-146.
214. **Seedorf H, Fricke WF, Veith B, Bruggemann H, Liesegang H, Strittmatter A, Miethke M, Buckel W, Hinderberger J, Li FL, Hagemeyer C, Thauer RK, Gottschalk G.** 2008. The genome of *Clostridium kluyveri*, a strict anaerobe with unique metabolic features. *Proceedings of the National Academy of Sciences of the United States of America* **105**:2128-2133.
215. **Kopke M, Held C, Hujer S, Liesegang H, Wiezer A, Wollherr A, Ehrenreich A, Liebl W, Gottschalk G, Durre P.** 2010. *Clostridium ljungdahlii* represents a microbial production platform based on syngas. *Proceedings of the National Academy of Sciences of the United States of America* **107**:13087-13092.
216. **Biegel E, Schmidt S, Gonzalez JM, Muller V.** 2011. Biochemistry, evolution and physiological function of the Rnf complex, a novel ion-motive electron transport complex in prokaryotes. *Cell Mol Life Sci* **68**:613-634.
217. **Poehlein A, Daniel R, Schink B, Simeonova DD.** 2013. Life based on phosphite: a genome-guided analysis of *Desulfotignum phosphitoxidans*. *Bmc Genomics* **14**.
218. **Feist AM, Palsson BO.** 2010. The biomass objective function. *Current opinion in microbiology* **13**:344-349.
219. **Thiele I, Palsson BO.** 2010. A protocol for generating a high-quality genome-scale metabolic reconstruction. *Nat. Protocols* **5**:93-121.
220. **Hyduke D, Schellenberger J, Que R, Fleming R, Thiele I, Orth J, Feist A, Zielinski D, Bordbar A, Lewis N, Rahmanian S, Kang J, Palsson B.** 2011. COBRA Toolbox 2.0.

221. **Pirt SJ.** 1965. The maintenance energy of bacteria in growing cultures. *Proc R Soc Lond B Biol Sci* **163**:224-231.
222. **Schauder R, Widdel F, Fuchs G.** 1987. Carbon assimilation pathways in sulfate-reducing bacteria II. Enzymes of a reductive citric acid cycle in the autotrophic *Desulfobacter hydrogenophilus*. *Arch. Microbiol.* **148**:218-225.
223. **Hoehler TM, Jørgensen BB.** 2013. Microbial life under extreme energy limitation. *Nat Rev Micro* **11**:83-94.
224. **van Bodegom P.** 2007. Microbial maintenance: a critical review on its quantification. *Microb Ecol* **53**:513-523.
225. **Davidson MM, Bisher ME, Pratt LM, Fong J, Southam G, Pfiffner SM, Reches Z, Onstott TC.** 2009. Sulfur Isotope Enrichment during Maintenance Metabolism in the Thermophilic Sulfate-Reducing Bacterium *Desulfotomaculum putei*. *Appl Environ Microbiol* **75**:5621-5630.
226. **Schonheit P, Kristjansson JK, Thauer RK.** 1982. Kinetic mechanism for the ability of sulfate reducers to outcompete methanogens for acetate. *Arch. Microbiol.* **132**:285-288.
227. **Stefanie JWH, Elferink O, Visser A, Hulshoff Pol LW, Stams AJM.** 1994. Sulfate reduction in methanogenic bioreactors. *FEMS Microbiology Reviews* **15**:119-136.
228. **Kristjansson JK, Schönheit P.** 1983. Why do sulfate-reducing bacteria outcompete methanogenic bacteria for substrates? *Oecologia* **60**:264-266.
229. **Jin Q.** 2012. Energy conservation of anaerobic respiration. *American Journal of Science* **312**:573-628.
230. **Edwards JS, Ramakrishna R, Palsson BO.** 2002. Characterizing the metabolic phenotype: a phenotype phase plane analysis. *Biotechnol Bioeng* **77**:27-36.
231. **Edwards JS, Ibarra RU, Palsson BO.** 2001. *In silico* predictions of *Escherichia coli* metabolic capabilities are consistent with experimental data. *Nat Biotechnol* **19**:125-130.
232. **Thiele I, Price ND, Vo TD, Palsson BO.** 2005. Candidate metabolic network states in human mitochondria. *J. Biol. Chem.* **280**:11683-11695.
233. **Zomorodi AR, Suthers PF, Ranganathan S, Maranas CD.** 2012. Mathematical optimization applications in metabolic networks. *Metab Eng* **14**:672-686.
234. **Yoon K-S, Ishii M, Kodama T, Igarashi Y.** 1997. Carboxylation Reactions of Pyruvate: Ferredoxin Oxidoreductase and 2-Oxoglutarate: Ferredoxin Oxidoreductase from *Hydrogenobacter thermophilus* TK-6. *Bioscience, Biotechnology, and Biochemistry* **61**:510-513.
235. **Villanueva L, Haveman SA, Summers ZM, Lovley DR.** 2008. Quantification of *Desulfovibrio vulgaris* dissimilatory sulfite reductase gene expression during electron donor- and electron acceptor-limited growth. *Appl Environ Microbiol* **74**:5850-5853.
236. **Keller KL, Rapp-Giles BJ, Semkiw ES, Porat I, Brown SD, Wall JD.** 2014. New Model for Electron Flow for Sulfate Reduction in *Desulfovibrio alaskensis* G20. *Appl Environ Microbiol* **80**:855-868.

237. **Meyer B, Kuehl JV, Deutschbauer AM, Arkin AP, Stahl DA.** 2013. Flexibility of Syntrophic Enzyme Systems in *Desulfovibrio* Species Ensures Their Adaptation Capability to Environmental Changes. *J Bacteriol* **195**:4900-4914.
238. **Carbonero F, Oakley BB, Purdy KJ.** 2014. Metabolic Flexibility as a Major Predictor of Spatial Distribution in Microbial Communities. *Plos One* **9**.
239. **Krogh A, Larsson B, von Heijne G, Sonnhammer ELL.** 2001. Predicting transmembrane protein topology with a hidden Markov model: Application to complete genomes. *J Mol Biol* **305**:567-580.
240. **Price M, Ray J, Wetmore KM, Kuehl JV, Bauer S, Deutschbauer AM, Arkin AP.** 2014. The genetic basis of energy conservation in the sulfate-reducing bacterium *Desulfovibrio alaskensis* G20.
241. **Ingvorsen K, Zehnder AJB, Jorgensen BB.** 1984. Kinetics of Sulfate and Acetate Uptake by *Desulfobacter postgatei*. *Appl Environ Microb* **47**:403-408.
242. **Widdel F, Pfennig N.** 1981. Studies on Dissimilatory Sulfate-Reducing Bacteria That Decompose Fatty-Acids .1. Isolation of New Sulfate-Reducing Bacteria Enriched with Acetate from Saline Environments - Description of *Desulfobacter postgatei* gen-nov, sp-nov. *Arch. Microbiol.* **129**:395-400.
243. **Wolfe AJ.** 2005. The acetate switch. *Microbiol Mol Biol R* **69**:12-+.
244. **Stahlmann J, Warthmann R, Cypionka H.** 1991. Na⁺-Dependent Accumulation of Sulfate and Thiosulfate in Marine Sulfate-Reducing Bacteria. *Arch. Microbiol.* **155**:554-558.
245. **Brandis-Heep A, Gebhardt NA, Thauer RK, Widdel F, Pfennig N.** 1983. Anaerobic Acetate Oxidation to CO₂ by *Desulfobacter postgatei* .1. Demonstration of All Enzymes Required for the Operation of the Citric-Acid Cycle. *Arch. Microbiol.* **136**:222-229.
246. **Möller-Zinkhan D, Thauer RK.** 1988. Membrane-bound NADPH dehydrogenase- and ferredoxin: NADP oxidoreductase activity involved in electron transport during acetate oxidation to CO₂ in *Desulfobacter postgatei*. *Arch. Microbiol.* **150**:145-154.
247. **Ivanovsky RN, Sintsov NV, Kondratieva EN.** 1980. ATP-linked citrate lyase activity in the green sulfur bacterium *Chlorobium limicola* forma *thiosulfatophilum*. *Arch. Microbiol.* **128**:239-241.
248. **Thauer RK, Moller-Zinkhan D, Spormann AM.** 1989. Biochemistry of acetate catabolism in anaerobic chemotrophic bacteria. *Annu Rev Microbiol* **43**:43-67.
249. **Atomi H.** 2002. Microbial enzymes involved in carbon dioxide fixation. *Journal of Bioscience and Bioengineering* **94**:497-505.
250. **Rabus R, Hansen TA, Widdel F.** 2006. Dissimilatory Sulfate- and Sulfur-Reducing Prokaryotes. *Prokaryotes: A Handbook on the Biology of Bacteria*, Vol 2, Third Edition:659-768.
251. **Costa C, Moura JJG, Moura I, Liu MY, Peck HD, Legall J, Wang YN, Huynh BH.** 1990. Hexaheme Nitrite Reductase from *Desulfovibrio desulfuricans*. Mössbauer and EPR Characterization of the Heme Groups. *J. Biol. Chem.* **265**:14382-14388.
252. **Mahadevan R, Lovley DR.** 2008. The degree of redundancy in metabolic genes is linked to mode of metabolism. *Biophys J* **94**:1216-1220.

253. **Segura D, Mahadevan R, Juárez K, Lovley DR.** 2008. Computational and Experimental Analysis of Redundancy in the Central Metabolism of *Geobacter sulfurreducens*. *Plos Comput Biol* **4**:e36.
254. **Yang TH, Coppi M, Lovley D, Sun J.** 2010. Metabolic response of *Geobacter sulfurreducens* towards electron donor/acceptor variation. *Microbial Cell Factories* **9**:90.
255. **Sousa FL, Thiergart T, Landan G, Nelson-Sathi S, Pereira IA, Allen JF, Lane N, Martin WF.** 2013. Early bioenergetic evolution. *Philosophical transactions of the Royal Society of London. Series B, Biological sciences* **368**:20130088.
256. **Ramos AR, Keller KL, Wall JD, Pereira IAC.** 2012. The membrane QmoABC complex interacts directly with the dissimilatory adenosine 5'-phosphosulfate reductase in sulfate reducing bacteria. *Front Microbiol* **3**.
257. **Pires RH, Lourenco AI, Morais F, Teixeira M, Xavier AV, Saraiva LM, Pereira IAC.** 2003. A novel membrane-bound respiratory complex from *Desulfovibrio desulfuricans* ATCC 27774. *Biochimica Et Biophysica Acta-Bioenergetics* **1605**:67-82.
258. **Krumholz LR, Wang L, Beck DAC, Wang T, Hackett M, Mooney B, Juba TR, McInerney MJ, Meyer B, Wall JD, Stahl DA.** 2013. Membrane protein complex of APS reductase and Qmo is present in *Desulfovibrio vulgaris* and *Desulfovibrio alaskensis*. *Microbiology* **159**:2162-2168.
259. **Grein F, Pereira IAC, Dahl C.** 2010. Biochemical Characterization of Individual Components of the *Allochromatium vinosum* DsrMKJOP Transmembrane Complex Aids Understanding of Complex Function *In Vivo*. *J Bacteriol* **192**:6369-6377.
260. **Klenk HP, Clayton RA, Tomb JF, White O, Nelson KE, Ketchum KA, Dodson RJ, Gwinn M, Hickey EK, Peterson JD, Richardson DL, Kerlavage AR, Graham DE, Kyrpides NC, Fleischmann RD, Quackenbush J, Lee NH, Sutton GG, Gill S, Kirkness EF, Dougherty BA, McKenney K, Adams MD, Loftus B, Peterson S, Reich CI, McNeil LK, Badger JH, Glodek A, Zhou LX, Overbeek R, Gocayne JD, Weidman JF, McDonald L, Utterback T, Cotton MD, Spriggs T, Artiach P, Kaine BP, Sykes SM, Sadow PW, D'Andrea KP, Bowman C, Fujii C, Garland SA, Mason TM, Olsen GJ, Fraser CM, Smith HO, Woese CR, Venter JC.** 1998. The complete genome sequence of the hyperthermophilic, sulphate-reducing archaeon *Archaeoglobus fulgidus*. *Nature* **394**:101-101.
261. **Junier P, Junier T, Podell S, Sims DR, Detter JC, Lykidis A, Han CS, Wigginton NS, Gaasterland T, Bernier-Latmani R.** 2010. The genome of the Gram positive metal- and sulfate-reducing bacterium *Desulfotomaculum reducens* strain MI-1. *Environmental Microbiology* **12**:2738-2754.
262. **Heidelberg JF, Seshadri R, Haveman SA, Hemme CL, Paulsen IT, Kolonay JF, Eisen JA, Ward N, Methe B, Brinkac LM, Daugherty SC, Deboy RT, Dodson RJ, Durkin AS, Madupu R, Nelson WC, Sullivan SA, Fouts D, Haft DH, Selengut J, Peterson JD, Davidsen TM, Zafar N, Zhou LW, Radune D, Dimitrov G, Hance M, Tran K, Khouri H, Gill J, Utterback TR, Feldblyum TV, Wall JD, Voordouw G, Fraser CM.** 2004. The genome sequence of the

- anaerobic, sulfate-reducing bacterium *Desulfovibrio vulgaris* Hildenborough. Nature Biotechnology **22**:554-559.
263. **Brown SD, Gilmour CC, Kucken AM, Wall JD, Elias DA, Brandt CC, Podar M, Chertkov O, Held B, Bruce DC, Detter JC, Tapia R, Han CS, Goodwin LA, Cheng JF, Pitluck S, Woyke T, Mikhailova N, Ivanova NN, Han J, Lucas S, Lapidus AL, Land ML, Hauser LJ, Palumbo AV.** 2011. Genome Sequence of the Mercury-Methylating Strain *Desulfovibrio desulfuricans* ND132. J Bacteriol **193**:2078-2079.
264. **Wang S, Huang H, Moll J, Thauer RK.** 2010. NADP⁺ Reduction with Reduced Ferredoxin and NADP⁺ Reduction with NADH Are Coupled via an Electron-Bifurcating Enzyme Complex in *Clostridium kluyveri*. J Bacteriol **192**:5115-5123.
265. **Andrews SC, Berks BC, McClay J, Ambler A, Quail MA, Golby P, Guest JR.** 1997. A 12-cistron *Escherichia coli* operon (hyf) encoding a putative proton-translocating formate hydrogenlyase system. Microbiology **143**:3633-3647.
266. **Kunkel A, Vorholt JA, Thauer RK, Hedderich R.** 1998. An *Escherichia coli* hydrogenase-3-type hydrogenase in methanogenic archaea. European Journal of Biochemistry **252**:467-476.
267. **Sapra R, Verhagen MFJM, Adams MWW.** 2000. Purification and characterization of a membrane-bound hydrogenase from the hyperthermophilic archaeon *Pyrococcus furiosus*. J Bacteriol **182**:3423-3428.
268. **Clark ME, He ZL, Redding AM, Joachimiak MP, Keasling JD, Zhou JZZ, Arkin AP, Mukhopadhyay A, Fields MW.** 2012. Transcriptomic and proteomic analyses of *Desulfovibrio vulgaris* biofilms: Carbon and energy flow contribute to the distinct biofilm growth state. BMC Genomics **13**.
269. **Yu NY, Wagner JR, Laird MR, Melli G, Rey S, Lo R, Dao P, Sahinalp SC, Ester M, Foster LJ, Brinkman FSL.** 2010. PSORTb 3.0: improved protein subcellular localization prediction with refined localization subcategories and predictive capabilities for all prokaryotes. Bioinformatics **26**:1608-1615.
270. **Barton L.** 1995. Sulfate-reducing bacteria. Plenum Press, New York.
271. **Dar SA, Kleerebezem R, Stams AJM, Kuenen JG, Muyzer G.** 2008. Competition and coexistence of sulfate-reducing bacteria, acetogens and methanogens in a lab-scale anaerobic bioreactor as affected by changing substrate to sulfate ratio. Appl Microbiol Biot **78**:1045-1055.
272. **Kobayashi K, Hasegawa H, Takagi M, Ishimoto M.** 1982. Proton translocation associated with sulfite reduction in a sulfate-reducing bacterium, *Desulfovibrio vulgaris*. Febs Letters **142**:235-237.
273. **Neidhardt FC, Ingraham JL, Schaechter M.** 1990. Physiology of the bacterial cell: a molecular approach. Sinauer Associates, Inc, Sunderland, Mass.
274. **Orth JD, Conrad TM, Na J, Lerman JA, Nam H, Feist AM, Palsson BO.** 2011. A comprehensive genome-scale reconstruction of *Escherichia coli* metabolism--2011. Mol Syst Biol **7**:65.